FINAL REPORT: ER-1127

Development of Effective Aerobic Cometabolic Systems for the In Situ Transformation of Problematic Chlorinated Solvent Mixtures

Lewis Semprini, Mark E. Dolan, Gary D. Hopkins, and Perry L. McCarty

Department of Civil, Construction & Environmental Engineering
Oregon State University, Corvallis, Oregon

February 2005

Distribution Statement A: Approved for Public Release, Distribution is Unlimited

This report was prepared under contract to the Department of Defense Strategic Environmental Research and Development Program (SERDP). The publication of this report does not indicate endorsement by the Department of Defense, nor should the contents be construed as reflecting the official policy or position of the Department of Defense. Reference herein to any specific commercial product, process, or service by trade name, trademark, manufacturer, or otherwise, does not necessarily constitute or imply its endorsement, recommendation, or favoring by the Department of Defense.

Table of Contents

LIST OF TABLES IV

LIST OF FIGURES VI

ACRONYMS XIII

ACKNOWLEDGEMENTS XIV

EXECUTIVE SUMMARY XV

1. OBJECTIVES 1

2. BACKGROUND 4

2.1 BIOAUGMENTATION STUDIES 10
2.2 MOLECULAR METHODS TO TRACK BIOAUGMENTED MICROORGANISMS 13

3. MATERIALS AND METHODS 17

3.1 CULTURE DEVELOPMENT 18
3.2 MOLECULAR METHODS 19
3.2.1 Sample Acquisition and Preparation 20
3.2.2. DNA Extraction Methods 21
3.2.3 Oligonucleotide Primer and Probe Design 21
3.2.4 PCR Conditions 23
3.2.5 Gel Electrophoresis 25
3.2.6 Creation of a Clone Library 25
3.2.7 T-RFLP Analysis 28
3.2.8 Quantitative Real Time PCR 28
3.2.9 FISH Analysis 30
3. 3 CULTURE KINETIC STUDIES 31
3.3.1 Chemicals Used 31
3.3.2 Growth of the Butane Culture(s) Media and Microcosm Tests 32
3.3.3 Batch Transformation Kinetic Tests in Media 33
3.4 MICROCOSM METHODS TEST 33
3.4.1 Microcosm Construction 33
3.4.2 Analytical Methods for the Media and Microcosm Studies 35
3.5 CONTINUOUS FLOW COLUMN STUDY METHODS 35
3.5.1 Construction of the Continuous Flow Column 35
3.5.2 Bromide Tracer Tests 38
3.5.3 Column Injection System 38
3.5.4 Analytical Methods 38
3.6 METHODS USED IN THE FIELD DEMONSTRATION 39
3.6.1 Test Leg Installation for the Field Experiments 39
3.6.2 Subsurface Hydrogeology 40
3.6.3 Groundwater Chemical Characteristics 42
3.6.4 Extraction System 42
3.6.5 Inducted Gradient Conditions of the Field Experiment 45
3.7 MODEL DEVELOPMENT 49
3.7.1 Monod/Michaelis-Menten Kinetics 50
3.7.2 Modeling Substrate Inhibition 51
3.7.3 Modeling Product Toxicity 52
3.7.4 Modeling Contaminant Transport 53
3.7.5 Combined Biotransformation and Transport Model 53
3.7.6 Verification of Model Performance 56

4. RESULTS OF LABORATORY STUDIES 64

4.1 CULTURE DEVELOPMENT 64
4.2 CLONE LIBRARY DEVELOPMENT 70
4.3 STUDIES OF 1,1,1-TCA TRANSFORMATION AND BUTANE UTILIZATION WITH AN ENRICHED CULTURE 76
4.3.1 Butane and 1,1,1-TCA Kinetic Experiments 82
4.3.2 The Simulation of Butane Utilization and 1,1,1-TCA Transformation in the BR3 Microcosm Set 97
4.4 MICROCOSM TESTS 1,1-DCE 108
4.4.1 Results 108
4.4.2 Discussion 123
4.5 GROWTH CHARACTERISTICS AND COMETABOLIC ACTIVITY OF STRAIN 183BP 124
4.5.1 Characteristics of Strain 183BP when Grown on Butane 124
4.5.2 Ethanol, Acetate, and Succinate as Substrates for the Strain 183BP Culture 129
4.5.3 Acetate as a Cosubstrate With Butane 137
4.5.4 C1 through C6 n-hydrocarbons as substrates for strain 183BP cultures 153
4.5.5 Batch Transformation Kinetic Tests in Media Using the Strain 183BP Culture 165
4.6 COMPARISON OF LABORATORY DATA AND MODEL SIMULATIONS FROM MICROCOSM EXPERIMENTS 171
4.6.1 Results from Microcosms with Indigenous Microorganisms (M1) and Mercury Killed Controls (M4) 171
4.6.2 Bioaugmented Culture Exposed to Butane and CAHs (M2, M3) 174
4.6.3 1,1-DCE Transformation Capacity Experiments in Microcosms 176
4.6.4 Model Simulations for Biotransformation in Microcosm M2B 182
4.6.5 Summary of Laboratory Experiments and Simulations 189
4.7 CONTINUOUS FLOW COLUMN STUDIES 190
4.7.1 Transport Study 190
4.7.2 Bioremediation Study 195
4.8 MODELING ANALYSIS OF THE CONTINUOUS FLOW COLUMN EXPERIMENT 208
4.8.1 Calibration of Biotransformation-Transport Model 208
4.8.2 Biotransformation-Transport Simulations for the First Phase of the 1,1,1-TCA Test 209
4.8.3 Biotransformation Model Simulations of the Second Phase 1,1,1-TCA Test 215

5. FIELD DEMONSTRATION RESULTS 230

5.1. THE FIRST SEASON OF FIELD TESTING 231
5.1.1 Results of Bromide Tracer Tests 234
5.1.2 Results of the CAH Transport Test and the Initial Bioaugmentation and Biostimulation Experiment (Days 0-20) 235
5.1.3 Summary of the Results from the First Season of Testing 247
5.2. RESULTS FROM THE SECOND SEASON OF FIELD TESTING 255
5.2.1 Results from the First 30 Days of Testing 255
5.2.2 Results from Days 30 to 70 263
5.2.3. Percentage Removals of 1,1,1-TCA and 1,1-DCE Achieved 268
5.2.4. Summary of Results from the Second Season of Field Testing 269
5.3 THE THIRD SEASON OF FIELD TESTING 269
5.3.1 First Bioaugmentation Event of the Third Field Season 272
5.3.1.1 Results from the First Bioaugmentation Event in the Third Field Season 273
5.3.1.2 Summary of the First Bioaugmentation Event of the Third Field Season 279
5.3.2 Second Bioaugmentation Event of the Third Field Season 289
5.3.2.1 Bioaugmentation Event 2: Chemical Results 290
5.3.2.2 Bioaugmentation Event 2: Microbial Results 299
5.3.2.3 Bioaugmentation Event 2: Discussion 305
5.3.3 Third Bioaugmentation Event of the Third Field Season 308
5.3.3.1 Bioaugmentation Event 3: Chemical Results 308
5.3.4 Fourth Bioaugmentation Event of the Third Field Season 317
5.3.4.1 Bioaugmentation Event 4: Chemical Results 317
5.3.4.2 Bioaugmentation Event 4: Microbial Results 326
5.3.4.3 Bioaugmentation Event 4: Discussion 332
5.3.4.4 Summary of Third Field Season Bioaugmentation Tests 336

6. RESULTS AND ACCOMPLISHMENTS: FIELD STUDIES 340
6.1 MODELING OF THE FIRST SEASON OF FIELD TESTS 340
6.2 DETERMINATION OF FLOW VELOCITY 341
6.3 DETERMINATION OF SORPTION PARAMETER VALUE 342
6.4 RESULTS OF THE MODELING ANALYSIS 348
6.5 SIMULATIONS TO PREDICT ACTIVITY AFTER BIOAUGMENTATION 356
6.6 SENSITIVITY ANALYSIS OF 1,1-DCE PRODUCT TOXICITY 356
6.7 SENSITIVITY OF 1,1-DCE TRANSFORMATION RATE 361
6.8 SENSITIVITY OF FIRST ORDER MASS TRANSFER RATE AND PULSING CYCLE 362
6.9 SUMMARY FROM THE MODELING OF THE FIRST SEASON TESTS 365
7. CONCLUSIONS 371
8. REFERENCES 373

List of Tables

TABLE 1 PHYSICAL AND CHEMICAL PROPERTIES OF 1,1-DCA, 1,1-DCE, AND 1,1,1-TCA. 7
TABLE 2. COMPARISON OF KINETIC PARAMETERS FOR 1,1-DCE AND 1,1,1-TCA TRANSFORMATION (ADAPTED FROM KIM ET AL., 2002B) 11
TABLE 3. ADDITIONAL BACTERIAL SEQUENCES THAT ARE 100% COMPLEMENTARY TO THE STRAIN 183BP-SPECIFIC PRIMER RAN191F 24
TABLE 4. ADDITIONAL BACTERIAL SEQUENCES THAT ARE 100% COMPLEMENTARY TO THE STRAIN 183BP-SPECIFIC PRIMER RAN443R 24
TABLE 5. 16S RDNA PRIMER SEQUENCES AND CONCENTRATIONS IN PCR REACTION MIXTURES 25
TABLE 6. ENZYME RECOGNITION SITES AND REACTION COMPONENTS FOR RESTRICTION ENDONUCLEASE DIGESTIONS 28
TABLE 7. GROWTH MEDIA COMPOSITION 33
TABLE 8 GROUNDWATER COMPOSITION 45
TABLE 9. FEATURES OF THE BIO-TRANSPORT MODEL 50
TABLE 10. INPUT VALUES FOR TRANSPORT COMPARISON 57
TABLE 11. STELLA INPUT VALUES FOR BIOTRANSFORMATION COMPARISON 60
TABLE 12. MODEL INPUT VALUES FOR BIOTRANSFORMATION COMPARISON 61
TABLE 13. PREDICTED LH-PCR AND T-RFLP RESULTS FOR THE FULLY-SEQUENCED CLONES AND SIMILAR KNOWN ORGANISMS FOUND IN GENEBANK SEARCH (HIGHER RELATIVE MATCH SCORE CORRESPONDS TO GREATER SIMILARITY) 72
TABLE 14. MNLI T-RFLP PREDICTED FRAGMENT LENGTHS AND RESULTS FOR SELECTED CLONES AND ISOLATES 73
TABLE 15. MICROCOSMS USED FOR THE EXPERIMENT OF CAH TRANSFORMATION 76
TABLE 16. MICROCOSMS USED FOR THE KINETIC EXPERIMENTS 82
TABLE 17. BUTANE HALF-SATURATION CONSTANT (K_S) ACHIEVED IN THE BR3 MICROCOSM SET 86
TABLE 18. 1,1,1-TCA HALF-SATURATION CONSTANT (K_S) ACHIEVED IN THE BR3 MICROCOSM SET 89
TABLE 19. BUTANE HALF-SATURATION CONSTANT (K_S) ACHIEVED IN THE BR4 MICROCOSM SET 93
TABLE 20. 1,1,1-TCA HALF-SATURATION CONSTANT (K_S) DETERMINED IN THE BR4 MICROCOSM SET 96
TABLE 21. AVERAGE VALUES OF BUTANE AND 1,1,1-TCA HALF-SATURATION CONSTANT DETERMINED IN ALL MICROCOSMS 96
TABLE 22. MEASURED PARAMETERS FOR MODEL DEVELOPMENT 97
TABLE 23. BUTANE MAXIMUM SPECIFIC RATE ($K_{MAX,BUT}$) AND CELL DECAY RATE (B) ACHIEVED IN THE BR3 MICROCOSM SET 101
TABLE 24. 1,1,1-TCA MAXIMUM SPECIFIC RATE ($K_{MAX,TCA}$) ACHIEVED IN THE BR3 MICROCOSM SET 104
TABLE 25. TRANSFORMATION CAPACITY RANGES (T_C) ACHIEVED IN THE BR3 MICROCOSM SET 107
TABLE 26. PARAMETERS FOR MODEL DEVELOPMENT IN THE BR3 MICROCOSM SET 107
TABLE 27. MICROCOSM CONDITIONS AND LAG TIMES TO 50% BUTANE REMOVAL 111
TABLE 28. COMPARISON OF T-RFLS IN THE SOURCE CULTURE, BIOAUGMENTATION CULTURE, AND INDIGENOUS AQUIFER SAMPLES 116
TABLE 29. SUMMARY OF THE FRAGMENTS FROM THE T-RFLP ANALYSIS FOR THE BIOAUGMENTED AND INDIGENOUS MICROCOSMS AFTER TWO ADDITIONS OF BUTANE 122
TABLE 30. STRAIN 183BP ESTIMATED TTRANSFORMATION CAPACITIES UNDER RESTING CONDITIONS AND WITH ALTERNATE SUBSTRATE ADDITION 131
TABLE 31. MASS OF TCA TRANSFORMED (μG) IN SUCCINATE-, ACETATE-, BUTANE-, AND NON-AMENDED SYSTEMS 134
TABLE 32. OPTICAL DENSITY, NITRATE, AND PH VALUES FOR SUCCINATE-, ACETATE-, BUTANE-, AND NON-AMENDED SYSTEMS AT THE END OF THE 600 H TEST 135
TABLE 33. AMENDMENT CONDITIONS USED TO TEST ACETATE AS A COSUBSTRATE WITH BUTANE TO SUPPORT TCA COMETABOLISM 138
TABLE 34. OPTICAL DENSITY, NITRATE, AND PH VALUES FOR ACETATE- AND BUTANE-FED SYSTEMS AT THE END OF THE 300 H TEST 140
TABLE 35. COMPARISON OF THE TCA MASS TRANSFORMED BY THE DIFFERENT RATIO OF BUTANE MASS 141

TABLE 36. INACTIVATION OF STRAIN 183BP CULTURES AS A RESULT OF DCE TRANSFORMATION MEASURED BY THE PERCENT DECREASE IN BUTANE UPTAKE RATES 151
TABLE 37. SUMMARY OF RESULTS TO COMPARE THE POTENTIAL OF SUBSTRATE AS INDUCERS OF 1,1,1-TCA[1] 164
TABLE 38. INPUT PARAMETERS FOR MODELING BIOTRANSFORMATION IN MEDIA 169
TABLE 39. MICROCOSM DESCRIPTIONS 171
TABLE 40. INPUT PARAMETERS FOR MODELING1,1-DCE PRODUCT TOXICITY 179
TABLE 41. INPUT VALUES FOR SIMULATING BIOTRANSFORMATION IN M2 AND M3 183
TABLE 42. INITIAL CELL CONCENTRATION FOR SIMULATING BIOTRANSFORMATION IN THE M2 AND M3 MICROCOSM 183
TABLE 43. SIMULATED TRANSPORT PARAMETERS FOR BROMIDE (CONSERVATIVE TRACER) AND 1,1,1-TCA 194
TABLE 44: SUMMARY OF COLUMN TESTS 208
TABLE 45. MODEL PARAMETERS USED FOR SIMULATING THE COLUMN STUDY 214
TABLE 46. INJECTION CONCENTRATIONS AND PROCESSES STUDIED DURING THE FIRST SEASON OF FIELD TESTING233
TABLE 47. BUTANE AND OXYGEN INJECTION PULSING DURATIONS AND CONCENTRATIONS 233
TABLE 48. 1,1-DCE, 1,1-DCA, AND 1,1,1-TCA INJECTION CONCENTRATIONS 234
TABLE 49. FRACTIONAL BREAKTHROUGHS OF BROMIDE AND 1,1,1-TCA, 1,1-DCA, AND 1,1-DCE PRIOR TO BIOTRANSFORMATION 242
TABLE 50. PERCENTAGE REMOVALS OF 1,1,1-TCA AND 1,1-DCE DURING DIFFERENT PERIODS OF THE FIRST SEASON OF FIELD TESTING BASED ON WELLS S1 AND S3 249
TABLE 51. INJECTION CONCENTRATIONS AND PROCESSES STUDIED DURING THE SECOND SEASON OF FIELD TESTING256
TABLE 52. PERCENTAGE REMOVALS OF 1,1,1-TCA AND 1,1-DCE DURING DIFFERENT PERIODS OF THE SECOND SEASON OF FIELD TESTING 268
TABLE 53. DURATION, CHEMICAL AMENDMENTS, AND PROCESSES STUDIED DURING THE BIOAUGMENTATION EVENTS IN THE THIRD SEASON OF FIELD TESTING 271
TABLE 54. CALCULATED GROUNDWATER CONCENTRATIONS OF AMENDED NUTRIENT SOLUTION 272
TABLE 55. SUMMARY OF CAH REMOVAL IN THE BIOAUGMENTED LEG DURING THE THIRD FIELD SEASON . 338
TABLE 56. AQUIFER HYDRAULIC CHARACTERISTICS 341
TABLE 57. RETARDATION FACTORS AND SOLIDS PARTITION COEFFICIENTS 346
TABLE 58. BIOTRANSFORMATION VALUES FOR SIMULATING FIELD DATA 348
TABLE 59. TRANSPORT PARAMETER VALUES FOR SIMULATING FIELD DATA 349

List of Figures

FIGURE 1. RECIRCULATION WELL SYSTEMS USED IN THE EDWARDS FIELD DEMONSTRATION OF IN SITU TCE TREATMENT WITH TOLUENE-UTILIZING MICROORGANISMS 5
FIGURE 2. PATHWAY FOR THE ABIOTIC AND BIOTIC TRANSFORMATION OF 1,1,1-TCA 8
FIGURE 3. KINETIC STUDIES OF BUTANE INHIBITION OF 1,1,1-TCA TRANSFORMATION AS DESCRIBED BY KIM ET AL. (2002) 12
FIGURE 4. COMMONLY USED APPROACHES IN MOLECULAR MICROBIAL ECOLOGY (ADAPTED FROM HEAD ET AL., 1998) 15
FIGURE 5. AN OVERVIEW OF THE PROJECT, INCLUDING MICROBIAL CHARACTERIZATION METHODS, LABORATORY STUDIES, AND BIOAUGMENTATION FIELD STUDIES 18
FIGURE 6. FLOWCHART OF PROBE (PRIMER) DESIGN AND SELECTION FOR TARGETING SPECIFIC PHYLOGENETIC GROUPS 22
FIGURE 7. FLOW CHART OF 16S RRNA GENE CLONE LIBRARY ANALYSIS STARTING WITH LIQUID CULTURES AND INCLUDING ARCHIVING, PLASMID PREPARATION, PCR SCREENING, AND RFLP ANALYSIS 27
FIGURE 8. ILLUSTRATION OF COLUMN PACKING PROCEDURE 36
FIGURE 9. COLUMN REACTOR SET-UP SHOWING THE DUAL PUMP INJECTION SYSTEM USED FOR DELIVERING DISSOLVED OXYGEN, BUTANE, 1,1,1-TCA AND 1,1-DCE ALONG WITH THE FLOW THROUGH DO METER 37
FIGURE 10 DIAGRAM OF THE EXPERIMENTAL WELL LEGS AT MOFFETT FEDERAL AIRFIELD 41
FIGURE 11. MODEL SIMULATIONS USING RESSQ OF THE STREAMLINES FOR FLOW EXPECTED FOR THE INJECTION AND EXTRACTION CONDITIONS OF THE FIELD DEMONSTRATION 46
FIGURE 12. A VERTICAL CROSS SECTION OF THE AQUIFER AN EXPERIMENTAL WELL LEG 46
FIGURE 13. THE INJECTION SYSTEM UNDER CONSTRUCTION AT THE TEST SITE 47
FIGURE 14 COMPARISON OF MODEL OUTPUT FOR SOLUTE TRANSPORT 58
FIGURE 15. COMPARISON OF MODEL OUTPUT FOR BIOTRANSFORMATION 62
FIGURE 16. COMPARISON OF MODEL OUTPUT FOR BIOTRANSFORMATION WITH HIGH 1,1,1-TCA PRODUCT TOXICITY 63
FIGURE 17 DIGITAL IMAGES OF DAPI-STAINED AUGMENTATION CULTURE 64
FIGURE 18. T-RFLP PROFILES FOR THE FROZEN SOURCE CULTURE, THE MICROCOSM BIOAUGMENTATION CULTURE (THE SOURCE CULTURE AFTER ONE GROWTH CYCLE ON BUTANE), AND THE NUMERICALLY DOMINANT CLONES FOUND IN THE CLONE LIBRARY 65
FIGURE 19. FOUR MICROBIAL CULTURES ENRICHED FROM THE SOURCE CULTURE ON BUTANE 68
FIGURE 20. SIGNIFICANT DIFFERENCES IN RESTING CELL CAH TRANSFORMATION ACTIVITY FOR FOUR MICROBIAL CULTURES DOMINATED BY EITHER THE ORGANISM WITH A T-RFL OF 183 BP (B6 AND B8) OR AN ORGANISM WITH A T-RFL OF 179 BP (B1 AND B4) 69
FIGURE 21. SCANNING ELECTRON MICROGRAPHS OF THE STRAIN 183BP CULTURE (LEFT FRAME, 5 □M BAR) AND THE STRAIN 179BP CULTURE (MIDDLE FRAME, 5 □M BAR AND RIGHT FRAME, 20□M BAR) SHOW AN EVEN DISTRIBUTION OF STRAIN 183BP CELLS ACROSS THE MEMBRANE AND CLUMPS OF AGGREGATED STRAIN 179BP CELLS AFTER GROWTH IN MINERAL MEDIA WITH A BUTANE HEADSPACE 69
FIGURE 22. RESULTS OF PHYLOGENETIC-SPECIFIC PCR AMPLIFICATION OF GROUNDWATER SAMPLES ACQUIRED FROM A WELL 0.5 M FROM THE INJECTION WELL 70
FIGURE 23. FLOW CHART OF 16S RRNA GENE CLONE LIBRARY ANALYSIS STARTING WITH LIQUID CULTURES AND INCLUDING ARCHIVING, PLASMID PREPARATION, PCR SCREENING, AND RFLP ANALYSIS 74
FIGURE 24. NUCLEOTIDE SEQUENCES FOR RRNA PROBES DESIGNED FOR FOUR OF THE DOMINANT CLONE GROUPS IN THE CLONE LIBRARY 75
FIGURE 25. COMPARISON OF MN(LL) T-RFLP PROFILES FOR THE SOURCE CULTURE AND THE NUMERICALLY DOMINANT CLONES FROM THE CLONE LIBRARY 75
FIGURE 26. BUTANE UTILIZATION AND LIMITED 1,1,1-TCA TRANSFORMATION ACHIEVED IN INDIGENOUS MICROCOSM BR2-C3 77
FIGURE 27. BUTANE UTILIZATION AND 1,1,1-TCA TRANSFORMATION ACHIEVED IN MEDIA-CULTURE INOCULATED MICROCOSM BR2-2 78
FIGURE 28. BUTANE UTILIZATION AND 1,1,1-TCA TRANSFORMATION ACHIEVED IN MEDIA-CULTURE INOCULATED MICROCOSM BR2-3 79
FIGURE 29. 1,1,1-TCA TRANSFORMATION RATE DATA FOR MICROCOSM BR2-2 DURING DAY 28 - 37 80

FIGURE 30. BUTANE UTILIZATION AND CHLORINATED COMPOUND TRANSFORMATION ACHIEVED IN THE MEDIA-CULTURE INOCULATED MICROCOSM BR2-2 81
FIGURE 31. OVERALL RESULTS FROM THE BUTANE KINETIC EXPERIMENTS CONDUCTED IN THE BIOAUGMENTED MICROCOSM BR3-2 82
FIGURE 32. EXPERIMENTAL DATA FROM THE BUTANE KINETIC EXPERIMENT CONDUCTED IN MICROCOSM BR3-2 ON DAY 5 83
FIGURE 33. EXPERIMENTAL DATA FROM THE BUTANE KINETIC EXPERIMENT CONDUCTED IN MICROCOSM BR3-2 ON DAY 6 84
FIGURE 34. EXPERIMENTAL DATA FROM THE BUTANE KINETIC EXPERIMENT CONDUCTED IN MICROCOSM BR3-2 FROM DAY 13 TO 14 85
FIGURE 35. OVERALL RESULTS FROM THE 1,1,1-TCA KINETIC EXPERIMENT CONDUCTED IN BIOAUGMENTED MICROCOSM BR3-2 87
FIGURE 36. EXPERIMENTAL DATA FROM THE 1,1,1-TCA KINETIC EXPERIMENT CONDUCTED IN MICROCOSM BR3-2 ON DAY 15 87
FIGURE 37. EXPERIMENTAL DATA FROM THE 1,1,1-TCA KINETIC EXPERIMENT CONDUCTED IN MICROCOSM BR3-2 FROM DAY 15 TO 16 88
FIGURE 38. OVERALL RESULTS FROM THE BUTANE AND 1,1,1-TCA KINETIC EXPERIMENTS CONDUCTED IN BIOAUGMENTED MICROCOSM BR4-5 90
FIGURE 39. EXPERIMENTAL DATA FROM THE BUTANE KINETIC EXPERIMENT CONDUCTED IN MICROCOSM BR4-5 ON DAY 4 91
FIGURE 40. EXPERIMENTAL DATA FROM THE BUTANE KINETIC EXPERIMENT CONDUCTED IN MICROCOSM BR4-5 ON DAY 13 92
FIGURE 41. EXPERIMENTAL DATA FROM THE 1,1,1-TCA KINETIC EXPERIMENT CONDUCTED IN MICROCOSM BR4-5 ON DAY 5 94
FIGURE 42. EXPERIMENTAL DATA FROM THE 1,1,1-TCA KINETIC EXPERIMENT CONDUCTED IN MICROCOSM BR4-5 FROM DAY 13 TO 14 95
FIGURE 43. BUTANE UTILIZATION DATA FROM MICROCOSM BR3-5 98
FIGURE 44. SIMULATION OF BUTANE UTILIZATION FOR MICROCOSM BR3-5 99
FIGURE 45. 1,1,1-TCA TRANSFORMATION DATA FROM MICROCOSM BR3-5 102
FIGURE 46. SIMULATION OF 1,1,1-TCA TRANSFORMATION FOR MICROCOSM BR3-5 103
FIGURE 47. SIMULATIONS OF BUTANE UTILIZATION AND 1,1,1-TCA TRANSFORMATION FOR MICROCOSM BR3-1 WITHOUT THE TERM FOR TRANSFORMATION CAPACITY 105
FIGURE 48. SIMULATIONS OF 1,1,1-TCA TRANSFORMATION FOR MICROCOSM BR3-5 OVER A RANGE OF TRANSFORMATION CAPACITIES 106
FIGURE 49. BUTANE MASS HISTORIES IN THE BIOAUGMENTED MICROCOSM SET NB, FED ONLY BUTANE 109
FIGURE 50. BUTANE (CLOSED SYMBOLS) AND 1,1-DCE (OPEN SYMBOLS) MASS HISTORIES IN THE BIOAUGMENTED MICROCOSMS SET PEB, PRE-EXPOSED TO 1,1-DCE WITH NO BUTANE INITIALLY PRESENT 110
FIGURE 51. BUTANE (CLOSED SYMBOLS) AND 1,1-DCE (OPEN SYMBOLS) MASS HISTORIES IN THE BIOAUGMENTED MICROCOSM SET EB, EXPOSED TO 1,1-DCE AND BUTANE SIMULTANEOUSLY 113
FIGURE 52. BUTANE (CLOSED SYMBOLS) AND 1,1-DCE (OPEN SYMBOLS) MASS HISTORIES IN NON-BIOAUGMENTED MICROCOSM SET EI, EXPOSED TO 1,1-DCE AND BUTANE SIMULTANEOUSLY 115
FIGURE 53. ELECTROPHEROGRAMS FROM THE MNLI DIGESTS OF SAMPLES FROM THE BIOAUGMENTED MICROCOSM B5 THAT WAS FED BUTANE AND NOT EXPOSED TO 1,1-DCE 118
FIGURE 55. ELECTROPHEROGRAMS FROM THE MNLI DIGESTS OF SAMPLES FROM THE BIOAUGMENTED MICROCOSM B8 THAT WAS SIMULTANEOUSLY EXPOSED TO 1,1-DCE AND BUTANE 120
FIGURE 56. ELECTROPHEROGRAMS FROM THE MNLI DIGESTS OF SAMPLES FROM THE NON-BIOAUGMENTED MICROCOSMS THAT WERE SIMULTANEOUSLY EXPOSED TO 1,1-DCE AND BUTANE 121
FIGURE 57. STRAIN 183BP CULTURE GROWTH ON BUTANE A) BUTANE UTILIZATION, B) CELL GROWTH MEASURED AS OPTICAL DENSITY, AND C) NITRATE CONSUMPTION 126
FIGURE 58. NITRATE REQUIREMENTS OF THE STRAIN 183BP CULTURE WHEN GROWN ON BUTANE 127
FIGURE 59. RELATIONSHIPS BETWEEN TSS, OD_{600}, AND PROTEIN CONCENTRATIONS FOR THE STRAIN 183BP CULTURE WHEN GROWN ON BUTANE IN MINERAL MEDIA 128
FIGURE 60. TCA TRANSFORMATION BY BUTANE-GROWN STRAIN 183BP RESTING CELLS WHERE A) RESTING CELLS WERE FED AN ALTERNATE SUBSTRATE, ACETATE OR ETHANOL, AFTER INITIAL TCA TRANSFORMATION, AND B) ONE GROUP OF RESTING CELLS WERE IMMEDIATELY EXPOSED TO TCA WHILE

Another Group Was Shaken for 24 Hours Under Aerobic Conditions In The Absence Of Butane Before TCA Exposure 130
Figure 61. TCA Transformation by a Butane-Grown Strain 183BP Culture in Mineral Media, Where the Culture is Amended a) Alternately with Succinate and Butane, b) Alternately with Acetate and Butane, and c) with Butane Alone 133
Figure 62. TCA Transformation by a Resting Butane-Grown Strain 183BP Culture in Mineral Media 134
Figure 63. Cumulative TCA Transformation by Strain 183BP Culture Amended with Alternate Substrates 136
Figure 64. Maximum TCA Transformation Rates Achieved by Strain 183BP Culture Amended with Alternate Substrates during the Four Phases of the Test 137
Figure 65. Average TCA Transformation and Average Butane Utilization by R183 a) Average TCA transformation in acetate-butane mixed substrate, and b) The average butane degradation curve in the mixed substrate system 139
Figure 66. Average TCA Cumulative Mass in Different Substrate Conditions 140
Figure 67. CAHs Transformation by R183 Culture a) CAHs concentration and butane mass in control, and b) CAHs transformation by the R183 resting cells 143
Figure 68. Combined Butane Utilization and CAH Transformation by a Strain 183BP Culture 145
Figure 69. CAHs Transformation by R179 a) CAHs and butane in controls, and (b) CAHs transformation in R179 resting cells 147
Figure 70. Butane Utilization and CAH Transformation by the Strain 179BP Culture 149
Figure 71. Butane Utilization by Strain 183BP Compared to Those Exposed to DCE and Non-Exposed Cultures 151
Figure 72. Butane Utilization by Strain 183BP Compared to Those Exposed to DCE and Non-Exposed Cultures 152
Figure 73. Butane Utilization by Strain 183BP Compared to Those Exposed to DCE and Non-Exposed Cultures 152
Figure 74. Inactivation of Strain 183 BP as a Result of DCE Transformation 153
Figure 75. Methane and Ethane as Potential Growth Substrates for the Strain 183BP Culture 155
Figure 76. Propane Utilization by the183BP Culture, a) Propane uptake, and b) TCA 157
Figure 77. Butane Utilization and TCA Transformation by Strain 183BP, a) Butane Uptake, and b) TCA Transformation 159
Figure 78. Pentane Utilization and TCA Transformation by Strain 183BP Culture, a) Pentane Uptake, and b) TCA Transformation Observed in Four TCA Additions 160
Figure 79. Hexane Utilization and TCA Transformation by Strain 183BP, a) Hexane Uptake, and b) TCA Transformation of Two TCA Additions over 3 days 162
Figure 80. Incubation of a CAH Mixture and Strain 183BP Cells in the Presence of Butane Resulted in Fast 1,1-DCE Transformation Followed by Butane, 1,1-DCA, and 1,1,1-TCA Transformation 166
Figure 81. Butane and 1,1-DCE Mass Profiles in 8 reactors containing Strain 183BP Cells, Those Used in the First Season Bioaugmentation at the Moffett Field Site, and a Mixture of 1,1-DCE, 1,1-DCA, and 1,1,1-TCA in the Presence of Butane Show Very Similar Activities 167
Figure 82. 1,1-DCA and 1,1,1-TCA Mass Profiles in 8 Reactors Containing Strain 183BP Cells, Those Used in the First Season Bioaugmentation at the Moffett Field Site, and a Mixture of 1,1-DCE, 1,1-DCA, and 1,1,1-TCA in the Presence of Butane Show Similar Activities 168
Figure 83. Model Simulations of Strain 183BP Transformation of Butane, 1,1-DCE, 1,1-DCA, and 1,1,1-TCA in Media Bottles 170
Figure 84. Poisoned Control Data for M1 (indigenous culture) 172
Figure 85. Laboratory data for M4 (mercury killed control) 173
Figure 86. Microcosm M2B Experimental Data 174
Figure 87. Results of Biotransformation Experiments for Microcosms M2 and M3 175
Figure 88. Simulation of Butane Utilization Prior to 1,1-DCE Transformation Capacity Experiments 176
Figure 89. Results of Transformation Capacity Experiments of 1,1-DCE 178
Figure 90. Simulations for Various K_{MDCE} Values Compared to Laboratory Data 181

FIGURE 91. COMPARISON OF LABORATORY DATA VERSUS MODEL OUTPUT FOR M2B 185
FIGURE 92. COMPARISON PLOT OF M2B DATA AND MODEL OUTPUT ASSUMING LOW K_{mDCE} (0.1 MMOL/MG/HR) 188
FIGURE 93. ELUTION DATA OF BROMIDE FROM THE COLUMN AND MODEL FIT AT A FLOW RATE OF 0.2ML/MIN 191
FIGURE 94. 1,1,1-TCA BREAKTHROUGH CURVE FIT TO EQUILIBRIUM AND NON-EQUILIBRIUM CDE 192
FIGURE 95. LONG-TERM BREAKTHROUGH OF 1,1,1-TCA PRIOR TO BIOAUGMENTATION AND BIOSTIMULATION 192
FIGURE 96. DISSOLVED OXYGEN BREAKTHROUGH: COLUMN EFFLUENT DATA FITTED TO 1-D CDE 193
FIGURE 97. PULSED BUTANE BREAKTHROUGH DATA THROUGH THE SOIL COLUMN 194
FIGURE 98. 1,1,1-TCA, BUTANE AND DISSOLVED OXYGEN PROFILE DURING THE FIRST PHASE OF BIOAUGMENTATION AND BIOSTIMULATION EXPERIMENT 196
FIGURE 99. 1,1,1-TCA, BUTANE, AND DO PROFILES DURING THE SECOND PHASE OF THE TEST 198
FIGURE 100. 1,1,1-TCA, BUTANE AND DO PROFILES DURING THE THIRD PHASE OF THE TEST: DEMONSTRATION OF BUTANE DEPENDENCE 200
FIGURE 101. 1,1,1-TCA, 1,1-DCE, BUTANE AND DO PROFILES DURING THE THIRD PHASE 203
FIGURE 102. REAL-TIME PCR MICROBIAL ANALYSIS DURING BIOSTIMULATION 204
FIGURE 103. MICROBIAL COMMUNITY COMPOSITION DETERMINED BY T-RFLP ANALYSIS DURING THE BIOAUGMENTATION TEST IN THE SOIL COLUMN FROM DAY 37 TO 134 207
FIGURE 104. COMPARISON OF THE BIOTRANSFORMATION AND CXTFIT MODELING FIT TO 1,1,1-TCA TRANSPORT TESTS 209
FIGURE 105. MODEL SIMULATIONS OF CONCENTRATION IN THE COLUMN EFFLUENT AND LABORATORY DATA DURING THE FIRST PHASE OF BIOTRANSFORMATION TEST (DAYS 0-30) 211
FIGURE 106 MODEL SIMULATIONS OF THE SPATIAL DISTRIBUTION IN CONCENTRATION AFTER 30 DAYS OF OPERATION IN PHASE I 212
FIGURE 107. MODEL SIMULATIONS OF CONCENTRATION IN THE COLUMN EFFLUENT AND LABORATORY DATA DURING THE SECOND PHASE OF BIOTRANSFORMATION TEST (DAYS 30-53) 216
FIGURE 108: MODEL SIMULATIONS OF THE SPATIAL DISTRIBUTION IN CONCENTRATION AFTER 53 DAYS OF OPERATION IN PHASE II 218
FIGURE 109. MODEL SIMULATIONS OF CONCENTRATION IN THE COLUMN EFFLUENT AND LABORATORY DATA DURING THE SECOND PHASE (LOW 1,1,1-TCA CONCENTRATION) OF BIOTRANSFORMATION TEST (DAYS 53-65) 221
FIGURE 110. MODEL SIMULATIONS OF THE SPATIAL DISTRIBUTION IN CONCENTRATION AFTER 65 DAYS OF OPERATION AT THE END OF PHASE II 223
FIGURE 111. MODEL SIMULATIONS OF CONCENTRATION IN THE COLUMN EFFLUENT AND LABORATORY DATA DURING THE THIRD PHASE OF BIOTRANSFORMATION TEST WHEN 1,1-DCE WAS INTRODUCED: TC ALTERED 226
FIGURE 112. MODEL SIMULATIONS OF THE SPATIAL DISTRIBUTION IN CONCENTRATION AFTER 135 DAYS OF OPERATION IN PHASE III: TC ALTERED 228
FIGURE 113. CONFIGURATION OF THE EXPERIMENTAL TEST LEGS 231
FIGURE 114. RESULTS OF THE BROMIDE TRACER TEST CONDUCTED ALONG THE EAST EXPERIMENTAL LEG IN THE FIRST SEASON OF FIELD TESTING 235
FIGURE 115. 1,11-TCA CONCENTRATION HISTORIES AT MONITORING LOCATIONS ALONG THE WEST (INDIGENOUS) LEG AND THE EAST (BIOAUGMENTED) LEG FOR THE FIRST 20 DAYS OF TESTING IN THE FIRST FIELD SEASON 237
FIGURE 116. 1,1-DCA CONCENTRATION HISTORIES AT MONITORING LOCATIONS ALONG THE WEST (INDIGENOUS) LEG AND THE EAST (BIOAUGMENTED) LEG FOR THE FIRST 20 DAYS OF TESTING IN THE FIRST FIELD SEASON 238
FIGURE 117. 1,1-DCE CONCENTRATION HISTORIES AT MONITORING LOCATIONS ALONG THE WEST (INDIGENOUS) LEG AND THE EAST (BIOAUGMENTED) LEG FOR THE FIRST 20 DAYS OF TESTING IN THE FIRST FIELD SEASON 239
FIGURE 118. DO CONCENTRATION HISTORIES AT MONITORING LOCATIONS ALONG THE WEST (INDIGENOUS) LEG AND THE EAST (BIOAUGMENTED) LEG FOR THE FIRST 20 DAYS OF TESTING IN THE FIRST FIELD SEASON 240

FIGURE 119. BUTANE CONCENTRATION HISTORIES AT MONITORING LOCATIONS ALONG THE WEST (INDIGENOUS) LEG AND THE EAST (BIOAUGMENTED) LEG FOR THE FIRST 20 DAYS OF TESTING IN THE FIRST FIELD SEASON 241
FIGURE 120. DO CONCENTRATION HISTORIES AT MONITORING LOCATIONS ALONG THE WEST (INDIGENOUS) LEG AND THE EAST (BIOAUGMENTED) LEG FOR THE PERIOD OF 20 TO 70 DAYS OF TESTING IN THE FIRST SEASON 250
FIGURE 121. BUTANE CONCENTRATION HISTORIES AT MONITORING LOCATIONS ALONG THE WEST (INDIGENOUS) LEG AND THE EAST (BIOAUGMENTED) LEG FOR THE PERIOD OF 20 TO 70 DAYS OF TESTING IN THE FIRST SEASON 251
FIGURE 122. 1,1,1-TCA CONCENTRATION HISTORIES AT MONITORING LOCATIONS ALONG THE WEST (INDIGENOUS) LEG AND THE EAST (BIOAUGMENTED) LEG FOR THE PERIOD OF 20 TO 70 DAYS OF TESTING IN THE FIRST SEASON 252
FIGURE 123. 1,1-DCA CONCENTRATION HISTORIES AT MONITORING LOCATIONS ALONG THE WEST (INDIGENOUS) LEG AND THE EAST (BIOAUGMENTED) LEG FOR THE PERIOD OF 20 TO 70 DAYS OF TESTING IN THE FIRST SEASON 253
FIGURE 124. 1,1-DCE CONCENTRATION HISTORIES AT MONITORING LOCATIONS ALONG THE WEST (INDIGENOUS) LEG AND THE EAST (BIOAUGMENTED) LEG FOR THE PERIOD OF 20 TO 70 DAYS OF TESTING IN THE FIRST SEASON 254
FIGURE 125. DISSOLVED OXYGEN CONCENTRATIONS IN THE WEST (INDIGENOUS) LEG AND THE EAST (BIOAUGMENTED) LEG DURING THE FIRST 30 DAYS OF THE SECOND SEASON OF FIELD TESTING 258
FIGURE 126. BUTANE CONCENTRATIONS IN THE WEST (INDIGENOUS) LEG AND THE EAST (BIOAUGMENTED) LEG DURING THE FIRST 30 DAYS OF THE SECOND SEASON OF FIELD TESTING 259
FIGURE 127. 1,1,1-TCA CONCENTRATIONS IN THE WEST (INDIGENOUS) LEG AND THE EAST (BIOAUGMENTED) LEG DURING THE FIRST 30 DAYS OF THE SECOND SEASON OF FIELD TESTING 260
FIGURE 128. 1,1-DCE CONCENTRATIONS IN THE WEST (INDIGENOUS) LEG AND THE EAST (BIOAUGMENTED) LEG DURING THE FIRST 30 DAYS OF THE SECOND SEASON OF FIELD TESTING 261
FIGURE 129. DISSOLVED OXYGEN CONCENTRATIONS IN THE WEST (INDIGENOUS) LEG AND THE EAST (BIOAUGMENTED) LEG DURING THE COMPLETE 70 DAYS OF THE SECOND SEASON OF FIELD TESTING .. 264
FIGURE 130. BUTANE CONCENTRATIONS IN THE WEST (INDIGENOUS) LEG AND THE EAST (BIOAUGMENTED) LEG DURING THE COMPLETE 70 DAYS OF THE SECOND SEASON OF FIELD TESTING 265
FIGURE 131. 1,1,1-TCA CONCENTRATIONS IN THE WEST (INDIGENOUS) LEG AND THE EAST (BIOAUGMENTED) LEG DURING THE COMPLETE 70 DAYS OF THE SECOND SEASON OF FIELD TESTING 266
FIGURE 132. 1,1-DCE CONCENTRATIONS IN THE WEST (INDIGENOUS) LEG AND THE EAST (BIOAUGMENTED) LEG DURING THE COMPLETE 70 DAYS OF THE SECOND SEASON OF FIELD TESTING 267
FIGURE 133. BUTANE AND OXYGEN PULSE TIMES AND TOTAL CYCLE TIMES FOR THE FIRST BIOAUGMENTATION EVENT OF THE THIRD FIELD SEASON 275
FIGURE 134. TCA BREAKTHROUGH IN THE ABSENCE OF BUTANE STIMULATION IN THE WEST (INDIGENOUS) LEG AND THE EAST (BIOAUGMENTED) LEG DURING THE FIRST BIOAUGMENTATION IN THE THIRD SEASON OF FIELD TESTING 280
FIGURE 135. BUTANE CONCENTRATIONS IN THE WEST (INDIGENOUS) LEG AND THE EAST (BIOAUGMENTED) LEG DURING THE FIRST BIOAUGMENTATION IN THE THIRD SEASON OF FIELD TESTING 281
FIGURE 136. DISSOLVED OXYGEN IN THE WEST (INDIGENOUS) LEG AND THE EAST (BIOAUGMENTED) LEG DURING THE FIRST BIOAUGMENTATION IN THE THIRD SEASON OF FIELD TESTING 282
FIGURE 137. TCA CONCENTRATIONS IN THE WEST (INDIGENOUS) LEG AND THE EAST (BIOAUGMENTED) LEG FROM DAY 10 THROUGH DAY 70 DURING THE FIRST BIOAUGMENTATION IN THE THIRD SEASON OF FIELD TESTING 283
FIGURE 138. DCA CONCENTRATIONS IN THE WEST (INDIGENOUS) LEG AND THE EAST (BIOAUGMENTED) LEG FROM DAY 10 THROUGH DAY 70 DURING THE FIRST BIOAUGMENTATION IN THE THIRD SEASON OF FIELD TESTING 284
FIGURE 139. TCA CONCENTRATIONS IN THE WEST (INDIGENOUS) LEG AND THE EAST (BIOAUGMENTED) LEG AT THE END OF THE FIRST BIOAUGMENTATION TEST IN THE THIRD SEASON OF FIELD TESTING 285
FIGURE 140. DCA CONCENTRATIONS IN THE WEST (INDIGENOUS) LEG AND THE EAST (BIOAUGMENTED) LEG AT THE END OF THE FIRST BIOAUGMENTATION TEST IN THE THIRD SEASON OF FIELD TESTING 286
FIGURE 141. BACKGROUND DCE CONTAMINATION CONCENTRATIONS IN THE WEST (INDIGENOUS) LEG AND THE EAST (BIOAUGMENTED) LEG DURING THE FIRST BIOAUGMENTATION EVENT IN THE THIRD SEASON OF FIELD TESTING 287

FIGURE 142. BROMIDE CONCENTRATIONS IN THE WEST (INDIGENOUS) LEG AT THE BEGINNING OF THE TEST AND IN THE EAST (BIOAUGMENTED) LEG DURING THE END OF THE FIRST BIOAUGMENTATION EVENT IN THE THIRD SEASON OF FIELD TESTING 288
FIGURE 143. TCA CONCENTRATIONS IN THE WEST (INDIGENOUS) LEG AND THE EAST (BIOAUGMENTED) LEG DURING THE FIRST BIOAUGMENTATION EVENT IN THE THIRD SEASON OF FIELD TESTING 289
FIGURE 144. BROMIDE CONCENTRATIONS IN THE WEST (INDIGENOUS) LEG AND THE EAST (BIOAUGMENTED) LEG DURING THE 28 DAYS OF THE SECOND BIOAUGMENTATION IN THE THIRD SEASON OF FIELD TESTING 293
FIGURE 145. BUTANE CONCENTRATIONS IN THE WEST (INDIGENOUS) LEG AND THE EAST (BIOAUGMENTED) LEG DURING THE 28 DAYS OF THE SECOND BIOAUGMENTATION IN THE THIRD SEASON OF FIELD TESTING 294
FIGURE 146. DISSOLVED OXYGEN CONCENTRATIONS IN THE WEST (INDIGENOUS) LEG AND THE EAST (BIOAUGMENTED) LEG DURING THE 28 DAYS OF THE SECOND BIOAUGMENTATION IN THE THIRD SEASON OF FIELD TESTING 295
FIGURE 147. TCA CONCENTRATIONS IN THE WEST (INDIGENOUS) LEG AND THE EAST (BIOAUGMENTED) LEG DURING THE 20 DAYS OF THE SECOND BIOAUGMENTATION IN THE THIRD SEASON OF FIELD TESTING 296
FIGURE 148. DCA CONCENTRATIONS IN THE WEST (INDIGENOUS) LEG AND THE EAST (BIOAUGMENTED) LEG DURING THE 20 DAYS OF THE SECOND BIOAUGMENTATION IN THE THIRD SEASON OF FIELD TESTING 297
FIGURE 149. DCE CONCENTRATIONS IN THE WEST (INDIGENOUS) LEG AND THE EAST (BIOAUGMENTED) LEG LATE IN THE SECOND BIOAUGMENTATION TEST IN THE THIRD SEASON OF FIELD TESTING 298
FIGURE 150. CELL DENSITIES FOUND IN GROUNDWATER OBTAINED FROM WELLS SE0.5 AND SE1 DURING THE SECOND BIOAUGMENTATION EVENT 300
FIGURE 151. T-RFLP PROFILES GENERATED FROM THE BIOAUGMENTATION CULTURE GROWN IN THE LABORATORY AND GROUNDWATER SAMPLES OBTAINED FROM WELLS SE0.5 AND SW0.5 DURING THE COURSE OF THE SECOND BIOAUGMENTATION EVENT 301
FIGURE 152. BAR GRAPH REPRESENTATION OF THE MAJOR PEAKS FOUND IN T-RFLP ANALYSES OF GROUNDWATER SAMPLES TAKEN FROM THE SE0.5 AND SE1 WELLS DURING THE SECOND BIOAUGMENTATION EVENT 303
FIGURE 153. BROMIDE CONCENTRATIONS IN THE WEST (INDIGENOUS) LEG AND THE EAST (BIOAUGMENTED) LEG DURING THE FIRST 4 DAYS OF THE THIRD BIOAUGMENTATION EVENT IN THE THIRD SEASON OF FIELD TESTING 311
FIGURE 154. BUTANE CONCENTRATIONS IN THE WEST (INDIGENOUS) LEG AND THE EAST (BIOAUGMENTED) LEG DURING THE THIRD BIOAUGMENTATION IN THE THIRD SEASON OF FIELD TESTING 312
FIGURE 155. DISSOLVED OXYGEN CONCENTRATIONS IN THE WEST (INDIGENOUS) LEG AND THE EAST (BIOAUGMENTED) LEG DURING THE THIRD BIOAUGMENTATION IN THE THIRD SEASON OF FIELD TESTING 313
FIGURE 156. TCA CONCENTRATIONS IN THE WEST (INDIGENOUS) LEG AND THE EAST (BIOAUGMENTED) LEG DURING THE THIRD BIOAUGMENTATION EVENT IN THE THIRD SEASON OF FIELD TESTING 314
FIGURE 157. DCA CONCENTRATIONS IN THE WEST (INDIGENOUS) LEG AND THE EAST (BIOAUGMENTED) LEG DURING THE THIRD BIOAUGMENTATION EVENT IN THE THIRD SEASON OF FIELD TESTING 315
FIGURE 158. DCE CONCENTRATIONS IN THE WEST (INDIGENOUS) LEG AND THE EAST (BIOAUGMENTED) LEG DURING THE THIRD BIOAUGMENTATION EVENT IN THE THIRD SEASON OF FIELD TESTING 316
FIGURE 159. BROMIDE CONCENTRATIONS IN THE WEST (INDIGENOUS) LEG AND THE EAST (BIOAUGMENTED) LEG DURING THE FOURTH BIOAUGMENTATION EVENT IN THE THIRD SEASON OF FIELD TESTING 320
FIGURE 160. BUTANE CONCENTRATIONS IN THE WEST (INDIGENOUS) LEG AND THE EAST (BIOAUGMENTED) LEG DURING THE FOURTH BIOAUGMENTATION EVENT IN THE THIRD SEASON OF FIELD TESTING 321
FIGURE 161. DISSOLVED OXYGEN CONCENTRATIONS IN THE WEST (INDIGENOUS) LEG AND THE EAST (BIOAUGMENTED) LEG DURING THE FOURTH BIOAUGMENTATION EVENT IN THE THIRD SEASON OF FIELD TESTING 322
FIGURE 162. TCA CONCENTRATIONS IN THE WEST (INDIGENOUS) LEG AND THE EAST (BIOAUGMENTED) LEG DURING THE FOURTH BIOAUGMENTATION EVENT IN THE THIRD SEASON OF FIELD TESTING 323
FIGURE 163. DCA CONCENTRATIONS IN THE WEST (INDIGENOUS) LEG AND THE EAST (BIOAUGMENTED) LEG DURING THE FOURTH BIOAUGMENTATION EVENT IN THE THIRD SEASON OF FIELD TESTING 324
FIGURE 164. DCE CONCENTRATIONS IN THE WEST (INDIGENOUS) LEG AND THE EAST (BIOAUGMENTED) LEG DURING THE FOURTH BIOAUGMENTATION EVENT IN THE THIRD SEASON OF FIELD TESTING 325
FIGURE 165. CELL DENSITIES FOUND IN GROUNDWATER OBTAINED FROM THE BIOAUGMENTED WELL LEG DURING THE FOURTH BIOAUGMENTATION EVENT BASED ON REAL-TIME PCR ANALYSES 328

FIGURE 166. T-RFLP PROFILES GENERATED FROM THE BIOAUGMENTATION CULTURE GROWN IN THE LABORATORY AND GROUNDWATER SAMPLES OBTAINED FROM WELLS SE0.5 AND SW0.5 DURING THE COURSE OF THE FOURTH BIOAUGMENTATION EVENT 329
FIGURE 167. BAR GRAPH REPRESENTATION OF THE MAJOR PEAKS FOUND IN T-RFLP ANALYSES OF GROUNDWATER SAMPLES TAKEN FROM THE SE0.5 WELL DURING THE FOURTH BIOAUGMENTATION EVENT 331
FIGURE 168. QUALITATIVE RESULTS OBTAINED FROM T-RFLP ANALYSES OF THE AMOUNT OF DNA IN A 47BP FRAGMENT, THE DOMINANT ORGANISM PRESENT IN THE BIOAUGMENTATION CULTURE, COMPARED TO THE TOTAL DNA OBTAINED 332
FIGURE 169. CAH REMOVAL EFFICIENCY AS A FUNCTION OF DISTANCE FROM THE INJECTION WELL FOR THE BIOAUGMENTED (CLOSED SYMBOLS) AND THE INDIGENOUS (OPEN SYMBOLS) WELL LEGS DURING THE FOURTH BIOAUGMENTATION EVENT OF THE THIRD FIELD SEASON 336
FIGURE 170. CONCEPTUAL MODEL OF MOFFETT FIELD TEST AQUIFER 340
FIGURE 171. BROMIDE TRACER TEST DATA AT THE THREE MONITORING WELLS S1 (1M); S2 (2.2M); S3 (4M) AND THE INJECTION WELL 341
FIGURE 172. COMPARISON OF TRACER DATA TO MODEL OUTPUT 342
FIGURE 173. BREAKTHROUGH CURVES OF 1,1-DCE, 1,1-DCA, AND 1,1,1-TCA 344
FIGURE 174. COMPARISON OF CAH BREAKTHROUGH DATA WITH MODEL OUTPUT FOR VARYING MASS TRANSFER RATE COEFFICIENT (F_K) AT S1 (1M) 347
FIGURE 175A. COMPARISON OF BUTANE AND OXYGEN FIELD DATA AND MODEL OUTPUT AT S1 (1M) 351
FIGURE 175B. COMPARISON OF 1,1-DCE AND 1,1,1-TCA CONCENTRATIONS FOR THE FIELD DATA AND MODEL OUTPUT AT S1 (1M) 352
FIGURE 175C. COMPARISON OF 1,1-DCA CONCENTRATIONS FOR THE FIELD DATA AND MODEL OUTPUT AT S1 (1M) 353
FIGURE 175D. MODEL OUTPUT OF CELL CONCENTRATION AT S1 (1M) 354
FIGURE 175E. MODEL OUTPUT OF CELL DISTRIBUTION OVER THE FIRST 2.6 M OF THE TEST ZONE ON DAY 20 AND 75 355
FIGURE 176. MODEL OUTPUT FOR SIMULATING UTILIZATION AND TRANSFORMATION AT S1 (1M) IF 25 MG/L OXYGEN IS INJECTED BETWEEN DAYS 75 AND 90 357
FIGURE 177. MODEL OUTPUT FOR SIMULATING UTILIZATION AND TRANSFORMATION AT S1 (1M) IF 50 MG/L BUTANE AND 50 MG/L OXYGEN ARE INJECTED BETWEEN DAYS 75 AND 90 358
FIGURE 178A. BUTANE AND OXYGEN OUTPUT FROM SENSITIVITY ANALYSIS OF 1,1-DCE PRODUCT TOXICITY AT S1 (1M) 359
FIGURE 178B. 1,1-DCE AND 1,1,1-TCA RESULTS FROM SENSITIVITY ANALYSIS OF 1,1-DCE PRODUCT TOXICITY AT S1 (1M) 360
FIGURE 178C. BIOMASS RESULTS FROM SENSITIVITY ANALYSIS OF 1,1-DCE PRODUCT TOXICITY AT S1 (1M) 361
FIGURE 179A. COMPARISON OF BUTANE AND OXYGEN UTILIZATIONS FROM FIELD BIOTRANSFORMATION ASSUMING DIFFERENT 1,1-DCE TRANSFORMATION RATES 363
FIGURE 179B. COMPARISON OF 1,1-DCE AND 1,1,1-TCA TRANSFORMATION FROM FIELD BIOTRANSFORMATION ASSUMING DIFFERENT 1,1-DCE TRANSFORMATION RATES 364
FIGURE 180A. COMPARISON OF BUTANE UTILIZATION AT S1 (1M) FOR EQUILIBRIUM (F_K = 2.0 DAY^{-1}) AND NON-EQUILIBRIUM (F_K = 0.2 DAY^{-1}) SORPTION WITH ELONGATED BUTANE AND OXYGEN PULSING DURATIONS 367
FIGURE 180B. COMPARISON OF OXYGEN UTILIZATION AT S1 (1M) FOR EQUILIBRIUM (F_K = 2.0 DAY^{-1}) AND NON-EQUILIBRIUM (F_K = 0.2 DAY^{-1}) SORPTION WITH ELONGATED BUTANE AND OXYGEN PULSING DURATIONS 368
FIGURE 180C. COMPARISON OF 1,1-DCE TRANSFORMATION AT S1 (1M) FOR EQUILIBRIUM (F_K = 2.0 DAY^{-1}) AND NON-EQUILIBRIUM (F_K = 0.2 DAY^{-1}) SORPTION WITH ELONGATED BUTANE AND OXYGEN PULSING DURATIONS 369
FIGURE 180D. COMPARISON OF 1,1,1-TCA TRANSFORMATION AT S1 (1M) FOR EQUILIBRIUM (F_K = 2.0 DAY^{-1}) AND NON-EQUILIBRIUM (F_K = 0.2 DAY^{-1}) SORPTION WITH ELONGATED BUTANE AND OXYGEN PULSING DURATIONS 370

ACRONYMS

ATU	allythiourea
CAH	chlorinated aliphatic hydrocarbon
CF	chloroform
1,1,1-DCA	1,1,1-dichloroethane
1,1-DCE	1,1-dichloroethene
cis-DCE	*cis*-1,2-dichloroethene
trans-DCE	trans-1,2-dichloroethene
DGGE	denaturing gradient gel electrophoresis
ECD	electron capture detector
FID	flame ionization detector
FISH	fluorescence in situ hybridization
MCL	maximum contaminant level
PCE	tetrachloroethene
PCR	polymerase chain reaction
PID	photoionization detector
pMMO	particulate methane monooxygenase
REP	repetitive extragenic palindromic
rRNA	ribosomal RNA
SSCP	single-strand-conformation polymorphism
Tc	transformation capacity
TGGE	temperature gradient gel electrophoresis
sMMO	soluble methane monooxygenase
1,1,1-TCA	1,1,1-trichloroethane
TCE	trichloroethene
T-RFLP	terminal restriction fragment length polymorphism
VC	vinyl chloride

ACKNOWLEDGEMENTS

The authors would like to acknowledge the support of our three project managers at the Air Force Research Laboratory: Ms. Alison Lightner, Captain David Kempisty, and 1st Lieutenant Kolin Newsome. Ms. Lightner was instrumental in getting the project started. Captain Kempisty helped during the middle years, and Lt. Newsome assisted with the completion of the project. We would also like to acknowledge the work of graduate students who completed their M.S. thesis work on the project, and whose results are presented in Sections 4 and 6. Their thesis abstracts are also presented in the Section 8. The students and their thesis titles are: Darin Rungkamol, "Aerobic Cometabolism of 1,1,1-Trichloroethane and Other Chlorinated Aliphatic Hydrocarbons by Indigenous and Bioaugmented Butane-Utilizers in Moffett Field Microcosms;" Maureen A. Mathias, "Modeling Cometabolic Transformation of a CAH Mixture by a Butane Utilizing Culture;" Hee K. Lim, "Microcosm Studies of Bioaugmentation with a Butane-Utilizing Mixed Culture: Microbial Community Structure and 1,1-DCE Cometabolism;" Bhargavi Maremanda, "Aerobic cometabolism of 1, 1, 1-Trichloroethane and 1, 1-Dichloroethene by a bioaugmented butane-utilizing culture in a continuous flow column;" Jun Li, "Molecular Analysis of Bacterial Community dynamics during Bioaugmentation Studies in a Soil Column and at a Field Test Site;" Chakkrid Sattayatewa, "Growth Characteristics and Chlorinated Hydrocarbon Transformation Ability of two *Rhodococcus* sp. Isolates;" Ju Yong Jeong, "Isolation and Molecular Characterization of Several Butane- and Butanol- Utilizing Microorganisms Obtained from a Bioremediation Test Site." We would also like to thank Dr. Steve Giovannoni for providing access to his laboratory for molecular analysis work and his helpful advice, and to Stephanie Connon and Kevin Vergin for their help with molecular methods, and to Dr. Mohammad Azizian and Dr. Young Kim for provided guidance to the MS students in the laboratory.

We would also like to thank NASA Ames Research Center in Sunnyvale, CA, for providing access to Moffett Field as the site of the field experiments; the Oakland Regional Water Quality Control Board of the State of California for permitting the field experiments, and for their overview of the test plans; and the EPA's Western Region Hazardous Substance Research Center for providing support for the laboratory column experiments presented in Chapter 4, and funding the kinetic studies that supported the modeling analysis of Chapter 6. We would also like to thank all of the experts on the SERDP Advisory Panels, who provided helpful suggestions and feedback throughout the study.

EXECUTIVE SUMMARY

Many sites in the DoD and DOE complex are contaminated with chlorinated solvent mixtures. Passive in-situ treatment via aerobic cometabolism is one means of potentially restoring the contaminated aquifers. The goal of the project was to develop a cometabolic culture that has potential for bioaugmentation and to evaluate its performance under laboratory conditions and under in-situ conditions in field demonstrations. Field demonstrations were conducted at the Moffett Field In-situ Test Facility, which served as a prototype for the development of in-situ cometabolic treatment systems that have been implemented in practice, such as the recirculation well system implemented at Edwards AFB. A bacterial mixed culture and pure cultures derived from the mixed culture that grew on butane and were effective at transforming 1,1,1,-trichloroethane (1,1,1-TCA), 1,1-dichloroethane (1,1-DCA), and 1,1-dichloroethene (1,1-DCE) were evaluated. This mixture of contaminants was of interest, since 1,1,1-TCA was a frequently used contaminant at DoD facilities and 1,1-DCE and 1,1-DCA are abiotic and biotic transformation products of 1,1,1-TCA. The project was conducted in response to the Statement of Need related to the development of in-situ biological barrier technologies for the clean-up of groundwater with chlorinated solvent contamination.

The specific objectives of this study were to: 1) develop a butane utilizing culture for bioaugmentation in laboratory and field experiments; 2) characterize the bioaugmentation culture using molecular methods, including a clone library, sequencing, and PCR based methods; 3) develop kinetic information for substrate utilization and the transformation of the CAH mixtures; 4) develop molecular based methods for tracking the cultures that were bioaugmented and biostimulated in laboratory and field studies; 5) conduct laboratory microcosm and continuous flow column studies to evaluate the performance of the bioaugmented culture under geochemical conditions mimicking those present at the field site; 6) conduct field demonstrations to evaluate the bioaugmentation approach and to determine the effectiveness in treating problematic mixtures of 1,1,1-TCA, 1,1-DCE, and 1,1-DCA using butane as cometabolic substrate, and compare the results to those achieved by indigenous butane-utilizers; 7) track microbial community changes and quantify members of the bioaugmented culture in situ using molecular based methods; 8) simulate the results of laboratory and field studies using a transport code for these cometabolic transformations.

Objective 1: Develop a butane utilizing culture for bioaugmentation in laboratory and field experiments. The culture selected as the source for bioaugmentation efforts at the Moffett Federal Airfield In-Situ Bioremediation Test Site, CA, was obtained from a Moffett soil/groundwater microcosm that was inoculated with a butane-utilizing enrichment culture acquired from Hanford, WA, capable of co-metabolically degrading the chlorinated solvents TCE, 1,1,1-TCA, and 1,1-DCE. At least three distinct morphologies existed in this enrichment culture: a small curved rod approximately 1 micron in length, a slightly larger and wider 1 to 2 micron rod, and an approximately 10 to 20 micron long filamentous organism. Transformation studies performed with the enrichment culture showed that effective transformation of 1,1-DCE, 1,1-DCA, and 1,1,1-TCA was achieved with the culture.

Objective 2: Characterize the bioaugmentation culture using molecular methods, including clone library, sequencing, and PCR based methods. Results of the clone library analysis showed the dominant clones in the enrichment culture consisted of *Hydrogenophaga, Rhodococcus, and Acidovorax* organisms. Terminal restriction fragment length polymorphism (T-RFLP) was also performed, and showed many of the organisms identified in the clone library could also be tracked using T-RFLP analysis. However, the results also indicated that not all of the organisms in the culture were identified using clone library methods, and at least one dominant organism based on T-RFLP analyses was not identified in the clone library. Two *Rhodococcus* spp. that were isolated from the enrichment culture had very different morphologies. The *Rhodococcus* sp. culture that corresponded to 179 base pairs (bp) in T-RFLP analysis grew in clumps in media and colonized surfaces, while the culture corresponding to 183bp in T-RFLP was rod shaped, grew planktonically, and did not stick to vessel walls. The 183bp culture was most closely related to *Rhodococcus* sp. USA-AN012, a nitrile-metabolizing actinomycete.

Objective 3: Develop kinetic information for substrate utilization and the transformation of the CAH mixtures. Kinetic studies performed with the enrichment culture and the two *Rhodococcus* pure cultures showed effective transformation of 1,1-DCE, 1,1-DCA, and 1,1,1-TCA, consistent with the work of Kim et al. (2002a, 2002b) 1,1-DCE was most rapidly transformed, followed by 1,1-DCA, and 1,1,1-TCA, and butane was shown to be a strong inhibitor of CAH transformation. Studies with the pure cultures showed the 183-BP culture was more effective at transforming 1,1-DCE and 1,1,1-TCA than the 179bp culture. Growth and transformation kinetic parameters and inhibition models developed by Kim et al. (2002a, 2002b) did a good job of fitting the results of the batch laboratory experiments with mixtures of 1,1-DCE, 1,1-DCA and TCA, and growth on butane. Studies with the 183bp microorganism also showed that other growth substrates could be used to stimulate 1,1,1-TCA transformation. Growth of the 183bp microorganism on pentane and hexane also resulted in effective 1,1,1-TCA transformation. Growth on other substrates, such as acetate and succinate, did not induce effective 1,1,1-TCA transformation.

Objective 4: Develop molecular based methods for tracking the cultures that were bioaugmented and biostimulated in laboratory and field studies. Several molecular techniques were used to track the cultures in laboratory microcosm studies and in the field study. Based on the 16S-rRNA sequences obtained from the clone library, the terminal fragment length in base pairs for specific microorganisms was determined using T-RFLP analysis, which permitted changes in community structure to be monitored. A SYBR Green real-time PCR method was used for quantifying the 183bp culture. Primers were developed for this organism based on the sequencing information obtained from the pure culture. The method was used to enumerate the 183bp microorganism in laboratory column studies and in the field study. Development of fluorescence in situ hybridization (FISH) for the *Rhodococcus* cultures was also undertaken, but proved unsuccessful. The *Rhodococcus* cultures are gram positive, and it proved difficult to permeate the cells with the probes to make FISH work with these microorganisms.

Objective 5: Conduct laboratory microcosm and continuous flow column studies to evaluate the performance of the bioaugmentation culture under geochemical conditions mimicking those present at the field site. A series of microcosm studies and a continuous flow

column were conducted to evaluate the performance of the enrichment culture and pure cultures under conditions encountered in the field. The cultures were added to batch microcosms containing Moffett subsurface solids and groundwater. Studies with the mixed culture show much more effective transformation of 1,1,1-TCA could be achieved in the bioaugmented microcosms compared to microcosms where indigenous butane-utilizers were stimulated. Microcosm studies also showed that 1,1-DCE could also be very effectively transformed, and enhanced transformation activity was maintained over a period of four months. Batch microcosm studied performed with the 183bp culture showed effective transformation of mixtures of 1,1-DCE, 1,1,1-DCA, and 1,1,1-TCA could be achieved over a period of 100 days. Model simulations show the kinetic models used for the simulation of the transformation of mixtures in media also worked well for simulating the results of the microcosm studies.

For the continuous flow column study, a 1-D column was packed with Moffett aquifer material and fed Moffett groundwater. The fluid residence time in the column was about 1.5 days. The column was bioaugmented at the column influent with a small mass (0.5 mg) of the 183-BP culture and pulse-fed butane and dissolved oxygen and 1,1,1-TCA. Butane was effectively utilized in the column and about 80% of the added 1,1,1-TCA was effectively transformed. When the 1,1,1-TCA concentration was increased, less 1,1,1-TCA was transformed, and upon lowering the concentration about 60 to 70 % of 1,1,1-TCA was again transformed. 1,1,1-TCA transformation was maintained in the column for a period of 120 days. When 1,1-DCE was added along with 1,1,1-TCA, concentrations of 1,1,1-TCA, oxygen, and butane increased, while about 50% of the 1,1-DCE was transformed. The results indicated that 1,1-DCE transformation product toxicity was occurring, and that effective 1,1,1-TCA transformation was difficult to maintain in the presence of 1,1-DCE. Overall, the results of the microcosm studies showed that the cultures that were developed could be successfully bioaugmented and effectively transform CAHs over prolonged periods. 1,1-DCE, while effectively transformed in batch kinetic studies, proved to be more difficult to transform in a continuous flow column, and its presence resulted in less effective butane utilization and 1,1,1-TCA transformation.

Objective 6: Conduct field demonstrations to evaluate the bioaugmentation approach and to determine the effectiveness in treating problematic mixtures of 1,1,1-TCA, 1,1-DCE, and 1,1-DCA using butane as cometabolic substrate, and compare these results to those achieved by indigenous butane-utilizers. Field studies were conducted over three seasons at the Moffett Field Test facility. Two experimental well test legs were installed in the shallow aquifer at the site, one for the bioaugmentation tests and another for tests with indigenous butane utilizers. In the first season of testing, the ability to treat a mixture of 1,1,1-DCE, 1,1,1-TCA, and 1,1-DCE was evaluated by adding known concentrations of the CAHs to the injected groundwater. The tests were conducted under forced gradient conditions of injection and extraction, with monitoring wells located between the injection and extraction wells. Upon the addition of six grams dry weight of the enrichment culture, containing the 183-BP culture, rapid uptake of butane was observed in the bioaugmented leg as compared to the indigenous leg. During the first 20 days of treatment in the bioaugmented leg, transformation of 1,1-DCE, 1,1-DCA, and 1,1,1-TCA was observed, as indicated by decreases in concentrations to below injection levels. Consistent with laboratory kinetic and microcosm studies, 1,1-DCE was most effectively transformed, followed by 1,1-DCA and 1,1,1-TCA. During the first 20 days of operation the approximate removals of 1,1,1-TCA, 1,1-DCA, and 1,1-DCE were 20%, 70%, and

80%, respectively. In contrast, there was little evidence of butane utilization or CAH transformation along the indigenous experimental leg during the first 20 days of the test. With prolonged treatment (over 40 days), effective butane and oxygen utilization and CAH transformation were all lost in the bioaugmented leg, with only about 10% of the 1,1-DCE being removed. This coincided with a change from short alternating pulse cycles of groundwater containing dissolved butane or dissolved oxygen (about 20 min butane/ 60 min oxygen), to very long cycles (2 hr butane/24 hr oxygen). Upon changing back to short pulse cycles, effective butane and oxygen removal was achieved, and 1,1-DCE removal increased to about 90% in the bioaugmented leg after 65 days of operation; however, effective removal of 1,1-DCA and 1,1,1-TCA was not achieved. The results from the first year of field tests indicated that bioaugmentation was effective during the early stages of the tests; however, with prolonged operation the treatment was only slightly more effective than that achieved in the indigenous leg.

The objective of the second season of testing was to determine if prolonged transformation of 1,1,1-TCA could be achieved, since it was the most difficult to treat of the three compounds tested. Along with oxygen, hydrogen peroxide was evaluated as a source of oxygen that permitted more butane to be added to the test legs. Prior to bioaugmentation, hydrogen peroxide was added to test its ability to deliver oxygen and to help reduce the biomass from the previous year's demonstration. An enrichment culture containing about 5 grams dry weight of 183bp and 172bp organisms was added to the bioaugmented test leg. Effective butane and oxygen consumption was observed on both experimental legs; however, 1,1,1-TCA removal was achieved only in the bioaugmented leg. About 70 % TCA removal was achieved during the first 30 days of testing at an injection concentration of 100 μg/L. When the concentration was increased to 160 μg/L, removal decreased to about 60 %. 1,1,1-TCA was continuously removed for a period of about 50 days. Hydrogen peroxide was shown to be an effective means of delivering oxygen; however, the addition of increasing amounts of butane did not result in more effective TCA transformation.

The objective of the third season of testing was to track the microbial communities during the test, and again evaluate the transformation of a mixture of the three CAHs. The microbial results are presented under Objective 7 below. Similar results to the first two field seasons were obtained for CAH transformation, with DCE being most effectively treated, followed by DCA, and finally, TCA. Long-term transformation was attained only for DCE during the third field season, which may have been due to in part to the high levels of DCE tested (up to 300 μg/L). TCA removal efficiencies of up to 75% were attained, but were not sustainable over the long-term. Similarly, DCA removal efficiencies of up to 95% were also observed, but a gradual loss in CAH transformation ability resulted in diminished removal efficiencies over time. Nutrient addition appeared to increase TCA removal by about 5 %, but a combination of lowering peroxide concentrations and adding nutrients at the same time made it difficult to attribute the increased efficiency to nutrient addition alone. Injection concentrations of DCE as high as 130 μg/L were effectively treated to below detection limits (~ 2 μg/L), safely below the EPA MCL for DCE of 7 μg/L. However, the limited transformation of TCA resulted in residual TCA concentrations that had the potential to abiotically transform to DCE, and thus re-contaminate the treatment zone.

A mild bleach solution was applied to the aquifer treatment zone prior to bioaugmentation on three occasions during the third year of testing. The bleach was added to act as a mild biocide to reduce the number of active butane-utilizing microorganisms that had been enriched in the treatment zone over the previous two years of bioaugmentation testing. This was done to lessen the competition for butane for the bioaugmentation culture and, hopefully, increase the chance of successful colonization and CAH transformation activity. When the bleach solution was allowed to reside in the aquifer for greater than 48 hrs under no-flow conditions, the butane-utilizing populations were reduced to levels found during the first year bioaugmentation tests, based on time to complete butane utilization in the indigenous leg.

Objective 7: Track microbial community changes and quantify members of the bioaugmented culture in situ using molecular based methods. Molecular-based methods were used to track the bioaugmented cultures and measure any changes that occurred during the course of the laboratory microcosm and field studies. Results from T-RFLP analysis of microcosm tests showed that a few organisms dominated the microbial community, and were maintained in the microcosms over extended periods. The 183bp microorganism, for example, was a dominant organism in studies of 1,1-DCE transformation, and was only present in the bioaugmented microcosms. The methods also showed some shifts in the community structure occurred during the course of the experiments. Quantitative real-time PCR (qPCR) analysis was used to enumerate the presence of the 183bp (*Rhodococcus* sp.) microorganism in the groundwater effluent from the continuous flow column tests. The bioaugmented culture was detected in the column effluent over a period of 135 days at cell concentrations ranging from 2.7E+2 to 3.1E+5 organisms per mL of column effluent. The cells represented only a small fraction of the total cells present.

Microbial community studies were conducted on groundwater samples obtained from the bioaugmented leg during the third year of testing. The dominant organisms observed in the laboratory-grown bioaugmentation cultures were not found in significant numbers in community analyses of groundwater samples taken after bioaugmentation. In each case, bioaugmentation imparted CAH transformation ability to the subsurface, but organisms from the bioaugmentation culture were not observed in T-RFLP analyses. This may have been due to selection and enrichment of different organism in the subsurface than under laboratory conditions, or it is possible that the dominant organisms in laboratory conditions effectively populated the aquifer solids, but few were present in the aqueous solution available for analysis. Organisms comprising less than 1% of the total bacterial population are not resolved in T-RFLP analyses, indicating that the bioaugmented organisms were not present in the aqueous phase in sufficient numbers compared to total populations to be detected in community analyses.

In both bioaugmentation events where microbial community analyses were conducted, a clear microbial community succession occurred from a dominant organism with a TFL of 277 bp to an organism with a TFL of 126 bp. The 277bp fragment was consistent with an *Acidovorax* sp. found in the clone library made from DNA obtained from the bioaugmentation source culture. The 277bp organism was dominant before bioaugmentation and through the initial phase of butane enrichment. However, after reaching complete butane utilization and maximum CAH transformation rates, the community shifted to domination by the 126bp organism and remained so until butane addition was terminated. The community shift to the 126bp organism was

accompanied by a gradual decrease in CAH removal efficiency, especially in the case of TCA transformation. Attempts to culture both the 277bp and 126bp organisms from field samples were unsuccessful, not surprisingly considering the significant differences between the subsurface and laboratory conditions.

Real-time PCR analysis for one member of the bioaugmentation culture showed effective microbial transport out to the second groundwater monitoring well located 2.2 m from the injection well. The cells may easily have been transported farther than that, but attenuation of the culture concentration with distance traveled resulted in levels too low to accurately measure at the monitoring well 4 m from the injection well. This finding was consistent with the field CAH results where high DCE concentrations pushed butane utilization and CAH removal farther out into the treatment zone, with significant amounts of CAH removal occurring past the first monitoring well. However, real-time PCR estimates of strain 183bp populations indicated that the bioaugmented organism comprised a small fraction of the total microbial population. In the second bioaugmentation event of the third season, immediately after bioaugmentation the strain 183bp population represented as much as a 3-5 % of the total microbial population, which was estimated from DAPI-stained cell counts. After a few days, the strain 183bp population fell to less than 0.1 % of the total population (100 to 800 cells/mL) and remained there before continuing to decline over time.

The fourth bioaugmentation event of the third season resulted in more stable and slightly higher concentrations of strain 183bp cells in groundwater samples, with samples from well SE0.5 having 10,000 cells/mL and samples from SE1 having about 2000-3000 cells/mL. Lesser concentrations were found out at the SE1.5 and SE2 wells. It is possible that higher numbers were present, but were preferentially attached to aquifer solids, which is consistent with modeling analyses that indicated that the numbers of bioaugmented organisms found in aqueous samples were too few to account for the CAH transformation observed.

Objective 8: Simulate the results of laboratory and field studies using a transport code for these cometabolic transformations. The transport code of Semprini and McCarty (1992) was modified to simulate the results of the continuous flow column studies and the first season field experiments. The modifications included allowing more that one CAH to be transformed, adding complex inhibition kinetics for cometabolism, and the process of transformation product toxicity. The code used kinetic parameters from detailed kinetics studies and those obtained from batch microcosm experiments. For the continuous flow column studies, the model yielded results similar to those observed in the column tests, predicting about 70% transformation of 1,1,1-TCA should be achieved. The model simulations showed the 1,1-DCE transformation toxicity was the likely cause of the transient responses observed in the columns of the decrease in butane utilization and 1,1,1-TCA transformation. Simulations of the results of the first season of field testing showed the initial decrease in 1,1-DCE, 1,1-DCA, and 1,1,1-TCA were consistent with field observations during the first 20 days of operation. As the test proceeded, the loss of transformation activity likely resulted from long pulse cycles, limited addition of butane, and 1,1-DCE transformation toxicity. The simulations of the latter stages of the field tests indicated the 1,1,1-TCA and 1,1-DCA would be transformed to greater extents than were observed, if the bioaugmented culture still dominated the population of butane-utilizers. The simulations

indicate that the microbial population likely shifted to the indigenous community that did not effectively transform these compounds.

Overall the results showed that bioaugmentation enhanced treatment performance; however, prolonged treatment of a mixture of 1,1-DCE, 1,1-DCA, and 1,1,1-TCA proved difficult to maintain. 1,1-DCE, the compound that has the lowest drinking water standard, could be effectively transformed, and bioaugmentation improved treatment. 1,1,1-TCA could also be transformed for extended periods, when present as a single contaminant. 1,1,1-TCA and 1,1-DCA transformation decreased in the presence of 1,1-DCE, which likely resulted from 1,1-DCE transformation toxicity. Since indigenous butane utilizers were present that were ineffective in transforming 1,1-DCA and 1,1,1-TCA, the shift to indigenous utilizers likely resulted in a decrease in performance when mixtures of 1,1-DCE, 1,1,1-TCA, and 1,1-DCA were present.

1. OBJECTIVES

Many sites in the DoD and DOE complex are contaminated with chlorinated solvent mixtures. Passive in-situ treatment via aerobic cometabolism is one means of potentially restoring the contaminated aquifers. McCarty et al. (1998) demonstrated the in-situ aerobic cometabolism of trichloroethylene (TCE) to treat a groundwater contaminated plume at Edwards AFB, CA. Toluene was used as an aerobic cometabolic substrate to drive TCE transformation. A passive bioremediation barrier was created using recirculation wells. The regional groundwater plume was effectively intercepted by the recirculation well treatment barrier, with 97 to 98% removal of TCE achieved for groundwater leaving the treatment zone. These results are very encouraging, and demonstrate that a properly designed recirculation system for in-situ biological treatment can be used as a passive barrier technology for treating groundwater plumes.

Despite the complexity of aerobic cometabolism, it has several advantages over other technologies as an in situ treatment process. It works well at low contaminant concentrations, since it is very compound specific, thus it is a good choice for creating passive barriers to treat the low concentration (~1 mg/L) distal ends of plumes. The concentration and type of growth substrate of the cometabolic substrate can be adjusted to achieve the desired degree of treatment. This is not true for biological treatment via anaerobic dehalogenation in which a high concentration of substrates might be required to reduce competing electron acceptors such as iron, nitrate, sulfate, and carbon dioxide for methanogenesis. Being an aerobic process groundwater quality is also maintained with dissolved oxygen present. The process may also be implemented to treat deep zones of contamination, for which other systems, such as passive iron walls, become costly to install.

Compound specificity is a potential disadvantage of aerobic cometabolism, since the treatment of mixtures of chlorinated aliphatic hydrocarbons (CAHs) becomes problematic. For example, toluene and phenol-utilizers are most effective in transforming chlorinated ethenes (such as TCE), but are not effective in transforming chlorinated methanes (chloroform), chlorinated ethanes (1,1,1-trichloroethane), or 1,1-dichloroethene (Semprini, 1997). The focus of this research is to overcome this limitation by developing novel cometabolic systems to treat CAH mixtures. Since the development of passive biological barrier systems, such as the recirculation system tested at Edwards AFB, results in bioactive zones close to wells, the bioaugmentation of cultures that have good cometabolism potential is a promising process. Thus, a goal of the project was to select a cometabolic culture that has potential for bioaugmentation and to evaluate its performance under laboratory conditions and under in-situ conditions in field demonstrations. Field demonstrations were conducted at the Moffett Field In-situ Test Facility, which serves as a prototype for the development of the recirculation well cometabolic treatment system, such as the one tested at Edwards AFB.

The objective was to evaluate the potential of bioaugmentation of a bacterial culture that grows on butane and is effective at transforming mixtures of contaminants, with a specific emphasis on 1,1,1,-trichloroethane (1,1,1-TCA), 1,1-dichloroethane (1,1-DCA), and 1,1-dichloroethene (1,1-DCE). This mixture of contaminants is of interest, since 1,1,1-TCA was a frequently used contaminant at DoD facilities; 1,1-DCE and 1,1-DCA are abiotic and biotic transformation

products of 1,1,1-TCA (Vogel and McCarty, 1987), and are often found together as a mixture of contaminants. Previous studies have shown that a bacterial enrichment culture that grew on butane was very effective in transforming 1,1-DCE, 1,1,1-TCA, and 1,1-DCA (Kim et al., 2002b), as well as a broad range of chlorinated ethenes, ethanes, and methanes (Kim et al., 2000). In addition, studies of Jitnuyanont et al. (2001) showed that when this culture was bioaugmented to microcosms constructed with groundwater and aquifer material from the Moffett field site, much better transformation was achieved than in microcosms where indigenous microorganisms were stimulated. Thus, the project focused on the bioaugmentation with a butane enrichment culture to achieve effective cometabolism. In the field studies, a comparison was made between transformation that was achieved in a test leg where indigenous butane utilizers were stimulated and that achieved in a leg bioaugmented with the enrichment culture.

The specific objectives of this study were:

1) **Develop a butane utilizing culture for bioaugmentation in laboratory and field experiments.**
   Pure and enriched cultures were isolated from the butane-utilizing enrichment culture of Kim et al. (2002b). Cultures were selected that performed well under the geochemical conditions of groundwater at the Moffett field test site, by adding the enrichment to microcosms constructed of Moffett groundwater and aquifer material and then culturing microorganisms that survived microcosm conditions.

2) **Characterize the bioaugmentation culture using molecular methods, including clone library, sequencing, and PCR based methods.**
   After enrichment cultures were obtained, a clone library was performed to identify microorganisms present in the enrichment using 16S rRNA-based methods. In addition, polymerase chain reaction (PCR) based methods, including Terminal Restriction Fragment Length Polymorphism (T-RFLP) were used to determine the microbial community structure. Pure cultures isolated from the bioaugmentation culture were also sequenced using 16S rRNA methods.

3) **Develop kinetic information for substrate utilization and the transformation of the CAH mixtures.**
   Kinetic parameters for the enrichment cultures were compared with detailed kinetic parameters derived by Kim et al. (2002b). Model simulations were then performed with results obtained from batch kinetic experiments.

4) **Develop molecular based methods for tracking the cultures that were bioaugmented and biostimulated in laboratory and field studies.**
   Specific primers were constructed for phylogenic-specific PCR amplification of members of the bioaugmentation culture in laboratory and field samples. These specific primers were used to develop quantitative real-time PCR (qPCR) methods to quantify the number of bioaugmented microorganisms present in laboratory and field tests. T-RFLP methods were developed to document the changes in microbial community structure during the tests.

5) **Conduct laboratory microcosm and continuous flow column studies to evaluate the performance of the bioaugmented culture under geochemical conditions mimicking those present at the field site.**
Microcosm studies were performed to evaluate the performance of the bioaugmented cultures under geochemical conditions of the field demonstration. A continuous flow column study with aquifer solids and groundwater from the field site was also performed under conditions that mimicked those of the field experiment.

6) **Conduct field demonstrations to evaluate the bioaugmentation approach and to determine the effectiveness in treating problematic mixtures of 1,1,1-TCA, 1,1-DCE, and 1,1-DCA using butane as cometabolic substrate, and compare these results to those achieved by indigenous butane-utilizers.**
A series of field experiments were performed to evaluate the cometabolic CAH transformation with bioaugmentation and in the absence of bioaugmentation. Two experimental test legs were operated with substrate addition, one was bioaugmented, and another where indigenous microorganisms were stimulated. Field experiments were conducted over three consecutive seasons.

7) **Tracking microbial community changes and quantifying members of the bioaugmented culture in situ using molecular based methods.**
PCR-based methods including T-RFLP and qPCR were used to evaluate changes in microbial community structure and to quantify the concentration of members of the bioaugmented culture in groundwater samples obtained during the field demonstration.

8) **Simulate the results of laboratory and field studies using a transport code for these cometabolic transformations.**
A transport code that includes the processes of inhibition and transformation toxicity was used to simulate the results of laboratory column experiments and the field experiments. Kinetic parameters values used in the transport code were derived from the laboratory studies.

The project was conducted in response to the Statement of Need related to the development of in situ biological barrier technologies for the clean-up of groundwater with chlorinated solvent contamination. The approach was to bioaugment microbial cultures in order to create effective reactive barriers for aerobic cometabolism through substrate and dissolved oxygen addition.

2. BACKGROUND

Aerobic cometabolism has been shown to be an effective treatment method in reducing CAH contamination (Semprini et al., 1991; Hopkins and McCarty, 1995; McCarty et al., 1998). Cometabolic transformation results from nonspecific enzymes fortuitously catalyzing reactions. Because these reactions do not provide energy or carbon, a primary growth substrate must be (at least) intermittently available to maintain a viable microbial population. In oxidative cometabolism, the enzymes use the primary growth substrate as an electron donor and oxygen as an electron acceptor.

The performance of cultures capable of cometabolic oxidative dechlorination has been studied for a variety of contaminants and primary growth substrates as reviewed by Arp et al. (2001) and Alvarez-Cohen and Spietel (2001). Examples of monooxygenase-inducing substrates for this purpose include methane, propane, ammonia, toluene, and phenol (Hamamura et al., 1999; Hamamura et al., 1997; Anderson and McCarty, 1997 Liu et al., 2001). Microorganisms that grow on butane have the ability to cometabolize a broad range of CAHs (Hamamura et al., 1999; Hamamura et al., 1997; Kim et al., 2000; Kim et al., 1997).

The development of biological in-situ barriers for the remediation of groundwater plumes contaminated with chlorinated solvents provides a potential low cost method for remediating groundwater contamination. This method is being considered for both anaerobic and aerobic treatment processes. Aerobic cometabolism which provides a method for rapid transformation of contaminants is one process for which in-situ biological barriers can be applied (Semprini, 1997). Aerobic cometabolism is best suited for in situ remediation for CAH contamination at concentrations of ~1 mg/L or less, but well above the drinking water standard for most of the compounds. Compounds for which aerobic cometabolism has been evaluated in laboratory and field studies include the chlorinated ethenes [TCE, *cis*-1,2-dichloroethene (*cis*-DCE) and trans-1,2-dichloroethene (trans-DCE), 1,1-DCE, and vinyl chloride (VC)]; the chlorinated ethanes (1,1,1-TCA) and the lower chlorinated ethane isomers]; and the chlorinated methanes [chloroform (CF) and the lower chlorinated methanes] (Semprini, 1997). The regulatory drivers for these environmental contaminants are maximum contaminant levels (MCLs) governed under the Safe Drinking Water Act (Source: http://www.epa.gov/safewater/mcl.html#3).

McCarty et al. (1998) conducted a field scale demonstration of TCE cometabolism by indigenous aerobic microorganisms grown on toluene. Groundwater contaminated with 500-1200 μg/L TCE was treated in-situ by cometabolic biodegradation through the injection of 7-13.4 mg/L toluene, oxygen, and groundwater circulated between two contaminated aquifers through two treatment wells located 10 m apart. The subsurface recirculation system consisting of two treatment wells (Figure 1). Each well was screened at two depths, with a submersible pump installed in-between. The pump drew TCE contaminated groundwater into the well, where the groundwater mixture of TCE, primary substrate and oxygen source was discharged into the aquifer from the second screened interval. An in-situ bioactive zone was created in the aquifer around the discharge screen of each treatment well. Thus, groundwater was caused to recirculate between the two aquifers. Water was never brought to the surface except for sampling, greatly reducing pumping costs and completely eliminating treatment and disposal requirements.

Figure 1. Recirculation Well Systems Used in the Edwards Field Demonstration of In Situ TCE Treatment with Toluene-Utilizing Microorganisms

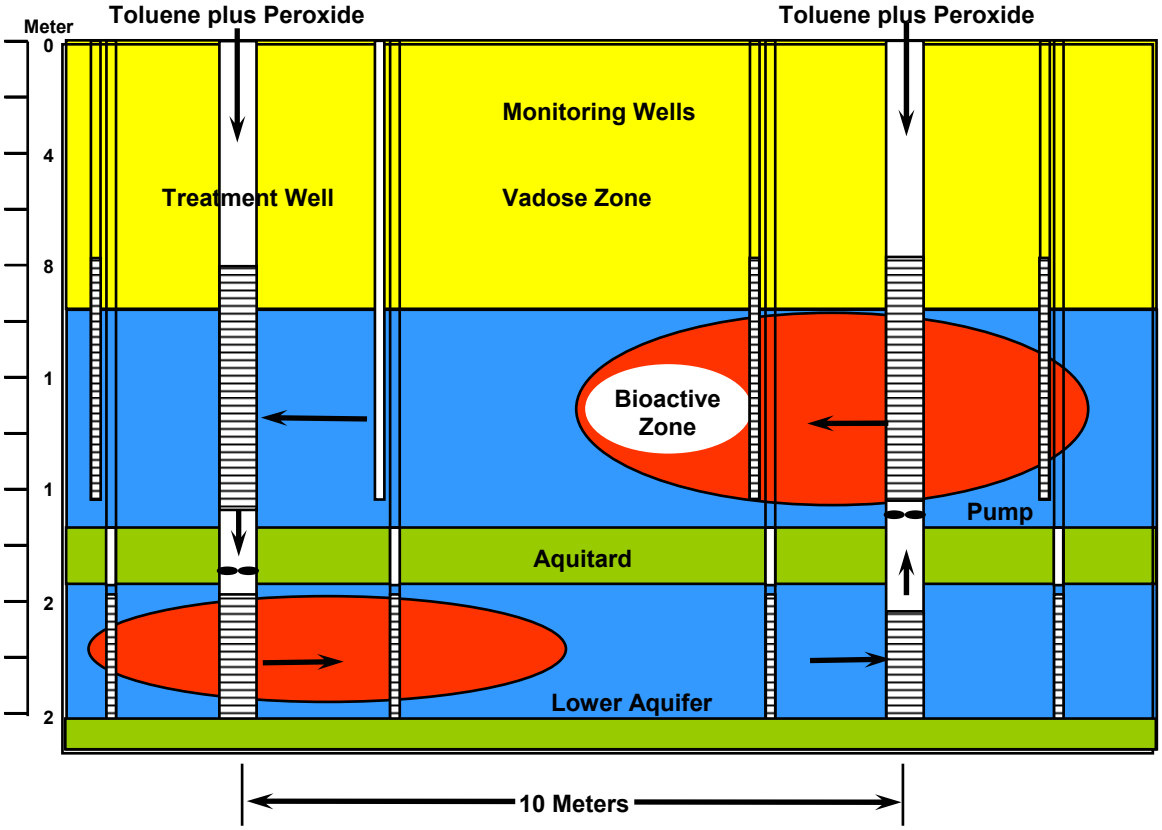

The recirculation systems tested at Edwards successfully demonstrated passive barrier treatment of the TCE plume. With multiple passes through the treatment zones, a TCE concentration of 1000 µg/L in the groundwater entering the treatment zone was reduced to an average concentration of 18-24 µg/L for the groundwater leaving the zone, resulting in an overall TCE removal of 97 to 98%.

The potential advantages of such a system over traditional pump-and-treat systems as summarized by McCarty et al. (1998) are (1) cost for pumping groundwater to the surface is avoided, (2) no above ground treatment system is required to treat groundwater contaminants, (3) TCE is destroyed in the process and not simply concentrated on another medium for disposal, (4) disposal of treated groundwater is not an issue, and (5) uncontaminated groundwater is not contaminated by being brought into the TCE contaminated zone as generally occurs in pump-and-treat systems.

One potential disadvantage of this biological treatment system is that toluene is a regulated chemical, although the above study did demonstrate that the removal of toluene to 1.1 ± 1.6 µg/L was well below the drinking water standard of 1000 µg/L. However, in some cases regulatory

approval to add toluene may still prove difficult to achieve. Another potential problem is that toluene and phenol stimulated microorganisms are not effective in degrading chlorinated methanes, such as CF, or chlorinated ethanes, such as 1,1,1-TCA (Chang and Alvarez-Cohen, 1996), as well as 1,1-DCE (Hopkins and McCarty, 1995), a chlorinated ethene that is often present with 1,1,1-TCA as an abiotic transformation product (Vogel and McCarty, 1987). This research focused on butane as a cometabolic substrate, which is more effective in stimulating microorganisms that are capable of treating CAH mixtures of 1,1,1-TCA, 1,1-DCE, and 1,1-DCA (Kim et al., 2002b).

As shown in Figure 1, bioactive zones are created close to the recirculation wells. Thus, the bioaugmentation of a culture that has better transformation abilities than indigenous cultures is a potential process that can be implemented in these systems. This study also focused on the bioaugmentation of butane-utilizing cultures that effectively transform 1,1,1-TCA, 1,1-DCE, and 1,1-DCA, with the objective of evaluating their effectiveness in creating recirculating in situ barriers.

Semprini (1997) reviewed the results of field studies that have been conducted evaluating aerobic cometabolic treatment. Many of these field studies have been conducted at a test site Moffett Field Test Facility, CA. The Moffett Field Facility was used in this study to evaluate potential systems for the treatment of problematic CAH mixtures of interest. Studies at the Moffett Field test site have evaluated the aerobic cometabolism of CAHs, focusing on TCE and its anaerobic transformation products. These studies included the initial studies with methane-utilizers (Roberts et al., 1990; Semprini et al. (1990; 1991), studies with phenol-utilizers (Hopkins et al., 1993a; 1993b), and toluene utilizers (Hopkins and McCarty, 1995). The operation of the Moffett Field test zone served as a pilot for the recirculation system depicted in Figure 1. The contaminants of interest were injected and transported under forced gradient conditions through the biostimulated test zone. The concentration responses at monitoring wells 1, 2, and 4 meters from the injection well were monitored to determine the transformation extents achieved during transport through the biostimulated zone. The biostimulated zone is representative of conditions created in the aquifer near the injection points of the recirculation systems show in Figure 1.

The Moffett Field site has proven invaluable in determining if cometabolic systems are effective for specific contaminants and contaminant mixtures. Hopkins and McCarty (1995) summarized the results of chlorinated ethene testing with methane, phenol, and toluene-utilizers. Methane-utilizers effectively transformed VC, and *trans*-DCE, and were less effective at transforming cis-DCE, and TCE. Phenol-utilizers effectively transformed TCE, *cis*-DCE, and VC, and were less effective at transforming 1,1-DCE and *trans*-DCE. Toluene-utilizers had similar abilities as phenol-utilizers for all common compounds tested. In all of the Moffett Field tests, 1,1,1-TCA was present as a background contaminant. None of the systems tested (methane, phenol, toluene) were effective in transforming 1,1,1-TCA. There has been little success in transforming chlorinated ethanes with phenol or toluene-utilizers (Alvarez-Cohen and Chang, 1995). Laboratory studies with methane-utilizers that express soluble methane monooxygenase (sMMO) have demonstrated effective 1,1,1-TCA transformation ability, while those expressing particulate methane monooxygenase (pMMO) showed little activity (Oldenhuis et al., 1991, Chang and Alvarez-Cohen, 1996). Methane-utilizers at Moffett Field likely produced pMMO

instead of sMMO (Semprini, 1997). Since the subsurface conditions at Moffett Field did not favor sMMO stimulation, the use of methane-utilizers for cometabolizing 1,1,1-TCA was diminished. In our study, we focused on butane-utilizers, that have good 1,1,1-TCA transformation abilities.

The Moffett Site has proven useful in studying many of the processes that have been incorporated in the Field Scale Demonstration at Edwards AFB. The alternate pulsing of cometabolic substrate and oxygenated water, for example, was developed and tested as a practical means of helping to distribute the microbial population using the Moffett Test Zone (Roberts et al., 1990; Semprini and McCarty, 1991). It also served as a means to study the process of competitive inhibition between the cometabolic substrates and the CAHs tested (Semprini et al., 1991; Semprini and McCarty, 1992).

Problems associated with the transformation of CAH mixtures were also illustrated in the field studies conducted at Moffett Field. In studies with toluene utilizers, 1,1-DCE strongly inhibited the transformation of TCE (Hopkins and McCarty, 1995). Results of the model simulations indicated that 1,1-DCE both competitively inhibited TCE transformation and produced very high transformation product toxicity (Shim, 1998).

Our study focused on a CAH mixture consisting of 1,1-DCA, 1,1-DCE, and 1,1,1-TCA, as these three compounds are often found together at contaminated sites. In a groundwater survey of 158 sites, Westrick et al. (1984) found that 1,1-DCA, 1,1-DCE, and 1,1,1-TCA existed in 1.8, 6.3, and 16.5% of their samples, respectively. Squillace et al. (2002) ranked these CAHs among the top 14 compounds that contributed to greater than 95% of the detections in the 402 most common mixtures identified in their survey. 1,1-dichloroethene, produced as an abiotic transformation product of 1,1,1-TCA contamination, is also a frequently detected contaminant. In a study of CAH contaminated plumes by Lawrence Livermore National Laboratory (UCRL-AR-133361) of 30 sites with contamination above 1000 μg/L 1,1,1-TCA was the second most frequently observed contaminant (TCE the first), and 1,1-DCE was third most frequently observed along with tetrachloroethene (PCE) and 1,2-cis-dichloroethene.

Their relatively high solubility in water and low affinity for sediment sorption make CAHs easily transported through soils and groundwater. Table 1 presents the physical and chemical properties of the CAHs investigated in this study as well as the maximum.

Table 1 Physical and Chemical Properties of 1,1-DCA, 1,1-DCE, and 1,1,1-TCA

CAH	Mol. Wt. (g/mol)	Specific Gravity[a]	Water Solubility[b] (mg/L)	Vapor Pressure[b] (mm Hg @ 20°C)	MCL[c] (μg/L)
1,1-DCA	98.96	1.174	5500	182	-
1,1-DCE	96.94	1.218	2250	600	7
1,1,1-TCA	133.4	1.35	1500	123	200

a. Fetter (1993)
b. US EPA (1990)
c. US EPA (2001)

Although most chlorinated contamination consists of CAH mixtures, few studies have been conducted on such compositions (Shim et al., 2001). Our study investigated the transformation of 1,1-DCA, 1,1-DCE and 1,1,1-TCA, three CAHs that are frequently found together due to biotic and abiotic transformation of the latter into the former two, respectively. Vogel and McCarty (1987) determined the pathway for the transformation processes (Figure 2).

Figure 2. Pathway for the Abiotic and Biotic Transformation of 1,1,1-TCA (from Vogel and McCarty, 1987)

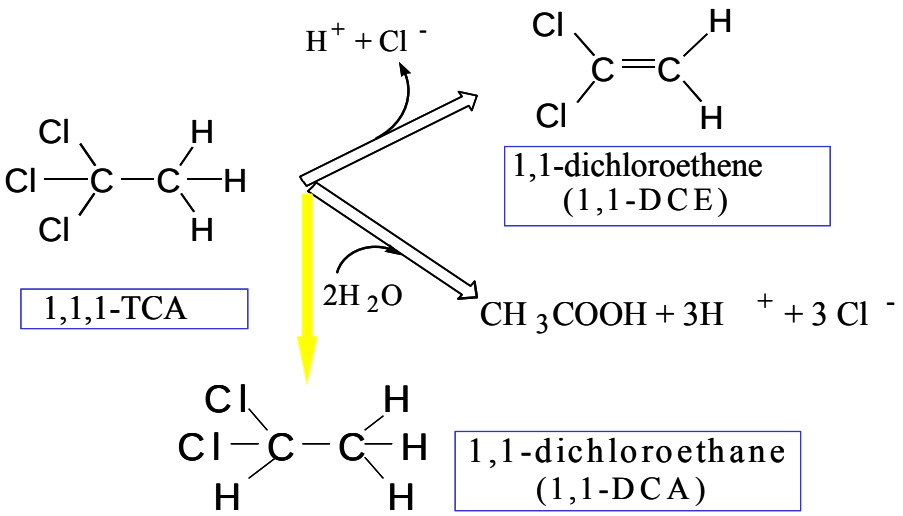

The pathway shows that 1,1,1-TCA is abiotically transformed into 1,1-DCE and acetic acid. The pseudo-first order rate constant for transformation to 1,1-DCE was reported as 0.04 yr^{-1}. 1,1-DCA can simultaneously be produced through reductive dehalogenation.

In previous work conducted at OSU, we found that butane grown cultures have great potential for dechlorination of methanes, ethanes, and ethenes (Kim et al., 1997). This growth substrate proved to be one of the best (compared to propane, methane, ammonia, phenol, etc.) for transforming CF and 1,1,1-TCA. In concurrence with transformation, we observed utilization of butane and oxygen and reasoned that a monooxygenase enzyme likely initiated degradation. Studies with pure cultures of butane utilizing microorganisms conducted by Hamamura et al. (1997; 1999) showed that butane monooxygenase enzymes were responsible for the transformation of CF and other CAHs. Hamamura et al. (1999) demonstrated the presence of butane monooxygenase by the molecular oxygen required for butane degradation, 1-butanol production during butane degradation, and acetylene inhibition on both butane oxidation and 1-butanol production. In that research, butane monooxygenase diversity among butane-grown bacteria *Pseudomonas butanovora*, *Mycobacterium vaccae* JOB5 and an environmental isolate, CF8, was characterized at the physiological level. The response to the monooxygenase inactivator, ethylene, and the inhibitor, allylthiourea (ATU), differentiated butane degradation among the three bacteria.

That work promoted our interest in using butane as the primary growth substrate for the transformation 1,1-DCA, 1,1-DCE, and 1,1,1-TCA. Kim et al. (2000) surveyed the cometabolic

potential of a broad range of chlorinated ethenes, ethanes, and methanes, with a butane enrichment culture. The enrichment culture had the ability to transform TCE and less chlorinated ethenes, including 1,1-DCE, 1,1,1-TCA, and less chlorinated ethanes such as 1,1-DCA, CF, and less chlorinated methanes.

Cometabolic biotransformation is a complex process at the whole cell and enzyme level. Processes include substrate inhibition (Kindred and Celia, 1989; Broholm et al., 1992; Keenan et al., 1994; Ely et al., 1995; and Kim et al., 2002), product toxicity (Chang and Criddle, 1997; Alvarez-Cohen and McCarty, 1991; Kim et al., 2000), and reducing energy limitations (Chang and Alvarez-Cohen, 1995; Ely et al., 1995; Sipkema et al., 2000). Arp et al. (2001) and Alvarez-Cohen and Speitel (2001) provided a review and discussion of these processes and the models representing them.

During transformation reactions, products may develop that pose toxic threats to cells or enzymes, thereby inactivating them. This phenomenon is termed *transformation product toxicity* and may be assigned one of several parameters to account for cell/enzyme death in mathematical models. Transformation capacity (T_c) represents one such parameter, defined as the quantity of a compound that a specific mass of microorganisms can degrade before they are inactivated by toxicity from transformation products. Units of transformation capacity are typically mass of degrading substrate per mass of cells. (Rittman and McCarty, 2001)

Various assumptions are made in using such parameters to simulate product toxicity. Alvarez-Cohen and Speitel (2001) reviewed interpretations for approximating inactivation, separating them into two classes. One class represents loss of full cellular function, while the other class assumes the loss of specific enzyme activity. The first class is most commonly used in modeling biodegradation and was incorporated in our study.

High transformation capacities (amount of CAH transformed/mg cells) have been obtained by butane-utilizing cultures for CF, 1,1,1-TCA and other chlorinated ethanes, and 1,1-DCE (Kim et al., 2000). Transformation capacities for CF, 1,1,1-TCA and 1,1-DCE of 0.071, 0.044 and 0.089 mg CAH/mg TSS of cells, respectively, were achieved which were a factor of four greater than those achieved with methanotrophs expressing sMMO (Chang and Alvarez-Cohen, 1996). The high capacities were achieved in resting cell studies without endogenous energy sources, such as formate.

Inhibition is an important process since the presence of the cometabolic substrate, which must be added, can hinder the transformation of the CAHs of interest. Substrate inhibition describes the hindrance of substrate transformation or utilization due to competition for or alteration of degradative enzymes. When an enzyme lacks specificity, *competitive inhibition* may occur in which one substrate binds to the catalytic site of the enzyme, thus preventing another substrate from reacting. A substrate may also bind to a non-reactive site on the enzyme, altering its conformation and creating *noncompetitive inhibition* which reduces the utilization of another substrate. Competitive and noncompetitive inhibition may occur simultaneously, causing a condition termed *mixed inhibition* (Rittman and McCarty, 2001). Competitive inhibition is the most frequent form of inhibition addressed in mathematically modeling cometabolic

biotransformation (Broholm et al., 1992; Semprini and McCarty, 1992; Chang and Alvarez-Cohen, 1995; Chang and Criddle, 1997; Lee et al., 2000).

Kim et al. (2002a; 2002b), conducted detailed kinetic studies in our laboratory with a butane-utilizing enrichment, which was the parent culture for this study. Inhibition types were determined and kinetic parameters for butane utilization, 1,1,1-TCA, 1,1-DCE, and 1,1-DCA transformation, and inhibition constants were developed. Table 2 presents a comparison of kinetic constants for the butane-utilizing culture compared to other cultures that have been studied in detail. The butane-utilizing culture had higher maximum utilization rates (k_{max}) for 1,1-DCE and lower K_s values than for cultures that grew on methane or ammonia, indicating it was much more effective at 1,1-DCE transformation. It was also as effective, if not more effective, in transforming 1,1,1-TCA. The transformation capacity of 1,1-DCE is also shown to be high for this culture.

Studies of Kim et al. (2002a, 2002b) also showed that CAHs competitively inhibited the transformation of other CAHs and butane, while butane showed mixed inhibitory effects toward the CAHs. Inhibition models were identified and detailed inhibition constants were obtained. Shown in Figure 3 is butane inhibition on the transformation of 1,1,1-TCA observed by Kim et al. (2002a). 1,1,1-TCA transformation was shown to be strongly inhibited by the presence of butane. Solid lines are the model fit of a mixed inhibition model for butane inhibition on 1,1,1-TCA transformation. The results indicate that effective utilization of butane to low concentrations is important to achieve good transformation of the CAHs of interest. 1,1-DCE and 1,1-DCA were also inhibited by butane to a lesser extent.

The kinetic inhibition models and parameter inputs into the models determined by Kim et al. (2002a; 200b) were used in the development of models to simulate the results of laboratory and field studies that were conducted. The results of these modeling studies are presented throughout this report.

2.1 Bioaugmentation Studies

Along with physicochemical, geological, and hydrological parameters, the feasibility of a given contaminated site to undergo in situ bioremediation is dependent upon the capacity of the indigenous microbial population to degrade the compound(s) of interest (Jenal-Wanner and McCarty, 1997). When the indigenous microbial population is not effective at a given site, bioaugmentation might be utilized (Steffan et al., 1999). Bioaugmentation involves the injection of desired exogenous microorganisms along with required nutrients directly into the contaminated zone. For the bioaugmentation method, there are two distinct approaches (Steffan et al., 1999). The first approach is adding the microorganisms to complement or replace the native microbial population. The goal of this approach is to achieve prolonged survival and growth of the added organisms and degradation of the target pollutants. The second bioaugmentation approach is adding large numbers of degradative bacteria to a contaminated site as biocatalysts to degrade a significant amount of target contaminant before becoming inactive or perishing, in which case long-term survival and growth of an active microbial population are not the primary goal. Our study was based on the first approach, with the objective of adding a culture that would survive and be effective for long periods.

Table 2. Comparison of Kinetic Parameters for 1,1-DCE and 1,1,1-TCA Transformation (adapted from Kim et al., 2002b)

Compound	Microorganisms	Growth Substrate	Additional Substrate	k_{max} (µmol/mg TSS/hr)[a]	K_s (µM)	k_1 (L/mg TSS/hr)[a]	T_c (µmol/mg TSS)	Reference
1,1-DCE	*M. trichosporium* OB3b, sMMO	methane	formate	0.36	5.1	0.07	-	1
	M. trichosporium OB3b PP358, sMMO	methane	formate	> 3.2	> 35	0.10	0.36	2
	M. trichosporium OB3b, pMMO	methane	formate	-	-	< 0.002	-	3
	Nitrosomonas europaea	ammonia	ammonia	0.43	9.2	0.05	0.023-0.04	4
	Butane-grown mixed culture	butane	none	1.3	1.5	0.87	0.52	this study
1,1,1-TCA	*M. trichosporium* OB3b, sMMO	methane	formate	1.4	214	0.007	-	1
	Mixed culture	methane	methane	-	-	0.00009	-	5
	Mixed culture	propane	none	-	-	0.003	-	6
	Butane-grown mixed culture	butane	none	0.19	12	0.02	-	this study

[a]: Cell mass is reported in mg TSS; unit conversions assume TSS is 50% protein. **Reference**: 1: Oldenhuis et al., 1991; 2: Aziz et al., 1999; 3. van Hylckama Vlieg et al., 1996; 4. Ely et al., 1997; 5. Strand et al., 1990. 6. Keenan et al., 1994.

Figure 3. Kinetic Studies of Butane Inhibition of 1,1,1-TCA Transformation as Described by Kim et al. (2002)

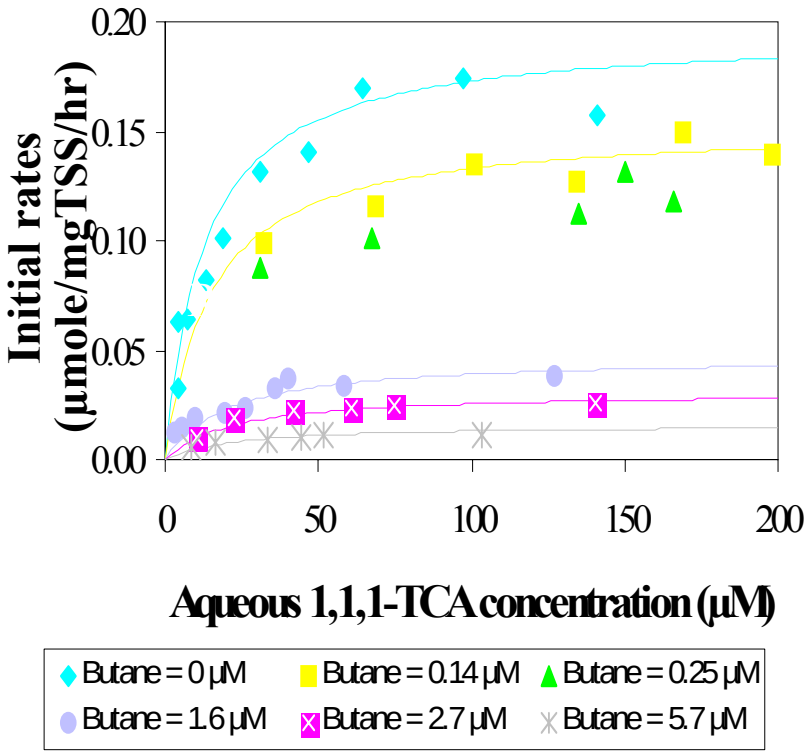

In situ bioaugmentation with a specialized microorganism, *Burkholderia cepacia* ENV435 was reported by Steffan et al (1999). In that work, groundwater contaminated with 1000-2500 µg/L chlorinated ethenes was treated by in situ bioaugmentation and the total mass of TCE, DCE, and VC in the treated area was reduced by as much as 78% within 2 days after injecting the organisms.

A pilot scale field study was previously conducted at the Moffett Field test site to determine if effective aerobic cometabolism of TCE could be accomplished through bioaugmentation of a genetically modified strain of *Burkholderia cepacia* G4 (McCarty et al., 1997). The modified strain that was bioaugmented, *B. Cepacia G4* $PR1_{301}$ ($PR1_{301}$), can degrade TCE effectively while growing on simple substrates such as lactate, instead of phenol or toluene, as is required for the unmodified strain. Strain-specific molecular probes were developed for monitoring the presence and movement of $PR1_{301}$ based on Rep-PCR.

Microcosm studies in small scale laboratory columns indicated that the bioaugmented organisms were present in column effluents as long as bioaugmentation continued, but not when it was discontinued. The $PR1_{301}$ did not maintain TCE degradative ability for long periods when lactate was used as a primary substrate (Munakata-Marr et al., 1997; Munakata-Marr, et al., 1996). In three field trials of bioaugmentation with $PR1_{301}$ and lactate addition, TCE was effectively

removed early in the tests. In addition, when phenol was added it was rapidly consumed, demonstrating the initial phase of bioaugmentation was successful in establishing a population at the site. However, as time proceeded, bioaugmentation with lactate feed alone became ineffective at TCE removal, reaching zero removal within a few weeks. The results suggest that predation of the introduced population or the inability of $PR1_{301}$ to effectively survive and out-compete native organisms for supplied substrate.

One of the major concerns in bioaugmentation is creating and maintaining the appropriate environment for the inoculated strain to grow and survive (Vogel, 1996). A microcosm study with the butane enrichment culture of Kim et al. (2002) was conducted by Jitnuyanont et al. (2001) to study the transformation of 1,1,1-TCA in bioaugmented and non-augmented microcosms. The augmented microcosms required less time to start utilization of butane than non-augmented microcosms. Initially the augmented microcosms were effective in transforming 1,1,1-TCA, but their transformation ability decreased with prolonged incubation. The non-augmented microcosms showed limited transformation ability in the beginning, but they improved with time. Thus, one of the major goals of our study was to obtain and characterize a butane-utilizing culture that was effective for long-term treatment under the geochemical conditions of the subsurface.

2.2 Molecular Methods to Track Bioaugmented Microorganisms

Culture independent studies are essential for determining how many different types of bacteria are present in bacterial communities, because less than 1% of bacteria in nature are believed to be cultured with currently available methods (Cottrell and Kirchman, 2000). Modern molecular techniques provide a means of tracking and quantifying a bioaugmented culture in the subsurface, as well as determining shifts in the microbial community that occur during biostimulation. For analysis of natural microbial populations in which unknown diversity must be evaluated, the methods using ribosomal RNA (rRNA) have been well established. rRNAs are evolutionarily and functionally homologous in all organisms; extremely conserved in overall structure, and rRNA genes lack artifacts of lateral transfer between contemporaneous organisms, thus relationships between rRNAs reflect evolutionary relationships of the organisms (Olsen et al., 1986). rRNA molecules are comprised of highly conserved sequence domains interspersed with more variable regions (Olsen et al., 1986). Detailed information about the variability or conservation of nucleotide positions in rRNA is important for several reasons; sites to which a function can be assigned are often conserved in structure, and conserved regions are very important in the search for the homologous sequence regions between different organisms. On the other hand, highly variable sequence regions can be used for the development of phylogenically-specific hybridization probes or PCR primers, applicable in the detection and identification of specific microorganisms (Peer et al., 1996). There are three rRNAs in bacteria, 5S (~120 nucleotides), 16S (~1600 nucleotides), and 23S (~3000 nucleotides). Among these, the 16S rRNA subunit is used the most due to its appropriate size. An outline of many of the procedures commonly used in molecular microbial ecology using 16s rRNA is depicted in Figure 3.

Fluorescence in situ hybridization (FISH) using 16S rRNA probes is one approach for determining bacterial community composition or identifying target organisms within a mixed

microbial community without requiring PCR. Cells are identified by hybridization of oligonucleotide probes that fluoresce when bound to the target rRNA molecules in the cell. By designing probes specific to hypervariable regions in the 16S subunit, specific phylogenic groups can be targeted. Cell numbers are generally obtained by manual counting using an epifluorescence microscope (Daims et al., 2001). The FISH technique provides definitive confirmation of the presence of active species in a consortium, since the probes target labile rRNA and not DNA. Furthermore, FISH data provide information that links morphology to identify (Ficker et al., 1999). In several environments, results from FISH analysis were similar to the community composition suggested by clone libraries (Ficker et al., 1999; Schramm et al., 1998). In our study, FISH probes were designed and tested for hybridization to strain 179BP and 183BP cultures without success. PCR primers based on the same oligonucleotide sequences as the FISH probes worked well in qPCR analyses, but we were unable to successfully fix the 183BP culture, *Rhodococcus sp,* to allow penetration of the probe for hybridization with the rRNA, although multiple methods were evaluated.

PCR-based community structure analyses consist of two major processes: PCR-clone-sequence approach and community finger printing methods. The starting point for both of these methods is the extraction of nucleic acids from environmental samples (Figure 4). The extracted DNA is subjected to PCR amplification using universal primers or primers designed to amplify rRNA genes from a particular group of organisms. Universally conserved sequences at the 5' and 3' ends allow amplification of nearly complete SSU rRNA genes from the DNA extracted from natural samples (Head et al., 1998). The PCR product can then be fingerprinted by using further methods, or cloned and sequenced so that a 16S rRNA gene library may be prepared. Once a sequence database has been generated from the clone library, phylogenic analysis can be carried out, and the diversity of microbial population can be determined (Head et al., 1998). In our study, a clone library was created to characterize and determine the phylogeny of the dominant microorganisms that were present.

There are several techniques for community fingerprinting: denaturing gradient gel electrophoresis (DGGE) (Ferris and Ward, 1997), temperature gradient gel electrophoresis (TGGE) (Felske et al, 1998), single-strand-conformation polymorphism (SSCP) (Schwieger and Tebbe, 1998), and T-RFLP (Liu et al., 1997; Löffler et al., 2000; Flynn et al., 2000; Dollhopf et al., 2001). The T-RFLP technique is currently one of the most powerful methods in microbial ecology for rapidly comparing the diversity of bacterial DNA (Dunbar et al., 2001). T-RFLP takes advantage of the high resolution and throughput of automated sequencing technologies to separate the polymorphic terminal fragments after restriction digestion (Flynn et al., 2000). It can access subtle genetic differences between strains as well as provide insight into the structure and function of bacterial communities (Marsh et al., 1999). In our study, we applied T-RFLP fingerprinting technique to compared bacterial community structure between different soil slurry samples collected from microcosms treated under various experimental conditions and between groundwater samples obtained over time during the field tests.

Figure 4. Commonly Used Approaches in Molecular Microbial Ecology (adapted from Head et al., 1998)

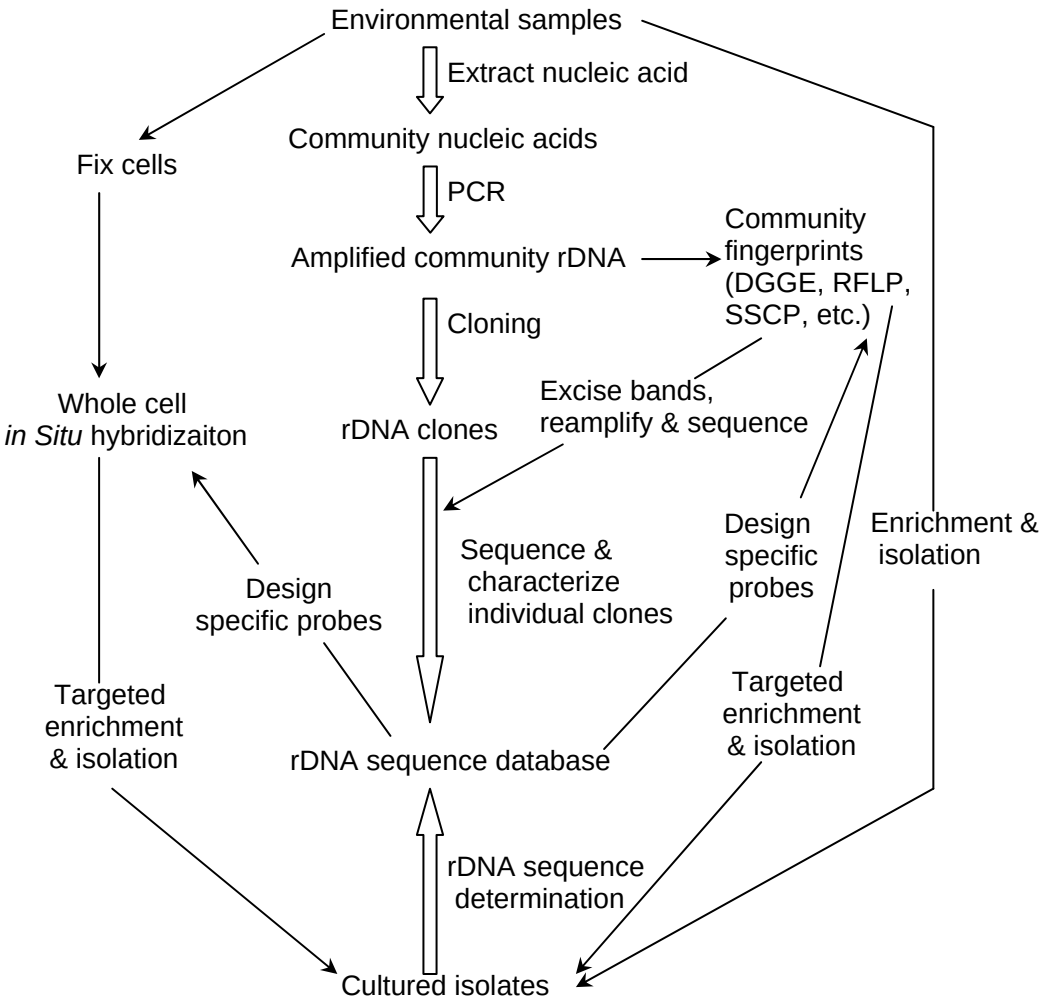

Limitations of PCR-based 16S rRNA analysis

Specific DNA probes were developed in our study to monitor the movement and survival of bacteria during bioaugmentation in field tests. In previous studies, Matheson et al. (1997) developed strain-specific DNA primers for tracking *B. cepacia G4* $PR1_{301}$ in laboratory microcosm studies and field bioaugmentation studies. The methods, as described by Matheson et al. (1997), involved the amplification of genomic DNA via repetitive sequence-based PCR (rep-PCR) using primers specific for repetitive extragenic palindromic (REP) elements, followed by cloning of the amplified fragments. Primers were developed specifically for $PR1_{301}$, and were successfully used to determine the persistence of the strain in aquifer sediment microcosms and in the Moffett Field aquifer in response to bioaugmentation. Similar primers for the butane culture were developed and used to track the culture in laboratory and field experiments. Details of primer development and PCR methods to study changes in the community structure are describe in sections 3.2.2, 3.2.6, 3.2.7, and 3.2.8 of the report.

In our project, efforts were made to model the cometabolic process both for laboratory batch and column experiments and for field experiments. Model simulations can help in the analysis of experimental results as well as in the design remediation systems. The modeling adapted the numerical code of Semprini and McCarty (1991; 1992) used to simulate the results of Moffett field experiments using methane as a cometabolic substrate. Basic features of the model regarding biostimulation included differential equations tracking concentrations of electron acceptor, electron donor, and biomass, as well as non-equilibrium sorption influences. Michaelis-Menten/Monod kinetics were based on the microbial growth rate depending on both electron donor (primary growth substrate) and electron acceptor concentrations. The model simulates cometabolism of two contaminants, including the effects of competitive inhibition, by using the ratio of half-saturation constants to estimate inhibition parameters.

Semprini and McCarty's model was expanded upon in our study to include more influential mechanisms such as mixed inhibition and product toxicity, extrapolating from biotransformation experiments and models reported by Kim et al. (2002a; 2003b). Because Kim's culture was the parent culture of the one used in our study, the parameter values reported by Kim were deemed as appropriate starting estimates for mathematically modeling CAH transformation by our culture. Some parameters were adjusted during simulation of batch laboratory results from the enrichment culture used in our studies. Details of the modeling study are presented in Sections 4 and 5 of the report.

3. MATERIALS AND METHODS

This section provides the materials and methods used for all aspects of the project including those for 1) culture development; 2) molecular methods including clone library, T-RFLP, and qPCR; 3) kinetic studies; 4) microcosm studies; 5) continuous flow column studies; 6) field studies; and 7) modeling studies.

A general diagram that indicates the relationships among the different studies is shown in Figure 5. The development of the culture for bioaugmentation consisted of isolation on agar plates and resuspending in media. The cultures were then grown in media on butane and assayed for their contaminant transformation abilities. A clone library was developed on the enrichment culture prior to the isolation of individual cultures. The clone library permitted the sequencing of dominant clones in the enrichment culture. The analysis permitted a comparison with the microorganisms that were obtained in pure culture in the isolation studies. T-RFLP was also developed for use in the culture isolation studies as well as in the microcosm, column, and field studies. The T-RFLP analysis was used to both track the bioaugmented microorganisms as well as to evaluate changes in community structure. PCR probes were developed that permitted quantification of the bioaugmented microorganisms. A fair amount of effort went into the development of FISH probes to track and quantify the bioaugmented culture. As will be discussed, these efforts failed as a result of the bioaugmented microorganisms being gram positive.

The performance of the bioaugmented culture was tested in media, in microcosms consisting of site groundwater and aquifer solids, and in a continuous flow column packed with aquifer material and fed groundwater. T-RFLP was used to track the community and the bioaugmented culture in all these studies. qPCR analysis was used to quantify the culture in the column studies.

The field study was conducted over three seasons of testing. As will be discussed the methods for conducting the field studies remained fairly unchanged throughout the course of the studies. Two test legs were operated, one that was bioaugmented and another where indigenous butane-utilizing cultures were stimulated. Some differences occurred among the tests, such as concentrations and the mixtures of the CAHs tested, the addition of minor nutrients, and levels of hydrogen peroxide added as a source of dissolved oxygen. All the analytical measurements for the field tests were conducted on site using an automated data acquisition system. Groundwater samples for microbial analysis were shipped to OSU and processes for T-RFLP and qPCR analysis.

This section provides general details of the methods used. Since studies were conducted over the course of four years, details on some tests that are very specific to those tests are presented along with the test results.

Figure 5. An Overview of the Project, Including Microbial Characterization Methods, Laboratory Studies, and Bioaugmentation Field Studies

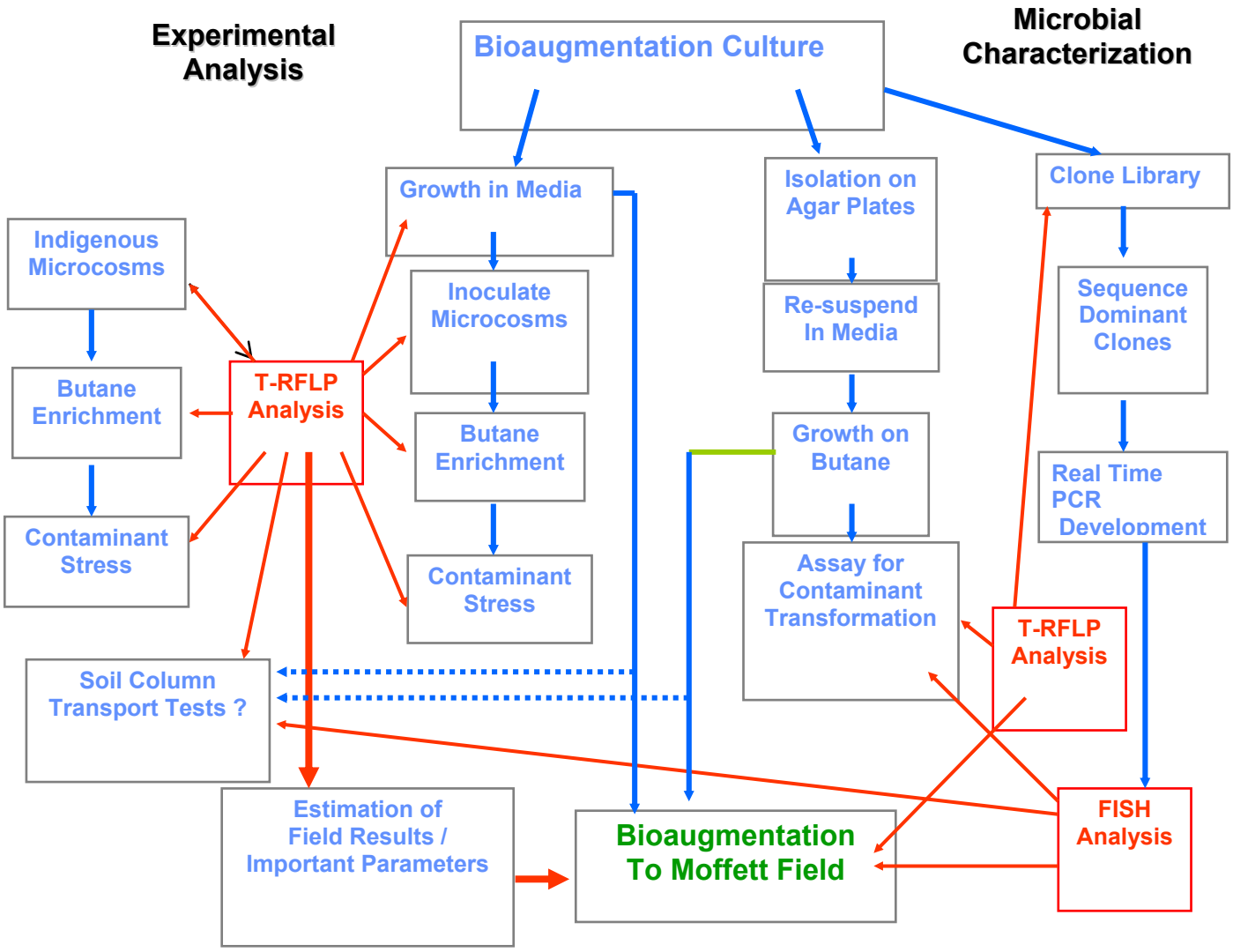

3.1 Culture Development

The culture selected as the source for bioaugmentation efforts at the Moffett Federal Airfield In-Situ Bioremediation Test Site, CA, was obtained from a Moffett soil/groundwater microcosm (B2-1) that was inoculated with a butane-utilizing enrichment culture of Kim e al. (2002a) that was capable of cometabolically degrading the chlorinated solvents TCE, 1,1,1-TCA, and 1,1-DCE. A soil/groundwater slurry was taken from the microcosm and the culture was grown in minimal salt media (MSM) with a 10% butane headspace. The culture was harvested, preserved

in DMSO, separated into 200 1-mL aliquots, and stored in liquid nitrogen for further use as inoculum for media, microcosm, and field bioaugmentation tests.

Frozen aliquots of the source culture were thawed and used as inoculum to grow bioaugmentation cultures for use in media, microcosm, and field tests. Initially, grow was accomplished using a 2 L stirred reactor containing a 1.8 L batch liquid phase comprised of mineral media and a 0.2 L gas headspace that was continually purged with a mixture of 4% butane in air. This system was scaled up to a 40L reactor with a 20 L aqueous batch volume and a continuously flushed 20 L butane-in-air headspace. However, these systems did not produce consistent microbial cultures. Large quantities of butane-utilizers were grown and the microbial compositions analyzed by T-RFLP and the cultures were found to be of different composition. Although many of the same organisms were present in more than one growth batch, different unknown organisms were always present and sometimes dominant and the known, or target, organisms were not in consistent proportions to the overall biomass.

To grow a significant mass of the 183 bp-enriched culture for bioaugmentation at Moffett Field, batch growth conditions were employed. Forty eight 700 mL bottles containing 300 mL mineral media and 400 mL headspace with 4% butane in repeated injections were incubated on shaker tables oscillating at 200 rpm at 20ºC. Additional oxygen was added as vacuum was created in the bottles due to butane and oxygen utilization. The batch cultures were harvested (approximately 4 g of culture dry weight) and concentrated into 35-5 mL cryogenic tubes and frozen in liquid nitrogen until needed. Molecular analysis of the stored culture showed a monoculture with a T-RFL of 183 bp. Samples from this frozen culture were thawed and tested for butane and CAH activity prior to delivery to Moffett Field for the first round of bioaugmentation. This procedure was used throughout the remainder of the field test with varying success at producing monocultures or limited mixed cultures.

Butane-utilizing microorganisms were isolated from the source culture by thawing an aliquot of the frozen source culture and inoculating it into mineral media in a 4% butane headspace, harvesting the resulting culture at log growth phase and serially plating the culture onto agar containing only mineral salts media. The plates were incubated at 20ºC and enriched in a 3% butane headspace. Individual colonies were chosen and serially plated for four or more generations on mineral salts agar in a butane-in-air headspace. Colonies were chosen and again inoculated into mineral media with a butane-in-air headspace. When grown to sufficient density, approximately 10- 1 mL samples of each culture were placed in cryogenic tubes with DMSO or glycerol added to a final concentration of 7% or 25%, respectively, and stored at -80ºC.

3.2 Molecular Methods

Molecular analyses used in this project included the creation of a clone library, T-RFLP, qPCR, and FISH analyses. The clone library was created using 16S rRNA genes amplified from an aliquot of the frozen source culture used to grow the bioaugmentation cultures for media tests, microcosms, and field bioaugmentations. T-RFLP analyses were used to observe microbial community composition in bioaugmentation cultures, microcosm samples, and field groundwater samples. qPCR was used to quantify the amount of strain 183BP cells in microcosm, soil column, and field groundwater samples. FISH analyses were conducted in the attempt to

microscopically observe and enumerate strain 183BP cells in lab microbial cultures and field samples; however, due to the difficulty of getting the probes into the cells, the attempts were fruitless.

3.2.1 Sample Acquisition and Preparation

Three different aqueous sample preparations were used dependent upon the sample types. Aqueous samples were collected from aqueous media-grown bacterial cultures, groundwater effluent from a soil column experiment, and groundwater pumped from monitoring wells at the field test site. All the concentrated cell samples then proceeded to DNA extraction using the same protocol. Sampling of cultures grown in the laboratory consisted of 0.1 to 1 mL of cell culture (dependent on the cell density) pipetted into a clean 1.5 mL microcentrifuge tube (Eppendorf, Germany) and centrifuged at 9000×*g* for 3 min. Supernatant was removed and the pellet was incubated in lysozyme buffer to begin the DNA extraction procedure.

Groundwater samples were collected in 250 mL polycarbonate bottles (Nalgene, Rochester, NY) from sampling wells at the Moffett bioaugmentation test site, CA and shipped in ice chests to Oregon State University. Cells were then concentrated from groundwater samples by filtration through 0.2 μm-pore-size white polycarbonate filter membranes (diameter, 25 mm; Osmonic Inc.) with 0.8 μm-pore-size nitrocellulose support membrane (diameter, 25 mm; Millipore) by applying a vacuum of 20 in. Hg. The polycarbonate filter membrane was then placed in a clean 1.5 mL microcentrifuge tube (Eppendorf, Germany) and incubated in lysozyme buffer to begin the DNA extraction procedure. Approximately 250 mL of effluent samples from the soil column were collected twice each week and were concentrated using the same method used for the groundwater samples.

Occasionally the presence of small soil and/or organic particles contained in the groundwater samples caused very serious clogging of the membrane during filtration. When filter clogging caused excessive filtration times, a centrifuge method for all concentration was applied. A 240-mL portion of the water sample was equally dispensed into 6×50 mL centrifuge tubes (VWR International, San Diego, CA) and centrifuged at 5000×*g* for 10 min. The supernatant from each tube was removed and the final 1.5 mL was transferred to a clean 1.5 mL microcentrifuge tube (Eppendorf, Germany) and centrifuged at 9000×*g* for 3 min. Approximately 200 μL of resulting sediments was taken from the bottom of each tube and combined in a new 1.5 mL tube and again centrifuged at 9000×*g* for 3 min. All the resulting sediments were placed into a new 1.5 mL microcentrifuge tube (Eppendorf, Germany). After the final centrifuge step, supernatant was removed and the sample was incubated in lysozyme buffer to begin the DNA extraction procedure.

Microcosm samples were acquired after vigorous mixing of the microcosm contents to obtain a representative microbial sample. A microcosm would be vigorously shaken and then left stationary on its side for 15 min to settle out the larger particles. A sterile disposable syringe was inserted through the septa and used to acquire a 1 mL sample of mixed sediment and groundwater. Unlike the other sample types, the microcosm samples contained significant amounts of sediment, requiring a different DNA extraction protocol.

3.2.2 DNA Extraction Methods

DNA extraction from aqueous samples obtained from the field site, the soil column and media-grown laboratory cultures was performed by following the protocol supplied with the DNeasy Tissue Kit (Qiagen, Valencia, CA). Briefly, concentrated cell pellets or the filter membrane containing cells were suspended in a cell lysis buffer (200 µL per tube) containing 20 mM Tris-Cl (pH 8.0), 2 mM EDTA, 1.2% Trition X-100 and 20 mg/mL lysozyme. After incubation at 37 ºC for 30 min, 25 µL proteinase K solution and 200 µL buffer AL were added the cell solution and heated to 70 ºC for another 30 min. Then, 200 µL of 100% ethanol was added to deproteinate the lysates. The mixture was pipetted into a DNeasy spin column placed in a 2 mL collection tube and centrifuged at 8000×*g* for 1 min. The spin column was transferred to a new collection tube, 500 µL buffer AW1 was added, and the tube was centrifuged at 8000×*g* for 1 min. Then the spin column was placed on a new collection tube and 500 µL buffer AW2 was added to center of the spin column. Then the tube was centrifuged at 14000×*g* for 3 min. After discarding the flow-through, the mixture was centrifuged at the same speed for 1 more min to allow complete ethanol evaporation/removal. The spin column was then transferred to a clean 1.5 mL microcentrifuge tube (Eppendorf, Germany) and DNA was eluted with 100 µL of elution buffer AE and stored at -20ºC.

DNA was extracted from microcosm soil slurry samples using FastDNA ® SPIN Sample kit (BIO 101 Inc., Vista, CA) according to the manufacturer's instructions with a following modification: To avoid inhibition of subsequent PCR by co-extractants, the DNA-bound silica matrix was rinsed 3 times with a 5.5 M guanidine thiocyanate (Fluka Chemical Corp., Milwaukee, WI) solution before SEWS-M reagent was added to the spin column. Extracted DNA was eluted in DES buffer supplied with the kit.

3.2.3 Oligonucleotide Primer and Probe Design

Primers were designed for use in qPCR analyses that were specific to hyper-variable region of the 16S rRNA gene of strain 183BP organisms to allow selective amplification of a target organism's DNA. The goal of probe (primer) design was to choose an ideal oligonucleotide sequence complementary to a region of the target organism sequence that allows at least one mismatch to the same region in all other non-target organisms. Since the primer design follows the same procedure as probe design, only the probe design procedure is described here. Potential 16S rRNA-targeted oligonucleotide probes applicable to the specific detection of strain 183BP were formulated using the probe design tool of the ARB program package (written by O. Strunk and W. Ludwig; available at http://www.arb-home.de). Operating under UNIX, LINUX, or Sun-Micro system, it is a graphically oriented software package for phylogenic analysis, sequence alignment and analysis and molecular probe design.

Figure 6 shows the procedure for probe design. Fragment sequences of strain 183BP were compiled using the ARB CONSENSUS function. To provide sufficient information from non-target, but phylogenetically similar sequences to strain 183BP, the partial sequence of strain 183BP (the first 1032 bases) was checked against the Genebank database using BLAST at NCBI (http://ncbi.nlm.nih.gov/BLAST). Fifty sequences sharing the highest similarities with strain 183BP were obtained from NCBI and imported into the ARB program along with the strain 183BP sequence. These sequences were added to a 16S rRNA database downloaded from RDP II (Hugenholtz, 2002; available online at http://rdp.cme.msu.edu/html/alignments.html), which contains more than 8000 sequences, most belonging to soil bacteria. The imported sequences

Figure 6. Flowchart of Probe (primer) Design and Selection for Targeting Specific Phylogenetic Groups

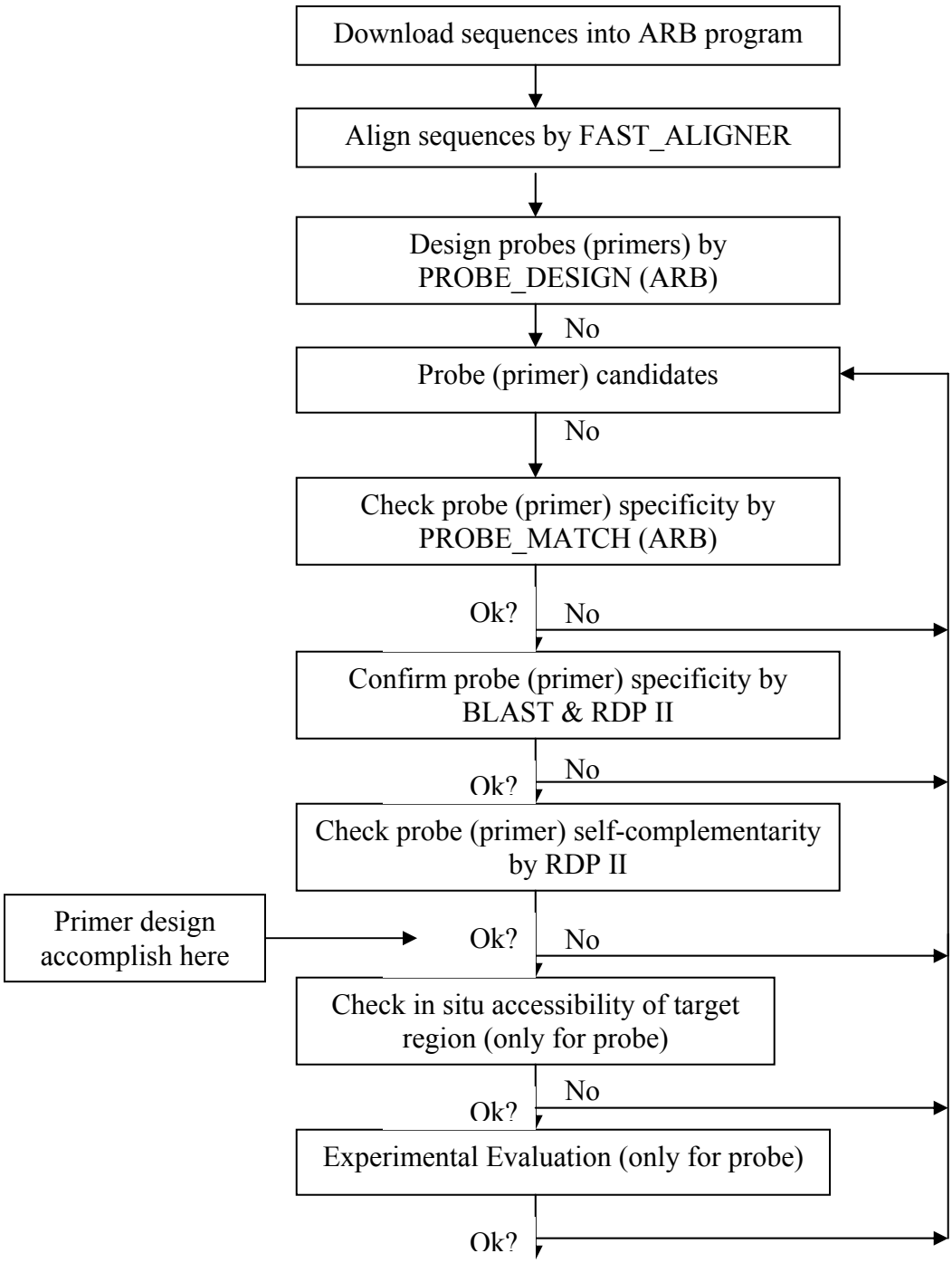

were automatically aligned using FAST ALINGER (version 1.03) against the existing sequences. The aligner needs a sequence as reference, which can be chosen from the consensus of the group containing the species, from the closest relative found by the selected PT_SERVER, or from a fixed species if no relative is found automatically. Ambiguously and incorrectly aligned positions were manually aligned on the basis of the conserved primary sequences and consensus of phylogenetically related sequences.

Based on the newly established 16S rRNA database, the probe design tool can select nucleotide sequence regions that allow discrimination of the target sequence from all non-target reference sequences. In the ARB program, PT_SERVER searches for patterns (such as regions specific to target sequences) in special searchable database files, which essentially are fragmented versions of standard ARB database files (Hugenholtz et al., 2001). Before performing the probe design, the searchable database file, PT_SERVER, must be updated from the newly modified ARB database. The 183BP sequence was highlighted as the design target while others were left unmarked. Several parameters need to be defined prior to probe design, such as G+C content, location (E. coli number), maximal hairpin bonds, melting temperature and probe length. In this case, they were defined as 50 to 100%, 1 to 10000, 0, 30 to 100 ˚C, and 18-mer, respectively. Potential probe (primer) candidates were evaluated by the PROBE_MATCH function in order to check their specificity from 0 - 5 mismatches. The criterion for the probe selection is that the probe should contain at least one mismatch to non-target sequences, ideally located in the middle of the target string to maximize the destabilizing effect of the mismatch.

Once a probe (primer) was characterized that had at least one mismatch to all non-target sequences in the database, probe specificity was checked against all available rRNA sequences in the public databases (Genebank and RDP II [available at http://rdp.cme.msu.edu/html/]). An exact match will have a score (bits) of twice the value of the number of nucleotides of the submitted probe sequence (Tables 3 and 4).

The hybridization and PCR reaction can be disrupted if the probe is self-complementary, i.e., forming hairpin turns or dimers. Thus, the probe sequence should be inspected by the PROBE_MATCH program in RDP II, where only pairings of 2 or more consecutive Watson-Crick pairs are accepted and the allowed size of the loop (of the potential hairpin) is between 2 and 4.

The accessibility of the probes (primer) was further evaluated by comparing the 16S rRNA target position of the probes with the in situ accessibility map of E. coli provided by Fuchs et al. (1998). They examined the accessibility of the E. coli rRNA to more than 200 oligonucleotide probes complementary to the entire length of the E. coli 16S rRNA molecule and mapped the regions with relatively high and low accessibility. However, this check provides only a very general idea about the putative fluorescence intensity of the individual probe because the secondary structure of E. coli 16S rRNA may differ from that of other bacteria strains, especially for bacteria strains phylogenetically distant to *E. coli*.

3.2.4 PCR Conditions

Each PCR reaction was carried out in a final volume of 50 µL reaction mixture contained 20 µK 2.5×PCR Eppendorf mastermix (Eppendorf, Westbury, NY) giving final concentrations in the PCR reaction of 1.25µ taq DNA polymerase, 50 mm KCl, 30 mm tris-HCl, 1.5 mm mg 2+, 0.1%

Table 3. Additional Bacterial Sequences that are 100% Complementary to the Strain 183BP-Specific Primer Ran191F

Genebank Accession #	Bacterial sequences producing significant alignments	Score (bits)	E value
X80625	*Rhodococcus* rubber strain DSM43338T	36	0.27
AY247275	*Rhodococcus* ruber M2	36	0.27
AF529079	*Rhodococcus* sp. an 16S rRNA gene	36	0.27
AY114177	*Rhodococcus* ruber strain AS 4.1038	36	0.27
AF420413	*Rhodococcus* sp. USA-AN012	36	0.27
AY114109	*Rhodococcus* sp. E33	36	0.27
AF447392	*Rhodococcus* aetherovorans strain Bc663	36	0.27
AF447391	*Rhodococcus* aetherovorans strain 10bc312	36	0.27
AF323255	Gram positive bacterium B1G-1B	36	0.27
AF131484	*Rhodococcus* sp. IM-43760	36	0.27
AF103733	*Rhodococcus* sp. YH1	36	0.27
AF350248	*Rhodococcus* ruber strain AS4.1187	36	0.27
AJ459106	*Rhodococcus* sp. HN	36	0.27
AY496284	*Rhodococcus* sp. SoD	36	0.27

Table 4. Additional Bacterial Sequences that are 100% Complementary to the Strain 183BP-Specific Primer Ran443R

Genebank Accession #	Bacterial sequences producing significant alignments	Score (bits)	E value
AF547972	Mycobacterium tokaiense strain CIP 106807	36	0.27
AF547950	Mycobacterium murale strain CIP 105980	36	0.27
AF420413	*Rhodococcus* sp. USA-AN012	36	0.27
AF447392	*Rhodococcus* aetherovorans strain Bc663	36	0.27
AF447391	*Rhodococcus* aetherovorans strain 10bc312	36	0.27
AF480590	a Mycobacterium tokaiense 16S rRNA gene	36	0.27
Y08857	a Mycobacterium sp. 16S rRNA gene	36	0.27
AB009578	Mycobacterium sp. PP1	36	0.27
AF353688	*Rhodococcus* sp. PR-N14	36	0.27
AF103733	*Rhodococcus* sp. YH1	36	0.27
AF350248	*Rhodococcus* ruber strain AS4.1187	36	0.27
AJ459106	*Rhodococcus* sp. HN	36	0.27

lgepal-ca630 and 200 µm each dATP, dctp, dGTP and dTTP, 20 – 40 pmol of each primer (a forward primer and a reverse primer, Table 5), and 2 µL of template DNA. All PCR Amplifications were performed with an Eppendorf Gradient Thermocycler (Eppendorf, Germany). The PCR reaction conditions consisted of one cycle of 95ºC for 2.5 min., 55ºC for 1 min., and 72ºC for 2 min., followed by 35 cycles of 95ºC for 0.5 min., 55ºC for 1 min., and 72ºC for 2 min., and final extension at 72ºC for 20 min. and cooling at 4ºC. The annealing temperature (55ºC) was the same for all primers used.

Molecular biology grade water was prepared by filtering nanopure water (NANO pure, Barnstesd International Inc., Boston, MA) through a 0.2 µm syringe filter (Millipore Corp., Billerica, MA), followed by UV-light exposure for 1 min. Molecular biology grade water (2 µL) and DNA template extracted from a pure strain 183BP culture were used as negative and positive controls, respectively, in PCR reactions.

Table 5. 16S rDNA Primer Sequences and Concentrations in PCR Reaction Mixtures

Primer	Primer Sequence	Amount (pmol)
Universal bacteria primers		
27F-B-FAM*	5'-AGR GTT YGA TYM TGG CTC AG-3'	40
338Rpl	5'-GCW GCC WCC CGT AGG WGT-3'	30
183BP-specific primers		
Ran191F	5'-GTT CCG GGG TGG AAA GGT-3'	20
Ran443R	5'-ACT CGC GCT TCG TCG GTA-3'	20

*27F-B-FAM primer is labeled with FAM dye at the 5' end for T-RFLP analysis
**All primers are purchased from Qiagen Inc., Valencia, CA.

3.2.5 Gel Electrophoresis

Five microliters of each PCR product was visualized on a 1% agarose gel (EMD Chemicals Inc., Gibbstown, NJ) prepared with 1×TAE buffer (0.04M Tris-acetate, 0.001M EDTA) and stained with 0.5 µg/mL ethidium bromide. MassRuler Low Range DNA Ladder (MBI Fermentas Inc, Hanover, MD) was loaded as a DNA mass marker. The DNA Ladder yields the following 11 discrete fragments (in base pairs): 1031, 900, 800, 700, 600, 500, 400, 300, 200, 100, and 80. Electrophoresis of 5µL MassRuler DNA Ladder results in bands containing 50, 45, 40, 35, 30, 50, 20, 15, 10, 5, 4 ng of DNA, respectively. Electrophoresis was conducted using 1×TAE at 220 volts for 40 min.

The resultant gels were imaged by BioDoc-It system (UVP Inc, Upland, CA) and the DNA band intensities in the electronic images were analyzed using the NIH Image J program (written by Wayne Rasband of the National Institute of Health; available at http://rsb.info.nih.gov/ij/ for free). Band intensities and sample volumes were used to estimate the required dilution to prepare samples for fragment analysis at Central Service Lab at Oregon State University.

3.2.6 Creation of a Clone Library

Genomic DNA was extracted from a frozen aliquot of the source culture using a DNeasy Tissue Kit (Qiagen, Valencia, CA) following the procedure described in Section 3.2.2. The extracted

DNA underwent PCR amplification of the 16S rRNA genes present using the universal bacterial primers 27F-B and 1492R using the protocol described in Section 3.2.3. The resulting PCR amplicons were purified using a QIAquick PCR Purification Kit (Qiagen, Valencia, CA) under manufactures recommendations and were then used as inserts for the clone library. A clone library of the 16S rRNA genes was developed using pGEM-T Easy Vector Systems (Promega, Madison, WI). PCR-amplified 16S rRNA genes were ligated into pGEM-T Easy vectors which were then transformed into JM109 high efficiency competent E. coli cells. The transformed cells were then smeared onto plates containing agar composed of Luria-Bertani (LB) broth, IPTG, Xgal, and ampicillin. Since the vector contained the ampicillin resistance gene, only transformed colonies should grow on the plates and since the inserted DNA should have knocked out the lac Z operon in the vector, successfully transformed colonies containing a DNA insert should appear white, instead of blue. One hundred white colonies were picked from the plates, re-plated and grown overnight, transferred to test tubes containing LB media and ampicillin, and again grown overnight before being aliquoted for archiving, plasmid prep, and screening (Figure 7).

The clones were first screened by RFLP analysis. DNA inserts were amplified using PCR with pUC/M13F and pUC/M13R primers whose recognition sites flanked the DNA insertion site in the vectors. The amplified inserts were then digested using the restriction endonuclease HaeIII. The resulting DNA fragments were separated on a 3% agarose gel and sized by comparison with a known DNA standard, Generuler 100bp DNA Ladder Plus (MBI Fermentas, Hanover, MD). Clones producing similar RFLP profiles were grouped and again eletrophoresed on a 3% agarose gel to compare lane-to-lane for similarity. Since the library was conducted to identify the major or dominant organisms in the source culture, a single representative clone was chosen from each of the 16 groups containing more than a single clone. Stored plasmid prep samples of the 16 clones were purified, diluted to an appropriate concentration, and sent to OSU's Central Services Laboratory for sequence analysis using an ABI 3700 sequencer. Most of the clones were only partially sequenced (~350 bp) over the approximate 1500 bp region of the DNA insert. However, the 16 representative clones also underwent T-RFLP analysis as described in Section 3.2.6 and clones matching the T-RFLs of the dominant organisms in the source culture were chosen for complete sequencing. The resulting sequence information was then used to design group-specific PCR primers and FISH probes for future molecular analyses of the cultures during bioaugmentation tests.

Figure 7. Flow Chart of 16S rRNA Gene Clone Library Analysis Starting with Liquid Cultures and Including Archiving, Plasmid Preparation, PCR Screening, and RFLP Analysis (Courtesy of Kevin Vergin and Stephen Giovannoni, Oregon State University)

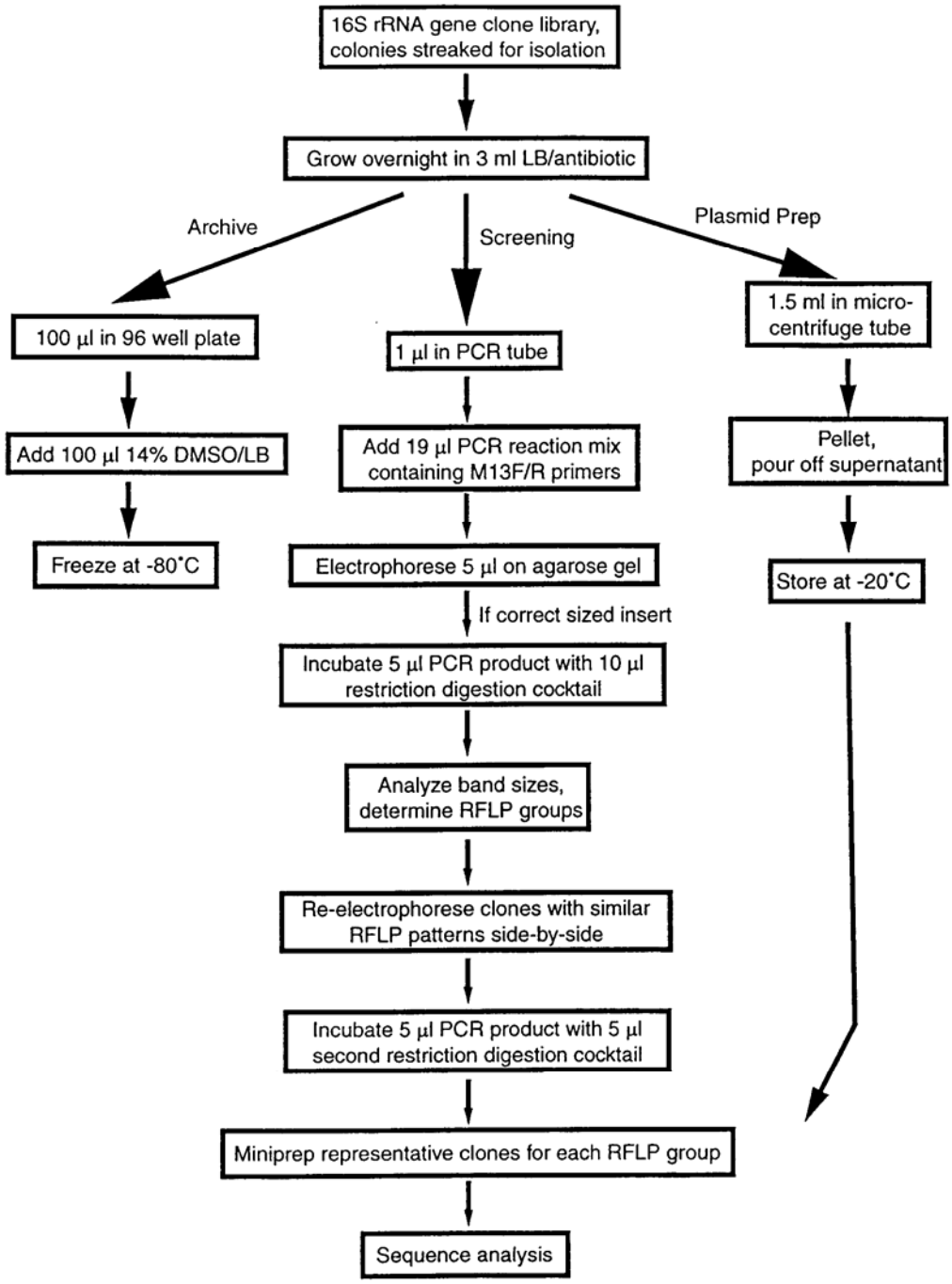

3.2.7 T-RFLP Analysis

PCR products amplified by the primer pair of 27F-B-FAM and 338R were digested at 37ºC for 4.5 hours with *Mnl*I or *Hin6*I restriction endonucleases (MBI Fermentas Inc, Hanover, MD). Digestion was followed by incubation at 80ºC for 10 min to terminate enzyme activity. Each enzyme was supplied in a concentration of 10 U/µL with an appropriate buffer. The recognition sites of these enzymes and the composition of the reaction mixtures are shown in the Table 6.

One microliter of each digested sample was taken and diluted to an approximate concentration of 1 ng DNA/µL with molecular biology grade water (The dilution ratio was calculated from DNA mass estimation after gel electrophoresis by Image J). One microliter of the diluted DNA sample was then taken and dried using a Vacufuge concentrator (Eppendorf, Germany) for 20 min and sent to the Central Service Laboratory at Oregon State University for fragment size analysis.

Table 6. Enzyme Recognition Sites and Reaction Components for Restriction Endonuclease Digestions

MnlI		Hin6I	
Recognition sites			
5'-C C T C$(N)_7$ ^-3' 3'-G G A G$(N)_6$ ^-5'		5'-G^C G C-3' 3'-C G C^G-5'	
Reaction mixture ingredients			
Reagent	Volume (µL)	Reagent	Volume (µL)
Enzyme (10 U/µL)	0.25	Enzyme (10 U/µL)	0.25
G^+ Buffer	2	Y^+ / Tango Buffer	2
PCR product	10	PCR product	10
Water	7.75	Water	7.75

Each sample was run on an ABI 377 slab gel platform with Filter set A as the dye set consisted of 6-FAM (blue) labeled samples and Rox (red) standard. GENESCAN400-ROX (fragment size: 50-, 60-, 90-, 100-, 120-, 150-, 160-, 180-, 200-, 220-, 240-, 260-, 280-, 290-, 300-, 320-, 340-, 360-, 380- and 400-bp; PE Applied Biosystems, Foster City, CA) was added into each sample as an internal lane standard. Fragment size was determined using GeneScan software, version 2.1 (PE Applied Biosystems, Foster City, CA). Results were obtained in the form of an electropherogram and a data table of fragment size and peak area.

The densitometric curve of selected T-RFLP files were transferred to GelComparII program (version 3.5, Applied Maths Inc., Belgium). Each gel was normalized according to the internal size standard and the banding patterns were compared using unweighted pair group method with arithmetic means clustering method and the Dice coefficient method.

3.2.8 Quantitative Real Time PCR

The SYBR Green qPCR was performed in a Sequence Detection System 7000 (PE Applied Biosystems, Foster City, CA). The SYBR Green PCR Master Mix (PE Applied Biosystems, Foster City, CA) contains SYBR Green I Dye, AmpliTaq Gold® DNA polymerase, dNTPs with dUTP, Passive Reference 1, and optimized buffer components. All amplification reactions were

carried out in a total volume of 25 µL in 96-Well Optical Reaction Plates and optical adhesive covers (PE Applied Biosystems, Foster City, CA). Each reaction contained 1 µL of DNA template, 12.5 µL of 2×SYBR Green I PCR Master Mix, 150 nM concentrations of forward and reverse primers, and to reach a total volume of 25 µL, molecular biology grade water. The cycling parameters were as follows: initial incubation at 50ºC for 2 minutes to active UNG and for 95ºC for 10 minutes to activate the Taq polymerase, thermal conditions followed 40 cycles of 95ºC for 15 seconds and 60ºC for 1 minute, during which a fluorescent measurement was taken from each well at each cycle.

For this study, an absolute quantitation method was used. Calibration curves were run in parallel and in triplicate with each analysis using the DNA extracted from a pure strain 183BP culture. The extracted DNA was then diluted in 10-fold series from 4.04×10^{-1} down to 4.04×10^{-6} per mL. Wells with no DNA template were used as negative controls. The cycle threshold (C_T), indicative of the quantity of target gene at which fluorescence exceeds a preset threshold, was set above the baseline where there was little change in the fluorescence signal. After exceeding the threshold, the sample was considered positive.

Amplification data collected by the 7000 Sequence Detector was then analyzed using the Sequence Detection System software (version 1.1; PE Applied Biosystems, Foster City, CA). The calibration curve was created by plotting the cycle threshold (C_T) against the log of the concentrations of strain 183BP. The coefficient of linear regression (R) for each standard curve was calculated.

Ten-fold serial dilutions of DNA extracted from a pure culture of strain 183BP containing [4.04 ± 2.18] $\times10^7$ cell/mL were prepared. Standard curves were performed in triplicates. Initially PCR was performed on triplicates of serial dilution in the same run, 1:1, 1:10 and 1:100. However, the C_T values of 1:1 and 1:10 dilution were very close. We believed that the presence of humic or other background compounds in the environmental samples inhibited the PCR reaction. A clear 1-log decrease in the sensitivity of 183BP detection was observed between 1:10 and 1:100 dilutions for most samples. Due to the high variability associated with 1:100 diluted samples, samples of 1:10 dilution were chosen for cell quantitation.

SYBR Green I is a double-stranded-DNA-binding stain. When unbound it has no detectable fluorescence; however, it does emit fluorescence when bound to any double-stranded (ds) DNA (Giulietti et al., 2001). Following amplification, a melting curve analysis was performed to verify the product specificity by its melting temperature (T_m) (Ririe et al., 1997). If SYBR-Green-I-bound dsDNA is heated, a rapid loss of SYBR Green I fluorescence can be observed near the denaturation temperature of the DNA strand. The melting curve and the value of T_m are dependent on the GC content, length and sequence of the amplicon. Thus, some non-target amplicons can be distinguished by the melting curve analysis. In the present study, T_m is determined during a phase of slow heating, from 60 to 95ºC, during which time there occurs a rapid decrease in the fluorescence due to the denaturation of the amplicons, resulting in the formation of single filaments of DNA and the detachment of SYBR Green I. The melting curves were visualized with the Sequence Detection System software (version 1.1; PE Applied Biosystems, Foster City, CA). Samples producing curves with more than one evident melting point were not used for analysis.

3.2.9 FISH Analysis

Oligonucleotide Probes And Stains

Once selected, the oligonucleotide probes were purchased (Operon Technologies, Inc., Alameda, CA) with a single amino linker attached at the 5' terminus and labeled with the cyanine monofunctional dye, Cy3. The probe was dispensed to 0.5 mL amber safe-lock microcentrifuge tubes (Eppendorf, Germany) with 170 pmol of probe per tube, were dried and stored at –20 °C. Prior to use, the probe stock solution was hydrated to a final probe concentration of 2 ng/µl using hybridization solution (0.9 M NaCl, 20 mM Tris-HCl [pH 7.4], 0.01% sodium dodecyl sulfate, and 15% or 35% formamide).

The DNA intercalating dye 4', 6'-diamidino-2'-phenylindole (DAPI; Sigma) was stored as a solution at 1 mg/mL at –20 °C. A final concentration of 5 µg/mL in hybridization wash solution (150 mM NaCl, 20 mM Tris/HCl [pH 7.4], 5 mM EDTA, and 0.01% sodium dodecyl sulfate) was placed in coplin jars at 4 °C and used to nonspecifically stain bacterial cells and any other DNA-containing organisms.

Sample Ixation And Filtration

Groundwater samples were fixed in paraformaldehyde for 4 hours at 4°C with a final solution concentration of 2% paraformaldehyde. After fixation, 20 mL individual sub-samples were filtered through 0.2 µm pore size white polycarbonate filter membrane (diameter, 25 mm; Osmonic Inc.) with 0.8 µm pore size nitrocellulose membrane support (diameter, 25 mm; Millipore Inc.) and glass microfibre filter backing (diameter, 25 mm; Whatman) by applying a slight vacuum at ~5 in. Hg. After filtration, the polycarbonate membrane was transferred from the filter stack to a microscope slide (size, 25×75×1 mm; Fisher Scientific) using Cryo-Babies (Diversified Biotech), was air-dried in the dark, and stored at –20 °C in a slide box containing desiccant.

Whole-Cell Hybridization and DAPI Staining

Prior to hybridization, the white polycarbonate membrane was cut into four parts and each quarter was fixed to a new slide with a Cryo-Babies (Hampton Research, Aliso Viejo, CA) on each end. Hybridization with oligonucleotide probes for each quarter membrane was performed in a 50 µl aliquot of hybridization solution (0.9 M NaCl, 20 mM Tris/HCl [pH 7.4], 0.01% sodium dodecyl sulfate, and 15% or 35% formamide, 2 ng/µl probe) pipetted directly onto the membrane. A glass cover slip (size, 24×60 mm or 22×22 mm; VWR International, San Diego, CA) was applied immediately on the top of the Cyro-Babies in order to create a layer of hybridization solution between the cover slip and the membrane. The slide was then placed in a sealed black chamber containing 3 small jars filled with nanopure water to maintain humidity, and incubated at 37 °C for 3 hours for media-grown cultures and 10-16 for environmental samples. Following hybridization, the slide was transferred to hybridization wash buffer (150 mM NaCl, 20 mM Tris/HCl [pH 7.4], 5 mM EDTA, and 0.01% sodium dodecyl sulfate) for 10 minutes. The same wash step was repeated once in a new hybridization wash buffer. The slide was then transferred into the 5 µg/mL DAPI solution and incubated for 10 minutes in the dark and then rinsed with DAPI wash (hybridization wash) for another 2 minutes, and finally air dried in the dark with the Cryo-Babies stickers removed. A drop of Citifluor antifadent (Ted Pella,

Inc., CA) was added to each membrane and then covered with a cover slip, sealed with nail polish, and stored at –20 °C with desiccant.

Cell Counts

Total cell counts and FISH-labeled cell counts were calculated by the method developed from Kepner and Pratt (1994). Cell counting was performed on randomly chosen field of view (FOV) for each test sample. The number of target cells per milliliter of groundwater sample was determined from values for the effective area of the filter, the area of FOV, the dilution of the sample applied, and the volume of diluted sample filtered, as follows:

$$\text{Total number of target (cell/mL)} = (N \times A_t)/(d \times V_f \times A_g)$$

Where, N: mean number of cell counted per FOV;
A_t: effective area of the filter (mm^2)
d : dilution factor (V_{final}/V_{sample})
V_f : volume of diluted sample filtered (mL)
A_g: area of FOV (mm^2)

Fluorescent Microscopy

Cy3-positive and DAPI-positive cells were counted for each field of view using a DMRB epifluorescence microscope (Leica Inc, Germany) coupled with an ORCA-ER CCD digital camera (Hamamatsu Inc., Japan) and filter sets appropriate for Cy3 and DAPI. Consistent exposure times for DAPI and Cy3 images were 1 and 5 seconds, respectively. Cy3 and DAPI images were processed by IPLab software (version 3.5.5, Scanalytics Inc, Fairfax, VA). Positive probe signals were determined by segmenting and overlaying Cy3 images on the corresponding DAPI image (the same FOV under the DAPI filter set) segmentations. Segmentations on the Cy3 images matching the corresponding segmentations on the DAPI images were counted as positive. Negative control counts were determined using the same technique and subtracted from positive probe counts to correct for autofluorescence and nonspecific binding.

3. 3 Culture Kinetic Studies

Described in this section are the methods used in the batch kinetic studies. The methods vary somewhat for the different studies (such as reactor volumes, cell densities, and cultures used); provided below is the method most typically used.

3.3.1 Chemicals Used

Chemicals used in all kinetic experiments included butane, 1,1-DCE, 1,1-DCA, and 1,1,1- TCA. N-Butane (Grade CP) was obtained from Airgas Co. (Corvallis, OR). 1,1,1-TCA (99.5%), 1,1-DCE (99%) and 1,1-DCA (>99%) were all purchased from Aldrich Chemical Co. (Milwaukee, WI).

Concentrations of 1,1-DCE, 1,1,-DCA, and 1,1,1-TCA were added during experiments using a saturated solutions of each CAH. This procedure eliminates the use of carrier solvents, such as methanol, for introduction of CAH into the microcosms. Saturated solutions were created in a serum bottle that was crimp-sealed and shaken vigorously for 6 hours to ensure saturation and

left quiescent overnight before use. These solutions were typically made by injecting neat chemicals into 27 mL vials containing approximately 25 mL of deionized water. Volumes of each neat CAH were added so that total mass in the saturated solution volume exceeded the solubility limit of each CAH.

3.3.2 Growth of the Butane Culture(s) Media and Microcosm Tests

The bacterial enrichment culture used for kinetic studies for the 1,1,1-TCA and 1,1-DCE tests was acquired from a previously prepared 1 mL aliquot of a frozen culture enriched from environmental samples from a Hanford, WA, DOE site. The culture was grown in batch by inoculating aliquot into a 2000-mL flask filled with 1800 mL of mineral salt media at room temperature. The composition of the growth media was that used by Kim et al (2002a) for growing the parent enrichment culture, which was adapted from the Xanthobacter Py2 media (Wiegant and de Bont , 1980), and is presented in Table 7. The growth reactor was continuously fed with butane and air. Headspace partial pressure of 2 to 4 % butane was maintained throughout the growth cycle.

For microcosm studies with the 183BP culture, a resuspended solution of previously frozen, concentrated cells was used as an inoculum. In order to create the frozen inoculum of cells, a pure culture obtained from plates was added to autoclaved 707 mL clear glass bottles containing growth media (Table 7) and capped with gray butyl rubber septa (Wheaton Glass Co., Millville, NJ). After inoculation, 15-30 mL of headspace (air) was removed and replaced with an equivalent volume of butane. The bottles were incubated at 20°C and shaken at approximately 200 rpm. All growth reactors were periodically fed oxygen to maintain atmospheric pressure within, and to ensure that oxygen limitation would not occur. Butane concentrations and optical densities (600 nm) were read periodically from representative bottles. The culture was grown in batch and stored frozen for use as inoculum in laboratory experiments and the field tests. When most of the butane had been utilized and optical density at 600 nm reached approximately 1.0, the cells were harvested. The aqueous cell mixture was centrifuged at 8000 rpm (Du pont Sorvall RC-5B) for 30 minutes. The supernatant was decanted and the concentrated cells were transferred into a 50 mL beaker. Glycerol was stirred in with the harvested cells at approximately 15% by volume to prevent cell damage during freezing. The cells/glycerol mixture was stored in cryogenic vials in a dewar filled with liquid nitrogen. Prior to freezing, a dry weight test was performed using a 1 mL sample of the harvested, condensed cells to determine approximate cell concentration.

Prior to using the cells, a cryogenic vial containing the frozen cells was removed from liquid nitrogen and allowed to thaw to room temperature for about 1 hour. 2.5 mL of the thawed cells were transferred into Eppendorf aliquots and spun at 14,000 rpm for 3 minutes in an Eppendorf 5415C centrifuge. The supernatant was decanted and replaced with autoclaved growth media (Table 7). The centrifuging and washing were repeated 2 times. The rinsed seed culture was diluted in 100 mL of growth media (Table 7). A 1 mL sample of this solution was injected into each microcosm. Dilution and dry weight analysis of the frozen culture indicated cell concentration within the reactors was approximately 1.5 mg/L.

Table 7. Growth Media Composition

Stock Solution	Compound	Concentration
Phosphate Buffer	***K_2HPO_4*3H_2O***	***2030.9 (mg/L)***
	NaH_2PO_4*H_20	***739.0 (mg/L)***
Sulfate Solution	***$MgSO_4$***	***60.2 (mg/L)***
Chloride Solution	***$CaCl_2$***	***11.1 (mg/L)***
Nitrate Solution	***$NaNO_3$***	***153.0 (mg/L)***
Trace Element Solution	***$FeSO_4$*7H_2O***	***6283.0 (μg/L)***
	$MnCl_2$*4H_2O	***300.8 (μg/L)***
	$ZnSO_4$*7H_2O	***146.6 (μg/L)***
	H_3BO_3	***61.8 (μg/L)***
	Na_2MoO_4*2H_20	***108.9 (μg/L)***
	$NiCl_2$*6H_2O	***23.8 (μg/L)***
	$CuCl_2$*2H_2O	***17.0 (μg/L)***
	$CoCl_2$*6H_2O	***23.8 (μg/L)***

Source: Rungakamol (2001)

3.3.3 Batch Transformation Kinetic Tests in Media

The culture's ability to transform the CAHs of interest and utilize butane as a carbon/energy source was measured in growth media (Table 7). These tests were performed in 27-mL serum vials containing 10 mL of bioaugmented cells in growth media, 17-mL of air, and with desired concentrations of 1,1-DCE, 1,1-DCA, 1,1,1-TCA, and butane. Degradation of the substrates over time was measured to develop transformation profiles.

Typically 10-mL of grown culture were added directly into 27-mL vials sealed with a gray butyl rubber septa cap. Volumes of saturated stock solutions of the CAHs were added to achieve the desired injection concentrations. For example 1,1-DCE (1 μL), 1,1-DCA (0.5 μL), and 1,1,1-TCA (2.4 μL) were injected to obtain approximate aqueous concentrations of 100, 200, and 200 μg/L, respectively. Approximate cell concentrations ranged 170 to 200 mg/L. Butane gas (0.7 mL) was injected to obtain approximately 4% volume headspace. The vials were shaken on a rotary at 200 rpm. Headspace gas samples were taken periodically using a 100 μL gas-tight syringe, and compound masses were measured by gas chromatography.

3.4 Microcosm Methods Test

3.4.1 Microcosm Construction

Microcosms were constructed using aquifer materials and groundwater acquired in aseptic manner from the Moffett Federal Airfield In-situ Bioremediation Test Site, CA. Aquifer material was collected during the installation of the injection and extraction wells for the field test experimental legs. Three phases were present in the microcosms: aquifer solids, groundwater, and a gaseous headspace. Microcosms were constructed under a laminar flow hood (The Baker Company, Sanford, MA) to minimize the potential for microbial contamination during assembly. Materials used in microcosm construction were autoclaved including bottles, caps, and all other instruments.

Three different microcosm studies were conducted during the course of the project. The first two studies evaluated 1,1,1-TCA and 1,1-DCE transformation in separate tests. These studies were

performed with the bioaugmentation of a highly enriched mixed culture**.** The third study was performed to evaluate the bioaugmentation with the Strain 183BP pure culture. In this study the transformation of CAH mixtures was evaluated. The difference methods used in microcosms studies are provide below.

Microcosm studies of 1,1-TCA and 1,1-DCE transformation (Study 1 and Study 2) were performed in 156-mL bottles with open-hole screw cap closures and gray butyl rubber septa (Wheaton Glass Co., Millville, NJ). The core materials used for microcosm fabrication were sieved (No. 8 sieve, 2.38-mm opening), combined and mixed before distributing to the microcosm bottles. Approximately 25 mL of aquifer material and 55 mL of Moffett groundwater were added to each microcosm. Groundwater nitrate concentrations ranged from 4.2 to 4.4 mg/L as NO_3^-. Bioaugmented microcosms were constructed as triplicates for all experimental conditions.

Butane (1.8 mL) was volumetrically injected into the 156-mL microcosm bottles using a 1-mL gas tight syringe (Precision Sampling Corp., Baton Rouge, LA). The bottles were shaken for 10 min. to allow the equilibration of substrate before initial gaseous samples were taken. The microcosms were incubated at 20 °C on a shaker table at 200 rpm for the duration of the study. Headspace vacuums created by the consumption of butane and oxygen were re-equilibrated to atmospheric pressure by injection of pure oxygen into the headspace. The saturated stock solution of the CAH of interest was injected into the microcosms through the rubber septa using a 25-µL microsyringe (Hamilton Co., Reno, NEV) to achieve the desired concentration. Headspace samples were taken periodically with a 100 µL gas-tight syringe and analyzed for butane and CAHs of interest using the procedures described below. The culture used to inculate the microcosm was a mixed enrichment culture from which the strain 183BP was isolated.

For the third study, the microcosms were constructed in 707-mL bottles with open-hole screw cap closures and gray butyl rubber septa (Wheaton Glass Co., Millville, NJ. Similar procedures were used in preparing the microcosms as those previously described. The microcosms contained approximately 100 mL of aquifer material and 400 mL of groundwater. The bioaugmented culture was inoculated into microcosm groups using a resuspended solution of previously frozen, concentrated cells of the strain 183BP. A cryogenic vial containing the frozen cells was removed from liquid nitrogen and allowed to thaw to room temperature for about 1 hour. 2.5 mL of the thawed cells were transferred into Eppendorf aliquots and spun at 14,000 rpm for 3 minutes in an Eppendorf 5415C centrifuge. The supernatant was decanted and replaced with autoclaved growth media (Table 7). The centrifuging and washing were repeated 2 times. The rinsed seed culture was diluted in 100 mL of growth media (Table 7). A 1 mL sample of this solution was injected into each microcosm. Dilution and dry weight analysis of the frozen culture indicated cell concentration within the reactors was approximately 1.5 mg/L.

Saturated stock solutions of 1,1-DCE (20 µL), 1,1-DCA (16 µL), and 1,1,1-TCA (65 µL) were injected using glass syringes to achieve aqueous concentrations of 100, 200, and 200 µg/L, respectively. These concentrations were in the range used in later field experiments. Four mL of butane (9.6 mg total mass, 0.91 mg/L aqueous concentration at equilibrium) was injected with a plastic syringe into all microcosm reactors.

In all the microcosm studies, immediately after substrate injection, each bottle was hand shaken for five minutes, and then sampled to determine compound headspace concentrations using gas chromatographic analysis (GC). The reactors were incubated at 20°C and stored upright on a shaker table at 100 rpm with periodic headspace sampling. Oxygen was added to the reactors according to stochiometric oxygen demand for butane consumption (4 mol O_2:1 mol butane). This was done by filling a glass syringe with oxygen and allowing headspace in the reactors to equilibrate to atmospheric pressure.

3.4.2 Analytical Methods for the Media and Microcosm Studies

Equilibrium partitioning between gaseous and aqueous phases within the media and microcosm reactors allowed compound masses to be determined. The gaseous concentrations of butane, 1,1-DCE, 1,1-DCA, and 1,1,1-TCA were measured based on GC analysis using calibration curves generated using external standards. Mass balances incorporating these gaseous concentrations, published Henry's constants (Mackay and Shiu, 1981; Gossett, 1987; Tovannabootr and Semprini, 1998), and solution volumes were used to determine the total mass remaining in the bottle. This method is further described by Kim et al. (2000) and Jitnuyanont et al. (2001).

To determine the gaseous concentration of butane, 1,1-DCE, and 1,1-DCA, a 100 µL of headspace sample was injected into Hewlett Packard (Wilmington, DE) 6890 GC equipped with a photo ionization detector (PID) and a flame ionization detector (FID) connected in series. Chromatographic separation was achieved using a 0.53 mm X 30 m GS-Q capillary column (J&W Scientific, Folsom, CA), operated isothermally at 250°C with helium gas as a carrier gas (15 mL/min). The PID was used to quantify 1,1-DCE, while the FID was used to quantify butane and 1,1-DCA. The column temperature was ramped after 1.5 minutes at 145°C to 205°C at an increasing rate of 40°C/min. Carrier gas was helium at a flow rate of 15 mL/min. 1,1,1-TCA was measured using a Hewlett Packard (Wilmington, DE) 5890 gas chromatograph equipped with a ^{63}Ni electron capture detector (ECD). Chromatographic separation was achieved using a HP-624 capillary, 30m x 0.25mm x 1.4mm film thickness. This column was operated isothermally at 100°C. The carrier gas was helium at a flow rate of 1.5 mL/min with an argon/methane mixture (95%:5%) as a make-up gas.

The aqueous concentration of nitrate was measured by Dionex DX 500 ion chromatograph (Dionex Co., Sunnyvale, CA) equipped with conductivity detector CD20. Aqueous samples (1 mL) were taken after the microcosms were allowed to settle for few minutes. The samples were centrifuged for 10 min and 500 µL of supernatant was used for IC analysis.

3.5 Continuous Flow Column Study Methods

3.5.1 Construction of the Continuous Flow Column

The continuous flow column study was conducted in a glass column reactor. The glass column (Internal dimensions: 2.5 cm diameter; 30 cm length; Volume = 150 mL) (Kontes, Vineland, NJ) was packed with aquifer material obtained from several core samples from Moffett Field test site. Figure 8 illustrates the column packing procedure. The aquifer solids were homogenized and then wet sieved using US sieve #50 (opening size: 297 microns) to remove large particles. Solids retained on this sieve were used to pack the column. The column was packed by flowing Moffett test site groundwater at a flow rate of 0.2 mL/min in an up-flow mode through the column. The

column was packed in 1-1.5 cm intervals. For each interval, a layer of aquifer material was added and the solids were compacted by tamping using a sterilized glass rod and hand vibrating. Additional layers were added to fill the column to top, while visually ensuring that the layers had no trapped air bubbles. Each layer was tamped and hand vibrated for a period of 1-2 min before adding groundwater through the column. This process of adding solids to the top of the column in a counter current manner washed out fine solids.

Figure 8. Illustration of Column Packing Procedure

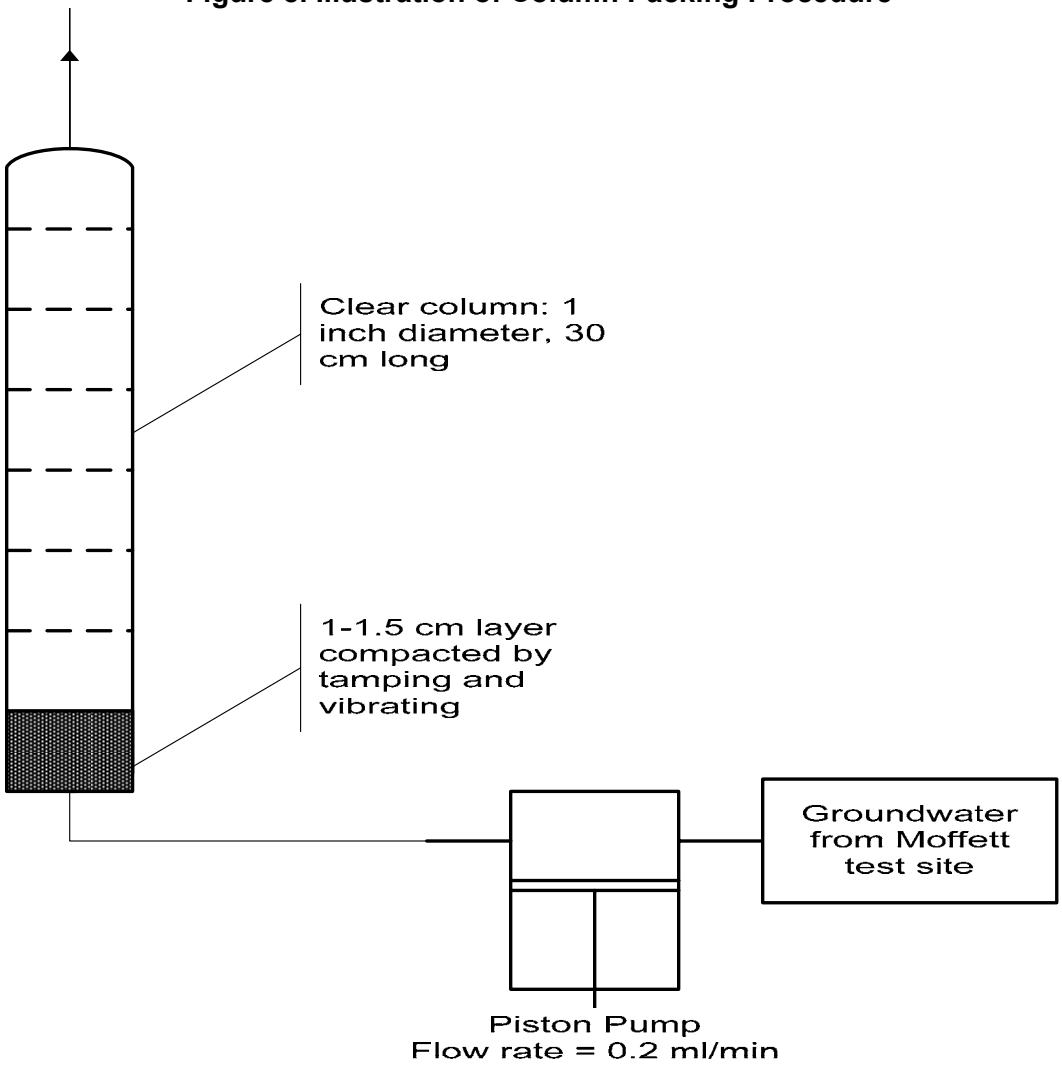

Figure 9. Column Reactor Set-Up Showing the Dual Pump Injection System used for Delivering Dissolved Oxygen, Butane, 1,1,1-TCA and 1,1-DCE Along with the Flow Through DO Meter

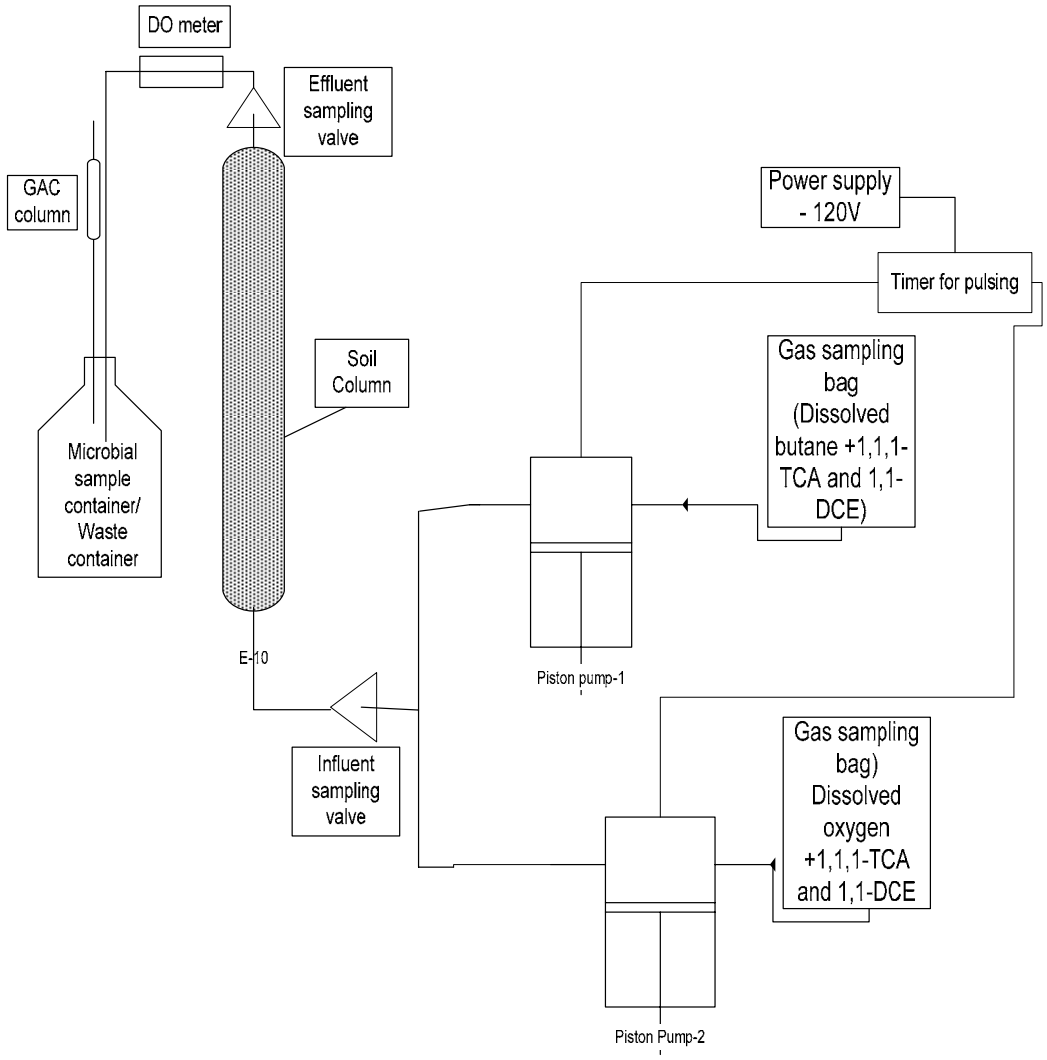

3.5.2 Bromide Tracer Tests

A bromide stock solution of 1000 mg/L was prepared in deionized water using potassium bromide (KBr). This stock solution was further diluted in site groundwater to obtain bromide ion concentration of 25 mg/L. The Feed solution (25 mg/L) was injected into the column by maintaining upward flow using a piston pump (Fluid Metering Inc., Syosset, NY, model #: QG6) at a rate of 0.2 mL/min.

3.5.3 Column Injection System

The injection system for the column study was constructed to alternatively pump groundwater from one reservoir containing oxygenated groundwater and another reservoir containing groundwater with dissolved butane. This was achieved by coupling two piston pumps to an electronic timer (ChronTrol, San Diego, CA; model: ChronTrol XT series timer) which alternates the injection of groundwater from each reservoir (Figure 9). 1,1,1-TCA and 1,1-DCE were added to the desired injection concentration in both reservoirs. The piston pumps (Fluid Metering Inc., Soyosset, NY, Model #: QG6) were connected to the column using short lengths of tygon tubing (Fisher Scientific, U.S.A) and 1/8 inch I.D. stainless steel tubing (V.W.R International, U.S.A). The solutions were pulse fed at alternating pulse cycles of 30 minutes for the butane solution and 120 minutes for the dissolved oxygen (DO) solution to achieve the desired stoicheometry of butane and oxygen addition. Most experiments were conducted at a flow rate of 0.2 mL/min.

DO and butane fed solutions were prepared by dissolving gaseous oxygen and butane in water. This was accomplished by purging groundwater with either oxygen or butane in an aeration vessel. The fed solution was then pumped into the two reservoirs which were metalized-film bags (Chromatography Research supplies, Louisville, KY; size: 9″*9″, volume = 1.6 L) respectively.

Groundwater (1.5-L) was oxygenated by sparged with pure oxygen (99 %) in a 2-L aeration vessel for about one hour to obtain a dissolved oxygen concentration near saturation (~40 mg/L). The DO solution was then transferred into a metallized-film bag reservoir using the compressed oxygen gas pressure.

Groundwater with dissolved butane was prepared as follows: 600 mL of groundwater was sparged with nitrogen for 30 minutes in a 1-L aeration vessel to remove oxygen. The de-oxygenated groundwater water was then sparged with butane for about 5 to 8 minutes and then stirred for 45 minutes to ensure the dissolution of butane. This was repeated two more times. Butane was transferred into the metallized-film bag reservoir by butane gas pressure in the aeration vessel.

Measured amounts of 1,1,1-TCA and 1,1-DCE saturated in deionized water were added to both DO and butane reservoirs through the polypropylene septum fitting using a glass syringe (Hamilton Co., Reno, NV), to achieve injection concentrations of ~200 μg/L or ~400 μg/L of 1,1,1-TCA and ~130 μg/L of 1,1-DCE.

3.5.4 Analytical Methods

Samples (1-mL) for bromide analysis were collected from both the influent and effluent sampling valves of the column in 1.5-mL polypropylene vials. Samples for dissolved butane,

1,1,1-TCA and 1,1-DCE concentration measurements were acquired in a 2 mL crimp top glass vials. Headspace analysis was used to determine the concentration of these compounds. A 1-mL sample was collected in the 2 mL crimped vial. Sample volumes were determined by weighing vials before and after collection. Two samples each from influent and effluent sampling ports were obtained, one for the butane analysis and another for 1,1,1-TCA and 1,1-DCE analysis. The microbial samples were collected for the real time PCR analysis in 500mL autoclaved bottles. The bottle was connected at the effluent end of the column after the DO probe.

Bromide concentrations were determined using Dionex (Sunnyvale, CA) 4000i Ion Chromatograph equipped with an auto sampler and a 4270 integrator. Chromatic separation was achieved using a Dionex Ionpac AS4A column, which utilized a regenerant that contained sulphuric acid (H_2SO_4) and an eluant consisting of sodium carbonate (Na_2CO_3) and sodium bi-carbonate ($NaHCO_3$). The eluant was pumped at a flow rate of 1.5mL/min. Samples were analyzed by dispensing aqueous samples into Dionex Polyvials with filter caps for the use on the auto sampler. The method was calibrated using external standards.

Butane, 1,1,1-TCA and 1,1-DCE headspace concentrations from the 2-mL sample vials were determine by gas chromatographic analysis. The samples were equilibrated at 20°C using a vortex mixer for 3 minutes at a speed setting of 7 to insure equilibrium partitioning between the gas and liquid phases. Headspace concentrations of butane, 1,1,1-TCA and 1,1-DCE were determined by injecting 100 μL of sample the GCs.

The butane gas concentration was determined with a Hewlett Packard (Wilmington, DE) 6890 gas chromatograph FID using the method previously described. 1,1,1-TCA and 1,1-DCE were measured using a Hewlett Packard (Wilmington, DE) 6890 gas chromatograph equipped with a ^{63}Ni ECD, as previously described. The concentrations in the groundwater sampled from the columns were computed via mass balance calculations using the published Henry's constants (Mackay and Shui; Gossett, 1987).

The DO concentration in the column effluent was measured using a in-line microelectrode DO probe. The DO meter was a Microelectrodes Inc., Bedford, NH (model #: 16-1730Flow-thru oxygen electrode). The DO probe was calibrated using water saturated with oxygen. Meter. The DO probe was installed after the effluent sampling valve.

3.6 Methods Used in the Field Demonstration

3.6.1 Test Leg Installation for the Field Experiments

New test legs were constructed at the Moffett Field Test Site for the field experiments. The new test legs were located directly west of the test legs used in previous field demonstrations. Since the groundwater flow direction is to the north at the site, this placement would ensure that groundwater infiltration from previous demonstrations would not have occurred at the locations of the new test legs. Two new test legs were installed: a control leg for tests without bioaugmentation, and the bioaugmentation test leg where the butane culture would be added. The installation of the two experimental legs permitted the comparison of results obtained with the stimulation of an indigenous population and to those obtained with bioaugumentation.

The well field for the two experimental legs is shown in Figure 10. The West Leg was used as the indigenous control leg, and the East Leg was the bioaugmentation leg. The legs were installed parallel to each other and 15 ft apart to avoid microbial contamination between the legs. Each leg consists of an extraction well, an injection well, and five monitoring wells in a direct line between these wells.

The injection and extraction wells were installed by a hollow-stem-auger drilling method. During the well installation, core samples were obtained by pushing a split spoon sampler containing 2 inch brass core sampling tubes ahead of the auger, using standard sampling techniques. The injection wells were fabricated out of 2-in. PVC, while the extraction wells were 6-inch PVC). The injection and extraction wells for each experimental leg were 7 m (24 ft.) apart and were slotted over a 5-ft interval, 15 to 20 ft. below ground surface (bgs). After installation with a hollow stem auger the screen section was backfilled with a medium sand. The internal volume of each injection well was reduced by 60 percent by inserting a 1.5 m length perforated 45 mm OD PVC hollow bar with a packer attached at the top. The injection solution was delivered via a 6 mm OD stainless steel (SS) tubing connected to the top of the PCV hollow bar packer.

The five monitoring wells were installed along each experimental leg as stainless steel sand-point-wells. Three of the sand-point-wells (1.25-inch), were for groundwater monitoring, and were slotted over a 2.0-ft. interval. They are located 4, 8, and 16 ft. from the injection well (Figure 10). The slotted interval was centered between 15.5 to17.5 ft (bgs). Two of the sand-point-wells (1.25-inch) which were used to obtain samples of attached microorganisms (to be filled with solid support media) were slotted over a 5-ft.. interval. They are located 2 and 5 ft.. from the injection wells. Coupons of glass beads and acid washed aquifer solids were lowered into these wells. These coupons were placed into and removed from the wells during the course of the field experiments. These drive point wells were installed with minimal disturbance of the aquifer by augering to 4 m and hand-driving the wellpoints in place. The groundwater monitoring wells were placed at a depth of 5.5 m, which resulted in the screened section being located in the most permeable zone consisting of sand and gravels. A 6 mm OD stainless steel tube containing a series of orifices along the slotted interval was placed in each sandpoint. The sandpoint was filled with 3 mm glass beads to the top of the well screen to reduce the internal pore volume by 60 percent. A packer was then slid over the 6 mm sampling tube.

3.6.2 Subsurface Hydrogeology

During the well installation aquifer core samples were obtained using a split spoon sampler with 2-inch brass sleeves. Methods for obtaining aseptic core samples were employed. The cores were shipped to Oregon State University where they were used in the microcosm studies and the continuous flow column experiment, as previous discussed.

Figure 10 Diagram of the Experimental Well Legs at Moffett Federal Airfield.

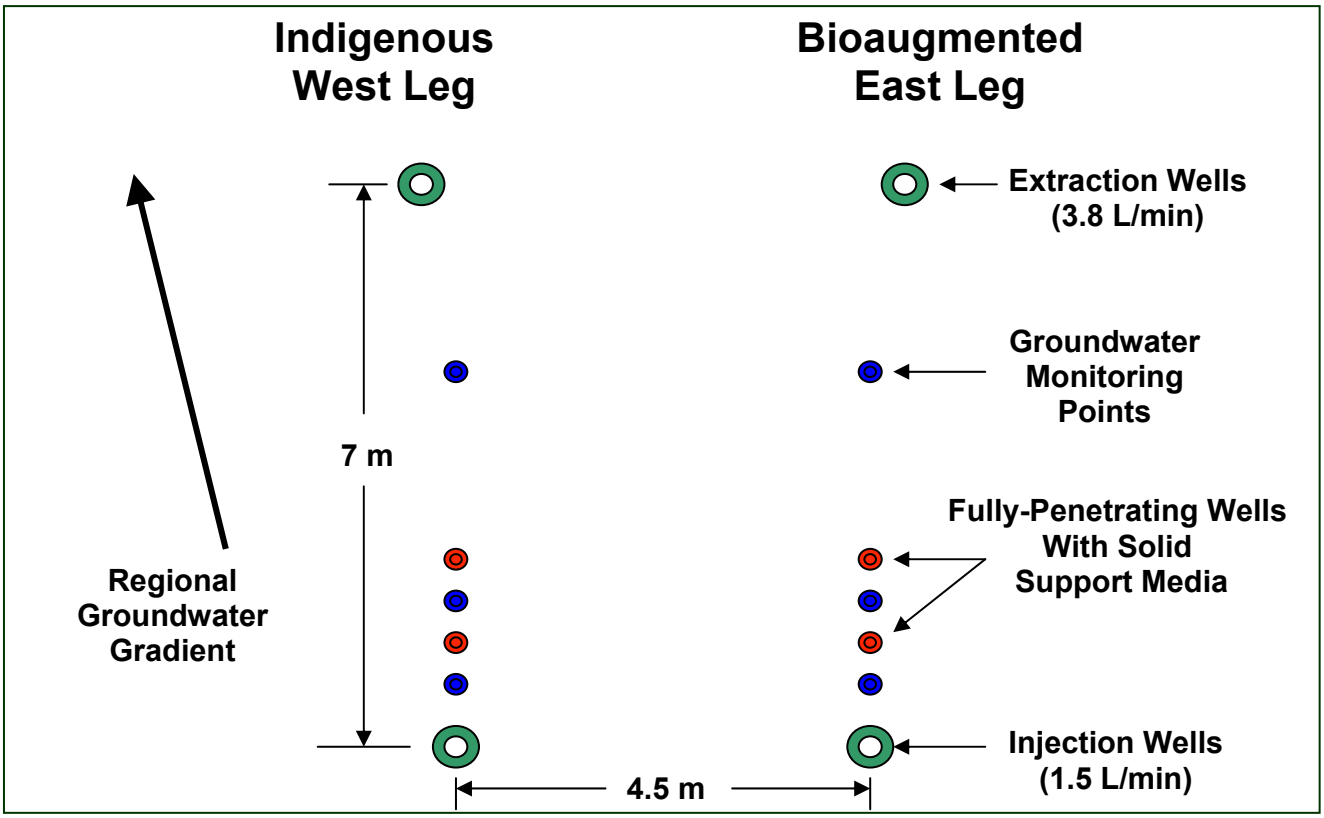

The subsurface hydraulic and geochemical characteristics of the site has been discussed in detail by Roberts et al. (1990). Results of drill cutting and core sample inspection indicate the new wellfield had similar hydrogeologic characteristics as those described by Roberts et al (1990). The site is located on the lower part of Stevens Creek alluvial fan, approximately 3 km south of the southwest extremity of San Francisco Bay, in a region were the aquifer is contaminated by several CAHs, including 1,1,1-TCA and 1,1-DCE. A vertical cross section of one of the well legs used in the study is shown in Figure 12. The well legs for the current tests were installed 3 and 6 meters west of the well leg SI – NI described in detail by Roberts et al (1990), based on well logs the new legs showed similar lithologic profiles. The uppermost 0.5 m consists of silty sand with pebbles up to 8 in. in diameter. This surface layer is underlain by approximately 4 m of silt and clay. The aquifer consists of fine-to-course grained sand and appears poorly sorted in the cores. The aquifer is approximately 1.5 m thick, and is located 4.3 to 5.8 m below the ground surface. A layer of greenish-gray silty clay underlies the aquifer.

As discussed by Roberts et al. (1990) the aquifer is confined with a piezometric surface about 2.5 meters above the top confining layer. The hydraulic gradient is to the north at 0.0032 ft/fl . Results of well test analysis discussed by Roberts indicated the aquifer is a confined leaky aquifer with a tranmissivity of 140 m^2/day, a storativity of 0.00013, and an r/B value of 0.05.

3.6.3 Groundwater Chemical Characteristics

Groundwater chemical characteristics at the site are discussed by Roberts et al. (1990). A summary of the chemical composition of the groundwater at the site is provided in Table 8. The groundwater hardness is 920 mg/L, and is classified as very hard. Bicarbonate is the major for of alkalinity at the measured pH of 6.5. Nitrate and phosphate were present at 10 mg/L and 0.1 mg/L, respectively. As discussed by Roberts et al. (1990) the groundwater has the chemical characteristic for suitable microbial growth.

The groundwater had low levels of CAH contamination. Only one CAH was detected in the ambient groundwater, which had a similar retention time as 1,1-DCE on the site GC analysis. If this compound was 1,1-DCE its concentration was in the range of 10 μg/L. No aromatic compounds (benzene, toluene, xylene) or chlorinated aromatics were present (Roberts et al., 1990).

3.6.4 Extraction System

The groundwater extraction system was designed to maintain a constant rate of fluid withdrawal and permit changes in rates, if desired. The inlet suction was located at a depth of 5.2 m, in the center of the well screen. Induced gradient conditions were maintained by extracting groundwater at a rate four times the injection rate in both experimental legs. Groundwater was typically extracted at a rate of 8 L/min in the East experimental leg, and 6 L/min from the west experimental leg to limit cross contamination among the legs. Results of bromide tracer tests indicated these rates limited cross contamination. Like in the previous field studies conducted at the site, groundwater was injected upgradient of the natural flow and extracted downgradient to ensure effective capture of the groundwater.

Groundwater was extracted using Grundfos 5E pump heads with ½ HP Franklin three phase motors. The motors were controlled by ABB 140 variable frequency drives. The use of variable speed drives and three phase motors provides control of the pump discharge rate by controlling the speed (RPM) of the motor. Signet low flow paddle wheel sensors connected to a Signet flow controller produced a direct reading of the instantaneous flowrate as well as recording of the accumulative extracted volume. For rapid visual confirmation of flow, a direct reading rotometer was installed on each flowrates extraction line. Extraction flow in excess of the injection flow rate was delivered to the top of a counter flow, air stripping column before being discharged to a storm drain.

Injection System

The injection system was designed to achieve constant injection rates desired, chemical concentrations, the pulse alternate injection of groundwater containing dissolved oxygen or dissolved methane. The system was designed to automatically shut down when the injection water was not being supplied due to a system malfunction. The extracted groundwater was used as the injection supply water. The injection system was of similar design to that described by Roberts et al. (1990). The injection system consists of a pulse timer that permitted the alternate injection of groundwater containing butane or oxygen (and/or hydrogen peroxide). Two separate injection systems were constructed, so that microbial contamination across the experimental legs would be minimized.

The two injection systems were identical and operated in parallel with groundwater supplied from the extraction well to the corresponding injection well (groundwater from the east extraction well was amended and injected into the east injection well, groundwater from the west extraction well was amended and injected into the west injection well). A photo of the injection system under construction is shown in Figure 13.

For injection, extracted groundwater was pumped through a rotometer and flowrate was adjusted to 1.25 L/min. Gas (oxygen or butane) was added at 250 mL/min through a low pressure solvent frit (to produce a fine bubble stream) and the mixture passed through a ¼ inch static mixer. The groundwater was then delivered to the top of a "gas absorption column," which was composed of a 3-in. diameter clear PVC pipe and fittings. At the top of the gas absorption column, excess gas was vented via a ¼ inch tube to a 1 ¼ ABS vent pipe which had a 25 CFM blower at one end. Also at the top was a liquid overflow which drained into the waste stream. Additional gas was added at the bottom of the gas absorption column at 150 mL/min, essentially producing a two stage gas saturation process.

The gases were delivered to the two systems via a common manifold which has a pressure regulator and a solenoid for each gas (butane, oxygen and nitrogen). The timing of the pulse duration and control of the pulse cycles was controlled by a Chrontroller. A cycle was composed of x minutes of butane, 4 minutes of nitrogen, y minutes of oxygen followed by 4 minutes of nitrogen. The nitrogen pulses were to eliminate explosive mixture in the gas vent system. The x and y durations were varied during the demonstrations.

Liquid chemical augmentations (stock solution of CAH; minor nutrients) were added just ahead of the injection pump, which was connected to the bottom of the gas separation column. A final rotometer was used to adjust the flowrate to 1.25 L/min., followed by a second static mixer. The pumps used were Ismatec gear pump heads driven by Cole Parmer magnetic drive motors.

The CAH solutions were prepared by adding pure (neat) solute to a "saturation flask," which was mixed using a magnetic stir bar. The saturation flask was a 125 mL erlenmeyer flask with upper and lower side arms and indentation baffles. The top of the saturation flask was fitted with a ground glass joint and a stopcock to add neat CAH. The lower sidearm of the saturation flask was connected to a supply reservoir of DI water and the upper side arm was connected to a variable speed, multichannel Ismatec pump that was used to add the CAH to the injection flow stream. The connection between the saturation flask and the pump was split into two streams before the pump to provide independent injection solutions for each of the well legs.

The inorganic solutions, including the bromide tracer and trace nutrients, were prepared in batches and pumped into the injection flow streams using a 20 RPM multichannel Ismatec pump. A single delivery tube was used, which was split into two streams before the pump and combined with the CAH solution before being added to the two injection flow streams. All tubing used in the injection system and delivery to the injection wells were ¼ in. stainless steel

Automated Sampling and Analytical Procurement

As previously discussed, two identical test legs each had an injection well, three sampling wells and an extraction well for a total of 10 monitoring locations. These 10 points were connected to

an Automated Sampling and Analytical Platform (ASAP, Analytical and Remedial Technology, Inc., Milpitas, CA) system, which automatically collected processed samples for gas chromatographic analysis, anion chromatographic analysis, dissolved oxygen and pH measurement. The ASAP incorporates an interface module used to control the peristaltic pump for purging the sample wells (~2L) and providing a representative groundwater sample to the ASAP system. Details of the ASAP are provided by McCarty et al. (1998), and are briefly described here.

The ASAP allowed continuous, near real-time sampling of approximately 30 samples per day using modules to process aqueous sample aliquots for introduction into attached analytical instrumentation. Analytical results were automatically stored in a computer database for both local and remote access and analysis including graphic display. The ASAP allowed remote control of sampling activities and provided automated calibrations and QA/QC analyses of known standards. Purgeable hydrocarbons (chlorinated and non-chlorinated aliphatic hydrocarbons) were analyzed by GC, inorganic ions through single-column ion chromatography, and dissolved oxygen and pH with probes.

For GC, the ASAP processed the sample by collecting a fixed volume (2.5 mL) of groundwater sample, stripping the volatile compounds from the sample, and collecting them on a pair of sorbant traps in series. The first trap was a standard method 624 trap, while the second trap was a custom Carbosieve-G trap. The second trap was intended to trap alkane gases that passed through the first trap. During the sorption step, the traps were operated at room temperature, while the desorption trap temperature was 210° F. The gas chromatograph was a Finnagan 9000 series GC equipped with a tandom PID/FID. A 30 m, thick film DB-5 mega bore GC column in series with a 15 m, thick film DB-624 mega bore column (J&W Scientific, Folsom, CA) provided good resolution of the compounds of interest. Chromjet integrators (Thermal Separation Products, San Jose, CA) provided integration of the detector signals and communicated with the ASAP computer for data storage and retrieval.

Inorganic ions (bromide) were processed by the ASAP high-performance liquid chromatography (HPLC) module using fixed-loop injection, a standard anion column and conductivity detector (Model 350) (both from Alltech Associates, Deerfield, IL), and a binary gradient HPLC pump (Thermal Separation Products, San Jose, CA). The eluent was 4 mM potassium acid phthalate. For anion chromatography, the ASAP collected a fixed volume of groundwater (approximately 15 ul), which was injected it into a direct reading ion chromatograph. The eluant was continuously purged with He gas. The hydrogen peroxide was added to prevent aerobic biologic growth in the eluant which, previous to this modification, was a very serious problem.

The ASAP system also collected data for dissolved oxygen and pH using probes and associated meters (Orion Research, Inc, Models 860 and 520A, respectively (Beverly, MA).

In the previous field tests at the site the addition of minor nutrients (N and P) was not needed to achieve affective stimulation of the indigenous microorganisms. However, for selected field tests a dilution of nutrients used to grow the butane culture (Table 7) was added to the injected groundwater.

Table 8 Groundwater Composition

Inorganic Constituents	Concentration
Cations:	
Calcium	10.0 meq/L
Magnesium	8.2 meq/L
Sodium	2.8meq/L
Potassium	<0.1 meq/L
Anions:	
Sulfate	15.6 meq/L
Bicarbonate	4.4 meq/L
Chloride	1.2 meq/L
Nitrate	0.1 meq/L

3.6.5 Induced Gradient Conditions of the Field Experiment

The field experiments were performed under induced gradient conditions created by the injection and extraction of groundwater. Groundwater was injected at a rate of 1.25 L/min. and extracted at a rate of 6 to 8 L/min.

Model simulations of streamline of flow are shown in Figure 11. Simulations were performed at the expected injection and extraction rates of the field tests with a hydraulic gradient of 0.0032 fl/ft in a northerly direction.. The results show separate flow paths between the injection and extraction wells of the two experimental legs. Thus we did not expect microbial or contaminant cross contamination to occur between the experimental legs. Results of bromide tracer tests also showed cross-contamination did not occur.

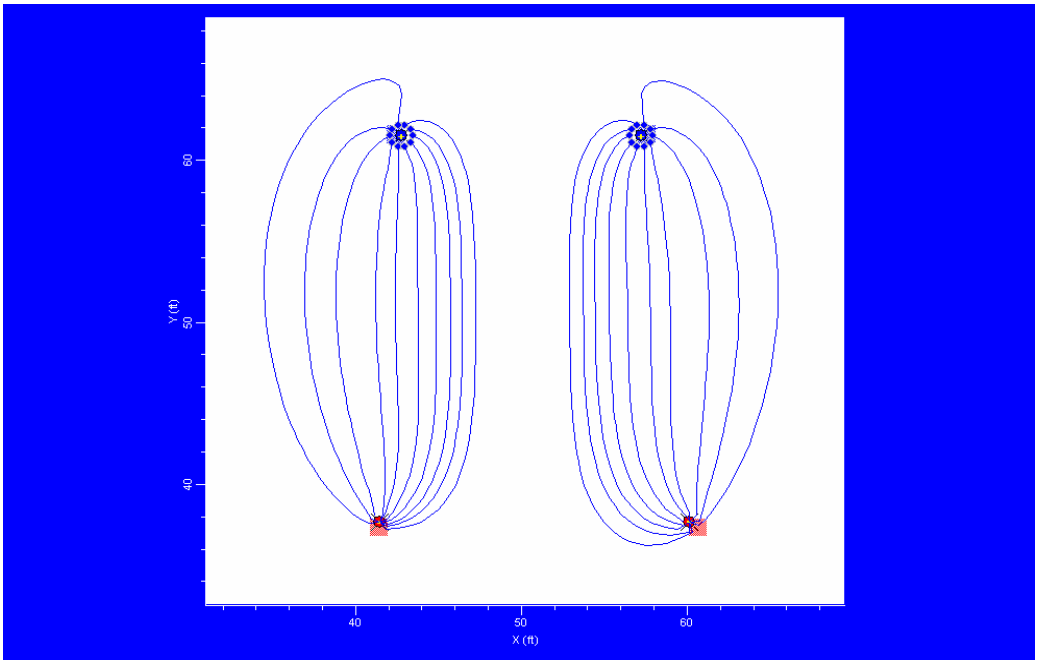

Figure 11. Model Simulations using RESSQ of the Streamlines for Flow Expected for the Injection and Extraction Conditions of the Field Demonstration

Figure 12. A Vertical Cross Section of the Aquifer an Experimental Well Leg

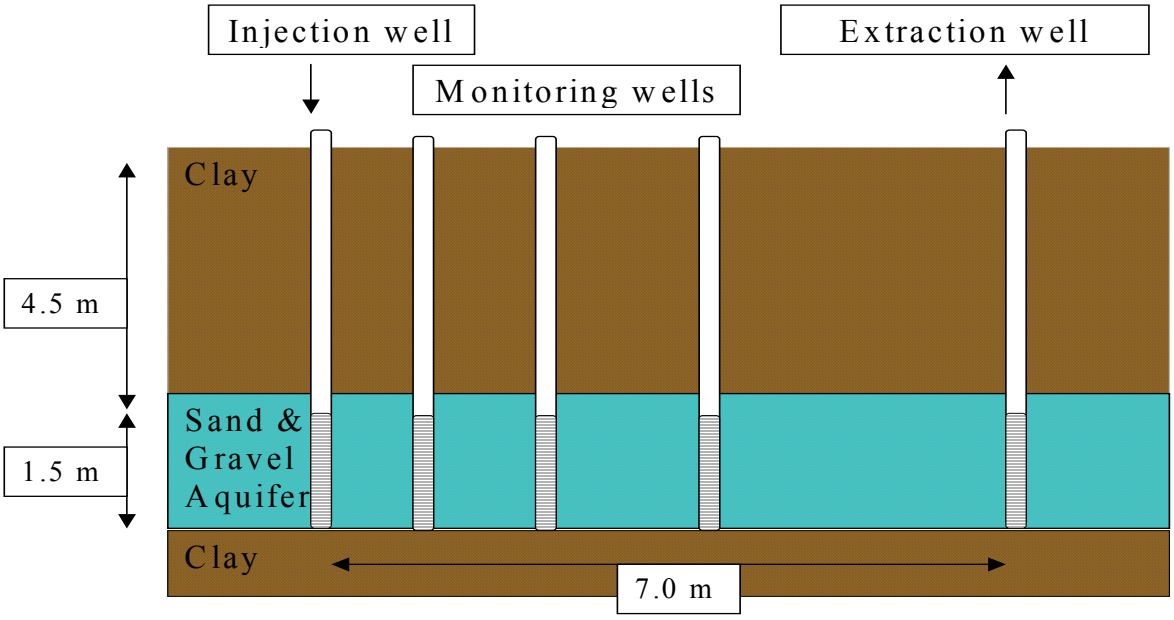

Figure 13. The Injection System under Construction at the Test Site

During the first season of field testing, a series of bromide tracer tests were performed to determine the rates of fluid injection and extraction that were required to effectively capture the injected groundwater at the extraction wells, while having no across contamination of groundwater between the experimental legs. If any cross contamination was to occur, it was to be from the indigenous leg to the bioaugmented leg. Like in the previous field studies conducted at the site, groundwater was injected upgradient in the natural flow and extracted downgradient to ensure effective capture of the groundwater. Based on the results of the series of bromide tracer tests the groundwater was typically injected at a rate of 6 L/min. into both injection wells and was typically extracted at a rate of 6 L/min. in the east experimental leg, and 8 L/min. from the west experimental leg. These injection and extraction rates limited cross contamination among the legs and resulted in effective recovery of the injected groundwater at the extraction wells.

All the field tests were conducted under the induced gradient conditions of injection and extraction as described above. The CAHs were continuously added to the injected fluid in a way that similar injection concentrations were achieved in both experimental legs. Groundwater containing dissolved butane or dissolved oxygen was added in alternating pulses, as described above. For example, in one set of experiments conducted during the first season of testing the butane pulse cycle was set at 12 min., followed by 10 min. nitrogen, followed by 45 min. of

oxygen. This pulse cycle was increased to 1 hr of butane, nine hours of oxygen, and 10 min. of nitrogen later in the test. Cycle times for butane and oxygen for the different experiments will be reported with the results of the individual experiments.

The concentrations of butane and oxygen in the injected fluid were determined from the periodic sampling of the injected fluid. Since the butane pulse cycles were typically short, there are much fewer values of the concentration of the injected fluid when butane was being added. The maximum injection concentration of butane measured during the first season of testing was approximately 35 mg/L, about 50% of its solubility in water. The maximum oxygen concentration was around 44 mg/L, close to its solubility limit in water. The average injection concentrations that were delivered depended on the duration of the pulse cycles, and other factors, including the efficiency of absorption, and temperature. During the first season of testing, when very little butane was being consumed by the indigenous experimental leg, the butane concentration in the field reached maximum concentrations of about 6 mg/L, which is consistent with a maximum injection concentration added of around 35 mg/L, and the a pulse cycle of about 12 minutes for butane in a total pulse duration of about 60 min.

For several experiments, hydrogen peroxide was added to increase the potential oxygen concentration in the injected fluid. A concentrated hydrogen peroxide solution (30%) was diluted in DI water and was fed with a metering pump into the injected fluid after oxygen was added. The effect of hydrogen peroxide addition was monitored by measuring the groundwater DO concentrations at the monitoring wells.

The field tests were typically conducted as a series of tests, as previously described by Semprini et al. (1990). Transport tests were conducted were bromide and the CAHs of interest were continuously injected under induced gradient conditions. Bromide and the CAHs were typically injected for a long enough period of time so that pseudo-steady-state breakthrough concentrations were achieved at the monitoring wells of each experimental leg. The breakthrough response as permitted estimates of retardation factors due to sorption of the CAHs to the aquifer solids.

The transport tests were followed by the bioaugmentation and biostumulation tests. The butane culture was bioaugmented to the East leg, while indigenous butane-utilizing microorganisms were stimulated in the West leg. The butane culture was grown at Oregon State University, as previously described, and shipped overnight on ice to Stanford University. For most bioaugmentations the culture was injected into the East Leg the day it arrived. The culture (typically 5 grams of cells on a dry weight basis), was delivered to the site concentrated in 2 liters of growth media. For bioaugmentation the cells and media were mixed in 17 liters of site groundwater, prior to injection. The cells were then added to the injected fluid over a period of several hours and delivered to the field through the injection well at the normal injection rate of 1.25 L/min. The period of inoculation varied for experiment to experiment, but was usually shorter than eight hours. Butane and oxygen addition to the injected fluid was started just prior to the injection of the culture. Tests in the indigenous leg were conducted using the same procedures as the bioaugmented leg, however this leg was not bioaugmented with cells.

Bioaugmentation, biostimulation and transformation tests were performed under constant conditions of operation until pseudo steady-state concentration were achieved at the monitoring locations. Transient tests were then initiated to determine the response of the system to changes in operating conditions. For example, in the first season of testing year the biostimulation/biotransformation tests started with a short butane/oxygen total pulse cycle of about 1 hr. After about 20 days of operation the total pulse cycle was increased to about 12 h. In the final stages of the test the pulse cycle was then decreased to about 1 hr. In the second season of testing the CAH injection concentrations were varied during the course of the experiment, and the oxygen levels were varied by injecting differ concentrations of hydrogen peroxide. In the final season of field testing bioaugmentation was repeated several times. Detailed descriptions of the different tests conditions will be provided when the results of the different seasons of field testing are presented.

Since the same experimental legs were used for the three seasons of field testing, attempts were made to lower the number of microorganisms in the test legs prior to bioaugmentation and biostimulation. The field seasons were separated by a period of six months or longer, during which neither butane nor oxygen was added. Hydrogen peroxide (16 mg/L) was added prior to the start of the second season of field testing in an attempt to lower the numbers of microorganism present. Prior to the start of the third season of field testing hydrogen peroxide was again added prior to bioaugmentation and biostimulation. Later in the third season of field testing household beach (Clorox®) was added at an injection concentration of 60 mg/L, prior to bioaugmentation and biostimulation. Similar hydrogen peroxide and bleach additions were performed both to the west and east experimental legs.

3.7 Model Development

Modeling studies focused on recreating the phenomena of aerobic cometabolism, substrate and CAH inhibition, transformation, product toxicity, and developing a numerical model to simulate observed laboratory and field performance. Two models were used for this purpose. Laboratory data were simulated using the biotransformation model developed by Kim et al. (2002b). The model was solved using Stella® software (High Performance System, Inc., Hanover, NH) with Runge-Kutta integration. (It is referred to as the Stella model throughout the report.) The field data were simulated using a modified form of the combined biotransformation/transport model presented by Semprini and McCarty (1991, 1992). (This model is referred to as the numerical bio-transport model throughout the report.) The features of the bio-transport model are presented in Table 9.

Biotransformation for both models used in our studies followed that introduced by Kim et al. (2002a, 2002b). The combined numerical bio-transport model expanded upon Kim et al. (2002b) kinetics to include the influence of an electron acceptor. The model presented below describes the expanded version.

Table 9. Features of the Bio-Transport Model

Monod/Michaelis-Menten Kinetics
Competitive Inhibition of CAHs on CAH Transformation
Competitive Inhibition of CAHs on Butane Utilization
Mixed Inhibition of Butane on CAH Transformation*
Transformation Product Toxicity
1-D Advective/Dispersive Transport
Equilibrium and Non-Equilibrium Sorption
Cyclic Pulsing of Electron Donor and Electron Acceptor at Boundaries

*The transport model also allowed for mixed inhibition of butane and CAHs by CAHs. However, Kim et al. (2002b) only butane mixed inhibition on 1,1-DCE to be relevant, so mixed inhibition of butane on 1,1-DCA and 1,1,1-TCA was omitted from our study.

3.7.1 Monod/Michaelis-Menten Kinetics

Michaelis-Menten/Monod kinetics provide the backbone for modeling biotransformation. The differential equations representing substrate utilization and microbial growth are:

Equation 1

$$\frac{dX}{dt} = Y\frac{dS}{dt} - bX$$

Equation 2

$$\frac{dS}{dt} = -X\frac{k_m S}{K_s + S}$$

where: S = substrate aqueous concentration (mg/L)
X = microbial concentration (mg/L)
k_m = maximum utilization rate of substrate (mg substrate/mg cells/day)
Y = yield coefficient (mg cells/mg growth substrate)
K_s = half-saturation constant of substrate (mg/L)
b = decay coefficient (day $^{-1}$)

Semprini and McCarty (1991) found that for aerobic cometabolism, the rate of microbial growth depends on both electron donor (primary growth substrate) and electron acceptor, and, therefore, provided dual Monod terms to equation 1 to describe this. The resulting equation is:

Equation 3

$$\frac{dX}{dt} = \left[Xk_{mD}Y\left(\frac{C_D}{K_{sD} + C_D}\right) - bX \right]\left(\frac{C_A}{K_{SA} + C_A}\right)$$

where: C_D = aqueous concentration of electron donor (ED) (mg/L)
C_A = aqueous concentration of electron acceptor (EA) (mg/L)
k_{mD} = maximum utilization rate of ED (mg ED/mg cells/day)
K_{sD} = half-saturation constant of ED (mg ED/L)
K_{sA} = half-saturation constant of EA (mg/L)

In their model, utilization of the electron donor (primary growth substrate) and electron acceptor were also represented by expanding equation 2 for dual Monod kinetics:

Equation 4

$$\frac{dC_D}{dt} = -k_{mD} X \left(\frac{C_D}{K_{sD} + C_D} \right) \left(\frac{C_A}{K_{SA} + C_A} \right)$$

Equation 5

$$\frac{dC_A}{dt} = -k_{mD} F_a X \left(\frac{C_D}{K_{sD} + C_D} \right) \left(\frac{C_A}{K_{SA} + C_A} \right)$$
$$- d_c f_d b X \left(\frac{C_A}{K_{SA} + C_A} \right)$$

where: F_a = stochiometric ratio of electron acceptor per electron donor utilized for cell synthesis (mg EA/mg ED)
d_c = cell decay oxygen demand (mg O_2/ mg cells)
f_d = fraction of biodegradable cells

3.7.2 Modeling Substrate Inhibition

Kim et al (2002a; b) presented the following equation for modeling competitive, noncompetitive, and mixed inhibition for the butane-utilizing enrichment. This culture was the parent culture used in the laboratory and field experiments. Competitive inhibition is the most frequent inhibition type included in mathematical simulations. Incorporating this into substrate utilization mathematics, Equation 2 becomes:

Equation 6

$$\frac{dS}{dt} = \frac{-Xk_m S}{K_s \left(1 + {I_c}/{K_{Ic}} \right) + S}$$

where: I_c = aqueous concentration of inhibitor (mg/L)
K_{Ic} = const. for competitive inhibition (mg inhibitor/L)

Note that in competitive inhibition, the half-saturation portion of the equation becomes a function of the inhibitor concentration.
Noncompetitive inhibition more specifically influences the maximum utilization rate, and equation 3.2.2 may be transformed to:

Equation 7

$$\frac{dS}{dt} = \frac{-Xk_m}{1 + {I_u}/{K_{Iu}}} \left(\frac{S}{K_s + S} \right)$$

where: I_u = aqueous concentration of noncompetitive inhibitor (mg/L)
K_{Iu} = constant for noncompetitive inhibition (mg inhibitor/L)

For the case of mixed inhibition, the mathematics have a combined form of equations 6 and 7, resulting in:

Equation 8

$$\frac{dS}{dt} = \frac{-Xk_m}{1+{I_u}/{K_{Iu}}}\left(\frac{S}{\frac{K_s}{1+{I_u}/{K_{Iu}}}\left(1+{I_c}/{K_{Ic}}\right)+S}\right)$$

Competitive and noncompetitive inhibition may or may not be caused by the same inhibitor. Terms for competitive and noncompetitive inhibition are additive, and Equation 8 may be extended to include several inhibitors. For example, transformation of 1,1,1-TCA may be inhibited by the presence of 1,1-DCE, butane, and 1,1-DCA through competitive, mixed, and competitive fashions, respectively. Expansion of the transformation equation would be:

Equation 9

$$\frac{dC_{TCA}}{dt} = \left(\frac{-Xk_{mTCA}}{1+{C_B}/{K_{Iu,B,TCA}}}\right)\left(\frac{C_A}{K_{sA}+C_A}\right)*$$

$$\left(\frac{C_{TCA}}{\frac{K_{sTCA}}{1+{C_B}/{K_{Iu,B,TCA}}}\left(1+{C_B}/{K_{Ic,B,TCA}}+{C_{DCE}}/{K_{Ic,DCE,TCA}}+{C_{DCA}}/{K_{Ic,DCA,TCA}}\right)+C_{TCA}}\right)$$

where: C = aqueous concentration of substrate (mg/L)

k_m = maximum utilization rate of 1,1,1-TCA (mg TCA/mg cells/day)

K_{sTCA} = half-saturation constant of 1,1,1-TCA (mg TCA/L)

$K_{iu,S,TCA}$ = constant for noncompetitive inhibition of 1,1,1-TCA by inhibitor "S" (mg inhibitor/L)

$K_{ic,S,TCA}$ = constant for competitive inhibition of 1,1,1-TCA by inhibitor "S" (mg inhibitor/L)

3.7.3 Modeling Product Toxicity

The model also incorporates transformation capacity (T_c) into the differential term for cell growth (Equation 3) to account for product toxicity. Competitive inhibition of butane by CAHs in the form of Equation 6 is included also:

Equation 10

$$\frac{dX}{dt} = \left[XYk_{mD}\left(\frac{C_D}{K_{sD}\left(1 + {I_c}/{K_{Ic}}\right) + C_D} \right) - bX - \frac{1}{T_{cS}}\frac{dC_S}{dt} \right] *$$

$$\left(\frac{C_A}{K_{SA} + C_A} \right)$$

where: T_{cS} = transformation capacity of non-growth substrate "S" (mg substrate/ mg cells)

T_c is specific for any parent compound and the culture exposed to it. Product toxicity from several non-growth substrates may be incorporated by adding a T_c term for each compound (Alvarez-Cohen and McCarty, 1991).

3.7.4 Modeling Contaminant Transport

Non-equilibrium sorption for one dimensional transport was defined in the numerical bio-transport model as a first-order rate process:

Equation 11

$$\frac{dS}{dt} = D_h \frac{\partial^2 S}{\partial x^2} - \frac{Q}{A\phi}\frac{dS}{dx} - \frac{\rho_b}{\phi} F_k \left(k_d S - S^* \right)$$

Equation 12

$$\frac{dS^*}{dt} = F_k \left(k_d S - S^* \right)$$

where: S^* = sorbed-phase concentration of substrate (mg substrate/kg soil)
S = aqueous concentration of substrate (mg/L)
F_k = rate coeff. for mass transfer between aqueous and sorbed phases (day^{-1})
D_h = hydrodynamic dispersion coefficient (m^2/day)
Q = average groundwater flow (m3/day)
A = cross-sectional area of aquifer, width x thickness (m^2)
ρ_b = bulk density of the aquifer solids (kg/L)
k_d = partition coefficient of sorbed substrate (L/kg)
ϕ = aquifer porosity

This form was chosen to provide a simple, non-equilibrium sorption process. Equilibrium sorption conditions may be simulated by assigning the mass transfer rate coefficient (F_k) a very high value.

3.7.5 Combined Biotransformation and Transport Model

The biotransformation and contaminant transport models presented above were combined to create separate equations for tracking the aqueous concentrations of the electron donor (butane), electron acceptor (oxygen), and CAHs (1,1-DCE, 1,1-DCA, and 1,1,1-TCA). Equation 11 was

added to Equations 4, 5, and 8 to represent utilization/transformation and transport of each compound. The latter term of Equation 11 was omitted from the combined equations for the electron donor and acceptor because of limited sorption capacity for butane and oxygen.

A Haldane constant was incorporated into the electron donor utilization equation, as some substrates can pose inhibition on themselves. For substrates such as butane for which this is not the case, a large value input for the Haldane constant can cancel out the effect of this parameter.

The combined biotransformation-transport equation for butane and oxygen utilization are presented below (Equations 13 and 14, respectively).

Equation 13

$$\frac{dC_{BUT}}{dt} = -Xk_{mBUT}\left(\frac{C_A}{K_{sA}+C_A}\right)*$$
$$\left(\frac{C_{BUT}}{K_{sBUT}\left(1+{C_{DCE}}/{K_{Ic,DCE,BUT}}+{C_{DCA}}/{K_{Ic,DCA,BUT}}+{C_{TCA}}/{K_{Ic,TCA,BUT}}\right)+{C_{BUT}^{2}}/{K_{HAL}}+C_{BUT}}\right)$$
$$+D_h\frac{\partial^2 C_{BUT}}{\partial x^2}-\frac{Q}{A\phi}\left(\frac{dC_{BUT}}{dx}\right)$$

Equation 14

$$\frac{dC_{O2}}{dt} = -F_a Xk_{mBUT}\left(\frac{C_{O2}}{K_{sO2}+C_{O2}}\right)*$$
$$\left(\frac{C_{BUT}}{K_{sBUT}\left(1+{C_{BUT}}/{K_{HAL}}+{C_{DCE}}/{K_{Ic,DCE,BUT}}+{C_{DCA}}/{K_{Ic,DCA,BUT}}+{C_{TCA}}/{K_{Ic,TCA,BUT}}\right)+C_{BUT}}\right)$$
$$-d_c f_d bX\left(\frac{C_{O2}}{K_{sO2}+C_{O2}}\right)+D_h\frac{\partial^2 C_{O2}}{\partial x^2}-\frac{Q}{A\phi}\left(\frac{dC_{O2}}{dx}\right)$$

Transformation of 1,1-DCE, 1,1-DCA, and 1,1,1-TCA including mixed inhibition by butane and competitive inhibition by CAHs are:

Equation 15

$$\frac{dC_1}{dt} = -X\left(\frac{k_{m1}}{1+{C_{BUT}}/{K_{Iu,BUT,1}}}\right)\left(\frac{C_{O2}}{K_{sO2}+C_{O2}}\right)$$

$$\left(\frac{C_1}{\frac{K_{s1}}{1+C_{BUT}/K_{Iu,BUT,1}}\left(1+C_{BUT}/K_{Ic,BUT,1}+C_2/K_{Ic,2,1}+C_3/K_{Ic,3,1}\right)+C_1} \right)$$

$$+D_h\frac{\partial^2 C_1}{\partial x^2}-\frac{Q}{A\phi}\left(\frac{dC_1}{dx}\right)-\frac{\rho_b}{\phi}F_{k1}\left(k_{d1}C_1-C_1^*\right)$$

where: C_1 = aqueous concentration of transforming CAH (mg/L)
C_1^* = sorbed phase concentration of transforming CAH (mg CAH/kg soil)
C_2 = aqueous concentration of second CAH (mg/L)
C_3 = aqueous concentration of third CAH (mg/L)
$K_{Iu,BUT,1}$ = uncompetitive inhibition constant of transforming CAH by butane (mg butane/L)
$K_{Ic,BUT,1}$ = competitive inhibition constant of transforming CAH by butane (mg butane/L)
$K_{Ic,2,1}$ = competitive inhibition constant of transforming CAH by second CAH (mg CAH#2/L)
$K_{Ic,3,1}$ = competitive inhibition constant of transforming CAH by third CAH (mg CAH#3/L)
k_{d1} = partition coefficient of transforming CAH (L/kg)
F_{k1} = rate coefficient for mass transfer between aqueous and solids (day^{-1})

The microbial culture was assumed to be an immobile, distributed mass. Therefore transport (Equation 11) was not included in defining microbial concentration profiles. Equation 10 was used alone, with expanded terms for product toxicity of all three CAHs studied. The resulting mathematical equation for microbial growth with competitive inhibition by CAHs is:

Equation 16

$$\frac{dX}{dt}=XYk_{mBUT}\left(\frac{C_{O2}}{K_{sO2}+C_{O2}}\right)*$$

$$\left(\frac{C_{BUT}}{K_{sBUT}\left(1+C_{DCE}/K_{Ic,DCE,BUT}+C_{DCA}/K_{Ic,DCA,BUT}+C_{TCA}/K_{Ic,TCA,BUT}\right)+C_{BUT}} \right)$$

$$-bX\left(\frac{C_{O2}}{K_{sO2}+C_{O2}}\right)$$

$$-\left(\frac{dC_{DCE}}{dt}\frac{1}{T_{cDCE}}+\frac{dC_{DCA}}{dt}\frac{1}{T_{cDCA}}+\frac{dC_{TCA}}{dt}\frac{1}{T_{cTCA}}\right)\left(\frac{C_{O2}}{K_{sO2}+C_{O2}}\right)$$

where: T_{cDCE} = transformation capacity of 1,1,1-DCE (mg DCE/mg cells)
T_{cDCA} = transformation capacity of 1,1,1-DCA (mg DCA/mg cells)
T_{cTCA} = transformation capacity of 1,1,1-TCA (mg TCA/mg cells)
$K_{Ic,DCE,BUT}$ = competitive inhibition constant of by 1,1-DCE (mg DCE/L)
$K_{Ic,DCA,BUT}$ = competitive inhibition constant of butane by 1,1-DCA (mg DCA/L)
$K_{Ic,TCA,BUT}$ = competitive inhibition constant of butane by 1,1,1-TCA (mg TCA/L)
dC_{TCA}/dt = Overall 1,1,1-TCA transformation rate for biotransformation only, as defined in equation 2.15 and omitting terms for transport and sorption (mg/L/day)
dC_{DCA}/dt = Overall 1,1-DCA transformation rate for biotransformation only as defined in equation 2.15 and omitting terms for transport and sorption (mg/L/day)
dC_{DCE}/dt = Overall 1,1-DCE transformation rate for biotransformation only as defined in equation 2.15 and omitting terms for transport and sorption (mg/L/day)

Finite difference forms of Equations 13 through 15 and 10 were solved simultaneously using Runge-Kutta numerical integration as described by Semprini and McCarty (1991,1992). Input for various parameters were a conglomeration of values obtained from field tests, laboratory experiments, and literature. The combined model allows for cyclic additions of electron donor and acceptor at varying concentrations and duration periods.

3.7.6 Verification of Model Performance

To ensure that our combined biodegradation/transport model was performing appropriately, simulations were run and the output was compared to that from other models. Comparisons included simulations for contaminant transport without biodegradation and biodegradation in batch systems.

The transport portion of our model was tested for adequate description of advection, dispersion, and sorption by comparing output from our model to the Ogatta-Banks (OB) approximation (Domenico and Schwartz, 1990. pg 375). The OB approximation defines solute transport with linear sorption as:

Equation 17

$$\frac{dC}{dt} = D_x \frac{d^2C}{R_f\, dx^2} - v_x \frac{dC}{R_f\, dx}$$

Equation 18

$$R_f = 1 + \left[\frac{1-\phi}{\phi}\right]\rho_b k_d$$

where: C = aqueous-phase concentration (mg/L)
v_x =average pore-water velocity (m/day)
$v_x = Q / (\Phi * A)$
Q = average flow within aquifer (m^3/day)
A = cross sectional area of aquifer, width * thickness (m^2)

D_h = hydrodynamic dispersion coefficient (m^2/day)
ρ_b = bulk density of solid matrix (kg/L)
R_f = retardation coefficient for linear sorption
k_d = partitioning coefficient from aqueous phase to solids phase (L/kg)
Φ = porosity

For solute transport with no sorption, R_f is set equal to 1. Solving for concentration as a function of time and distance, the Ogatta-Banks approximation becomes:

Equation 19

$$C = \frac{C_o}{2} erfc\left[\frac{R_f x - v_x t}{2\left(\alpha_d v_x t R_f\right)^{1/2}}\right]$$

where: C_o = initial aqueous concentration (mg/L)
α_d = dispersivity (m)
erfc = complementary error function

Simulations were run using our model (Equations 13 through 16) and the Ogatta-Banks approximation (Equation 19) for advective and dispersive transport of butane, oxygen, and 1,1,1-TCA. For our model, the transformation rate of 1,1,1-TCA (k_{mTCA}) was set to zero, thus shutting off biotransformation. Equilibrium sorption of 1,1,1-TCA was assumed by setting the solids' mass transfer rate coefficient (F_k) to a very high value (200 day-1), thus forcing equilibrium conditions. It was assumed that butane and oxygen would not be retarded. For the OB model, retardation was omitted by setting R_f to 1 for these substrates. Our model excludes sorption for the electron donor and acceptor, so no adaptation was necessary.

The input values are presented in Table 10 and represent approximate conditions at the Moffett Field Test Facility.

Table 10. Input Values for Transport Comparison

Average flow*, Q (m/day)	Aquifer Thickness, b (m)	Porosity, Φ (-)	Bulk Density, ρ_b (kg/L)	Dispersivity, α_d (m)	1,1,1-TCA Partitioning Coeff., k_d (L/kg)	1,1,1-TCA Retardation Factor, R_f (-)
2.16	1.5	0.333	1.6	.31	.2	1.96

**Based on this flow average linear velocity, v_x, of 4.32 m/day was input into the Ogatta Banks Approx.*

In running the simulation, concentrations/masses were recorded at distances 1.17 m, 2.3 m, and 3.5 m from the injection well with 1 hour time increments. The results are presented in Figure 14. The plots show aqueous concentrations of butane, oxygen, and 1,1,1-TCA over time for simulations by both the Ogatta-Banks approximation and our model. Note that there is excellent comparison for transport of all three substrates at all three locations. The minor shifts between the curves may be attributed to omitting a second term of the Ogatta-Banks approximation and the differences in boundary conditions between the two models. The close comparison confirmed that the transport portion of our model was performing adequately.

Figure 14. Comparison of Model Output for Solute Transport (OB Approx refers to Ogatta-Banks approximations output; Fortran Code refers to our model's output)

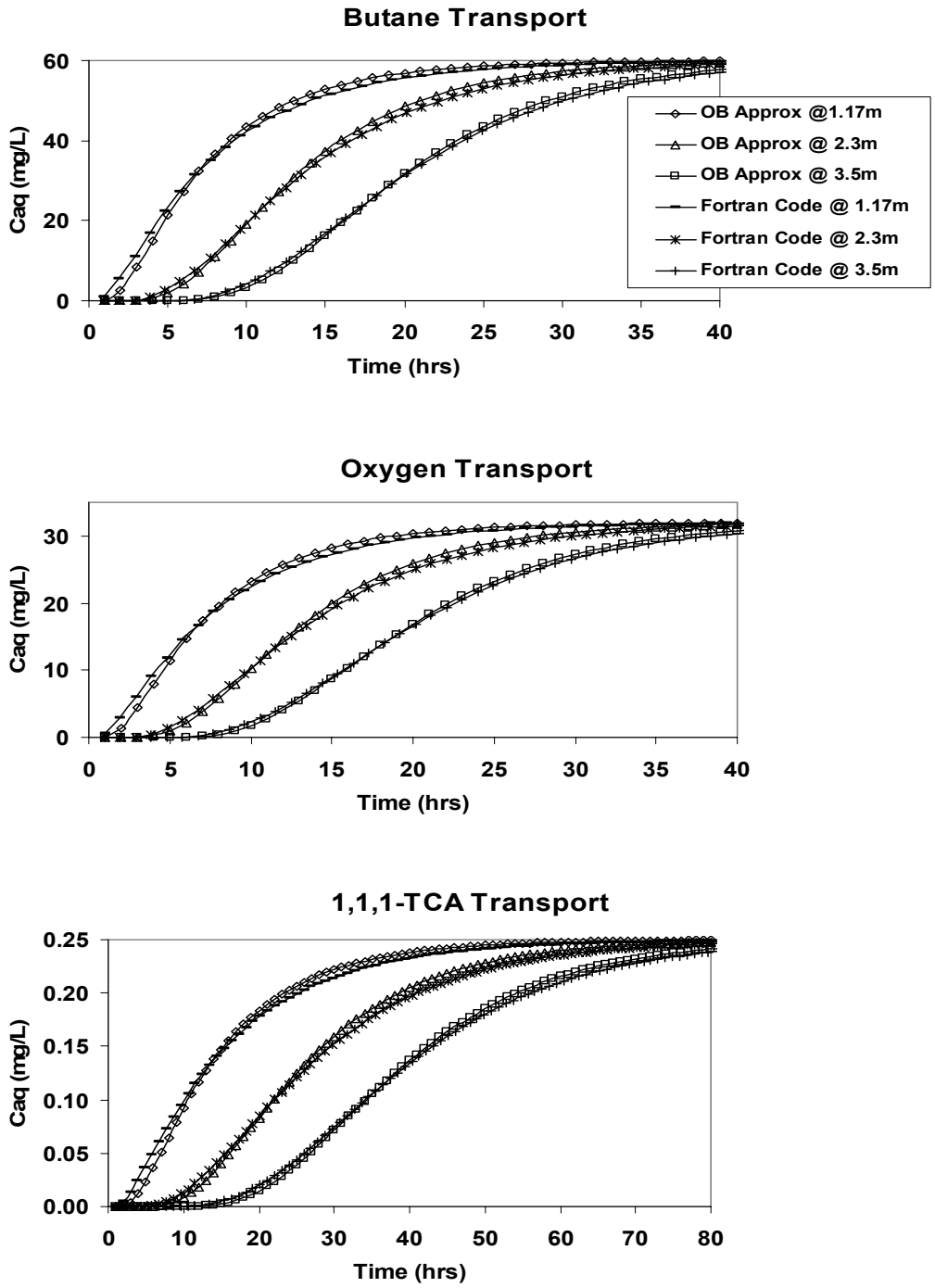

The biotransformation portion of our combined code was evaluated by turning off transport and comparing the biotransformation results to that of the cometabolism model introduced by Kim et al. (2002a, 2000). Simulations were conducted for biotransformation of 1,1-DCE and 1,1,1-TCA with butane as the electron donor.

Simulations were run for a 49.5 L volume of liquid (no gas phase present). This volume was based on an aquifer 2.4 m long, 1 m wide, and 1.5 m thick with porosity of 0.333. These characteristics represented settings for the Moffett Field Test Facility site where actual field experiments of transport with biodegradation were to be modeled (Section 5). A batch system in which only biodegradation occurred (no transport) was approximated in our model by setting flow, dispersion, and sorption values to zero. The voids surrounding the solids therefore provided an all liquid "batch" reactor.

Kinetic input values as defined by Kim et al (2002b) were assumed and are presented in Tables 11 and 12. These tables list input for the Stella model and the numerical bio-transport model.

To assure that the simulated batch bioreactor was uniform throughout the aquifer zone, output from our model was recorded at distances of 1 m, 1.5 m, and 2 m from the injection well. Results from all three locations were exactly the same.

Figure 15 compares output from both the Stella simulation and the numerical Bio-transport model's simulation as total substrate mass and cell concentration remaining over time. Overall there is good comparison between the two models, indicating that the numerical transport code adequately simulates biotransformation.

To stress the model, product toxicity of 1,1,1-TCA was assumed to be high (T_{cTCA} = 91.0 mg cells/ μmol TCA = 0.08 μmol TCA/ mg cells). This T_{cTCA} value compares to an order of magnitude difference in that used for laboratory and field data modeling (TcTCA =9.10 mg cells/μmol TCA = 0.082μmol TCA/mg cells). Figure 16 shows similar comparisons for these simulations as those presented in Figure 15. (T_{cTCA} = 9.1 mg cells/μmol/ TCA = 0.82 μmol TCA/mg cells). Thus the model appeared to be simulating the transformation capacity term well.

Table 11. Stella Input Values for Biotransformation Comparison

Parameter	Units	Value	Parameter	Units	Value
K_{ic}DCEBUT	µmol/L	8.7	KmaxBUT	µmol /mg/ hr	2.5
K_{ic}DCETCA	µmol /L	1.1	KmaxDCE	µmol /mg/ hr	2.8
			KmaxTCA	µmol /mg/ hr	0.2
K_{iu}BUTDCE	µmol /L	6.9			
K_{iu}BUTTCA	µmol /L	0.5	KsBUT	µmol /L	19.2
			KsDCE	µmol /L	1.48
K_{ic}TCABUT	µmol /L	313	KsTCA	µmol /L	12.2
K_{ic}TCADCE	µmol /L	17			
			TcDCE	µmol /mg	0.52
K_{ic}BUTDCE	µmol /L	0.33	TcTCA	µmol /mg	0.82*
X_0	mg/L	12	HccBUT	-	38
Y	mg/µmol	0.046	HccDCE	-	0.86
b	hr-1	.0042	HccTCA	-	0.55
V_L	L	49.5	V_G	L	0

Nomenclature is provided in Appendix C. * The value given was input for the shown in Figure 15. T_{cTCA} = 0.08 was input for simulation of the comparison shown in Figure 16.

Table 12. Model Input Values for Biotransformation Comparison

Parameter	Units	Value	Parameter	Units	Value
K_{ic}DCEBUT	mg/L	0.84	kmaxBUT	mg/mg/d	3.48
K_{ic}DCETCA	mg/L	0.11	KmaxDCE	mg/mg/d	6.51
			KmaxTCA	mg/mg/d	0.64
K_{iu}BUTDCE	mg/L	0.40			
K_{iu}BUTTCA	mg/L	0.03	KsBUT	mg/L	1.11
			KsDCE	mg/L	0.14
K_{ic}TCABUT	mg/L	41.75	KsTCA	mg/L	1.63
K_{ic}TCADCE	mg/L	2.27			
			TcDCE*	mg/mg	19.8
K_{ic}BUTDCE	mg/L	0.02	TcTCA*	mg/mg	9.1
X_0	mg/L	12	f_d	-	0.8
Y	mg/mg	0.79	F_a	g EA/g ED	4.0
B	d-1	0.10	d_c	g EA/ g cells	1.42
V_L	L	49.5	V_G	L	0

*Input values for transformation capacity are the inverse of the convention used; units here are in mg cells per mg substrate. The value given was input for simulation of the comparison shown in Figure 15. T_{cTCA} = 91.0 was input for simulation of the comparison shown in Figure 16.

Figure 15. Comparison of Model Output for Biotransformation (Fortran Output refers to our model results)

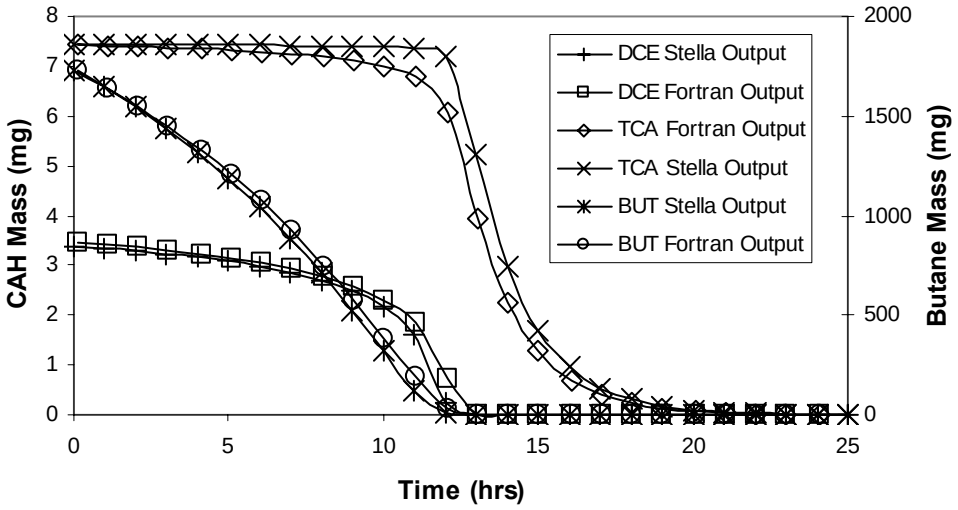

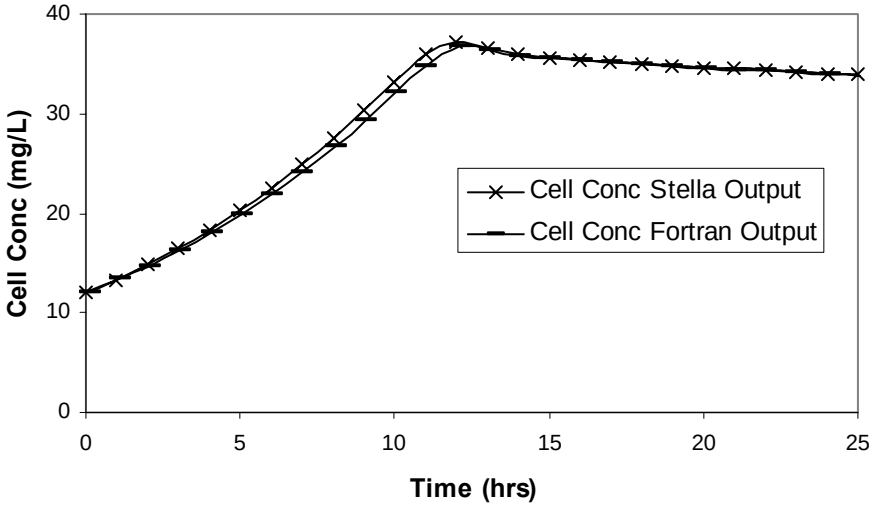

Figure 16. Comparison of Model Output for Biotransformation with High 1,1,1-TCA Product Toxicity (Fortran Output refers to our model results)

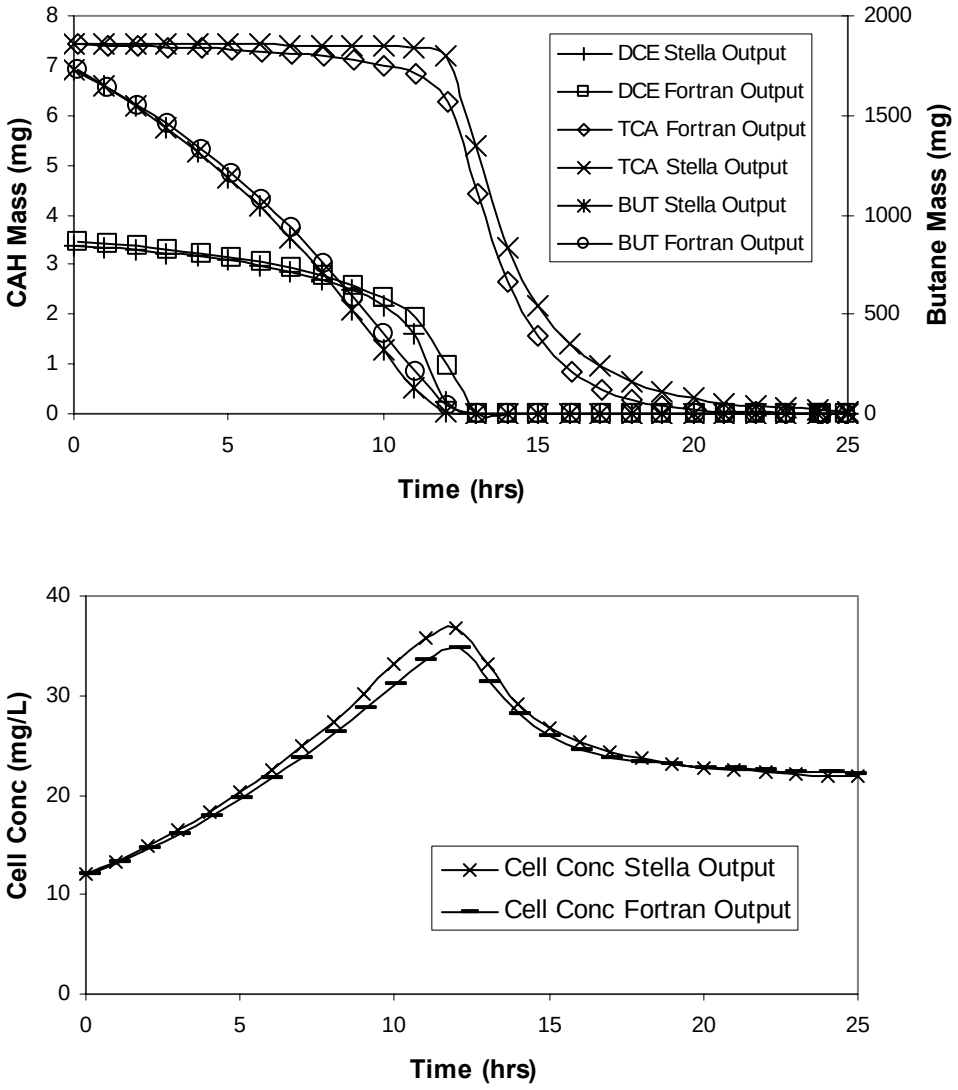

4. RESULTS OF LABORATORY STUDIES

4.1 Culture Development

The culture selected as the source for bioaugmentation efforts at the Moffett Federal Airfield In-Situ Bioremediation Test Site, CA, was obtained from a Moffett soil/groundwater microcosm (B2-1) that was inoculated with a butane-utilizing enrichment culture acquired from Hanford, WA, capable of co-metabolically degrading the chlorinated solvents TCE, 1,1,1-TCA, and 1,1-DCE. A soil/groundwater slurry was taken from the microcosm and the culture was grown in minimal salt media (MSM) with a 10% butane headspace. The culture was harvested, preserved in DMSO, separated into 200 – 1 mL aliquots and stored in liquid nitrogen for further use as inoculum for media, microcosm, and field bioaugmentation tests. Thus, by definition, the source culture contained organisms native to the Moffett site and also organisms not native to the site.

In order to visually inspect the morphological diversity of the augmentation culture, an aliquot was re-suspended into 100 mL MSM with a 10% butane headspace and grown for 3 days at 20°C. A sample was taken, subjected to DAPI staining, and viewed with fluorescence microscopy. At least three distinct morphologies were observed (Figure 17); a small curved rod approximately 1 micron in length, a slightly larger and wider 1 to 2 micron rod, and an approximately 10 to 20 micron long filamentous organism. The size differences may play a role in the ability to transport the organisms in the subsurface; however, not enough is known about the roles individual organisms play in butane oxidation and chlorinated solvent transformation to predict what effects selective transport may have on the effectiveness of bioremediation.

Figure 17 Digital Images of DAPI-Stained Augmentation Culture

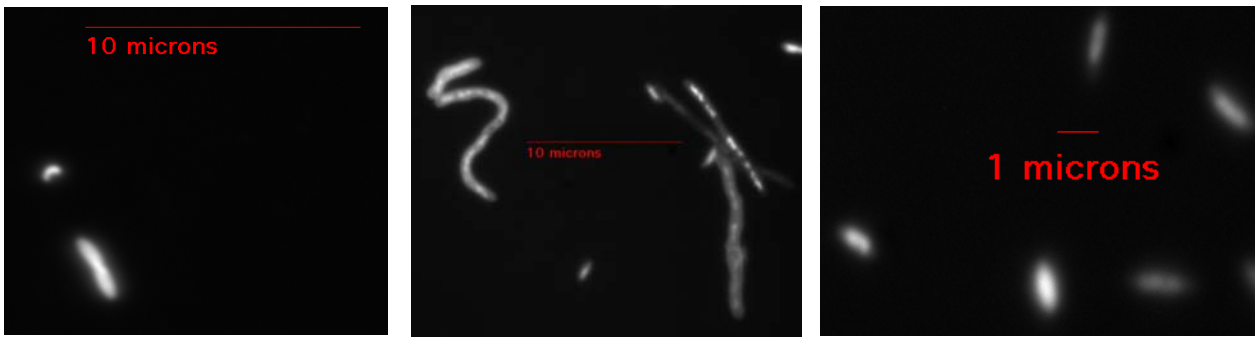

A comparison of T-RFLP results of frozen aliquots of the source culture and the culture after growth in mineral media reveals a significant bacterial community shift during the growth period (Figure 18). The frozen aliquots contained two clearly dominant peaks at 179 and 277 bp, consistent with the *Rhodococcus* and the *Acidovorax* clones, respectively (Section 4.2). Smaller peaks were present at 207 bp and 167 bp, consistent with the *Hydrogenophaga* clone and the unidentified deep subsurface proteobaterium clone, respectively. Other small peaks were observed at 100 bp (corresponding to a clone similar to an ultramicrobacterim species) and at 47

bp (no clone available). In contrast, after inoculating the growth reactor with one frozen aliquot and growing the culture to a cell density of about 100 mg/L dry weight, the dominant peak is at 207 bp, consistent with *Hydrogenophaga*, and the second largest peak is at 183 bp, a T-RF not currently represented by a clone. The third largest peak is at 167 bp, consistent with the unidentified deep subsurface proteobacter clone, and the peaks at 179 bp and 277 bp, that are consistent with *Rhodococcus* and *Acidovorax* respectively, are both very small. Subsequent growth reactor series have shown that the composition of the inoculum culture is not necessarily predictive of the culture composition after additional growth on butane. However, the activity of the cultures grown from frozen aliquots as measured by 1,1-DCE transformation rates were very similar even though the culture composition appeared to be different.

Figure 18. T-RFLP Profiles for the Frozen Source Culture, the Microcosm Bioaugmentation Culture (the Source Culture after One Growth Cycle on Butane), and the Numerically Dominant Clones Found in the Clone Library (Note the difference in relative peak size of the 179 bp and 183 bp fragments in the source culture and the bioaugmentation culture and the absence of a clone with terminal fragment length of 183 bp)

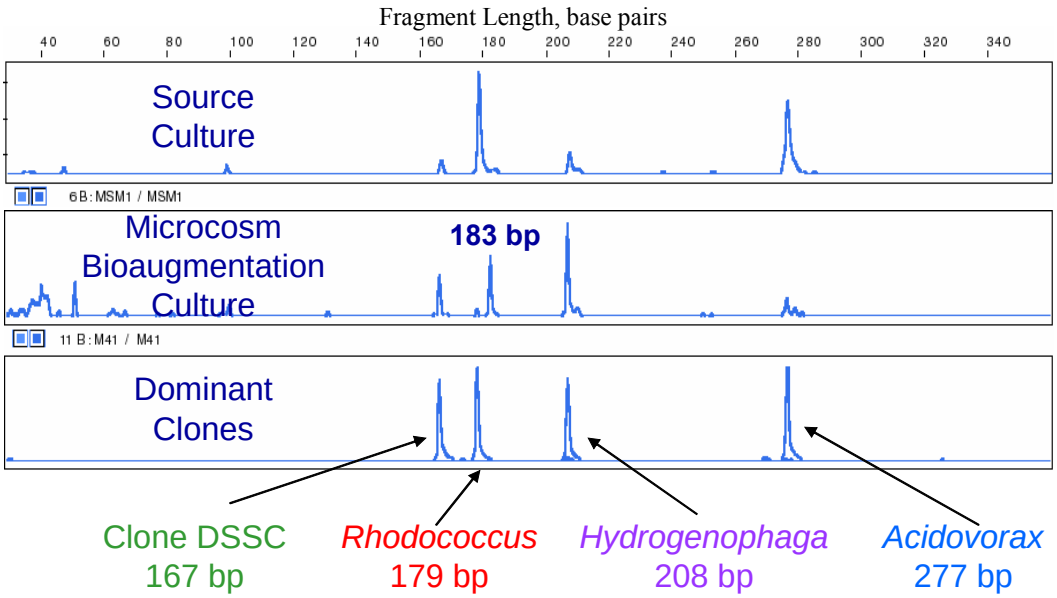

Isolation of Butane-Utilizing Microbial Cultures

Microcosm studies using a bioaugmentation culture grown from the source culture (section 4.5) indicated that the organism with a T-RFL of 183 bp was influential in butane utilization and DCE transformation. Microcosms able to transform high concentrations of DCE were enriched in the 183 bp organism compared to indigenous microcosms where this organism was never observed. Thus, efforts to isolate butane-utilizing CAH-transforming organisms from the source culture with an emphasis on obtaining the organism with a T-RFL of 183 bp were undertaken.

A frozen aliquot of the bioaugmentation culture was enriched in a 4% butane headspace, harvested at log growth phase and serially plated onto plates with agar containing only mineral

salts media. The plates were incubated at 20ºC and fed a 3% butane headspace. Individual colonies were harvested and serially plated for four or more generations. T-RFLP analyses of the resulting cultures revealed cultures enriched for the organism with a T-RFL of 183 bp (cultures B6 and B8) and for an organism with a T-RFL 179 bp (cultures B1 and B4), consistent with the *Rhodococcus* clone (Figure 19). The enriched cultures were tested for butane uptake rates and rates of 1,1,1-TCA and 1,1-DCE transformation. The results indicated that the cultures enriched for the 183 bp organism were able to oxidize butane at faster specific rates than the cultures enriched for an organism consistent with the *Rhodococcus* clone (data not shown). Cultures B6 and B8 were also able to degrade about 3 to 4 times more 1,1-DCE and 1,1,1-TCA at faster rates than cultures B1 and B4 (Figure 20). Dilutions from these enrichment cultures were streak-plated and grown in a butane headspace, enriched to monocultures, aliquoted into cryogenic tubes with 7% DMSO, and stored at -80ºC. These cultures, hereafter referred to as strain 183BP and strain 179BP, were used to grow bioaugmentation cultures for subsequent experiments.

The strain 179BP and 183BP cultures were grown in media and observed to have very different morphologies. The strain 179BP organism grew in clumps in media and colonized surfaces where the strain 183BP organism grew planktonically and did not stick to vessel walls, indicating that strain183BP may transport better in the subsurface. When viewed using scanning electron microscopy, the strain 183BP culture was evenly distributed and not aggregated whereas the strain 179BP culture grew almost exclusively in aggregates (Figure 21). The 16S rRNA gene from the strain 183BP culture was sequenced and found to be a close relative to a *Rhodococcus* sp., *Rhodococcus* sp. USA-AN012, a nitrile-metabolizing actinomycetes. The sequence information from the hypervariable regions of the organism's 16S rRNA gene was used to design two different rRNA probes for FISH analyses and to design phylogenetic-specific primers for PCR amplification reactions (see section 3.2.2). Searches of a database of known bacterial 16rDNA sequences (GenBank) found 10 other organisms (*Rhodococcus* sp and *mycobacterium* sp.) with identical sequences in the probe recognition sites, so the probes are not uniquely specific.

The primers, designed to amplify strain 183BP organisms (and very closely related species), were tested in the laboratory on strain 183BP cultures of various cell density and on cultures not expected to contain strain 183BP cells with good results. The primers were then tested for phylogenetic-specific PCR amplification of Moffett field samples (Figure 22). Negative controls (an anaerobic dehalogenating culture) produced very faint bands (intensity < 0.1) as did samples acquired from the bioaugmented leg prior to the October 2003 bioaugmentation and from samples acquired from the control leg. Samples taken from the first fully penetrating well on the bioaugmented leg one and two days after bioaugmentation produced very bright bands (intensity = 1.5 to 2.0), indicating successful transport of the organisms at least 0.5 m from the injection well. However, T-RFLP analyses of the same samples did not show the presence of strain 183BP. Presumably this was due to the relative numbers of strain 183BP organisms to other organisms in the sample. T-RFLP analyses are good for identifying dominant organisms in a mixed microbial community, but are not good at identifying organisms that make up a small part (<1%) of the total community DNA. The primers were also used in quantitative real time PCR analyses of strain 183BP populations in field samples.

Culture Growth for Bioaugmentation to Moffett Field

Frozen aliquots of the source culture were thawed and used as inoculum to grow bioaugmentation cultures for use in media, microcosm, and field tests. Initially, growth was accomplished using a 2 L stirred reactor containing a 1 L batch liquid phase comprised of mineral media and a 1 L gas headspace that was continually purged with a mixture of 4% butane in air. This system was scaled up to a 40 L reactor with a 20 L aqueous batch volume and a continuously flushed 20 L butane-in-air headspace. This system was used to grow the initial bioaugmentation culture for the field test conducted in 200 L. However, efforts at large-scale growth of a culture with consistent composition was spotty. Although these systems did not produce consistent microbial cultures, we were able to grow a significant mass of organisms with the ability to rapidly degrade 1,1-DCE. However, since one objective of the project was to track the culture in the subsurface after bioaugmentation, growth of specific desired organisms was needed. Large quantities of butane-utilizers were grown and the microbial compositions analyzed by T-RFLP and the cultures were found to be of variable composition. Although many of the same organisms were present in more than one growth batch, different unknown organisms were always present and sometimes dominant and the known, or target, organisms were not in consistent proportions to the overall biomass.

Since the strain 183BP culture was identified as an important butane-utilizing, CAH-transforming culture in microcosm experiments and was not found in indigenous samples, it was deemed a desirable member of a potential bioaugmentation culture. In order to control the growth conditions to favor growth of a significant mass of the strain 183BP culture for bioaugmentation at the Moffett field site, batch growth conditions were employed. Forty eight 700 mL bottles containing 300 mL mineral media and 400 mL headspace with 4% butane in repeated injections were incubated on shaker tables oscillating at 200 rpm at 20ºC. Additional oxygen was added as vacuum was created in the bottles due to butane and oxygen utilization. The batch cultures were harvested (approximately 4 to 5 g of culture dry weight) and concentrated for storage and/or shipment to the field site. Initially, concentrated cultures were stored in 5 mL cryogenic tubes and frozen in liquid nitrogen until needed. However, it was found that even with DMSO or glycerol added as a cryopreservative, strain 183BP did not survive extended periods in the freezer. This was first noticed when repeatedly thawing a strain 183BP cell line for use in ongoing media-based CAH transformation tests and finding significant decreases in activity with increased time of storage. After the first season of field tests, bioaugmentation cultures were grown in batch and concentrated in one or two 500 mL centrifuge bottles, refrigerated and shipped to the Moffett site on ice. This procedure was used throughout the remainder of the field tests with varying success at producing monocultures or limited mixed cultures. T-RFLP analyses were used to determine the microbial composition of bioaugmentation cultures used in microcosm and field tests. Both limited mixed cultures and essentially monocultures of strain 183BP were used for different field and microcosm tests.

Figure 19. Four Microbial Cultures Enriched from the Source Culture on Butane (two of the cultures, cultures B6 and B8, were enriched in an organism with a T-RFL of 183 bp while the other two, cultures B1 and B4, were enriched in an organism with a T-RFL of 179 bp, which was consistent with the T-RFL of a clone identified as a *Rhodococcus* sp.)

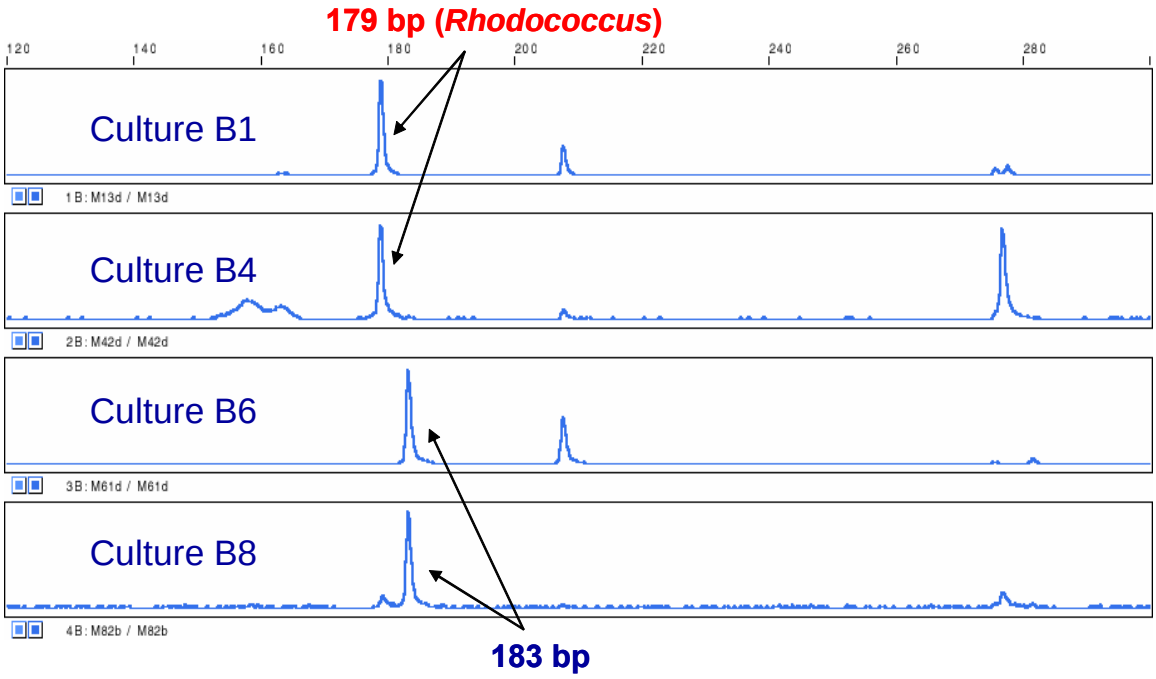

Figure 20. Significant Differences in Resting Cell CAH Transformation Activity for Four Microbial Cultures Dominated by Either the Organism with a T-RFL of 183 bp (B6 and B8) or an Organism with a T-RFL of 179 bp (B1 and B4) (note the difference in time scale for the transformation of 1,1-DCE compared to 1,1,1-TCA)

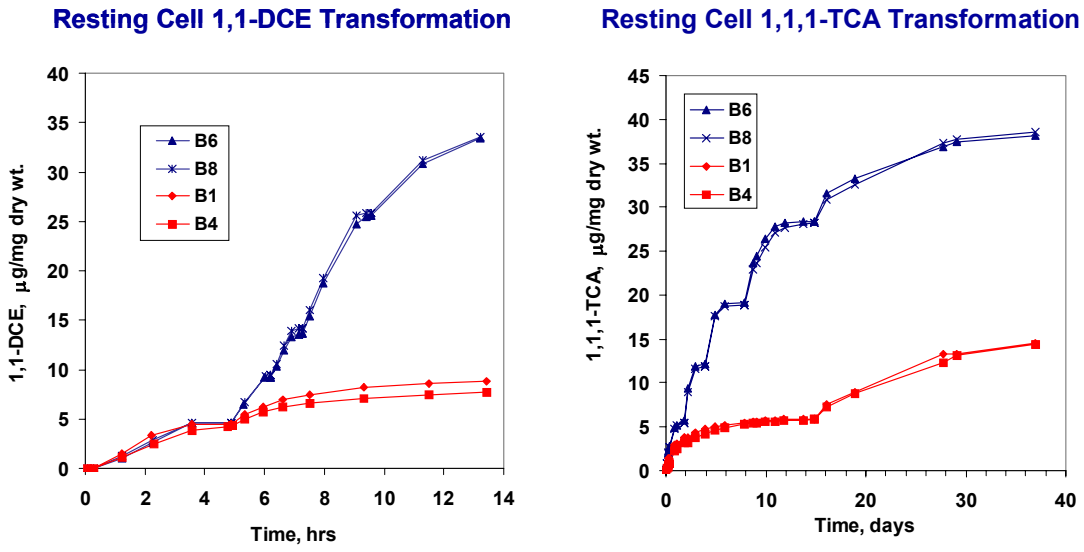

Figure 21. Scanning Electron Micrographs of the Strain 183BP Culture (left frame, 5 □m bar) and the Strain 179BP Culture (middle frame, 5 □m bar and right frame, 20□m bar) Show an Even Distribution of Strain 183BP Cells across the Membrane and Clumps of Aggregated Strain 179BP Cells after Growth in Mineral Media with a Butane Headspace

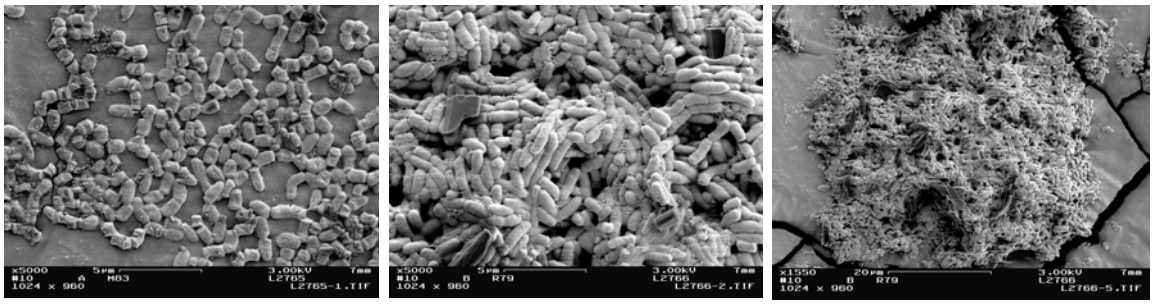

Figure 22. Results of Phylogenetic-Specific PCR Amplification of Groundwater Samples Acquired from a Well 0.5 m from the Injection Well

Lanes 2–9: PCR results using universal bacterial primers 27F and 1492R.
Lanes 11–18: PCR results using 183 bp-specific primers 191F and 434 R.
Lanes 1, 10, and 19: DNA mass standard
Lanes 2,3 and 11,12: Bioaugmented leg before most recent bioaugmentation.
Lanes 4,5 and 13,14: Bioaugmented leg one day after bioaugmentation.
Lanes 6,7 and 15,16: Bioaugmented leg two days after bioaugmentation.
Lanes 8,9 and 17,18: Indigenous leg before most recent bioaugmentation.

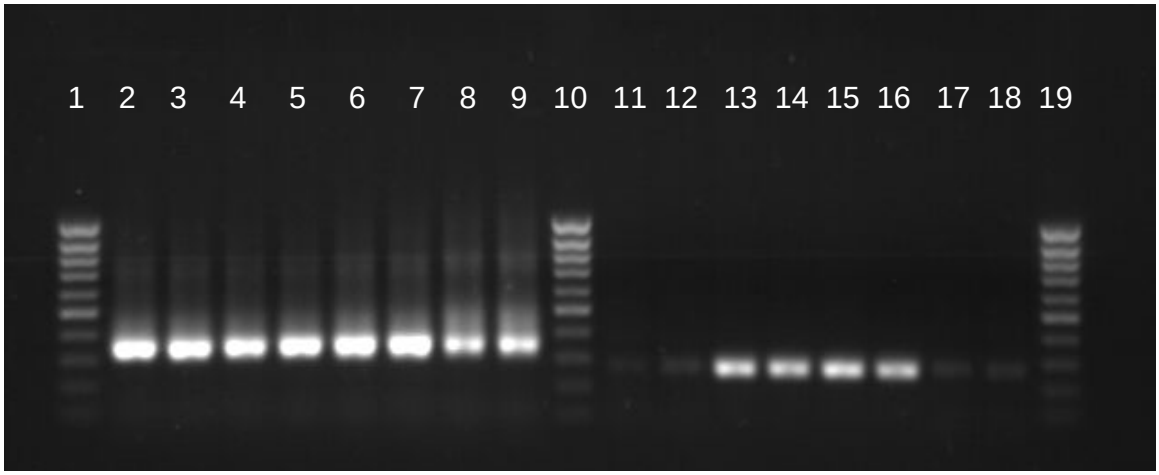

4.2 Clone Library Development

In order to track members of the augmentation culture in the subsurface, a clone library of the 16S rRNA genes of the augmentation culture was developed. This allowed identification of specific organisms in the mixed culture without the need to isolate each organism. The steps involved in clone library development can be seen in Figure 23. DNA was extracted from two aliquots of the liquid nitrogen stored augmentation culture and amplified using PCR conditions described in section 3.2.4 and using the primers EubA (5'-AAGGAGGTGATCCANCCVCA-3') and EubB (5'-AGRGTTYGATYMTGGCTCAG-3'). The resulting amplicons were purified using QIAquick PCR Purification Kit (Qiagen, Valencia, CA) and electrophoresed on a 1% agarose gel with negative and positive controls to verify the success of the DNA extraction and PCR amplification. The PCR products were then ligated into the pGEM-T-easy vectors (Promega, Madison, WI) and the vectors were transformed into high efficiency competent JM109 *E. coli* cells. The transformed cells were streaked onto plates and grown overnight. Ninety six successful clones, as determined by colorimetric reactions, were harvested from the plates and grown in LB/ampicillin media for archiving and screening. Eighty-eight of the ninety-six colonies contained an insert of the proper length. Restriction digest analysis (*Hae*III) of the 88 colonies revealed 35 distinct banding patterns with 16 patterns repeated two or more times. An internal primer, 700R, was used to sequence a representative clone from each of the 16 groups. Visual inspection of the augmentation culture using DAPI staining and fluorescence microscopy found only two or three dominant morphologies. Molecular analysis suggests the augmentation culture is more complex than was apparent from visual inspection.

After restriction fragment length polymorphism (RFLP) analysis, partial sequencing, and searching a database of known organisms (Genbank), sixty two of the eighty six clones were found to be similar (98% identity over 500 base pairs) to one of four groups of bacteria (Table 13). T-RFLP analyses conducted on the 16 representative clones showed actual terminal fragment lengths were within 2 bp of the computer-predicted fragment lengths (Table 14). The four groups included *Acidovorax* (24 clones) and *Hydrogenophaga* (21 clones), both gram negative facultative chemolithotrophs known for hydrogen oxidation, *Rhodococcus* (12 clones), a gram positive bacterium known for hydrocarbon degradation and in some cases have been implicated in chlorinated solvent transformation, or an unidentified bacterium found in a deep subsurface clay (5 clones). A comparison of the T-RFLP profile for the source culture and the combined profiles of the four dominant clone group representatives can be seen in Figure 24. A representative clone from each group was chosen and the full 16S rRNA gene segment between EubB and EubA primer sites was sequenced.

The full sequences were then used in another database search and the above results were confirmed with very high matches between the clones and known organism sequences (Table 14). The sequence information was used to design fluorescent rRNA probes and PCR primers specific to each of the four clones (Figure 25). A search of the database for known organisms that would match the designed probe sequences found no complete matches for any of the probes. The closest matches found were 2 mismatches each for probes 12c (*Hydrogenophaga*), 11a (*Rhodococcus*), and 8a (unknown beta proteobacterium) and 1 mismatch for probe 5a (*Acidovorax*). The probes and primers were synthesized and available for use in fluorescent in situ hybridization (FISH) analysis and real time PCR analyses.

The sequence information was also used to choose restriction enzymes for the T-RFLP analyses. Computer analyses (Omiga 2.0, Genetics Computer Group, Madison, WC) of the fully sequenced clones and similar organisms selected from the database search was used to select two restriction enzymes, MnlI and Hin6I, that would yield distinctly different terminal fragment lengths for each of the clones and for all but the most closely related organisms (Table 13).

Table 13. Predicted LH-PCR and T-RFLP results for the fully-sequenced clones and similar known organisms found in Genebank search (higher relative match score corresponds to greater similarity)

Rel. Score	Organism	LH-PCR	MnII T-RFLP	Hin6I T-RFLP	HaeIII T-RFLP
	Clone 12c	**340**	**209**	**151**	**69**
2835	*Hydrogenophaga palleronii*	340	209	151	69
2652	*Hydrogenophaga flava*	340	209	203	69
2422	Nitrogen-fixing bacterium MI753	340	209	203	69
2571	*Pseudomonas spinosa*	340	209	203	217
2458	*Xylophilus ampelinus*	340	209	203	217
2482	*Acidovorax sp. IMI 357678*	340	132	203	198
2244	*Delftia acidovorans*	340	166	203	198
	Clone 5a	**340**	**277**	**203**	**198**
2870	*Acidovorax facilis*	340	277	203	198
2767	Unidentified bacterium	340	277	203	198
2674	Type 0803 filamentous bacterium	340	277	203	198
2581	*Xylophilus ampelinus*	340	209	203	217
2413	*Aquaspirillum sinuosum*	340	209	203	217
2438	Nitrogen-fixing bacterium MI753	340	209	203	69
2169	*Hydrogenophaga palleronii*	340	209	151	69
2545	*Acidovorax sp. IMI 357678*	340	132	203	198
2377	*Comamonas sp. 12022*	340	277	203	198
2327	*Delftia acidovorans*	340	166	203	198
	Clone 11a	**340**	**179**	**340**	**67**
2872	*Rhodococcus sp.*	340	179	340	67
2811	*R.opacus*	340	179	340	67
2633	*N.calcarea*	340	179	340	67
2753	*R.marinonascens*	340	277	340	67
2393	*N.otitidiscaviarum*	340	277	340	67
2496	*N.restrica*	340	277	340	217
2498	*N.corynebacteroides*	340	277	171	67
2323	*Nocardia crassostrae*	340	129	340	67
2654	*R.erythreus*	340	11	340	67
	Clone 8a	**342**	**168**	**65**	**219**
1590	Uncultured bacterium H20	342	168	65	219
1542	Uncultured proteobacterium A13	342	168	65	219
1542	Uncultured bacterium S28	342	168	65	219
1594	Beta proteobacterium A0823	342	279	65	219
1104	*Bordetella avium*	342	211	342	200
1104	*B.bronchiseptica*	342	212	342	77

Table 14. MnII T-RFLP Predicted Fragment Lengths and Results for Selected Clones and Isolates

No. of Clones Tested (Total)	GenBank Database Comparison:	Predicted MnII T-RFLP	Actual MnII T-RFLP
6 (21)	*Hydrogenophaga palleronii*	209	207.3 - 207.7
3 (24)	*Acidovorax*	277	277.1 - 277.3
2 (12)	*Rhodococcus*	179	178.9, 179.0
2 (5)	Unidentified bacterium (deep clay)	168	167.0, 167.2
1 (3)	*Ferribacterium*		237.2
1 (2)	*ultramicrobacterium* (proteobacterium)		100.4
1 (2)	*Hydrogenophaga palleronii ???*		208.7
	Isolate 1		178.8
	Isolate 2		178.9
	Isolate 3		178.9
	Isolate 4		178.9

Figure 23. Flow Chart of 16S rRNA Gene Clone Library Analysis Starting with Liquid Cultures and Including Archiving, Plasmid Preparation, PCR Screening, and RFLP Analysis (courtesy of Kevin Vergin and Stephen Giovannoni, Oregon State University)

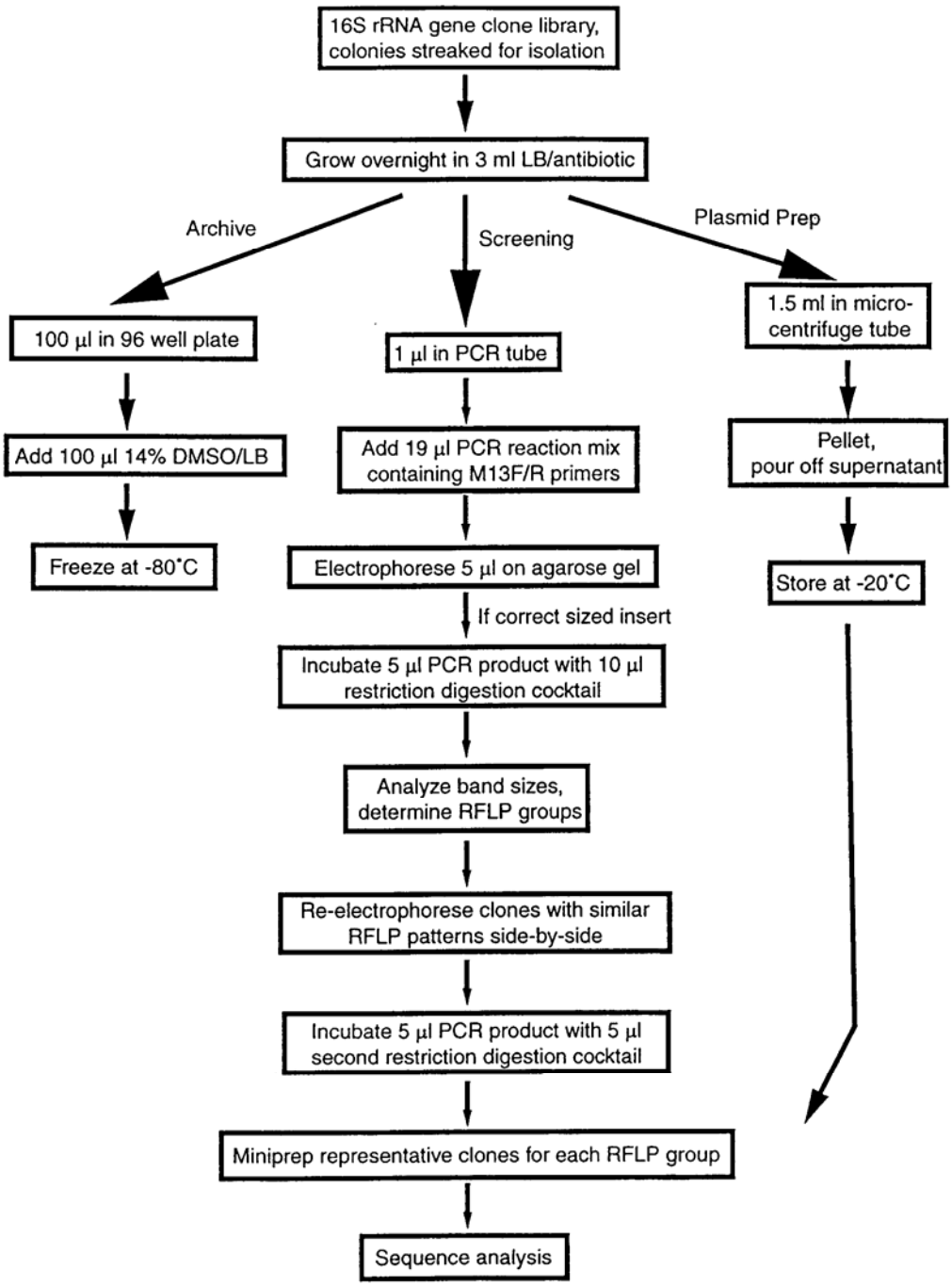

Figure 24. Nucleotide Sequences for rRNA Probes Designed for Four of the Dominant Clone Groups in the Clone Library

Probe 5a (*Acidovorax*)
5' GUACAUGUCAAAGGCGGGUA 3'

Probe 8a (Unknown beta proteobacterium)
5' UCGGGCGGCAGCGCGGUCUU 3'

Probe 12c (*Hydrogenophaga*)
5' GGCCUGCGCUGGCGCUCAUG 3'

Probe 11a (*Rhodococcus*)
5' AGCCGAAAGUCAUACCCGGU 3'

Figure 25. Comparison of Mn(II) T-RFLP Profiles for the Source Culture and the Numerically Dominant Clones from the Clone Library

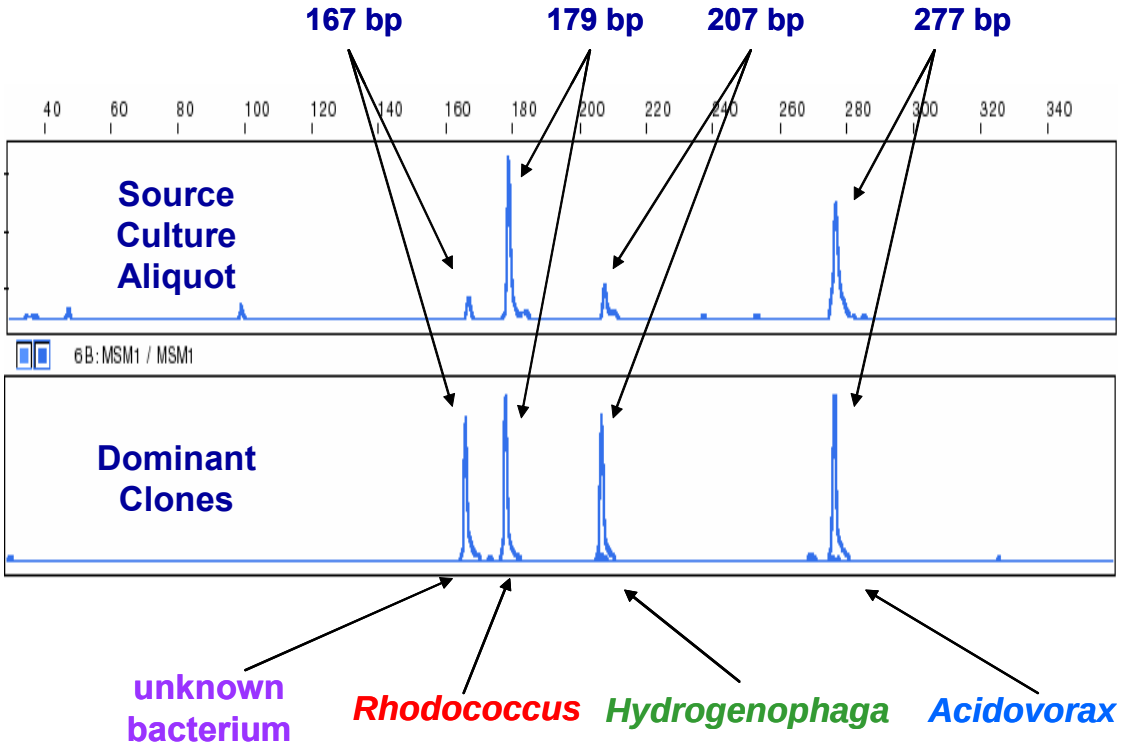

4.3 Studies of 1,1,1-TCA Transformation and Butane Utilization with an Enriched Culture

The objective of these experiments was to compare the 1,1,1-TCA transformation ability between indigenous microorganisms from Moffett test site and butane-utilizers bioaugmented to Moffett Field microcosms. The transformation of CAH mixtures of 1,1,1-TCA, TCE, and 1,1-DCE was also evaluated in bioaugmented microcosms. Microcosms were constructed in 125 mL media bottles sealed with grey butyl rubber lined caps. They were filled with 100 mL of Moffett groundwater and aquifer material. The conditions of the microcosms are shown in Table 15. A media-culture for bioaugmentation was obtained from a growth reactor inoculated with the frozen butane-utilizing mixed culture. The enrichment was harvested from the batch growth reactor at the measured optical density (OD_{600}) of 0.25 and density of 120 mg TSS /L. The cells were not washed before bioaugmentation. Microcosm studies were performed with the enrichment culture described in section 3.1. A microcosm study was performed to evaluate TCA transformation by the culture. Table 15 presents the microcosm setting setting for these initial tests.

Table 15. Microcosms Used for the Experiment of CAH Transformation

Microcosm	Contents	Substrate	CAHs	Description
BR2-C3	GW/Soil	Butane	1,1,1-TCA	Indigenous microcosm
BR2-2	GW/Soil	Butane	1,1,1-TCA, 1,1-DCE, TCE	Inoculated with 100 μL of media-culture
BR2-3	GW/Soil	Butane	1,1,1-TCA, 1,1-DCE, TCE	Inoculated with 500 μL of media-culture

Figure 26 presents the butane utilization and 1,1,1-TCA transformation achieved in non bioaugmented microcosm BR2-C3. No 1,1,1-TCA transformation was observed even after four additions of butane. With long-term exposure to 1,1,1-TCA, the rate of butane utilization slowed.

The butane utilization and 1,1,1-TCA transformation achieved in microcosm BR2-2 bioaugmented microcosm is presented in Figure 27. 1,1,1-TCA was added to the microcosm along with butane. Butane was consumed in 5 days, and 1,1,1-TCA transformation was then observed. On day 18, 1,1,1-TCA transformation ceased after 0.2 mg of 1,1,1-TCA was transformed. More butane was then added to enhance the transformation. On day 26 and 44, the successive additions of TCA were repeated. The total mass of TCA transformed was 0.36 and 0.25 mg, respectively. On day 28, after butane was consumed, 1,1,1-TCA transformation accelerated. This is most likely due to butane competitive inhibitory effect on 1,1,1-TCA transformation. The transformation rate decreased gradually with continued additions of 1,1,1-TCA. The butane utilization also slowed down around day 37 after continued 1,1,1-TCA.transformation.

Figure 26. Butane Utilization and Limited 1,1,1-TCA Transformation Achieved in Indigenous Microcosm BR2-C3

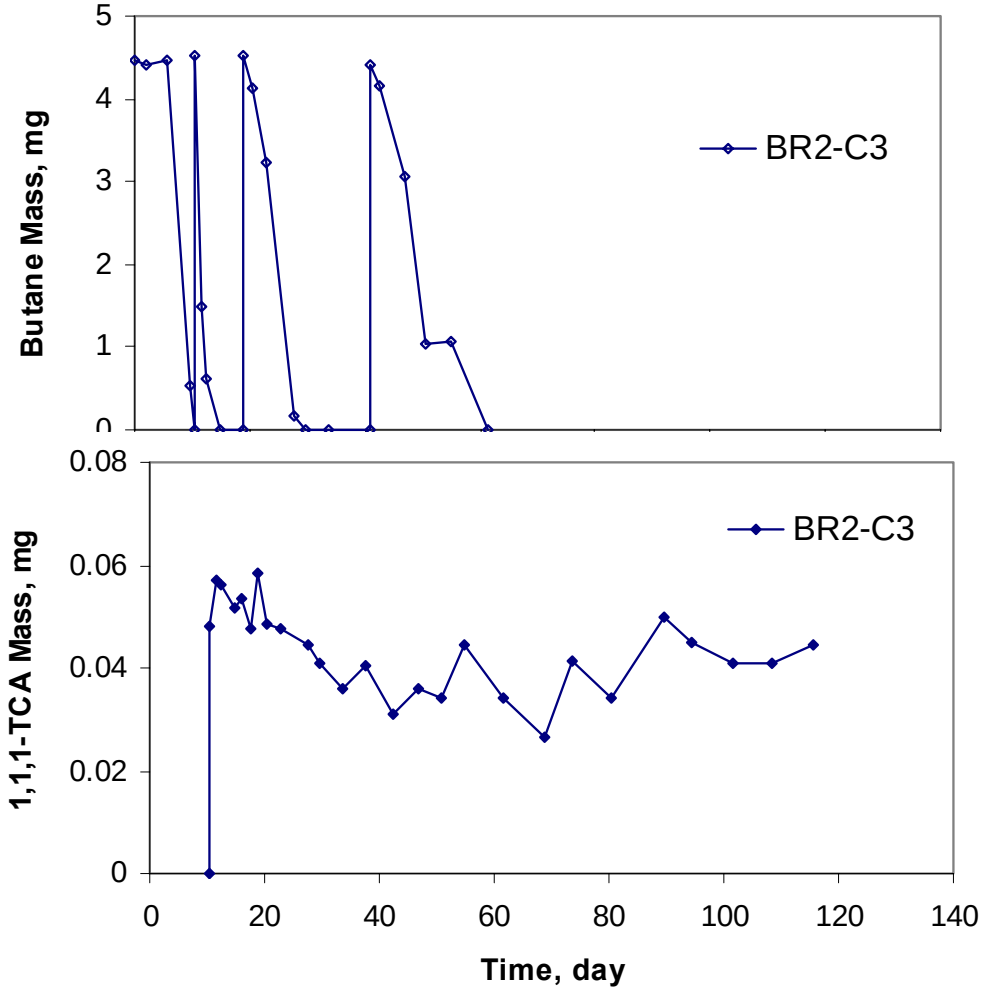

Figure 27. Butane Utilization and 1,1,1-TCA Transformation Achieved in Media-Culture Inoculated Microcosm BR2-2

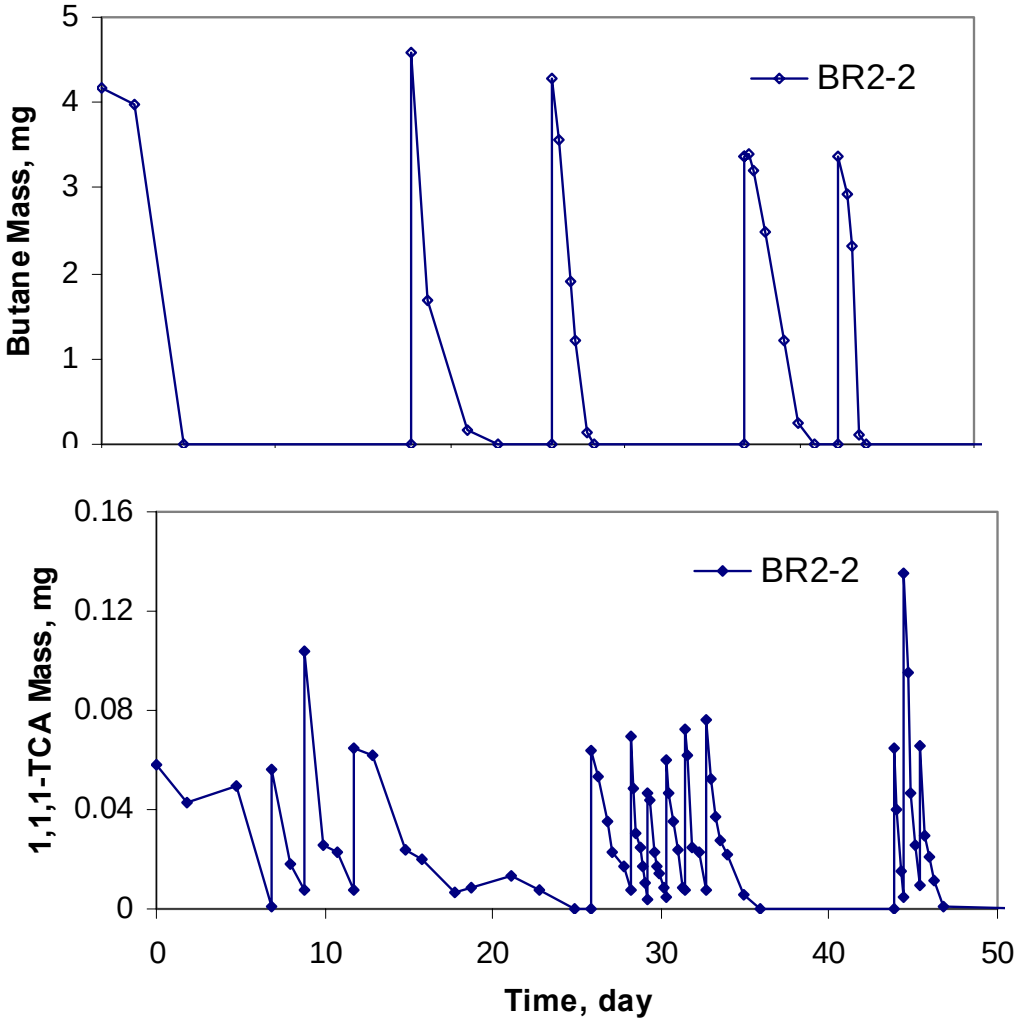

Figure 28. Butane Utilization and 1,1,1-TCA Transformation Achieved in Media-Culture Inoculated Microcosm BR2-3

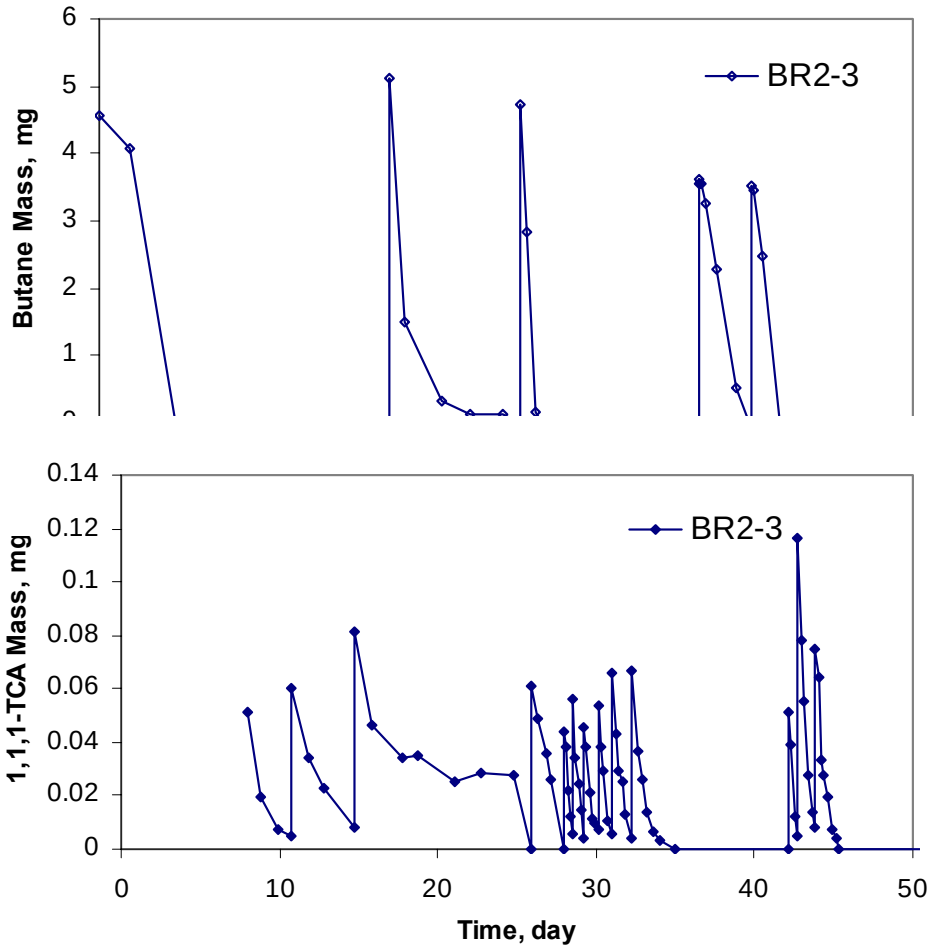

Figure 28 presents the butane utilization and 1,1,1-TCA transformation achieved in microcosm BR2-3. Microcosm BR2-3 had the five times amount of inoculation as microcosm BR2-2. Unlike microcosm BR2-2, only butane was initially added to microcosm BR2-3, and it was consumed in 5 days, the same as microcosm BR2-2. After the butane was consumed, 1,1,1-TCA was added to the microcosm. Similar to microcosm BR2-2, 1,1,1-TCA transformation ceased on day 18. The mass of transformed 1,1,1-TCA was 0.15 mg. The re-addition of butane was conducted to enhance the transformation. The 1,1,1-TCA experiments were repeated day 26, and 42. The total mass of TCA transformed was 0.3 and 0.23 mg, respectively. After day 37, the butane uptake rate had slowed down. Similar to microcosm BR2-2, the competitive inhibition of 1,1,1-TCA transformation by butane and a decrease in transformation rate with continued addition of 1,1,1-TCA were also observed in microcosm BR2-3.

Figure 29. 1,1,1-TCA Transformation Rate Data for Microcosm BR2-2 during Day 28 - 37

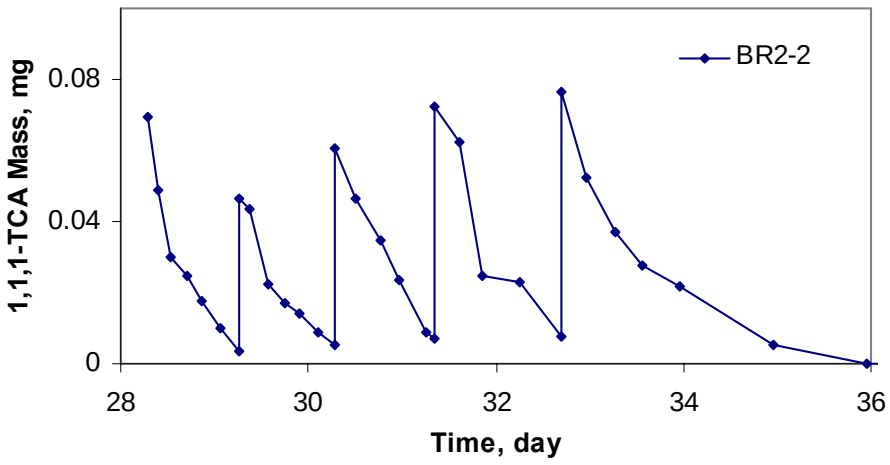

Figure 29 presents the experimental data during on day 28 to 37 for microcosm BR2-2. The gradual slowing in 1,1,1-TCA transformation rates can be seen.

Figure 30 presents the utilization of butane and transformation of chlorinated solvent mixtures of 1,1,1-TCA, TCE and 1,1-DCE achieved in microcosm BR2-2 after 52 days of incubation. On day 53, butane was added along with 1,1,1-TCA, TCE, and 1,1-DCE. Butane utilization occurred within 3 days. 1,1-DCE, and 1,1,1-TCA were transformed within 2 and 4 days, respectively. However, the TCE transformation ceased after 90% of the TCE was transformed. On day 58, the microcosm was purged under a laminar flow hood to remove TCE, and more butane was added to increase the amount of biomass. The experiment was repeated on day 60. Butane was consumed within 2 days. 1,1-DCE, 1,1,1-TCA and 70% of TCE were transformed within 13 hours, 3 days and 6 days, respectively. After 66 days of incubation, the utilization of butane and the transformation of chlorinated solvents slowed down. Butane utilization and 1,1-DCE transformation occurred within 4 days. 1,1,1-TCA and 87% of TCE was transformed within 10 days. Inhibition of 1,1,1-TCA and TCE transformation by butane and 1,1-DCE was observed.

Figure 30. Butane Utilization and Chlorinated Compound Transformation Achieved in the Media-Culture Inoculated Microcosm BR2-2

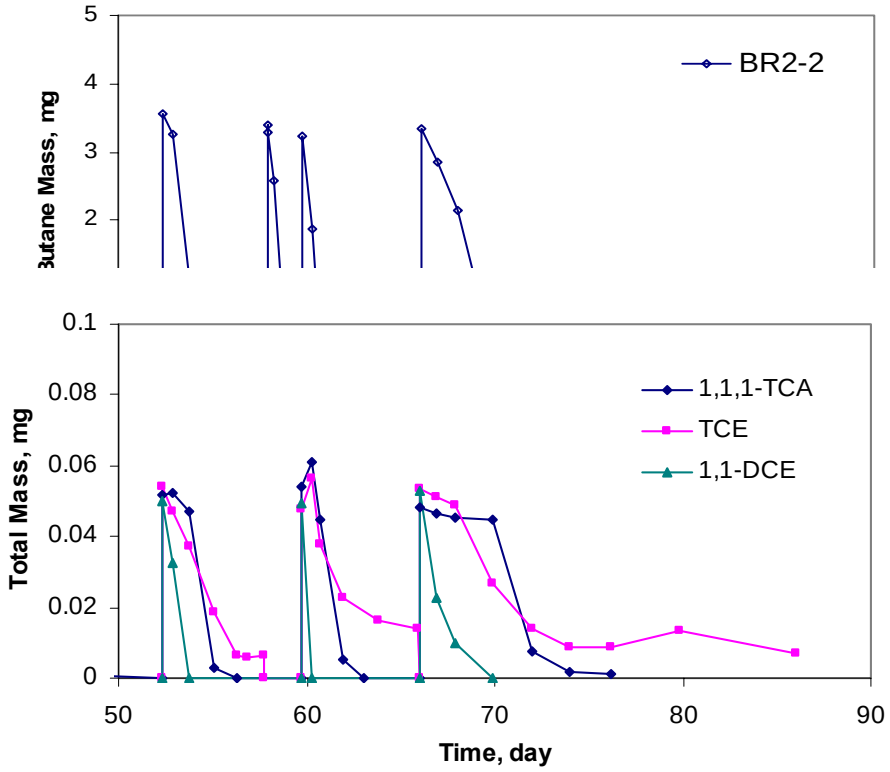

The microcosms bioaugmented with the frozen butane-utilizing culture showed the same performance as previous microcosms inoculated with a cell slurry. Long-term transformation of 1,1,1-TCA in the absence of butane utilization was achieved at rapid rates. The transformation of a mixture of 1,1,1-TCA, 1,1-DCE and TCE was observed. The transformation rate of 1,1-DCE was the fastest, while the transformation rates of 1,1,1-TCA and TCE were slower. After transforming the mixture of these chlorinated solvents, the rates of butane utilization and chlorinated solvent transformation slowed down. This is probably due to the transformation product toxicity, especially that of 1,1-DCE.

4.3.1 Butane and 1,1,1-TCA Kinetic Experiments

Table 16. Microcosms Used for the Kinetic Experiments

Microcosm	Contents	Substrate	CAHs	Description
BRC-1 to BRC5	GW/Soil	Butane	1,1,1-TCA	Indigenous microcosm
BR3-1 to BR3-5	GW/Soil	Butane	1,1,1-TCA	Inoculated with 500 µl of media-culture, and having initial biomass of 0.47 mg/L
BR4-1 to BR4-5	GW/Soil	Butane	1,1,1-TCA	Inoculated with 500 µl of media-culture, and having initial biomass of 0.45 mg/L
BR4-M	Growth media	Butane	1,1,1-TCA	Inoculated with 500 µl of media-culture, and having initial biomass of 0.45 mg/L

Studies were conducted over a range of butane and 1,1,1-TCA concentrations to determine the half-saturation constants (K_s) of indigenous and bioaugmented butane-utilizers under microcosm conditions. The microcosms constructed for this experiment are presented Table 16. The microcosm fabrication was the same as for the previous experiment. The bioaugmented cultures of the BR3 and BR4 microcosm sets, and microcosm BR4-M were obtained from reactors inoculated with the frozen butane-utilizing culture but at different times. These studies help demonstrate the reproducibility of the bioaugmentation process.

Figure 31. Overall Results from the Butane Kinetic Experiments Conducted in the Bioaugmented Microcosm BR3-2

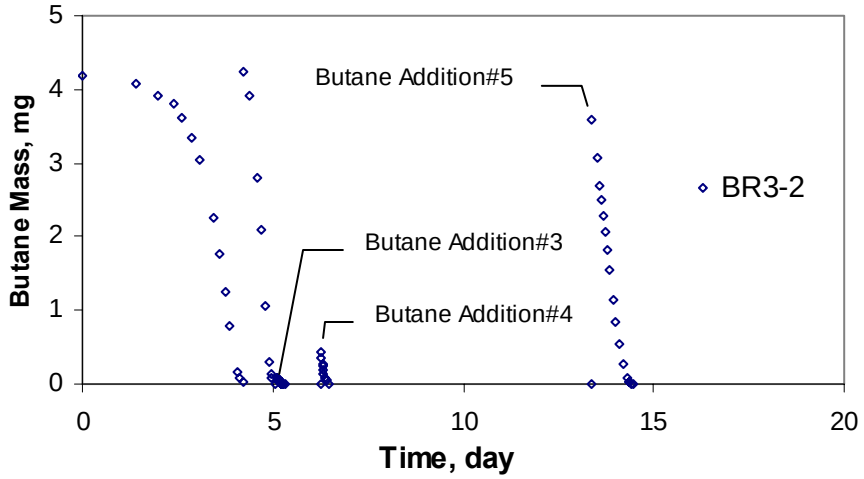

Figure 31 presents the overall results from the butane kinetic experiments conducted in inoculated microcosm BR3-2. Two additions of butane (4 mg) were added to each microcosm to stimulate the microbial population. To determine a butane K_s value, a kinetic experiment was conducted on day 5, starting at an aqueous concentration of 40 μg/L. Butane utilization followed first-order kinetics as shown in Figure 32.

Figure 32. Experimental Data from the Butane Kinetic Experiment Conducted in Microcosm BR3-2 on Day 5

a) The third addition of butane

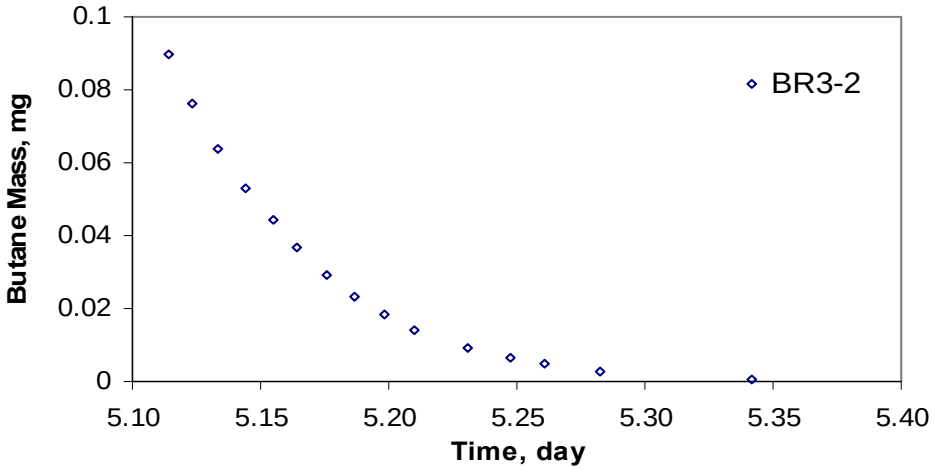

b) Butar

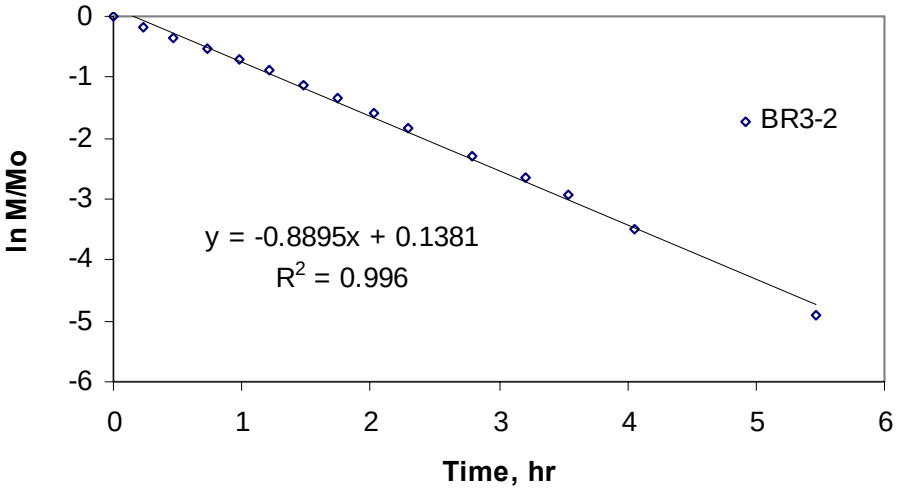

Figure 33. Experimental Data from the Butane Kinetic Experiment Conducted in Microcosm BR3-2 on Day 6

a) The fourth addition of butane

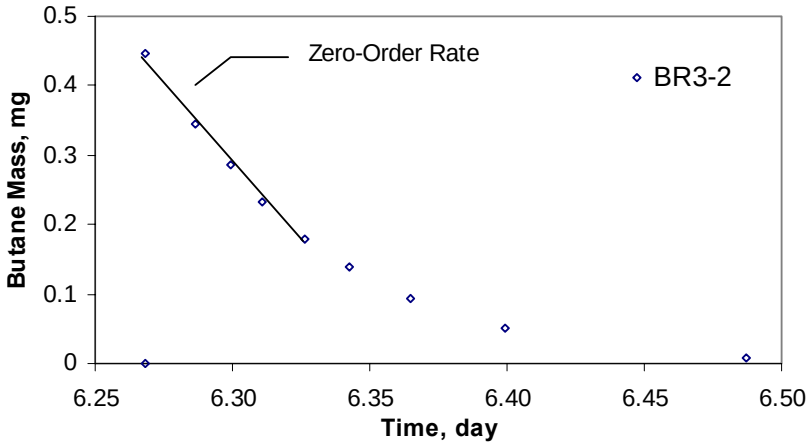

b) Initial butane utilization following zero-order kinetics

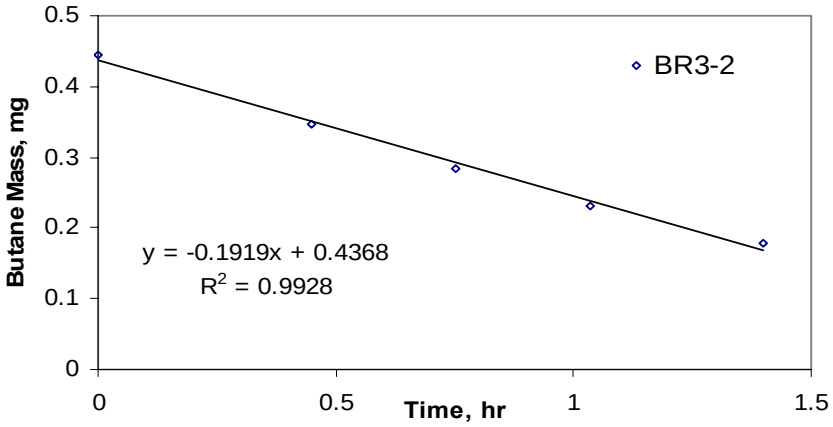

c) Latter butane utilization following first-order kinetics

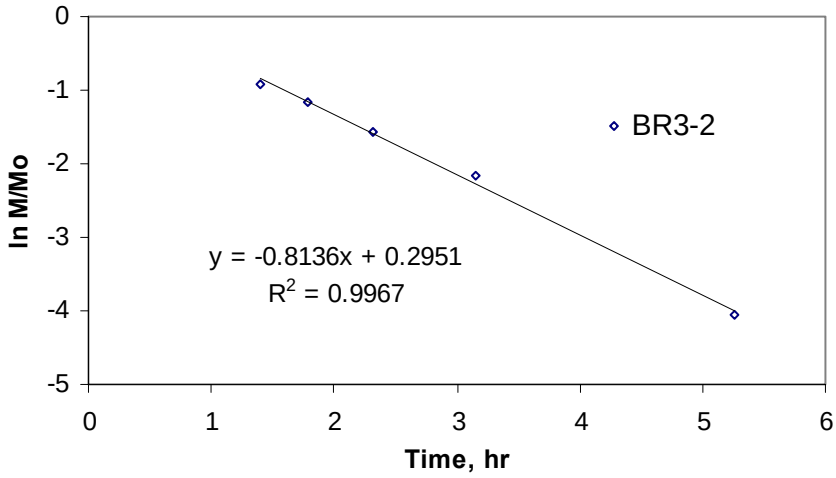

Figure 34. Experimental Data from the Butane Kinetic Experiment Conducted in Microcosm BR3-2 from Day 13 to 14

a) The fifth addition of butane

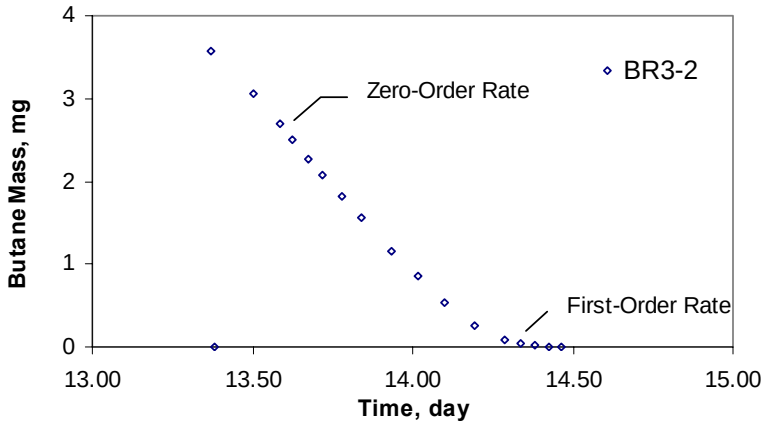

b) Initial butane utilization following zero-order kinetics

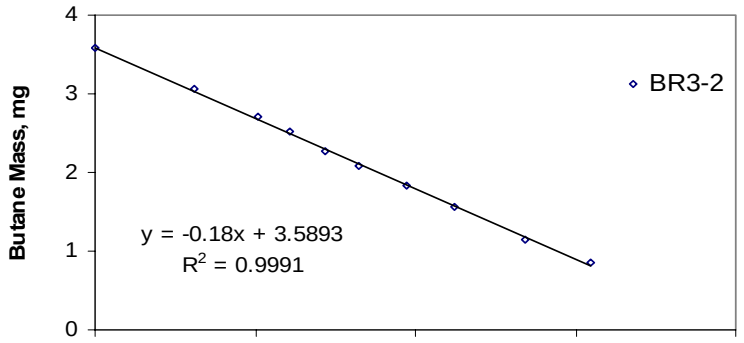

c) Latter bu

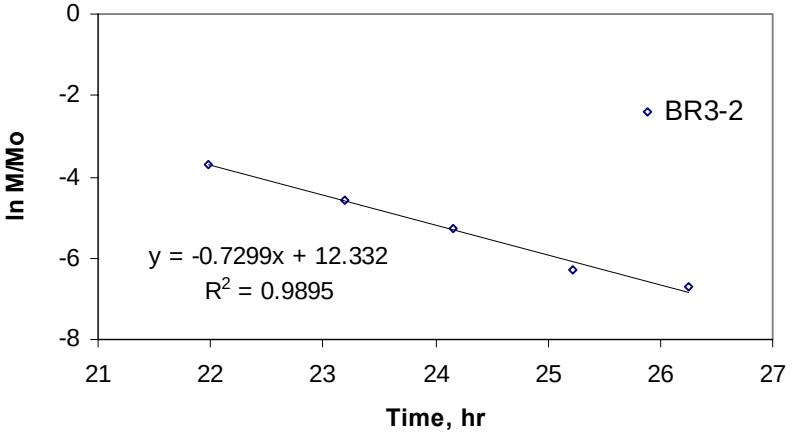

Another kinetic experiment was then conducted on day 6 at a higher butane concentration (200 μg/L). As shown in Figure 33, the first five data points tend to follow zero-order kinetics and the remaining seem to follow first-order kinetics. On day 13, another kinetic test was performed at an aqueous concentration of 1800 μg/L. Butane transformation rates covered both zero-order and first-order ranges, as shown in Figure 34. Table 17 presents the K_s values for butane and the initial aqueous concentration of butane. The K_s values obtained from both experiments were similar. The average K_s value for the BR3 microcosm set is 0.11 ± 0.014 mg/L.

Table 17. Butane Half-Saturation Constant (K_s) Achieved in the BR3 Microcosm Set

Microcosm	The 4th addition of butane		The 5th addition of butane	
	C_l (μg/L)	K_s (mg/L)	C_l (μg/L)	K_s (mg/L)
BR3-1	196	0.119	1514	0.077
BR3-2	196	0.104	1577	0.109
BR3-3	196	0.109	1711	0.102
BR3-4	193	0.11	1711	0.113
BR3-5	175	0.12	1709	0.132
Average		0.11 ± 0.007		0.11 ± 0.02

After the fifth addition of butane was completely consumed, a 1,1,1-TCA kinetic test was started on day 15. The 1,1,1-TCA kinetic experiments were conducted in a similar manner as the butane experiments. Figure 35 presents the overall results from the 1,1,1-TCA kinetic experiments conducted in microcosm BR3-2. 1,1,1-TCA transformation at an initial concentration of 100 μg/L followed first-order kinetics, as shown in Figure 36. Thus the K_s value could not be determined from this 1,1,1-TCA test. Another kinetic experiment was performed at a higher aqueous concentration. As shown in Figure 37, the transformation of 1,1,1-TCA at 700 μg/L followed zero-order kinetics initially, and then followed first-order kinetic after the 1,1,1-TCA was lower than 250 μg/L. This indicates that the K_s value is between 250 and 700 μg/L. Table 18 presents the K_s values along with the initial aqueous concentration of 1,1,1-TCA from the the BP3 microcosm set. All microcosms had similar K_s values. The average K_s value is 0.37 ± 0.051 mg/L. The results show that the bioaugmentation process yields similar K_s values for both butane and 1,1,1-TCA.

Figure 35. Overall Results from the 1,1,1-TCA Kinetic Experiment Conducted in Bioaugmented Microcosm BR3-2

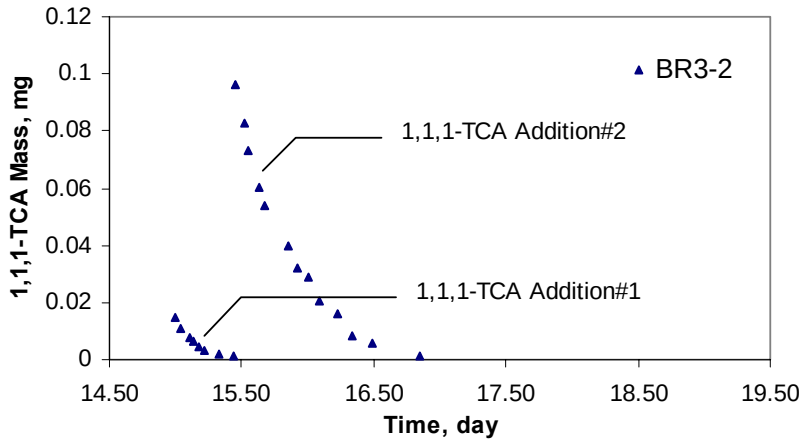

Figure 36. Experimental Data from the 1,1,1-TCA Kinetic Experiment Conducted in Microcosm BR3-2 on Day 15

a) The first addition of 1,1,1-TCA

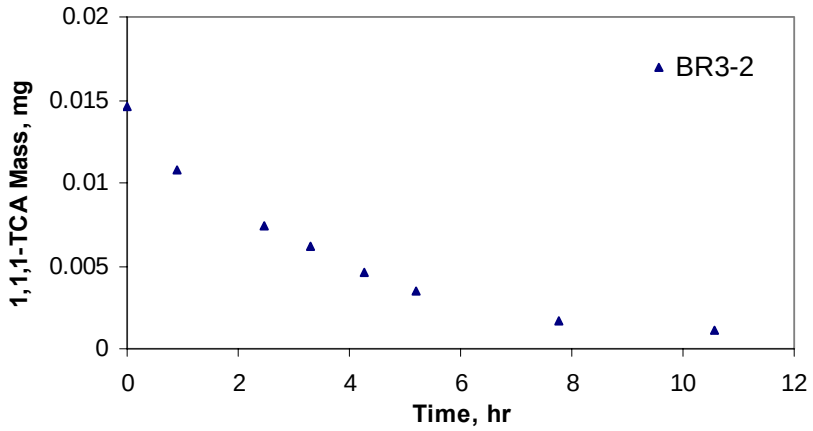

b) 1,1,1-TCA transformation following first-order kinetics

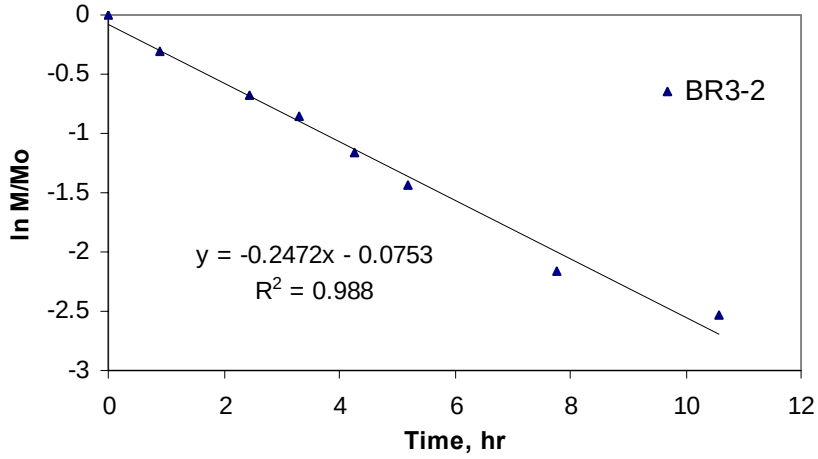

Figure 37. Experimental Data from the 1,1,1-TCA Kinetic Experiment Conducted in Microcosm BR3-2 from Day 15 to 16

a) The second addition of 1,1,1-TCA

b) Initial 1,1,1-TCA transformation following zero-order kinetics

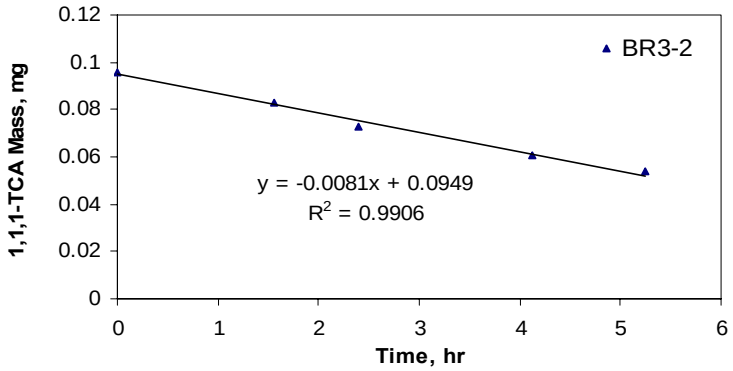

c) 1,1,1-TCA transformation following first-order kinetics

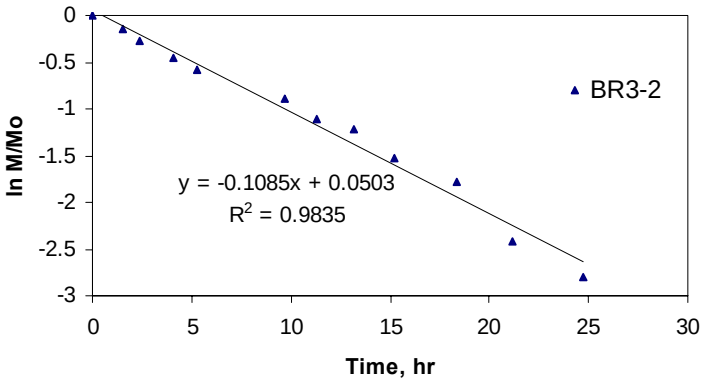

Table 18. 1,1,1-TCA Half-Saturation Constant (K_s) Achieved in the BR3 Microcosm Set

Microcosm	The 2nd addition of 1,1,1-TCA	
	C_l (μg/L)	K_s (mg/L)
BR3-1	680	0.400
BR3-2	731	0.443
BR3-3	698	0.324
BR3-4	720	0.335
BR3-5	711	0.345
Average		0.37 ± 0.051

Kinetic experiments were also conducted in the BR4 microcosm set. The overall results from the kinetic experiments for both butane and 1,1,1-TCA in microcosm BR4-5 are presented in Figure 38. The first two additions of butane were performed to stimulate the microbial population. The butane kinetic experiments were conducted with the third and fifth additions of butane. As shown in Figure 39 and 40, the data from both experiments followed zero-order kinetics initially and then first-order kinetics. The initial concentration ranged from 230 to 330 μg/L. Table 19 presents the K_s values for butane from the BR4 microcosm set and the initial concentrations of butane. The similar results from all microcosms indicate the reproducibility of bioaugmentation process. The average K_s value for the BR4 microcosm set is 0.11 ± 0.012 mg/L. Microcosm BR4-M, which contained growth media, had a slightly lower K_s value than the other microcosms.

After the third and fifth additions of butane were consumed, kinetic experiments with 1,1,1-TCA were performed on day 5 and 13. As shown in Figures 41 and 42, 1,1,1-TCA transformation at low concentrations followed first-order kinetics while transformation at high concentrations was approximated by zero-order kinetics. On day 5, after six data points were collected, 1,1,1-TCA in the microcosms was purged. The 1,1,1-TCA K_s values obtained from the BR4 microcosm set are presented in Table 20. The average K_s value for the BR4 microcosm set is 0.35 ± 0.114 mg/L. The similar K_s values indicate reproducible bioaugmentation was achieved in all the microcosms.

Figure 38. Overall Results from the Butane and 1,1,1-TCA Kinetic Experiments Conducted in Bioaugmented Microcosm BR4-5

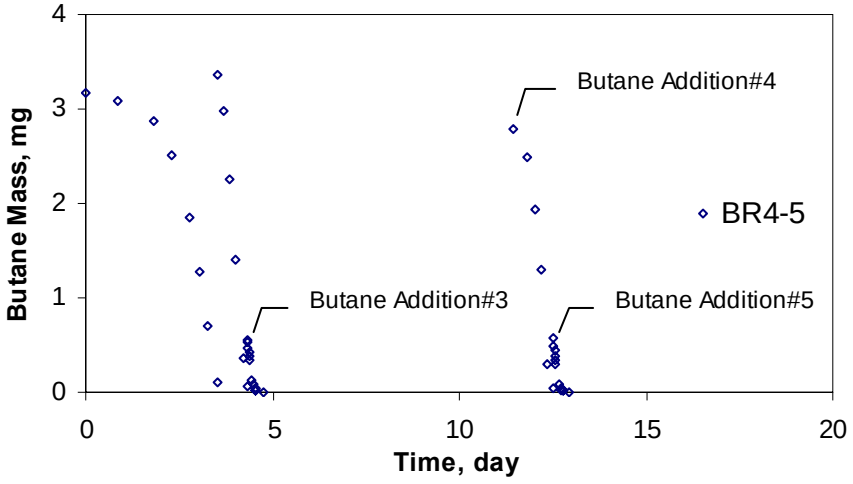

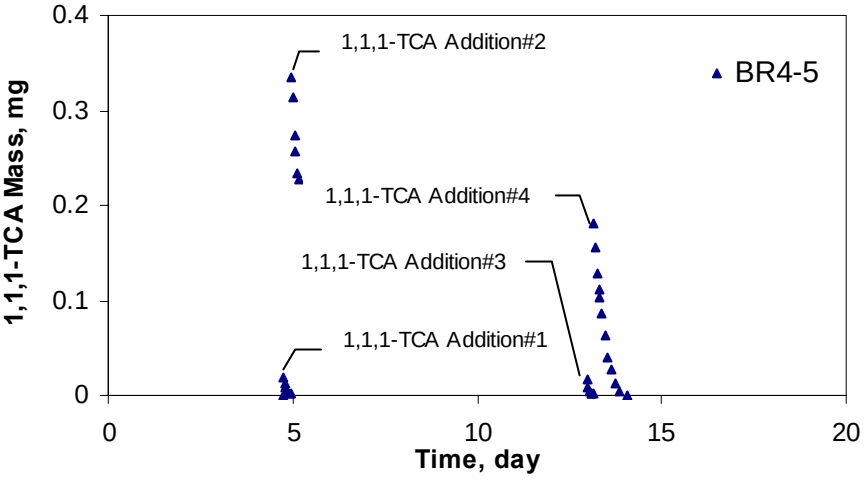

Figure 39. Experimental Data from the Butane Kinetic Experiment Conducted in Microcosm BR4-5 on Day 4

a) The third addition of butane

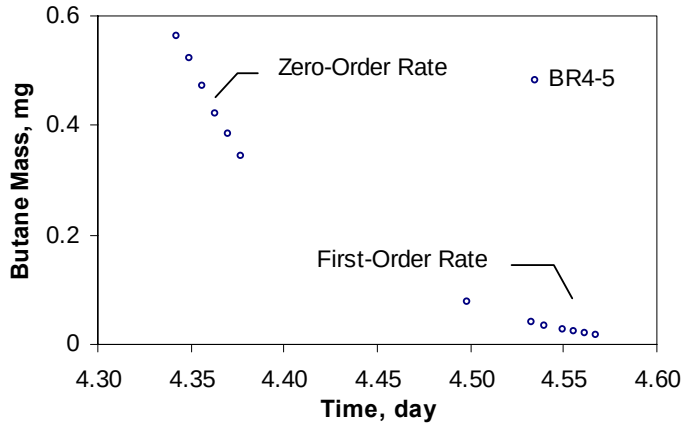

b) Initial butane utilization following zero-order kinetics

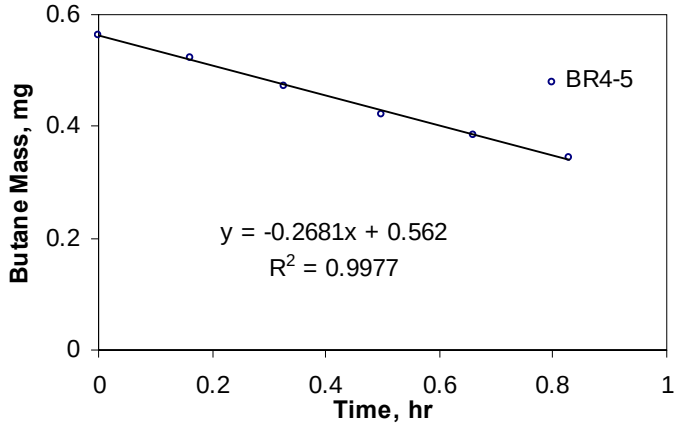

c) Butane utilization following first-order kinetics

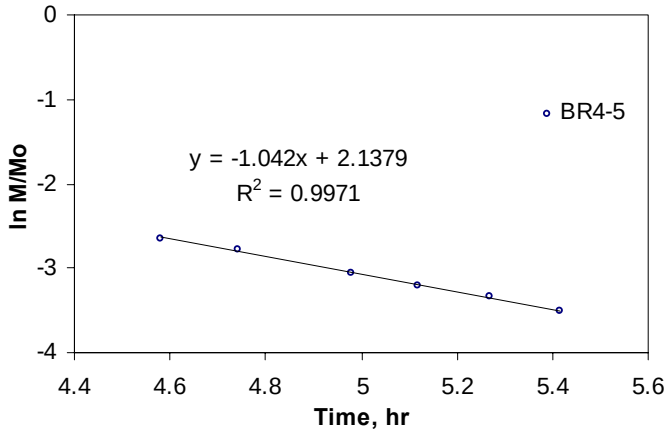

Figure 40. Experimental Data from the Butane Kinetic Experiment Conducted in Microcosm BR4-5 on Day 13

a) The fifth addition of butane

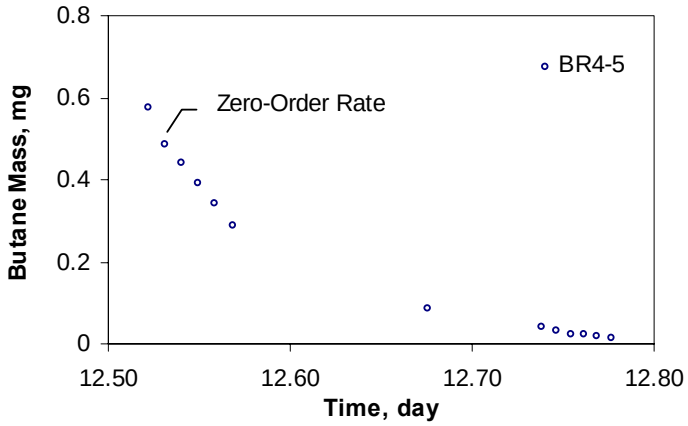

b) Initial butane utilization following zero-order kinetics

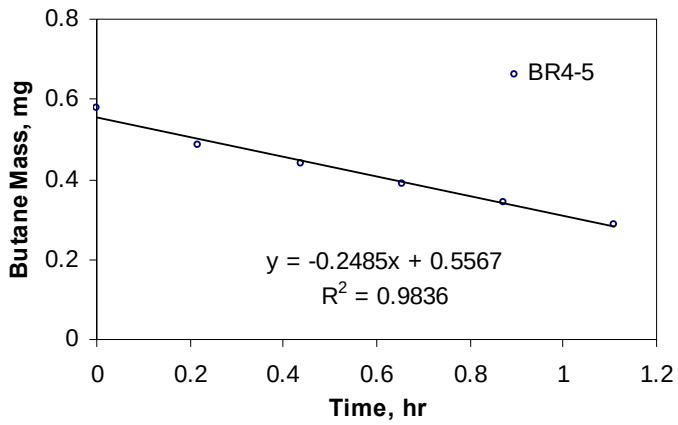

c) Butane utilization following first-order kinetics

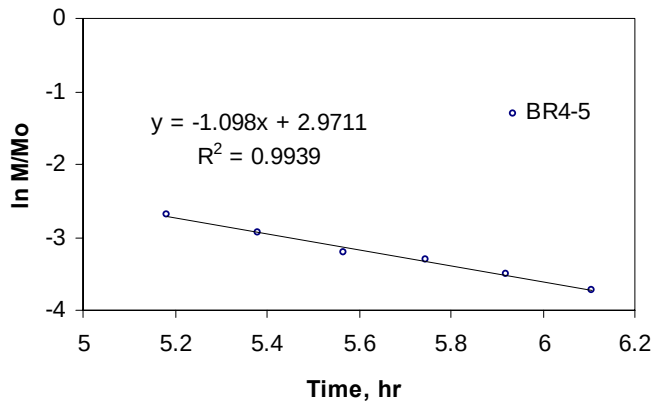

Table 19. Butane Half-Saturation Constant (K_s) Achieved in the BR4 Microcosm Set

Microcosm	The 3rd addition of butane		The 5th addition of butane	
	C_l (μg/L)	K_s (mg/L)	C_l (μg/L)	K_s (mg/L)
BR4-M	326	0.061	242	0.071
BR4-1	271	0.095	267	0.105
BR4-2	253	0.108	233	0.093
BR4-3	264	0.129	232	0.116
BR4-4	284	0.127	248	0.117
BR4-5	248	0.113	254	0.100
Average		0.12 ± 0.014		0.11 ± 0.01

Table 20 presents the average butane and 1,1,1-TCA K_s values achieved in the BR3 and BR4 microcosm sets and microcosm BR4-M. The microcosms were all bioaugmented with the same frozen culture, but from batches of cells grown at different time and with different frozen cells. They all had the similar K_s values for butane and 1,1,1-TCA. The results indicate a very reproducible bioaugmentation process, using the procedures that were established.

Figure 41. Experimental Data from the 1,1,1-TCA Kinetic Experiment Conducted in Microcosm BR4-5 on Day 5

a) The first and second additions of 1,1,1-TCA

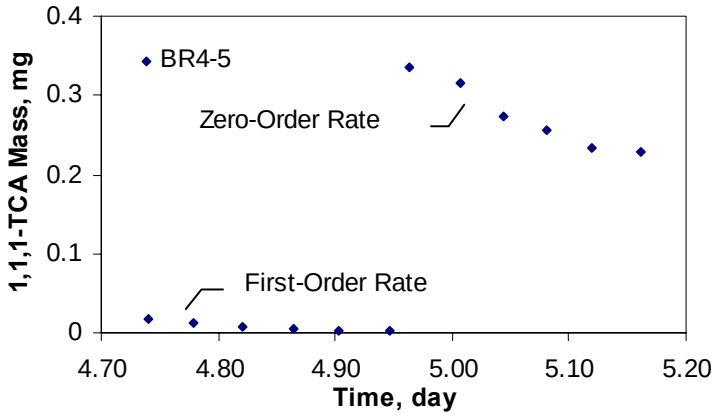

b) 1,1,1-TCA transformation following first-order kinetics

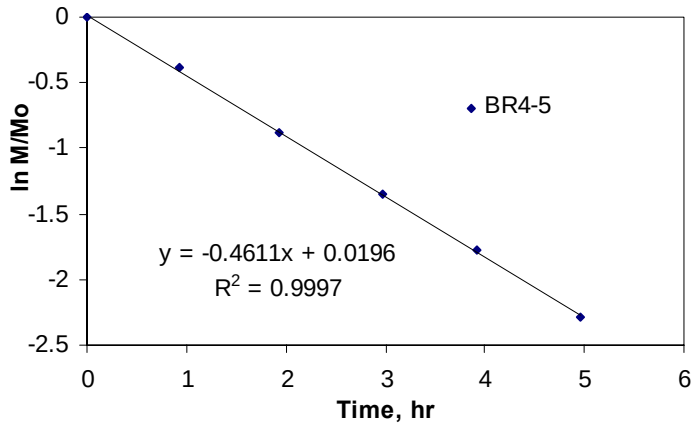

c) 1,1,1-TCA transformation following zero-order kinetics

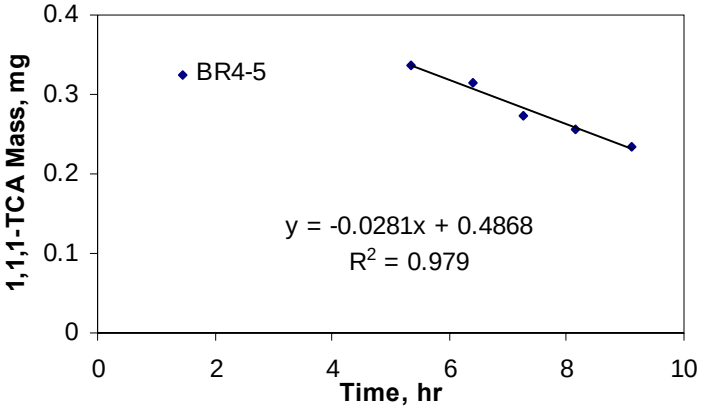

Figure 42. Experimental Data from the 1,1,1-TCA Kinetic Experiment Conducted in Microcosm BR4-5 from Day 13 to 14

a) The third and fourth additions of 1,1,1-TCA

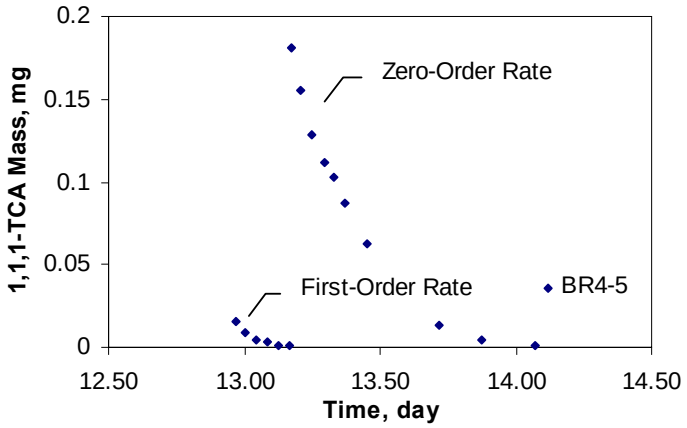

b) 1,1,1-TCA transformation following first-order kinetics

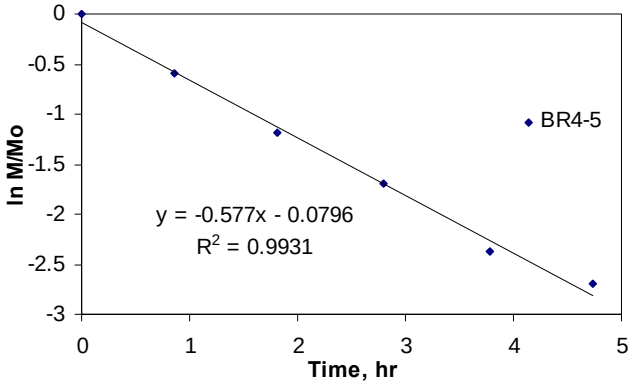

c) 1,1,1-TCA transformation following zero-order kinetics

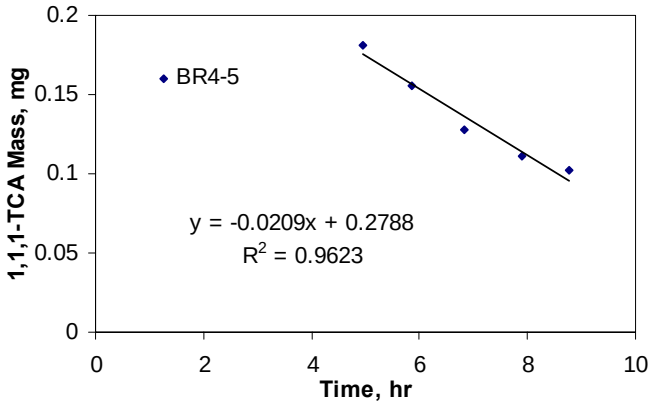

Table 20. 1,1,1-TCA Half-Saturation Constant (K_s) Determined in the BR4 Microcosm Set

a) The first and second additions of 1,1,1-TCA

Microcosm	Low C_l (µg/L)	High C_l (µg/L)	K_s (mg/L)
BR4-M	112	2394	0.306
BR4-1	110	2633	0.519
BR4-2	154	2615	0.480
BR4-3	120	2399	0.259
BR4-4	136	2543	0.464
BR4-5	139	2557	0.427
Average			0.430 ± 0.101

b) The third and fourth additions of 1,1,1-TCA

Microcosm	Low C_l (µg/L)	High C_l (µg/L)	K_s (mg/L)
BR4-M	89	1386	0.206
BR4-1	88	1663	0.365
BR4-2	102	1297	0.263
BR4-3	106	1326	0.186
BR4-4	58	1467	0.289
BR4-5	121	1381	0.276
Average			0.28 ± 0.064

Table 21. Average Values of Butane and 1,1,1-TCA Half-Saturation Constant Determined in All Microcosms

Microcosm	Butane K_s (mg/L)	1,1,1-TCA K_s (mg/L)
BR3 set	0.11 ± 0.014	0.37 ± 0.051
BR4 set	0.11 ± 0.012	0.35 ± 0114
BR4-M	0.07 ± 0.007	0.26 ± 0.07

Model Development

Kinetic parameters including the maximum specific rate of butane utilization ($k_{max,But}$) and 1,1,1-TCA transformation ($k_{max,TCA}$), cell decay rate (b), and/or transformation capacity (T_c) for non-augmented and bioaugmented microcosms test were determined through simulations of butane utilization and 1,1,1-TCA transformation, using the non-steady-state model described in Section 3. The results of microcosm studies in the BR3, BR4 and B4 bioaugmented microcosm sets and the BRC indigenous microcosm set were selected for these simulations.

Table 22. Measured Parameters for Model Development

Parameter	Microcosm			
	BR3 set	BR4 set	B4 set	BRC set
X_0, mg/L	0.47	0.45	unknown	unknown
Y, mg/mg	0.7	0.7	0.7	0.7
$K_{s,But}$, mg/L	0.11	0.11	0.11	0.11
$K_{s,TCA}$, mg/L	0.37	0.37	0.37	0.37
V_L, L	0.1	0.1	0.075	0.1
V_g, L	0.057	0.057	0.082	0.057
$H_{cc,But}$, mg-L/mg-L	38.05	38.05	38.05	38.05
$H_{cc,TCA}$, mg-L/mg-L	0.55	0.55	0.55	0.55

Measured parameters including initial biomass (X_0) in the bioaugmented microcosms, the mass of butane and 1,1,1-TCA added, butane and 1,1,1-TCA half-saturation constants ($K_{s,But}$ and $K_{s,TCA}$), cellular yield (Y), volume in liquid and gas phases (V_L and V_g), and Henry partition coefficient for butane and 1,1,1-TCA ($H_{cc,But}$ and $H_{cc,TCA}$) were not varied in the fitting exercise. These values are presented in Table 22. The values of $K_{s,But}$ and $K_{s,TCA}$ were obtained from the kinetic experiments previously described, while the value of Y was determined from growth studies with the frozen butane-utilizing culture. The unknown parameter values of the maximum specific rate of butane utilization ($k_{max,But}$) and 1,1,1-TCA transformation ($k_{max,TCA}$), cell decay rate (b), and/or transformation capacity (T_c) were varied using a heuristic approach to obtain a good fit between model predictions and experimental observations. The errors of unknown parameters were expressed in terms of standard deviation based on modeling of the five replicate microcosms.

4.3.2 The Simulation of Butane Utilization and 1,1,1-TCA Transformation in the BR3 Microcosm Set

Figure 43 presents the butane utilization data from microcosm BR3-5 and model simulations. The data was divided into 4 sections (A, B, C, and D). The A section presented the data from the first and second additions of butane, while the B, C, and D sections included the data from the third, fourth, and fifth additions of butane, respectively. The values of $k_{max,But}$ and b were varied to obtain a good fit between model predictions and experimental data shown in section A. The data of the other sections were then modeled using these values, once they were fixed.

Figure 43. Butane Utilization Data from Microcosm BR3-5

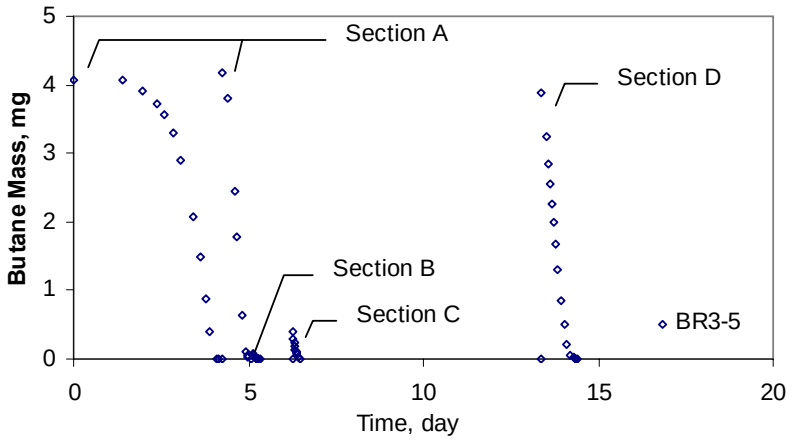

Figure 44. Simulation of Butane Utilization for Microcosm BR3-5

Simulation of butane utilization for microcosm BR3-5 for all additions of butane

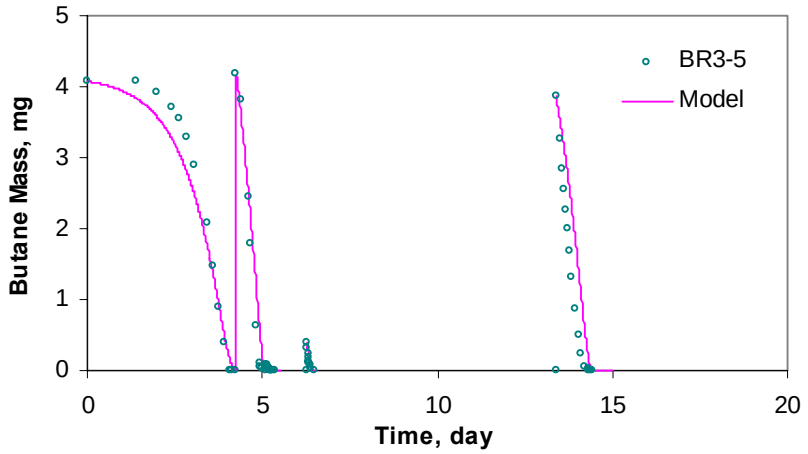

Section A: The first and second additions of butane from day 0 to 5

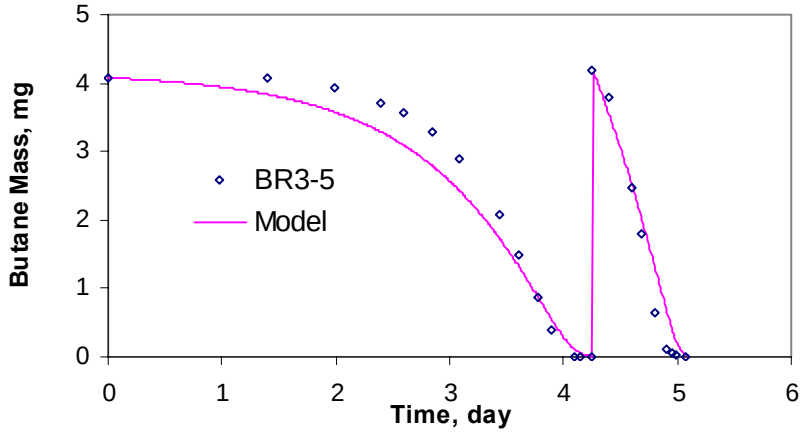

Section B: The third addition of butane on day 5

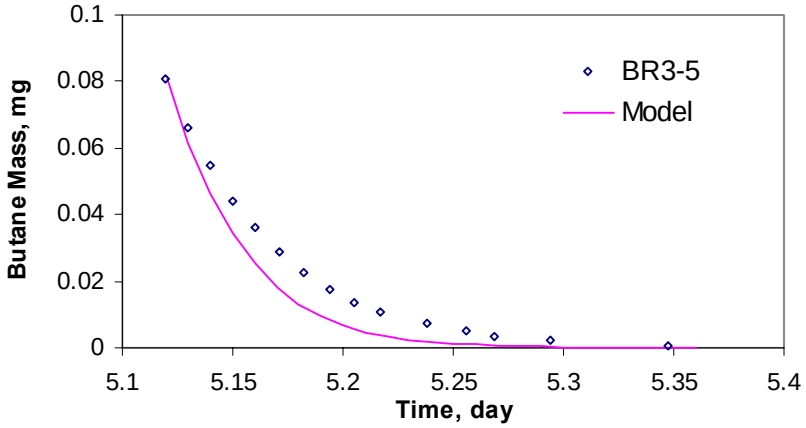

Section C: The fourth addition of butane on day 6

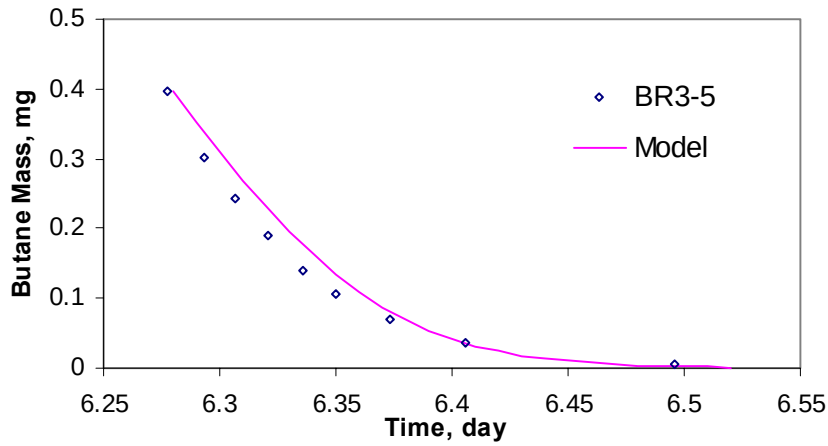

Section D: The fifth addition of butane from day 13.38 to 14.44

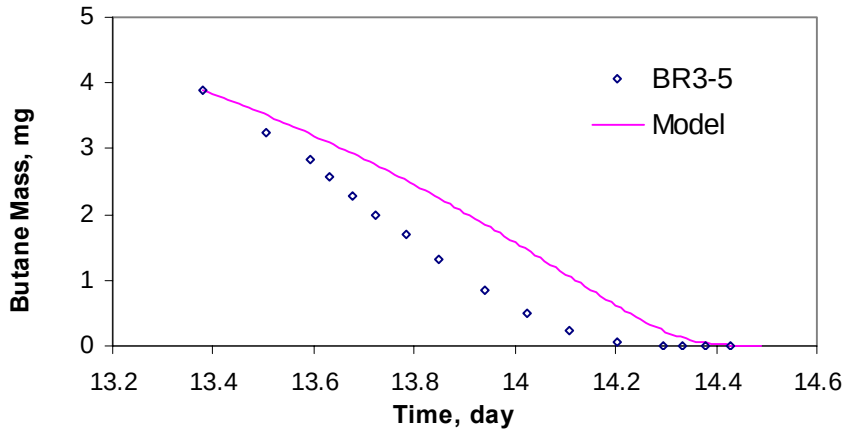

The simulation of butane utilization for microcosm BR3-5 is presented in Figure 44. The model fit data well at low concentration as well as high concentration. The initial concentration ranged from 35 to 1800 μg/L. The $K_{s,But}$ values obtained from the kinetic experiments provided good matches of the simulation to the microcosm results, as presented in section C. The model started deviating from the experimental data in section D. This probably results from fitting cell decay rate (b) with only early time data. Thus the value of cell decay rate (b) may have some error. The results from the model simulation for the other microcosms were similar (simulations not shown). The values for the butane maximum specific rate ($k_{max,But}$) and cell decay rate (b) of the BR3 bioaugmented microcosm set are shown in Table 23. Both values obtained from all microcosms were similar. This indicates the reproducibility of the bioaugmentation process. The average values for the butane maximum specific utilization rate ($k_{max,But}$) and cell decay rate (b) were 1.76 ± 0.023 mg/mg-day and 0.15 ± 0.006 day^{-1}, respectively.

Table 23. Butane Maximum Specific Rate ($k_{max,But}$) and Cell Decay Rate (b) Achieved in the BR3 Microcosm Set

Microcosm	$k_{max,But}$ (mg/mg-day)	b (day^{-1})
BR3-1	1.79	0.15
BR3-2	1.74	0.15
BR3-3	1.76	0.15
BR3-4	1.73	0.14
BR3-5	1.76	0.14
Average	1.76 ± 0.023	0.15 ± 0.006

The 1,1,1-TCA transformation data from microcosm BR3-5 presented in Figure 45 was also simulated. To simplify the modeling, the effect of transformation product toxicity was not considered. Similar to butane utilization modeling, the data were divided into 2 sections (E and F). The E and F sections presented the data from the first and second additions of 1,1,1-TCA. All parameters previously determined for butane were used in the simulation. The only unknown parameter was $k_{max,TCA}$. The variation of $k_{max,TCA}$ values was performed until the model best fit the data in section E of the figure. This value was then used to model section F.

Figure 45. 1,1,1-TCA Transformation Data from Microcosm BR3-5

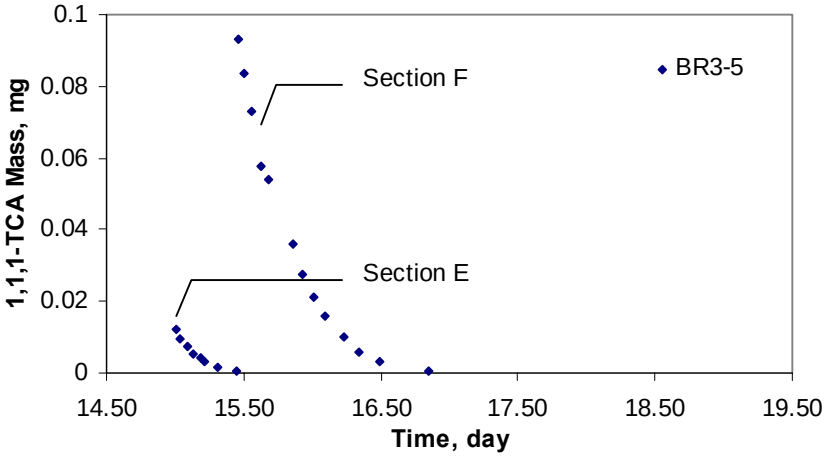

Figure 48 presents the simulation of 1,1,1-TCA transformation for microcosm BR3-5. A good fit between the model simulation and data is achieved in both sections of low and high concentrations. The initial concentration of data ranged from 90 to 750 μg/L. The 1,1,1-TCA maximum specific rate ($k_{max,TCA}$) values for microcosm set BR3 are shown in Table 24. All microcosms had similar values, except microcosm BR3-1, which had the lowest 1,1,1-TCA k_{max}. The $k_{max,TCA}$ values of microcosm set BR3 varied more than the $k_{max,But}$ values. The value of 1,1,1-TCA maximum specific rate ($k_{max,TCA}$) ranged from 0.05 to 0.12 mg/mg-day.

Figure 46. Simulation of 1,1,1-TCA Transformation for Microcosm BR3-5

Complete simulation of 1,1,1-TCA transformation for microcosm BR3-5

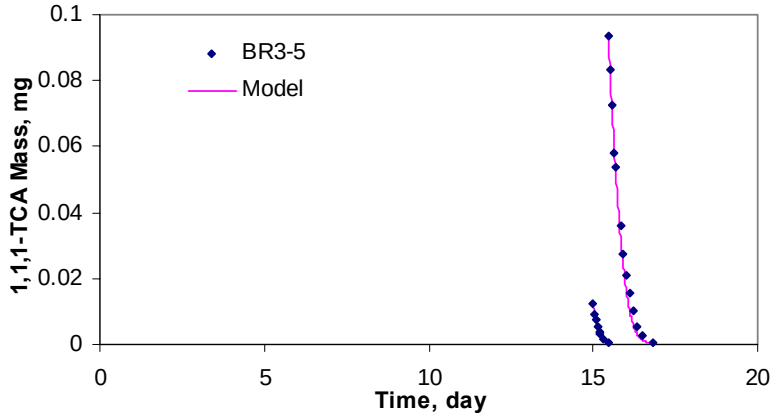

Section E: The first addition of 1,1,1-TCA on day 15

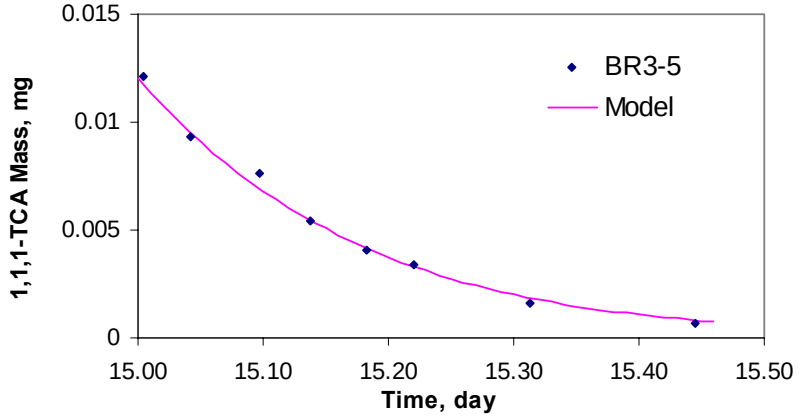

Section F: The second addition of 1,1,1-TCA from day 15 to 16

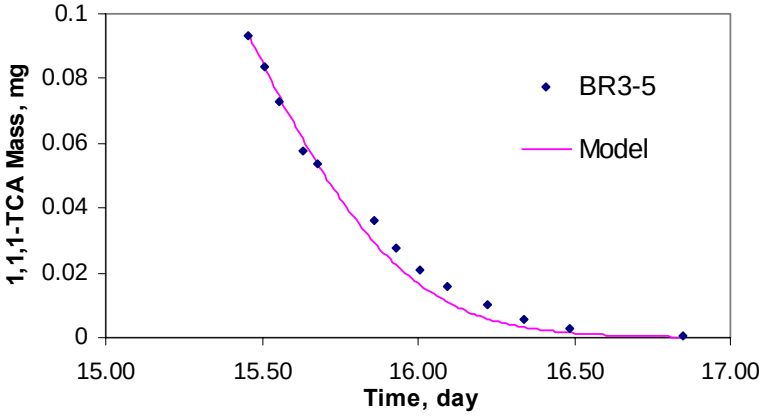

Table 24. 1,1,1-TCA Maximum Specific Rate ($k_{max,TCA}$) Achieved in the BR3 Microcosm Set

Microcosm	$k_{max,TCA}$ (mg/mg-day)
BR3-1	0.05
BR3-2	0.12
BR3-3	0.11
BR3-4	0.09
BR3-5	0.09
Average	0.09 ± 0.027

A good fit between model simulation and data at both low and high concentrations was achieved in all microcosms BR3-1 to BR3-5 (data not shown). The butane and 1,1,1-TCA data for microcosm BR-1 is shown in Figure 47. The deviation of model from the data occurred at late time. This is probably due to the error is the cell decay rate (b) that were obtained from fitting the data at early time. However, the reasonable fit between the model and experimental data from all microcosms was still obtained. This supports the model assumption that the effect of product transformation toxicity at the concentration tested was negligible, and the enzyme for 1,1,1-TCA transformation remained active for long time periods.

Simulations of 1,1,1-TCA transformation were also conducted to determine if inclusion of transformation capacity value (T_c) improved results. Values of T_c were varied to see if better fits were obtained.

Figure 47. Simulations of Butane Utilization and 1,1,1-TCA Transformation for Microcosm BR3-1 Without the Term for Transformation Capacity

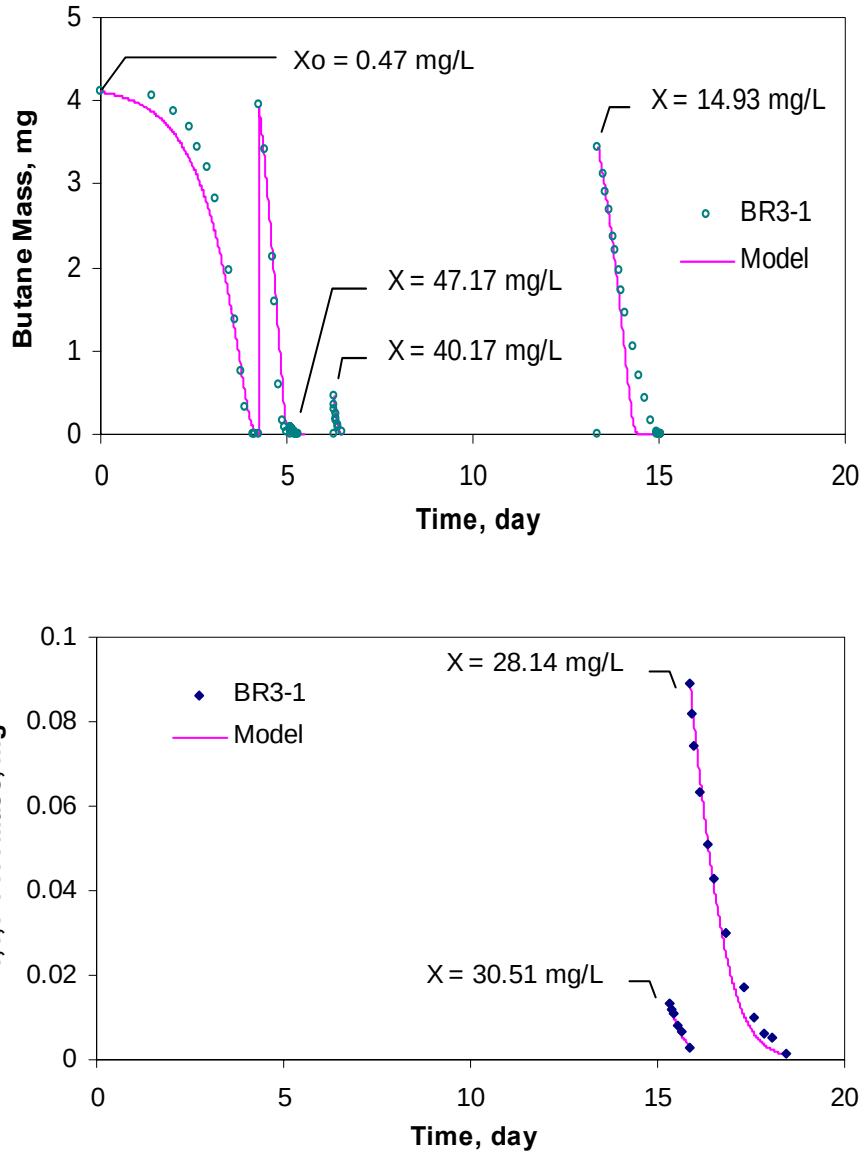

Figure 48. Simulations of 1,1,1-TCA Transformation for Microcosm BR3-5 over a Range of Transformation Capacities

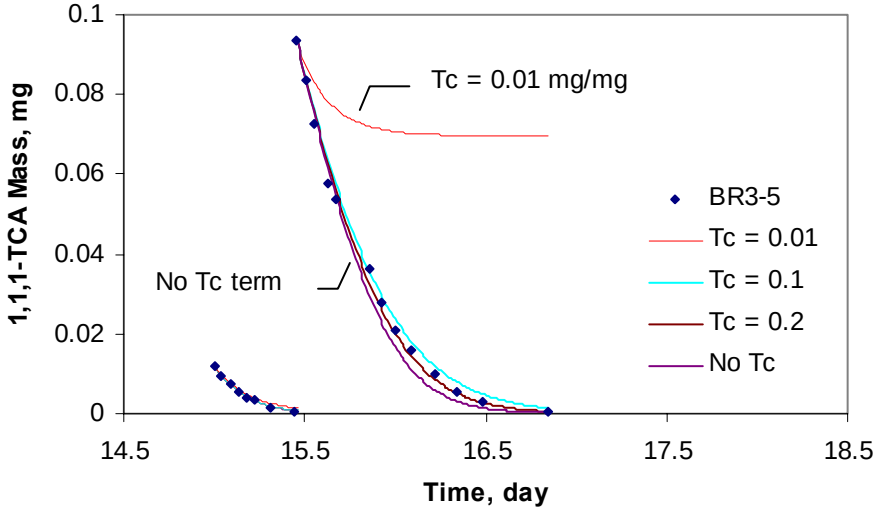

Section	Biomass (X) at starting of model simulation (mg/L)			
	$T_c = 0.01$	$T_c = 0.1$	$T_c = 0.2$	No T_c term
E	36.63	36.63	36.63	36.63
F	24.02	33.12	33.65	34.19

Figure 48 presents the results of model simulation over a range of transformation capacities along with the biomass (X) at starting of model simulation for microcosm BR3-5. The low T_c value of 0.01 mg 1,1,1- TCA/mg cell caused a significant decrease in biomass. Similar biomass values were obtained from simulations with $T_c \geq 0.1$ and those without a T_c term ($T_c = \infty$). Little improvement was obtained by including the transformation capacity term. The results from the data at low concentrations tested were not sensitive to the transformation capacity term. Thus fits to transformation capacity model were obtained from the data at high concentration. The maximum concentration of tested 1,1,1-TCA was approximately 700 µg/L. Even at these high concentrations there was little sensitivity to transformation capacity. Little sensitivity to transformation capacity was also due to the amount of biomass available, as illustrated in following calculations:

Initial biomass = $X_0 * V_l$
= (36 mg/L)(0.1 L)
= 3.6 mg cells

Mass of transformed 1,1,1-TCA = $C_l * V_l$
= (0.7 mg/L)(0.1 L)
= 0.07 mg TCA

Destroyed cells = Mass of transformed 1,1,1-TCA / T_c
= (0.07 mg TCA)/(0.1 mg TCA/mg cells)
= 0.7 mg cells << 3.9 mg cells

Compared to the initial biomass, the amount of destroyed cells was small. As a result, the simulation was not very sensitivity to the transformation capacity. A range of transformation capacity (T_c) values obtained from microcosm BR3 set are presented in Table 25 since there is little sensitivity to the transformation capacity. The average value of transformation capacity was 0.11 ± 0.064 mg 1,1,1-TCA/mg cell. All parameters used in the model simulation for microcosm set BR3 are presented in Table 26.

Table 25. Transformation Capacity Ranges (T_c) achieved in the BR3 Microcosm Set

Microcosm	Maximum $C_{l,TCA}$ tested (μg/L)	T_c (mg TCA/mg cells)
BR3-1	680	0.1 - 0.2
BR3-2	731	0.05 - 0.07
BR3-3	690	0.04 - 0.06
BR3-4	720	0.1 - 0.2
BR3-5	711	0.1 - 0.2
Average		0.11 ± 0.064

Table 26. Parameters for Model Development in the Br3 Microcosm Set

Parameter	Microcosm set BR3
X_0, mg/L	0.47
Y, mg/mg	0.7
b, day^{-1}	0.15 ± 0.006
$K_{s,But}$, mg/L	0.11
$k_{max,But}$, mg/mg-day	1.76 ± 0.023
$K_{s,TCA}$, mg/L	0.37
$k_{max,TCA}$, mg/mg-day	0.09 ± 0.027
T_c, mg /mg	0.11 ± 0.064

4.4 Microcosm Tests 1,1-DCE

The objectives of this study were to evaluate the cometabolic 1,1-DCE transformation abilities of indigenous and bioaugmented butane-utilizers in microcosms constructed with aquifer groundwater/soil originated from the Moffett Field site and to characterize the microbial community structures that develop in the microcosms.

The microcosms, consisting of aquifer solids, groundwater and air, were fed butane as a primary substrate and 1,1-DCE as a contaminant using methods previously described by Jitnuyanont et al (2001). Butane and 1,1-DCE concentration were monitored to evaluate cometabolic transformation efficiency. In some microcosms indigenous microorganisms present in the aquifer solids and ground water were stimulated. Other microcosms were bioaugmented with an enrichment culture known to actively cometabolize 1,1-DCE. At various times throughout the study, microcosm samples were obtained and subjected to terminal restriction fragment length polymorphism analysis (T-RFLP) of 16S rRNA genes, and evaluated for microbial community composition and potential microbial community changes due to 1,1-DCE transformation stress.

4.4.1 Results

Butane Utilization and 1,1-DCE Transformation

Triplicate bioaugmented microcosms were operated under three sets of experimental conditions. In one set, the microcosms were fed butane, but were never exposed to 1,1-DCE to evaluate what microbial community would develop post-bioaugmentation in the absence of 1,1-DCE transformation stress. Another set was fed butane and increasing doses of 1,1-DCE to evaluate the microbial community that developed under increasing 1,1-DCE transformation stress. A final set was pre-exposed to 1,1-DCE in the absence of butane to evaluate the resting cell transformation capacity of the bioaugmented culture. After 29 days of 1,1-DCE exposure, this set was fed butane to determine if butane-utilizing organisms were still viable, and if so, whether they were capable of 1,1-DCE cometabolism.

Microcosm set NB, made up of microcosms B5, B6 and B7, was bioaugmented with the butane-utilizing enrichment culture and received butane, but received no 1,1-DCE as co-substrate (Table 27). The microcosms received 68-71μmol of butane per feeding and had six repeated butane feedings over 199 days. Butane utilization occurred essentially without lag upon the first feeding, and rapid butane utilization occurred for all sequential feedings (Fig. 49). The general trend was similar for all triplicate microcosms. Samples were taken for microbial analysis from each microcosm before and after the third butane feeding and after the sixth feeding (Figure 49).

Figure 49. Butane Mass Histories in the Bioaugmented Microcosm Set NB, Fed Only Butane

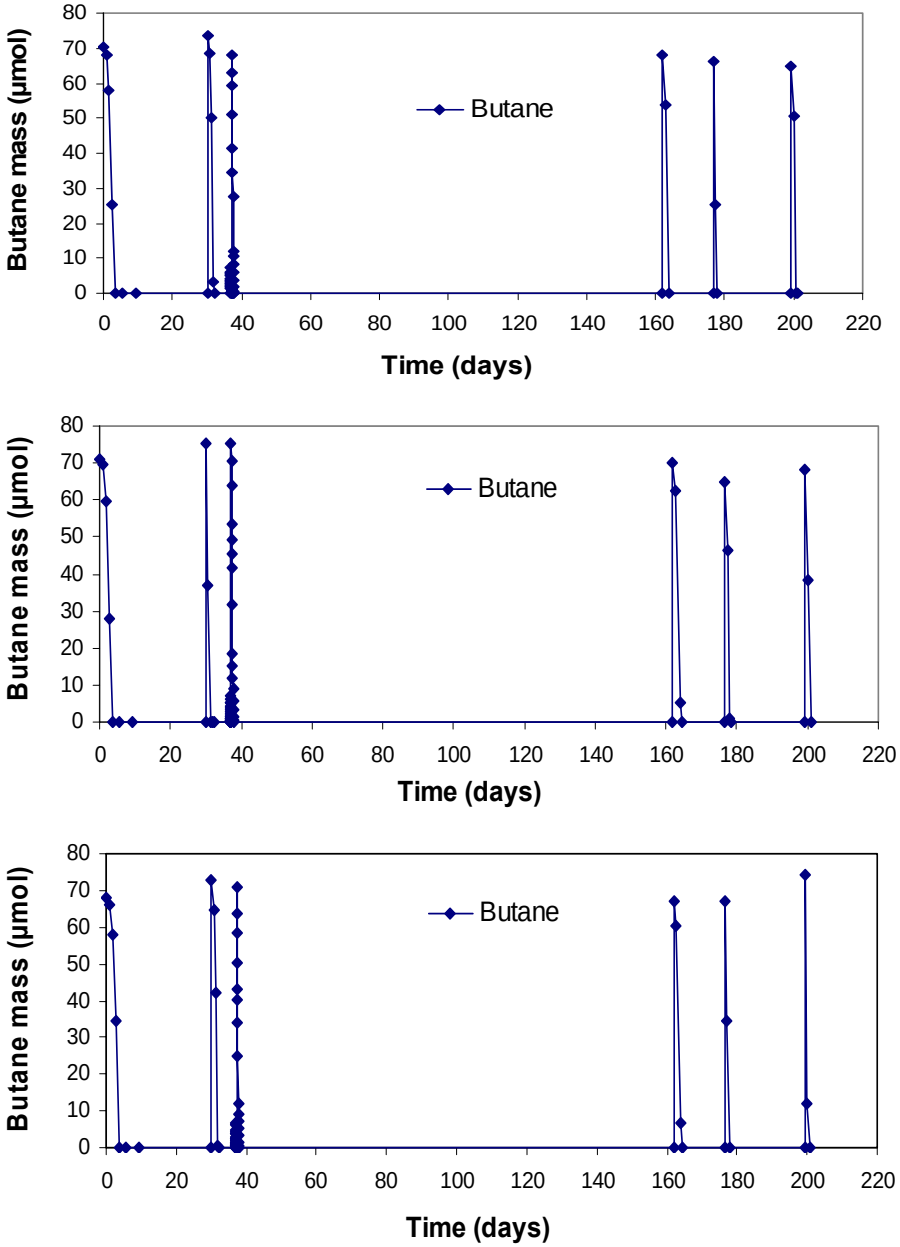

Triplicate microcosms B2, B3 and B4 made up microcosm set PEB and were bioaugmented with the butane-utilizing enrichment culture and exposed to the co-substrate 1,1-DCE in the absence of butane for 29 days to observe the effect of 1,1-DCE preexposure. Butane was added after 29 days of incubation to determine if butane utilizers were still present and active and to see if they maintained their ability to transform 1,1-DCE. The initial decrease in 1,1-DCE mass essentially stopped after the first few hours of exposure (Figure 50) with 89% of the initial 1,1-DCE mass remaining after 4 hours. This trend was reproducible in the triplicates; with reductions of 11%, 11%, and 13% of the initial 1,1-DCE mass in B2, B3, and B4, respectively. After 3 days, 77-79% of the initial 1,1-DCE mass remained in the microcosms and no significant change of 1,1-DCE mass occurred over the next 26 days.

Figure 50. Butane (closed symbols) and 1,1-DCE (open symbols) Mass Histories in the Bioaugmented Microcosms Set PEB, Pre-Exposed to 1,1-DCE with No Butane Initially Present

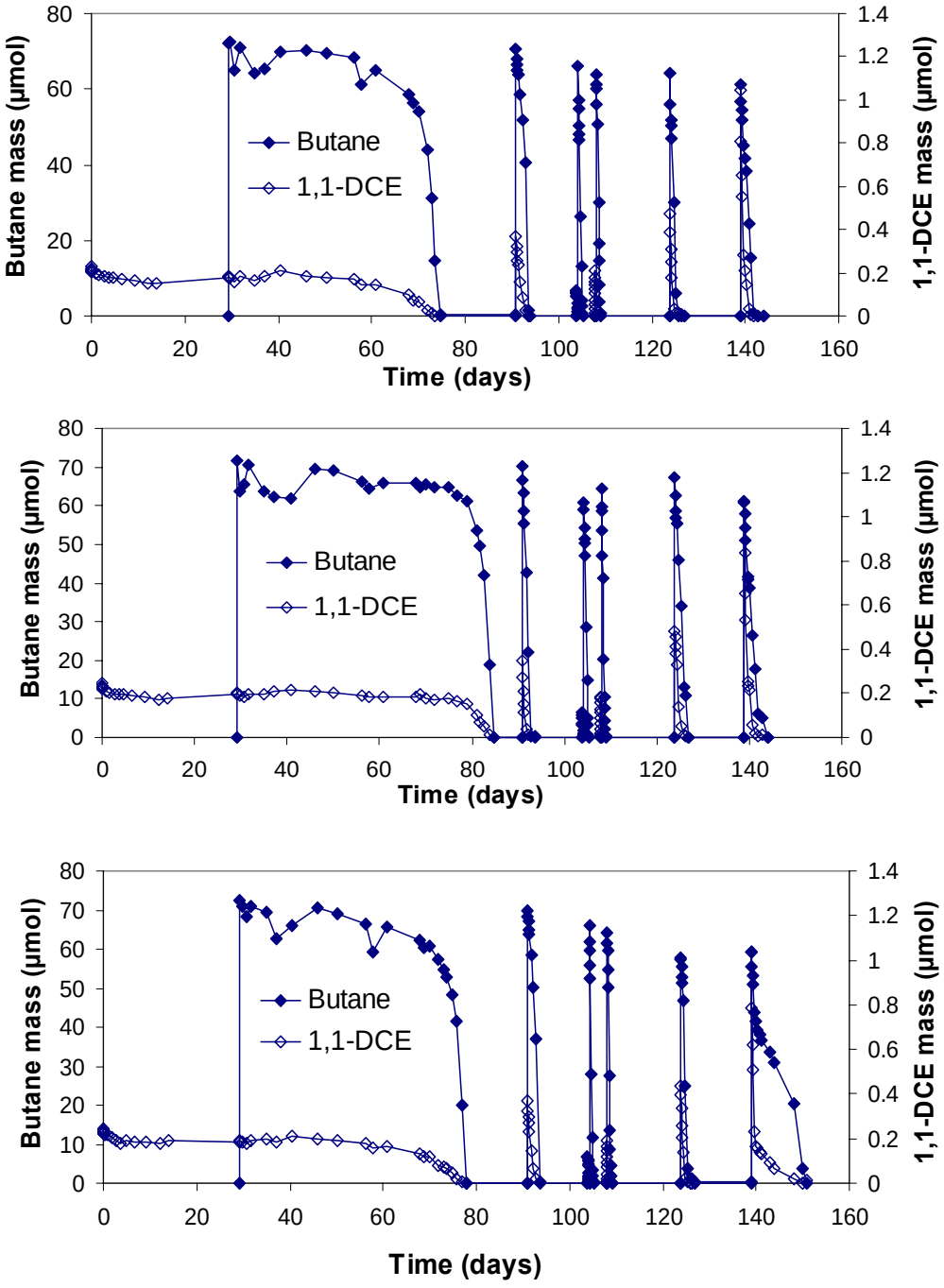

We cannot conclude that the initial rapid loss of 1,1-DCE was attributed to biotransformation of 1,1-DCE or sorption onto the aquifer solids; however, the mass transformed is in the range of the transformation capacity for 1,1-DCE estimated by Kim *et al* for their enrichment culture (2002). To test for cometabolism ability, butane (72-73µmol) was added on day 29. A lag time of 46 to 62 days was required for complete butane utilization in the microcosms. 1,1-DCE was concurrently transformed with butane with the complete removal of both substrates requiring the same amount of time. When compared to the results of microcosms not-exposed to 1,1-DCE (microcosm set NB), stimulation of butane utilizers in microcosm set PEB required greater lag times (Table 27). The long lag period suggests that 1,1-DCE transformation product toxicity may have greatly reduced the butane-utilizing microbial population as a result of extended exposure to 1,1-DCE in the absence of butane. However, the next addition of butane (70-71µmol) and 1,1-DCE (0.35-0.37µmol) on day 91 was completely removed within 3 days with subsequent feeding resulting in similar rapid removal. The 1,1-DCE dose was doubled on day 124 and doubled again on day 139, while butane feed remained constant. The increasing amounts of 1,1-DCE were effectively transformed in all three microcosms, with a longer time required in B4 at the highest 1,1-DCE concentration.

Microcosm set EB, containing triplicate microcosms B8, B9 and B10, were bioaugmented with the butane-grown mixed culture and simultaneously fed butane and 1,1-DCE (Table 27). Five butane feedings (70 µmol) were performed over 70 days, while the 1,1-DCE dose ranged from 0.17µmol to 1.99µmol (Figure 51). As shown in Table 1, a shorter lag period for 1,1-DCE transformation and butane utilization was observed here compared to the 1,1-DCE pre-exposed microcosm set PEB (Figure 50).

Table 27. Microcosm Conditions and Lag Times to 50% Butane Removal

Microcosm	Description of test	Substrate	Time (days)
Set PEB: B2, B3 & B4	Bioaugmented microcosms pre-exposed to 1,1-DCE, with butane added after 29 days of incubation.	Butane & 1,1-DCE	48 ± 6
Set EB: B8, B9 & B10	Bioaugmented microcosms exposed to 1,1-DCE and butane simultaneously.	Butane & 1,1-DCE	10.9 ± 2.3
Set NB: B5, B6 & B7	Bioaugmented microcosms fed butane with no exposure to 1,1-DCE.	Butane	2.6 ± 0.2
Set EI: I6, I7 & I8	Non-bioaugmented microcosms exposed to 1,1-DCE and butane simultaneously.	Butane & 1,1-DCE	>25

In microcosm set EB the amount of 1,1-DCE was gradually elevated to eight times the initial dose (0.25 to 2.0 µmol). The rate of butane utilization and 1,1-DCE transformation increased with repeated exposures to butane and 1,1-DCE, and this trend was very reproducible and consistent in the triplicate microcosms. Among triplicates, microcosm B10 performed best in transforming 1,1-DCE, with a maximum transformation yield was 0.025 µmol 1,1-DCE/µmol

butane (0.042 mg 1,1-DCE/mg butane). The triplicate microcosms showed similar responses for the last exposure with not all of the 1,1-DCE or butane transformed.. In microcosm B10, butane consumption and 1,1-DCE transformation was observed after day 266,, while no butane or 1,1-DCE removal was observed in B8 and B9 (data is not shown), indicating that high concentrations of 1,1-DCE were able to interrupt and possibly irreversibly inactivate 8.5
butane utilization in the microcosms.

Figure 51. Butane (closed symbols) and 1,1-DCE (open symbols) Mass Histories in the Bioaugmented Microcosm Set EB, Exposed to 1,1-DCE and Butane Simultaneously

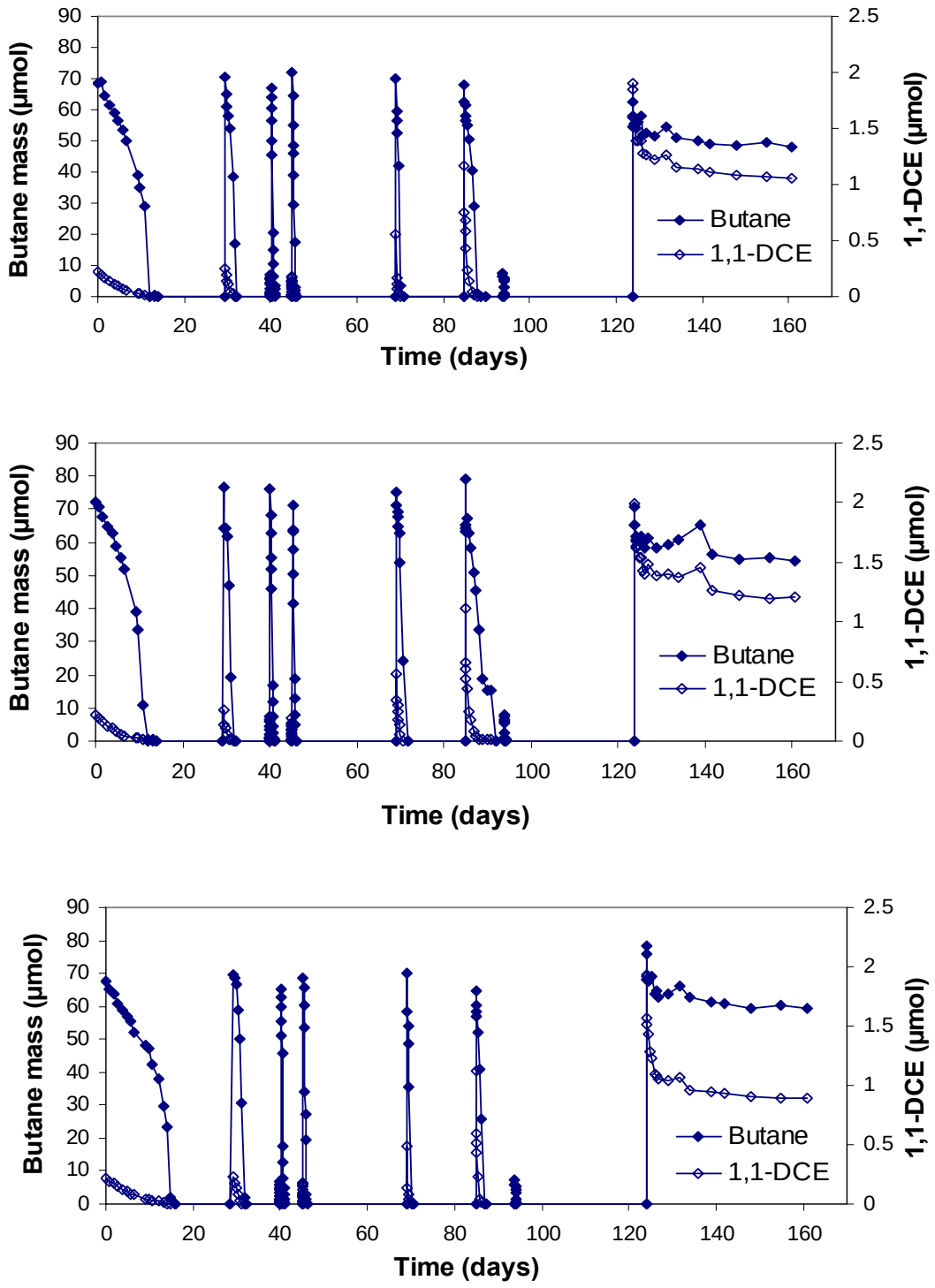

The results obtained with the non-bioaugmented microcosm set EI are shown in Figure 52. Microcosms I6, I7, and I8 were simultaneously fed butane and 1,1-DCE. The lag time required for butane utilization and 1,1-DCE transformation was between 25 to 60 days. Unfortunately, sampling errors disrupted data collection during this period. However, the lag period was longer than that observed in similarly treated bioaugmented microcosms (~ 11 days). The maximum transformation yield of 0.0043 µmol 1,1-DCE/µmol butane was significantly less than that achieved in the bioaugmented microcosms (0.025 µmol 1,1-DCE/µmol butane). 1,1-DCE was also concurrently transformed with butane in these microcosms, but transformation was not as well replicated among triplicate microcosms as observed in the bioaugmented microcosms. Butane utilization also appeared to be more inhibited at lower 1,1-DCE concentrations than in the bioaugmented microcosms.

Figure 52. Butane (closed symbols) and 1,1-DCE (open symbols) Mass Histories in Non-Bioaugmented Microcosm Set EI, Exposed to 1,1-DCE and Butane Simultaneously

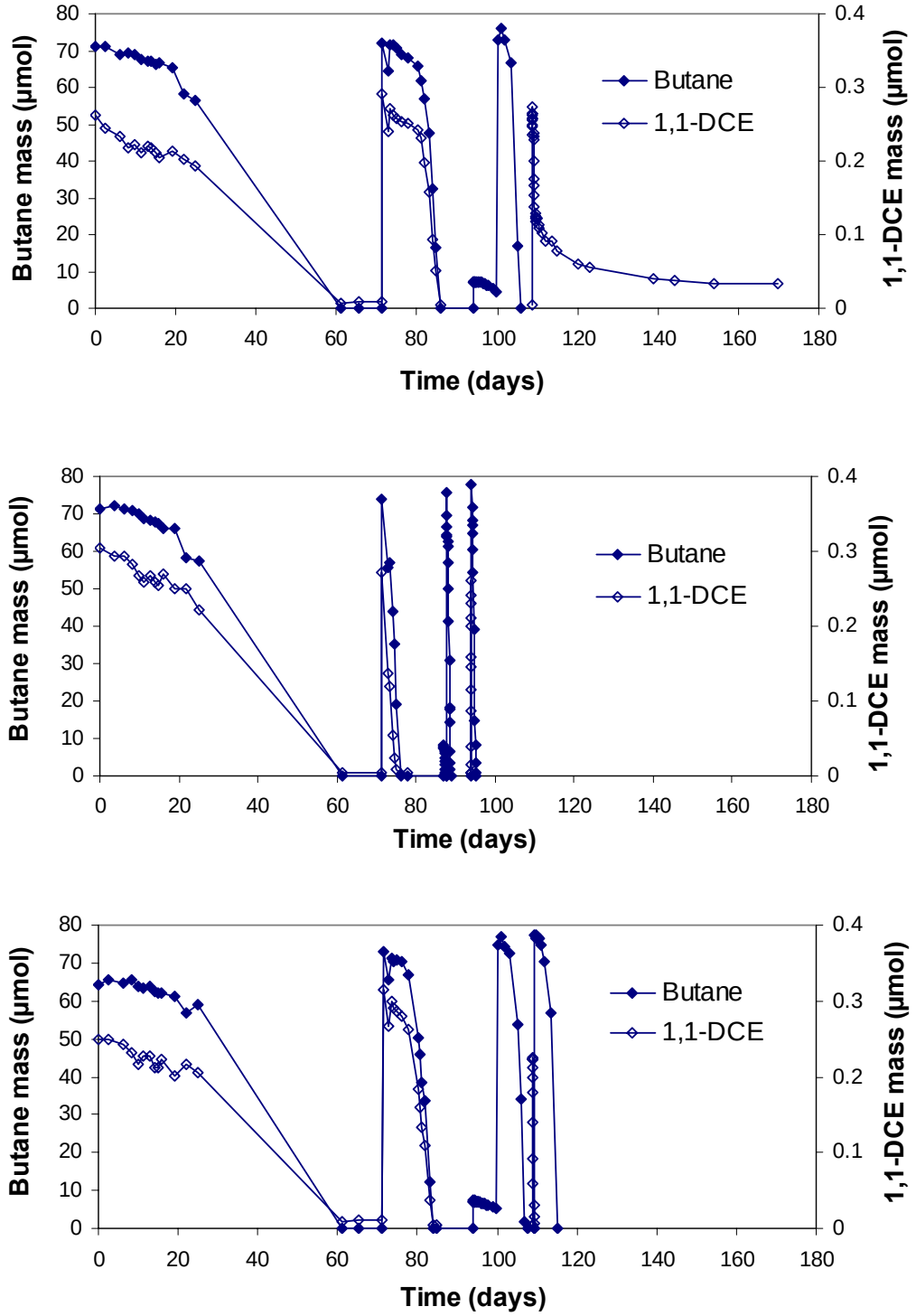

Characterizing Microbial Community Shifts Using T-RFLP Analyses

Comparison of major T-RFLs in the source culture, the bioaugmentation culture used to bioaugment the microcosms, and the indigenous aquifer samples is shown in Table 28. The bioaugmentation culture was grown on butane in mineral media from the source culture. A T-RFL of 167 BP is present in the three cultures and a T-RFL of 183 BP is shown only in the source culture and bioaugmentation culture. T-RFL of 169.7 BP is uniquely present only in the indigenous aquifer sample.

Table 28. Comparison of T-RFLs in the Source Culture, Bioaugmentation Culture, and Indigenous Aquifer Samples

T-RFL (base pair)	Source culture (%) *	Bioaugmented culture (%) **	Indigenous (%) ***
40.79	-	6.26	-
41.60	-	4.68	-
42.67	-	5.01	-
46.40	-	0.77	-
47.43	1.14	-	-
48.21	-	-	3.21
51.44	-	4.78	-
63.72	-	3.48	
67.34	-	0.92	-
99.16	1.86	-	-
100.46	-	2.27	-
131.79	-	0.85	-
167.22	4.67	10.21	2.35
168.63	-	-	0.85
169.73	-	-	40.52
173.10	-	-	1.65
178.97	35.13	1.58	-
183.24	1.37	14.86	-
184.36	1.71	-	-
206.51	-	0.88	-
207.60	0.49	26.34	-
210.60	2.8	4.61	-
211.23	-	-	2.44
212.78	-	-	0.90
213.43	-	-	2.85
237.55	-	-	2.39
239.61	-	-	2.26
251.00	-	-	1.75
253.69	-	-	2.84
255.21	-	-	2.06
275.55	-	1.08	-
276.61	42.98	6.44	-
277.28	-	-	6.24
278.49	-	-	2.26
279.46	-	3.84	13.45
281.53	-	1.14	12.81
283.51	-	-	4.01

* DNA extraction from the source culture.
** DNA extraction after growth of the source culture on butane.
*** DNA extraction from the microcosm aquifer solids and groundwater.

Slurry samples for microbial community analysis were taken at selected times as indicated by the arrows in Fig. 1, 2, 3 and 4. Results of T-RFLP analyses with MnlI digests are shown in Figure 53 for the bioaugmented microcosm B5 from microcosm set NB fed only butane. The size of the 169.7 BP peak decreases with time, while the peak at 183 BP becomes more dominant with the sequential utilization of butane. A similar trend was also observed in samples from microcosms B6 and B7. The bioaugmented microorganism(s) corresponding to the T-RFL of 183 BP peak appears to play an important role in butane utilization.

Electropherograms produced from samples taken from bioaugmented microcosm B2 which was pre-exposed to 1,1-DCE (set PEB) are shown in Figure 54. The initially dominant 169.7 BP peak became smaller while a T-RFL of 179 BP became dominant after butane was utilized and 1,1-DCE transformed. Microcosm B4 showed a similar pattern to microcosm B2. Microcosm B3 produced a different pattern with the T-RFL at 277.7 BP becoming dominant after butane was utilized and 1,1-DCE transformed. This peak dominated in further treatments with higher doses of 1,1-DCE. No T-RFL of 183 BP was observed in any profiles from 1,1-DCE pre-exposed microcosm set PEB, indicating that microorganisms corresponding to 183 BP were not likely responsible for 1,1-DCE cometabolism in these microcosms. In microcosms fed only butane the 183 BP peak dominated in all triplicate microcosms samples (Figure 53), while in those pre-exposed to 1,1-DCE peaks at 179 BP and 277.7 BP dominated.

Figure 53. Electropherograms from the MnII Digests of Samples from the Bioaugmented Microcosm B5 that was Fed Butane and Not Exposed to 1,1-DCE

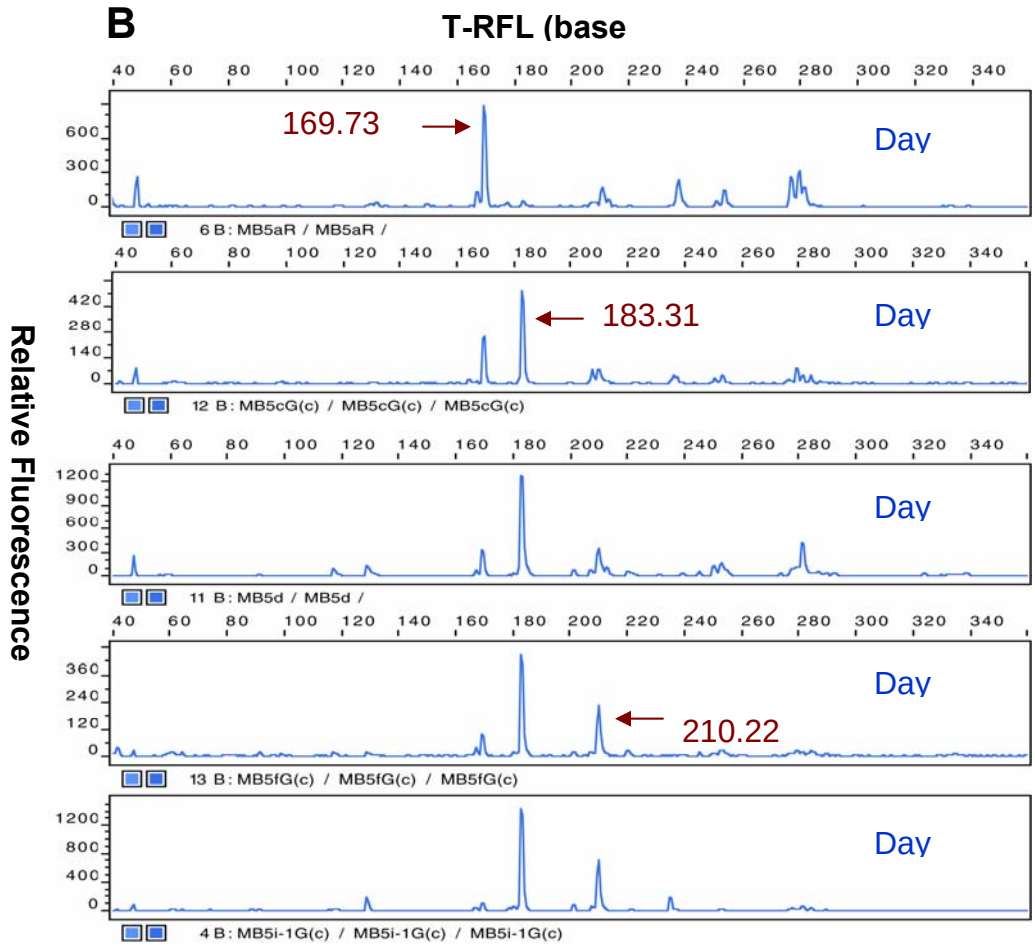

Figure 54. Electropherograms from the MnlI digests of samples from the bioaugmented microcosm B2 that was pre-exposed to 1,1-DCE.

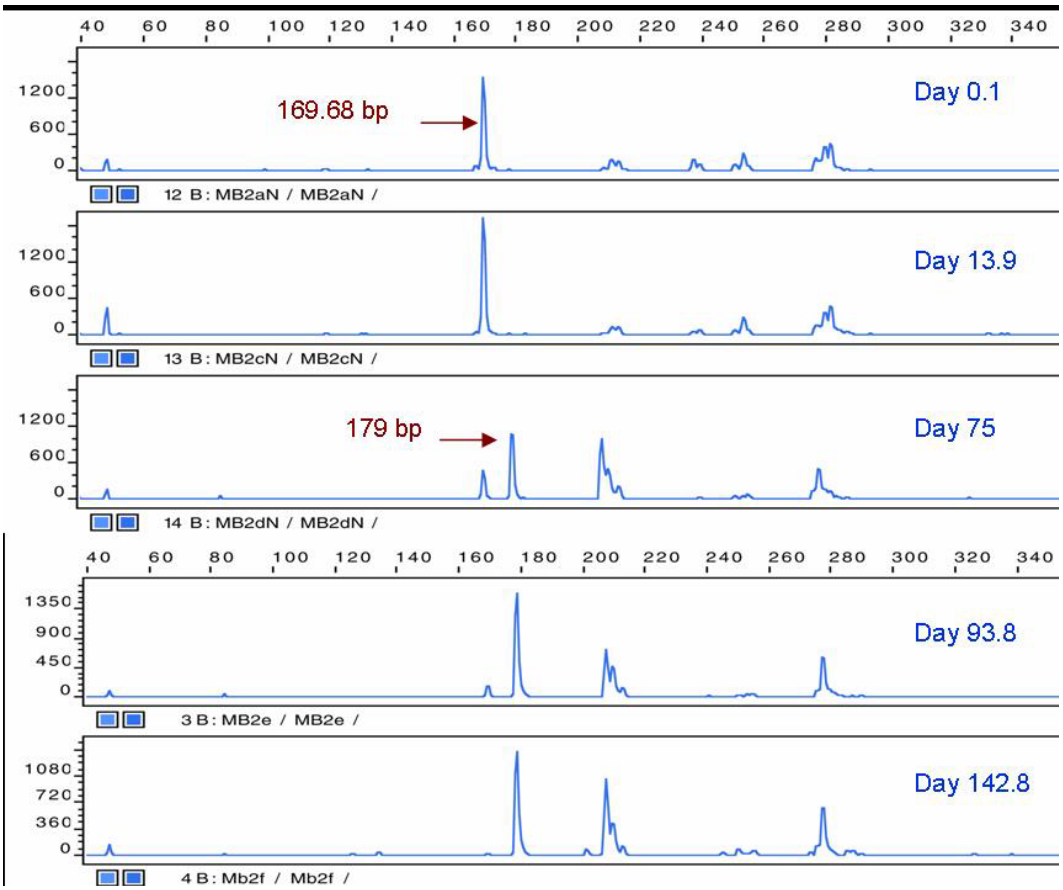

Figure 55 shows the electropherograms for microcosm B8 from set EB that was bioaugmented and simultaneously fed butane and 1,1-DCE. Prior to significant butane utilization or 1,1-DCE transformation (day 0.1) the 169 BP peak dominated. A peak at 183 BP became dominant with successive stimulations with butane and 1,1-DCE although other peaks were also consistently present such as the peak at 179 BP.

Figure 55. Electropherograms from the MnII Digests of Samples from the Bioaugmented Microcosm B8 that was Simultaneously Exposed to 1,1-DCE and Butane

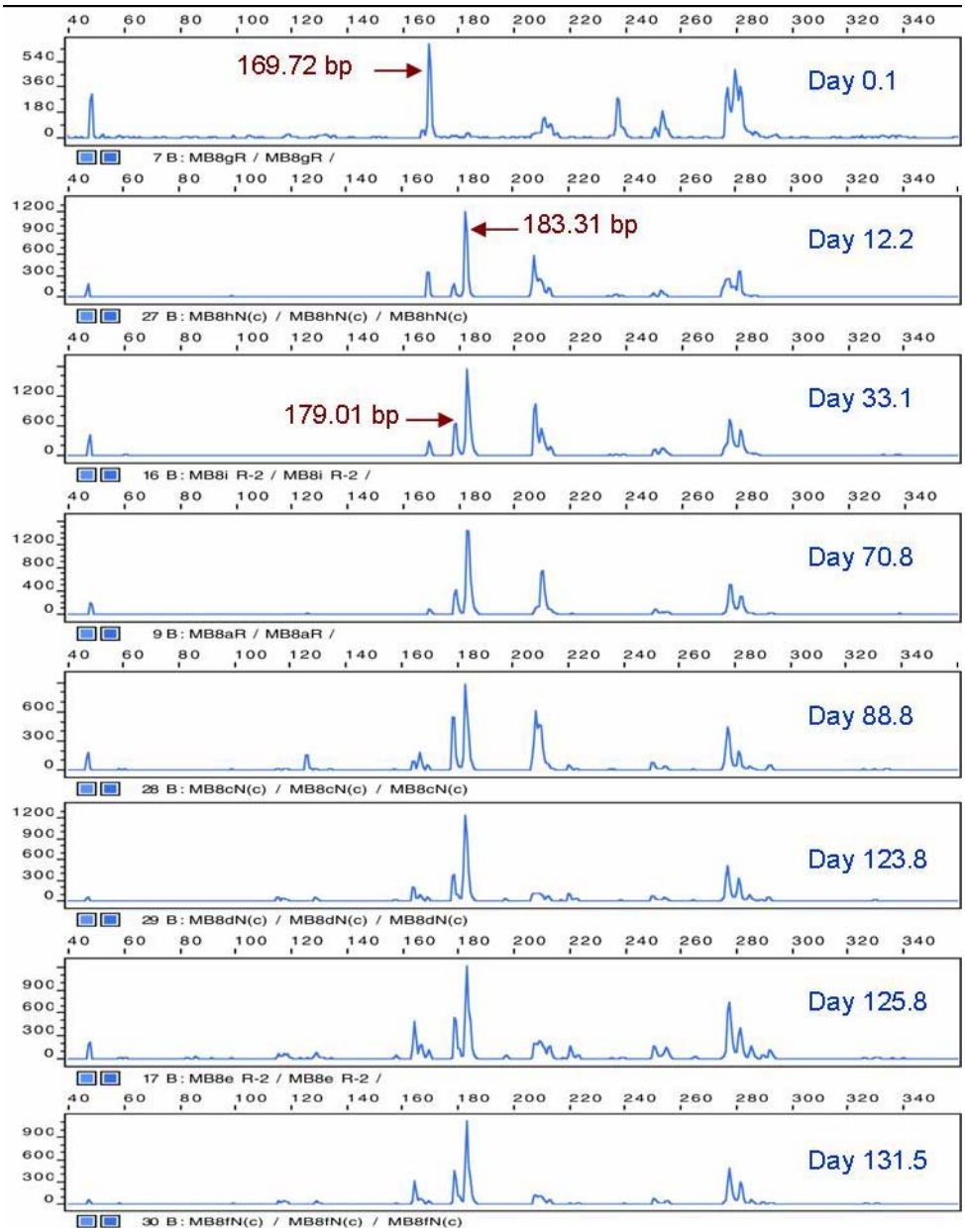

Microbial profiles produced from samples taken from microcosms B9 and B10 showed similar patterns as microcosm B8 with only minor differences. In microcosm B9, the 210 BP peak accounted for 30% of the total peak area, while the 183 BP peak represented 26% on day 94 (Data is not shown). The 179 BP peak was not found in microcosm B9 samples. After extended incubation resulted in the complete transformation of the highest level of 1,1-DCE in microcosm B10 (day 266) a 207.7 BP peak became dominant. A T-RFL of 207.7 BP was also present in the source culture and a clone with that T-RFL was found similar to *Hydrogenophaga* sp. Unfortunately, samples for T-RFLP analysis were not taken from microcosms B8 and B9 at this time for comparison purposes.

The non-bioaugmented microcosm set EI did not produce consistent microbial profiles in the triplicate microcosms. A 85 BP fragment dominated the profile in microcosm I6, a 277.9 BP fragment dominated microcosm I7, and a 207.5 BP fragment dominated in microcosm I8 (Figure 56). All three fragments were present in each of the microcosms, but appeared to be present in variable quantities. Although T-RFLP is not strictly a quantitative analysis, the similarity of results for the other microcosms give credence to differing microbial compositions in the indigenous microcosms. The different 1,1-DCE transformation efficiencies observed in microcosms I6 and I8 relative to I7 (Figure 52) may have been the result of enrichment of different microcorganisms. This microcosm set was not as efficient at 1,1-DCE cometabolism as either of the bioaugmented microcosm sets PEB or EB.

Figure 56. Electropherograms from the MnII Digests of Samples from the Non-Bioaugmented Microcosms that were Simultaneously Exposed to 1,1-DCE and Butane

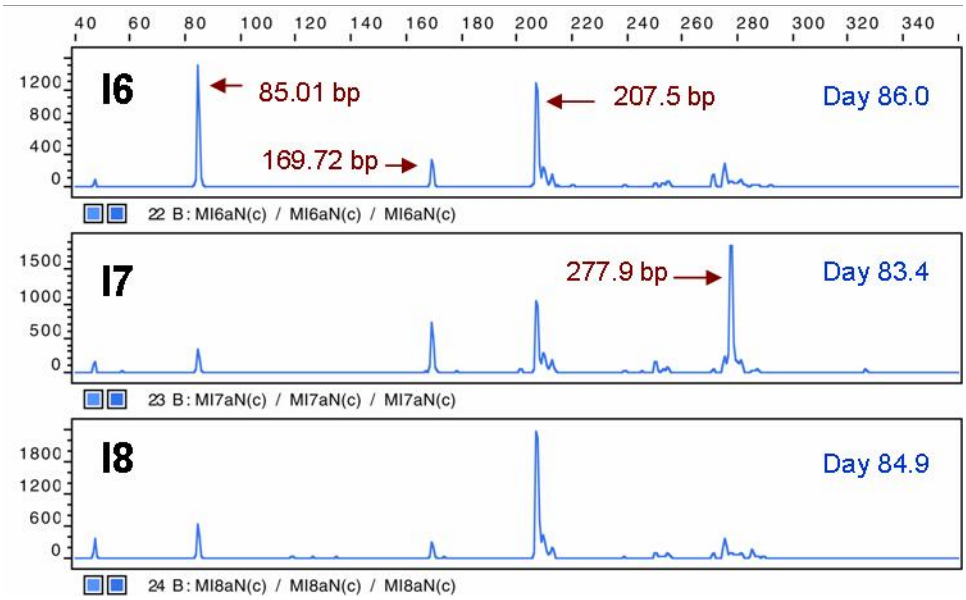

A summary of the terminal fragment lengths and percent of total peak areas found in samples after utilization of two additions of butane with various exposures to 1,1-DCE are presented in Table 29. The 183 BP represents the greatest fractional peak area of the bioaugmented microcosm set NB with no-exposure to 1,1-DCE. T-RFs of 183 BP and 207 BP were the major fragments found in the bioaugmented microcosm set EB, which were exposed to 1,1-DCE in the presence of butane. Bioaugmented microcosms which were pre-exposed to 1,1-DCE in the absence of butane produced major fragments at 179 BP or 277 BP, while the non-bioaugmented microcosm set EI showed a dominant peak at 207.7 BP. No peaks were observed at 183 BP in non-bioaugmented microcosms.

Table 29. Summary of the Fragments from the T-RFLP Analysis for the Bioaugmented and Indigenous Microcosms after Two Additions of Butane

T-RFL (bp)	[1]PE(B) (% peak area)			[2]E(B) (% peak area)			[3]NE(B) (% peak area)			[4]E(I) (% peak area)		
	B2	**B3**	**B4**	**B8**	**B9**	**B10**	**B5**	**B6**	**B7**	**I6**	**I7**	**I8**
47.6	1.1	2.5	1.5	2.1	3.3	2.0	2.3	1.3	2.1	1.0	1.2	2.8
58.7								0.6				
60.6								0.8				
74.3								0.4				
84.9	0.7	2.7								22.1	3.7	6.9
91.6									0.7			
117.5							1.5	2.3	5.7			
118.7								1.7	2.2			0.7
126.7												0.6
129.2							2.1	4.0	2.1			
130.1							1.5	1.6	1.4			
158.6								0.6				
167.5							1.7	2.3	1.4			
169.6	3.5	3.4	5.5	3.1	7.9	3.4	6.7	4.9	4.5	6.7	10.7	4.2
179.0	32.6	2.2	35.4	7.4	3.7	8.1						
180.5								1.4	1.4			
183.3				24.1	22.5	16.5	29.2	19.8	16.2			
201.6							1.7				1.0	
207.6	18.3	7.8	11.2	13.7	12.9	19.5	2.1	4.8	3.4	31.6	17.3	42.1
210.1	12.7	7.3	13.0	10.1	10.2	8.8	9.8	1.4	8.3	8.2	7.4	10.3
210.8						3.9						
211.7								2.2	0.6			
213.2	4.1	3.8	4.9	3.0	4.4	3.4	2.9	3.4	3.4	4.4	4.4	4.2
220.5							1.1	1.2	1.4			
221.8									1.0			
238.1									1.0			
245.4							1.2		0.9			
250.7				1.9	1.5	1.9	3.7	7.1	5.1	1.4	2.9	2.0
253.4		2.1	1.6	2.4	2.2	2.5	4.8	1.9	3.9	1.2	1.3	1.1
255.0	1.8		2.0	1.4	1.4		2.6	3.9	1.3	2.5	1.7	2.6
255.3									1.8			1.5
271.6										3.4	0.8	7.2
275.7	1.6		1.6	1.7	1.8	1.5				8.1	3.7	
275.8						1.5						
276.7	2.0		1.9	2.4	2.2							
277.7	16.0	65.6	15.2	11.8	9.9	14.8		4.4		1.0	37.4	
278.2							3.0		3.3	3.3		4.0
279.5	3.7		3.5	3.1	3.3	4.2	1.6	2.0	1.6			
280.0							3.7	2.5	4.4	1.8		1.6
281.5	2.0	2.6	2.6	9.6	10.1	8.3	12.6	11.8	11.2	3.1	4.5	2.9
284.8				1.2	1.6							
285.6								4.3	1.2			3.0
286.9				1.0	1.1							
287.2							2.2		1.6		1.2	1.0
289.7								2.1	1.3			1.2
292.4							2.0	0.6	1.9			
292.7								1.2				
324.1								1.6	1.1			
326.8											0.9	
332.9								1.9				
338.7									2.5			

Portion of each fragment to total peak area was calculated in percentage after ~140 μmol of butane utilization except fpr B5, B6, and B7. For microcosms B5, B6, and B7, the T-RFLP results after ~280 μmol of butane utilization were compared.

[1]PE(B): Bioaugmented microcosms were pre-exposed to 1,1-DCE with butane added after 29 days of incubation.

[2]E(B): Bioaugmented microcosms were exposed to 1,1-DCE along with a growth substrate.

[3]NE(B): Bioaugmented microcosms were fed butane with no exposure to 1,1-DCE.

[4]E(I): Non-bioaugmented microcosms were exposed to 1,1-DCE butane as a growth substrate.

4.4.2 Discussion

The microcosm studies demonstrated that both indigenous and bioaugmented butane utilizers could be stimulated in Moffett Field microcosms. Both bioaugmented and native butane utilizers were capable of cometabolizing 1,1-DCE. The lag period was much greater in the non-bioaugmented microcosms (indigenous microorganisms) simultaneously exposed to 1,1-DCE than in bioaugmented microcosms. The bioaugmented microcosms not exposed to 1,1-DCE had essentially no lag period to butane utilization (2.6 days), while bioaugmented microcosms simultaneously exposed to butane and 1,1-DCE had lags of approximately 11 days and those pre-exposed to 1,1-DCE and then fed butane had lag periods around 50 days. The longer lag periods likely resulted from 1,1-DCE transformation toxicity, with the presence of butane appearing to attenuate the toxic effects. Triplicate microcosms showed very reproducible lag periods and rates of butane consumption and 1,1-DCE transformation. Some differences resulted with prolonged stimulation and increases in 1,1-DCE concentration. For example, the best 1,1-DCE transformation ability was achieved in bioaugmented microcosm B10, with a T_y of 0.025 µmol 1,1-DCE/µmol butane (0.042 mg 1,1-DCE/mg butane). T-RFLP analysis also showed differences in the microbial communities resulting from bioaugmentation and operation under different environmental conditions.

In the non-bioaugmented microcosms fed butane and 1,1-DCE simultaneously, T-RFLs of 81 BP, 207.5 BP, or 277.9 were fairly dominant. A T-RFL of 183 BP was clearly dominant in the bioaugmented microcosms stimulated by butane alone and reasonably dominant in bioaugmented microcosms stimulated simultaneously with butane and 1,1-DCE. The microorganism represented by the 183 BP T-RF was likely associated with butane utilization and 1,1-DCE transformation. Microbial profiles in microcosm set PEB, pre-exposed to 1,1-DCE, were significantly different from those stimulated simultaneously with butane and 1,1-DCE. The 183 BP T-RFL was not presented in the pre-exposed microcosms, but instead, a T-RFL of 179 BP was dominant in microcosms B2 and B4 microcosms and a 277.8 BP peak was dominant in B3. One possible explanation is that product toxicity from 1,1-DCE transformation caused a shift in the microbial community. In studies of van Hylckama Vlieg et al. (1997), the cell activity and viability rapidly decreased during transformation of 1,1-DCE. Cell death was the predominant toxic effect resulting from 1,1-DCE rather than cell inactivation (van Hylckama Vlieg *et al*., 1997). Since acyl chlorides are generated upon the rearrangement or hydrolysis of the epoxides of 1,1-DCE and TCE, acyl chlorides may be the reactive products that cause the loss of viability. These are highly electrophilic compounds that can alkylate nucleophilic groups in nucleic acids and proteins and thus inhibit essential metabolic processes (van Hylckama Vlieg *et al*., 1997). Reactivation of the microbial populations would likely require growth of new cells rather than reactivation of inactivated cells. This loss in cell viability was indicated by the extended lag times to butane utilization and 1,1-DCE transformation in microcosms pre-exposed to 1,1-DCE.

The bioaugmented butane utilizers were capable of transforming greater amounts of 1,1-DCE than the indigenous butane utilizers. An organism(s) with a T-RFL of 183 BP, present in the bioaugmented culture, was generally dominant in all bioaugmented microcosms not pre-exposed to 1,1-DCE indicating that the bioaugmented microorganisms successfully out-competed indigenous microorganisms for the supplied butane, a necessary component of bioaugmentation required for effective bioremediation of 1,1-DCE.

Since the T-RFLP method is not able to differentiate at the species level, and since the method is not able to distinguish between multiple organisms with the same T-RFL, only general microbial community differences can be assessed. Furthermore, the biases attributed to PCR-based molecular analysis can also be important. However, in spite of these shortcomings, several conclusions can be drawn from this work. T-RFLP analysis was able to track microbial community shifts during stimulation with butane and 1,1-DCE, and to show the presence of bioaugmented microorganisms. The T-RFLP results showed good similarity among microcosm replicates. Since T-RFLP was successfully used to track certain bioaugmented microorganisms, it may be possible to determine the fate of bioaugmented microorganisms in the field using this method. T-RFLP may also be combined with more quantitative methods for tracking specific microorganisms such as fluorescence in-situ hybridization (FISH) analysis or real time quantitative PCR.

In this study, bioaugmentation reduced the lag period to butane utilization and 1,1-DCE transformation and enhanced 1,1-DCE cometabolism. High 1,1-DCE transformation yields were achieved in the bioaugmented microcosms and bioaugmented microcosms were maintained for over 200 days with successive feedings of butane and increasing 1,1-DCE concentrations. Similar microbial communities resulted in bioaugmented microcosms initially exposed to butane alone and those exposed to butane and 1,1-DCE, with a dominant T-RF of 183 BP observed. 1,1-DCE transformation product toxicity in the absence of butane likely caused significant increases in lag time to butane utilization and 1,1-DCE transformation. 1,1-DCE transformation product toxicity likely also influenced the different microbial community compositions that were observed with different exposure patterns.

4.5 Growth Characteristics and Cometabolic Activity of Strain 183BP

The butane-utilizing bacterium, strain 183BP, was isolated from a butane-utilizing, CAH-cometabolizing mixed culture enriched from environmental samples obtained from Hanford, WA. Evaluation of the isolate's growth and cometabolic transformation abilities when grown on butane, organic acids, and other hydrocarbon substrates was studied. Strain 183BP was grown in mineral media with a 3% butane-in-air headspace and the relationships between optical density (OD), total suspended solids (TSS), protein concentration, butane utilization, and nitrate uptake were determined. Since enzyme inhibition between primary and cometabolic substrates has been shown to frequently limit cometabolic transformation efficiencies, substrates not expected to induce the monooxygenase enzyme system responsible for hydrocarbon utilization and CAH cometabolism, such as ethanol, acetate, and succinate, were also evaluated as potential growth substrates. The non-hydrocarbon substrates were also tested for their ability to support cometabolic CAH transformation, either as a sole metabolic substrate, as a mixed substrate with butane also present, or in alternate feed cycles with butane. The straight chain, saturated hydrocarbons methane, ethane, propane, butane, pentane, and hexane were also evaluated as potential primary substrates and supporters of cometabolic transformation of TCA.

4.5.1 Characteristics of Strain 183BP when Grown on Butane

This experiment was conducted to determine the growth stoichiometry for the strain 183BP culture when grown on butane. Five parameters were followed during growth of strain 183BP on butane; optical density at 600 nm wavelength (OD_{600}), protein concentration, total suspended solid (TSS), and butane and nitrate concentrations. Optical density is a quick and reliable way to

measure the population of bacteria suspended in aqueous media and requires a small sample volume (~1 mL) compared to that required for TSS (up to 100s of mL). When correlated to TSS and protein measurements, OD_{600} can provide a reasonable estimation of culture concentrations. Protein concentrations are used to estimate viable cell populations since protein is reasonably labile and would degrade upon cell decay and lysis, which OD_{600} and TSS measurements may not reflect. Nitrate, the sole nitrogen source provided for cell synthesis, was monitored to determine the amount of nitrogen required for cell growth and maintenance. In this experiment, relationships between TSS concentration, optical density, protein concentration, butane consumption, and nitrate uptake were evaluated and yield coefficients calculated.

Each result was produced with strain 183BP cells grown from dilute solution (OD_{600} <0.25) to an OD_{600} of about 1.3 in one growth phase (one addition of substrate).
Figure 57 shows the relationship between cell growth measured by OD_{600} and butane consumption. The lag time to observable butane utilization was about 75 hr and 83 mg of butane was completely utilized by 150 hours. There was a coinciding increase in OD_{600} between 90 and 150 hr, reaching a maximum of about 1.0. Nitrate concentrations were observed to decrease with increasing OD_{600} and butane consumption. Nitrogen utilization ceased upon complete butane utilization. The relationship between butane consumption and nitrate uptake was linear (Figure 58) with 1.05 mg of nitrate required per mg of butane consumed (0.24 mg nitrate-N/mg butane). Since less phosphate buffer was used in the media to allow better resolution of the nitrate and nitrite peaks during IC analysis, pH was checked at the beginning and at the end of the growth cycle and found to be 7 and 6.3, respectively.

Figure 57. Strain 183BP Culture Growth on Butane a) Butane Utilization, b) Cell Growth Measured as Optical Density, and c) Nitrate Consumption. The three symbols represent triplicate bottles.

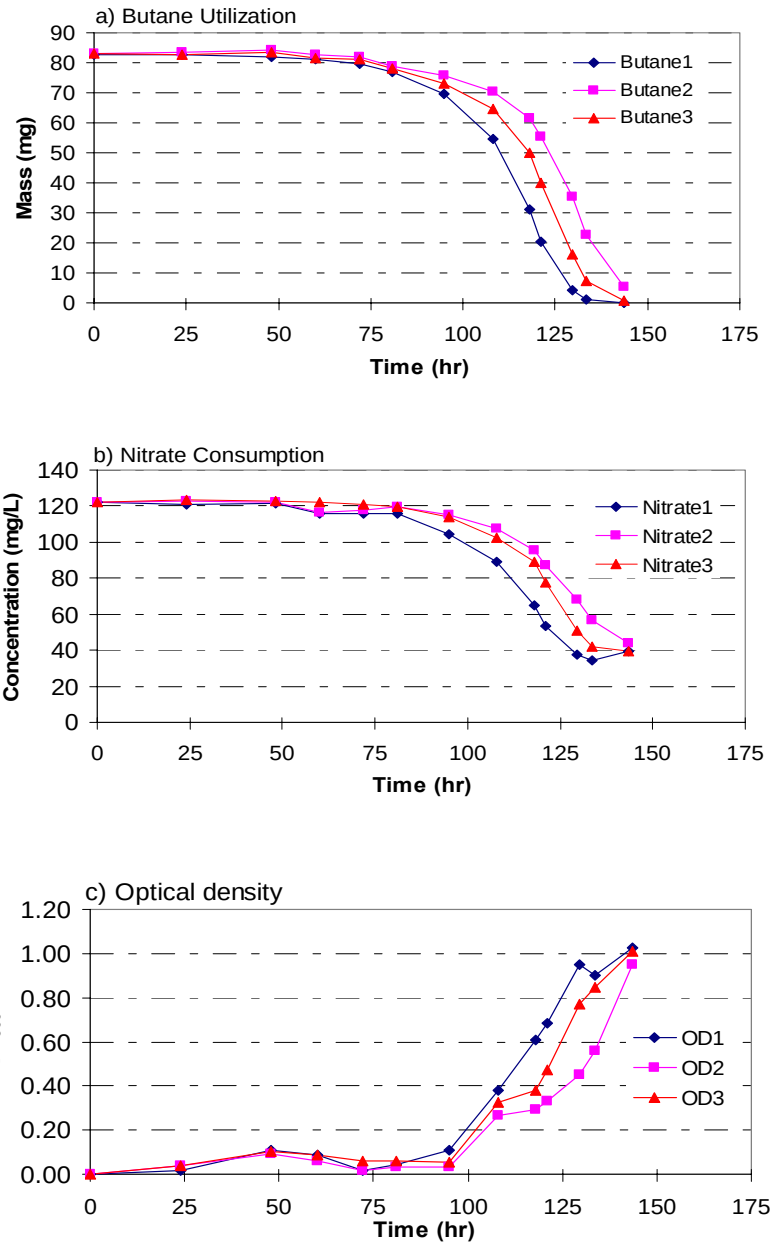

Figure 58. Nitrate Requirements of the Strain 183BP Culture when Grown on Butane. The plots are based on triplicate bottles under identical conditions, with a single linear regression of the entire data set.

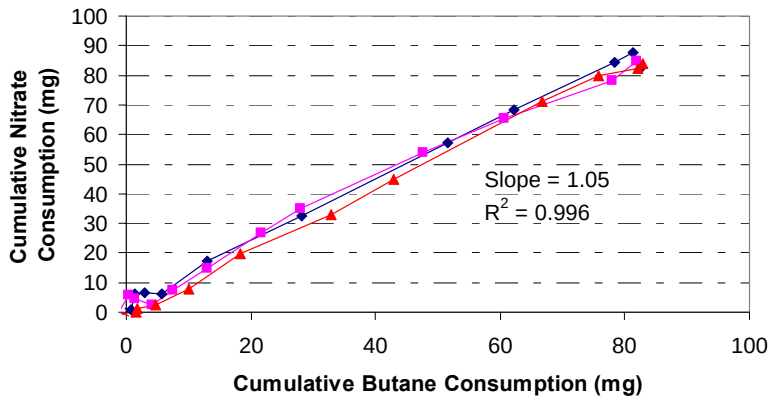

Total suspended solids (TSS), OD_{600}, and protein concentrations were compared during growth of strain 183BP on butane (Figure 59). Relationships between the measured parameters were obtained by least square error regression and are presented in equations 4.5.1, 4.5.2, and 4.5.3. Linear relationships provided good correlations of the parameters during exponential growth of the culture. These relationships have not been tested and may not be the same during steady state conditions or in systems experiencing stationary phase growth which may exhibit higher TSS and OD_{600} and lower protein concentrations due to increases in decayed cellular material.

$$TSS(mg/L) = 255 \times OD_{600} - 8.00 \qquad \text{Equation (4.5.1)}$$

$$TSS(mg/L) = 2.92 \times \Pr(mg/L) - 7.14 \qquad \text{Equation (4.5.2)}$$

$$\Pr otein(ug/mL) = 85.86 \times OD_{600} + 1.97 \qquad \text{Equation (4.5.3)}$$

The cellular yield coefficient is defined as the amount of cell mass or product formed related to a consumed substrate (generally, a carbon or nitrogen source or oxygen) or to intracellular ATP production (IUPAC, 1997). The average yield coefficient, Y, and 95% confidence interval for strain 183BP was found to be 0.73 ± 0.08 mg TSS/mg butane based on butane consumption and TSS analyses.

Figure 59. Relationships between TSS, OD_{600}, and Protein Concentrations for the Strain 183BP Culture when Grown on Butane in Mineral Media. Linear expressions relating the growth parameters were developed by least squares regression.

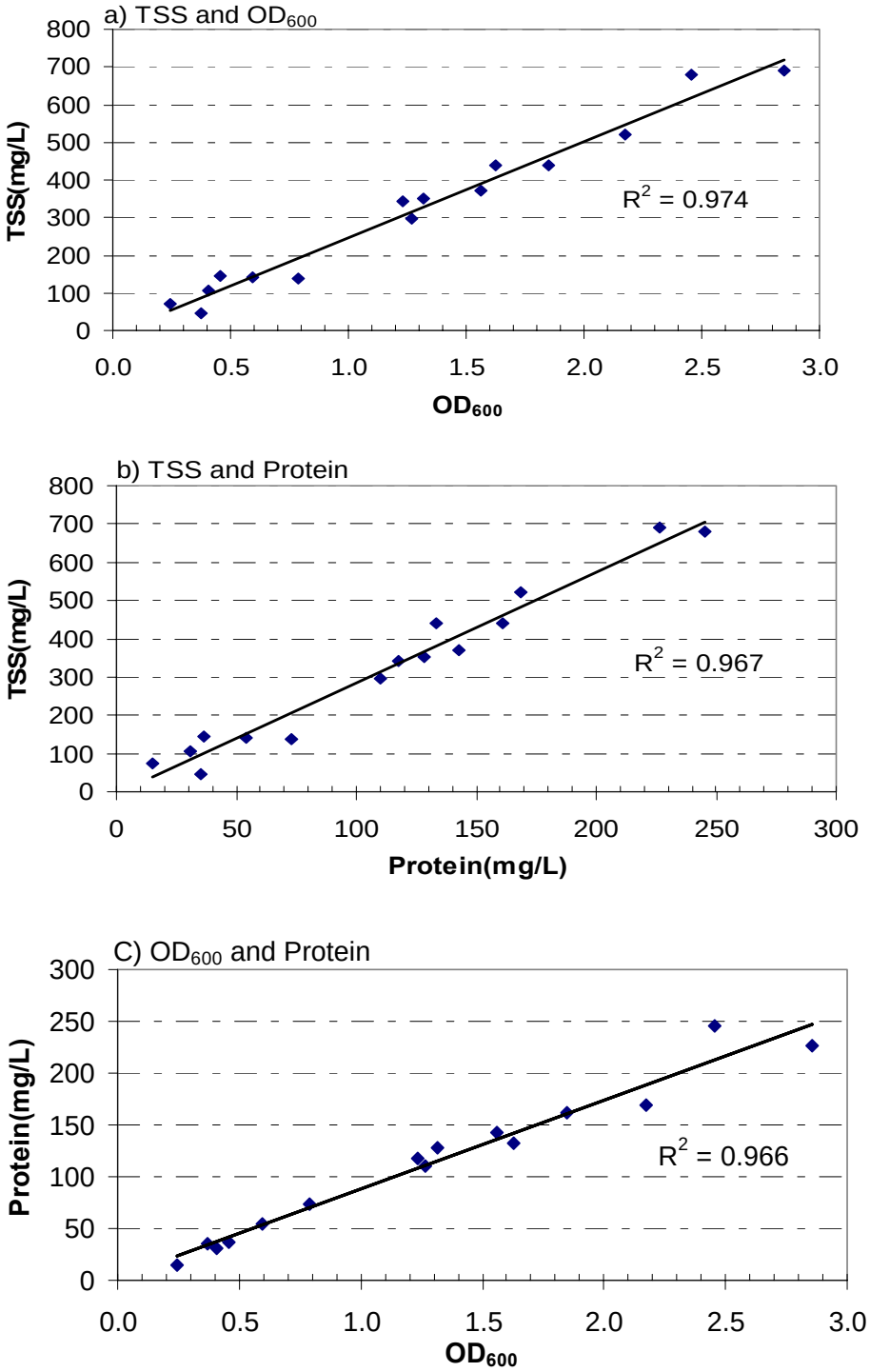

4.5.2 Ethanol, Acetate, and Succinate as Substrates for the Strain 183BP Culture

Butane is known to induce a monooxygenase enzyme system (MO) that also has the capacity to transform CAHs. However, the presence of butane is also known to inhibit cometabolic transformation of CAHs (Kim et al., 2000). The CAHs, 1,1-DCE, 1,1-DCA, and 1,1,1-TCA could all be transformed by the mixed butane-utilizing culture that produced the strain 183BP isolate. In tests performed with the butane-utilizing mixed culture, the presence of butane was found to most adversely affect the rate of TCA transformation, presumably due to competition for the monooxygenase enzyme. In the study conducted here, alternate growth supporting non-hydrocarbon substrates were examined for their ability to support TCA transformation by providing energy for the microorganisms while eliminating competition for the MO system. Acetate, a common, small molecule weight carboxylic acid, was of interest since most aerobic organisms are capable of using acetate as a carbon source and energy substrate. Other primary alcohols and carboxylic acid acids have also been found to be growth substrates for other butane-utilizing organisms (Hamamura et al., 1999 and 2000). In this study, acetate, ethanol, and succinate were investigated as alternative substrates for strain 183BP to support microbial growth and TCA transformation. Additionally, strain 183BP was alternately fed butane and non-hydrocarbon substrates in efforts to increase MO expression and minimize competitive inhibition effects to achieve greater CAH transformation.

First, acetate and ethanol were tested for their ability to support continued TCA transformation using a butane-grown culture. The strain 183BP culture was grown in mineral media with butane (10% in the headspace) in a 750 mL bottle, containing 300 mL of fresh mineral media. When the OD_{600} reached approximately 1.5, individual aliquots of 1 mL were inoculated into 27 mL vials containing 9 mL of fresh mineral media. The vials were sealed with aluminum crimp-tops and butyl rubber septa. Atmospheric pressure and aerobic conditions were maintained in the bottles by periodic re-equilibration with pure O_2 gas. TCA was added to the bottles and TCA transformation was monitored over time. After almost complete TCA transformation, TCA was added again with either acetate or ethanol also added as an alternate substrate (Figure 59). TCA transformation in these bottles was compared to that obtained in resting cell cultures operated in the same manner but without alternate substrate addition (Figure 60).

Figure 60. TCA Transformation by Butane-Grown Strain 183BP Resting Cells Where a) Resting Cells Were Fed an Alternate Substrate, Acetate or Ethanol, after Initial TCA Transformation, and B) One Group of Resting Cells Were Immediately Exposed to TCA While Another Group Was Shaken for 24 Hours Under Aerobic Conditions In The Absence Of Butane Before TCA Exposure; Neither Group Receive An Alternate Substrate Addition. (Error Bars Represent 95% Confidence Intervals Based On Triplicate Vials.)

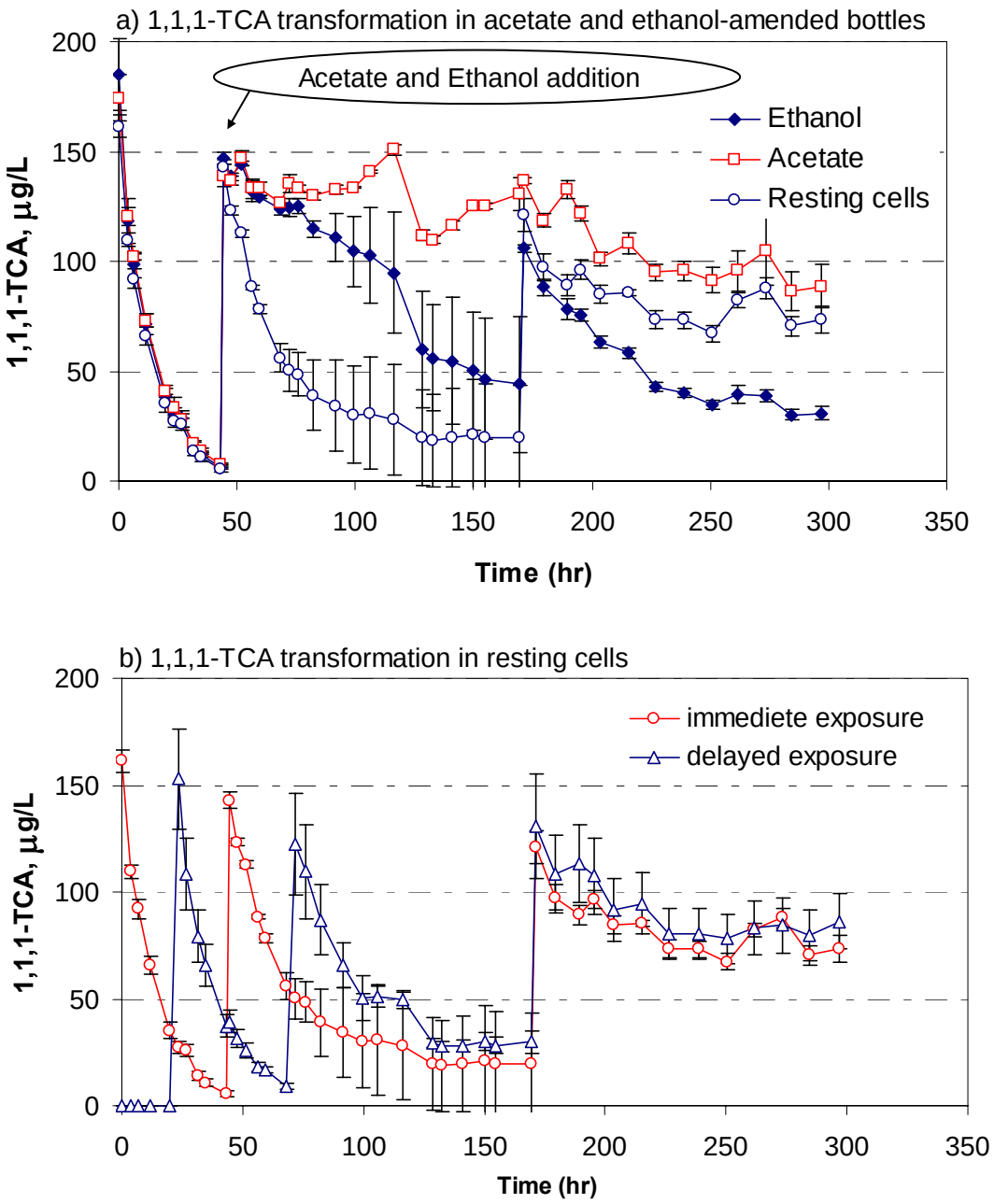

Addition of acetic acid caused the pH to drop to around 4, resulting in termination of all activity in the acetate-amended bottles. At 190 hr, pH was increased to pH = 7 with the addition of NaOH. After pH neutralization, an increase in OD_{600} was observed with a final OD_{600} in the acetate-amended bottles of 0.72 corresponding to a TSS of 175 mg/L indicating cell growth on acetate occurred. However, TCA transformation was not recovered after the initial drop in pH.

In the ethanol-amended vials, TCA transformation continued after ethanol amendment, but at a slower rate than in resting cell bottles. However, the resting cell bottles begin to slow significantly around 100 hr of incubation, while the ethanol-amended bottles continued slow, but steady, TCA transformation through approximately 250 hr. Optical density in ethanol-fed bottles increased over the test period to OD_{600} = 0.59 corresponding to a TSS of 140 mg/L, indicating that strain 183BP could grow on ethanol and provide slow, continued TCA transformation.

One triplicate group of resting cells was exposed to TCA immediately, while another set was shaken for 24 hr in the presence of O_2 and the absence of growth or cometabolic substrates. Previous studies have indicated that other MO expressing organisms can lose MO activity by "self oxidation" in the absence of substrate. Here, cells immediately exposed to TCA transformed essentially the same amount of TCA at similar rates to cells shaken for 24 hr before exposure to TCA, indicating that short-term self-oxidation was not a significant concern with this culture.

Resting cells were able to degrade approximately 190 μg of TCA resulting in an estimated TCA transformation capacity, T_c, of about 330 μg TCA/mg cells based on TSS estimated from OD_{600} measurements of initial cell concentrations (Table 30). Ethanol-amended cells transformed slightly more TCA than resting cells; however, since growth on ethanol resulted in higher biomass, the T_c of ethanol-amended cells was less than half of that for resting cells. Acetate-amended cells transformed the least TCA, but were negatively influenced by the precipitous pH drop.

Table 30. Strain 183BP Estimated Ttransformation Capacities under Resting Conditions and with Alternate Substrate Addition

Conditions	Average OD_{600}	Estimated TSS[1] (mg/L)	Average TCA transformed (μg)	T_c[2] (μg TCA/mg cells)
Initial	0.25 ± 0.04	56	-	-
Ethanol	0.59 ± 0.01	140	210	150
Acetate	0.72 ± 0.10	175	130	75
Immediate exposure	0.17 ± 0.03	35	195	338
Delayed exposure	0.17 ± 0.04	35	185	318

1. TSS values estimated from the correlation between TSS and OD_{600} as shown in equation 3.1
2. T_C calculated from estimated TSS values

When used alone, neither alternate substrate provided significantly greater TCA transformation than resting cells. However, significant cell growth occurred as a result of alternate substrate addition, creating a possibility of greater TCA transformation if re-induction of the MO enzyme system were accomplished. In the following test, TCA transformation was observed in vials alternately fed acetate and butane or succinate and butane to vials fed only butane and to vials containing resting cells. At issue was whether TCA transformation ability could be maintained or increased by alternate feed cycles of butane, an inducer and competitor for the monooxygenase system, and a growth substrate that does not compete for the monooxygenase enzyme, but does support microbial growth.

Strain 183BP was grown on butane in mineral media to an OD_{600} of 1.5 and 3 mL aliquots were harvested and inoculated into 27 mL vials containing 7 mL of fresh media without growth substrates. TCA was introduced to the vials to produce an aqueous concentration of 1300 μg/L at the beginning of the test and re-added when appropriate throughout the 600 hr test. TCA transformation in resting cells was monitored over time until the transformation rate slowed (Figure 61 and 62). Substrates were then added at about 150 hr and TCA transformation was again monitored. At approximately 260 hr, butane was added to all of the bottles, including the resting cell incubations, to stimulate monooxygenase activity, followed by another round of TCA transformation and alternate substrate addition. Butane addition was 0.5 mL, or approximate 1.2 mg, at each amendment and succinate and acetate addition were 4.4 mg and 4.1 mg respectively, or roughly the same electron equivalents as the butane addition.

Figure 61. TCA Transformation by a Butane-Grown Strain 183BP Culture in Mineral Media, Where the Culture is Amended a) Alternately with Succinate and Butane, b) Alternately with Acetate and Butane, and c) with Butane Alone. (Error bars represent 95% confidence interval based on triplicate vials.)

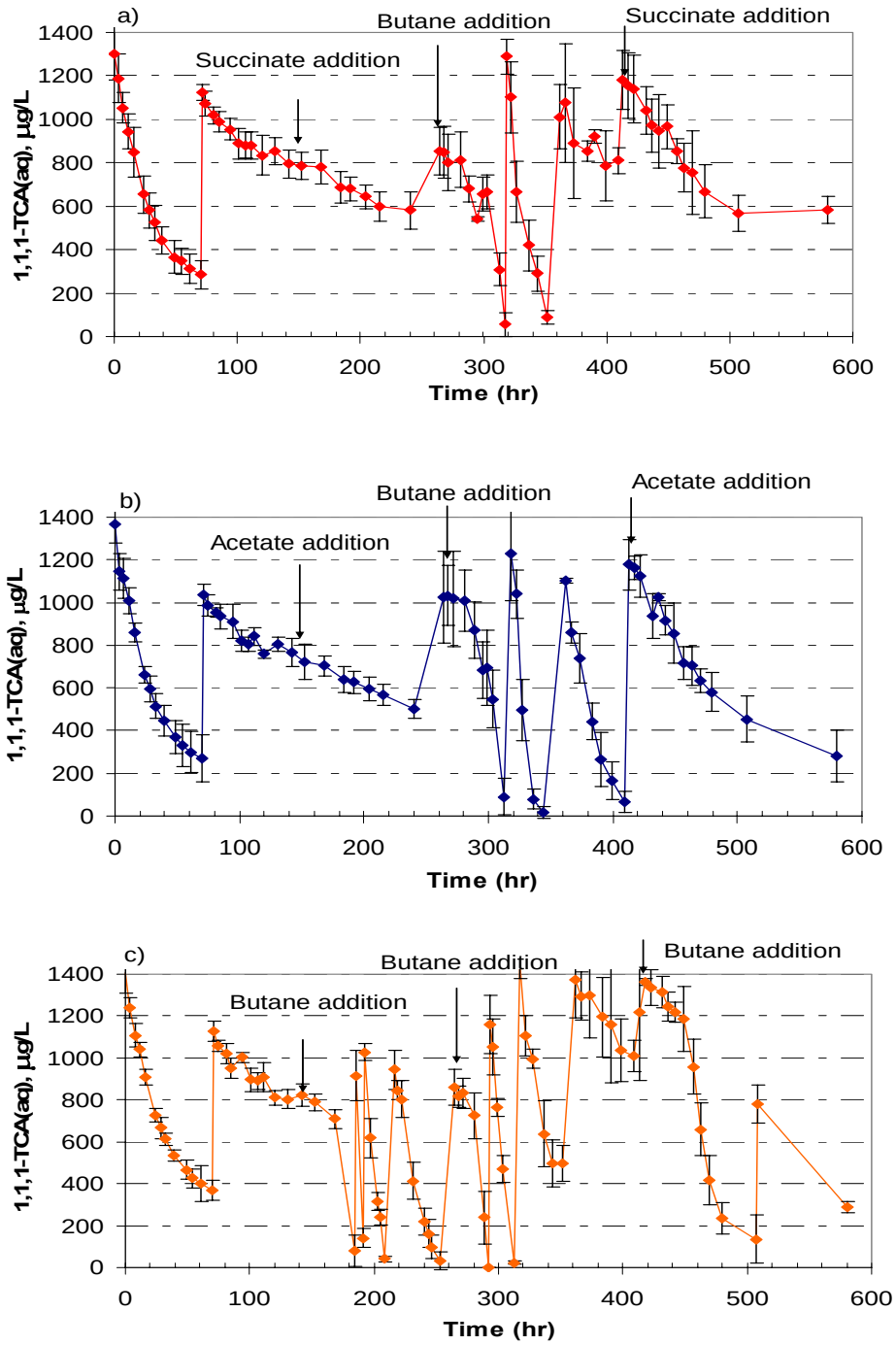

Initial TCA transformation was essentially the same in all vials through the first 150 hr, when the respective substrates were added to the vials (Figures 61 and 62). In the acetate- and succinate-amended bottles, TCA transformation continued at a rate essentially identical to that before

substrate addition, but observable turbidity increased. TCA transformation rates in butane-fed vials increased dramatically after a short lag period required for butane utilization.

Figure 62. TCA Transformation by a Resting Butane-Grown Strain 183BP Culture in Mineral Media. The culture received one additional butane amendment at 260 hr. (Error bars represent 95% confidence interval based on triplicate bottles.)

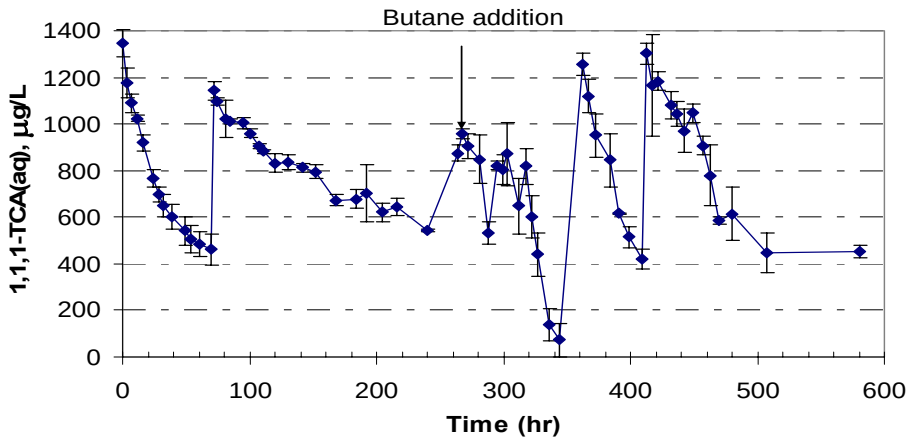

After approximately 100 hr of monitoring the effects of alternate substrate addition, butane was added to all of the vials, including those containing resting cells, to induce greater MO activity. TCA transformation rates increased in all of the vials after an initial lag period required to consume the butane. This lag period was shortest for the butane-fed system (complete utilization in 32 hr), followed by the acetate- (~55 hr) and succinate-fed systems (~60 hr) and the resting cell system (> 90 hr). Successive additions of TCA were transformed following butane addition in all of the systems. During this period of butane addition and TCA transformation, acetate-amended cultures transformed slightly more TCA than the butane-fed cultures at 64 µg compared to 61.8 µg (Table 31). Succinate-amended cultures managed an average of 41 µg TCA transformed while resting cells transformed only 30.6 µg.

Table 31. Mass of TCA Transformed (µg) in Succinate-, Acetate-, Butane-, and Non-Amended Systems

Conditions	Succinate	Acetate	Butane	Resting Cells
No substrate	26.9	27.3	26.8	24.7
Substrate addition	4.4	5.3	68.5	5.4
Butane activation	40.9	64.0	61.8	30.6
Substrate addition	23.6	23.4	34.6	17.6
Total	96	119	197	78

As TCA transformation rates again slowed, substrates were added again at approximately 410 h. TCA transformation in acetate- and succinate- amended vials continue at pre-amendment rates. Butane-fed vials also showed continued slow TCA transformation until the butane was consumed and the TCA transformation rate increased significantly. TCA transformation in resting cell vials continued at a rate approximately equal to that in the acetate-amended vials. By 500 h, the succinate-amended vials and the resting cell vials had both ceased TCA transformation activity. Continued, but slow, TCA transformation occurred in acetate- and butane-fed vials through 600 h.

Nitrate was measured at the end of the test and found to be completely depleted in all of the succinate vials, in 2 of the 3 acetate vials and in 2 of the 3 butane vials (Table 32). Since nitrate limitations can significantly decrease butane and TCA oxidation rates (data not shown), rates obtained in the last phase of the test may have been influenced by nitrogen limitation. Optical density measurements suggested the greatest biomass growth occurred in the acetate-amended bottles with about 340 mg TSS/L produced from two acetate and one butane feedings. The butane-fed systems similarly increased biomass by about 310 mg TSS/L, while succinate-fed bottles only increased about 250 mg/L. Resting cell vials showed an increase of about 130 mg TSS/L due to the one addition of butane. All of the vials maintained pH between 6 and 7 throughout the test.

Table 32. Optical Density, Nitrate, and pH Values for Succinate-, Acetate-, Butane-, and Non-Amended Systems at the End of the 600 h Test

	Average OD_{600} ± 95% CI	Estimated TSS[1] (mg/L)	NO_3^- (mg/L)	pH
Initial	0.80 ± 0.01	195	80	7.0
Succinate	1.77 ± 0.04	445	0	6.8
Acetate	2.13 ± 0.04	535	0 (2 of 3)	6.9
Butane	2.01 ± 0.06	505	0 (2 of 3)	6.2
Resting cell	1.31 ± 0.02	325	30	6.4

1. TSS values estimated from the correlation between TSS and OD_{600} as shown in equation 3.1

The butane-fed system was the most efficient at TCA transformation with a total of 197 μg of TCA transformed throughout the experiment (Figure 63). Considerable TCA transformation inhibition was observed when butane was added to the bottles, but butane was consumed quickly (about 30 hr) followed but a much longer time of TCA transformation in the absence of butane (about 120 hr). Resting cells transformed the least TCA (78 μg) while succinate (96 μg) and acetate systems (119 μg) showed enhanced TCA transformation compared to resting cells, but significantly less effective transformation than in butane-fed vials.

Figure 63. Cumulative TCA Transformation by Strain 183BP Culture Amended with Alternate Substrates. (Error bars are based on 95% confidence interval.)

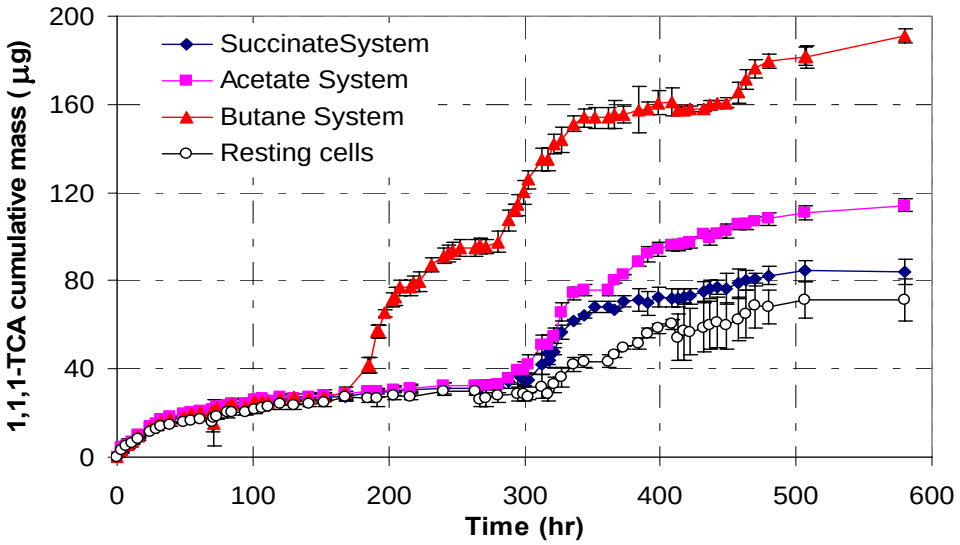

Positive cell growth was observed in both the succinate- and acetate-fed systems. However, TCA transformation rates did not increase with increasing cell densities, but continued at the same rate as that before the amendment, indicating that succinate and acetate do not induce MO expression, and also do not inhibit TCA transformation. Upon re-activation with butane at 260 hr, TCA transformation rates in the acetate-amended vials were greater than those in butane-fed vials (Figure 64) indicating that the increased biomass resulting from acetate utilization did produce MO upon induction with butane. TCA transformation rates in succinate-fed bottles increased to rate equivalent to those in butane-fed bottles, or approximately 80% of the acetate-fed rates. The higher rates obtained in the acetate-fed system may have been due to a greater biomass yield on acetate compared to succinate and butane. Resting cell transformation rates also increased significantly upon the addition of butane, but to a lesser degree than the other systems and with a greater lag time required to utilize the amended butane.

Figure 64. Maximum TCA Transformation Rates Achieved by Strain 183BP Culture Amended with Alternate Substrates during the Four Phases of the Test. The addition of alternate substrates generally resulted in lower TCA transformation rates. (Error bars are based on 95% confidence interval.)

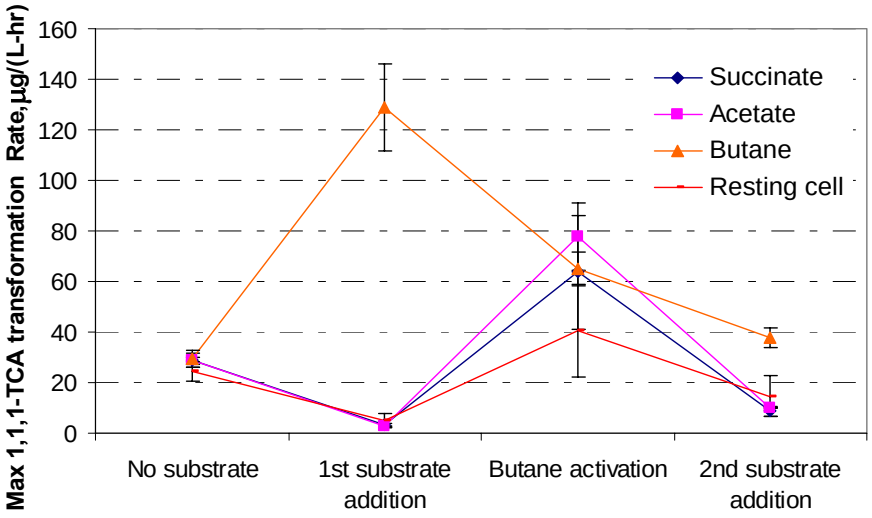

Overall, the inhibition of TCA transformation by the presence of butane was less significant than the induction of higher TCA transformation rates once the butane was consumed. Although the use of alternate substrates resulted in greater TCA transformation than occurred in resting cell systems, significantly more TCA was transformed in the butane-fed system. In this test, TCA transformation was allowed to proceed until the transformation rates were quite slow, presumably due to loss of MO activity, before subsequent substrate addition. It is possible that earlier addition of the alternate growth substrate would allow for increased biomass production during an active phase of TCA transformation, which could then be stimulated to produce more MO during the next butane addition.

4.5.3 Acetate as a Cosubstrate With Butane

Results from the previous experiments showed that strain 183BP grew well with acetate, but that TCA transformation ability was not increased, since the MO enzyme system was apparently not induced by acetate or TCA itself. In this experiment, various concentrations of butane were added with acetate to determine if low levels of butane were sufficient to induce MO activity, and thus greater TCA transformation, in acetate-grown cells.

Strain 183BP was grown on butane in mineral media to an OD_{600} of 1.4 and 3 mL aliquots were harvested and inoculated into 27 mL vials containing 7 mL of fresh media without growth substrates. TCA was introduced to the vials to produce an aqueous concentration of 1200 µg/L at the beginning of the test and re-added when appropriate throughout the 300 hr test. Acetate and butane were added together to the vials (Table 33) resulting in four substrate conditions; acetate alone, low butane and acetate, medium butane and acetate, and high butane without acetate. After inoculation and initial TCA transformation, the vials were alternately fed with the

butane/acetate mixture followed by butane addition without acetate and then another butane/acetate feed cycle.

Table 33. Amendment Conditions Used to Test Acetate as a Cosubstrate with Butane to Support TCA Cometabolism

Conditions	Butane (mg)	Acetate* (mg)
No Butane	0	8.0
Low Butane	0.15	7.6
Medium Butane	0.3	6.4
High Butane	1.7	0

*number based on available at a acetate concentration of 100 mM

TCA was initially transformed by strain 183BP resting cells for approximately 50 hr, when the mixed substrates were added to the vials. The vials exhibiting the least resting cell TCA transformation were fed the high butane-no acetate feed. Butane consumption required about 50 hr in all of the vials, regardless of the butane concentration added (Figure 65). TCA transformation continued in all of the vials once the added butane was consumed, with the most TCA transformation occurring in the vials fed the most butane. TCA transformation slowed to a halt around 135 hr and 1.7 mg of butane was added to all of the vials. Time to complete butane utilization was shortest for the vials previously fed high butane concentrations, approximately the same for the two systems previously fed intermediate levels of butane and slowest for the vials fed acetate without butane. TCA transformation was stimulated in all vials fed butane with the same relative order of transformation found for butane utilization. TCA was completely removed by 210 hr in all of the vials except those previously fed only acetate. A mixture of butane, acetate and TCA was again fed to the vials at 210 hr, but only slow butane utilization with little TCA transformation occurred. Nitrate concentrations were found to be low at the end of the test (Table 34) and may have limited growth in the latter portion of the test.

Figure 65. Average TCA Transformation and Average Butane Utilization by R183 a) Average TCA transformation in acetate-butane mixed substrate, and b) The average butane degradation curve in the mixed substrate system. (The error bars are based on 95% confidence interval.)

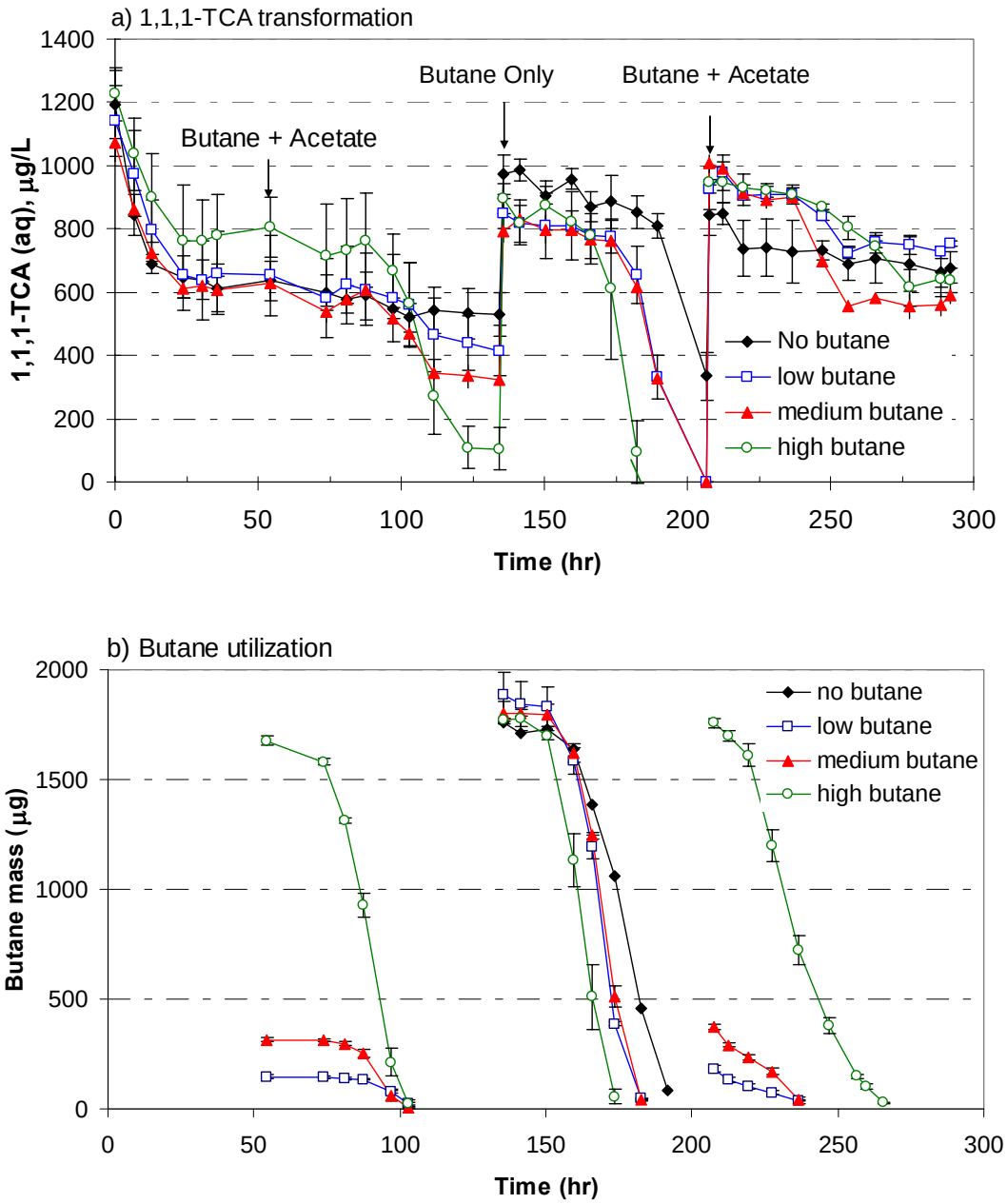

Table 34. Optical Density, Nitrate, and pH Values for Acetate- and Butane-Fed Systems at the End of the 300 h Test

Conditions	OD_{600}	Estimated TSS[1] (mg/L)	Nitrate (mg/L)	pH
Beginning	0.54 ± 0.01	130	55.1 ± 0.6	7.0
No Butane	2.37 ± 0.07	600	1.3 ± 0.4	7.1
Low Butane	2.34 ± 0.08	590	1.0 ± 0.4	7.1
Medium Butane	2.26 ± 0.07	570	1.0 ± 0.4	7.1
High Butane	2.20± 0.14	550	0.5 ± 0.1	6.2

1. TSS values estimated from the correlation between TSS and OD_{600} as shown in equation 3.1

Cumulative TCA transformation is presented in Figure 66. The system fed high butane concentrations clearly transformed the most TCA throughout the test. Increasing butane concentrations in the feed solution resulted in increased cumulative TCA transformation, with the most dramatic differences occurring during feed cycles incorporating both acetate and butane. OD_{600} measurements at the end of the experiment were the greatest in the acetate-fed system and least in the butane-fed system, although the difference was only about 10%. Although the system fed butane alone performed the best, significant TCA transformation was obtained in systems fed significantly less butane (Table 35) producing the highest transformation yields of 0.23 mg TCA/mg butane for the low butane system, 0.14 mg TCA/mg butane for the medium butane system, and a low of 0.027 mg TCA/mg butane for the butane alone system.

Figure 66. Average TCA Cumulative Mass in Different Substrate Conditions. The error bars are based on 95% confidence interval.

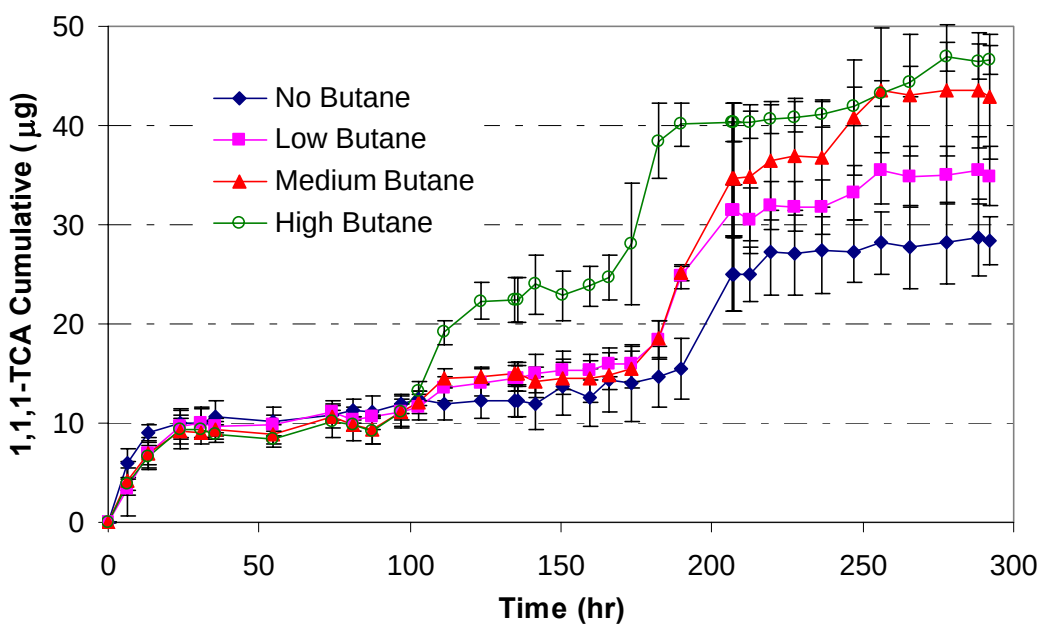

Table 35. Comparison of the TCA Mass Transformed by the Different Ratio of Butane Mass

Butane (mg)	TCA transformed mass (μg)				
	No Substrate	Mixed substrate	Butane only	Mixed substrate	Total
0	10	2.2	13.3	2.8	28
0.15	9.8	6.2	15.5	3.5	35
0.3	8.9	6.6	19.1	7.8	43
1.7	8.4	14	17.9	6.3	47

Comparison of two Rhodococcus sp. ability to transform DCE, DCA, and TCA

Two butane-utilizing bacterial strains, strain 183BP and strain 179BP, were isolated from a butane-utilizing, CAH-cometabolizing mixed culture enriched from environmental samples obtained from Hanford, WA. Both strains were characterized based on their 16S rRNA gene sequences and found to have high similarity with known *Rhodococcus* species. Strain 179BP was found to be 98% similar to both *Rhodococcus koreensis* and *Rhodococcus opacus*, while strain 183BP was 100% similar to *Rhodococcus sp*. USA-AN012. Strain 179BP , like strain 183BP, was able to grown on butane and cometabolically transform CAHs. However, when grown in mineral media on butane, strain 179BP formed tightly clumped filamentous aggregates while strain183BP grew planktonically as small stubby rods. In this experiment, the ability of a butane-grown strain 179BP culture to transform CAHs was compared to that of a butane-grown strain 183BP culture. The CAHs used were 1,1-DCE, 1,1-DCA, and 1,1,1-TCA.

The cultures were grown on butane in mineral media to OD_{600} of approximately 1.4 for strain 183BP and 1.0 for strain 179BP. Reactor bottles were prepared by adding 3 mL of culture into 27 mL vials containing 7 mL of fresh media. The average initial OD_{600} was 0.46 (corresponding to an initial TSS of 110 mg/L and initial protein concentration of 42 mg/L) for strain 183BP and 0.30 for strain 179BP (correlations of TSS and protein to optical density were not conducted on strain 179BP). For each culture, autoclaved-cell controls, resting cells without butane addition, and active cells with butane addition were tested in triplicate. CAHs were added to all test bottles. Approximately 1900 mg of butane was added to each of the active bottles to initiate the test. DCE, DCA, and TCA were added to the bottles to produce aqueous concentrations of 750 μg/L, 500 μg/L and 500 μg/L respectively for strain 183BP tests and approximately 450 μg/L for all CAHs for strain 179BP tests. Butane degradation and CAH transformation were monitored over time and are presented in Figures 67 – 70. After the initial butane was consumed and CAH transformation slowed, additional butane was added with the process repeated as necessary.

Control bottles of strain 183BP exhibited reasonably small initial losses (~10-15%) over the first 20 hours of the experiment (Figure 67a) and were generally stable thereafter, with the exception of DCE which showed additional losses throughout the experiment. Strain 183BP resting cells were capable of almost complete transformation of the added DCE within 5 hr (Figure 67b). However, DCE transformation inactivated the cells and no additional CAH transformation was

observed after 5 hr. DCA and TCA were only slightly transformed which was consistent with the butane-fed bottles where DCE was preferentially transformed before DCA and finally TCA (Figure 68). Taking into account control bottle losses, strain 183BP resting cells transformed 15.3 μg of DCE, 0.83 μg of DCA, and 1.4 μg of TCA, resulting in a DCE transformation capacity of 14 μg DCE/mg TSS in the presence of DCE and TCA. OD_{600} in the resting cell bottles decreased slightly to 0.42 by 26 hr.

Figure 67. CAHs Transformation by R183 Culture a) CAHs concentration and butane mass in control, and b) CAHs transformation by the R183 resting cells. (Error bars are based on 95% confidence interval.)

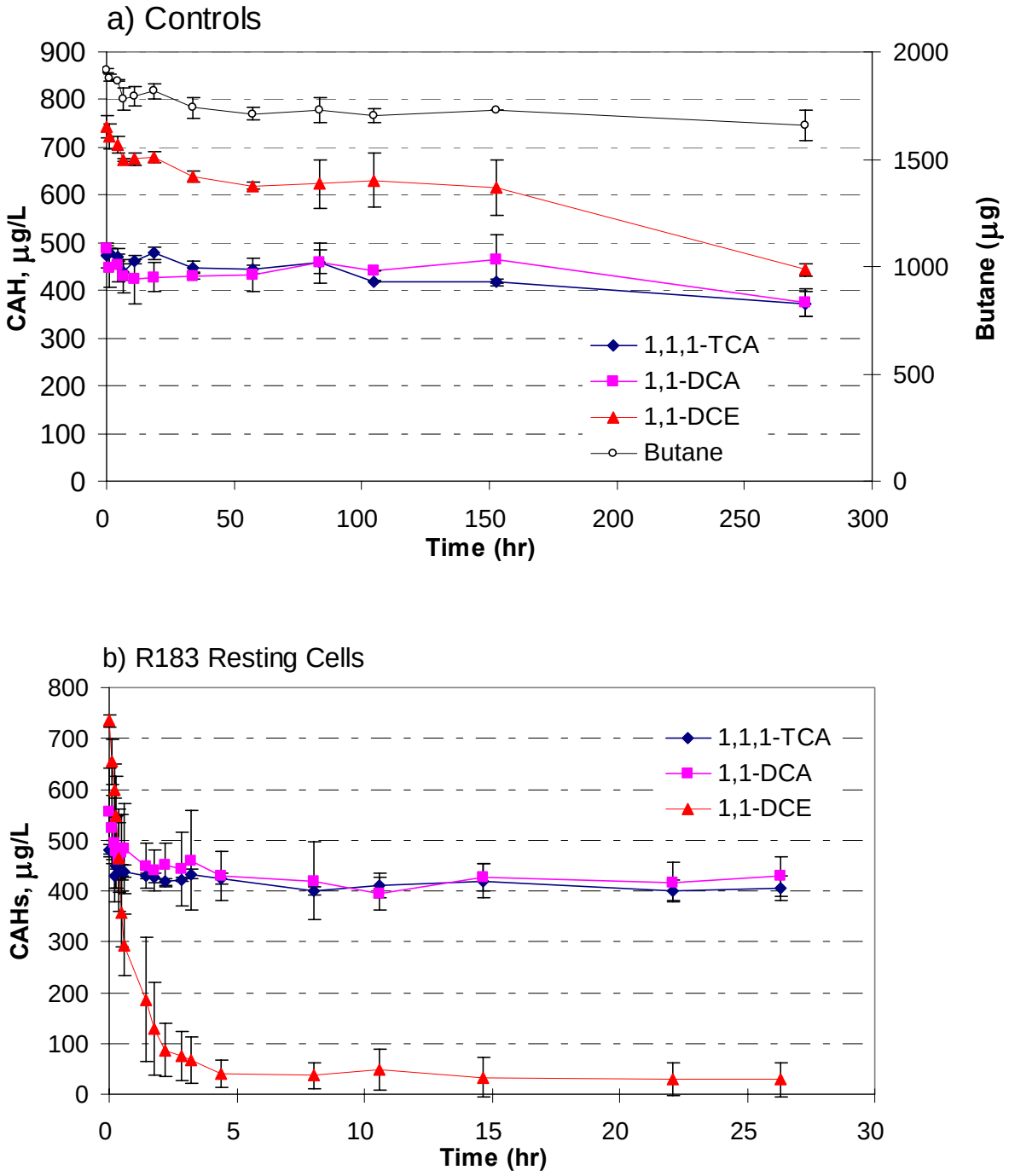

Figure 68 presents CAH transformation by strain 183BP in a butane-fed system. DCE was transformed concurrently with butane and was completely transformed before butane was completely utilized illustrating the fast kinetics of DCE transformation for this culture, even in the presence of butane. Significant transformation of DCA and TCA did not occur before butane was completely utilized indicating that the presence of butane was inhibitory to DCA and TCA transformation. Rapid DCA transformation began immediately upon the removal of butane around 50 hr. TCA transformation also initiated upon the removal of butane at about 50 hr, but proceeded at a significantly slower rate. The initial butane addition was sufficient to allow complete DCE transformation in all three bottles and almost complete DCA transformation in 2 of the 3 bottles. Additional butane was added to the bottles and DCA was effectively transformed as soon as the butane was removed to low levels. TCA continued to be slowly transformed through the second cycle of butane addition, but slowed to a halt around 150 hr. A third addition of butane resulted in increased TCA transformation rates once the butane was consumed. It was only after the DCE and DCA were completely transformed that high rates of TCA transformation occurred and complete transformation was attained in only one of the three bottles. On average, 6.79 μg of TCA, 3.26 μg of DCA, and 18.57 μg of DCE were transformed by the butane-fed strain 183BP culture during the study. OD_{600} increased to 1.58 after the three butane additions, corresponding to a culture density of 385 mg TSS/L based upon the correlation between OD_{600} and TSS developed for this culture.

Figure 68. Combined Butane Utilization and CAH Transformation by a Strain 183BP Culture. a) Butane utilization, b) DCE transformation, c) DCA transformation, and d) TCA transformation. The three symbols represent triplicate bottles.

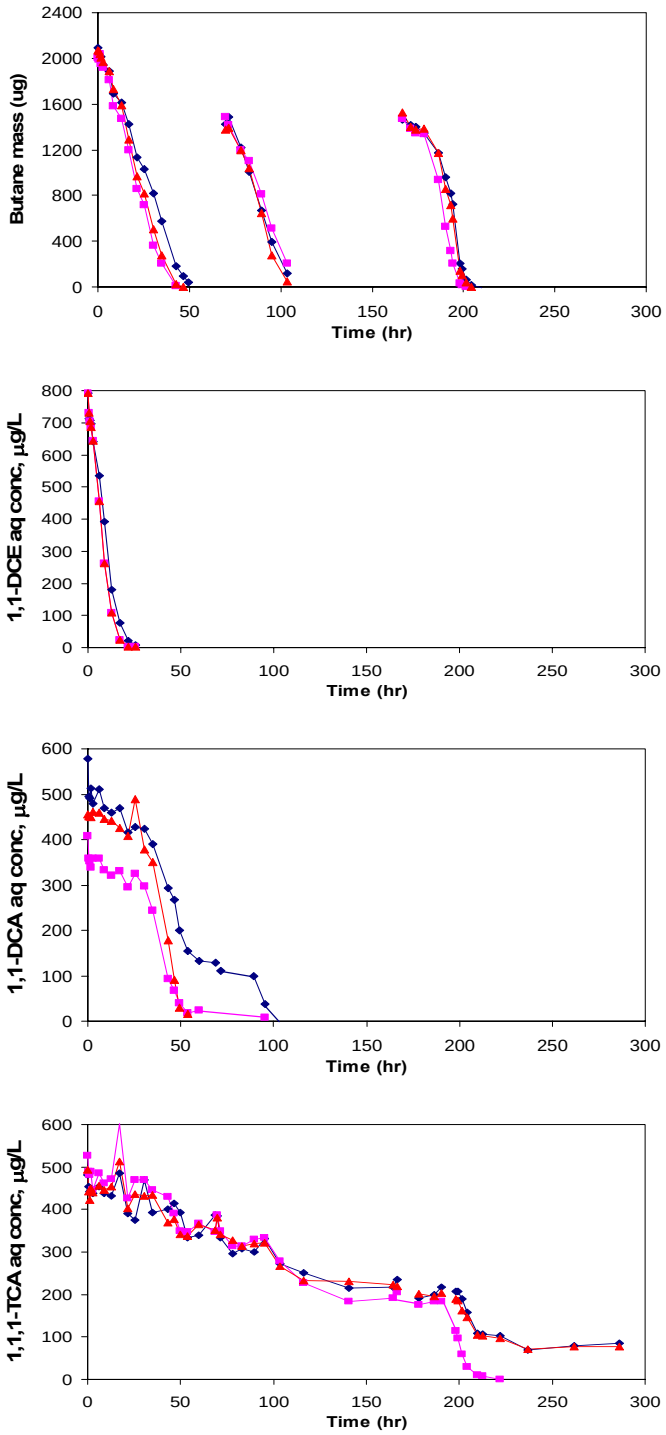

Similar to the results from strain 183BP controls, control bottles of strain 179BP exhibited reasonably small initial losses (~20-30%) over the first 200 hours of the experiment (Figure 69a) and were generally stable thereafter, with the exception of DCE and TCA which both showed additional losses throughout the 1300 hr experiment. By the end of the test about 42% of the TCA and 60 % of the DCA were remaining in the control bottles. Strain 179BP resting cells transformed a little less than one half of the added DCE within 5 hr (Figure 69b) and less than 20% of the DCA and 10% of the TCA provided. DCE transformation inactivated the cells and no additional CAH transformation was observed after 5 hr. Taking into account DCE losses in the control system over the same (10 hr) time period, the DCE transformation capacity of the resting cell strain 179BP culture was calculated to be 3.8 μg DCE/mg TSS, based on an estimated resting cell mass of 110 mg TSS/L, the same as that estimated for strain 183BP tests since they were grown on the same amount of butane and processed the same.

Figure 69. CAHs Transformation by R179 a) CAHs and butane in controls, and (b) CAHs transformation in R179 resting cells

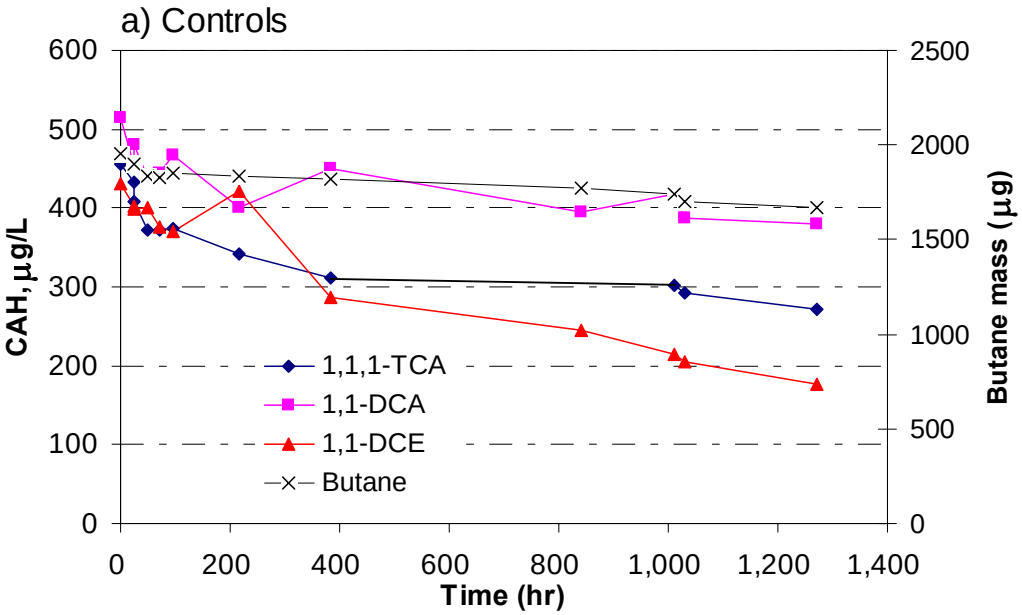

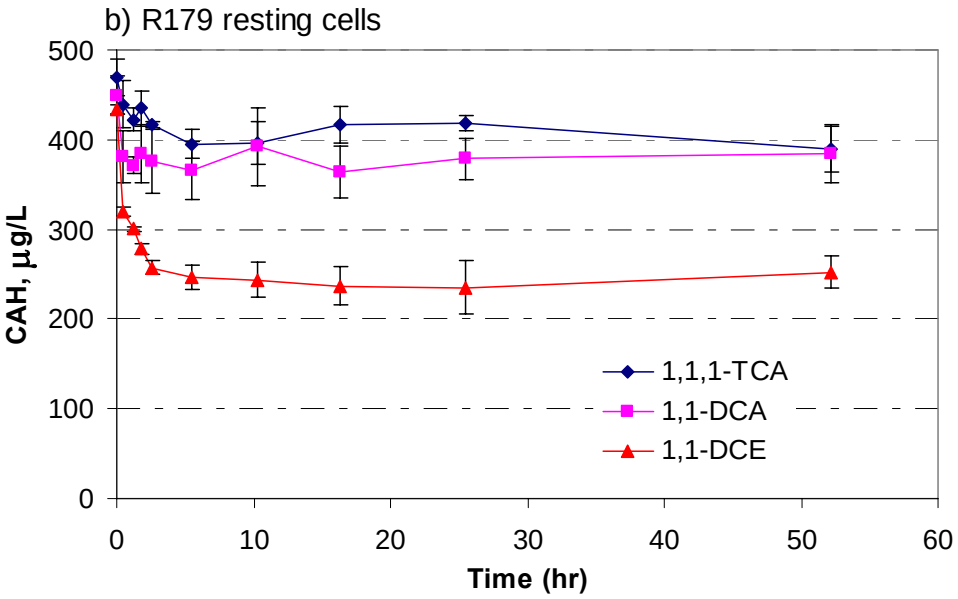

In the butane-fed system, only one of the three bottles of was able to completely transform DCE and completely utilize the provided butane (Figure 70). In the initial 20 hr of the test, both DCE and butane are rapidly transformed in all three bottles while TCA and DCA undergo more limited transformation. After this initial period, butane utilization rates decline drastically and DCE transformation rates also slow significantly. By approximately 200 hr, butane consumption and DCE transformation had slow nearly to a halt in two of the three bottles, with approximately 80 μg/L DCE remaining in solution. Over the remaining 900 hr of the test DCE concentrations in these bottles were reduced to about 20 μg/L and a small decrease in butane concentration was also observed. Although slow butane oxidizing activity may have remained, similar losses were seen in the control bottles so the removal could not be directly attributed to biological activity. In the third bottle, slow DCE transformation and butane utilization occurs for another 200 hr before all of the DCE is removed and rates of butane utilization begin to increase, presumably due to increased microbial growth and/or absence of DCE transformation product toxicity in the system. Butane consumption was complete by approximately 550 hr during which time DCA was also completely transformed. Only very slow transformation of TCA was occurring, so more butane was added around 700 hr and around 900 hr rapid transformation of TCA began resulting in the removal of about 75% of the remaining TCA by 1100 hr.

Figure 70. Butane Utilization and CAH Transformation by the Strain 179BP Culture. The three symbols represent triplicate bottles under identical conditions, a) Butane utilization, b) DCE transformation, c) DCA transformation, and d) TCA transformation.

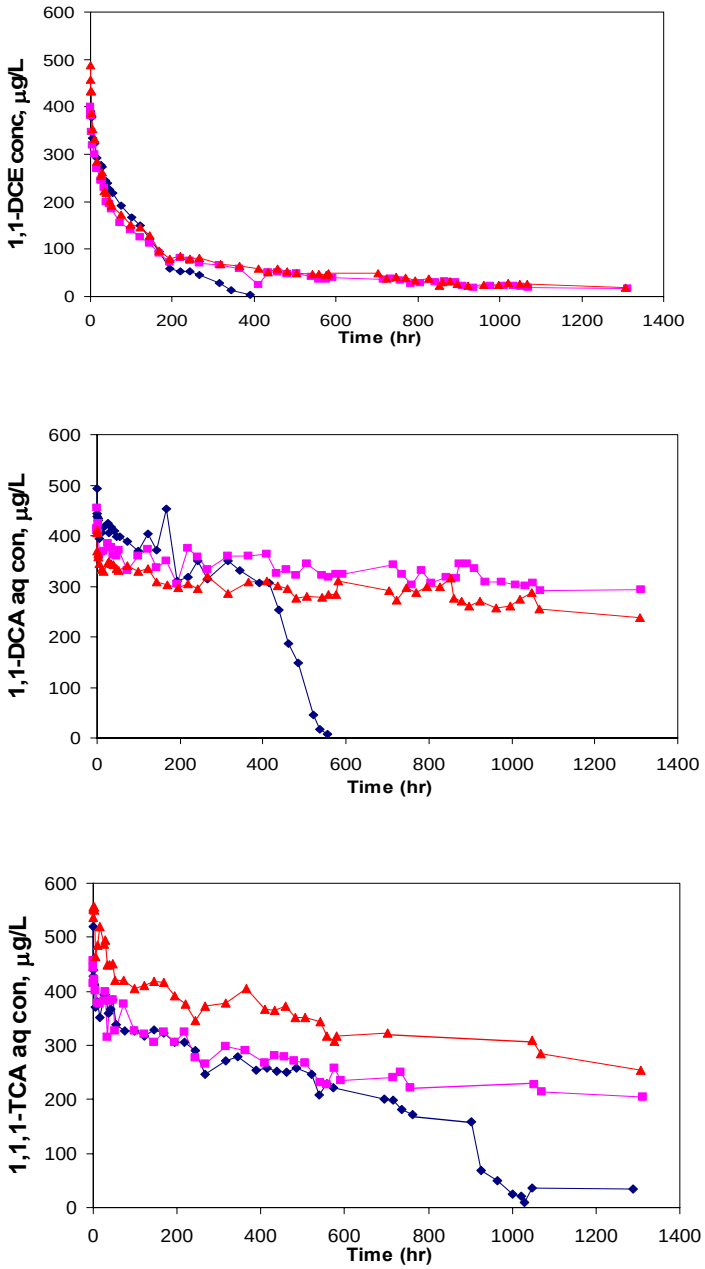

Overall, strain 183BP cells were able to transform the mixture of CAHs faster and more effectively with significantly less sensitivity to DCE transformation product toxicity than the strain 179BP culture. Strain 179BP cells were significantly slower at DCE transformation and butane utilization than strain 183BP cells. DCE (10 μg) was completely transformed in one test bottle containing strain 179BP over a period of 400 hrs. 1,1-DCE (18 μg) was completely transformed within 30 hrs in all three bottles containing strain 183BP. Also, resting cells of strain 183BP were able to transform 3.5 times as much DCE before inactivation than strain 179BP cells. Similar to the strain 183BP results, butane and DCE were concurrently transformed with complete DCE transformation occurring before complete butane utilization in the one strain 179BP bottle. DCA showed little activity until butane was significantly utilized, after which complete DCA transformation and additional butane was required for efficient TCA transformation.

To investigate the amount of cell inactivation caused by DCE transformation, tests were conducted using butane oxidation rates as a measure of general cell activity. Cultures of strain 183BP cells were used to transform different amounts of DCE, after which their butane utilization rates were measured and compared to those of the same cultures treated in an identical manner except without DCE addition. The percent reduction in butane oxidation rate was taken as the percent of cells inactivated by DCE transformation effects.

To initiate the experiment, 5 mL of fresh butane-grown strain 183BP cells were added to 27 mL vials containing 5 mL of fresh mineral media. The vials were crimped sealed with PTFE-lined butyl rubber septa. A DCE-saturated solution was introduced into one half of the vials and the gas phase DCE aqueous concentrations were monitored over time. After DCE was completely transformed by the strain 183BP resting cells, 200 μL of butane was added to each bottle. Butane concentration was monitored and initial butane uptake rates were determined. Bottles treated identically except without DCE exposure were considered to be the baseline or 100% active cell condition. Initial aqueous phase DCE concentrations were 200, 480, and 900 μg/L with triplicate bottles at each concentration and three additional bottles prepared for each condition which were not exposed to DCE. The initial biomass concentration (TSS) used in the 200 and 480 μg/L DCE tests was 145 mg/L. For the final test at 900 μg/L DCE, the initial biomass was increased to 220 mg/L.

At the three different initial DCE concentration conditions, 200 μg/L was completely transformed within 45 min of addition, while transformation of 480 μg/L required 95 hr and transformation of 900 mg/L required 80 hr by a denser culture. After transformation of the DCE, butane utilization rates were measured in both DCE-exposed cultures and unexposed cultures. The results are shown in figures 71, 72, 73, and 74. The rate of butane utilization was slower in each case for cells that had transformed DCE. The cultures had less than 25% of their butane oxidizing capability remaining after transformation of the the 900 μg/L DCE solution (Table 38). The relationship between percent inactivation and DCE mass transformed or specific DCE mass transformed (μg DCE/mg TSS) was approximately linear (Figure 74), but insufficient variations of cell densities and DCE concentrations were tested to verify the linearity of the relationship.

Figure 71. Butane Utilization by Strain 183BP Compared to Those Exposed to DCE and Non-Exposed Cultures. Circles are no-cell controls, triangles are cultures not exposed to DCE, and squares are cultures after transformation of a 900 µg/L DCE solution. Symbols are the average of triplicate bottles with error bars representing 95% confidence intervals. The regressed slope represents the measured butane utilization rate in µg/min.

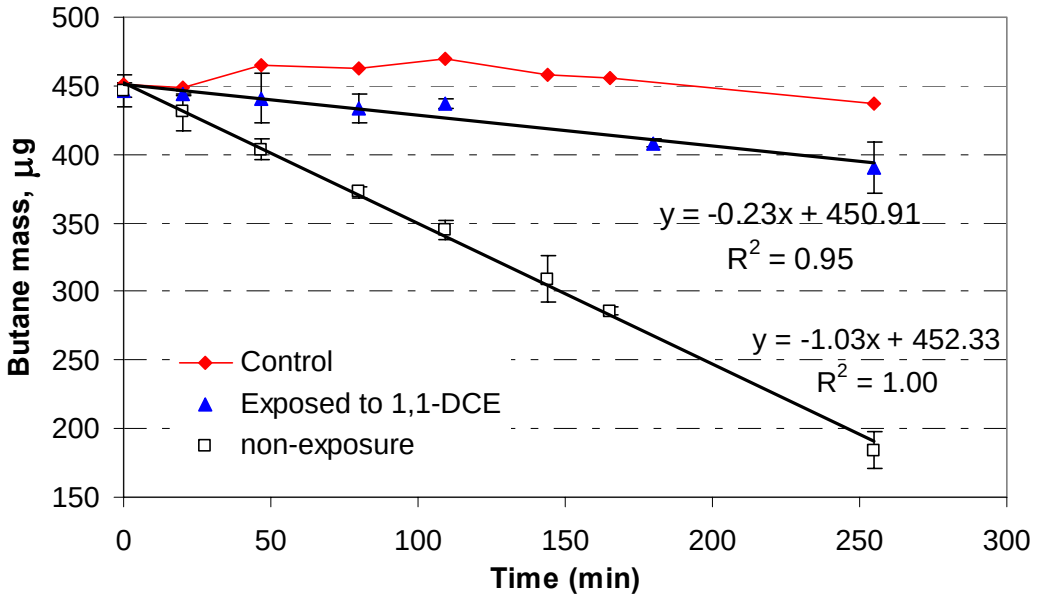

Table 36. Inactivation of Strain 183BP Cultures as a Result of DCE Transformation Measured by the Percent Decrease in Butane Uptake Rates

DCE (µg/L)	DCE transformed (µg)	DCE transformed (µg/mg cells)	Butane Initial Rate		Percent inactivation
			Not exposed to DCE (µg/min)	Exposed to DCE (µg/min)	
900	22.8	10.4	1.02	0.23	77.5
480	12.2	8.4	0.87	0.36	58.6
200	5.1	3.5	0.76	0.47	38.2

Figure 72. Butane Utilization by Strain 183BP Compared to Those Exposed to DCE and Non-Exposed Cultures. Circles are no-cell controls, triangles are cultures not exposed to DCE, and squares are cultures after transformation of a 480 □g/L DCE solution. Symbols are the average of triplicate bottles with error bars representing 95% confidence intervals. The regressed slope represents the measured butane utilization rate in □g/min.

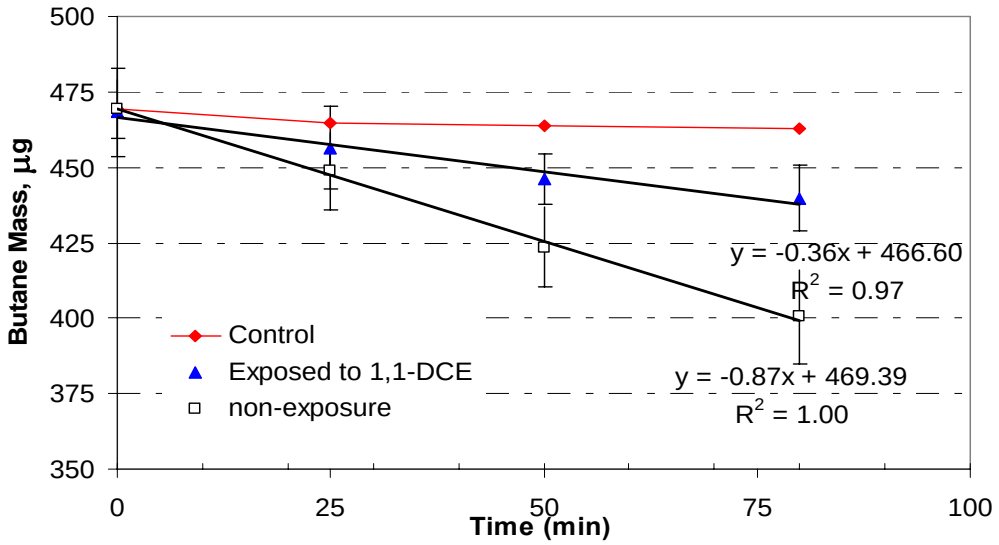

Figure 73. Butane Utilization by Strain 183BP Compared to Those Exposed to DCE and Non-Exposed Cultures. Circles are no-cell controls, triangles are cultures not exposed to DCE, and squares are cultures after the transformation of a 200 µg/L DCE solution. Symbols are the average of triplicate bottles with error bars representing 95% confidence intervals. The regressed slope represents the measured butane utilization rate in µg/min.

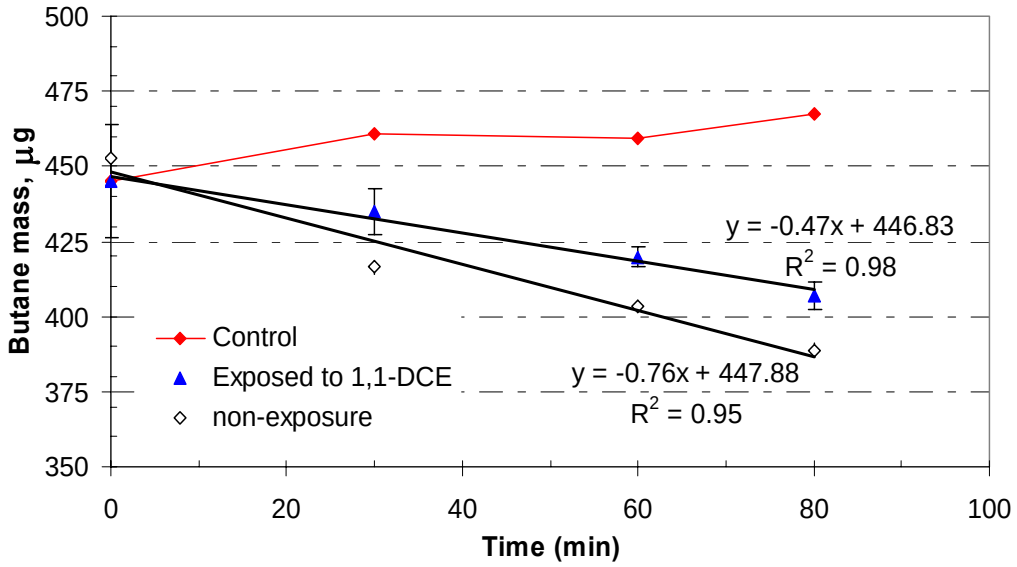

Overall, transformation of increasing amounts of DCE resulted in decreasing cellular butane uptake activity. Greater than 75% cell inactivation followed transformation of 10.4 μg DCE/mg cells. Extending the linear regression in Figure 75, 100% inactivation would occur at approximately 13.5 μg DCE/mg TSS. Estimates of the DCE transformation capacity of the strain 183BP culture presented in the previous section were found to be 14 μg DCE/ mg TSS, in very close agreement with the linear extrapolation.

Figure 74. Inactivation of Strain 183 BP as a Result of DCE Transformation

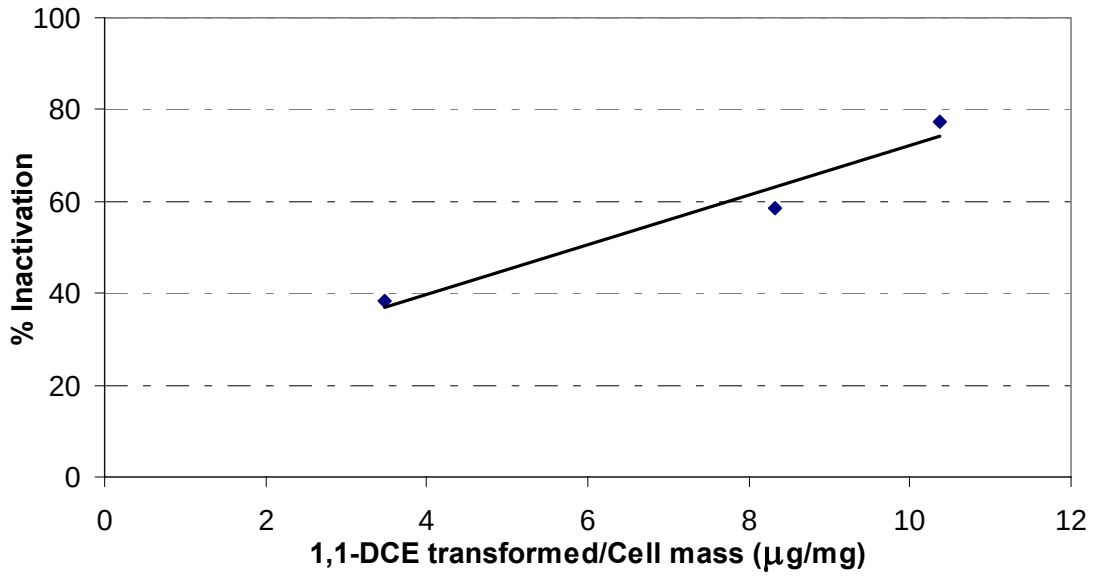

4.5.4 C1 through C6 n-hydrocarbons as substrates for strain 183BP cultures

Strain 183BP was known to cometabolize CAHs when grown on butane, but little was known about the culture's ability to utilize other hydrocarbons as substrates and whether or not other substrates could induce TCA transformation. In these experiments the straight-chain C1 through C6 hydrocarbons, methane, ethane, propane, butane, pentane, and hexane were compared as potential growth substrates for strain 183BP and as inducers of TCA transformation ability. A small inoculum of the strain 183BP culture was incubated in the presence of each potential substrate and the bottles were monitored for substrate utilization over time. Upon complete utilization of the substrate, TCA was added to the bottles and transformation was monitored. If the added TCA was completely transformed, TCA was again added with the procedure repeated until the culture ceased TCA transformation. Each substrate was tested in triplicate bottles.

The 183BP culture was grown on butane from a frozen stock culture to an OD_{600} of 1.2. To initiate the experiment, 0.5 mL of the culture was inoculated into 27 mL vials containing 9.5 mL of fresh mineral media. The average of the initial OD_{600} measurements was 0.175 corresponding to an initial protein concentration of 17 mg/L and a TSS concentration of 36 mg/L (using the relationships developed earlier for strain 183BP cells). Approximately 2.4 mg of substrate was

added to each bottle and the bottles were shaken at 200 rpm at 20°C and monitored over time for substrate utilization. When substrates were completely utilized, aqueous samples were taken to measure OD_{600} and protein concentration. TCA was added to each bottle to achieve a final aqueous concentration of approximately 500 μg/L and gas phase TCA was monitored over time.

The results of the experiments are shown in Figures 76 through 80. The strain 183BP culture was able to utilize all of the substrates except methane and possibly ethane. Little or no methane was utilized in over 10 days of incubation (Figure 76a) with the strain 183BP culture while protein concentrations dropped from an initial value of 17 mg/L to 11 mg/L and OD_{600} fell from 0.175 to 0.04 over the same 10 days presumably due to endogenous respiration. Ethane degradation was not consistent among triplicate bottles (Figure 76b). In one bottle only 20% of the 2.2 mg of the added ethane was degraded in over 10 days of incubation while the optical density decreased to 0.05 and the protein concentration decreased to about 11 mg/L. In the other two bottles, greater than 80% of the ethane was degraded over the same period with a lag time to 50% removal of greater than 140 hr, which was significantly longer than that for the C3 through C6 substrates. Protein concentrations increased very slightly to 18 mg/L and OD_{600} also slightly increased to 0.2 to 0.26, resulting in a calculated yield of approximately 0.01 mg protein/mg ethane or 0.01 mg cells/mg ethane. Based on protein measurements, the strain 183BP culture did not appear to grow on ethane, but rather cometabolized the ethane. Optical density measurements suggested a slight increase in biomass, but optical density is not as good an indicator of active biomass as protein measurement. TCA was not added to the bottles enriched with methane or ethane since neither substrate appeared to support growth of the strain 183BP culture.

Figure 75. Methane and Ethane as Potential Growth Substrates for the Strain 183BP Culture. a) Triplicate bottles with no evidence of methane utilization, and b) Two of three ethane-fed bottles slowly transformed a portion of the ethane.

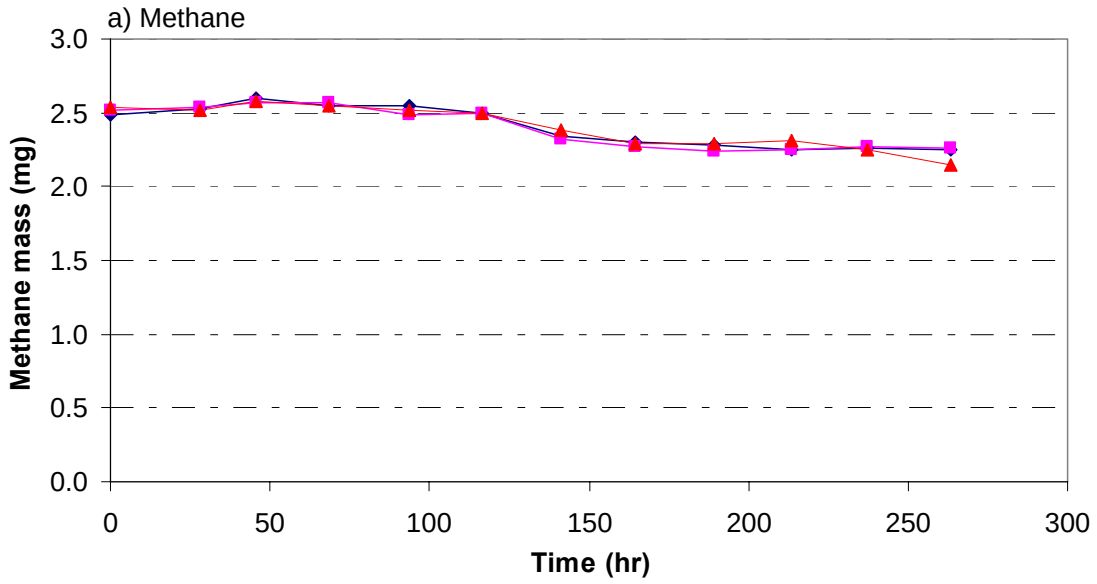

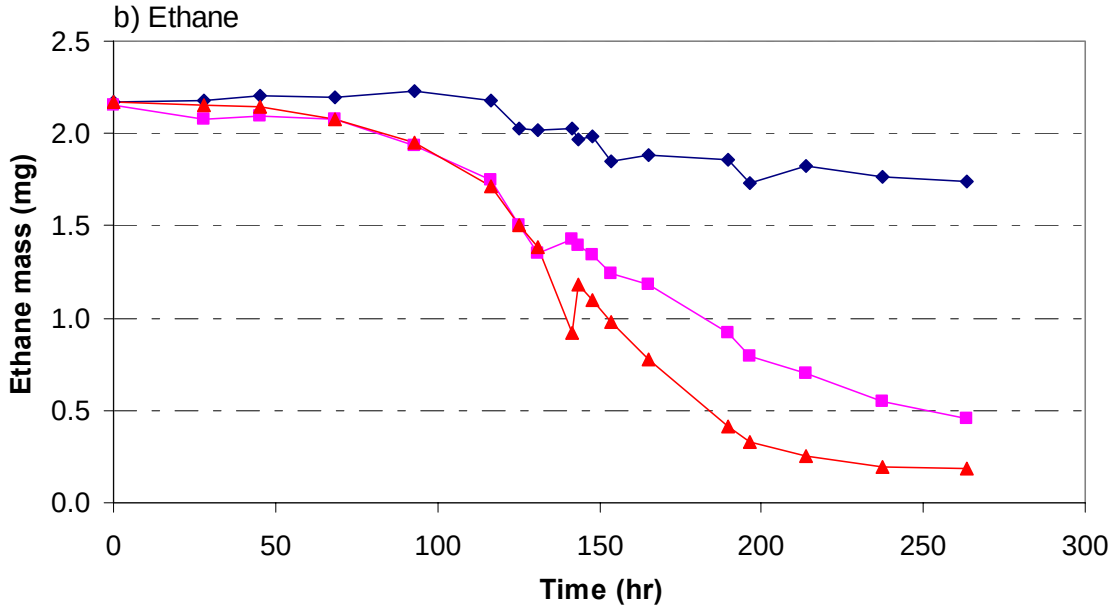

Propane utilization by the strain 183BP culture was consistent in triplicate bottles (Figure 76a), with rapid onset of utilization and requiring approximately 70 hr for 50% propane consumption. However, propane was not completely utilized by the strain 183BP culture. After 2 days of rapid propane utilization, the rate slowed to a halt after about 6 days with 85% of initial propane mass utilized. Cell growth was observed during propane utilization with an increase in OD_{600} to 0.76 and a 37 mg/L increase in protein concentration. The observed yield coefficient was 0.79 mg cells/mg propane (estimated form the TSS/OD_{600} relationship developed in an earlier section) or 0.20 mg protein/mg propane. The maximum propane utilization rate of 31 μg/hr occurred at about 2 days. As propane utilization decreased, TCA was added to the bottles, but no TCA transformation occurred and propane utilization rates essentially stopped (Figure 76b). It is not clear whether propane could support TCA cometabolism or not, since propane was not being utilized during the period that TCA was being tested.

Figure 76. Propane Utilization by the183BP Culture, a) Propane uptake, and b) TCA

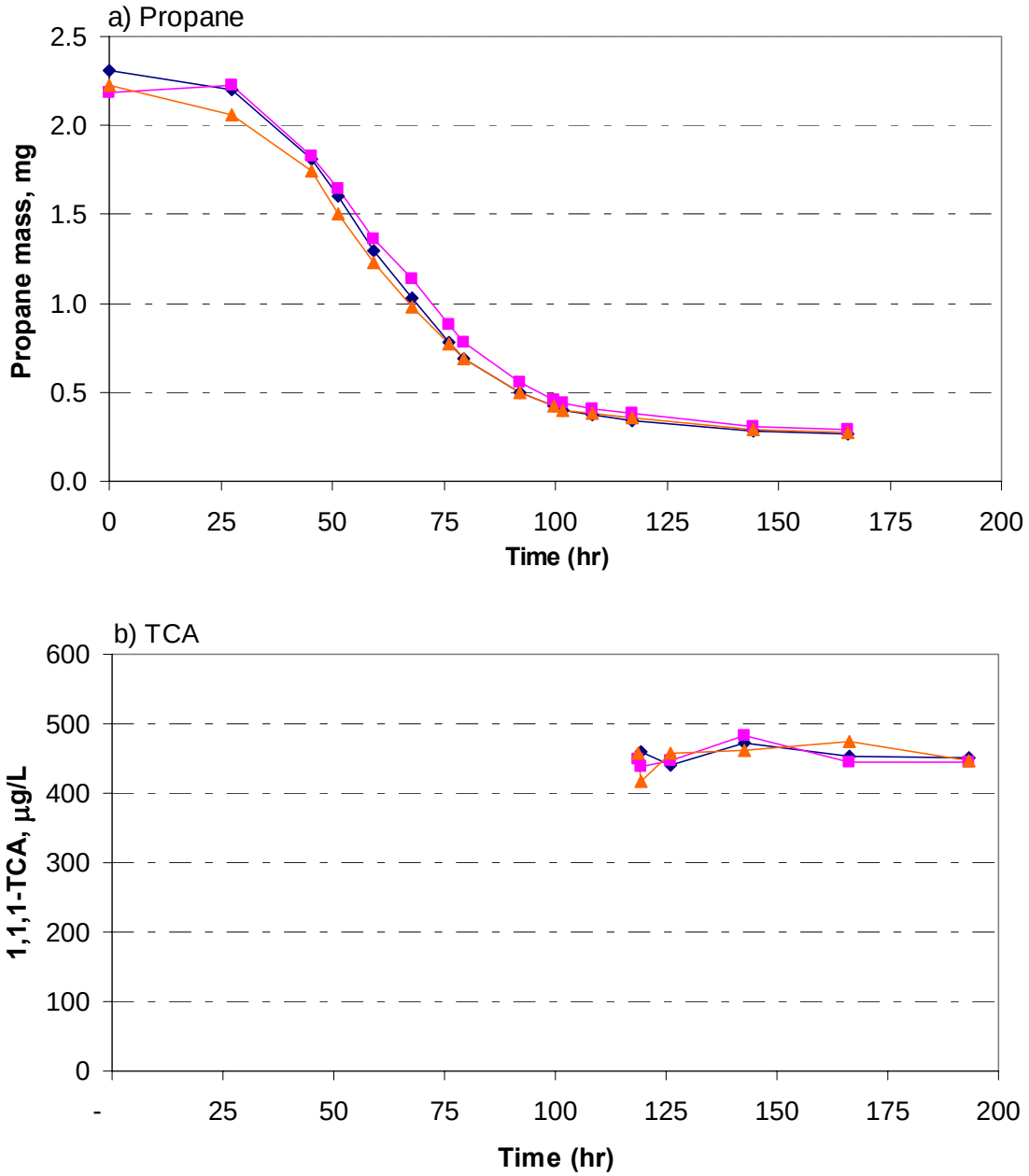

It is possible that nitrogen was a limiting nutrient. Initial nitrate concentration was approximately 200 mg/L providing 2 mg nitrate per bottle. Nitrogen requirements for strain 183BP cells grown on butane were found to be 1.05 mg nitrate/mg butane. If the same relationship held for growth on propane, approximately 2.4 mg nitrate would be required for complete propane utilization. Unfortunately, nitrate concentrations were not measured at the end of the test, so nitrogen limitations could not be confirmed.

Butane utilization was immediate and proceeded to 50% butane consumption by 55 hr, significantly faster than that for ethane or propane (Figure 76a). Samples taken to measure growth at 85% butane consumption resulted in an increase in OD_{600} to 0.77 and an increase in protein concentration of about 43 mg/L. The apparent yield coefficient was found to be 0.76 mg cells/mg butane or 0.22 protein/mg butane which was on the high end of the yield determined in previous tests using butane as a growth substrate ($Y = 0.73 \pm 0.08$ mg cells/mg butane). The maximum butane utilization rate was greater than 50 μg/hr, which was 1.5 times faster than the maximum rate of propane utilization.

TCA was added to the bottles 70 hr into the test after 85% butane consumption. TCA transformation began immediately, but slowly, with the rate increasing as the remaining butane was consumed (Figure 77b). Upon complete TCA transformation, additional TCA was added to the bottles. Less than 1 hr was required to completely transform the additional TCA, resulting in a maximum TCA transformation rate greater than 9.9 μg/hr, or about 19% of the maximum butane utilization rate. Since the TCA transformation rate was so high, the third TCA addition was increased to provide an aqueous concentration of 750 μg/L. TCA transformation stopped after about 75 to 80% TCA was transformed. A transformation capacity, T_c, defined as the maximum amount of TCA transformed per unit cell mass was calculated based on a cell mass estimated form the total butane utilized and the apparent yield coefficient of 0.77 mg cells/mg butane. A T_c of 16 μg TCA/mg cells (or 40 μg TCA/mg protein) and a transformation yield, T_y, of 12 μg TCA/mg butane was estimated for this culture.

Figure 77. Butane Utilization and TCA Transformation by Strain 183BP, a) Butane Uptake, and b) TCA Transformation

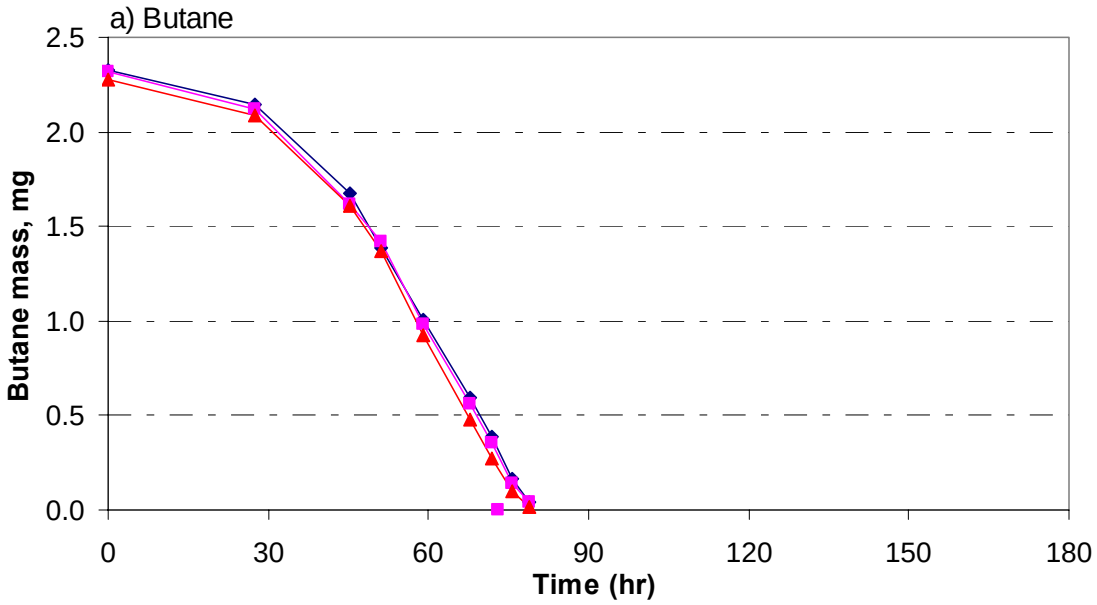

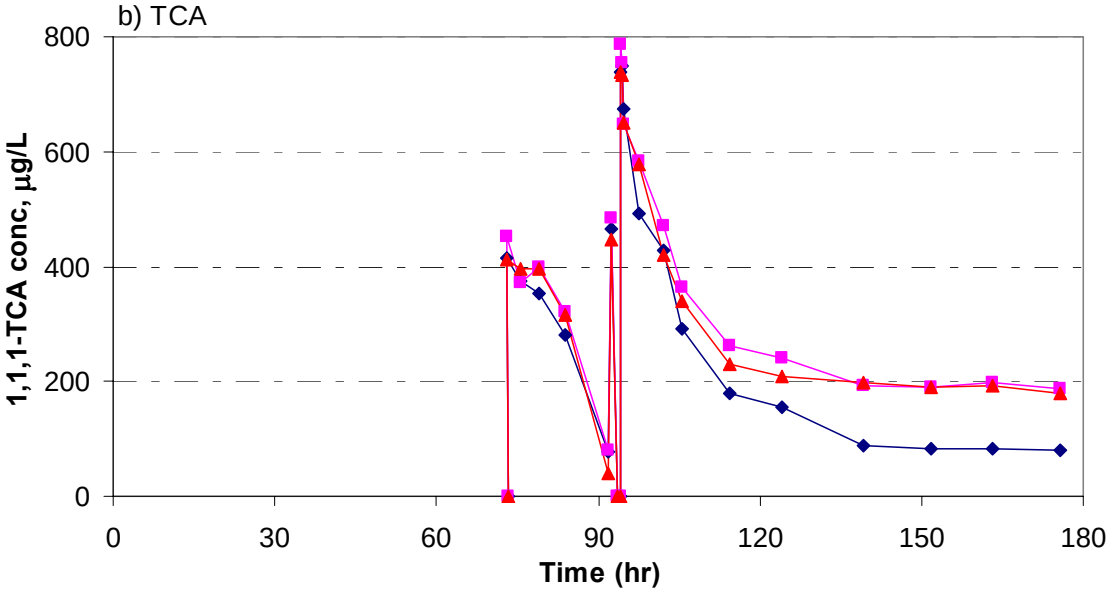

Pentane was also utilized immediately after addition and was completely utilized by about 75 to 80 hr (Figure 78a). OD_{600} increased to 0.9 and protein concentration increased to 60 mg/L, resulting in calculated yield coefficients of 0.77 mg cells/mg pentane and 0.25 mg protein/mg pentane. The strain 183BP culture required about 50 hr to utilize 50% of the pentane and had a maximum pentane utilization rate of 62 µg/hr, which was slightly higher than that for butane.

Figure 78. Pentane Utilization and TCA Transformation by Strain 183BP Culture, a) Pentane Uptake, and b) TCA Transformation Observed in Four TCA Additions

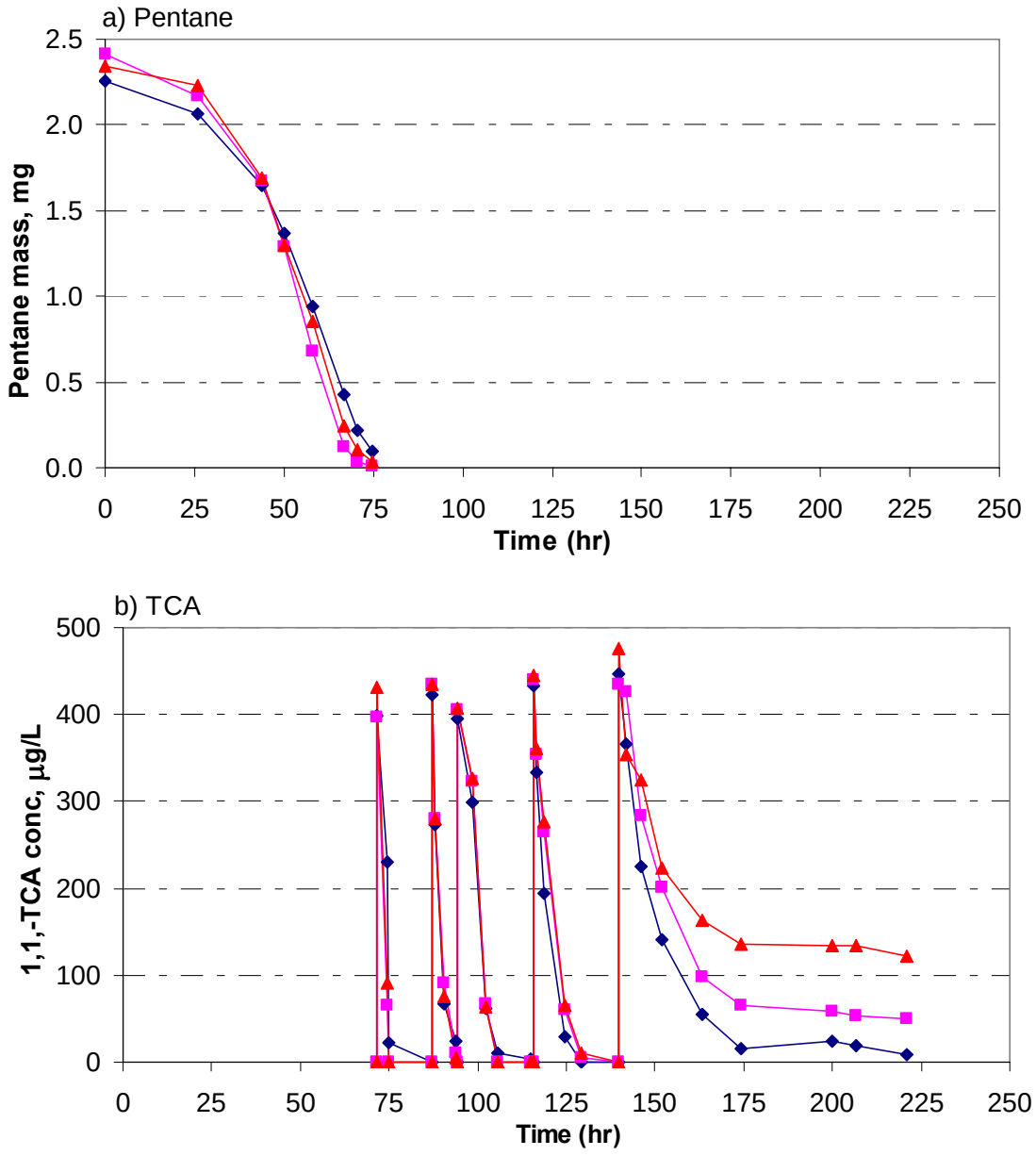

After complete pentane utilization, TCA was added to the bottles and TCA transformation was monitored over time. TCA was completely transformed and was re-added to the bottles four

times before TCA transformation stopped at approximately 175 hr (Figure 78b). A maximum TCA transformation rate of 2.0 μg TCA/hr was obtained after the first TCA addition. Although the maximum TCA transformation rate was less than in the butane grown culture, 40.5 μg of TCA was transformed before exhausting the culture, compared to 28.6 μg for the butane grown culture. The transformation capacity, T_c, with pentane was 26 μg TCA/mg cells and the transformation yield, T_y, was 17 μg TCA/ mg pentane.

Hexane was the longest carbon chain tested as a growth substrate for the strain 183BP culture. Like butane and pentane, hexane was also immediately transformed, but it took 56 hr to reach 50% removal and more than 120 hr for complete utilization (Figure 79a). OD_{600} increased to 0.93 and protein concentration increased to 79.9 mg/L, resulting in calculated yield value of 0.76 mg cells/mg hexane and 0.25 mg protein/mg hexane.

Figure 79. Hexane Utilization and TCA Transformation by Strain 183BP, a) Hexane Uptake, and b) TCA Transformation of Two TCA Additions over 3 days

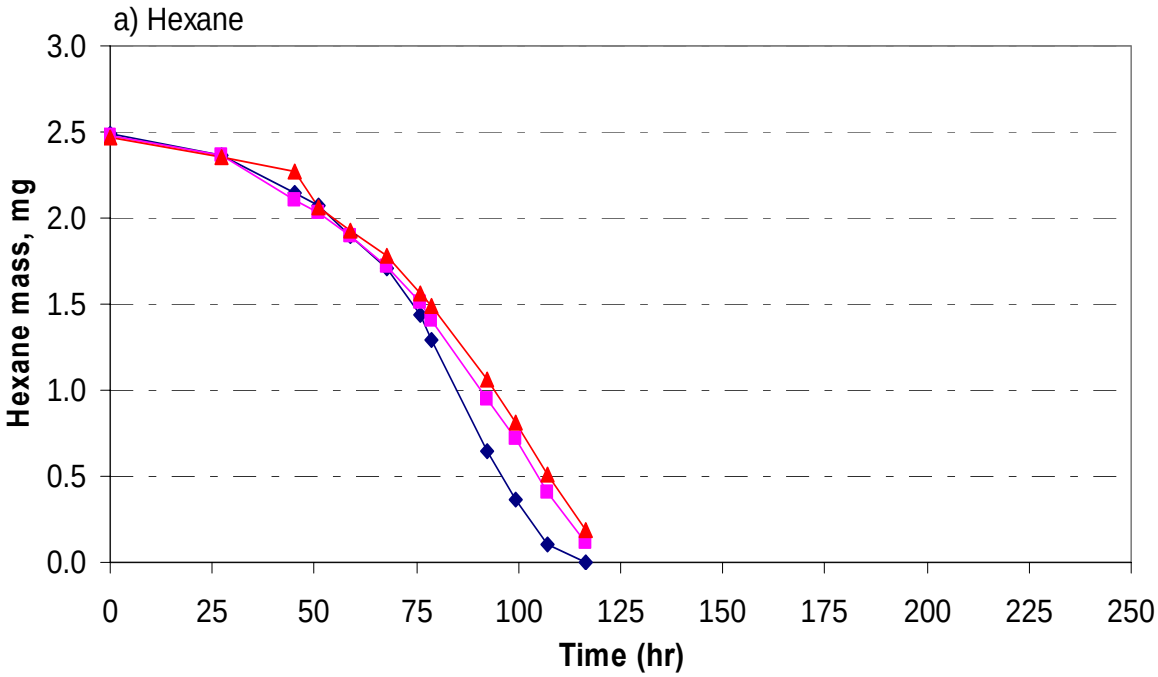

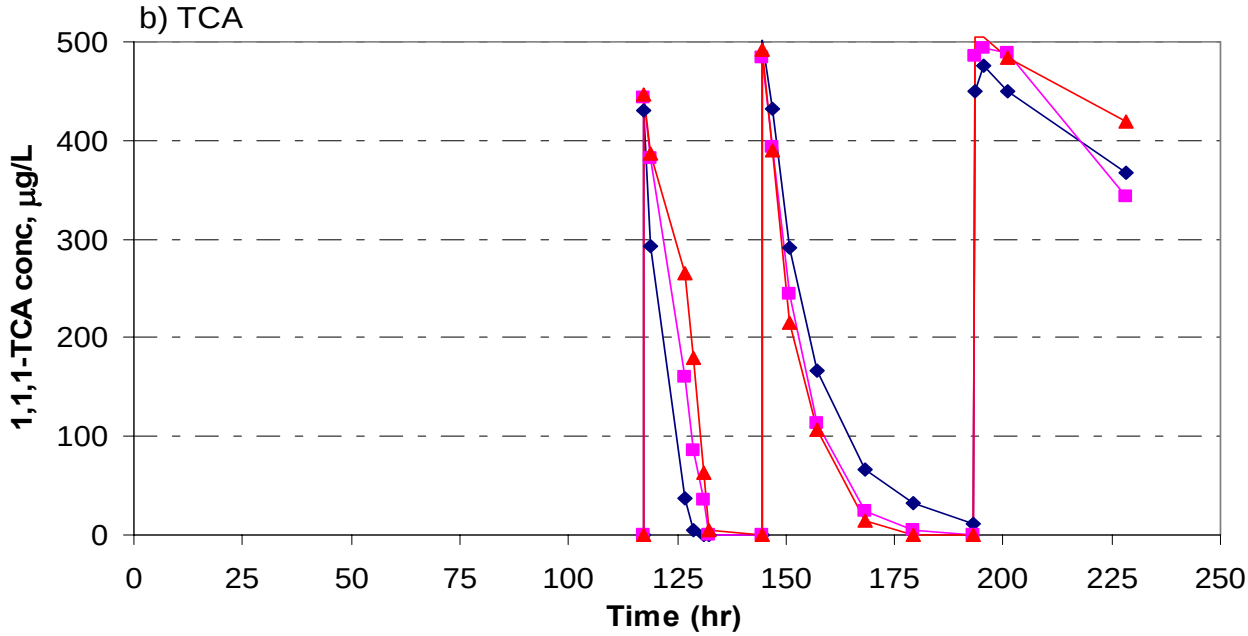

After hexane was completely transformed, TCA was added to the bottles and TCA transformation was monitored over time (Figure 79b). TCA transformation occurred immediately and slowed after the third addition of TCA resulting in 20.6 μg TCA transformed. A transformation capacity, T_c of 11 μg TCA/mg cells and a transformation yield, T_y, of 8 μg TCA/mg hexane were calculated.

Table 37 presents a summary of the experiment results. Although ethane and propane were present at higher aqueous concentrations, the fastest substrate utilization rates were obtained with growth on butane and pentane (50 μg/hr and 62 μg/hr respectively). The slower utilization of hexane may have been due to lower aqueous concentrations, however further experimentation would be required to verify this. Y_{OD600} and Y_{pr} were similar for the C3 through C6 substrates. While propane, butane, pentane, and hexane all supported strain 183BP growth, only butane, pentane, and hexane supported cometabolic TCA transformation.

The highest maximum transformation rates were observed after growth on butane, but pentane-grown cells transformed the most total TCA. Transformation capacity was the greatest for pentane-grown cells (26 μg/mg), followed by that for butane-grown cells (16 μg/mg) and hexane-grown cells (11 μg/mg). Transformation yields followed the same progression with pentane-grown cells (17 μg/mg), butane-grown (17 μg/mg), and hexane-grown (8 μg/mg). Viability of the cells after TCA transformation was not evaluated and nitrate levels were not measured at the end of the test, so substrate and/or TCA transformation may have been limited by nitrogen deficiencies.

Table 37. Summary of Results to Compare the Potential of Substrate as Inducers of 1,1,1-TCA[1]

	Initial	Methane	Ethane	Propane	Butane	Pentane	Hexane
Initial Substrate mass, mg		2.5	2.2	2.3	2.3	2.4	2.5
H_{cc}[2] @25°C		27	20	29	39	50	56
Aqueous solubility[2] @25°C, mg/L		24	61	62	61	41	13
Initial substrate, mg/L		5	6.8	4.6	3.4	2.8	2.6
Time to 50% concentration, hr		-	140	70	55	52	80
Time to complete utilization, hr		-	-	-	80	75	120
Total Substrate removal, mg		-	-	2.0	2.3	2.4	2.5
Max substrate degradation rate, μg/hr		-	-	31	50	62	37
OD^4_{600}	0.18	0.04 ± 0	0.23± 0.12	0.76 ± 0.02	0.77 ± 0.01	0.90 ± 0.01	0.93 ± 0.04
Protein[4], mg/L	17	10.9 ± 10	18.1 ± 4.8	54.0 ± 1.0	60.2 ± 5.7	77.4 ± 6.6	79.9 ± 10.6
TSS^4_{OD600}, mg/L	38	1 ± 0	45 ± 22	160 ± 5	165 ± 5	190 ± 5	200 ± 10
Y_{OD600}, mg Cells/mg Substrate		0.00	0.07	0.79	0.76	0.77	0.76
Y_{pr}, mg Protein/mg Substrate		0.10	0.01	0.20	0.22	0.25	0.25
TCA transformed mass, μg		-	-	-	28.6	40.4	20.6
TCA maximum rate, μg/hr		-	-	-	≥9.3	2.0	0.6
T_c, μg TCA/mg cells		-	-	-	16[3]	26	11
T_y, μg TCA/mg Substrate		-	-	-	12[3]	17	8

1. Values are the average of triplicate bottles except in the case of ethanol where only the two bottles showing activity were averaged.
2. Calculation based on the values in "Environmental Organic Chemistry", Schwarzenbach, R., P., Gshwend, P., M., and Imboden, D., D.
3. Value calculated from TSS estimates based on complete butane utilization and yield coefficient
4. Value ± 95% confidence interval

4.5.5 Batch Transformation Kinetic Tests in Media Using the Strain 183BP Culture

The strain 183BP culture's ability to degrade 1,1,1-TCA, 1,1-DCE, and 1,1-DCA while utilizing butane as a carbon/energy source was measured in mineral salts media (MSM). Vials with a total volume of 27 mL containing 10 mL of strain 183BP cells in growth media, 17 mL of air, and concentrations of 1,1-DCE, 1,1-DCA, 1,1,1-TCA, and butane served as the media reactors. Degradation of the substrates over time was recorded to develop transformation profiles.

Cells used in this experiment were from the culture used to bioaugment the Moffett field site in Season I. Cells were harvested from 8 different batch growth bottles before centrifugation and concentration for delivery to the field. The cells were mixed together and 10 mL were placed into each 27 mL vial. Approximate initial cell concentration was 85 mg/L dry weight. CAHs were injected to the vials to obtain approximate aqueous concentrations of 1,1-DCE, 1,1-DCA, and 1,1,1-TCA of 100, 200, and 200 μg/L, respectively. Butane was injected to obtain approximately 4% v/v in the headspace. The vials were shaken at 200 rpm in a 20°C room. Gas samples were taken periodically using a 100 μL gas-tight syringe and analyzed by gas chromatography.

Overall, the eight reactors behaved very similarly, with 1,1-DCE being quickly transformed, followed by butane, 1,1-DCA, and 1,1,1-TCA as shown in Figure 80 for one of the vials. The slower transformation of 1,1-DCA and especially 1,1,1-TCA may be attributed to inhibition by butane, with faster transformation of these CAHs occurring after a significant portion of the butane had been utilized. All of the vials produced similar results, as seen in Figures 81 and 82. Note that there is good reproducibility in these trends. For example, the reactors which showed slower butane utilization (183G-1A and B) also had slower transformation of all three CAHs

Stella modeling software was used to simulate biotransformation observed in the media reactors (Section 3). Kinetic parameters previously defined for the parent culture that strain 183BP was isolated from (Kim et al., 2002) were assumed as starting values for our model simulations (Table 38). Some values (the decay constant "b", the transformation capacity of 1,1,1-TCA "T_{cTCA}", and the constant for noncompetitive inhibition of 1,1-DCA by butane "$K_{IuBUTDCA}$") were adjusted to achieve a better fit of the experimental data. The initial cell concentration used, 85 mg/L, was based on dry weight analyses.

Results of model simulations using Kim's et al. (2002) input values and again using the adjusted parameter values are presented in Figure 83. A good match between model output and test data for butane, 1,1-DCE and 1,1,1-TCA was found using previously determined model input parameters (Figure 83A). However, the model significantly overestimated the rate of 1,1-DCA transformation in the presence of butane. By decreasing the constant for noncompetitive inhibition of 1,1-DCA by butane from 3.5 to 0.4 μmol/L a better fit was obtained between model output and experimental data for all four compounds (Figure 83B).

Butane was present at a much higher initial mass than the three CAHs and was rapidly transformed resulting in a high k_{max} value (2.5 μmol/mg/hr). 1,1-DCE was rapidly transformed, while 1,1-DCA and 1,1,1-TCA transformation were deterred by butane inhibition and generally slower transformation rates. The k_{max} value used to simulate 1,1-DCE transformation was even greater than that used for the growth substrate butane. The high k_{max} value for 1,1-DCE (2.8

μmol/mg/hr) reflects the significantly faster transformation of this compound as opposed to the lower k_{max} values for 1,1-DCA, 1,1,1-TCA (0.49 and 0.205 μmol/mg/hr, respectively) and their slower overall transformation. The lower noncompetitive inhibition constants of butane on 1,1-DCA and 1,1,1-TCA (0.4 and 0.5 μmol/L) resulted in model predictions of greater inhibition of their transformation by the presence of butane. As butane was consumed transformation rates of 1,1-DCA and 1,1,1-TCA increased.

Overall, these reactors provided a good indication of the culture's CAH biodegradation ability and can be used to gauge the behavior found upon bioaugmentation of this culture in the first season study conducted at the Moffett field site. The simulations suggested that the model performed well in predicting the culture's behavior. The input values defined in the media experiments were used to simulate strain 183BP behavior in subsequent microcosm experiments.

Figure 80. Incubation of a CAH Mixture and Strain 183BP Cells in the Presence of Butane Resulted in Fast 1,1-DCE Transformation Followed by Butane, 1,1-DCA, and 1,1,1-TCA Transformation

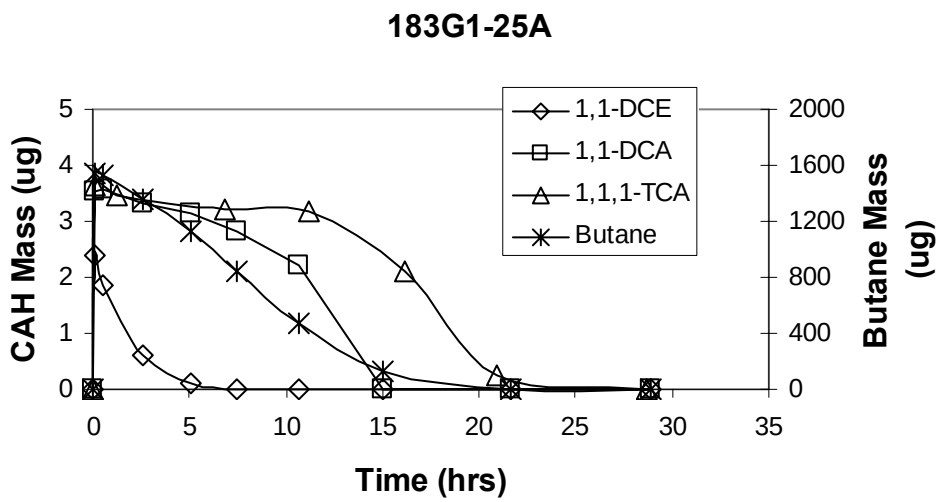

Figure 81. Butane and 1,1-DCE Mass Profiles in 8 reactors containing Strain 183BP Cells, Those Used in the First Season Bioaugmentation at the Moffett Field Site, and a Mixture of 1,1-DCE, 1,1-DCA, and 1,1,1-TCA in the Presence of Butane Show Very Similar Activities. 1,1-DCE transformation is complete before the complete utilization of butane.

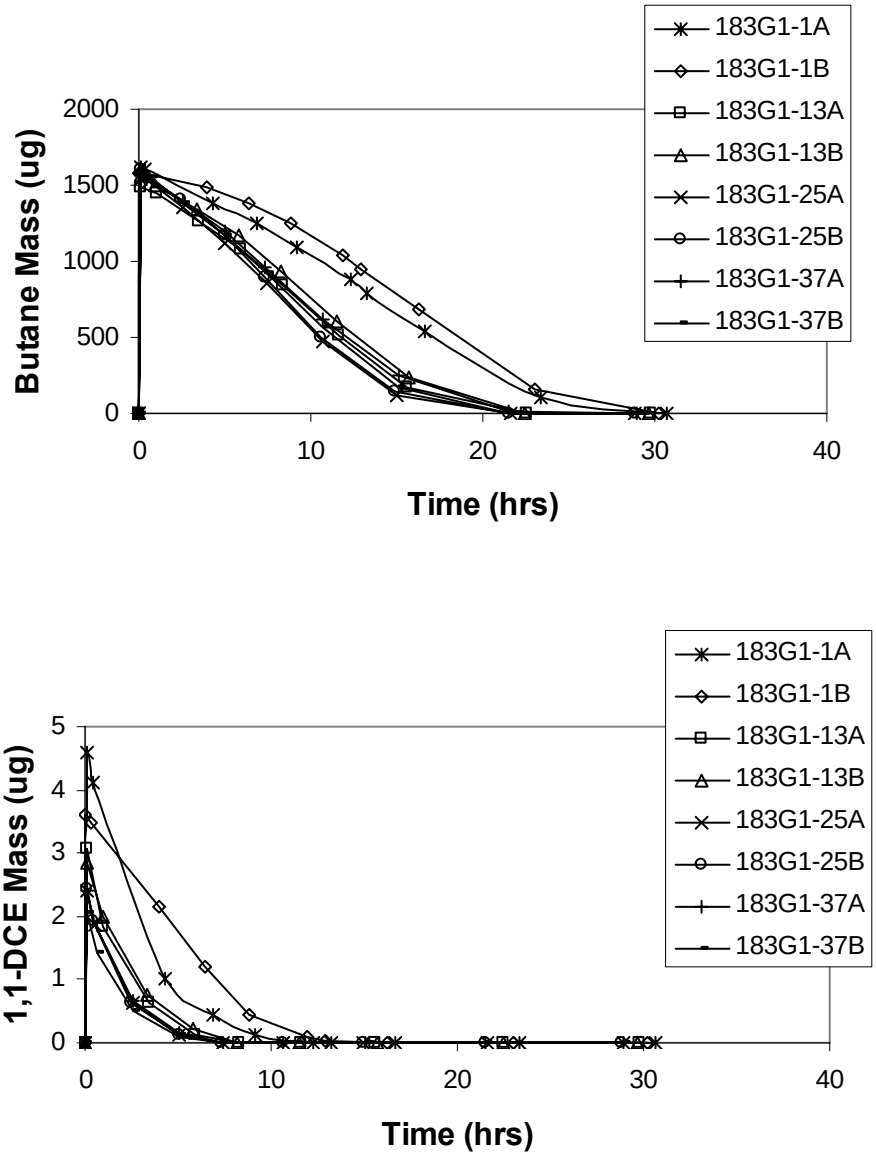

Figure 82. 1,1-DCA and 1,1,1-TCA Mass Profiles in 8 Reactors Containing Strain 183BP Cells, Those Used in the First Season Bioaugmentation at the Moffett Field Site, and a Mixture of 1,1-DCE, 1,1-DCA, and 1,1,1-TCA in the Presence of Butane Show Similar Activities. 1,1-DCA and 1,1,1-TCA transformation rates increased significantly around 10-15 hr and 17-23 hr, respectively, corresponding to points of about 66% and >90% butane removal in the vials.

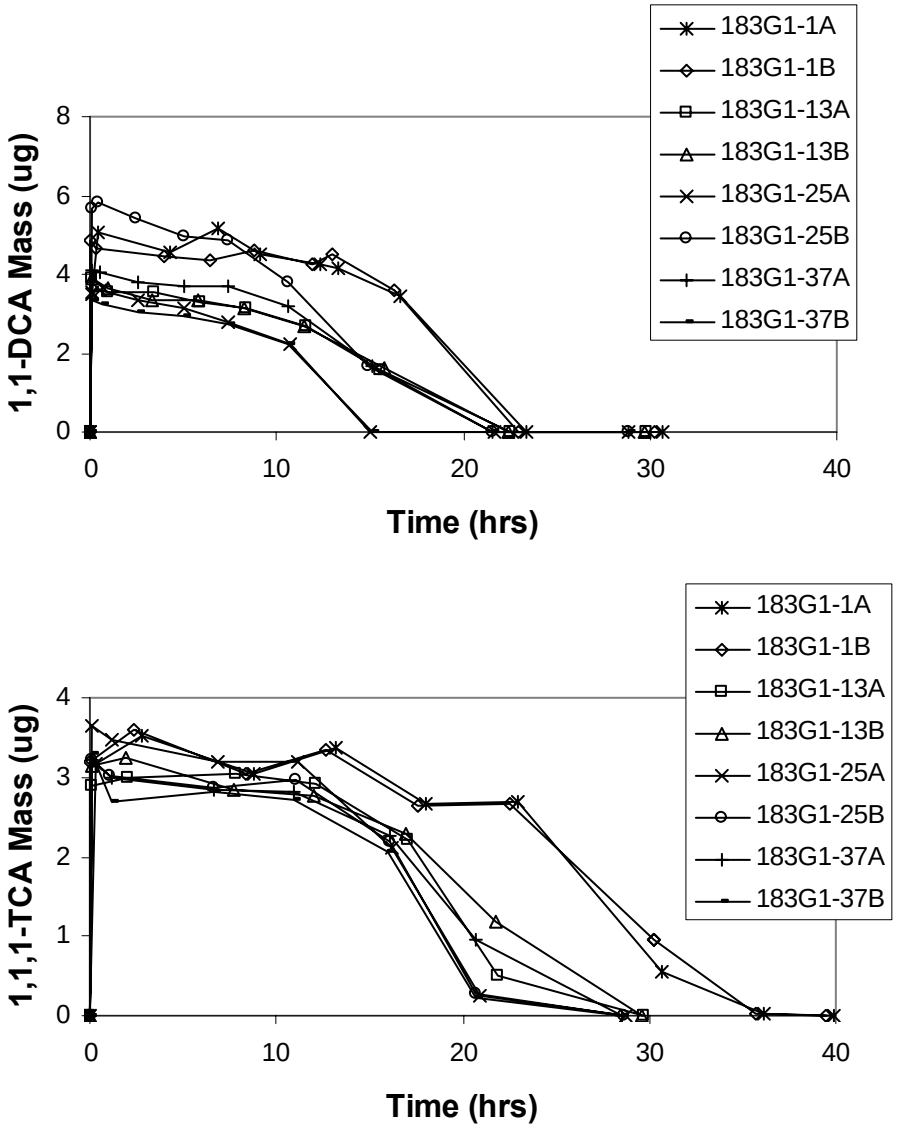

Table 38. Input Parameters for Modeling Biotransformation in Media

Parameter	Units	Value	Parameter	Units	Value
K_{ic}DCABUT	μmol /L	39.87*	X_0	mg/L	85
K_{ic}DCADCE	μmol /L	18*	Y	mg/μmol	0.046*
K_{ic}DCATCA	μmol /L	16*	b	hr-1	.0016*
					.0035**
K_{ic}DCEBUT	μmol /L	8.7*			
K_{ic}DCEDCA	μmol /L	3.6*	V_L	L	.017
K_{ic}DCETCA	μmol /L	1.1*	V_G	L	.010
K_{ic}TCABUT	μmol /L	313*	kmaxBUT	μmol /mg/hr	2.5*
K_{ic}TCADCA	μmol /L	9.8*	kmaxDCA	μmol /mg/hr	0.49*
K_{ic}TCADCE	μmol /L	17*	kmaxDCE	μmol /mg/hr	2.8*
			kmaxTCA	μmol /mg/hr	0.20*
K_{iu}BUTDCA	μmol /L	3.5*			
		0.4**	KsBUT	μmol /L	19.2*
K_{iu}BUTDCE	μmol /L	6.9*	KsDCA	μmol /L	19.2*
K_{iu}BUTTCA	μmol /L	0.5*	KsDCE	μmol /L	1.48*
			KsTCA	μmol /L	12.2*
K_{ic}BUTDCE	μmol /L	403			
			TcDCA	μmol /mg	1.99*
Hcc_{DCA}	-	0.18	TcDCE	μmol /mg	0.52*
Hcc_{DCE}	-	0.86			0.175**
$HccT_{CA}$	-	0.55	TcTCA	μmol /mg	0.52*
Hcc_{BUT}	-	38			0.82**

**Input value per Kim et al. (2002b)*
***Input value adjusted to better fit media reactor data*

Figure 83. Model Simulations of Strain 183BP Transformation of Butane, 1,1-DCE, 1,1-DCA, and 1,1,1-TCA in Media Bottles. A) Simulation using model parameters developed by Kim et al. (2002b) for the parent culture that strain 183BP was isolated from. B) Simulation using the adjusted model parameters developed in this study. Data points depict actual laboratory data. Lines depict model output.

A)

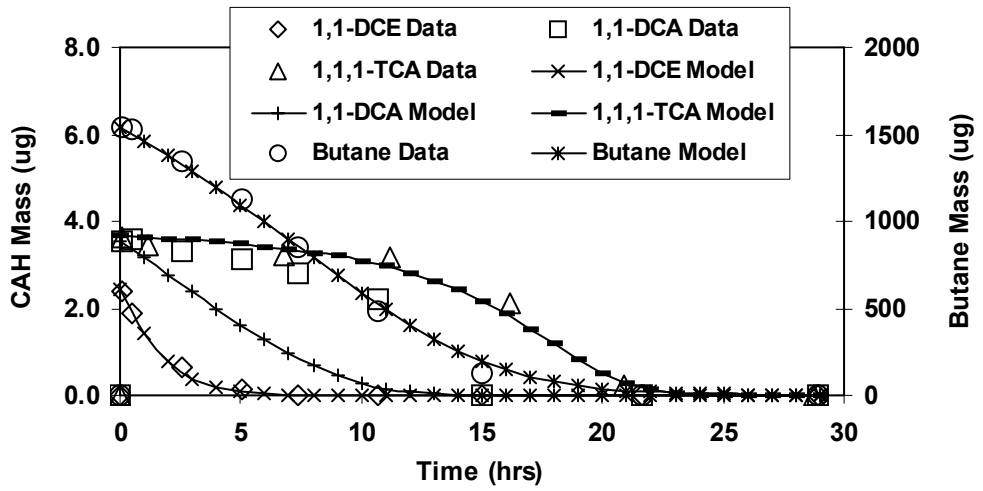

B)

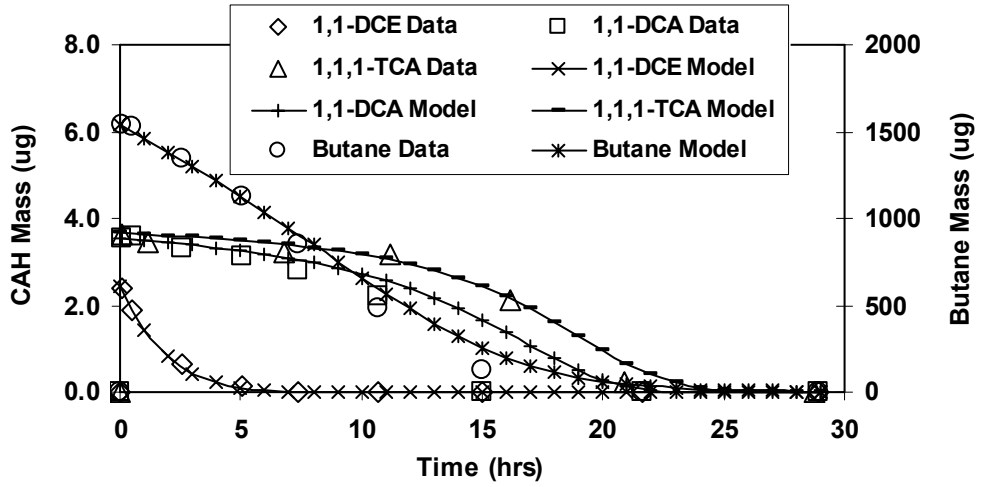

4.6 Comparison of Laboratory Data and Model Simulations from Microcosm Experiments

Soil and groundwater microcosm reactors were used to measure biotransformation of butane and the CAH mixture by the pure culture. Behavior within the microcosms was simulated using the Stella model discussed in Section 3. Presented here are the results of all microcosm experiments and the model simulations.

4.6.1 Results from Microcosms with Indigenous Microorganisms (M1) and Mercury Killed Controls (M4)

Table 39. Microcosm Descriptions

Microcosm Group	Culture[a]	Compound included				Experiment		
		BUT	1,1-DCE	1,1-DCA	1,1,1-TCA	BioT[b]	MTL[c]	TcDCE[c]
M1	*I*	*x*	*x*	*x*	*x*	*x*	-	-
M2	*B*	*x*	*x*	*x*	*x*	*x*	*x*	*x*
M3	*B*	*x*	*x*	*x*	*x*	*x*	*x*	*x*
M4[e]	*B*	*x*	*x*	*x*	*x*	*x*	-	-
M5	*B*	*x*	-	-	-	*x*	-	-

a. I represents the indigenous culture. B represents the bioaugmentation culture.
b. Biotransformation Experiment (Section 3.4.2)
c. Mass Transfer Limitation Experiment (Section 3.4.3)
d. 1,1-DCE Product Toxicity Experiment (Section 3.4.4)
e. Mercury killed control

To serve as controls, the culture indigenous to Moffett Field (microcosm group M1) and the bioaugmented culture killed with mercury (microcosm group M4) were studied for biotransformation activity. Data for M1 and M4 are presented in Figures 84 and 85 respectively. Butane is represented as mass in the gaseous phase, while the CAHs are represented by total mass within the reactors. Microcosms M1 (no po---) showed that for a period of 100 days, the indigenous organisms did not utilize butane or transform any of the CAHs. The mercury killed control microcosms (M4) showed negligible losses over time. Note the reproducibility of the data. These results indicated that transformation of the compounds seen in the other microcosms (M2, M3, and M5) were primarily due to the behavior of the bioaugmented culture--not transformation by the indigenous organisms or seepage losses from the reactors.

Figure 84. Poisoned Control Data for M1 (indigenous culture)

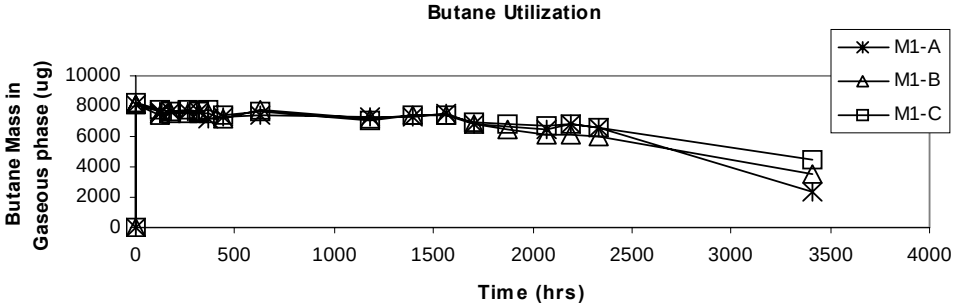

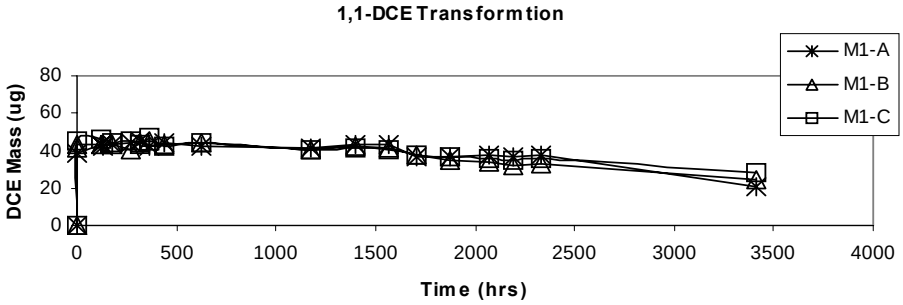

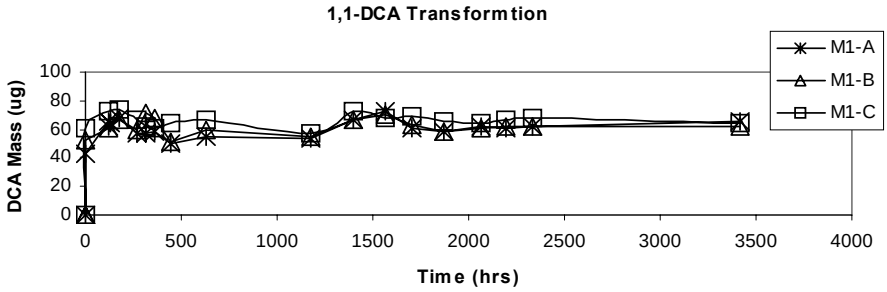

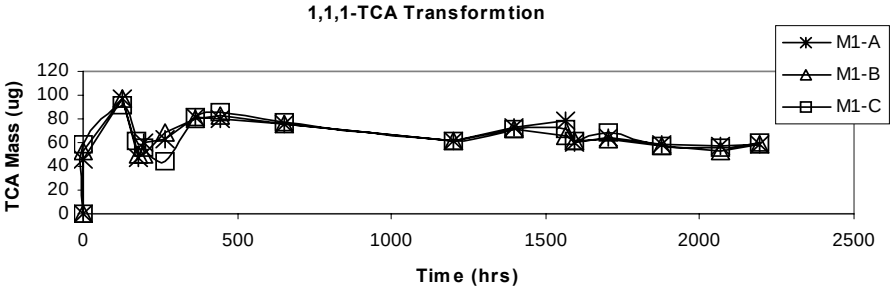

Figure 85. Laboratory data for M4 (mercury killed control)

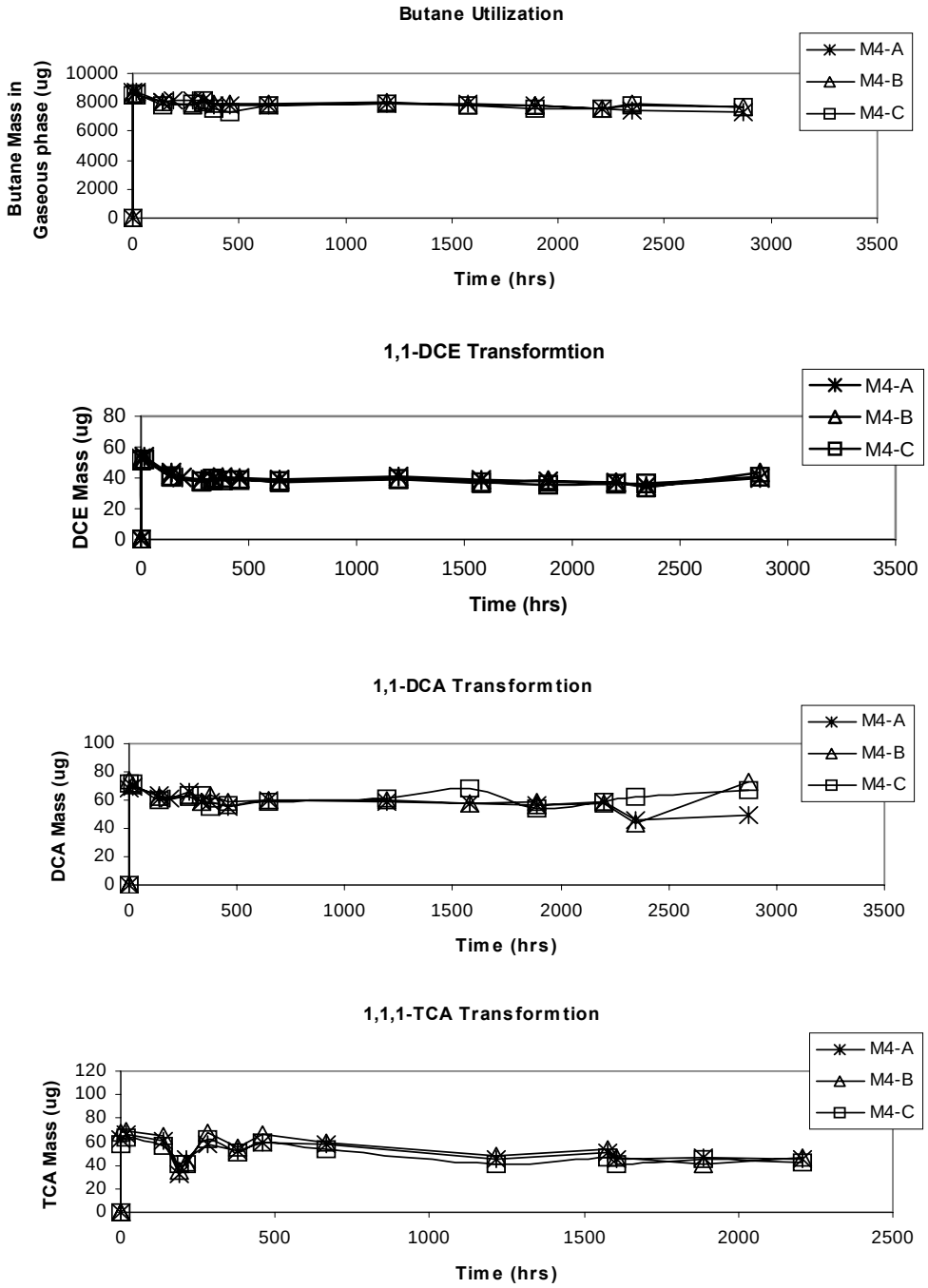

4.6.2 Bioaugmented Culture Exposed to Butane and CAHs (M2, M3)

Biodegradation of butane and the CAH mixture by the bioaugmented culture was studied in microcosms M2 and M3. The two groups differed in that the CAHs were added to the M3 group approximately 12 hours after butane, while butane and the CAHs were added simultaneously to the M2 group. This was done to study the effect of the butane pre-exposure on the thawed cells. All microcosms were exposed to 5 repeat additions of the compounds. Transformation over time was measured for each reactor using headspace analysis.

These microcosm experiments indicated that the bioaugmented culture was capable of butane utilization and biotransformation of the CAH mixture. Data from these microcosms and the control microcosms (M1 and M4), in which no butane utilization or CAH transformation was observed, supported this conclusion. The total mass remaining in each microcosm over time was determined based on equilibrium partitioning between phases. Results for one test reactor (M2B) are presented in Figure 86. As seen in the media experiments, microcosm data showed that 1,1-DCE is quickly degraded. Butane strongly inhibited the transformation of 1,1-DCA and 1,1,1-TCA. The decreased time for complete removal of all compounds as seen throughout repeat compound additions is indicative of the growing cell population.

A comparison of mass profiles for all reactors is presented in Figure 87. Note that there is good reproducibility of trends. For example, in microcosm M3A, slower CAH transformation occurred with a lag in butane. This trend is repeated in later additions as well, and may be attributed to a lower cell mass within this reactor. After the addition of the fifth substrate, transformation and utilization in microcosm M2C was lost. This was most likely due to nutrient limitations within the reactor.

Figure 86. Microcosm M2B Experimental Data

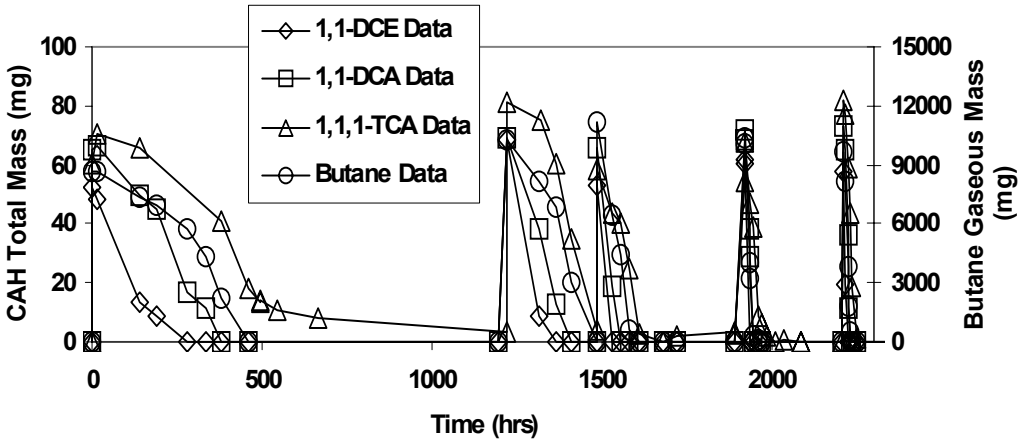

Figure 87. Results of Biotransformation Experiments for Microcosms M2 and M3.
Butane is reported as mass in the gaseous phase.

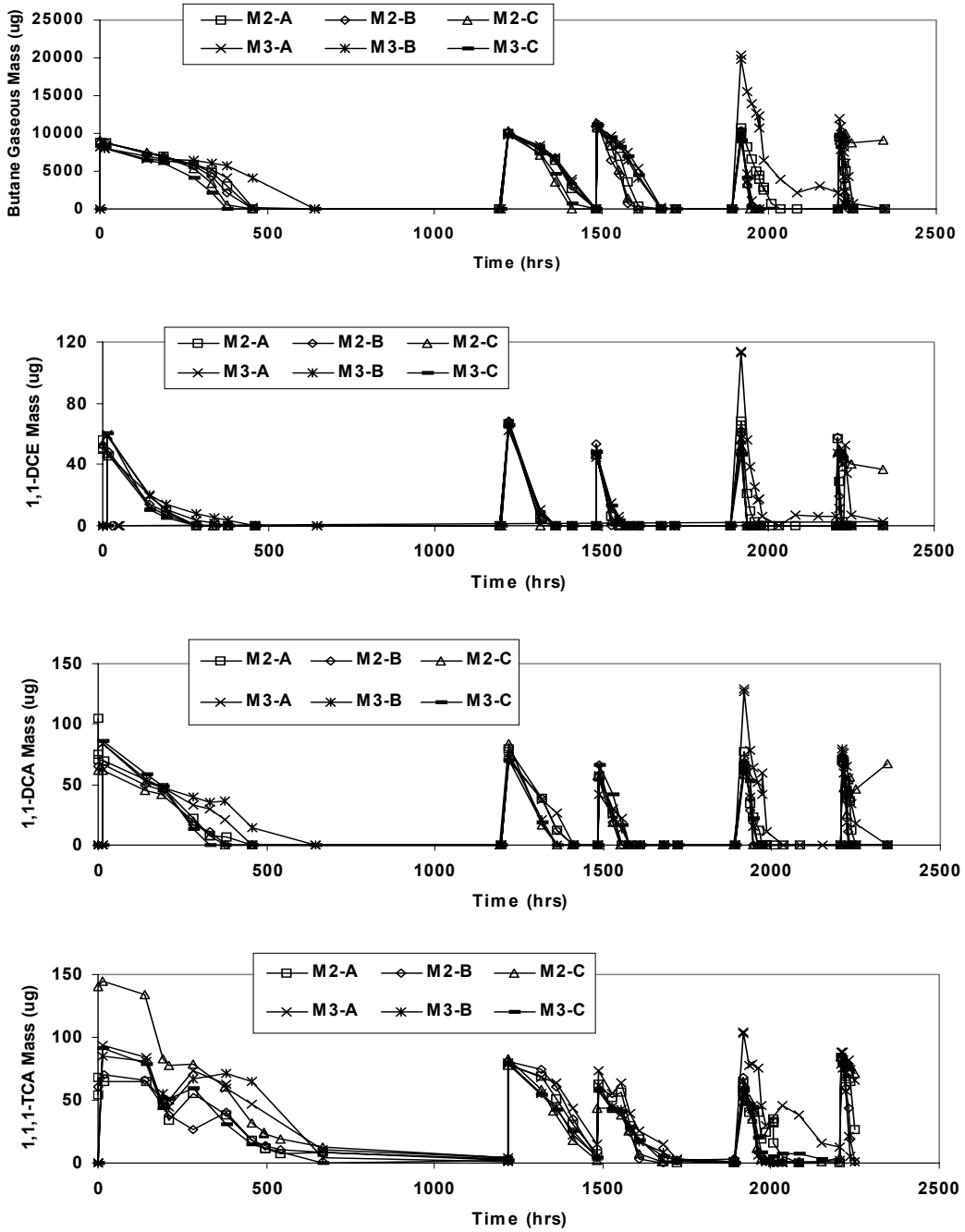

4.6.3 1,1-DCE Transformation Capacity Experiments in Microcosms

After five additions of butane and the CAH mixture had been degraded and transformed, preliminary model simulations indicated that the product toxicity of 1,1-DCE for our culture was much greater than that reported by Kim et al. (2000). Kim reported a 1,1-DCE transformation capacity (T_{cDCE}) value of 0.52 μmol DCE/mg cells (0.05 mg/mg), while our simulations showed that a value of 0.175 μmol DCE/mg cells (0.017 mg/mg) more adequately fit our laboratory data.

A new set of laboratory experiments was run on four of the bioaugmented microcosms (M2A, M2B, M3A, and M3B) to measure the actual transformation capacity of 1,1-DCE of the culture. This was done by determining the approximate cell mass present in the reactors based on butane utilization simulations, assuming a T_{cDCE} value of 0.52 μmol/mg, and calculating an approximate mass of 1,1-DCE required to eradicate all the cells.

To determine the required 1,1-DCE amount, repeat additions of butane were injected into the microcosms to stimulate the cells (which had been resting for several weeks) and develop utilization profiles. These profiles were simulated using the Stella model to determine approximate cell mass within the reactors. Laboratory data and model output for the latter two butane additions prior to product toxicity experiments are shown in Figure 88. The models represent butane utilization for various initial cell concentrations. Microcosm M2A was treated as an outlier and eliminated from further toxicity experiments. It is important to note, however, that the model provides a good fit of data from all four reactors.

Based on the three other microcosms (M2B, M3A, and M3B), 123 mg/L was assumed for the cell concentration at the start of the 1,1-DCE product toxicity tests, which corresponded to a cell mass of 41.2 mg within the reactors (aqueous volume = 0.40 L).

Figure 88. Simulation of Butane Utilization Prior to 1,1-DCE Transformation Capacity Experiments. Model fits to the microcosm data were used to estimate cell mass.

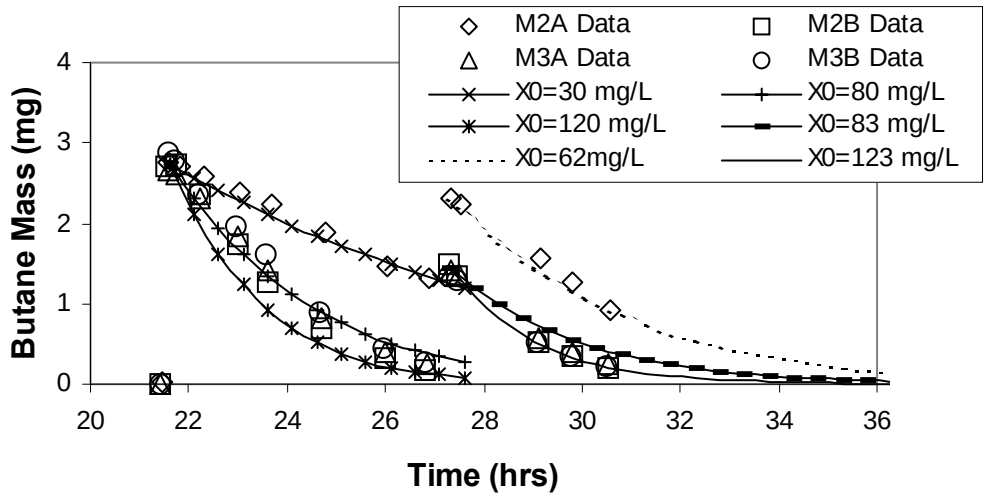

Previous simulations of the CAH mixture's transformation in microcosms indicated that a T_{cDCE} value of 0.175 μmol DCE/mg cells (0.017 mg/mg) better fits transformation data from our culture. Assuming T_{cDCE} = 0.017 mg DCE/mg cells, the required amount of 1,1-DCE to kill 41.2 mg cells is 717 μg 1,1-DCE:

$$M_{DCE} = Tc_{DCE} * X = 0.02 * 41.2 = 717 \mu g \ of \ 1{,}1 - DCE$$

where: M_{DCE} = total mass of 1,1-DCE within the microcosm (μg)
T_{cDCE} = transformation capacity of 1,1-DCE (μg DCE/mg cells)
X = cell mass (mg/L)

The three microcosms (M2B, M3A, and M3B) were then exposed to this elevated 1,1-DCE mass and transformation over time was measured. Approximately 1200 μg 1,1-DCE and 110 μg 1,1,1-TCA were added to the microcosm, which were then incubated at 150 rpm so that no mass transfer limitations would occur.

Figure 89 displays the laboratory data for the reactors and model output from simulations, including both T_{cDCE} values. Input values for the simulations are provided in Table 40. The plots show the mass of 1,1,1-TCA and 1,1-DCE remaining in the microcosms during the transformation test. The data are very reproducible. 1,1-DCE was rapidly transformed during the first 5 to 6 hours of these experiments, after which transformation ceased. 1,1,1-TCA transformation was never observed. This may be due to the time lag for 1,1,1-TCA transformation as opposed to 1,1-DCE. 1,1-DCE effectively eradicated all cells, preventing 1,1,1-TCA from ever being transformed. This, along with the model output, indicates that a lower T_{cDCE} value (0.175 μmol/mg = 0.017 mg/mg) better describes product toxicity for our culture. This lower T_{cDCE} value was therefore used in future model simulations. Note that at the lower T_{cDCE} value, the model also predicted that no 1,1,1-TCA transformation would occur.

Figure 89. Results of Transformation Capacity Experiments of 1,1-DCE

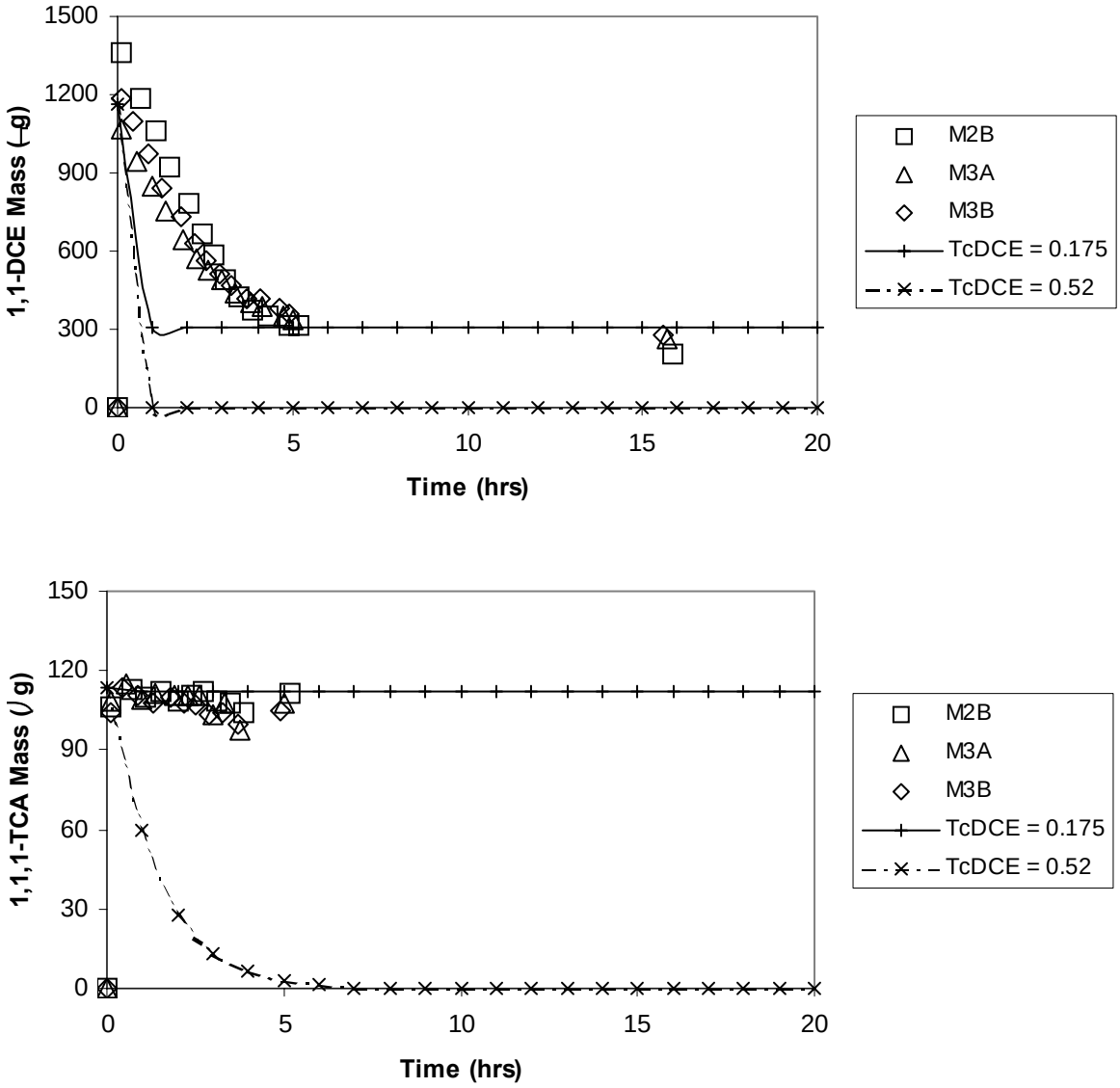

Table 40. Input Parameters for Modeling1,1-DCE Product Toxicity

Parameter	Units	Value	Parameter	Units	Value
K_{ic}DCABUT	μmol/L	403	X_0	mg/L	123*
K_{ic}DCADCE	μmol /L	18			
K_{ic}DCATCA	μmol /L	16	Y	mg/μmol	.046
			b	hr^{-1}	0.0035
K_{ic}DCEBUT	μmol /L	8.7			
K_{ic}DCEDCA	μmol /L	3.6	V_L	L	.400
K_{ic}DCETCA	μmol /L	1.1	V_G	L	.267
K_{ic}TCABUT	μmol /L	313	kmaxBUT	μmol /mg/hr	2.5
K_{ic}TCADCA	μmol /L	9.8	kmaxDCA	μmol /mg/hr	0.49
K_{ic}TCADCE	μmol /L	17	kmaxDCE	μmol /mg/hr	2.8
			kmaxTCA	μmol /mg/hr	0.2
K_{iu}BUTDCA	μmol /L	4.0			
K_{iu}BUTDCE	μmol /L	6.9	KsBUT	μmol /L	19.2
K_{iu}BUTTCA	μmol /L	0.5	KsDCA	μmol /L	19.2
			KsDCE	μmol /L	1.48
K_{ic}BUTDCE	μmol /L	0.33	KsTCA	μmol /L	12.2
Hcc_{DCA}	-	0.18	TcDCA	μmol /mg	1.99
Hcc_{DCE}	-	0.86	TcDCE	μmol /mg	0.52
$HccT_{CA}$	-	0.55			0.175
Hcc_{BUT}	-	38	TcTCA	μmol /mg	0.82

Nomenclature provided in Appendix C
**Initial cell concentration for 1,1-DCE toxicity experiments only. Initial cell concentrations for butane utilization models prior to toxicity experiment as noted in the legend of Figure 88.*

As seen in Figure 89, the model predicts that 1,1-DCE transformation should have occurred much faster than that shown by actual data. This indicated that the 1,1-DCE maximum transformation rate was less than that used as an input value in the model (k_{mDCE} = 2.8 μmol/mg/hr). Therefore, simulations were run at lower k_{mDCE} values (0.28 and 0.10 μmol/mg/hr) in attempt to better fit this observation. Figure 90 shows 1,1-DCE and 1,1,1-TCA transformation simulated with various k_{mDCE} values and compares the output to the actual data measured in the reactors. All other input values followed those listed in Table 40.

Comparison of the model outputs indicated that a k_{mDCE} value an order of magnitude less than that defined by Kim et al (2002b). more accurately describes the laboratory microcosm tests. Note that even at varying utilization rates, the effect of product toxicity remains constant; there is no degradation after 5 hours. It is difficult to determine what factors result in the possible lower k_{mDCE} needed to match the laboratory data. It may have been that enzyme activity was lower than in resting cell tests of k_{mDCE} (Section 4.6.2), or the culture actually has lower k_{mDCE} values than Kim's culture. Later microcosm tests evaluated the sensitivity to the k_{mDCE} value.

Figure 90. Simulations for Various k_{mDCE} Values Compared to Laboratory Data

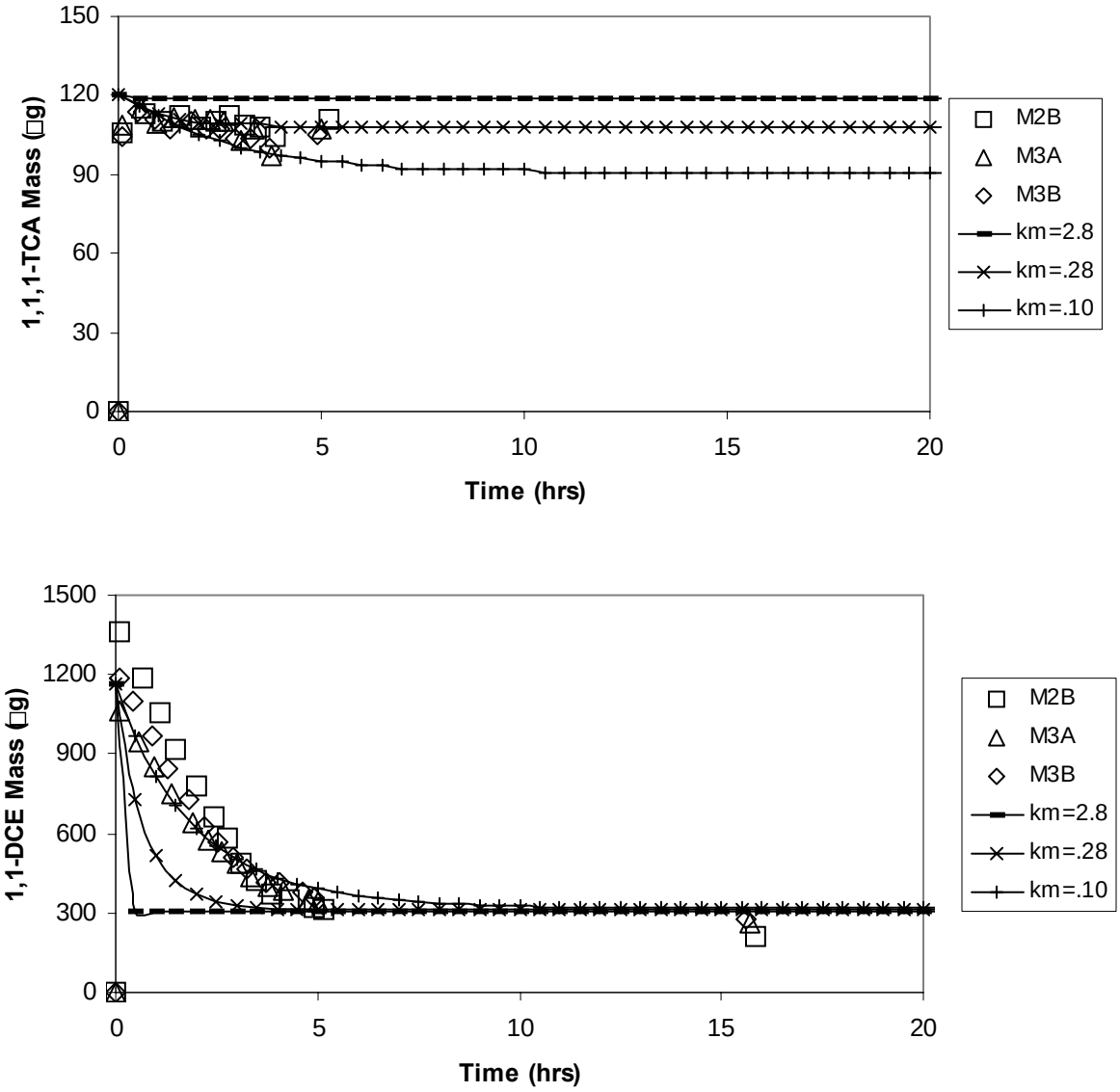

4.6.4 Model Simulations for Biotransformation in Microcosm M2B

The Stella biotransformation model was used to simulate the laboratory data of microcosm M2B. The input values for the model are listed in Table 41, and were based on those defined by Kim et al (2002b), with the exception of T_{cTCA}, T_{cDCE}, K_{Ga}.

Initial cell masses for simulating biotransformation of each compound addition are listed in Table 42. For simulating utilization of the first butane addition, X_0 was assigned a value of 4.1 mg/L. This value compares to the estimated initial cell mass of 1.5 mg/L. The first simulation (S1) was allowed to run until the time of the second addition of butane (about 1200 hours). The cell concentration remaining when butane was completely utilized (approximately 500 hrs) was input as the initial cell concentration for simulation of utilization of the second butane addition (S2). This pattern was followed for the remaining simulations. Initial cell concentrations were assigned this way because it was assumed that the decay term for the model is not appropriate for long periods when the cells are not exposed to the primary growth substrate. This lower cell decay is still hard to explain unless product toxicities were actually less that those assumed.

As experiments indicated (data not shown), non-equilibrium partitioning between the gaseous and aqueous phases occurred in the reactors during biotransformation of the first three compound additions (S1 through S3). Therefore, mass transfer limitations (MTL) were included in these model simulations as done with the simulations of microcosms M5 (data not shown). A mass transfer coefficient ($K_{Ga} = 0.03\ hr^{-1}$) was used.

Table 41. Input Values for Simulating Biotransformation in M2 and M3

Parameter	Units	Value	Parameter	Units	Value
K_{ic}DCABUT	μmol/L	403	X_0	mg/L	varies*
K_{ic}DCADCE	μmol /L	18	Y	mg/μmol	.046
K_{ic}DCATCA	μmol /L	16	b	hr^{-1}	0.0035**
K_{ic}DCEBUT	μmol /L	8.7	K_{Ga}	hr^{-1}	0.03***
K_{ic}DCEDCA	μmol /L	3.6			
K_{ic}DCETCA	μmol /L	1.1	V_L	L	.400
			V_G	L	.267
K_{ic}TCABUT	μmol /L	313			
K_{ic}TCADCA	μmol /L	9.8	kmaxBUT	μmol /mg/hr	2.5
K_{ic}TCADCE	μmol /L	17	kmaxDCA	μmol /mg/hr	0.49
			kmaxDCE	μmol /mg/hr	2.8
K_{iu}BUTDCA	μmol /L	4.0**	kmaxTCA	μmol /mg/hr	0.2
K_{iu}BUTDCE	μmol /L	6.9			
K_{iu}BUTTCA	μmol /L	0.5	KsBUT	μmol /L	19.2
			KsDCA	μmol /L	19.2
K_{ic}BUTDCE	μmol /L	0.33	KsDCE	μmol /L	1.48
			KsTCA	μmol /L	12.2
Hcc_{DCA}	-	0.18			
Hcc_{DCE}	-	0.86	TcDCA	μmol /mg	1.99
$HccT_{CA}$	-	0.55	TcDCE	μmol /mg	0.175**
Hcc_{BUT}	-	38	TcTCA	μmol /mg	0.82**

Nomenclature provided in Appendix C
**Initial cell concentration varied for each simulation. See Table 42*
***Values adjusted to better fit microcosm data.*
****Mass Transfer Limitation was assumed for simulations S1, S2, and S3 only.*

Table 42. Initial Cell Concentration for Simulating Biotransformation in the M2 and M3 Microcosm

Spike #	Approx Time since Last Spike (hrs)	MTL included in Simulation?	X_0 (mg/L)
S1	-	Y	4.1
S2	1200	Y	7.0
S3	270	Y	9.2
S4	430	N	12.7
S5	92	N	17.7

Figure 91 displays the modeling and microcosms results, showing the total mass within the microcosm over time for five additions of butane and the three CAHs. Butane mass from the gaseous phase is presented instead of total mass due to MTL occurring between fluid phases. Of interest here is the model's ability to mimick transformation orders and inhibition influences of each compound. Note that as the laboratory studies showed, the model predicted 1,1-DCE to be quickly degraded, followed by 1,1-DCA and 1,1,1-TCA transformation. Butane showed very strong inhibitory affects on 1,1-DCA and 1,1,1-TCA, with faster transformation of these CAHs occurring after butane concentrations were decreased by greater than 50%. The decrease in time for complete biotransformation of all compounds for consecutive substrate additions was indicative of the growing cell mass within the reactors, as seen in Figure 91c.

The sharp peaks at hours 1220, 1485, 1920, and 2210 represented the adjusted cell concentrations input into the model to best fit the data. (See first paragraph of this Section.) The sharp decline after each of these peaks resulted from the extreme product toxicity of 1,1-DCE.

Figure 91. Comparison of Laboratory Data Versus Model Output for M2B, A) 0 to 1700 hrs

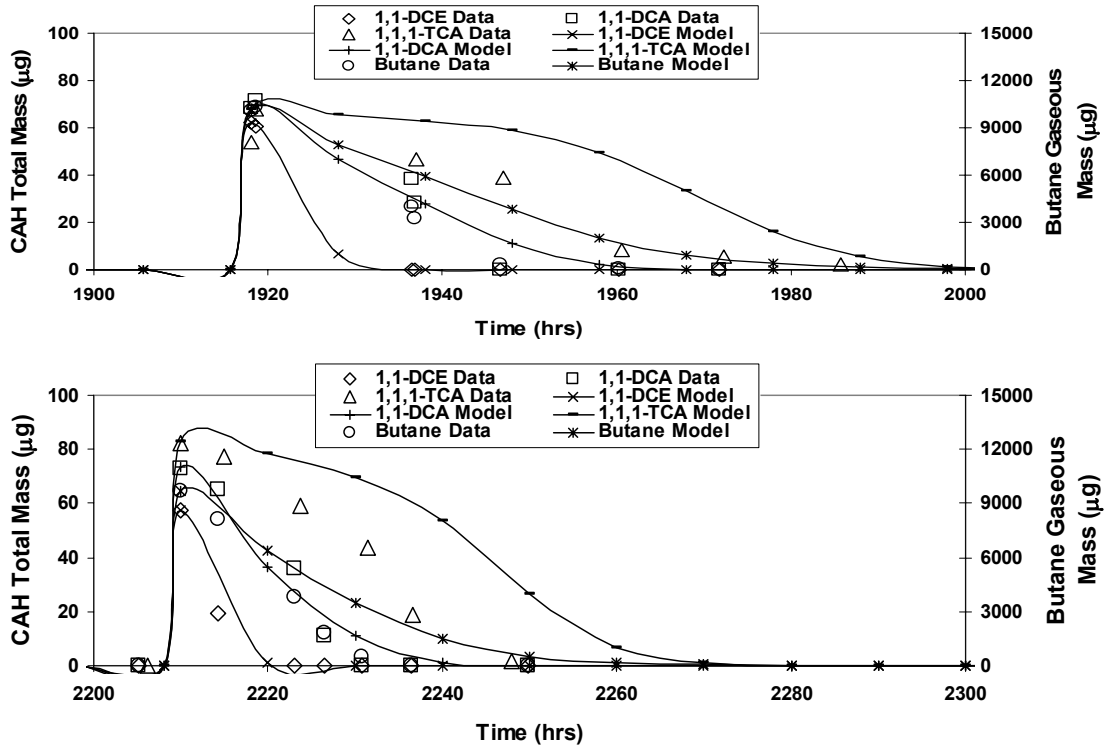

b). 1900 to 2300 hrs.

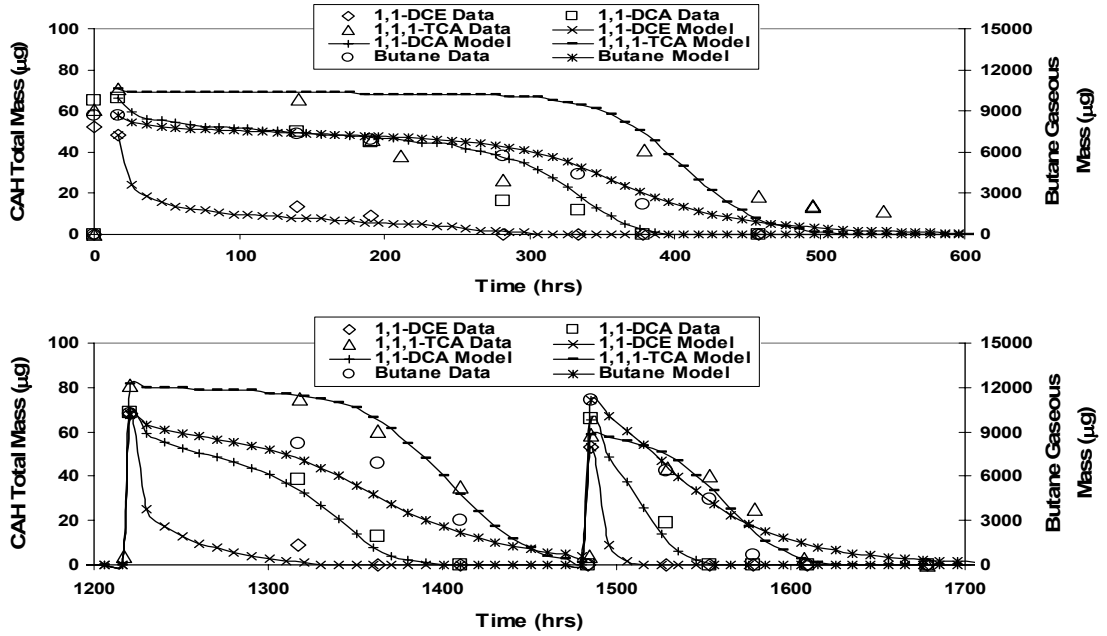

Figure 91c Cell concentrations calculated by the Stella model for M2B biotransformation.

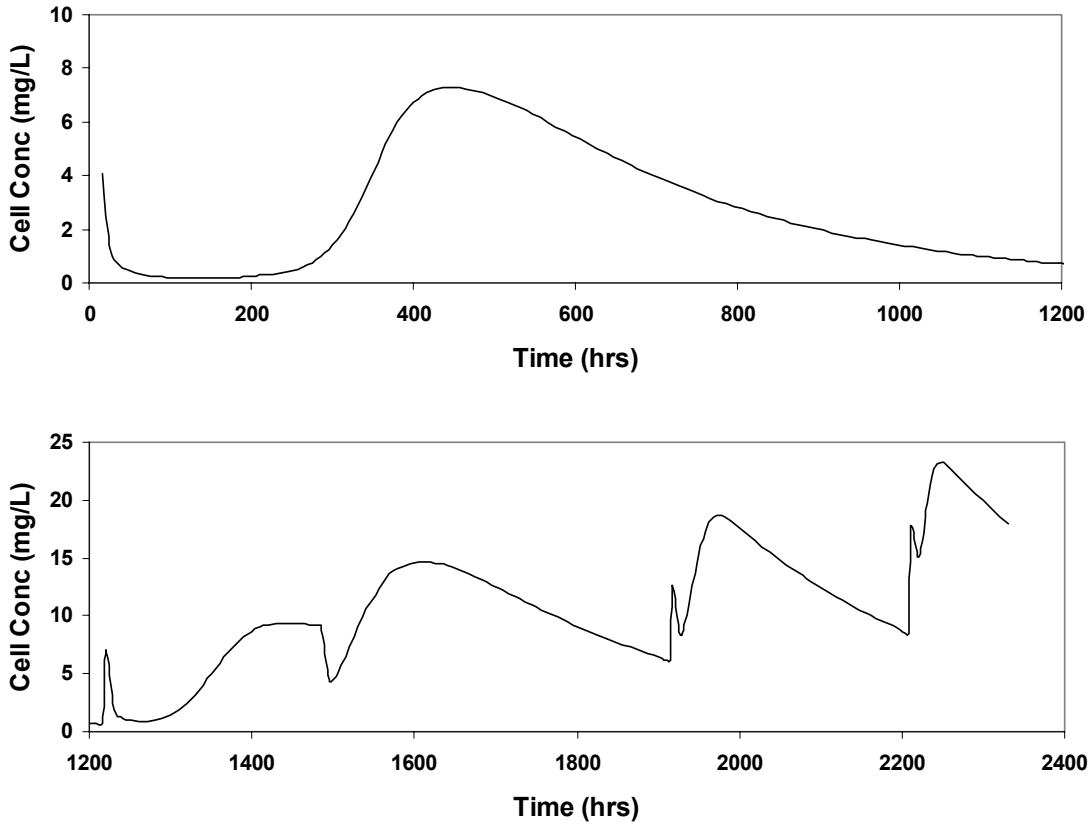

Biotransformation simulations were also run for M2B at the lower 1,1-DCE transformation rate (k_{mDCE} = 0.1 μmol/mg/hr), which more closely fit the product toxicity experimental data (Section 4.6.3). This value was an order of magnitude lower than the k_{mDCE} value (2.8 μmol/mg.day) defined by Kim et al (2002b). The nitial cell concentration was adjusted to most appropriately fit the 1,1-DCE transformation data. The model results are compared to the laboratory data for the first two substrate additions in Figure 92. Other parameter values were the same as those presented in Table 42 with the exception of k_{mDCE} and the noncompetitive inhibition constant of butane on 1,1-DCA ($K_{IuBUTDCA}$). This latter parameter was assigned a value of 0.4 μmol/mg which was used to fit transformation data from the media experiments (Mark's Section). This value was required for the model to simulate the order of CAH transformation observed: 1,1-DCE transformed first, followed by 1,1-DCA and 1,1,1-TCA. (Using the value from previous M2B simulations, $K_{IuBUTDCA}$ = 4.0 μmol/mg, the model resulted in 1,1-DCA transformation occurring before that of 1,1-DCE.)

In observing Figure 92, even though the transformation orders are correct, using the lower k_{mDCE} value resulted in more rapid butane utilization and 1,1-DCE and 1,1,1-TCA transformation. Varying initial cell concentrations did not improve the model fit. Higher initial cell concentrations resulted in butane consumption occurring even faster than 1,1-DCE

transformation. Lower initial cell concentrations did not improve the fit of the data; running the model with an initial cell concentration of 0.02 mg/L, an unreasonably small amount, resulted in overestimation of the transformation times (results not shown).

These contrasts illustrate the complexity of the system and the sensitivity and limitations of the model. It is reasonable to suspect that because the culture used in this study was different from that used by Kim et al. (2002a, 2000b), other parameter values may also be different from those assumed from Kim et al. What would have been more useful for modeling these simulations is to have had previously defined values specific for this study's culture.

Figure 92. Comparison Plot of M2B Data and Model Output Assuming Low k_{mDCE} (0.1 µmol/mg/hr)

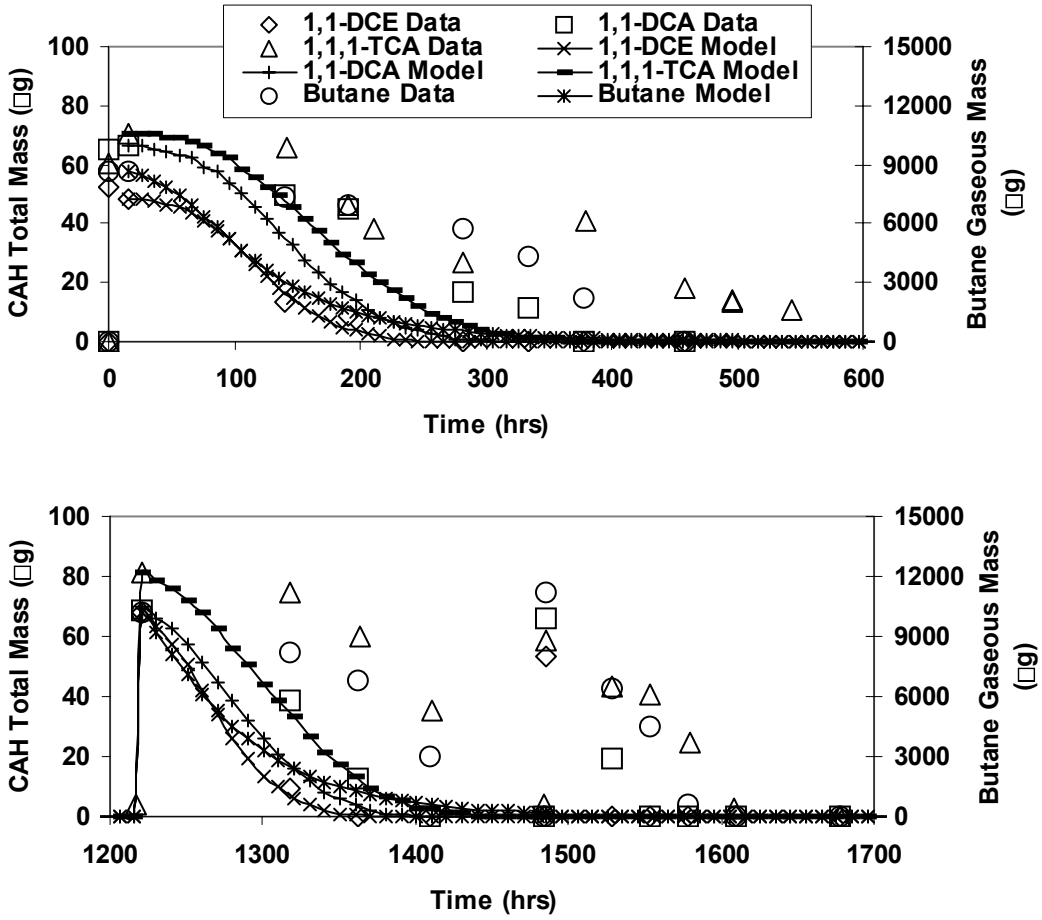

4.6.5 Summary of Laboratory Experiments and Simulations

Laboratory experiments in both growth media and microcosms showed that the culture is capable of cometabolic biotransformation of 1,1-DCE, 1,1-DCA, and 1,1,1-TCA with butane as the primary growth substrate (electron donor). The media reactors and the bioaugmented microcosms (M2 and M3) showed rapid transformation of 1,1-DCE, followed by slower transformation of 1,1-DCA and 1,1,1-TCA. This slower transformation is attributed to butane inhibition and slower reaction kinetics. These trends are very reproducible as noted by the similarity within all the reactors. The lack of biotransformation in the control microcosms (M1 and M4) confirmed that transformation is due to cometabolic reactions by this culture; transformation is not due to seepage losses from the reactors or to any species indigenous to Moffett Field.

Modeling of the activity seen in the media reactors indicated that Kim et al's (2002b) parameter values proved to be good initial estimates for the kinetics for the culture. It was only necessary to adjust the noncompetitive inhibition constant of butane on 1,1-DCA ($K_{IuBUTDCA}$), the transformation capacities of 1,1-DCE and 1,1,1-TCA (T_{cDCE}, T_{cTCA}), and the decay constant (b) to better fit the transformation data.

Laboratory tests that were run to better define the T_{cDCE} value specific to our culture indicated that 1,1-DCE product toxicity was greater than that reported by Kim et al (2002b). Simulations of butane utilization in the absence of the CAHs and prior to the product toxicity tests showed a good fit to the laboratory data. This verified that the Stella model's input values for butane utilization values were adequate. The product toxicity simulations showed that a T_{cDCE} value of 0.175 μmol DCE/mg cells more appropriately described our culture's product toxicity. However, comparison of the model output to the data suggested that the transformation rate of 1,1-DCE (k_{mDCE}) was much slower than that initially assumed (2.8 μmol/mg/hr). A k_{mDCE} value one order of magnitude lower more closely described the data (0.1μmol/mg/hr), although it is difficult to know what caused the requirement of a lower k_{mDCE}.

Laboratory experiments confirmed that mass transfer limitations (MTL) were occurring during transformation of the first three substrate additions. Incorporating a mass transfer coefficient (K_{Ga}) for butane into the Stella model allowed an improved match between model output and laboratory data for both butane utilization in microcosms M5 and butane utilization and CAH transformation in microcosms M2 and M3. A K_{Ga} value of 0.03 hr^{-1} was required.

Using the kinetic, inhibition, and product toxicity values defined by Kim et al. (2002a, 2002b) and the adjusted values noted above, model simulations showed a fairly good match for the trends of biotransformation observed in microcosms M2 and M3. The similarities included the order of transformation (1,1-DCE transformed first, followed by 1,1-DCA and then 1,1,1-TCA), the strong inhibition of butane on 1,1-DCA and 1,1,1-TCA (resulting in the delayed transformation), and the extreme product toxicity of 1,1-DCE (seen by a sharp decline in the simulated cell concentration after 1,1-DCE transformation).

The overall importance of these laboratory experiments and the model simulations was demonstrating the model's ability to mimic such trends using laboratory values defined from

independent experiments. The values were then carried over to simulate the result of the first season's field experiments (Section 9).

4.7 Continuous Flow Column Studies

This section presents the results from the biotransformation experiments conducted with a continuous flow column. Bioaugmentation was performed with *Rhodococcus sp.,* a culture previously described. Methods used in the continuous flow column study are described in Section 3. Prior to conducting the bioaugmentation and biotransformation experiments, the transport of dissolved butane and oxygen was studied.

4.7.1 Transport Study

Experiments were conducted to determine transport characteristics of the packed column prior to the bioaugmentation and biotransformation experiments. Bromide (25 mg/L) was added as a conservative tracer to the groundwater that was continuously injected at a flow rate of 0.2 mL/min. The resulting normalized breakthrough curve of the effluent bromide concentration to the influent concentration (C/C_o) is shown in Figure 93. The C/Co value of 0.5 represents one pore volume of fluid flow (Domenico and Schwartz, 1990) for advective-dispersive transport. Based on the tracer test flow rate and total internal volume of the column (150 mL), the porosity (n) was estimated as 26%. The length of the input pulse interval of bromide was 3.95 pore volumes. In order to predict the dispersion coefficient, the CXTFIT2 model, version 2.1 (Van Genuchten, 1981) was used to fit the data to advection-dispersion equation. The simulation resulted in a good fit (R^2 >0.99) to the bromide data, yielding a porosity of 26% and a dispersion coefficient of 1.93E-3 cm^2/sec corresponding to a dispersivity of 0.75 cm. This dispersivity value corresponds to a sandy-gravel aquifer material (Domenico and Schwartz, 1990). Any evidence of dead zones or rate-limited transport were not indicated, since a very good fit was obtained with a standard 1-1 advection and dispersion model. The model also fit the elution of bromide from the column very well.

Figure 93. Elution Data of Bromide from the Column and Model Fit at a Flow Rate of 0.2mL/min

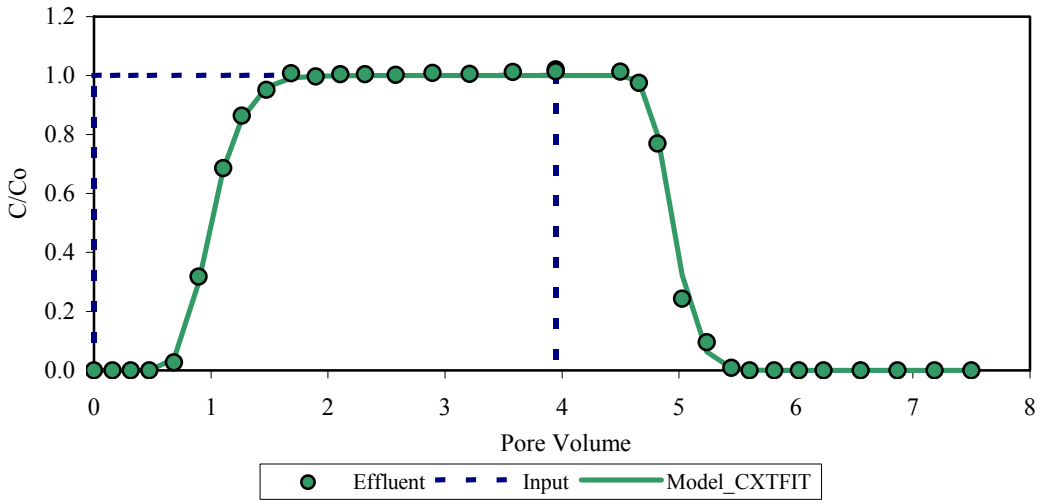

The transport of 1,1,1-TCA was modeled using the values of dispersion coefficient and porosity obtained from bromide tracer experiment. 1,1,1-TCA was injected into the soil column at an influent concentration of 200 ug/L using a peristaltic pump (flow rate = 0.2 mL/min). The number of pore volumes to achieve 50% breakthrough was 2.6, showing retardation of 1,1,1-TCA compared to the bromide tracer. 1,1,1-TCA transport data, however, did not fit the simple 1- dimensional (1-D) equilibrium sorption-convection-dispersion equation (CDE) that was used to fit bromide data (Figure 94). A chemical and physical non-equilibrium CDE transport model with retardation was therefore used to fit the 1,1, 1-TCA data, and a good fit was achieved. (Figure 94). This indicated the presence of mobile and immobile zones within the packed reactor and non-equilibrium sorption, which resulted in more dispersion and extended tailing in the breakthrough curve. Table 43 presents a comparison of modeling results obtained from CXTFIT.

In order to start the bioremediation phase of the experiment, it was necessary to ensure that 1,1,1-TCA was not transformed. Thus, 1,1,1-TCA was continuously added for a period of 42 days at an influent concentration of 200 μg/L. The effluent concentrations matched the influent (Figure 95), indicating minimal biotic or abiotic transformation of 1,1,1-TCA was occurring. The results also demonstrate our ability to maintain constant 1,1,1-TCA concentration in the influent fed to the column.

A transport study of butane and oxygen (electron acceptor) were also conducted in the packed column. The breakthrough curve along with the CXTFIT model fit of dissolved oxygen is as shown in Figure 96. Dissolved oxygen was delivered to the column at an input concentration of 17.6 mg/L, and the flow rate was 0.2 mL/min.

Figure 94. 1,1,1-TCA Breakthrough Curve Fit to Equilibrium and Non-Equilibrium CDE

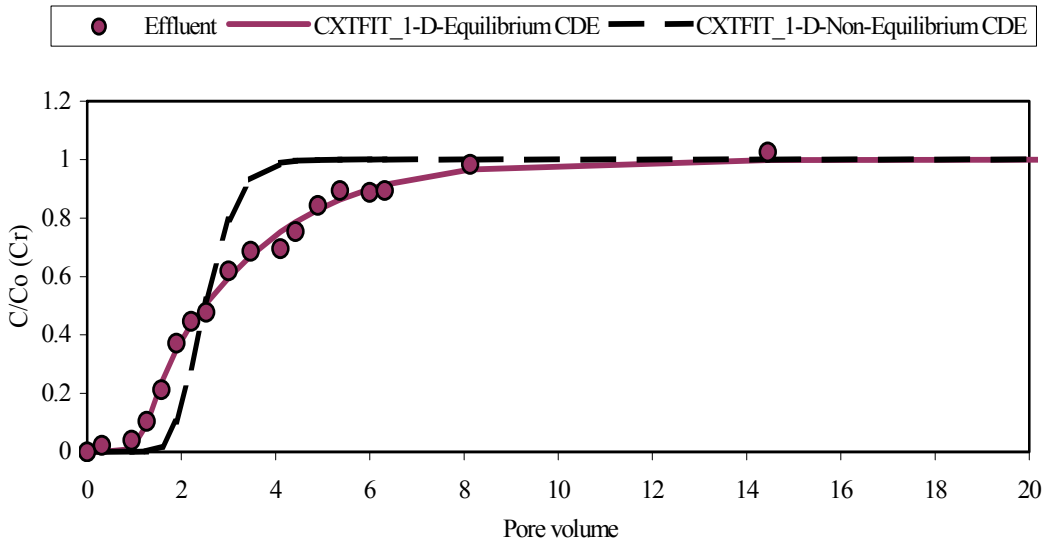

Figure 95. Long-Term Breakthrough of 1,1,1-TCA Prior to Bioaugmentation and Biostimulation

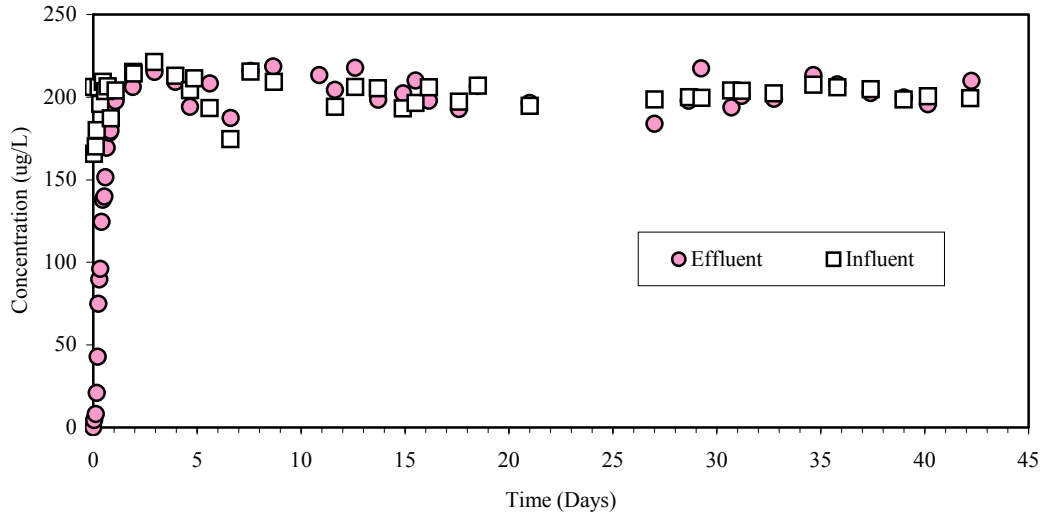

The initial decrease in concentration likely indicated a preexisting dissolved oxygen distribution in the column. Unlike bromide, dissolved oxygen concentrations did not reach the injected values during the test, possibly indicating some consumption of oxygen during transport through the column. The effluent dissolved oxygen data was modeled using CXTFIT (1-D equilibrium CDE), and dissolved oxygen transport was considered to be conservative.The modeling results suggest that oxygen was retarded. However, in the absence of biological transformations, The retardation of dissolved oxygen may be due to trapped gas bubbles, which affects transport. If bubbles were present, compounds can be retarded based on their Henry's coefficient given by Equation 4.7.1 (Fry et al., 1995). The retardation factor for dissolved oxygen was predicted to be 2.19 by the CXTFIT2 model. Based on retardation model presented by Fry et al., 1995, an estimate can be made for the amount of trapped gas present in the column. Based on a Henry's

dimensionless constant of 30.3 for oxygen, as little as 4% of the void space filled as bubbles could result in a retardation factor of 2.2.

Equation 4.7.1

$$R = 1 + H' {}^{Vg}\!/_{Vw}$$

Where R = Retardation present in the column
H′ = Dimensionless Henry's constant
Vg = Volume of trapped gas per volume of pore space
Vw = Volume of water per volume of pore space

Figure 96. Dissolved Oxygen Breakthrough: Column Effluent Data Fitted to 1-D CDE

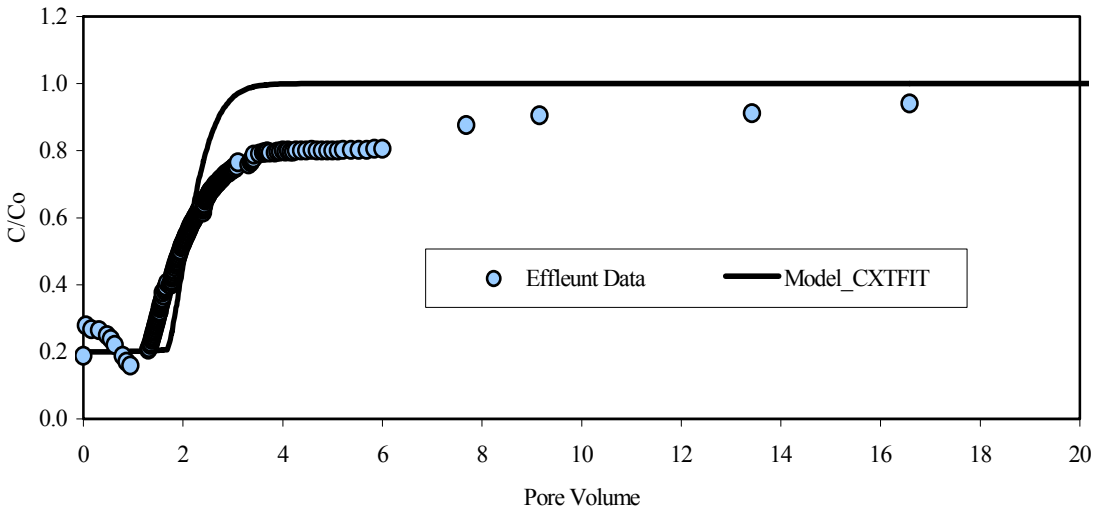

The butane transport test was conducted at a flow rate four times higher than the other experiments. Butane was added as a pulse to ensure no biostimulation of butane-utilizers prior to bioaugmentation. The butane breakthrough data is shown in Figure 97. 99.95% of the mass injected into the column was recovered, indicating butane utilization was not occurring. The model fit to butane transport data revealed that butane was more retarded than dissolved oxygen or 1,1,1-TCA, with a retardation factor of 6.5. As reported earlier, the retardation may have been due to the presence of trapped gases. Butane's dimensionless Henry's constant of 38.05 is in the range of oxygen (30.3), thus it would also be retarded by approximately a factor of 2.0 if gas bubbles were present. Furthermore, the retardation factor for butane was greater than 1,1,1-TCA. The octanol water partitioning coefficient for butane (776) is higher than 1,1,1-TCA (320). Compounds with high octanol water partitioning coefficient would be expected to be more strongly sorbed to the aquifer material. Thus, the butane results are consistent with greater retardation. The combined effects of partitioning into gas bubbles and sorption onto aquifer solids could potentially have resulted in a retardation factor for butane of 6.5, as obtained from CXTFIT2 model simulations. Table 43 presents the modeling results obtained for bromide,

1,1,1-TCA, dissolved oxygen and butane. The partitioning coefficient and mass transfer coefficient fit to 1,1,1-TCA and butane elution curves indicate the presence of mobile and immobile zones that exist within the column pack. The lower mass transfer coefficient for butane compared to 1,1,1-TCA may be associated with higher flow velocity of the butane test. If gas bubbles represent 4% of the void space, the actual porosity of the column would be around 0.30 compared to the 0.26 value obtained from bromide tracer test.

Figure 97. Pulsed Butane Breakthrough Data through the Soil Column

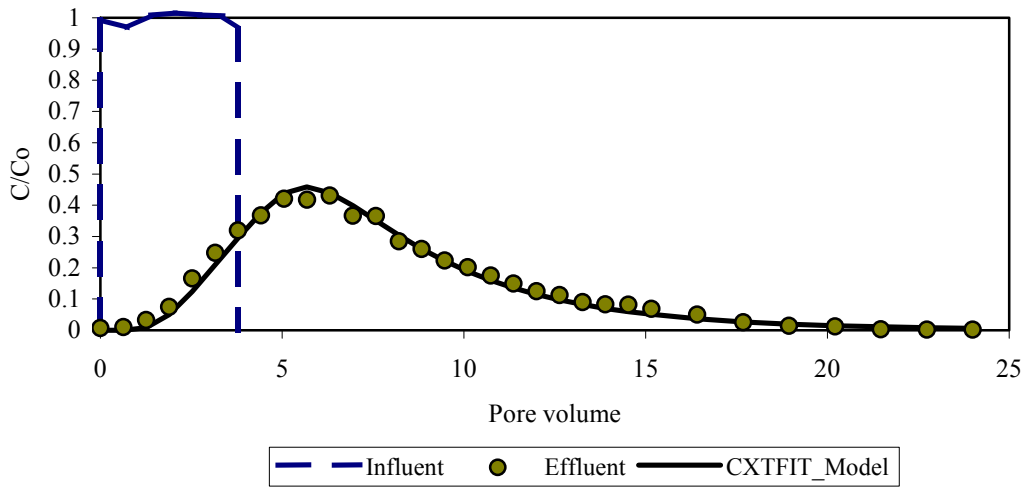

Table 43. Simulated Transport Parameters for Bromide (Conservative Tracer) and 1,1,1-TCA

Parameter	Bromide	1,1,1-TCA	Butane	Oxygen
Flow rate [mL/min]:	0.2	0.2	0.8	0.2
n: Porosity [-]:	0.26	0.26	0.26	0.26
D_x: Dispersion coefficient [cm^2/sec]	1.96E-03	1.96E-03	1.17E-2	1.96E-03
L: Length of the column [cm]:	30	30	30	30
v_x: Avg Groundwater velocity [cm/sec]:	2.60E-03	2.60E-03	1.04E-02	2.60E-03
R: Retardation Factor [-]	1	3.17	6.5	2.19
β: Partitioning Coefficient [-]	-	0.48	0.50	-
ω: Mass Transfer Coefficient [-]	-	1.37	0.15	-
α: Dispersivity [cm]	7.50E-01	7.50E-01	7.50E-01	7.50E-01

4.7.2 Bioremediation Study

Phase I: Bioaugmentation and Biostimulation Study

Prior to bioaugmentation, the flow through the column was kept constant for a period of 7 days at a flow rate of 0.2 mL/min. This flow rate provided for a fluid residence time in the column of 3.2 hours. During this time, 1,1,1-TCA influent concentration (200 μg/L) matched the effluent concentration demonstrating no transformation was occurring. On day 7, the column was fed with a two-hour pulse of dissolved oxygen (~24 mg/L) followed by half hour pulse of dissolved butane (18 mg/L). The pulses were cycled continuously with the feed piston pumps and timer (as shown in Figure 24). On day 8, the butane-utilizing culture was added at the column influent via the sampling port. The butane-utilizers used for bioaugmentation were grown in batch culture on butane and oxygen (see Section 5.3). About 2.5 mL of culture was added in increments of 0.5 mL over a span of 2.0 hours. The total mass of the cells added was 0.9 mg, on a dry mass basis.

After bioaugmentation of the column no significant decrease in 1,1,1-TCA concentration was observed for a period of about 2 days. During the first few days, butane was detected in the column effluent (Figure 3.6 b), after which, butane was removed below detection levels (around day 10). Upon the removal of butane to low levels, 1,1,1-TCA transformation was initiated. The concentration of dissolved oxygen decreased dramatically after the cyclic pulsing of DO and butane was initiated on day 7 (Figure 98c). A further reduction in the effluent DO concentration was observed after bioaugmentation (days 12-16), which corresponds to the stimulation of the butane-utilizers. DO concentration in the column effluent follows changes in the influent butane concentration. The lowest values were obtained at the higher influent butane concentration (11-16 days) and then increased when butane influent concentration were lowered after day 16. The decrease in 1,1,1-TCA concentration coincided with the decrease in oxygen and the stimulation of the butane-utilizing population. The ratio of DO to butane consumption during this period of time was 4.5 mg O_2:1 mg butane. This is in the range expected for the oxidation of butane to CO_2 and H_2O.

A maximum 1,1,1-TCA removal efficiency of ~84% was achieved about 8 days after bioaugmentation (day 16). The flow and influent concentration characteristics were kept fairly constant for a period of 20 days. Butane concentration of the influent pulse during this time ranged from 20-30 mg/L corresponding to a pulse averaged concentration of 3.5 mg/L. 1,1,1-TCA concentrations indicated that a steady-state removal of 80% was maintained from days 16 to 30. During this period butane was effectively consumed as the effluent butane concentration fell below detection (0.05 mg/L) most of the time. A period of butane breakthrough was observed at 12 to13 days that corresponded to a period of low DO concentrations, and high influent butane concentrations. The decrease in 1,1,1-TCA concentration stopped during this period, and resumed when butane was reduced to low concentration. Overall, the transformation yield during this phase was 0.06 mg of 1,1,1-TCA/mg of butane.

Figure 98. 1,1,1-TCA, Butane and Dissolved Oxygen Profile during the First Phase of Bioaugmentation and Biostimulation Experiment

a. 1,1,1-TCA Profile

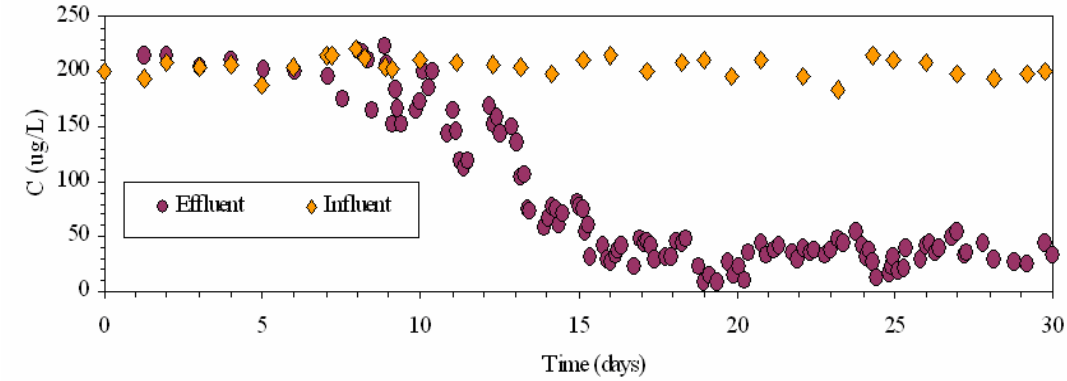

b. Butane Profile

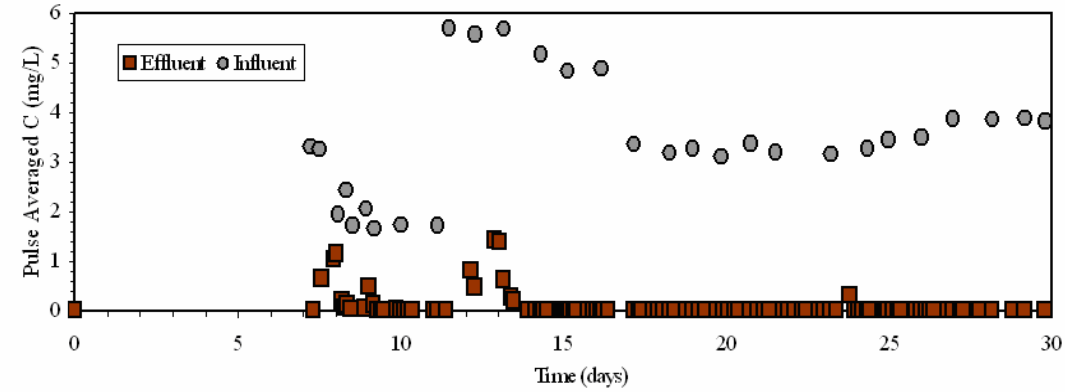

c. DO Profile

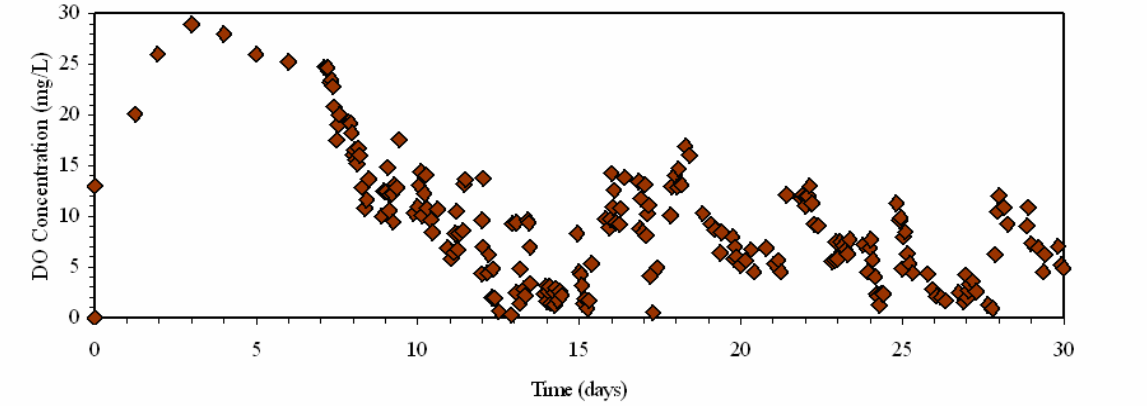

Phase II: High 1,1,1-TCA Concentration Test

Phase I showed that the biostimulated column achieved approximately 80% removal of 1,1,1-TCA at an influent concentration of 200 ug/L. However, to assess the transformation ability a higher concentration of 1,1,1-TCA (~430 ug/L) was fed during the second phase of the experiment (Figure 99a).

The response to the increase in the influent concentration of 1,1,1-TCA was appreciable. An increase in the effluent concentration of 1,1,1-TCA was observed over a period of 18 days (Figure 99a--days 36 to 53). The removal efficiency of 1,1,1-TCA during the period of the high concentration influent fluctuated from a high of 84% to a low of 24%. As in the phase I, the presence of butane at the effluent sampling port induced some perturbations in the measured 1,1,1-TCA concentrations at the effluent end (Figure 99b--days 34 to 36 and days 47 to 49). From 47 to 49 days, the DO concentrations were also driven to almost anaerobic conditions (Figure 99c). This resulted from the influent DO concentration being low (data not shown). Nevertheless, even when higher concentrations of DO were achieved around 50 days, the overall trend shows a decrease in 1,1,1-TCA removal efficiency over the period of 30 to 52 days (Figure 99a and c) based on a percentage removal basis. However, the transformation yield of the butane-utilizing culture were maintained during this period was 0.17 mg of 1,1,1-TCA/mg of butane, which is higher that what was observed during phase I.

To test whether effective transformation could be re-established, the 1,1,1-TCA influent concentration was reduced to 200 ug/L on day 53 (Figure 99a). Removal efficiency was reduced from 84% (average of phase I) to about 59% from day 56 to day 65 and steady-state concentrations were maintained, and during this same period, effective butane removal was also achieved and excess DO was maintained in the column effluent.

The decrease in removal efficiency at the end of phase II compared to phase I was about 15%. The exact reason for this is not known. One possibility is that native butane-utilizers were stimulated between phase I and II that did not effectively transform 1,1,1-TCA. Transformation of 1,1,1-TCA did improve after the concentration was lowered, on a percentage removal basis. The mass of 1,1,1-TCA injected during the period of days 45-53 (influent concentration of 1,1,1,-TCA ~ 430 ug/L) was 990 ug. Approximated one third (362 ug) was removed. However, from day 55 to day 63 when the injection concentration was lowered, an injected mass of 460 ug of 1,1,1-TCA was added of which 282 ug was estimated to be removed. This represents about 50% of the 1,1,1-TCA mass

Figure 99. 1,1,1-TCA, Butane, and DO Profiles during the Second Phase of the Test. The concentration of 1,1,1-TCA was doubled on day 30 and reduced back to 200 ug/L on day 53.

a. 1,1,1-TCA Profile

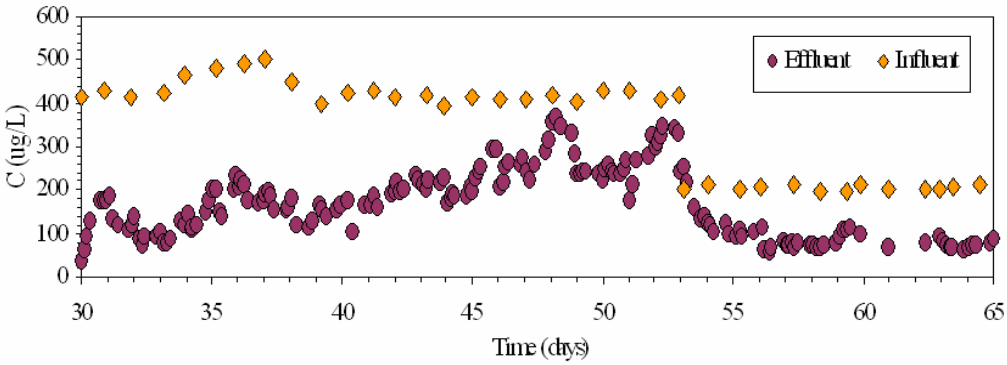

b. Butane Profile

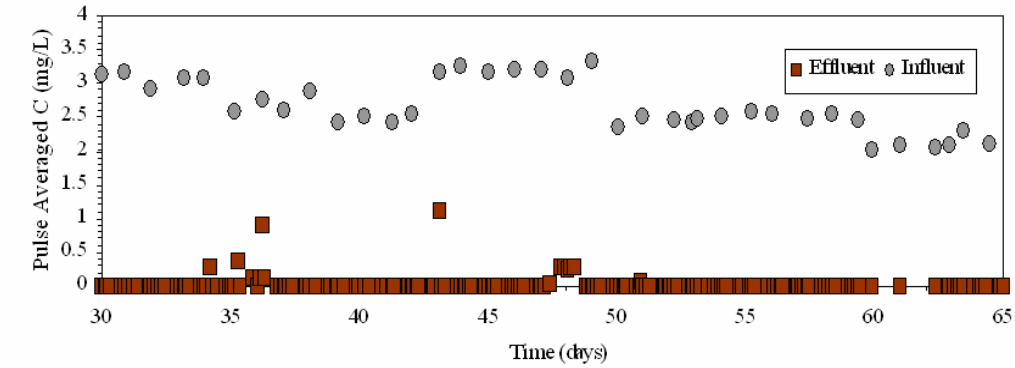

c. DO Profile

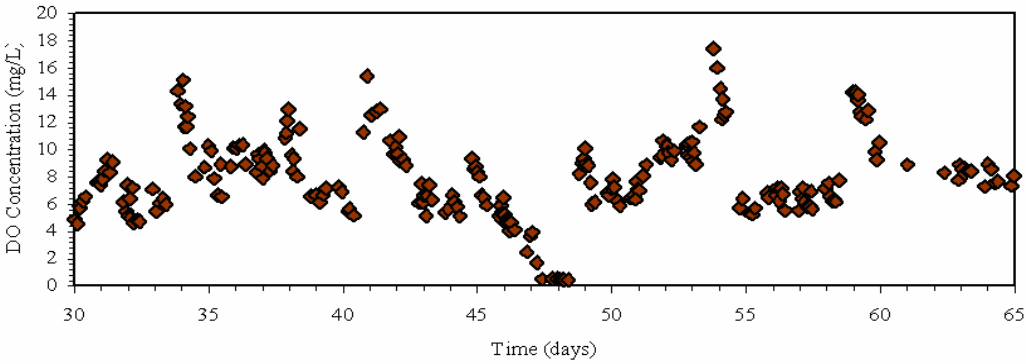

added. The transformation yield of the culture added during the low 1,1,1-TCA concentration test was 0.09 mg of 1,1,1-TCA/ mg of butane. Thus, based on total mass removal and transformation yield, the biostimulated column was potentially more effective at the higher concentration, than when the concentration was lowered.

Phase III: Test to Demonstrate Electron Donor (Butane) Dependence on the Transformation of 1,1,1-TCA and Presence of 1,1-DCE as a Co-Contaminant

To demonstrate dependence of 1,1,1-TCA transformation on butane consumption, the butane addition was turned off on day 66 (Figure 100a) while dissolved oxygen and 1,1,1-TCA addition continued. This resulted in an increase of the effluent concentration of 1,1,1-TCA from days 66 to 79. The 1,1,1-TCA effluent concentration remained ~22% lower than influent value, which would correspond to a first-order transformation rate of 0.07 hr^{-1}, based on a hydraulic residence time of 3.2 hours. In order to check whether this residual transformation activity was real, the pump delivering DO and 1,1,1-TCA was turned off for 48 hours (days 79 to 81) to permit a longer residence time in the column. If first order removal occurred during this period, the effluent concentration should have decreased to 7 ug/L. However, upon initiating the flow (day 81), the measured effluent concentration was ~165 ug/L, indicating that little transformation, had occurred. As expected, the DO concentrations during this period (days 66-81) increased when butane was not added (Figure 100c).

On day 85, butane addition was restarted to test whether butane-utilization and 1,1,1-TCA transformation could be restored (Figure 100a--days 88 to 110). Butane-utilization resulted as indicated by the lack of butane-breakthrough and the reduction in DO concentration. 1,1,1-TCA concentration decreases were observed coincident with DO concentration decreases. Steady-state 1,1,1-TCA removals of ~69% were observed. This removal efficiency, however, was lower than what was observed in phase I.

Figure 100. 1,1,1-TCA, Butane and DO Profiles during the Third Phase of the Test: Demonstration of Butane Dependence

a. 1,1,1-TCA Profile

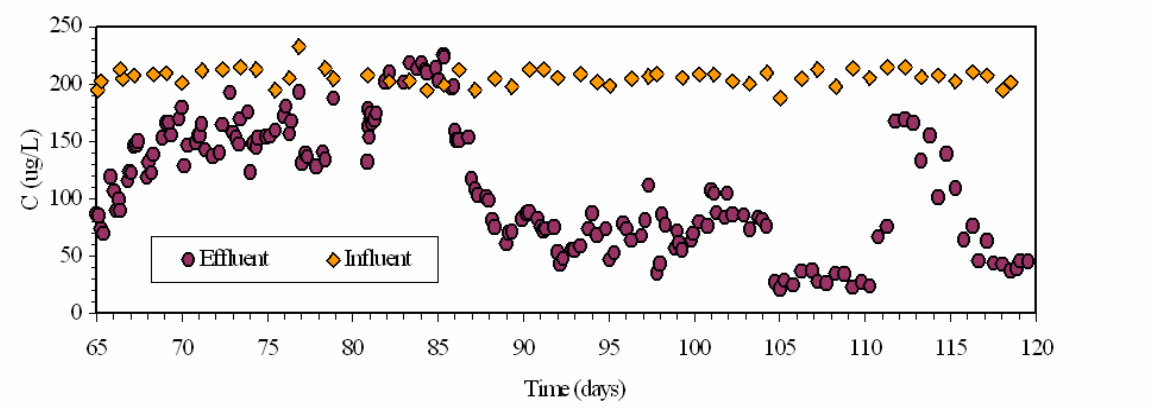

b. Butane Profile

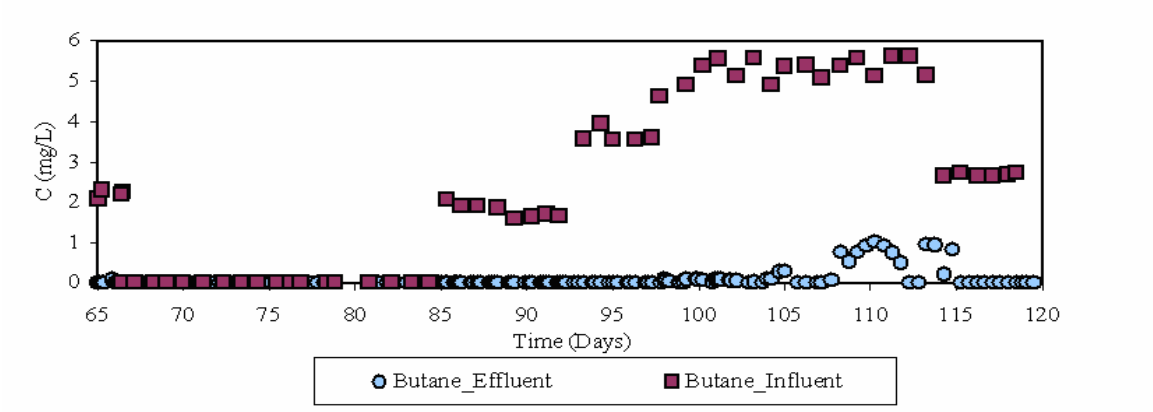

c. DO Profile

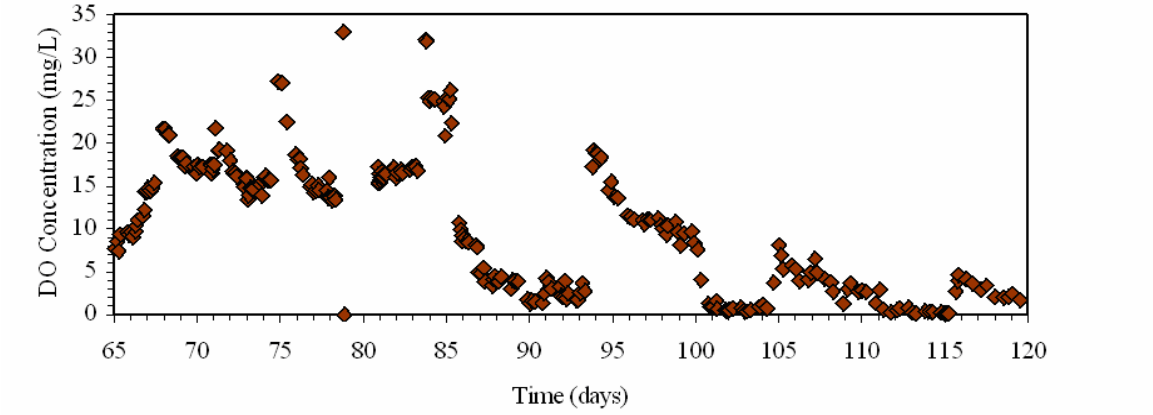

The average butane concentrations were doubled (from 93 day to 97). The increase in butane concentration did not immediately increase 1,1,1-TCA removal. Thus, the pulse cycle of butane was increased from 30 minutes to 40 minutes (Figure 100a-- days 97 to 114), which resulted in an increase in the mass of butane added by about 40%. The pulse averaged concentration of butane during this period was 5.5 mg/L. This resulted in better 1,1,1-TCA removal (days 104 to 111) with a percentage removal of 84%. On day 108, however butane was detected in the column effluent. Consistent with observations in phases I and II, the presence of butane resulted in increases in 1,1,1-TCA concentration. Thus, butane was inhibiting 1,1,1-TCA transformation. Low DO concentrations were also observed prior to butane breakthrough, which likely caused the incomplete consumption of butane. In order to restore DO levels in the column, the butane pulse interval was lowered by 20 minutes (i.e., 20 minutes of butane and 2 hours of DO) on day 114 resulting in time averaged butane concentration of 2.5 mg/L. This resulted in a decrease in butane concentrations below detection in the column effluent, and a corresponding decrease in 1,1,1-TCA concentrations in the effluent. DO concentration increased from 3 mg/L to 19 mg/L during this period and about 78% removal of 1,1,1-TCA was observed. Removal was close to that achieved during the first period of the test.

The last objective was to study the effect of adding of 1,1-DCE along with 1,1,1-TCA to the column. 1,1-DCE was injected into the column at an influent concentration of 130 ug/L starting on day 120 (Figure 101). For the initial period of about 4 days, 1,1-DCE was not detected in the effluent, but then an increasing trend was observed (Figure 101). A steady-state removal efficiency for 1,1-DCE of 74% and a transformation yield of 0.06 mg of 1,1-DCE/ mg of butane was achieved. With the onset of 1,1-DCE in the column effluent, butane was also detected (Figure 101b). Hence, the addition and transformation of 1,1-DCE proved to inhibit butane-utilization, as shown by Kim et al., 2002b. During this period, butane concentration in the column effluent averaged about 1.5 mg/L, thus only 50% removal was achieved. The decrease in butane-utilization resulted in a steady increase in DO concentrations and a more immediate increase in 1,1,1-TCA concentrations. After 10 days of 1,1-DCE addition, 1,1,1-TCA effluent concentration rose to influent levels, indicating 1,1,1-TCA was not being transformed.

Figure 101. 1,1,1-TCA, 1,1-DCE, Butane and DO Profiles during the Third Phase

a. 1,1,1-TCA and 1,1-DCE Profile

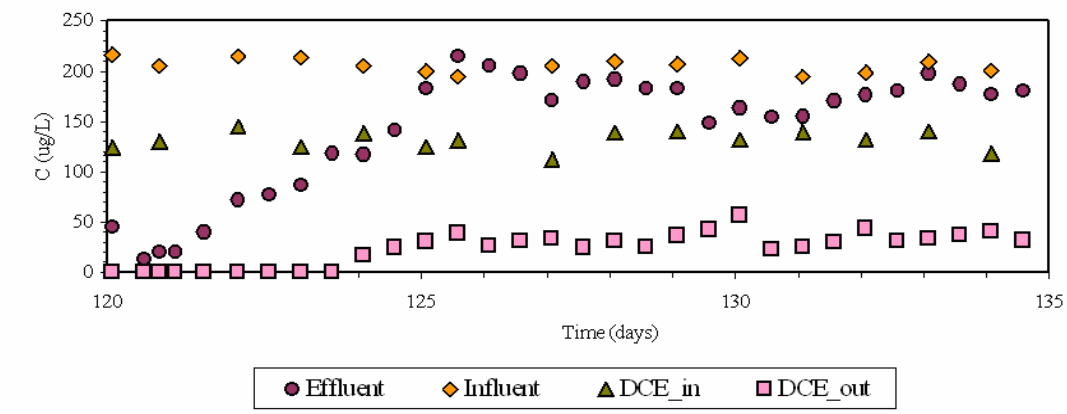

b.

Butane Profile

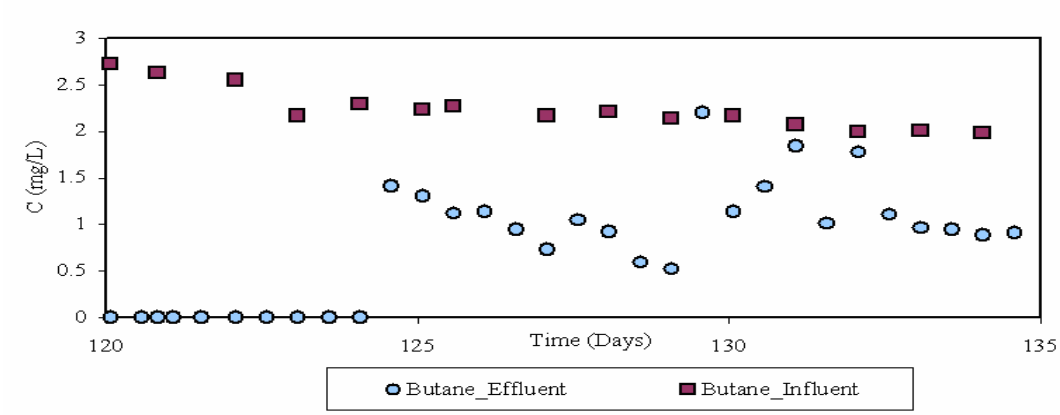

c.

DO Profile

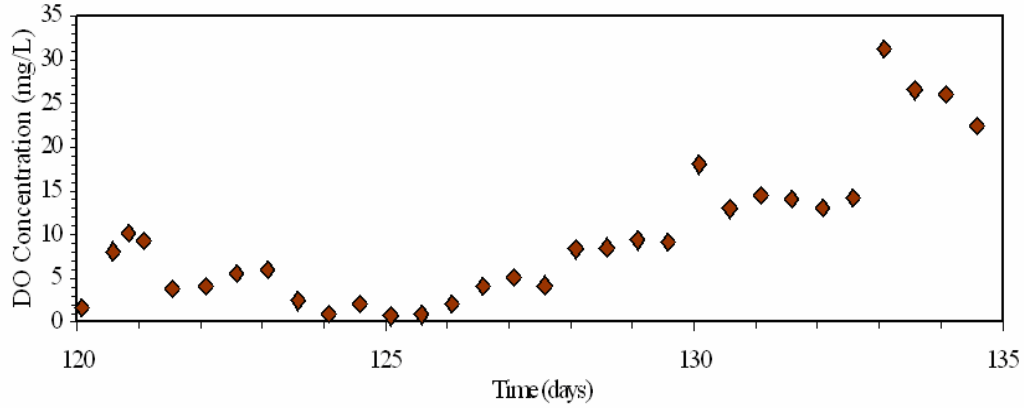

Figure 102. Real-Time PCR Microbial Analysis during Biostimulation

a. Real-time PCR Microbial Profile of 183bp *Rhodococcus* sp.

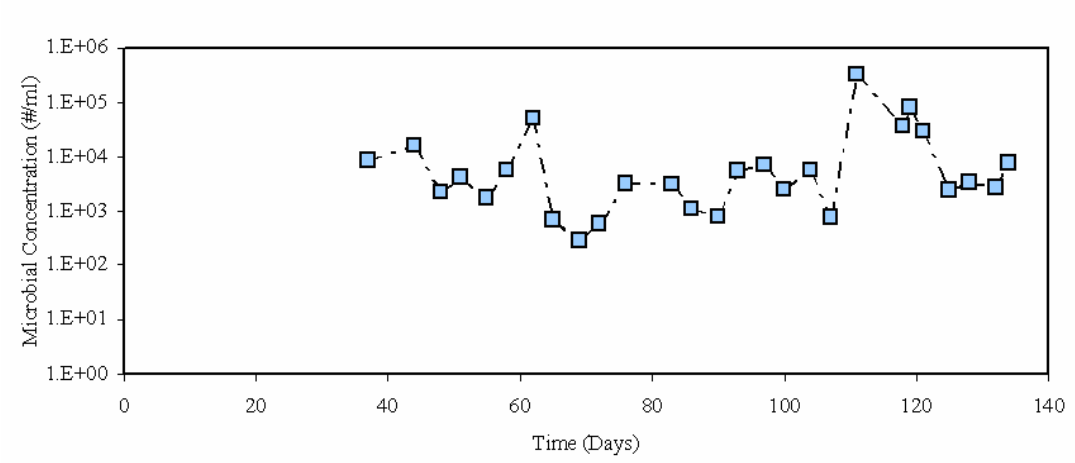

b.

Butane Profile

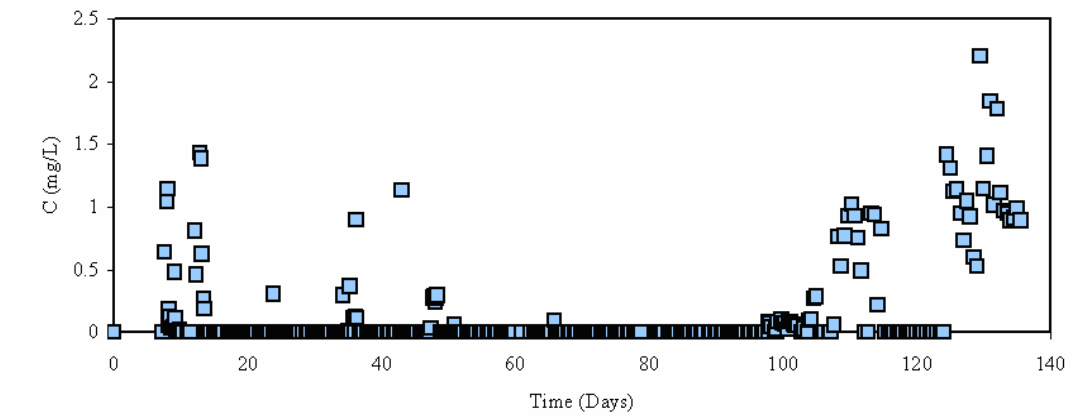

c.

Dissolved Oxygen Profile

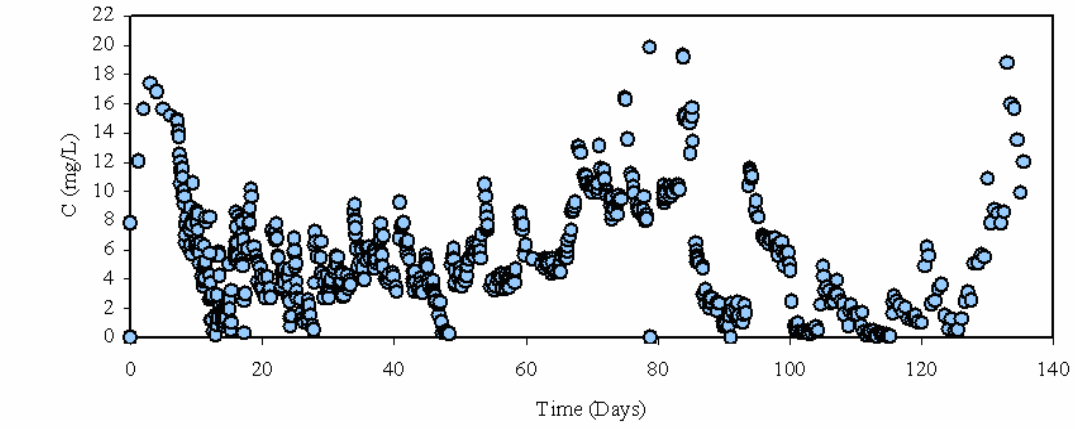

Real-Time PCR Microbial Analysis

The column effluent was collected (from days 36 to 135) and tested for the presence of the bioaugmented *Rhodococcus sp.* using real-time PCR analysis. Overall, the bioaugmented culture was maintained for a period of 135 days. Even during days 66-85 when the butane addition was turned-off, the (*Rhodococcus sp.*) culture was observed in the column effluent. Cell concentrations ranged from 2.7E+2 to 3.1E+5 organisms per mL of column effluent. The cell concentration appeared to be sensitive to the presence of butane and low oxygen concentration. This is evident over days 110-120, when butane could be detected in the column effluent. This corresponded to a period of low DO concentration in the column (Figure 102c) and high 1,1,1-TCA concentration.

The high cell concentration in the column effluent possibly results from detachment from the aquifer solids in response to the low dissolved oxygen concentration around day 100. (Madigan et al., 2000). The results, however, show a fairly stable amount of *Rhodococcus sp.* microorganisms in the column effluent over a period of around 100 days of operation.

T-RFLP Analyses and Microbial Community Composition

T-RFLP analysis was conducted on the soil column effluent samples using universal bacterial primers (27F-B-FAM and 338Rpl) and *Mnl*I and *Hin6*I restriction enzymes. However, analyses were primarily based upon the *Mnl*I T-RFLP profiles since they provided the highest discrimination of fragments due to increased frequency of recognition sites and the short length of the amplicons used.

Similar to the field groundwater samples, no fragments of 183 bp length were observed in any of the effluent samples throughout the test. However, unlike the field test, T-RFLP profiles of the bacterial community in the soil column exhibited greater diversity without clear species dominance or succession. The 126-bp peak, one of the major T-RFLP fragments found in field groundwater samples, was present only in trace amounts. Only one sample obtained on day 76 showed a 277-bp-dominance T-RFLP profile.

From day 37 to day 51 when the influent 1,1,1-TCA concentration was about 400 µg/L and only 13% was removed , it was shown that 47- and 253-bp fragments were the largest peaks and accounted for about 9% and 12% of the total area of all the detected peaks, respectively (Figure 103). Although the 47-bp fragment never obtained dominance, it accounted for a fairly stable percentage of total peak areas throughout the test period. The area percentage of the 167-bp peak was about 10% for day 37 and day 44 but diminished by day 51. Similar patterns were observed for the 278-bp fragment.

On day 53, 1,1,1-TCA concentration was dropped down to 200 µg/L and maintained there through day 65. The utilization rates for the influent butane and DO were about 100% and 74%, respectively. During this period, the 253-bp fragment became the largest peak on day 62 and day 65 and increased from about 7% of the total peak area on day 55 to 30% on day 65. The 47-bp peak also increased from day 53 to day 65, but encompassed a smaller percentage of the total population. On day 58, upon recovery of TCA treatment, a 165-bp fragment was found during day 57 to day 65 to be the largest peak in the profile, at 15.6% of total peak area.

The T-RFLP data showed a more diverse community structure when butane delivery was interrupted between day 66 and day 85. For instance, 130 peaks were detected in the sample collected on day 69; whereas, the average number of detected peaks in all effluent samples was 51. On day 76 in the absence of butane and little TCA removal, the 277-bp peak was dominant and accounted for about 22% of the total peak area. Upon restart of butane addition on day 85, about 75% reduction in the species diversity was observed immediately. Three peaks at 237-, 279- and 283-bp dominated the bacterial community on day 86 and accounted for 23.2%, 20.4% and 16.4% of the total peak area, respectively. On day 93 and 97, 44.6% and ~20%, respectively, of the total peak area was attributed to a 274-bp fragment, that, although present in most samples, had not gained prominence previously. Two unique features of the T-RFLP pattern were observed from the sample obtained on day 100: 1) The least diversity of any sample with only 16 different fragments; and, 2) the 279-bp fragment accounted for 64.9% of the total peak area, the largest percentage found during the test. Beginning on day 120, 1,1-DCE was delivered to the column simultaneously with 1,1,1-TCA. After about 10 days, TCA removal had dropped significantly, but DCE transformation continued and the microbial community was dominated by fragments of 237-, 253-, and 279-bp.

The effects of butane removal can be seen in the T-RFLP analyses. The number of the bacterial species detected increased by at least 100% over the average 51 peaks per sample after butane addition was stopped. Presumably, this was the result of switching from a concentrated source of a single organic substrate to multiple low-concentration sources of complex organics from cell lysis and decay.

Figure 103. Microbial Community Composition Determined by T-RFLP Analysis during the Bioaugmentation Test in the Soil Column from Day 37 to 134

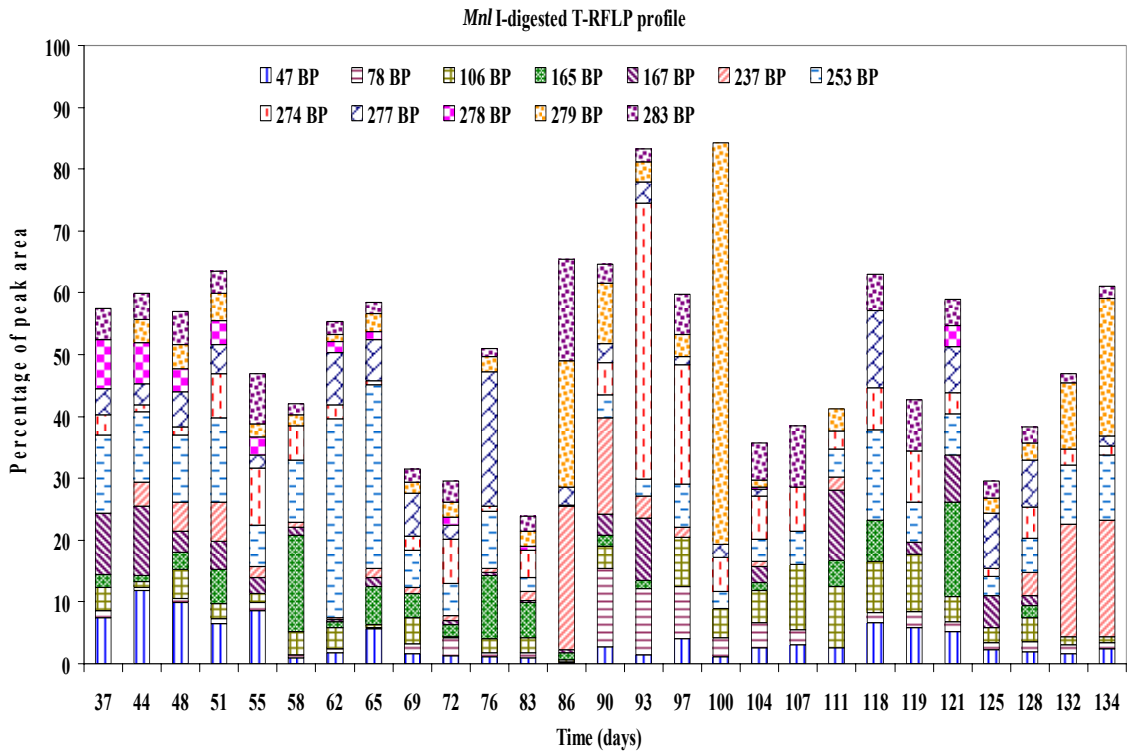

Summary of Biotransformation Column Tests

The butane-utilizing culture was successfully bioaugmented into the column reactor packed with aquifer material from the Moffett Field test site. This culture was able to cometabolically transform 1,1,1-TCA and 1,1-DCE using butane as a primary growth substrate. The transformation of 1,1,1-TCA was very sensitive to the presence of butane in the column. The butane-utilizing culture could withstand induced perturbations of varying 1,1,1-TCA, butane and DO concentrations. The presence and transformation of 1,1-DCE inhibited butane and DO utilization and 1,1,1-TCA transformation. These results are consistent with studies of Kim et al.(2000), (2002b) and those obtained in microcosms previously described..

Table 44 presents a summary of the column tests conducted with the percentage removal of 1,1,1-TCA (and 1,1-DCE) and transformation yield of the butane-utilizing culture in each stage of the experiment. These results suggest that if injected butane and dissolved oxygen concentrations could be maintained consistently, butane-utilizers can transform 1,1,1-TCA effectively. Based on the transformation yield, the culture performed better when the concentration of 1,1,1-TCA was increased as seen in Table 44. The transformation of 1,1,1-TCA was almost as effective at the end of the test as at the start of the test. This is also indicated in the transformation yield which remained almost constant except when 1,1,1-TCA and butane concentrations were increased days 30-53 and 105-110, respectively. Introduction of 1,1-DCE along with 1,1,1-TCA reduced the transformation of 1,1,1-TCA by about 65-70%.

Table 44: Summary of Column Tests

Phase	Days	Removal Efficiency (%)		Transformation Yield (mg/mg)	Notes
		1,1,1-TCA	1,1-DCE		
Phase I					
	0-30	84	-	0.06	1,1,1-TCA C = 200 ug/L
Phase II					
	30-53	84-24	-	0.17	1,1,1-TCA C ~ 430 ug/L
	53-65	59	-	0.09	1,1,1-TCA C = 200 ug/L
Phase III					
	66-81	~22	-	-	Butane Pulse Shut Off;
					1,1,1-TCA C = 200 ug/L
	85-105	69	-	0.06	1,1,1-TCA C = 200 ug/L
	105-110	84		0.04	1,1,1-TCA C = 200 ug/L
	116-120	78		0.05	1,1,1-TCA C = 200 ug/L
	120-135	0-5	75	0.06	1,1,1-TCA C = 200 ug/L
					1,1-DCE C = 130 ug/L

4.8 Modeling Analysis of the Continuous Flow Column Experiment

The biotransformation-transport model of Semprini and McCarty (1991, 1992) was used to simulate the results obtained from the laboratory column experiments after bioaugmentation. This model has the ability to pulse the electron donor/acceptor as was done in the column studies. The biotransformation model was used to simulate butane utilization, DO consumption, and 1,1,1-TCA and 1,1-DCE transformation. The biomass distribution both spatially and with respect to time was predicted. The non-steady-state equations used in the model are presented in Section 3.7.

4.8.1 Calibration of Biotransformation-Transport Model

In order to calibrate the biotransformation model for the column flow conditions, the transport of 1,1,1-TCA was modeled. The results from both CXTFIT and biotransformation models were compared, as shown in Figure 104. The dispersion coefficient and porosity obtained from CXTFIT model were used in the biotransformation model. The transformation parameter $K_{m,TCA}$ (maximum utilization rate of 1,1,1-TCA) was assumed to be zero to simulate 1,1,1-TCA transport only. The biotransformation model simulated the transport reasonably well, with a retardation factor of 2.69, and first-order-rate coefficient for sorption (f_k=3.0 day^{-1}). The combined equation for transport and biodegradation used by this model to predict liquid concentrations is also shown in Table 45 (a). The $K_{m,TCA}$ was set equal to zero for the transport simulation, to turn off the biotransformation term.

Figure 104. Comparison of the Biotransformation and CXTFIT Modeling Fit to 1,1,1-TCA Transport Tests

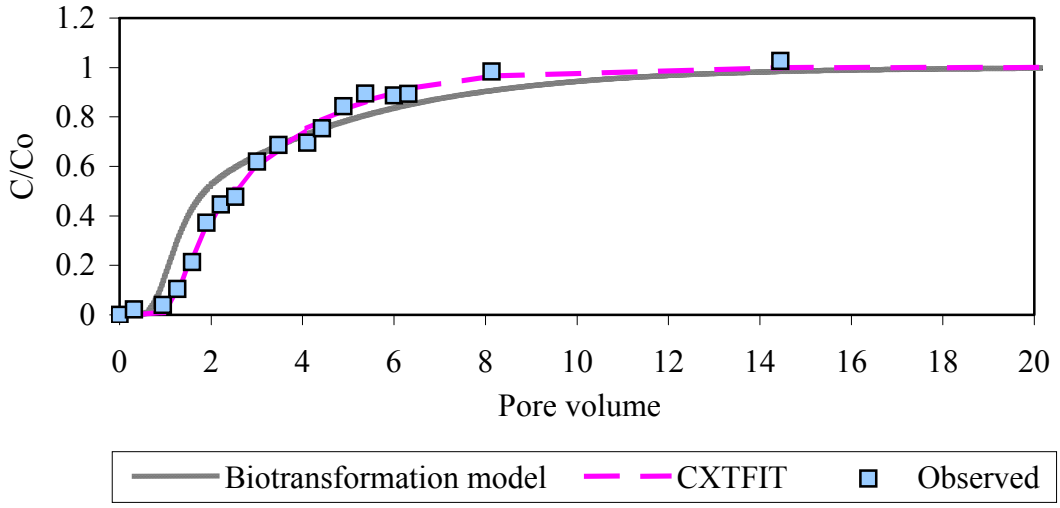

4.8.2 Biotransformation-Transport Simulations for the First Phase of the 1,1,1-TCA Test

The biotransformation model was then used to simulate the first 30 days of the Phase I biostimulation with butane. The model simulations during this period are presented in Figures 105 and 106. The numerical values used in the model, such as the inhibition constants, half saturation constants, etc., were obtained from previous work done with the culture bioaugmented into the column reactor (Kim et al., 2002b). These values are summarized in Table 45.

Time zero in Figure 105a represents day 8, i.e., the day when the culture was added to the column. An initial uniformly distributed biomass of 0.9 mg/L was used to simulate the column test. The biotransformation model fit 1,1,1-TCA transformation laboratory column test well. The model predicted that a residual butane concentration of approximately 0.5 mg/L would exist in the column effluent (Figure 105b). However, the concentration of butane in the laboratory column data was below detection level (0.05 mg/L). Differences in the model and actual data may be due to the retardation of butane in the column. The combined biotransformation /transport model does not allow retardation of butane and oxygen. The model fit the dissolved oxygen data from the column effluent well as shown in Figure 105. The high concentration seen initially in the modeled DO concentrations may be due to the retardation of oxygen or possibly indicates less dissolved oxygen was actually added to the column. indicated The maximum microbial biomass concentration at the end of the column occurred at about six days (Figure 105d). This corresponds to the period after rapid decreases in butane were predicted. The biomass then decreases with time as butane is consumed closer to the column influent. At about the same time, butane was also being consumed effectively (Figure 105b) and DO and 1,1,1-TCA concentrations decreased in the column effluent (Figure 105c). The observations are consistent with the lab data.

The spatial microbial population profile (Figure 106d) after 30 days of operation indicated that the biomass is concentrated within the initial one-third of the column. Thus most of the transformation of 1,1,1-TCA was occurring in that zone (Figure 106a). This is clearly evident in the spatial butane and oxygen profiles (Figures 106 b and c) where their concentrations also reduced in approximately the same region. The increase in the DO concentration seen where 1,1,1-TCA is transformed and butane is consumed (Figure 106c) is due to the dynamic pulsing of butane and oxygen in the model, since Figure 106c represents a snapshot at a particular time. However, the simulated concentration of 1,1,1-TCA increases away from the concentrated biomass region as simulated in Figure 106c. This simulated rebound could be the result of rate limited desorption of 1,1,1-TCA from the solids. It may also be associated with the dynamic pulsing of butane and oxygen. The model predicts that the dynamic alternate pulsing of butane and oxygen containing groundwater prevented biomass growth near the column influent.

Figure 105. Model Simulations of Concentration in the Column Effluent and Laboratory Data during the First Phase of Biotransformation Test (Days 0-30)

a. 1,1,1-TCA

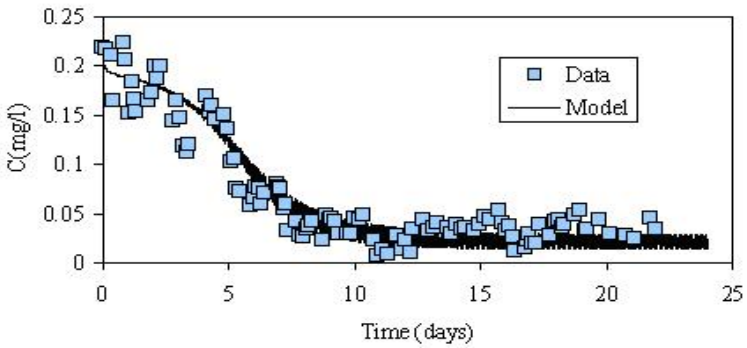

b. Butane

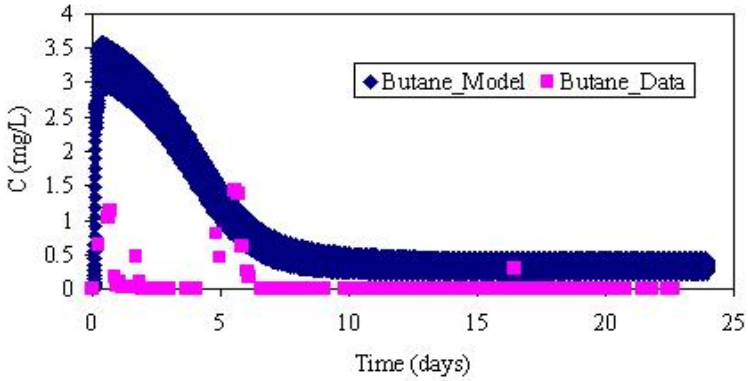

c. Dissolved Oxygen

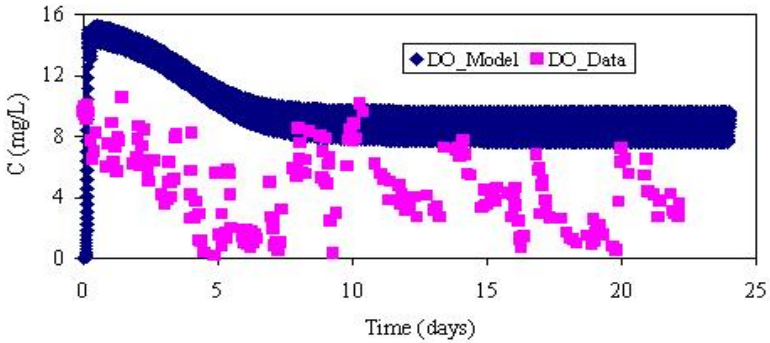

d. Biomass

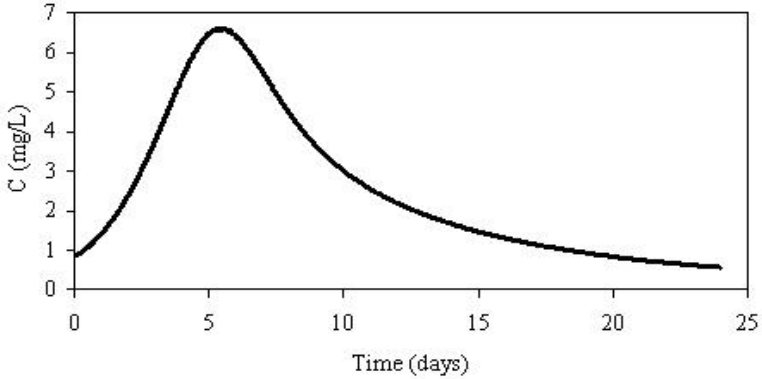

Figure 106. Model Simulations of the Spatial Distribution in Concentration after 30 days of Operation in Phase I

a. 1,1,1-TCA

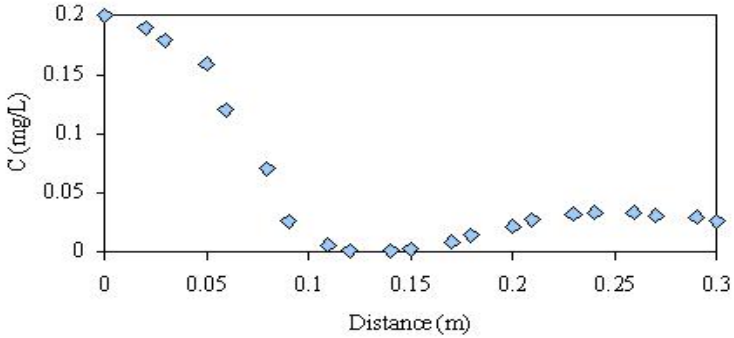

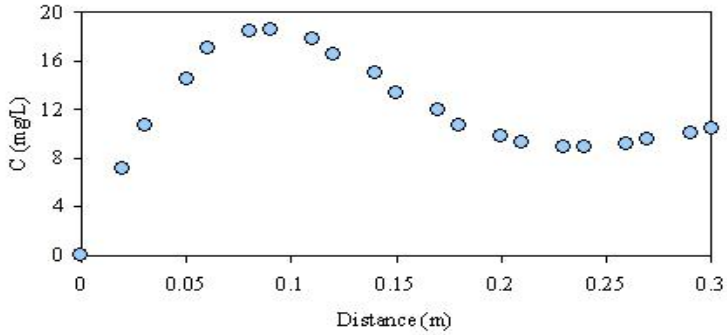

b. Butane

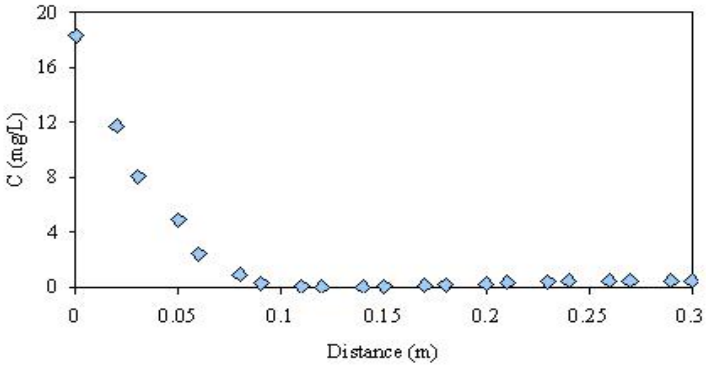

d. Biomass

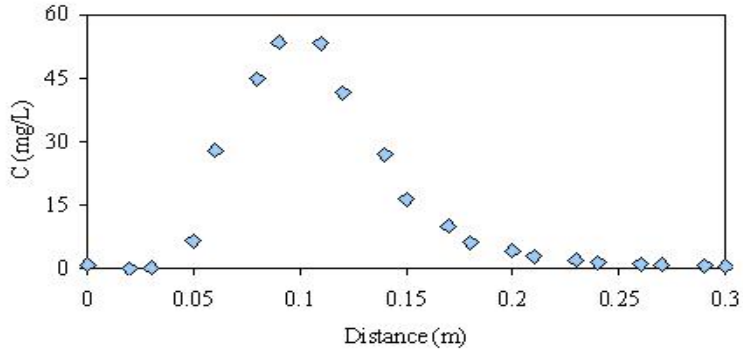

c. Dissolved Oxygen

Table 45. Model Parameters Used for Simulating the Column Study

Parameter	Value
Transport Parameters	
Volumetric Flow Rate	2.88E-4 m3/day
Porosity	0.26 [-]
Cross-Sectional Area	4.909E-4 m2
Bulk Density of Solids	1.6 Kg/L
Dispersion Coefficient	0.0169 m2/Day
Partitioning Coefficient	
1,1,1-TCA	0.352 L/Kg
Biotransformation Parameters	
$K_{ic, TCA, but}$	41.79 mg/L
$K_{ic, TCA,DCE}$	2.27 mg/L
$K_{iu, but,DCE}$	0.4 mg/L
$K_{iu, but, TCA}$	0.03 mg/L
$K_{ic, but, DCE}$	0.02mg/L
$K_{m, but}$	3.48 mg/mg/day
$K_{m, TCA}$	0.64 mg/mg/day
$K_{m, DCE}$	6.5 mg/mg/day
$K_{s, but}$	1.11 mg/L
$K_{s, TCA}$	1.63 mg/L
$K_{s, DCE}$	0.14 mg/L
$K_{s, O2}$	1 mg/L
$T_{c, TCA}$	
Phase I	0.16 mg/mg
Phase II (High Concentration)	0.08 mg/mg
Phase II (Low Concentration)	0.06 mg/mg
Phase III (with DCE)	0.14 mg/mg
$T_{c, DCE}$	
Phase III (with DCE)	0.03 mg/mg

4.8.3 Biotransformation Model Simulations of the Second Phase 1,1,1-TCA Test

a. High 1,1,1-TCA Concentration Test

Model simulations for the high 1,1,1-TCA concentration test are shown in Figures 107 and 108. The model parameters used to simulate the phase I of the 1,1,1-TCA test did not result in a good fit to the laboratory observations for the Phase II high concentration of 1,1,1-TCA (430 ug/L) test. The model predicts more transformation than was observed based on the column effluent concentrations. One possibility is that the performance of butane-utilizers was affected due to the presence of high 1,1,1-TCA influent concentrations. When the transformation capacity of 1,1,1-TCA was decreased from 0.16 mg/mg to 0.08 mg/mg (Table 45), the model provided a better fit to the effluent 1,1,1-TCA concentrations. The simulated effluent 1,1,1-TCA concentrations were fairly constant compared to column data. Transients in column operation, such as the low influent DO concentrations, resulting in low DO effluent values around day 47 (Figure 107c) were not included in the model simulations. Thus, transient changes that might lead to high 1,1,1-TCA concentrations were not simulated. The continuous butane breakthrough predicted by the biotransformation model (Days 35 to 53 in Figure 107b) was not observed in the laboratory column effluent. The removal of 1,1,1-TCA decreased during days 45-53, and corresponded to a period of low effluent DO concentrations.

Figure 107. Model Simulations of Concentration in the Column Effluent and Laboratory Data during the Second Phase of Biotransformation Test (Days 30-53)

a. 1,1,1-TCA

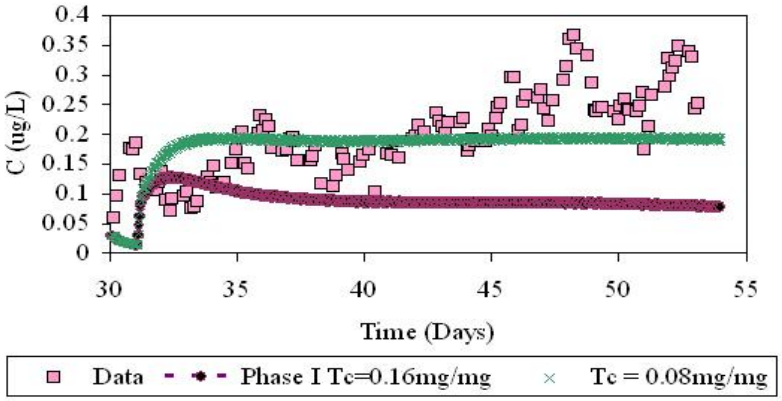

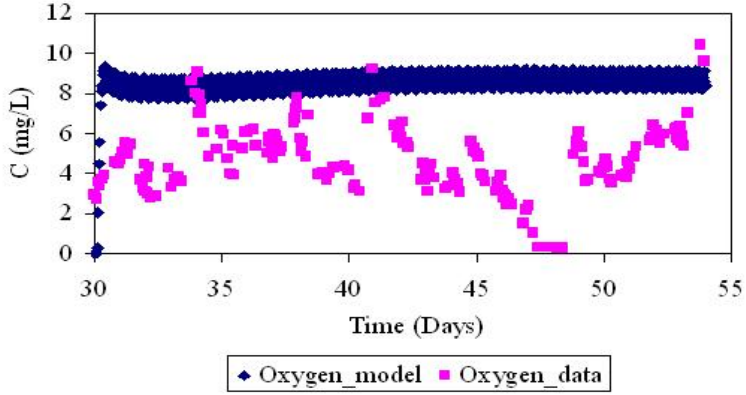

a. Butane

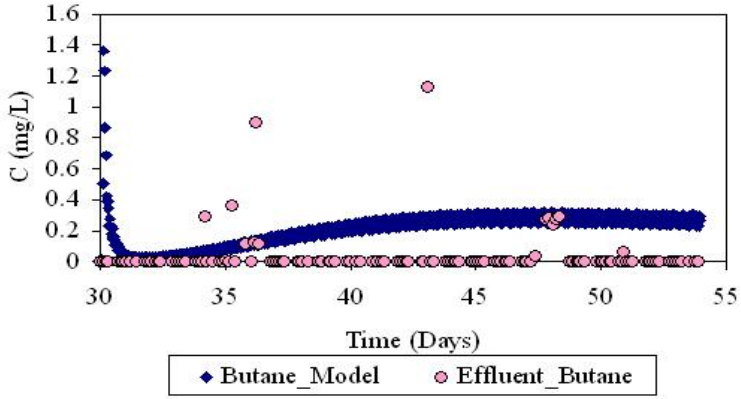

d. Biomass

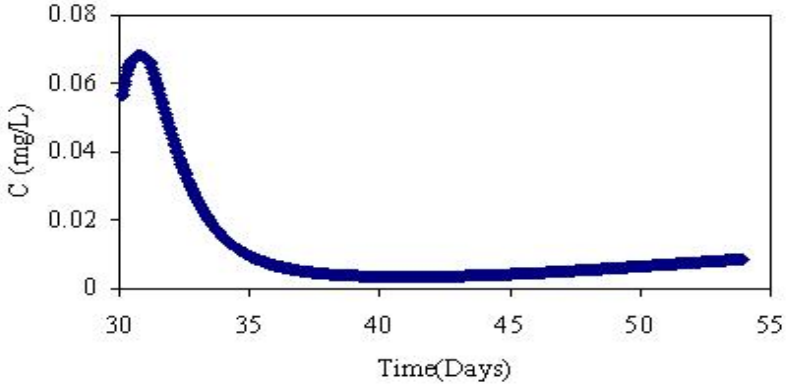

c. Dissolved Oxygen

Figure 108: Model Simulations of the Spatial Distribution in Concentration after 53 days of Operation in Phase II

a. 1,1,1-TCA

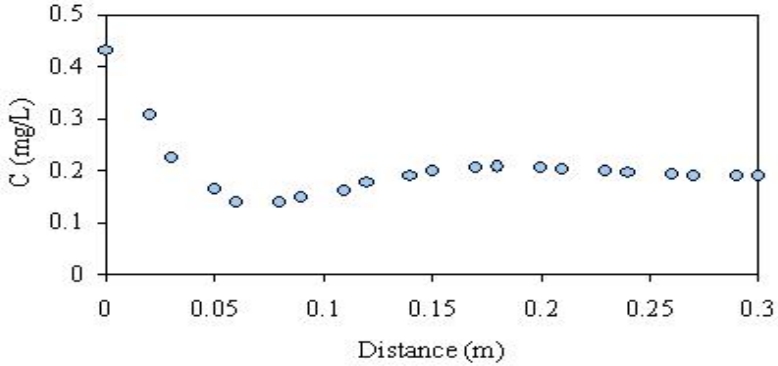

b. Butane

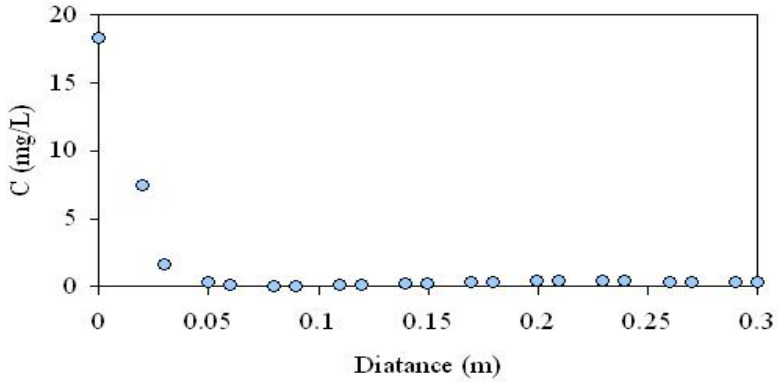

c. Dissolved Oxygen

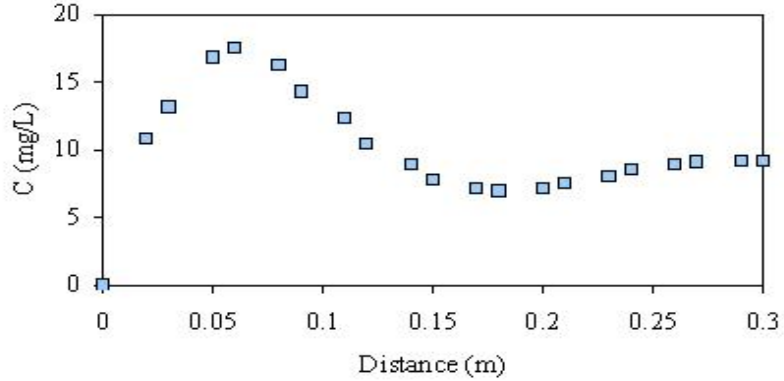

d. Biomass

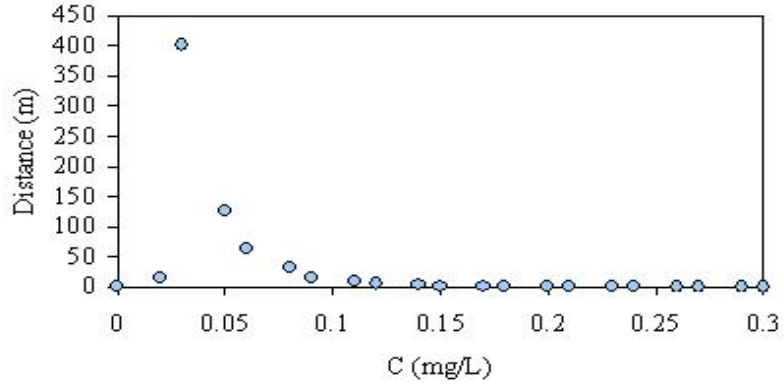

During this period, butane breakthrough was predicted by the model and pulses of butane was also observed in the column effluent (Figure 107b). This indicated that the presence of butane and low DO concentration inhibited the transformation of 1,1,1-TCA. Inhibition by butane was also observed in the microcosm studies. Overall, a reduction in removal efficiency was observed in both model simulations and the experimental results. In this phase, the model simulations of electron acceptor (dissolved oxygen) was not consistent with the observed data, and over predicts concentrations. One possibility is that the oxygen concentration in the influent groundwater was actually lower than that used in the model.

b. Low 1,1,1-TCA concentration test

Model simulations were then performed on the second phase of the test when the concentration of 1,1,1-TCA was lowered to 200 ug/L. The results are presented in Figure 109 and 110. Simulations conducted with the transformation capacity (Tc) used in the first phase (0.16 mg/mg) did not fit the transformation of 1,1,1-TCA observed in the column. Lower Tc value was used (0.06 mg/mg, Figure 4.6a). The results show that the performance of butane-utilizers was reduced from the previous phases. A reduction in Tc required to fit the observation indicates that the microorganisms' ability to transform 1,1,1-TCA was reduced. Another possibility is that two populations of butane-utilizers exist: one that degrades 1,1,1-TCA effectively, and another that does not degrade 1,1,1-TCA very well. The combined transport/biotransformation model does not have the capability of simulating two different microbial populations. Model simulations performed with a lower K_m and TCA to mimic this possibility showed similar results as those achieved by the reduction of the Tc value (data not shown).

Figure 109. Model Simulations of Concentration in the Column Effluent and Laboratory Data during the Second Phase (Low 1,1,1-TCA concentration) of Biotransformation Test (Days 53-65)

a. 1,1,1-TCA

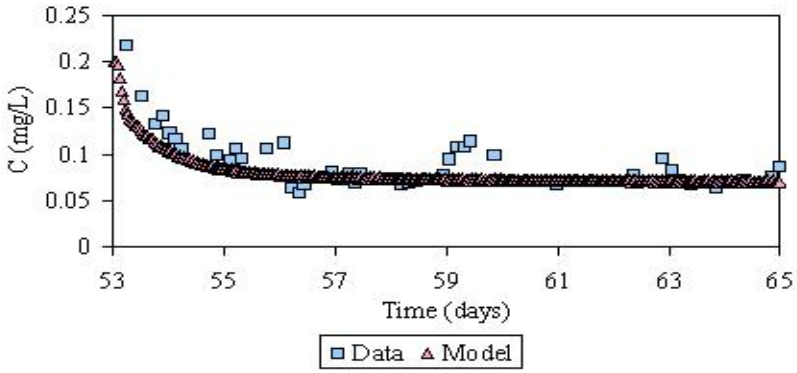

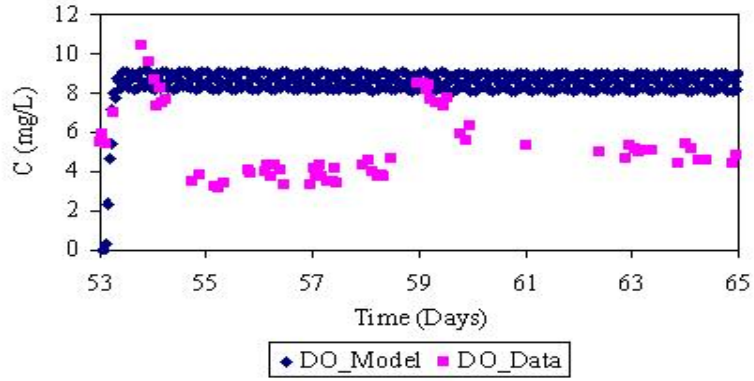

c. Butane

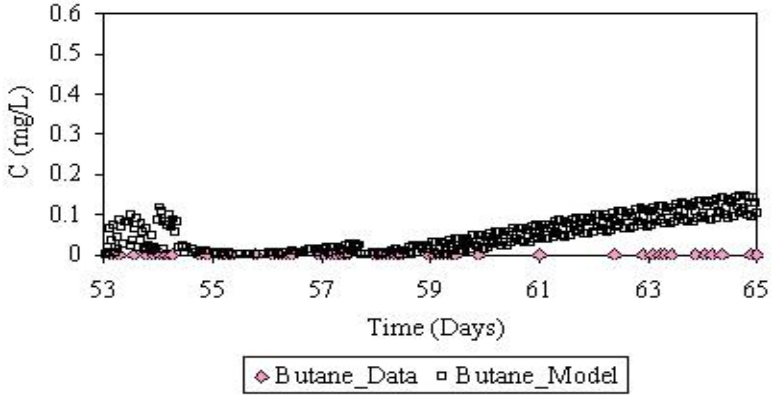

d. Biomass

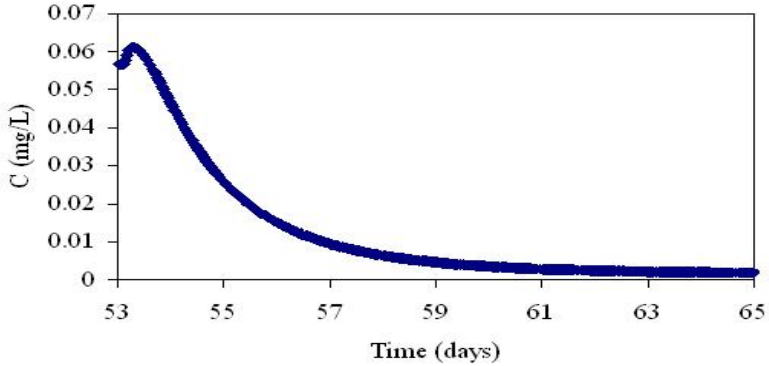

c. Dissolved Oxygen

Figure 110. Model Simulations of the Spatial Distribution in Concentration after 65 days of Operation at the End of Phase II

a. 1,1,1-TCA

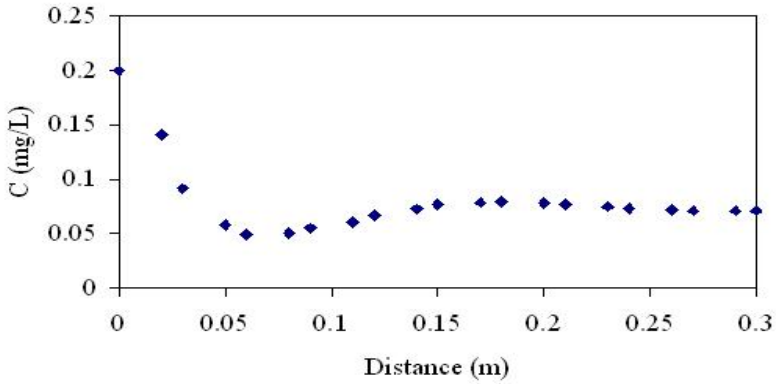

b. Butane

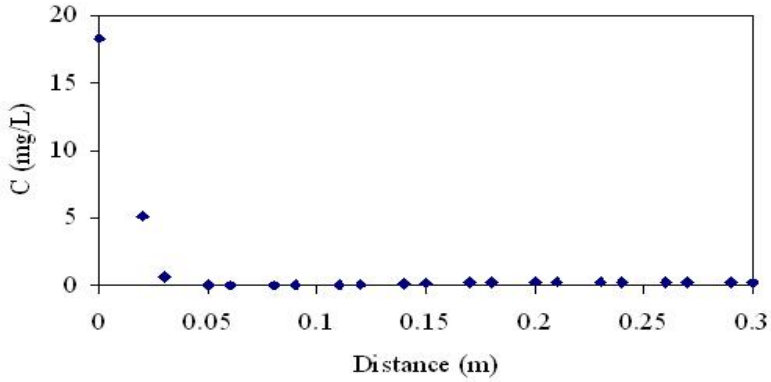

c. Dissolved Oxygen

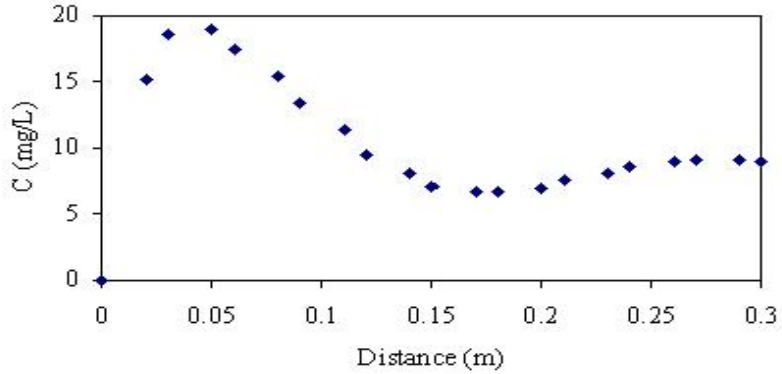

d. Biomass

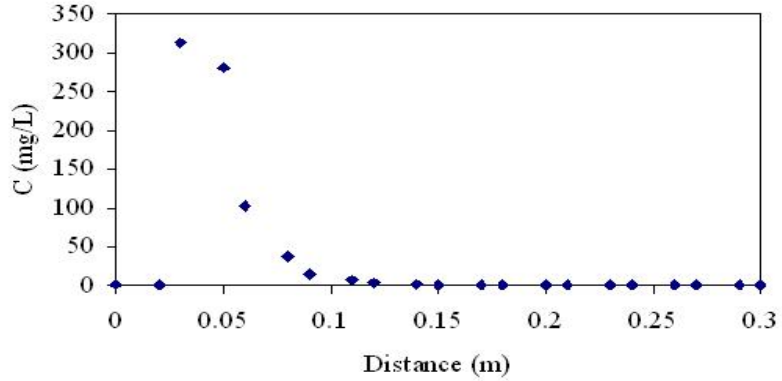

Figure 110 shows the spatial distribution of 1,1,1-TCA, butane, dissolved oxygen, and biomass. The general trends observed were similar to those observed in previous simulations.

Biotransformation-Transport Model Fit to 1,1,1-TCA and 1,1-DCE Third Phase Test

The last part of the biotransformation test, where 1,1-DCE was added along with 1,1,1-TCA, was also simulated. The results of temporal and spatial simulations are plotted in Figure 111, and 111, respectively. On day 120 1,1-DCE was injected into the column. The model simulations followed the general temporal trend in 1,1,1-TCA and 1,1-DCE effluent concentration, as observed in the experimental data. In the model simulations, the transformation of 1,1,1-TCA and 1,1-DCE was modeled by changing the transformation capacity value in the biotransformation model. The Tc for 1,1,1-TCA and 1,1-DCE were 0.14 mg/mg and 0.03 mg/mg, respectively. The model fit the temporal effluent concentration of 1,1,1-TCA and 1,1-DCE well. The low transformation capacity value of 0.03 mg/mg used to fit the transformation of 1,1-DCE and high value used for 1,1,1-TCA were consistent with the modeling analysis of microcosms where transformation capacity of 1,1-DCE was 0.017 mg/mg. This indicated that the transformation of 1,1-DCE is more toxic than the transformation of 1,1,1-TCA. In the model, a mass transfer rate sorption parameter value of 2 day^{-1} and a sorption coefficient of 0.5 L/Kg were used for 1,1-DCE. Model simulations of the butane and dissolved oxygen column effluent concentrations also fit the experimental data well. Again, the concentration of dissolved oxygen was over predicted.

The spatial distribution of the chlorinated solvents, substrates, and biomass are shown in Figure 112. The spatial profiles for the substrates and chlorinated solvents follow similar patterns as observed in Phase I and Phase II. The decrease in the biomass concentration seen in Figure 112d, is the result of toxicity of 1,1-DCE.

Overall, the presence of 1,1-DCE inhibited transformation of 1,1,1-TCA and butane utilization. This is consistent with the field experiments conducted at Moffett Site, California, using phenol and toluene as primary substrates (Hopkins and McCarty 1995), and in the field studies with the butane culture that will be discussed in Section 5.

Figure 111. Model Simulations of Concentration in the Column Effluent and Laboratory Data during the Third Phase of Biotransformation Test when 1,1-DCE was introduced: Tc altered

a .1,1,1-TCA and 1,1-DCE

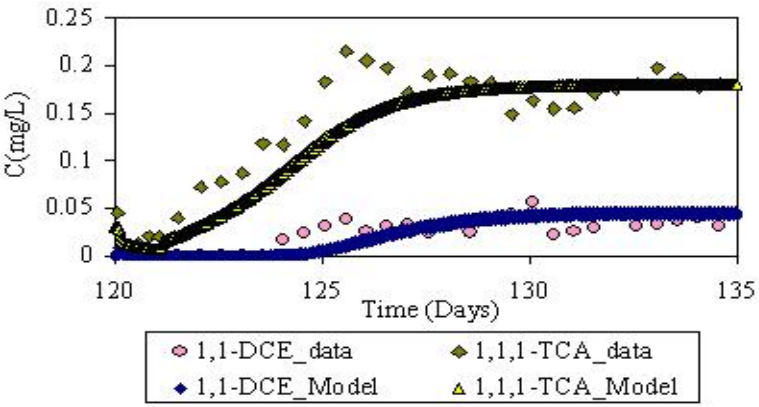

b. Butane

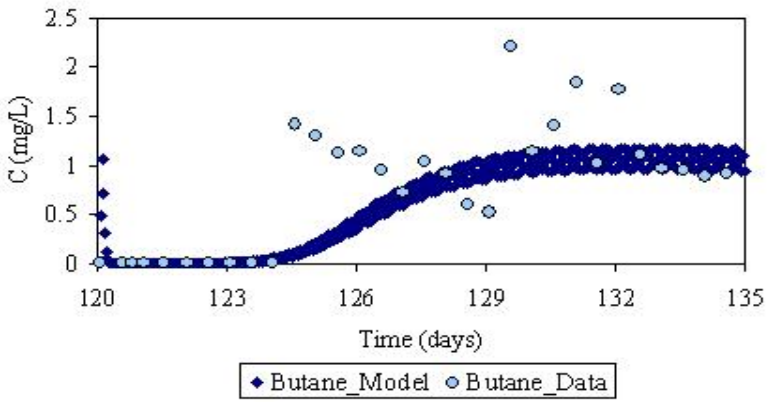

c. Dissolved Oxygen

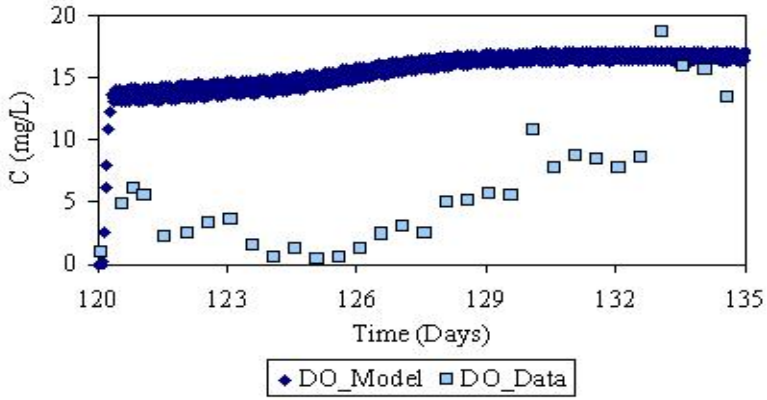

d. Biomass

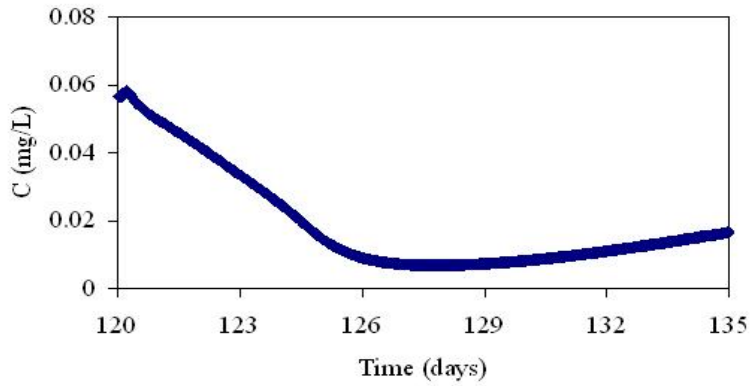

Figure 112. Model Simulations of the Spatial Distribution in Concentration after 135 Days of Operation in Phase III: Tc altered

a. 1,1,1-TCA and 1,1-DCE

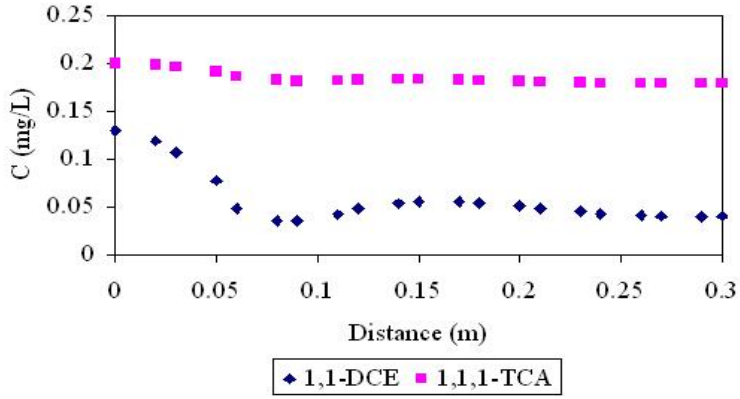

b. Butane

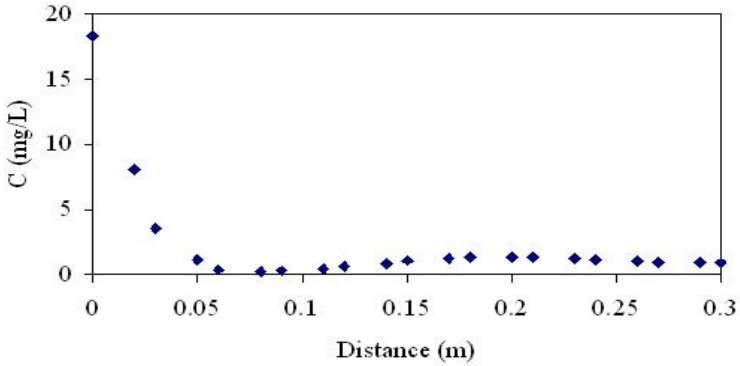

c. Dissolved Oxygen

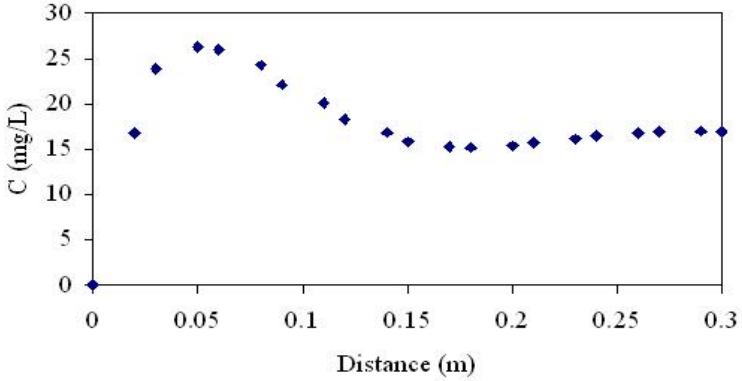

d. Biomass

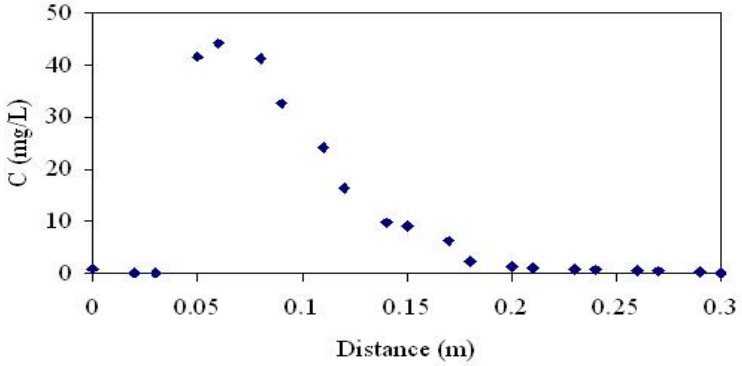

5. FIELD DEMONSTRATION RESULTS

The results from the three seasons of field testing are presented in this section. The objectives of the different seasons of field testing were as follows:

During the first season of testing the first bioaugementation test was performed with the 183BP enrichment culture, and the transformation of a mixture of 1,1,1-TCA, 1,1-DCA, and 1,1-DCE was evaluated. Experiments were also conducted on a control leg were indigenous microorganisms were stimulated. Experimental conditions of the control leg and the bioaugmented leg were essentially the same, with regards to the addition of butane as a substrate, dissolved oxygen, and the concentrations of the three CAHs. The experiments were conducted over a period of 70 days, to evaluate the long term performance of the bioagumented leg and to determine if any biotransformation activity was achieved along the indigenous leg.

During the second season of field testing, the transformation of 1,1,1-TCA was evaluated, since the results of the first season of testing indicated that it was the most difficult compound to transform. Tests similar to those of the first season were performed. The bioaugmented enrichment culture contained two cultures, the strain 172BP and the strain 183 BP. The control leg was operated in the same manner as the first year's tests. The tests also evaluated whether the addition of hydrogen peroxide as a source of oxygen, which permitted more butane addition, resulted in more effective 1,1,1-TCA transformation.

In the third season of field testing the tracking of the bioaugmented culture using molecular methods was performed using Real Time PCR and T-RFLP methods. The community shifts that occurred upon bioaugmentation and biostimulation were also tracked. Successived bioaugmentation tests were performed and the transformation of mixtures of 1,1,1-TCA, 1,1-DCA, and 1,1-DCE was evaluated.

The field experiments were performed in a shallow aquifer at Moffett Field Test Facility in California. As described in the Methods section, the test zone was confined to a 1.5 m thickness of alluvial sands and gravels between silty-clay aquitards. Details of the Moffett subsurface have been previously described by Roberts et al. (1990). Flow gradients were induced by injection and extraction wells spaced seven meters apart. Each experimental leg had three groundwater monitoring wells, S1, S2, and S3, that were spaced 1 m, 2.2 m, and 4 m from the injection well, respectively, to provide sampling access. Both experimental legs had identical well configurations. A schematic of the field test zone is presented in Figure 113. Details of the methods used in the field tests are provided in Section 3 (Methods Section).

Figure 113. Configuration of the Experimental Test Legs

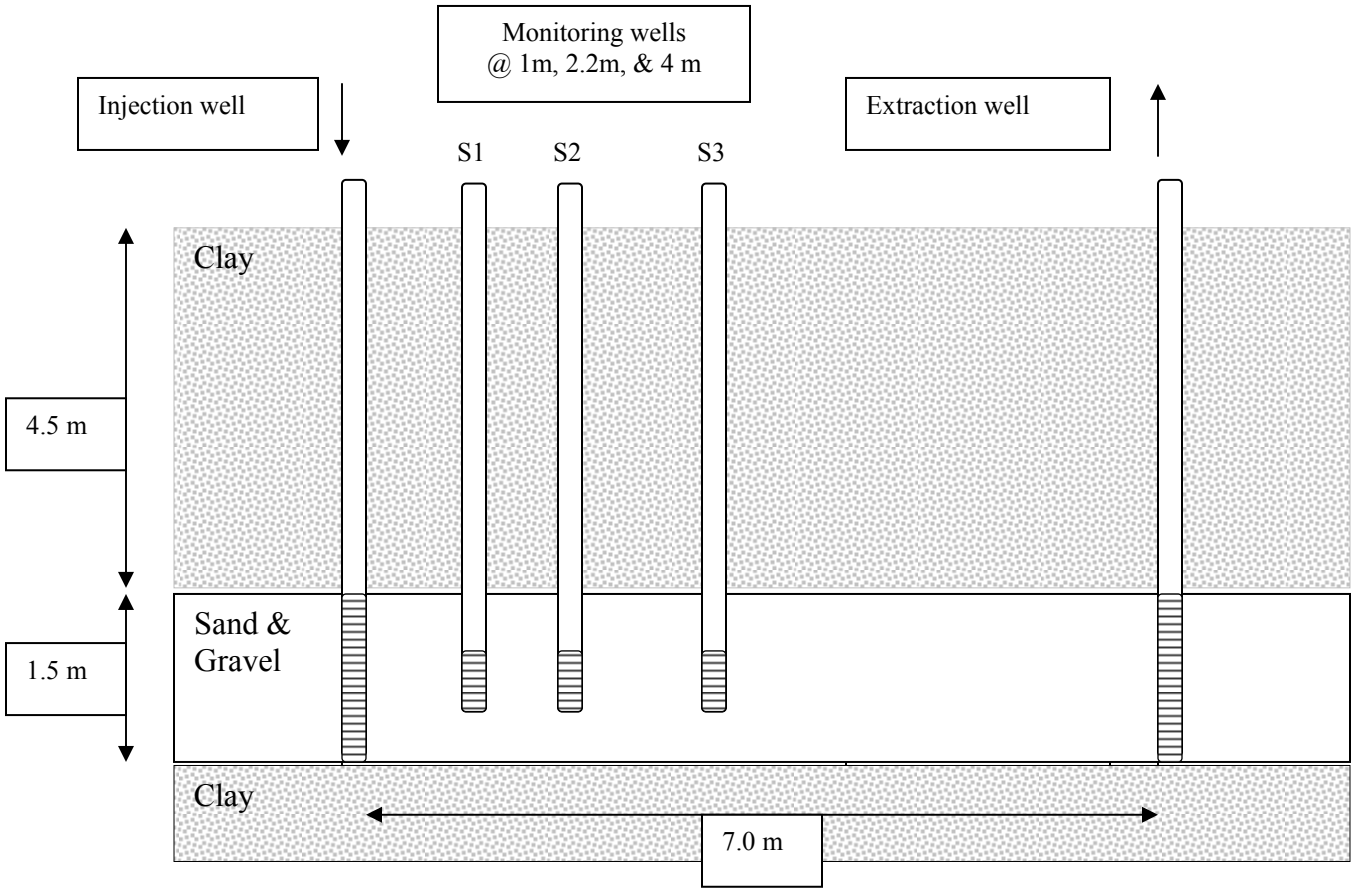

As described in the methods section, the injection system allowed for alternating, pulsed additions of butane and oxygen and continuous additions of 1,1-DCE, 1,1-DCA, 1,1,1-TCA. During the bioremediation experiments, the concentrations and pulsing durations of butane and oxygen were varied periodically in attempt to improve bioremediation. Injection concentrations of the CAHs were held approximately constant.

5.1. The First Season of Field Testing

The focus of the first season of field testing was to bioaugment the butane-utilizing enrichment culture containing 183BP that is capable of 1,1,1-TCA, 1,1-DCE, and 1,1-DCA transformation. The east leg was bioaugmented with the enrichment culture, while in the west leg indigenous butane-utilizing microorganisms were stimulated. Both legs were operated under similar induced gradient conditions of injection and extraction. The first series of tests were bromide tracer tests performed to determine if cross contamination occurred between the two experimental legs. The results of these tests show that if the injection rates on both legs were 1.25 L/min and extraction rates were around 4 L/min, cross contamination did not occur. At these rates effective capture of the injected groundwater by the extraction wells was also achieved.

The first season of field tests commenced in October, 2001, and consisted of a sequence of field tests along the east and west legs. The following sequence of tests were performed:

1) Tracer tests where bromide was added under induced gradient conditions to study transport characteristics of the test zone, and to determine if cross contamination of injected groundwater occurred between the experimental legs.
2) Addition of 1,1,1-TCA, 1,1-DCA, and 1,1-DCE prior to biostimulation and bioaugmentation to determine their transport characteristics and to evaluate if transformation occurred in the absence of biostimulation.
3) Bioaugmentation of the east leg with strain 183 BP and biostimulation of the east and west legs through the addition of butane and oxygen in short alternating pulses.
4) Long term biostimulation of both experimental legs through the addition of butane and oxygen with long pulse cycles, and the evaluation of the transformation of the CAH mixture in both experimental legs.
5) Evaluation of short term pulsing of butane and oxygen to supply more butane to the test legs and to restore the transformation of the CAH mixture

Table 46 present the conditions of the field tests during the first season of testing and outlines the sequence of tests described above. CAHs were continuously injected into the test zone at concentrations ranging from about 50 μg/L for 1,1-DCE to 140 μg/L for 1,1,1-TCA. During the biostimluation and biotransformation tests butane and oxygen were added in alternating pulses. The average concentrations presented in Table 47 represents the pulse averaged concentration, based on the injected concentration and the duration of the pulse interval for butane or oxygen, compared to the total pulse interval. Alternate pulsing of the butane and oxygen were performed to help prevent biological growth close to the injection well, and to distribute biomass along the test leg.

Table 46. Injection Concentrations and Processes Studied during the First Season of Field Testing

Duration	Chemicals Injected	Average Concentration	Process Studied
10/22-11/28/02	Bromide	150 mg/L	Transport characteristics of the experimental legs.
12/26-1/3/02 (0 – 9 days)	Bromide 1,1,1-TCA 1,1-DCA 1,1-DCE	150 mg/L 140 μg/L 130 μg/L 50 μg/L	1,1,1-TCA, 1,1-DCA, 1,1-DCE transport and transformation prior to biostimulation.
1/3/-1/23/02 (9-20 days)	Bromide Oxygen Butane 1,1,1-TCA 1,1-DCA 1,1-DCE	150 mg/L 20 mg/L[1] 8.75[1] mg/L 140 μg/L 140 μg/L 50 μg/L	Bioaugmentation east and biostimulation of both legs with short pulse cycles for transformation of the CAH mixture.
1/23-2/12/02 (20-40)	Bromide Oxygen Butane 1,1,1-TCA 1,1-DCA 1,1-DCE	150 mg/L 20 mg/L[1] 3.5[1] mg/L 140 μg/L 140 μg/L 50 μg/L	Long term biotransformation with long pulse cycles of butane and oxygen.
2/12-3/17/02 (40-70)	Oxygen Butane 1,1,1-TCA 1,1-DCA 1,1-DCE	20 mg/L 8.75 mg/L 140 μg/L 140 μg/L 50 μg/L	Biotransformation achieved upon returning to short total pulse cycles with more butane addition.

Presented in Table 47 is more detailed information on the pulse frequency of the butane and oxygen pulse cycles. Changes in the injection concentrations of the CAHs over the course of the experiments are also presented. These data were used in the modeling analysis of the results of the first season of testing presented in Section 6.

Table 47. Butane and Oxygen Injection Pulsing Durations and Concentrations

Days 9-20: 15/45 min BUT/O_2	Days 9-20: 35/25 mg/L BUT/O_2
Days 20-30: 2/22 hr BUT/O_2	Days 20-23: 35/25 mg/L BUT/O_2
Days 30-40: 1/23 hr BUT/O_2	Days 23-30: 35/5 mg/L BUT/O_2
Days 40-75: 15/45 min BUT/O_2	Days 30-40: 35/18 mg/L BUT/O_2
	Days 40-75: 20/25 mg/L BUT/O_2

Pulsing durations are read as from day 9 to day 20, butane was injected for 15 minutes, followed by 45 minutes of oxygen. Pulsing concentrations are read as from day 9 to day 20, butane was injected at 35 mg/L and oxygen was injected at 25 mg/L.

Table 48. 1,1-DCE, 1,1-DCA, and 1,1,1-TCA Injection Concentrations

1,1-DCE Injection	1,1-DCA Injection	1,1,1-TCA Injection
Days 0-9: 50 μg/L	Days 0-9: 130 μg/L	Days 0-9: 140 μg/L
Days 9-75: 65 μg/L	Days 9-20: 200 μg/L	Days 9-30: 140 μg/L
	Days 20-35: 100 μg/L	Days 30-75: 175 μg/L
	Days 35-60: 175 μg/L	
	Days 60-75: 150 μg/L	

Injections are read as from day 0 to day 9, approximately 45 μg/L 1,1-DCE, 130 μg/L, 1,1-DCA, and 140 μg/L 1,1,1-TCA was delivered into the aquifer.

5.1.1 Results of Bromide Tracer Tests

The results of bromide tracer tests are discussed in detail in Section 10, which presents the modeling analysis of the first years' demonstration. The results of a tracer test conducted along the east experimental leg during the first stages of field testing is shown in Figure 114. The bromide tracer was continuously added to the east experimental leg and bromide breakthrough concentrations were determined at monitoring wells and extraction wells of the both experimental legs. Groundwater was injected and extracted at rates of 1.0 L/min and 3.8 L/min, respectively along both experimental legs. Effective transport was observed between the injection and the monitoring wells of the east leg, and no bromide was observed in the monitoring wells or the extraction well of the west leg. With continuous injection, bromide concentrations achieved breakthroughs to the injected fluid concentration of 100 %, 85%, and 95 % at the S1, S2, and S3 east monitoring wells, respectively. The reason for the less effective breakthrough at the S2 east monitoring well compared to the S3 east well, is not known, but likely results from aquifer heterogeneities. Similar observations were reported by Roberts et al. (1990) in previous tests conducted at the site. Tracer tests conducted throughout the course of the field demonstration consistently showed less effective breakthrough at the S2 monitoring well.

The tracer tests showed fluid residence times from the injection well to the S1 east monitoring well (1 meter from the injection well) of about 10 hours, while to that of the S3 east monitoring well (3.8 meters from the injection well) was about 36 hours. Mass balances indicated that the extraction well recovered about 80% of the injected fluid.

A bromide tracer test was also performed on the west leg (data not shown) at an injection rate of 1.5 L/min and an extraction rate of 4.8 L/min. Rates were increases from the earlier tracer test to try to achieve better recovery at the extraction well. Both experimental legs were operated at the same injection and extraction rates. Bromide breakthrough was more variable along the west leg with only 60 % of the injected concentration achieved at the S2 west observation well (two meters from the injection well). Also the extraction well had less effect in capturing the injected fluid. Bromide was also observed in the groundwater extracted from the east experimental leg, indicating that cross contamination was occurring between the experimental legs under the operating conditions of this test.

Based on these results, the injection and extraction rates were optimized so that cross over did not occur. In order minimize the potential for cross contamination in either direction, the extraction rate on the west leg and the east leg were increased. The injection and extraction rates for the bioaugmentation and biostimulation tests were set at between 1.25 and 1.5 L/min in both injection wells and extraction rates were around 6.0 to 8.0 L/min in the extraction wells. Under these conditions cross contamination between the experimental legs did not occur. The east leg was chosen for use in the bioaugmentation tests, since more complete breakthrough of the injected fluid was observed at its monitoring wells.

Figure 114. Results of the Bromide Tracer Test Conducted along the East Experimental Leg in the First Season of Field Testing

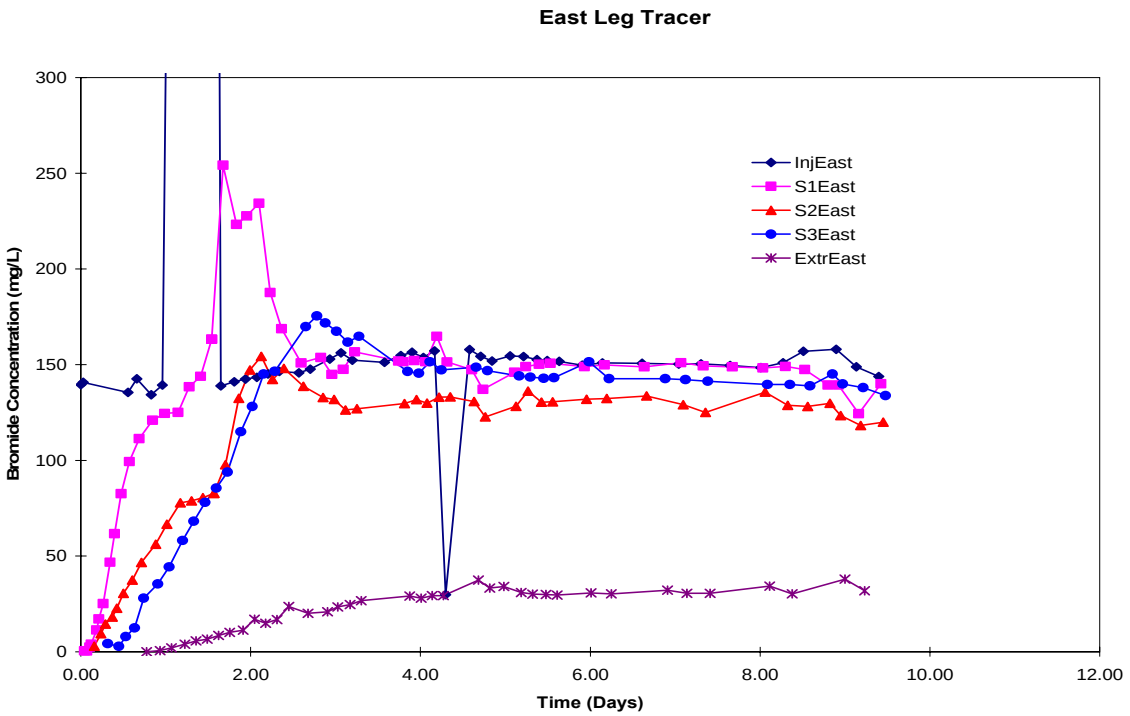

5.1.2 Results of the CAH Transport Test and the Initial Bioaugmentation and Biostimulation Experiment (Days 0-20)

The CAH transport experiment was initiated in December 2001. The tests were conducted with an injection rates of 1.5 L/min and extraction rates of 6 L/min at the east extraction well and 8 L/min on the west Extraction well. 1,1,1-TCA,1,1-DCA, and 1,1-DCE were simultaneously injected into both experimental legs, while bromide was added to the east leg. The concentrations histories at the monitoring locations along the west (indigenous) leg and the east (bioaugmented) for 1,1,1-TCA is presented in Figure 115. It should be noted that bioagumentation and biostimulation started on the ninth day of these tests. The breakthrough toward the injection concentration is shown for most locations, except along the S2 well in the indigenous west leg, where the concentration reached only 50% of the injected concentration after 10 days of addition. The percentage breakthroughs of 1,1,1-TCA observed along the east

are very consistent with those achieved in the bromide tracer test that was running concurrently. 1,1,1-TCA concentrations along the west (indigenous) leg more quickly responded to changes in the injection concentration, compared to the east leg. For example, the concentrations increased more rapidly when 1,1,1-TCA was first injected, and responded more quickly to the perturbation in the injected concentration at about 2.5 days. The concentrations reached pseudo-steady-state levels after about 10 to 15 days of injection in both experimental legs.

Results of the 1,1-DCA breakthroughs is shown Figure 116. Results are consistent with those observed for 1,1,1-TCA. Concentrations respond more quickly to changes in the injection concentration along the west (indigenous) leg. For example, the decrease in injection concentration over the period of about 6 to 7 days is more quickly and dramatically observed along the west leg. Over the period of 10 to 15 days, pseudo-steady-state concentrations are achieved along both experimental legs, with injected 1,1-DCA concentrations observed at the S1 wells of both experimental legs.

1,1-DCE breakthroughs are shown in Figure 117. Results are consistent with those observed for 1,1,1-TCA and 1,1-DCA. As will be discussed, 1,1,-DCE was observed to respond most rapidly to bioagumentation and biostimulation of the east leg, as shown by the decreases in concentration observed after day 10. The breakthroughs prior to bioaugmentation were consistent to those observed for 1,1,1-TCA and 1,1-DCA. The S1 wells concentrations of both experimental legs reached the injected concentration on day 9, just prior to the bioaugmentation of the east leg.

The percentage breakthrough achieved over a period of 10 to 15 days for 1,1,1-TCA and 1,1-DCA, and days 6 to 8 for 1,1-DCE, are provided in Table 49. 1,1-DCE brerakthrough was determine over an earlier time period, since it most rapid responded to bioaugmentation and biostimulation. The greatest fractional breakthroughs are observed in the S1 wells, that are nearest the injection well. Along the west leg, all the CAHs show the best breakthrough was achieved at the S1 well and the poorest at the S2 well. 1,1-DCE has lower fractional breakthroughs than 1,1,1-TCA and 1,1-DCA, since values were determined after a shorter period of injection (6 to 8 days) . It should be noted that breakthroughs on the west leg, which did not respond to biostimulation reached injection concentrations in the S1 and S3 wells over the period of 10 to 15 days. Concentrations reached only 50 to 60% of the injection concentration in the west S3 well for all the CAHs as a result of groundwater dilution. The results at all locations indicate that the CAHs were not transformed to a measurable extent prior to bioaugmentation or biostimulation. Percentage breakthroughs of the CAHs were similar to bromide conservative tracer on the east leg, indicating biotransformation was not occurring. Bromide was not injected into the west leg during these tests, since measurements were being made of potential cross contamination of injected fluid from the east to the west leg. The consistent breakthrough to injected concentrations at the S1 and S3 wells indicate little transformation was occurring along this experimental leg. Bromide tracer test results also show no cross contamination occurred during the test.

Figure 115. 1,11-TCA Concentration Histories at Monitoring Locations along the West (Indigenous) Leg and the East (Bioaugmented) Leg for the first 20 Days of Testing in the First Field Season

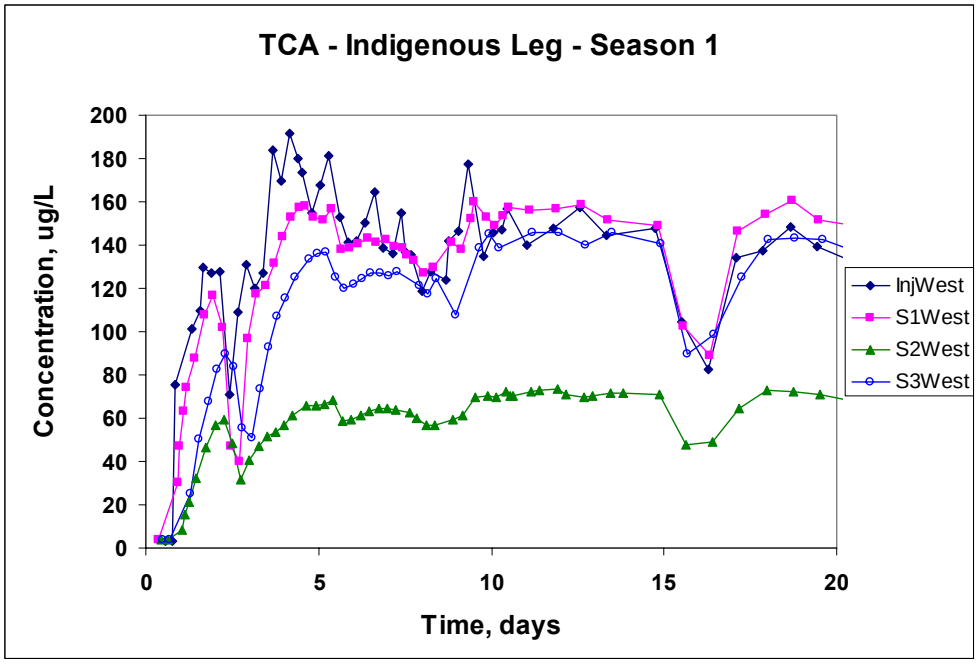

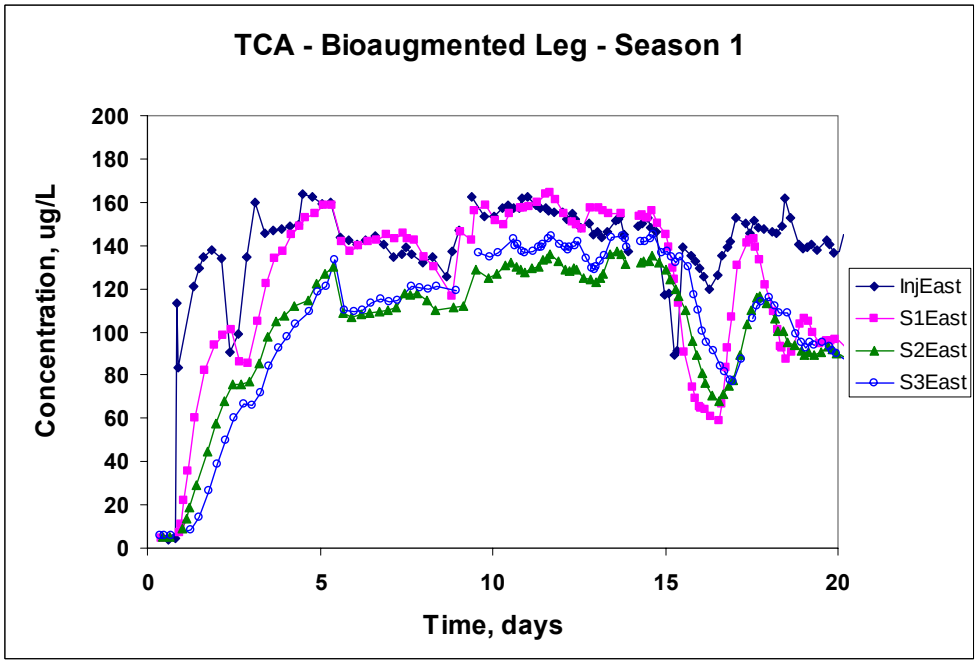

Figure 116. 1,1-DCA Concentration Histories at Monitoring Locations along the West (Indigenous) Leg and the East (Bioaugmented) Leg for the First 20 Days of Testing in the First Field Season

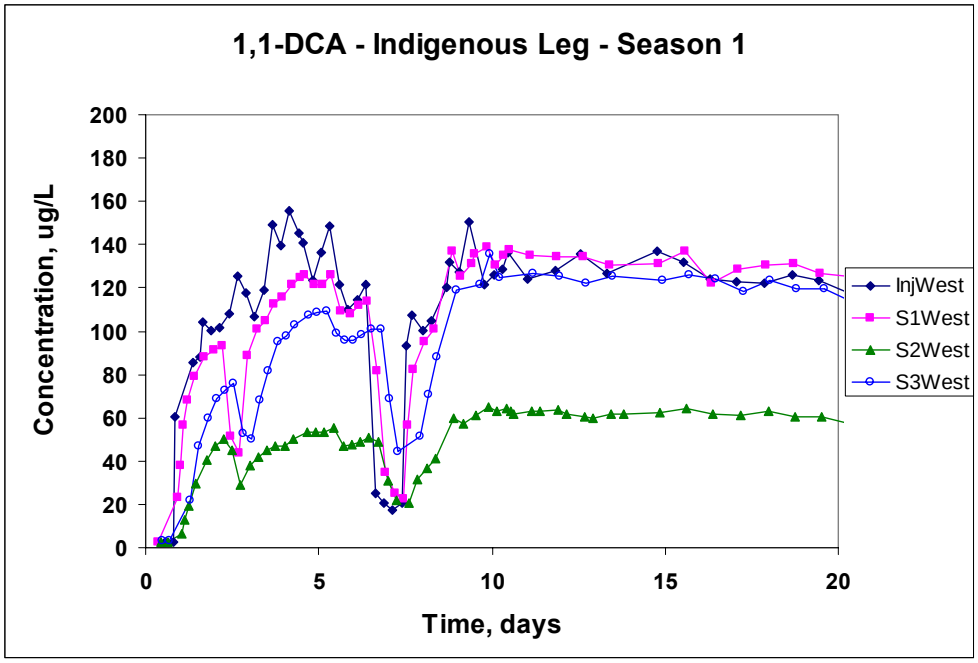

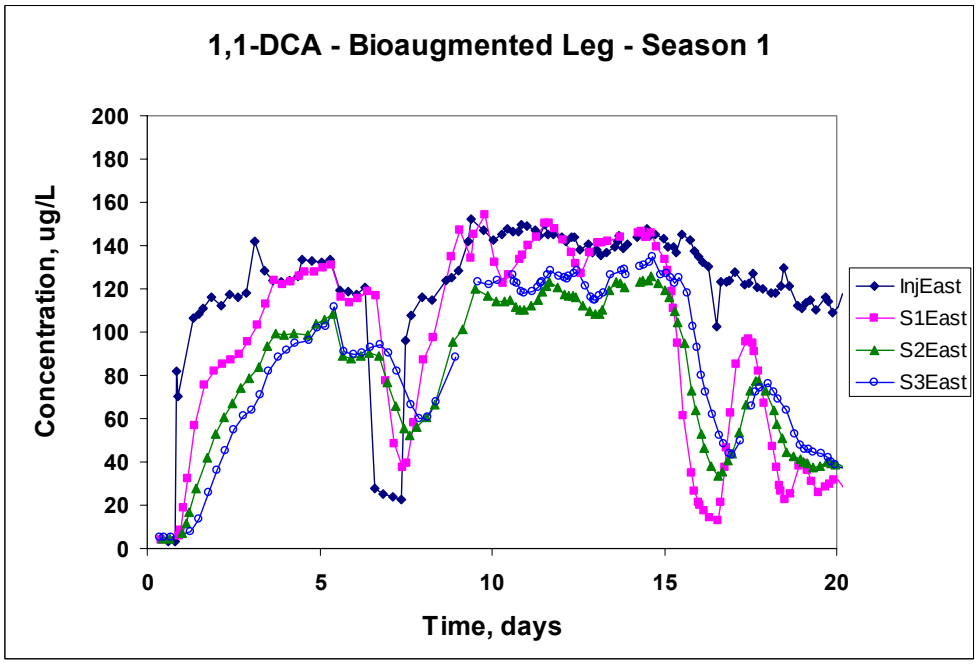

Figure 117. 1,1-DCE Concentration Histories at Monitoring Locations along the West (Indigenous) Leg and the East (Bioaugmented) Leg for the First 20 Days of Testing in the First Field Season

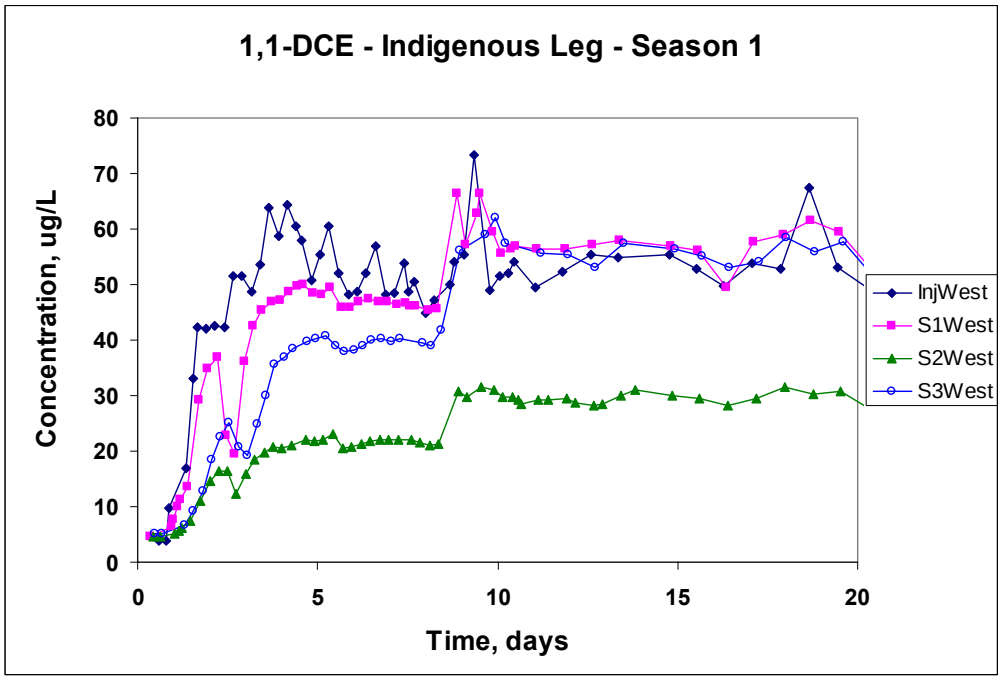

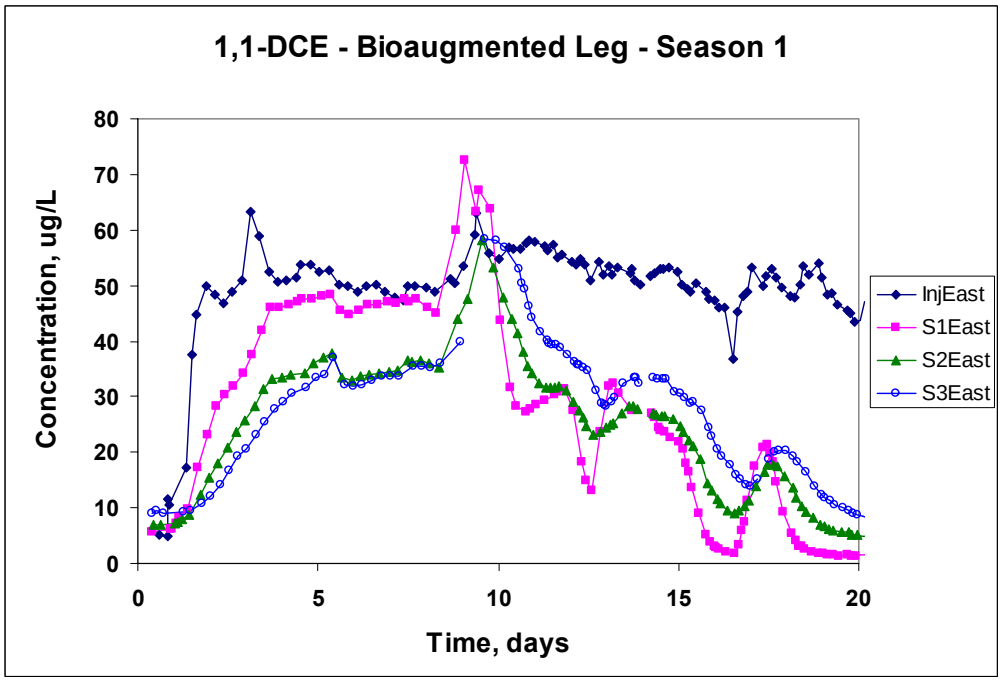

Figure 118. DO Concentration Histories at Monitoring Locations along the West (Indigenous) Leg and the East (Bioaugmented) Leg for the First 20 Days of Testing in the First Field Season

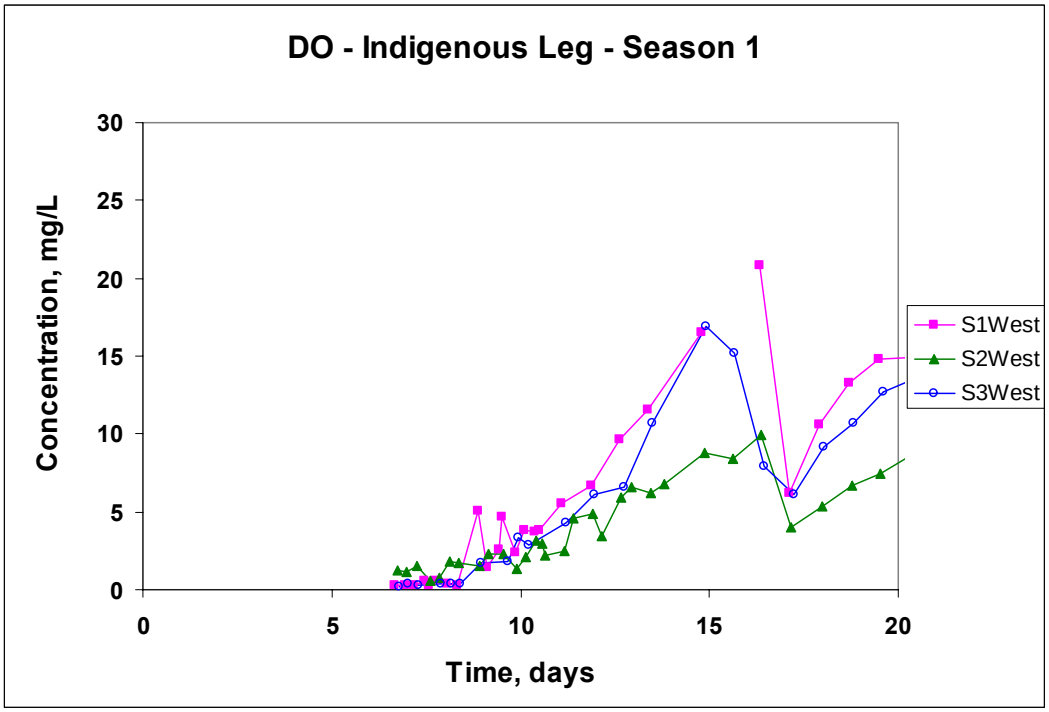

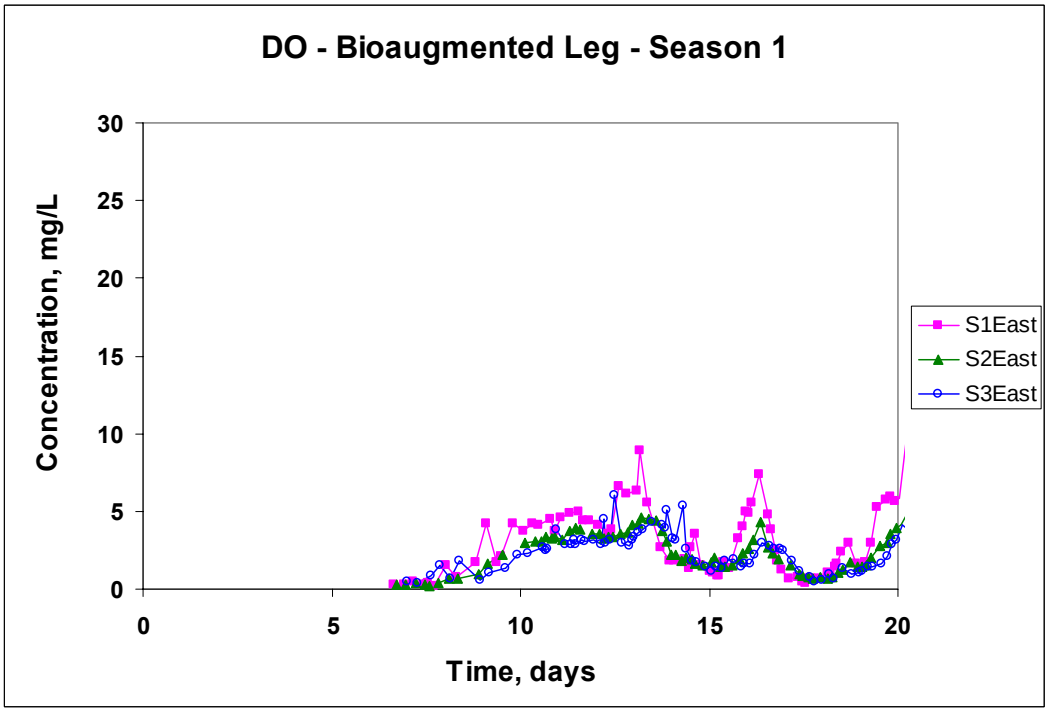

Figure 119. Butane Concentration Histories at Monitoring Locations along the West (Indigenous) Leg and the East (Bioaugmented) Leg for the First 20 Days of Testing in the First Field Season

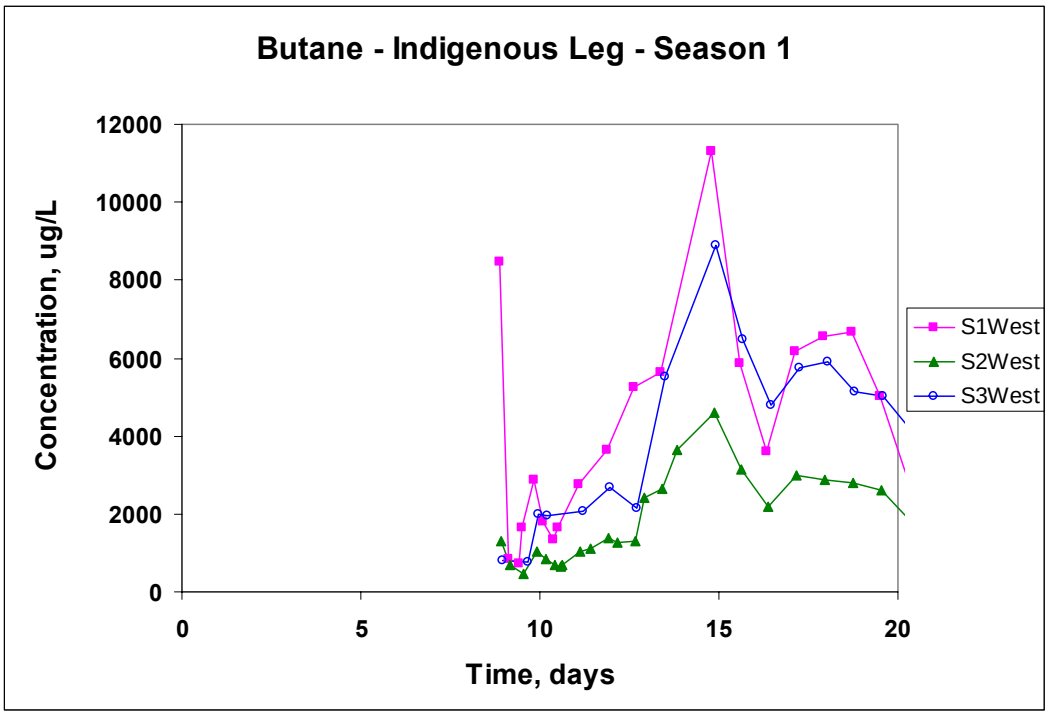

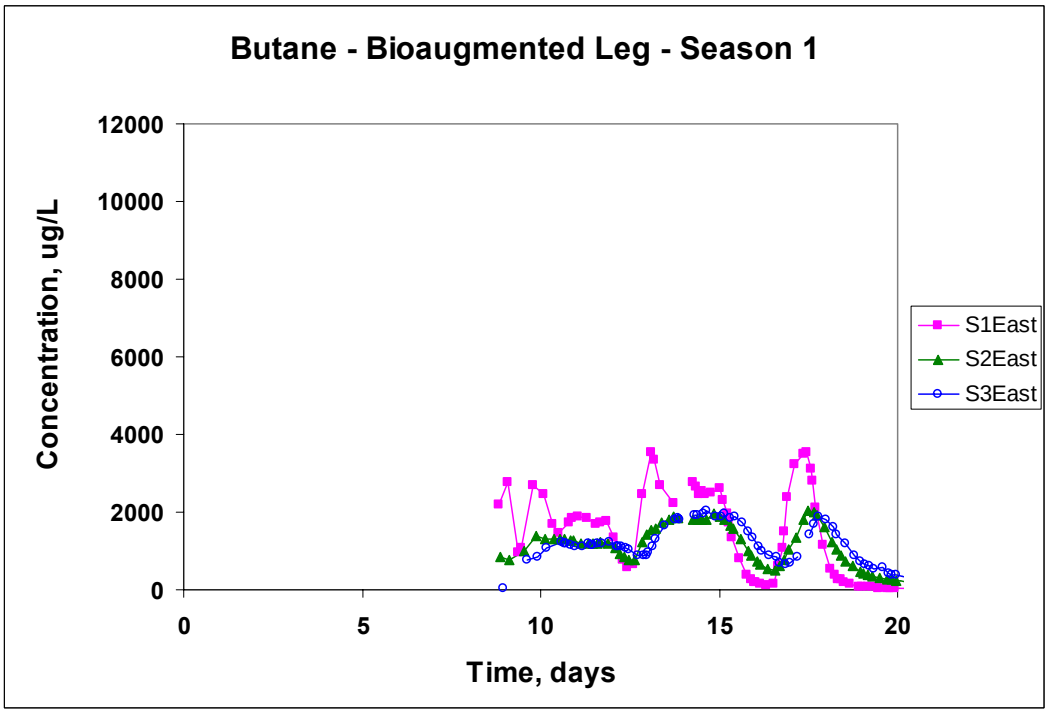

Table 49. Fractional Breakthroughs of Bromide and 1,1,1-TCA, 1,1-DCA, and 1,1-DCE Prior to Biotransformation

	Bromide % Breakthrough	1,1,1-TCA[1] % Breakthrough	1,1-DCA[1] % Breakthrough	1,1-DCE[2] % Breakthrough
West S1	N.D.	100	100	92 (100)
West S2	N.D.	50	50	38 (60)
West S3	N.D	95	95	77 (100)
East S1		100	100	96
East S2		90	87	76
East S3		93	93	76

1 Estimated over a period of 10 to 15 days
2 Estimated over a period of 6 to 9 day; values in paranthesis determined over a period of (10 to 15 days)

The enrichment culture containing the 183BP organism was then injected into the east leg, with continued injection of 1,1-DCE, 1,1-DCA, and 1,1,1-TCA and alternating injections of butane and oxygen. Dissolved oxygen addition to the injected groundwater was started on day 7 and butane addition was started on day 9, about 12 hours prior to bioaugmentation.

The culture was added to the site by diluting 4 g of the harvested cells in 25 L of Moffett groundwater and dispensing it via the injection well over a 4-hour period. The injected cell concentration was approximately 12 mg/L and the injection flow was approximately 1.35 L/min.

The breakthrough of dissolved oxygen at the observation wells of both experimental legs is shown in Figure 118. Initial dissolved oxygen concentrations were below detection in both experimental legs. Oxygen began to breakthrough at the observation wells prior to the bioaugmentration of the culture 9 days into the test. A dramatic difference between the west (indigenous) leg and the east (bioaugmented) leg is that the increase in DO concentrations is much greater in the west leg as time proceeds. The lower DO levels in the bioaugmented east leg was one of the first indications of the more rapid biostimulation of the east leg after bioaugmentation and the start of butane addition on day 9.

The breakthrough of dissolved butane along both experimental legs is shown in Figure 119. Analysis for butane was started after butane was added, so initial samples showed the presence of some butane. Butane is shown to increase to much higher and consistent concentrations on the indigenous west leg compared to the to the bioaugmented east leg.

The initial response to bioaugmentation to the east leg with the 183BP culture is best indicated from the concentration responses of the oxygen, butane, and 1,1-DCE on the east leg and comparisons to the responses observed along the west leg. The only difference in treatment in the two legs was that the east leg was bioaugmented. 1,1-DCE concentrations (Figure 117) in

the bioaugmented east leg began to decrease at 10 days and continued to decrease with concentration reduced from the injected concentration of 60 μg/L to 2 μg/L, by 20 day (10 days after bioaugmentation). In contrast 1,1-DCE concentration remained constant in the west indigenous leg. Butane concentrations also decreased to near detection at the west S1 well 20 days into the test, while the concentrations ranged from 2 to 6 mg/L in the indigenous leg. Dilution at the S2 well of the west indigenous leg is also observed in the butane concentrations. The DO concentrations were also greatly reduced in the bioaugmented leg.

1,1-DCA concentrations (Figure 116) were also dramatically reduced in the east bioaugmented leg starting at about 15 days. It is interesting to note that the rapid reduction in 1,1-DCA concentrations coincided with the decrease in butane concentrations to low levels over the same time period. At 20 days, the concentrations were reduced from an injected concentration of 120 μg/L to 40 μg/L at the east S1 observation well. In contrast, 1,1-DCA concentrations were not reduced in the west indigenous leg over the period of 10 to 20 days. .

1,1,1-TCA (115) also show some decrease in concentration starting 15 days in the east bioaugmented leg. Like 1,1-DCA, the decrease in 1,1,1-TCA concentration coincided with the reduction in butane concentration to low levels during the same period. At 20 days, the 1,1,1-TCA concentrations were reduced from the injected concentration of 140 μg/L to 100 μg/L at the east S1 observation well.

The transformation of the CAHs was correlated with the reduction of butane to low concentrations. The opposite response was observed in the east bioaugmented leg over the period of about 17 to 18 days, with butane concentrations increasing in all three monitoring locations, while DO concentrations (Figure 118) were reduced to less than 1 mg/L. This is indicated by a temporal pulse of butane concentration moving through the east leg. We do not know if the butane pulse results from a malfunction of the injection system, or DO concentration being driven to low levels. The concentrations of 1,1,1-TCA, 1,1-DCA, and 1,1-DCE all increased during this period of high butane concentrations despite their injection concentrations being constant. The greatest perturbation in concentrations of the CAHs and butane occurred at the S1 well. 1,1,1-TCA, and 1,1-DCA were perturbed to a greater extent than 1,1-DCE, which is consistent with our laboratory studies, discussed in Section 8, that indicated their transformation was more strongly inhibited by butane. The concentrations of butane and the CAHs all decrease after about 18 days, while the oxygen concentrations increase.

The response along the east leg shows cometabolic transformation of 1,1,1-TCA, 1,1-DCA, and 1,1-DCE in the bioaugmented west leg, corresponding to butane and oxygen utilization. In contrast, biostimulation of the west leg was not yet evident, as indicated by the concentrations of butane and oxygen observed, and no decreases in concentration of any of the CAHs. The results also show that most, if not all, of the reduction in concentrations of butane, DO, and the CAHs occurred within the first meter of transport in the test zone of the east leg (S1 monitoring well). The reductions in concentration at the S2 and S3 well appear to result for the transport downgradient of groundwater treated within the first meter. For example, this is also indicated by the delayed increases and decreases in concentration, such as those observed over the period of 17 to 20 days in the tests.

On day 21 of the test the alternating pulse cycles of butane and oxygen were lengthen to 2 hr of butane and 22 hr of oxygen. This was a dramatic increase in pulse cycle compared to that used in the initial phase of the biostimulation test. The pulse cycle was increased, since all the utilization of butane and transformation of the CAHs were occurring with first meter of transport in the east leg, Thus there was a concern about potential biofouling the aquifer near the injection well. Longer pulse cycles had been successful used in previous demonstrations at the Moffett test site, and modeling studies of Semprini and McCarty (1992) had shown that the alternate pulsing helped distribute the stimulated biomass.

Figure 120 shows the DO concentrations at the monitoring locations of the east and west legs over the period from 20 to 70 days. DO concentrations begin to oscillate in response to the longer pulse cycle. DO concentrations at the S1 and S3 west leg range from 0 to 20 mg/L during the period of 22 to 34 days. Similar oscillations are observed along the east leg. A change in the pulse cycling is also indicated at around 33 days by the decreased DO oscillations in both experimental legs. At this time the butane pulse intervals was changed from 2 hours to 1 hour, and the DO interval remained 23 hours (Table 47). This change was made as CAH transformation ability was gradually lost, as will be discussed. At 40 days, the pulse cycle was changed to the short pulse cycles used at the beginning of the experiment (Table 47), of 15 minutes butane and 45 minutes of DO, to determine if CAH transformation could be restored to levels achieved during the period of 15 to 20 days. With this change, the oscillations in the DO concentrations essentially ceased. DO concentration gradually decreased in the west indigenous leg over the period of 40 to 70 days, as a result of the biostimulation of indigenous butane-utiizing microorganisms. DO concentrations also decreased in the east bioaugmented leg when the cycle is changed at 40 days in response to the addition of more butane. Excess oxygen was maintained in the test zone of both legs over the period of 40 to 70 days.

Butane concentrations are shown in Figure 121 over the period of 20 to 70 days. The oscillations in the butane concentrations in response to the change to the longer pulse cycles is evident in both experimental legs over the period of 22 to 38 days. The oscillations are greater in the indigenous east leg, compared to the west bioaugmented leg. This results form less butane consumption along the west leg, and may also result from that leg responding more rapidly to changes in the injection concentrations, as was discussed earlier in relation to the breakthrough of CAHs at the monitoring locations. What is evident is that the change to longer pulsed resulted in increases in butane concentration along the bioaugmented east leg over the period of 22 to 38 days. Butane concentrations of less that 100 μg/L around 20 days increased to maximum concentrations of around 2 to 3 mg/L. Butane concentrations also increased at the S2 and S3 monitoring wells. The results show that the change to the longer pulse cycle affected butane utilization, and, as will be discussed, was associated with a loss in transformation of the CAHs.

With the return to the shorter pulse cycles at 40 days, oscillations in butane concentrations decreased. Butane concentrations in both the indigenous and bioaugmented legs stabilized at the S1 observation well at around 3 mg/L at around 50 days. The observations at the bioagumented leg, indicate that butane consumption had greatly diminished compared to the period 20 days into the test, when concentrations at all locations were below 400 μg/L. The results indicate that the population of butane utilizing microorganisms diminished greatly over the period when the butane pulse cycles were lengthened.

In both experimental legs the butane concentrations decreased at the S2 and S3 monitoring locations over the period from about 45 to 50 days, followed by decreases in concentration at the S1 location at about 50 days. The decreases in at the S1 bioaugmented leg were more rapid, than the gradual increase observed along the indigenous west leg. The butane concentration response with the change to the shorter pulse cycles were characteristic of those observed when a test leg is being biostimulated from low microbial biomass to a greater biomass. For example, similar temporal response along the test legs were observed when indigenous methane-utilizers were stimulated at the Moffett test site (Semprini et al., 1990). As illustrated here with butane, methane concentrations in those tests decreased more rapidly at the more distant monitoring locations, followed by the closer monitoring location as a result of biostimulation of indigenous microorganisms throughout the test zone. As biostimulation proceeds, biological growth occurs closer to the injection well, and the substrate concentrations then decrease later in the monitoring well closer to the injection well (S1 in this case). This type of respond has also been predicted in the modeling of the results of the methane biostimulation tests (Semprini and McCarty (1991), and modeling of the results of these tests (Section 10). The butane temporal responses are also consistent with the responses of DO, which show decreases in DO as a result of greater butane utilization. The response of both DO and butane indicate a significant decrease in the biomass of butane-utilizers occurred during the period of 20 to 40 days, when butane and oxygen were added in long pulse cycles, and an increase in biomass with return to the longer pulse cycle.

The temporal responses at the monitoring locations of 1,1,1-TCA, 1,1-DCA, and 1,1-DCE over the period of 20 to 70 days, are shown in Figures 122, 123, and 124, respectively. 1,1,1-TCA concentrations remain fairly unchanged in the indigenous west leg over the entire period, with little evidence of 1,1,1-TCA transformation. Even when indigenous butane-utilizers were effectively stimulated over the period of 60 to 70 days, 1,1,1-TCA concentrations did not significantly decrease, indicating that indigenous butane-utilizers did not transform 1,1,1-TCA, or transformed 1,1,1-TCA at very slow rates.

In the bioagumented leg, 1,1,1-TCA removals that were achieved at 20 days, were lost upon the change to the long pulse cycle. Concentrations in the S1 well increased soon after the long pulse cycles were initiated (around 22 days), and correspond to the increases in butane concentrations. Concentrations also increased at the S2 and S3 locations. Concentrations of 1,1,1-TCA, did not decrease upon the change to the shorter pulse cycles. At the end of the test, over the period of 65 to 70 days, butane is being as effectively removed in the period of 20 days into the test. 1,1,1-TCA concentration, however, did not show a significant 1,1,1-TCA decrease.

The temporal response of 1,1-DCA at the monitoring locations is shown in Figure 123. In the indigenous leg 1,1-DCA concentrations show little difference, compared to the injected concentration over the period of 20 to 70 days. The injected concentrations change significantly over the course of the experiments, and the concentrations at the monitoring locations reflect these changes. For example, over the period of 20 to 40 days the concentrations gradually increased, and concentrations at the monitoring locations increased, while over the period of 40 to 60 days, injection concentration decreased and the monitoring concentrations also decreased. An increase in the injection concentrations at 60 days, resulted in a corresponding increases at the monitoring locations. The data at the end of the experiment (60 to 70 days), when butane was being effectively indicates little removal of 1,1-DCA was observed. Concentrations at the S1

and S2 wells, over the period of 65 to 69 days, when pseudo steady-state conditions were obtained, indicate no removal of 1,1-DCA, since concentrations are essentially identical to the injection concentrations. Lower concentrations in the S3 well result from dilution by the native groundwater.

In the bioaugmented leg, the increase in 1,1-DCA concentrations in response to the change in pulse cycle over the period of 20 to 40 days is evident. The concentrations increased most rapidly in the S1 well, followed the S2 and S3 wells. After the period of long term pulses (40 days into the test), the concentration at the monitoring locations indicate little if any removal of 1,1-DCA in the bioaugmented leg. Upon changing to short pulse cycles at 40 days, concentrations at the observation locations track the changes in the injection concentration. At the end of the test (65 to 68 days) the concentrations at the S1 well and S3 wells were in the range of the injected concentration, indicating 1,1-DCA was not being removed to a significant extent in the test zone, despite the effective removal of butane. While the pulsing conditions were nearly identical to the those earlier in the tests (20 days), 1,1-DCA was not being transformed, as was observed earlier in the test.

The temporal response of 1,1-DCE is shown in Figure 124. At the indigenous leg, 1,1-DCE concentrations tracked the injected concentrations, and indicated little transformation through the period of long pulse cycles (40 days). The 1,1-DCE concentration, however, began to decrease at the S2 and S3 wells around 45 days, upon changing to the short pulse cycle. Decreases in concentration started at around 55 days in the S1 well. The decreases are consistent with the removal of butane concentrations to low levels that were first achieved at the S2 and S3 wells, followed by the S1 well. The results indicate the transformation of 1,1-DCE in the indigenous test leg in response to the stimulation of indigenous butane-utilizing microorganisms. The reduction in 1,1-DCE concentration is shown to be correlated with the decrease in butane concentrations in the indigenous leg. It is also important to note that by the end of the test, 1,1-DCE show oscillations in concentration with changes from 0 to 30 μg/L. Less oscillations in concentrations and lower average values were observed the S2 and S3 wells. The results are consistent with butane concentrations, which show oscillations in concentrations at the S1 well, but reduction in concentrations to very low levels in well S2 and S3. The greater oscillations at S1 are likely a result of inhibition by butane on the rates of 1,1-DCE transformation.

In the bioaugmented leg, the concentrations in 1,1-DCE increased during the period of 20 to 40 days. 1,1-DCE concentrations decreased more slowly than 1,1-DCA. This likely resulted from the more rapid transformation of 1,1-DCE that was observed. Thus, if the biomass of butane-utilizers was decreasing during this period, enhanced biotransformation rates may have been maintained longer, resulting in a slower rate of increase to the injected concentrations. At 40 days, the concentrations at the S1 reached the injected concentrations, indicating little transformation was occurring within 1 meter of transport in the test leg. After the short pulses and more butane was delivered to the test leg, concentrations decreased at the S2 and S3 monitoring location, followed by the S1 location. The results are consistent with butane responses, which show butane concentrations decreasing over the same period that 1,1-DCE concentrations decreased. For example, the decrease in 1,1-DCE over the period of 45 to 50 days in the S2 and S3 wells, corresponds to a decrease in butane concentration over the same period. A similar correlation was observed at the S1 well. The results indicate a more

distributed biostimulation of the test leg at this time, and 1,1-DCE transformation being associated to that biostimulation. It is also interesting to note greater oscillations in 1,1-DCE were observed at the end of the test 60 to 70 days, than was observe in the earlier phase of the test, for example 17 to 20 days (Figures 118 and 124). Oscillations in 1,1-DCE concentration at the S1 east well at later time are similar to those observed in the S1 west well. These oscillations are likely the result of butane inhibition on 1,1-DCE transformation.

5.1.3 Summary of the Results from the First Season of Testing

The first season of field testing demonstrated that parallel field tests could be performed along two test legs at the field site. The west leg served at the indigenous test leg, while the east was the bioagumented test leg. Bromide tracer tests demonstrated that the test legs could be hydraulically operated so that cross contamination would not occur between the experimental legs. Nearly complete breakthrough of the bromide tracer occurred at the S1 and S3 monitoring wells of both experimental legs, while incomplete breakthrough occurred at the S2 well. This was observed in earlier studies at Moffett, resulting from the heterogeneous alluvial deposits in the subsurface. The results of the tracer tests showed that controlled tests could be performed at the site.

1,1,1-TCA, 1,1-DCA, and 1,1-DCE transport tests prior to the bioaugmentation and biostimulation tests showed their retardation compared to the bromide tracer. With continuous addition their breakthrough concentrations approached the injected concentrations in the S1 and S2 well of both experimental legs, indicating that they were not transformed prior to bioaugmentation and biostimulation of the test leg.

Upon bioaugmentation of the east leg, effective uptake of butane and oxygen were observed within a few days in contrast to the indigenous leg, where little evidence of butane or oxygen uptake was observed 10 days after butane or oxygen addition was started. 1,1-DCE concentrations decreased in the bioaugmented leg within a few days, followed by decreases in 1,1-DCA, and 1,1,1-TCA. The decreases in 1,1-DCA and 1,1,1-TCA were correlated to a decrease in butane concentrations in the test leg. Transient increases in butane concentration in the test leg were also associated with increases in concentration of the CAHs, as a result of inhibition and possibly low DO concentrations.

Table 50 presents estimates of the percentage removal of the CAHs that was achieved in the test legs. In the bioaugmented leg, all three CAHs were being removed 20 days into the test (10 days after bioaugmentation), to different extends. 1,1-DCE was removed to the greatest extent, followed by 1,1-DCA and 1,1,1-TCA. All the removal was achieved within the first meter of travel within the test zone, consistent with butane removal. The results indicate that the bioaugmented biomass did not travel far in the test zone. This combined with the short pulse interval resulted in effective transformation within 1 meter of travel. In contrast, no removal of the CAHs occurred in the indigenous west leg over the same period. The results are consistent with butane and oxygen concentrations along the leg, which showed little removal. The results show that bioaugmentation of the 183 BP culture was effective in decreasing lag times for biostimulation as well as promoting the biotransformation of 1,1-DCE, 1,1-DCA, and 1,1,1-TCA. The results are also consistent with the results of laboratory studies with the 183 BP culture that showed 1,1-DCE was the most rapidly transformed, followed by 1,1-DCA, and 1,1,1-TCA. The results are also consistent with the results of laboratory studies which showed

that 1,1-DCA and 1,1,1-TCA transformation was inhibited by the presence of butane, and removal of butane to low concentrations was required for effective transformation to be achieved.

The effective transformation of CAHs that was achieved in the bioaugmented leg early in the tests, was lost during a period when long terms pulses of butane (1 to 2 hours) and oxygen (23 hours) were initiated. It was a mistake to make such a large change in the pulse cycle so early in the test. However, we do not know whether transformation activity would have been lost even if the short duration pulse cycles were maintained. Results of a modeling analysis of the results of these tests (Section 10) indicated that less butane was introduced during the longer pulse cycles, and this was partly the reason for the loss in activity, combined with 1,1-DCE transformation toxicity. The bioaugmented population may also have been established close to the injection well. Thus, the change to the long pulse cycle may have limited the oxygen and butane required for their maintaince. 38 days into the test, the CAH removals were greatly decreased in the bioaugmented leg, with essentially no removal of 1,1,1-TCA being achieved, and with very limited removal of 1,1-DCA and 1,1-DCE. Of the three CAHs, 1,1-DCE was removed to the most significant extent. In contrast, little removal of CAHs was achieved on the west indigenous leg over the same time period.

The initiation of the short pulse cycles after 40 days of operation resulted in 1,1-DCE removal in both the bioaugmented and indigenous legs. The results demonstrated that indigenous butane utilizers were present in the aquifer, that were capable of 1,1-DCE transformation. 1,1-DCE was more effectively transformed along the bioaugmented leg than the indigenous leg (Table 50). 1,1-DCA or 1,1,1-TCA was not removed along the indigenous leg, and limited removal was observed along the bioaugmented leg. Butane and CAH removal differed spatially along the bioaugmented legs during the later period of short pulses (40 to 70 days) compared to the earlier period (10 to 20 days). Butane uptake and CAH removal was more distributed along the test zone during the latter period. For example, in the latter test 1,1-DCA and 1,1-DCE removal increase from the S1 to the S3 wells. The results indicate more distributed biostimulation of the test zone, likely with indigenous butane-utilizing microorganisms that have limited ability to transform 1,1-DCA and 1,1,1-TCA.

A possible scenario that occurred along the bioaugmented leg was as follows. Bioaugmentation was successful in early in the test and effective CAHs transformation was achieved. Most the bioaugmented and biostimulated biomass was within 1 meter of transport of the injection well. After the initiation of the long pulse cycles, the biomass of bioaugmented culture, gradually decreased, corresponding to a loss in CAH removal. This likely resulted from less butane being delivered, the long pulse interval minimizing growth near the injection well where the bioaugmented culture resided, combined with 1,1-DCE transformation toxicity decreasing the biomass. Upon switching to the short pulse cycle indigenous butane-utilizers were stimulated in the indigenous leg, which had the ability to transform 1,1-DCE, but not 1,1-DCA or 1,1,1-TCA. A limited biomass of the bioaugmented culture may have also been present that resulted in some 1,1-DCA and 1,1,1-TCA removal and more effective 1,1-DCE removal compared to the indigenous leg. The results would indicate that maintaining an effective bioaugmented culture requires maintaining effective substrate and oxygen deliver to the aquifer region where the bioaugmented culture was established. Unfortunately we do not have molecular analysis of the shifts in the community structure during the first year of the study to support these observations.

Table 50. Percentage Removals of 1,1,1-TCA and 1,1-DCE during Different Periods of the First Season of Field Testing Based on Wells S1 and S3

Bioaugmented East Leg	1,1,1-TCA % Removal	1,1-DCA % Removal	1,1-DCE % Removal
Well S1			
20 days	30	69	83
38 days	0	0	12
65 days	0	0	73

Indigenous West Leg	1,1,1-TCA % Removal	1,1-DCA % Removal	1,1-DCE % Removal
Well S1			
20 days	0	0	0
50 days	0	0	0
65 days	0	10	66

Bioaugmented East Leg	1,1,1-TCA % Removal		1,1-DCE % Removal
Well S3			
20 days	25	65	83
38 days	5	10	27
65 days	5	25	93

Indigenous West Leg	1,1,1-TCA % Removal		1,1-DCE % Removal
Well S3			
30 days	0	0	0
50 days	0	0	0
65 days	0	0	82

Figure 120. DO Concentration Histories at Monitoring Locations along the West (Indigenous) Leg and the East (Bioaugmented) Leg for the Period of 20 to 70 Days of Testing in the First Season

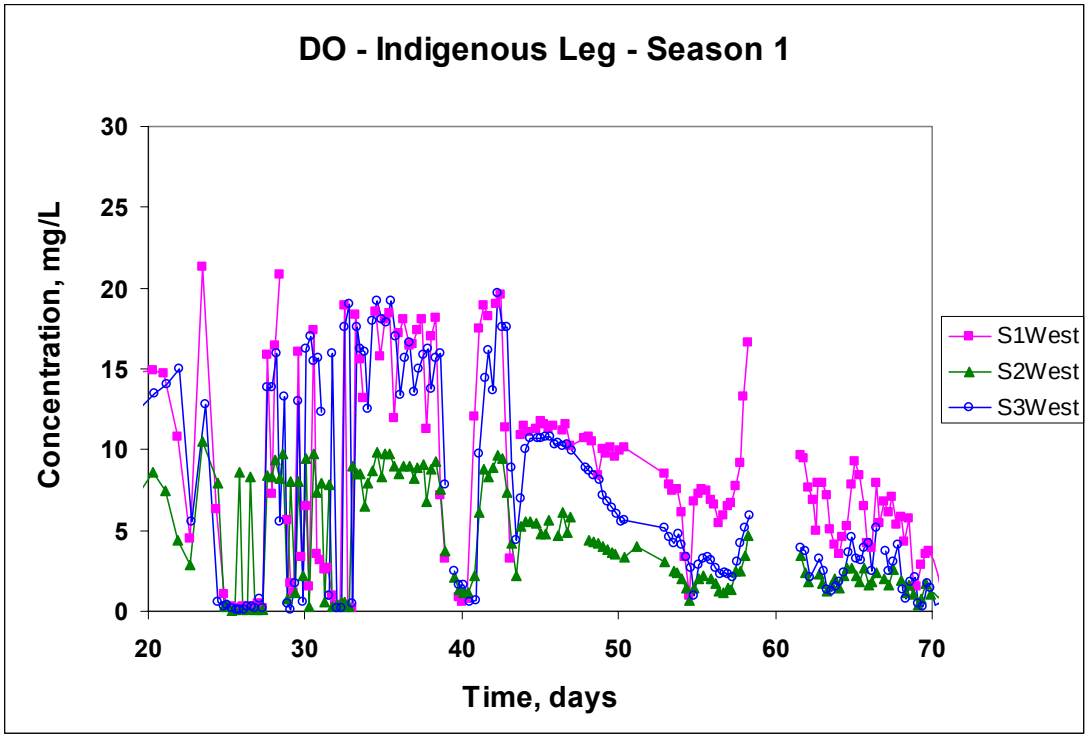

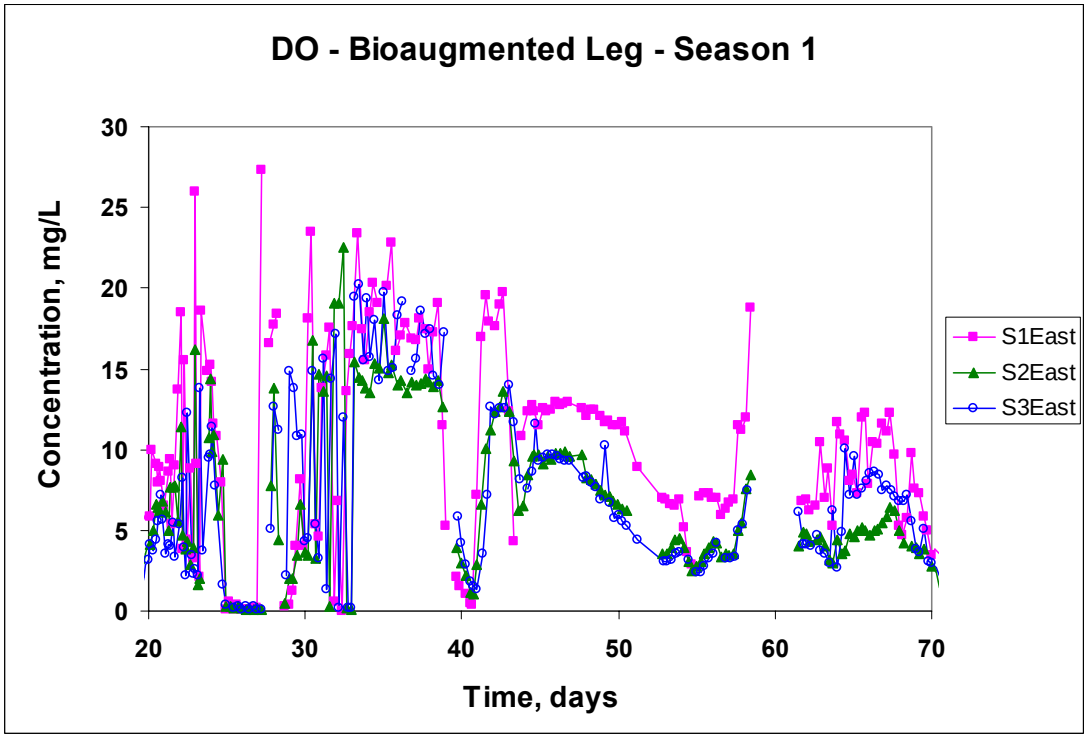

Figure 121. Butane Concentration Histories at Monitoring Locations along the West (Indigenous) Leg and the East (Bioaugmented) Leg for the Period of 20 to 70 Days of Testing in the First Season

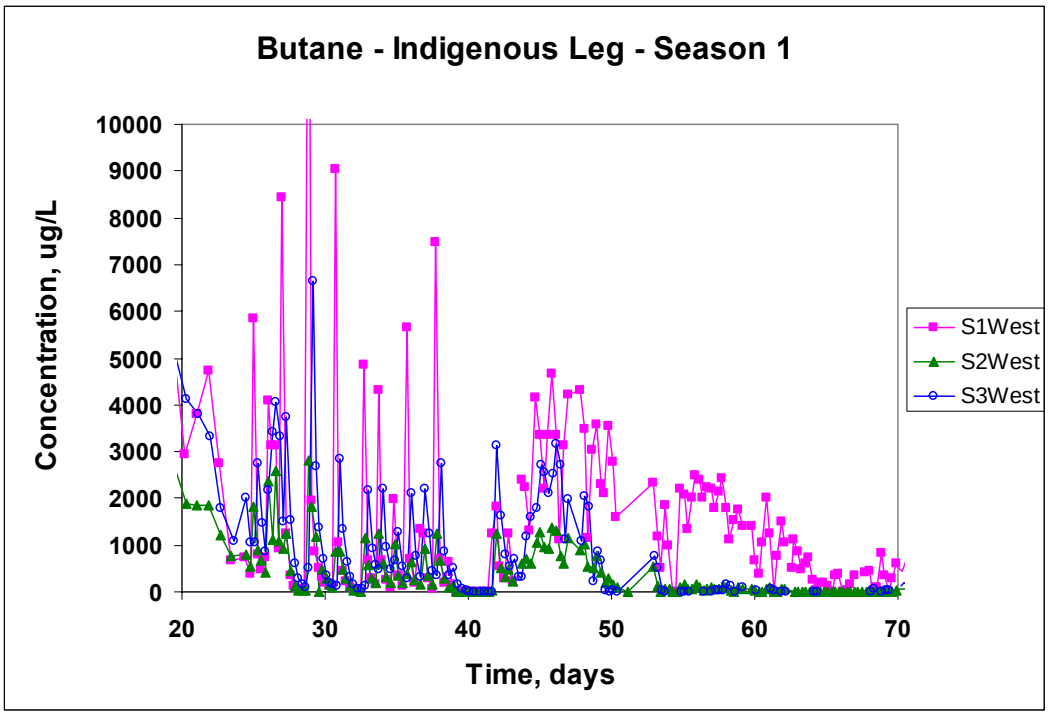

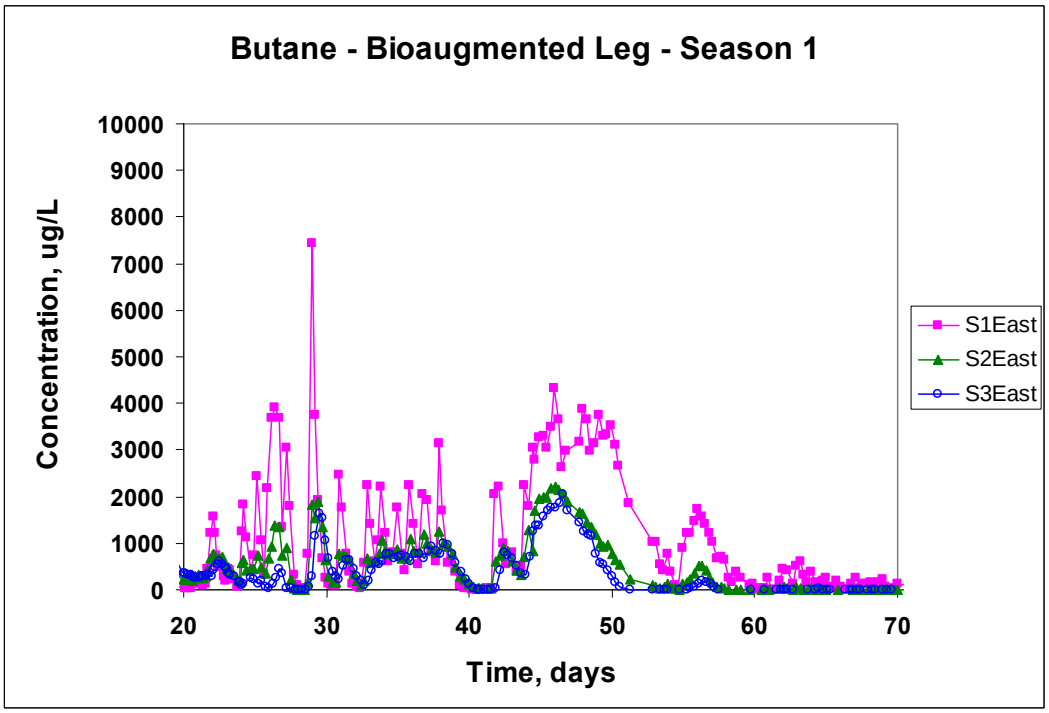

Figure 122. 1,1,1-TCA Concentration Histories at Monitoring Locations along the West (Indigenous) Leg and the East (Bioaugmented) Leg for the Period of 20 to 70 Days of Testing in the First Season

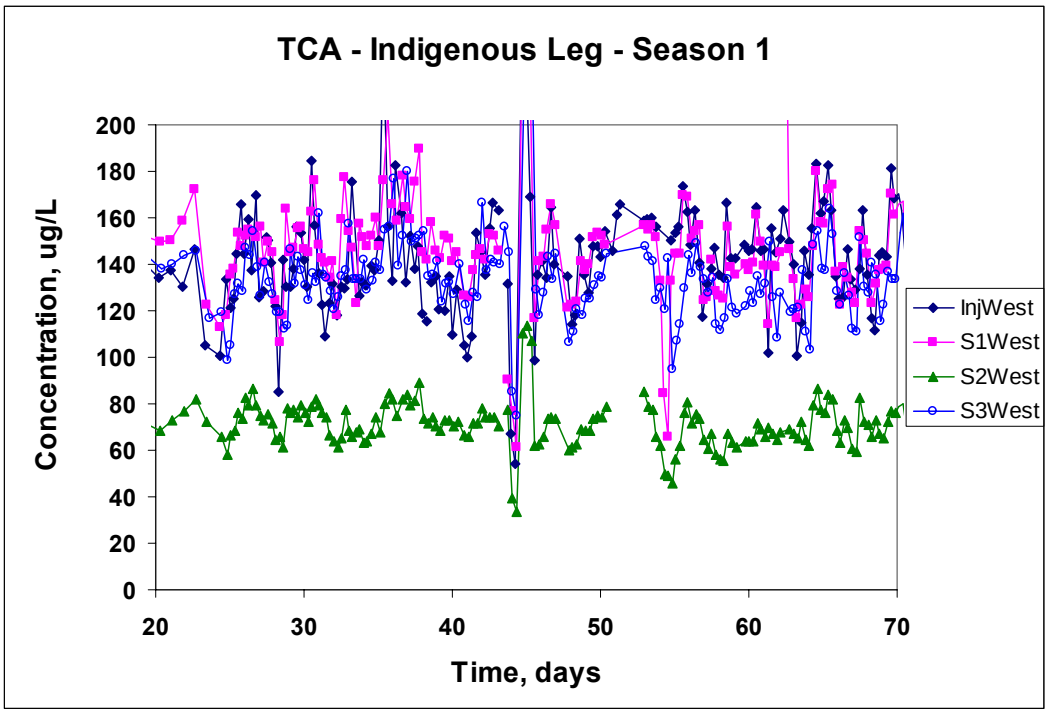

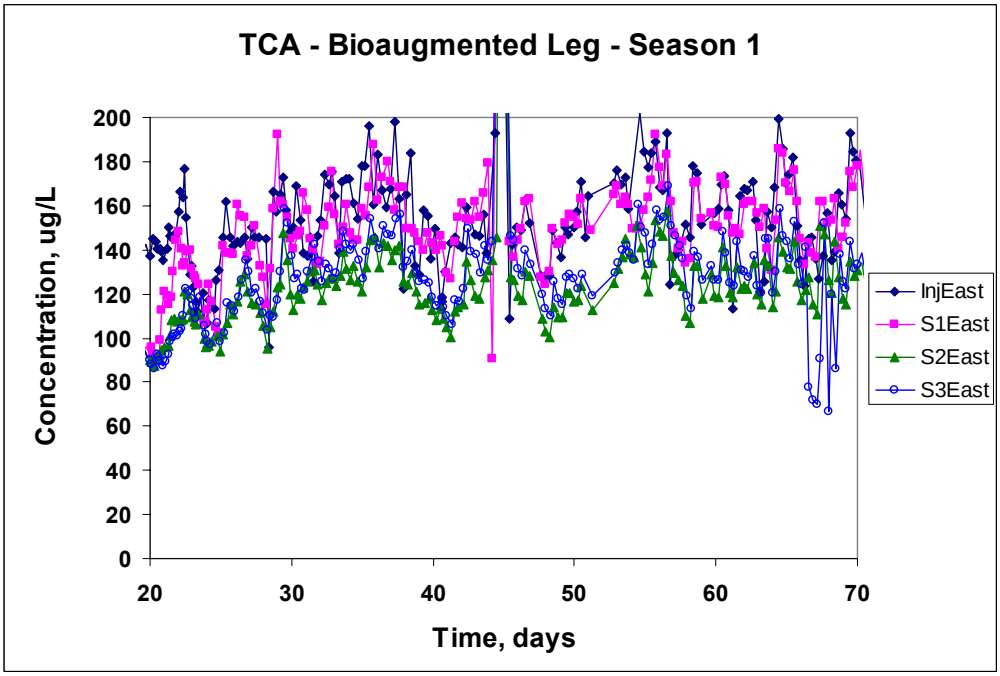

Figure 123. 1,1-DCA Concentration Histories at Monitoring Locations along the West (Indigenous) Leg and the East (Bioaugmented) Leg for the Period of 20 to 70 Days of Testing in the First Season

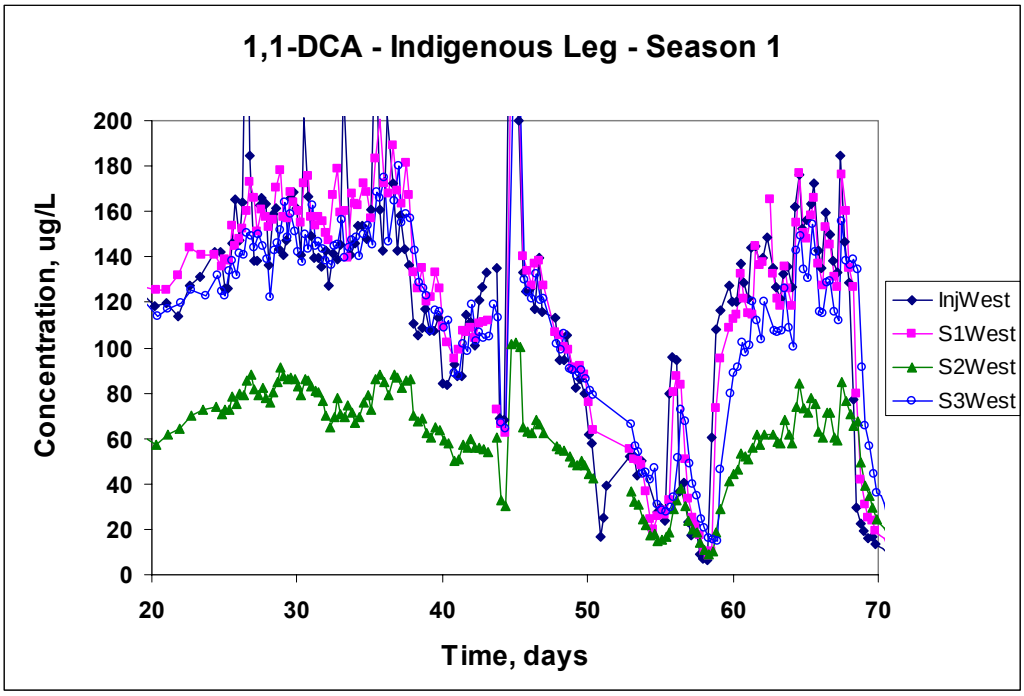

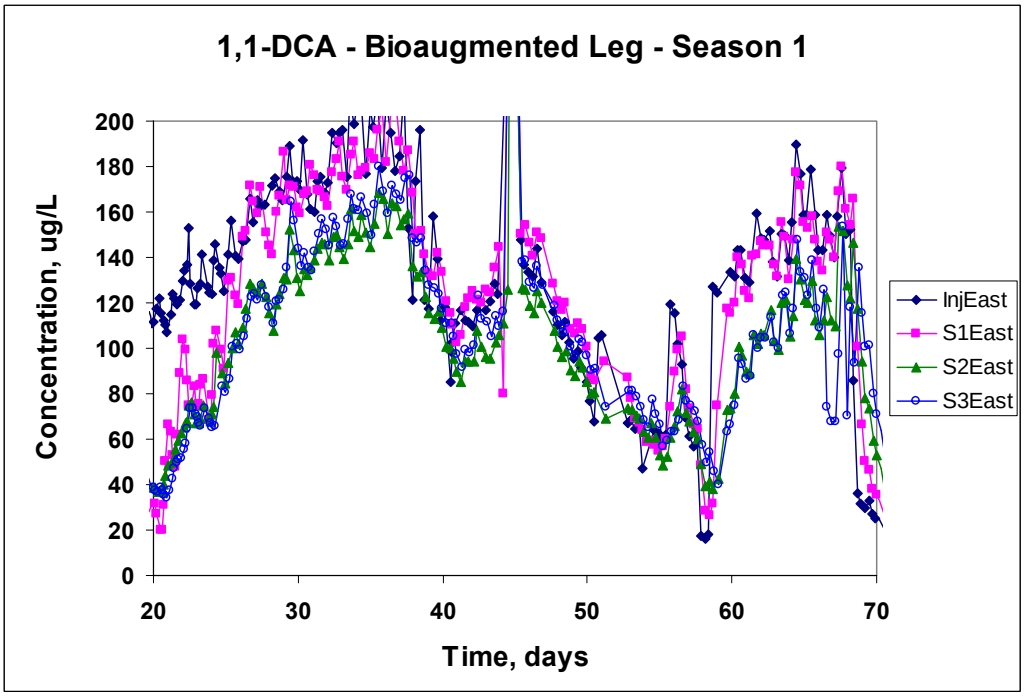

Figure 124. 1,1-DCE Concentration Histories at Monitoring Locations along the West (Indigenous) Leg and the East (Bioaugmented) Leg for the Period of 20 to 70 Days of Testing in the First Season

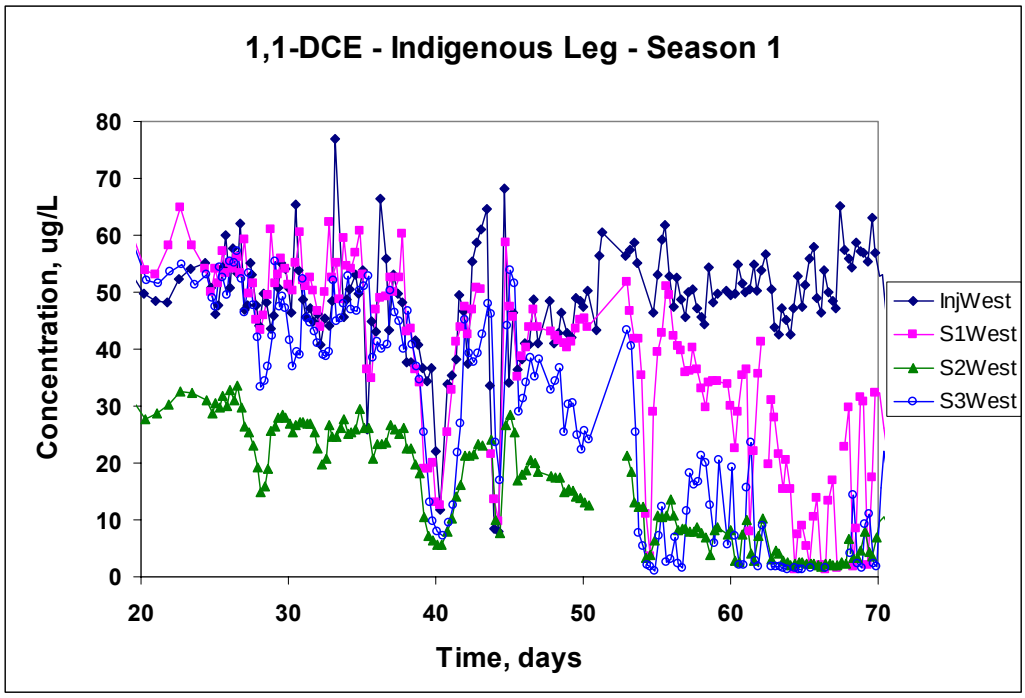

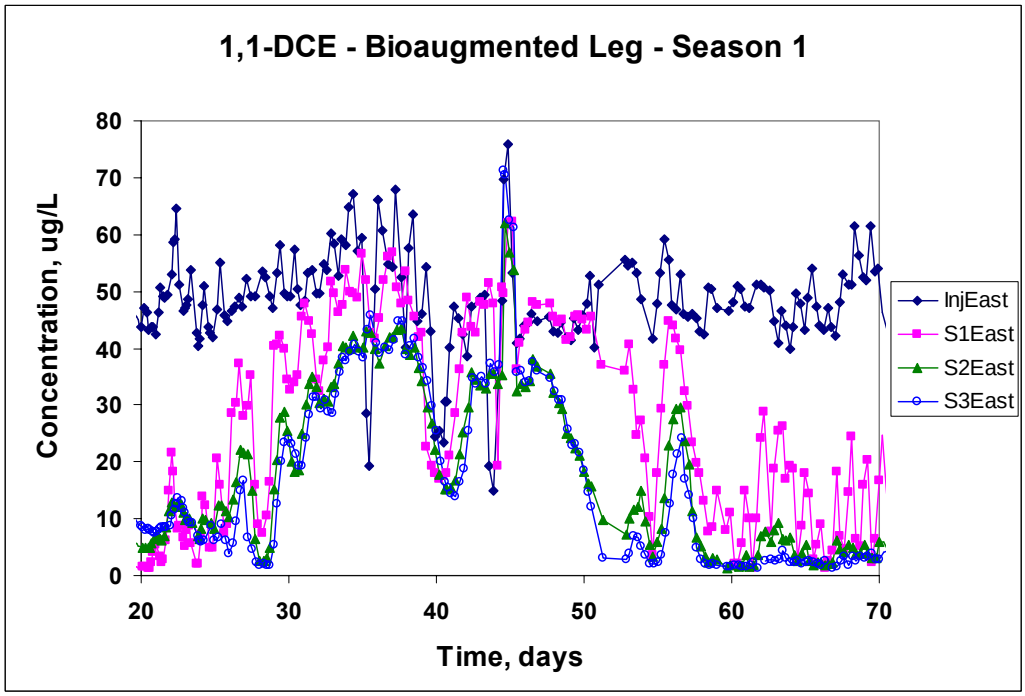

5.2. Results from the Second Season of Field Testing

The focus of the second season of field testing was to bioaugment the butane-utilizing enrichment culture containing strain 172BP and 183BP that are capable of 1,1,1-trichloroethane (1,1,1-TCA), 1,1-dichloroethene (1,1-DCE), and 1,1-dichloroethane (1,1-DCA) transformation. 1,1,1-TCA was the main contaminant of interest, since it was the contaminant that was least successfully transformed during the first season of testing. 1,1-DCE was also monitored, since it was present as a background contaminant at low concentrations in the site groundwater. The west experimental leg remained the leg where indigenous microorganisms were stimulated. It was operated using the same conditions and protocols as the bioaugmented east leg. As in the first season of testing, both experimental legs were operated under induced gradient conditions of injection and extraction. Injection rates on both legs were 1.25 L/min and extraction rates were 8 L/min.

The second season of field tests commenced in late September, 2002, about seven months after the completion of the first season of testing. During this period between seasons butane or oxygen were not added to the test legs. The following sequence of field tests were performed in both the east and west experimental legs during the second season of testing.

1) Addition of hydrogen peroxide to the test zone under induced gradient conditions to study hydrogen peroxide decomposition to dissolved oxygen (DO) in the test zone and to decrease the biomass presence near the injection well from the prior tests.
2) Addition of hydrogen peroxide and 1,1,1-TCA as a control phase of the test prior to the bioaugmentation of the culture to the east test leg and biostimulation of the west leg.
3) Bioaugmentation of the culture (east leg) in the presence of 1,1,1-TCA, butane, and oxygen.
4) Long-term biostimulation of the both test legs with butane, oxygen, and hydrogen peroxide (DO) injection to evaluate long term 1,1,1-TCA transformation.
5) Increase the amount of hydrogen peroxide and butane added to the treatment zone of both test legs to increase active biomass, to determine if more effective 1,1,1-TCA transformation could be achieved.

5.2.1 Results from the First 30 Days of Testingg

Table 51 presents the conditions of the tests during the second season of testing and represents the sequence of tests outlined above. In the second season of testing 1,1,1-TCA was the main contaminant that was studied with concentrations ranging from 100 to 140 μg/L. Hydrogen peroxide was added in concentrations ranging from 10 mg/L to 45 mg/L, while average butane concentration added ranged from 4 to 8 mg/L. Butane concentrations are estimates based on the pulse cycle times of butane and oxygen, and the butane concentrations injected.

Table 51. Injection Concentrations and Processes Studied during the Second Season of Field Testing

Duration	Chemicals Injected	Average Concentration	Process Studied
9/28-10/7/02 (0 to 8 days)	H_2O_2	10 mg/L	H_2O_2 decompostion to oxygen and disinfection
10/7-10/21/02 (9 to 23 days)	[1]H_2O_2 [2]Oxygen 1,1,1-TCA Bromide	10 mg/L 30 mg/L 115 μg/L 140 mg/L	1,1,1-TCA transport and transformation prior to bioaugmentation and butane addition
10/22-11/17/02 (23 to 40 days)	Oxygen 1,1,1-TCA Butane Bromide	30 mg/L 100 μg/L 4 mg/L 100 mg/L	Bioaugmentation, biostimulation, and biotransformation
11/17-12/5/02 (48-71 days)	Oxygen H_2O_2 1,1,1-TCA Butane	30 mg/L 15 to 45 mg/L 140 μg/L 6 to 8 mg/L	Long term biostimulation and biotransformation with H_2O_2 addition and increased butane addition

[1]added until day 17; [2]added day 17 to 23

Bromide tracer tests were also conducted on the east leg of the test site during the second season of field testing. The tests results (not shown) were used to determine the fraction breakthrough of the injection fluid at the monitoring locations. Essentially 100% breakthrough was observed at the S1 east monitoring well, while 70%, and 90% was achieved at the S2 east, and S3 east monitoring wells, respectively. Thus, these dilution estimates will be used when determining the degree of transformation observed upon biostimulation of the test zone.

Figures 125. through 128 show the DO, butane, 1,1,1-TCA, and 1,1-DCE concentrations, respectively during the first 30 days of the second season of testing, at the monitoring well locations. The west (indigenous) leg and east (bioaugmented) leg are presented together for comparison purposes. The tests were initiated with the introduction of hydrogen peroxide in order to evaluate it transformation to dissolved oxygen, and also as a means of potentially lowering the biomass present from the previous year's bioaugmentation and biostimulation tests. Hydrogen peroxide was not measured in the groundwater, however its breakdown product, dissolved oxygen, was measured. The DO concentration at the monitoring wells of the east and west legs are shown in Figure 125. Hydrogen peroxide (10 mg/L), in the absence of butane, was added during first 15 days of the test. DO concentrations of approximately 5 mg/L were observed at the monitoring wells, which is in agreement with the amount that would be stoichiometrically expected from the breakdown of H_2O_2 to ½ mole O_2 and a mole of H_2O. The results indicated the hydrogen peroxide decomposes to oxygen by the time of transport to the first monitoring well, S1. Both experimental legs show nearly identical results. Hydrogen peroxide was also added during the period that 1,1,1-TCA was injected, prior to oxygen or butane addition. As will be discussed, the presence of hydrogen peroxide did not cause any observable transformation of 1,1,1-TCA.

The change from the addition of hydrogen peroxide to the addition of dissolved oxygen (DO) occurred around day 17. DO additions were started on day 17, so that bioaugmentation would occur in the presence of DO, and not hydrogen peroxide. This was done to prevent hydrogen peroxide from harming the culture. The breakthrough of the dissolved oxygen to higher concentrations around day 20 was observed in both experimental legs. Consistent with the results of the bromide tracer tests, dissolved oxygen breakthrough to a lower concentration at the S2 east well was a result of dilution by native groundwater. DO is also observed to breakthrough to lower concentration, at the S2 west well, which is consistent with 1,1,1-TCA breakthrough concentrations, as well as tracer tests performed on the west leg during the third season of field testing. The DO concentration decreases observed after about 25 days resulted from the biostimulation of the test zone due to butane addition.

Bioaugmentation of the test leg was started on day 23. The butane culture was grown at Oregon State University as previously described and shipped overnight in media to Stanford University. Three grams each of the two cultures, stain 172 BP and 183 BP, were each delivered to the field site. They were diluted into 48 liters of site groundwater and injected over a period of several hours into the east leg injection well. The injection rate was maintained at 1.25 L/min, the same rate of injection that was used in the field tests.

Butane concentrations for both the west (indigenous) leg and the east (bioaugmented) leg are shown in Figure 126. Butane addition was started on day 22 just prior to the bioaugmentation of the test zone on day 23. Butane was observed to breakthrough to a maximum of about 4 mg/L in the west leg, and about 3 mg/L in the east leg. The lesser degree of breakthrough in the east leg, likely results from the bioaugmentation of microorganisms on day 23. Butane concentrations decrease to below detection by day 25, in the bioaugmented east leg, and day 26 in the indigenous west leg. It is also interesting to note that butane increased to over 3 mg/L in the S3 west leg, while concentration never increased above 1 mg/L in the east leg. The more rapid consumption of butane in the east leg likely resulted from the bioaugmentation of the test leg. It is interesting to note that butane is also rapidly consumed in the indigenous west leg. This is in comparison to the much longer period required during the first season of field testing, as discussed in Section 5.1. The results indicate that a greater biomass of butane-utilizing organisms were present at the start of the second season of testing. A significant number of butane utilizers survived the extended period of starvation of seven months when neither butane nor oxygen was fed to the test zone. Also, the addition of hydrogen peroxide at the beginning of the experiment did not appear to disinfect the test leg.

Figure 125. Dissolved Oxygen Concentrations in the West (Indigenous) Leg and the East (Bioaugmented) Leg during the First 30 days of the Second Season of Field Testing

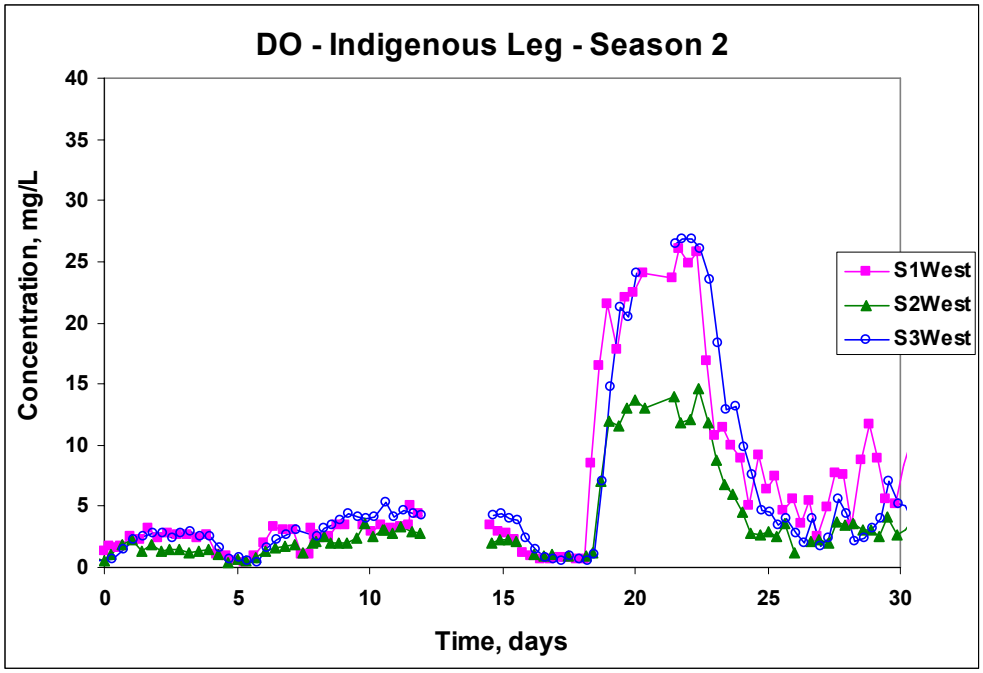

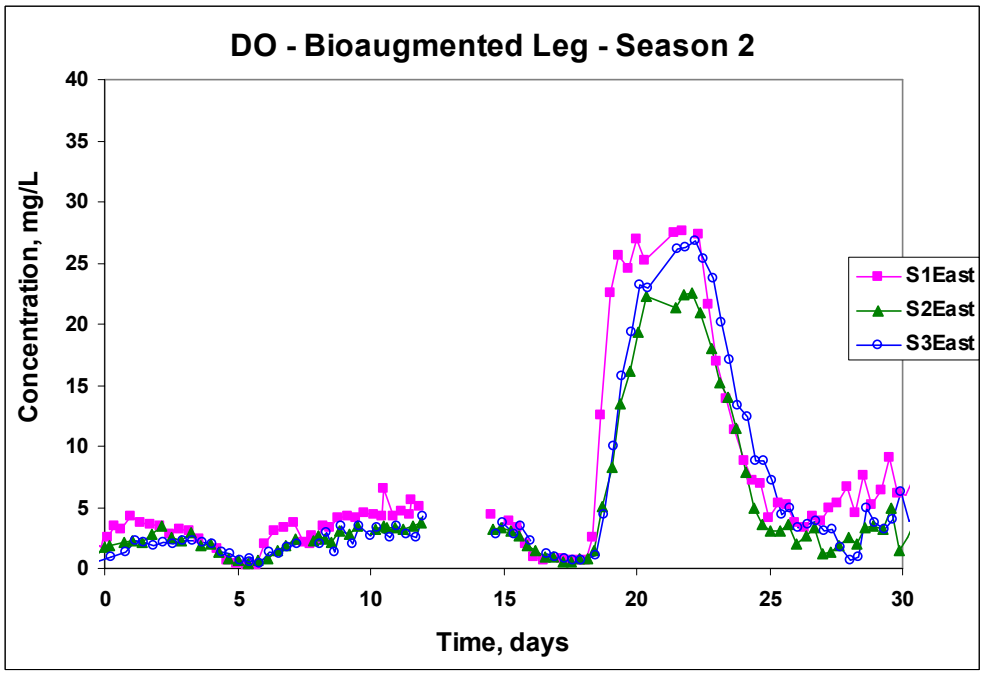

Figure 126. Butane Concentrations in the West (Indigenous) Leg and the East (Bioaugmented) Leg during the First 30 days of the Second Season of Field Testing

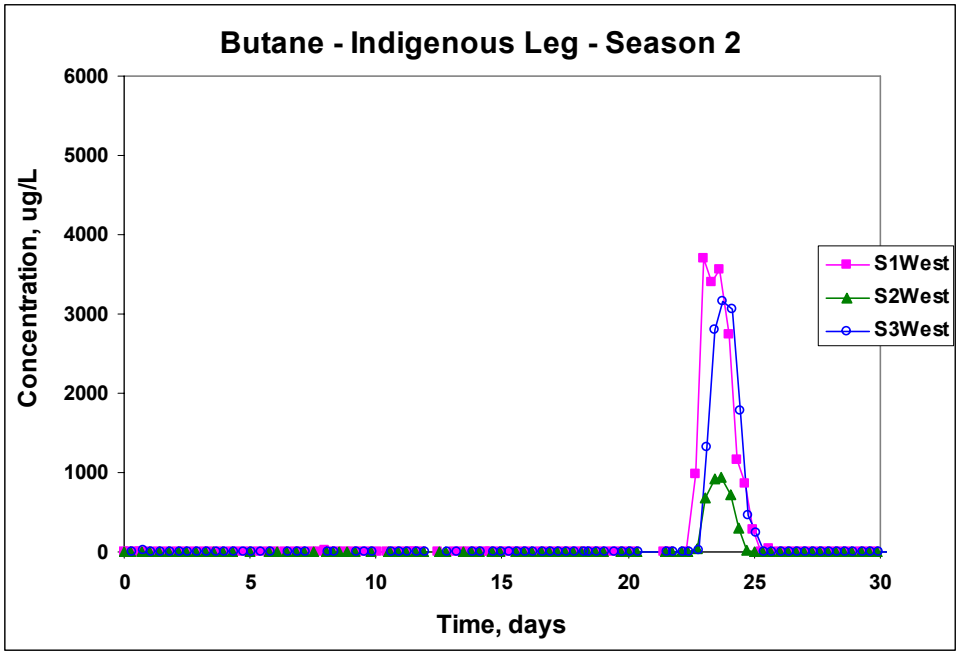

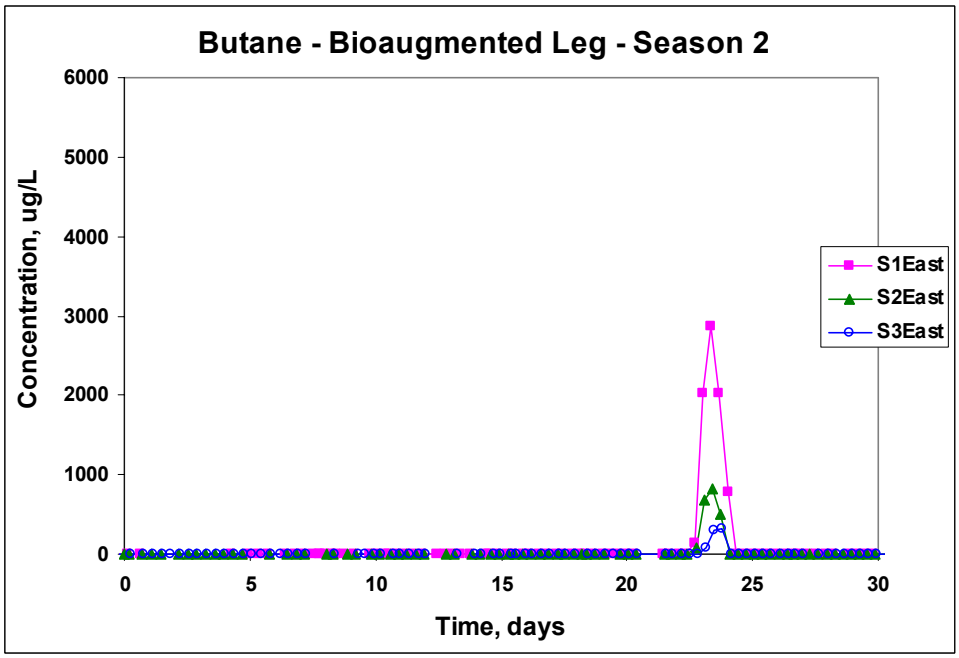

Figure 127. 1,1,1-TCA Concentrations in the West (Indigenous) Leg and the East (Bioaugmented) Leg during the First 30 days of the Second Season of Field Testing

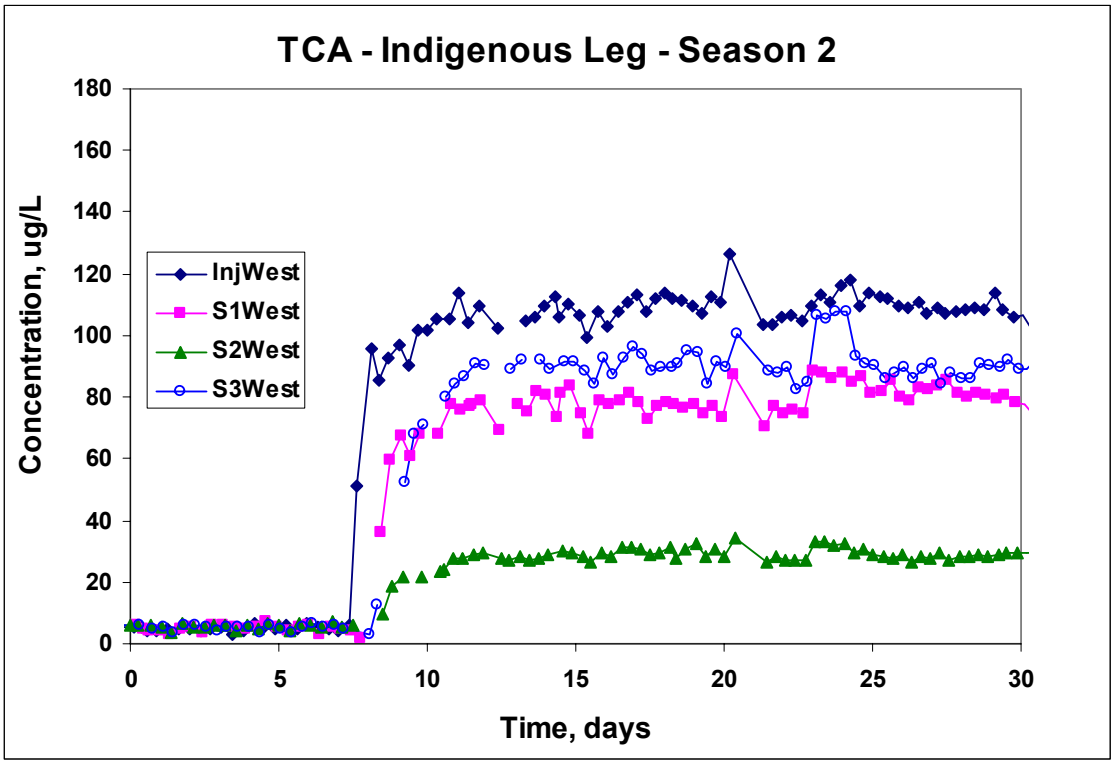

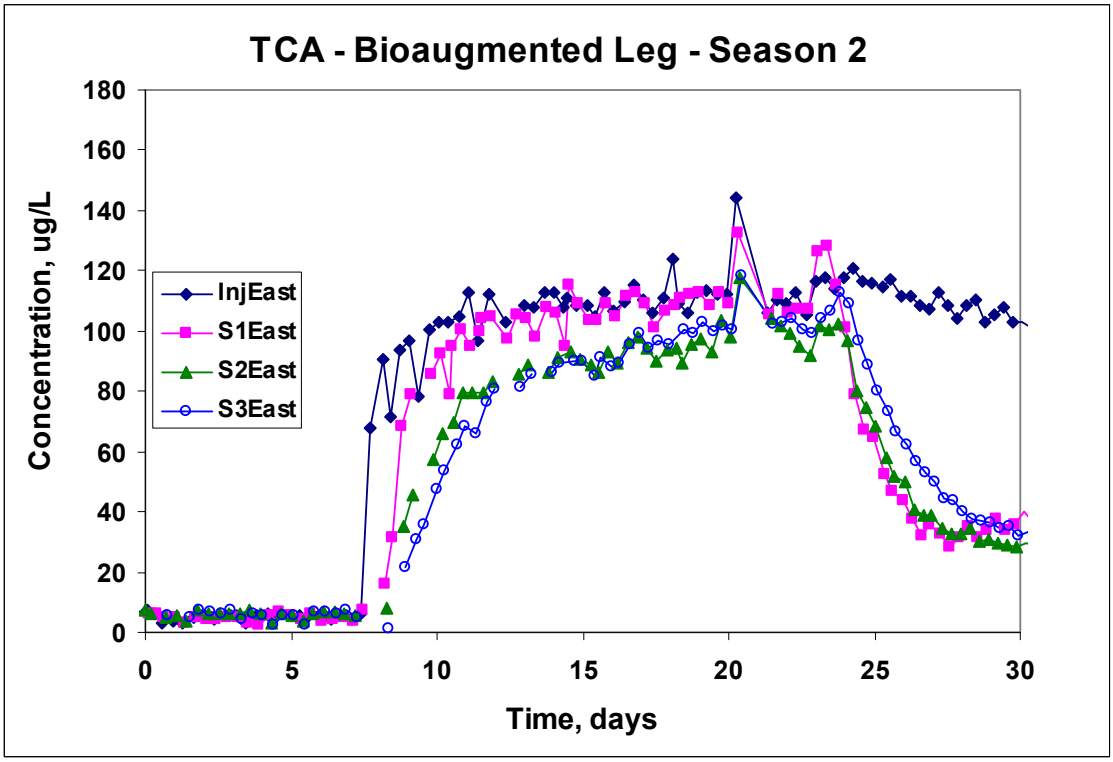

Figure 128. 1,1-DCE Concentrations in the West (Indigenous) Leg and the East (Bioaugmented) Leg during the First 30 days of the Second Season of Field Testing

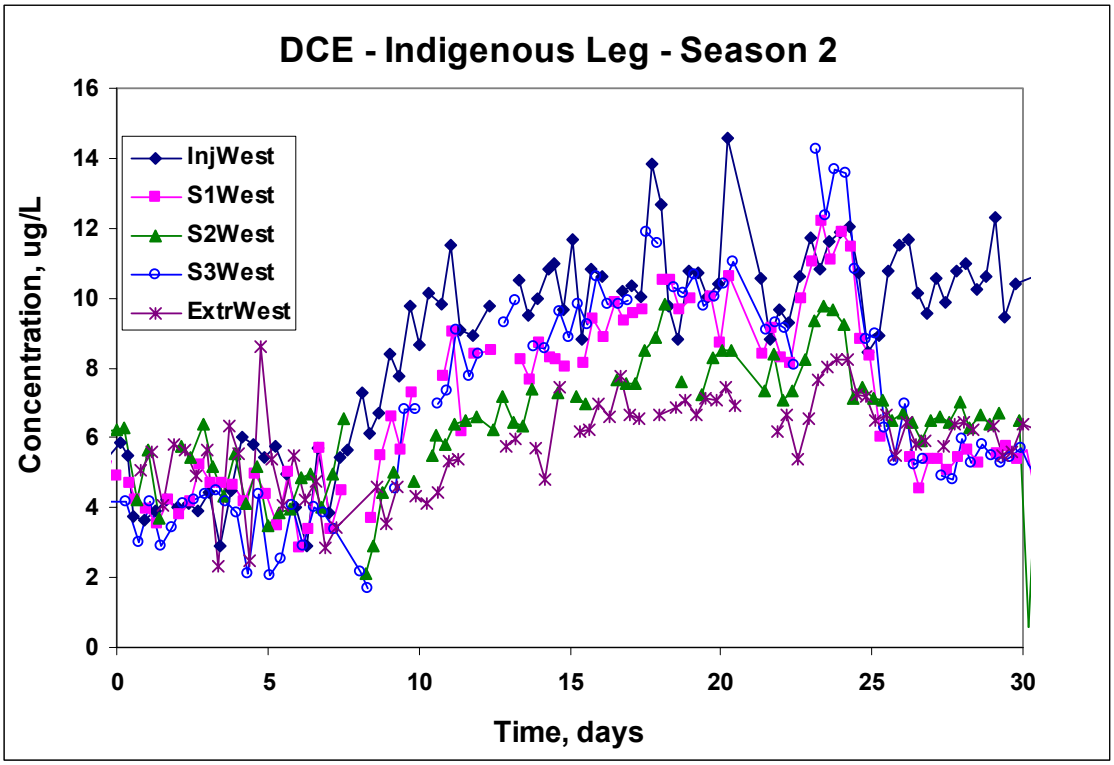

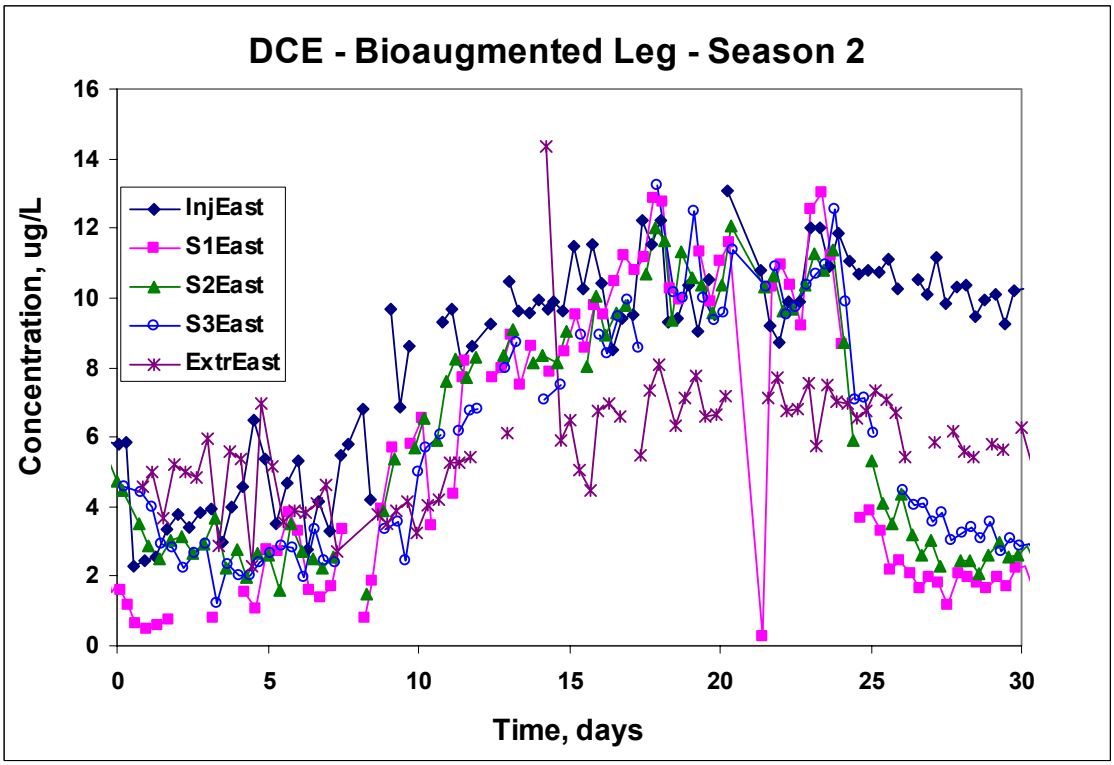

The temporal response of 1,1,1-TCA at the monitoring wells is shown in Figure 127. 1,1,1-TCA addition to the test zone was started around day 8, in the presence of hydrogen peroxide. The sequential breakthrough of 1,1,1-TCA at the monitoring locations is shown. Retardation in 1,1,1-TCA transport is consistent with the results of the first season of field testing. Prior to biostimulation, 1,1,1-TCA breakthrough to concentrations indicate essentially no transformation prior to bioaugmentation or butane addition. In the east leg the maximum concentrations were observed after about 20 days. The S1 west well breakthrough to the injection concentration, and maintains this concentration until the tests zone was biostimulated. The 80% and 90% breakthrough of 1,1,1-TCA at the S2 and S3 west monitoring wells is consistent with the results of bromide tracer tests, and result from dilution by the native groundwater. In the west leg 1,1,1-TCA never reaches injection concentrations at any of the observation locations. The greatest fractional breakthrough was about 85% at the S3 monitoring well, while the lowest degree of breakthrough was about 32 %, at the S2 monitoring well. The S1 well has a breakthrough concentration of about 80%. The lower breakthrough along this leg results from dilution by the native groundwater and not transformation. Unfortunately bromide tracer test data was not collected on the west leg during this period of the test for comparison purposes. However, the lack of complete breakthrough of DO at the S3 well on the west leg, is consistent with dilution by native groundwater. Also bromide tracer tests conducted on the west leg during the third season of field testing show groundwater dilution similar to the extents indicated here.

The concentrations of 1,1,1-TCA decreased in the west Experimental leg in response to bioaugmentation and biostimulation of the test zone. The concentration began to rapidly decrease around 24 days, coinciding with decreases in oxygen and butane concentrations in response to bioaugmentation and biostimulation of the test zone. The concentrations decreased most rapidly at the S1 well and most of the biotransformation was observed by transport to the S1 well. Butane is also observed to be completely removed by the S1 well indicating that most of the biological activity is within 1 meter of the injection well. Despite the uptake of butane and dissolved oxygen, 1,1,1-TCA concentrations did not decrease in the indigenous west leg. The concentration remained constant at all the observation locations. The results indicate that the indigenous butane-utilizers were not transforming 1,1,1-TCA.

Figure 128 presents 1,1-DCE concentrations in the test zone. 1,1-DCE was present as a background contaminant in the field at a concentration of about 6 μg/L. For example as shown in Figure 128 1,1-DCE was present at all the monitoring locations at early time, during the period when CAHs were not being added to the test legs. 1,1-DCE also present in the extracted groundwater that is used to make up the injected groundwater. When 1,1-TCA addition was started, around day 8, 1,1-DCE concentrations also increased in the injected fluid and also increased at the monitoring locations. 1,1-DCE was therefore present in the 1,1,1-TCA stock solution that was being added at the site. As observed in the 1,1,1-TCA addition tests, concentrations more closely approached the injection concentration along the east leg. With bioaugmentation and biostimulation of the east leg the concentration of 1,1-DCE decreased significantly from the injection concentration. Consistent with the 1,1,1-TCA observation the concentration decreased most rapidly in at the S1 east well, and more slowly in the S3 east well. The 1,1-DCE concentrations were reduced from 10 μg/L to about 2 μg/L 30 days into the test. 1,1-DCE concentrations were also observed to decrease in the indigenous west leg from 10 mg/L to about 6 μg/L, indicating some transformation of 1,1-DCE was occurring. Like observed in the

east leg, most of the transformation was observed within the first meter of transport through the test legs. The results are consistent with the results from the first season of testing, that indicated 1,1-DCE could be also transformed during transport through the west leg of indigenous butane utilizers, as well as by the east leg that had been bioaugmented. More effective 1,1-DCE removal, however, was achieved in the bioaugmented east leg.

5.2.2 Results from Days 30 to 70

Figure 129 through 132 present the temporal responses for the complete 70 days of the test. During the period from 30 to 70 days, changes in operating conditions were made to try to improve the amount of transformation achieved. In addition performance of the system over a period of about 2 months of operation was assessed. The DO concentration history indicates some of the operating condition changes that were made and also provides some insight to conditions that affect the performance of the system. During the first 40 days of the test, DO was injected with no addition of hydrogen peroxide. At around 32 day, the dissolved oxygen concentration decreased to below the detection limit (0.2 mg/L) in both experimental legs. The reason for these low DO concentrations is not completely know, but may have resulted from the increase in biomass in the experimental legs, resulting in more DO consumption. Lower DO injection concentrations were also observed during this period. Around 32 day, butane was also detected at monitoring wells in both experimental legs, as shown in Figure 130. Concentrations were typically below 1 mg/L, but there are several observations above 2 mg/L. The 1,1,1-TCA and 1,1-DCE concentrations (Figure 131 and 132) also increased in the east leg during this period when DO concentrations were low, and butane concentrations increased. The results show the transformation of 1,1,1-TCA and 1,1-DCE were correlated with DO concentrations and butane concentrations. This likely results from two factors, the transformation process being aerobic and requiring oxygen, and the strong inhibition the presence of butane has on the transformation process. The low DO and increase in butane does not result in an increase in 1,1,1-TCA in the west leg, and increases in 1,1-DCE are difficult to quantify. During the period of 38 to 45 days, DO measurements were lost, due to a malfunctioning DO probe. During this period butane was however effectively removed in experimental legs, and 1,1,1-TCA and 1,1-DCE transformation continued.

During the period from 40 to 70 days, hydrogen peroxide addition was started and DO addition was continued. Hydrogen peroxide was initially added at 5 mg/L from day 40 to day 48, and was increased to: 15 mg/L over the period of 48 to 52 days; 30 mg/L from 52 to 60 days; and to 45 mg/L at 60 days. In response to increases in the concentration of hydrogen peroxide added, the length of the butane pulse cycle was also increased, to delivery more butane to the tests legs. The addition of hydrogen peroxide resulted in sufficient DO to be observed in both experimental legs over the period of 48 to 68 days. The lower values observed in the S3 west well, result from dilution by the native groundwater, as previously observed with 1,1,1-TCA and DO. A period of breakthrough of butane was observed around 68 day in both experimental legs, however, these observations are not correlated with low DO values, and were likely caused by a malfunction in the butane delivery system.

Figure 129. Dissolved Oxygen Concentrations in the West (Indigenous) Leg and the East (Bioaugmented) Leg during the Complete 70 Days of the Second Season of Field Testing

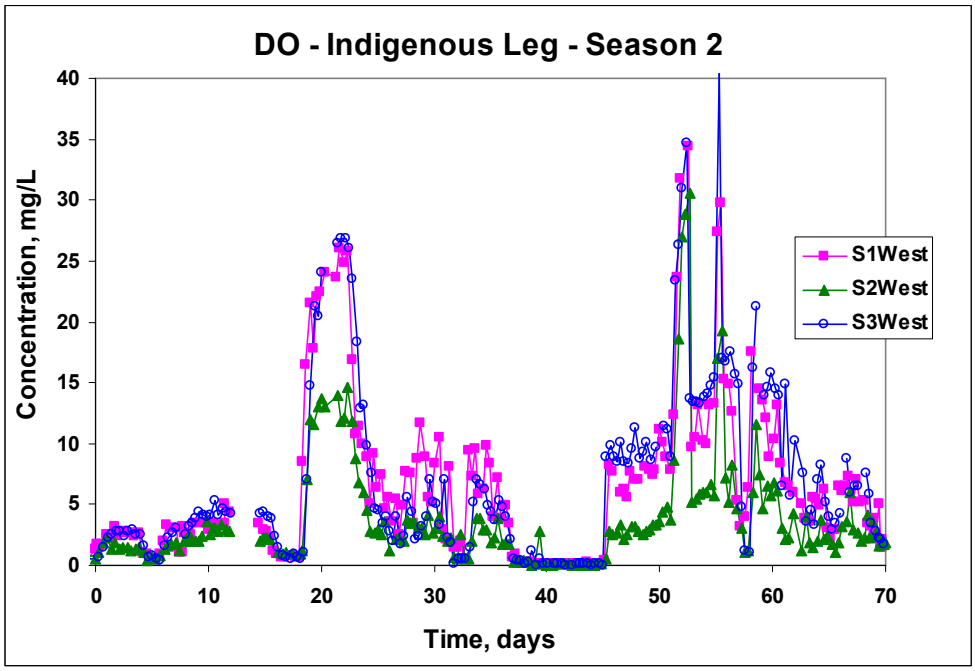

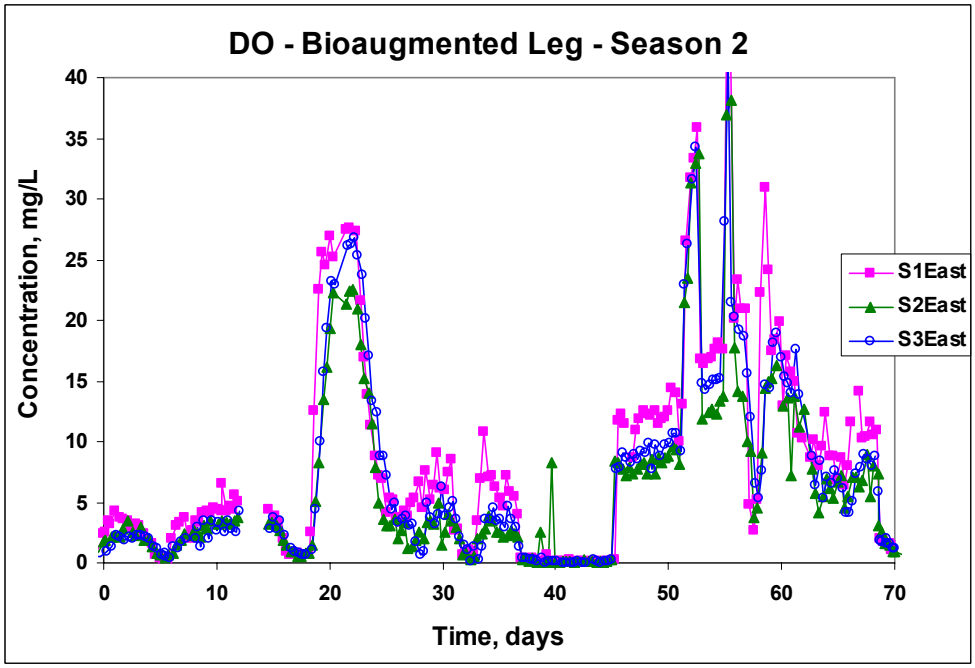

Figure 130. Butane Concentrations in the West (Indigenous) Leg and the East (Bioaugmented) Leg during the Complete 70 Days of the Second Season of Field Testing

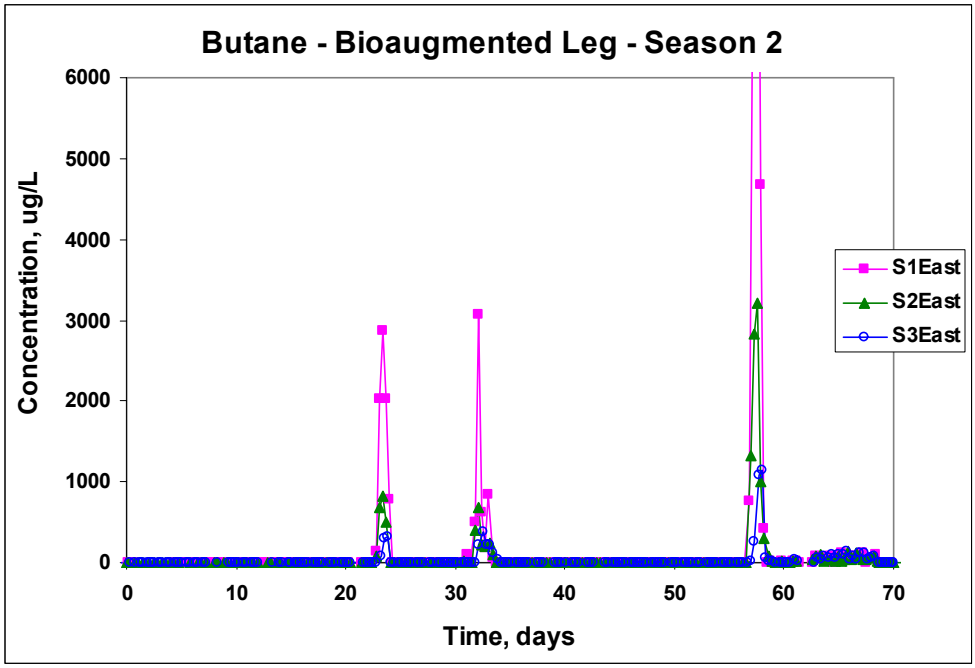

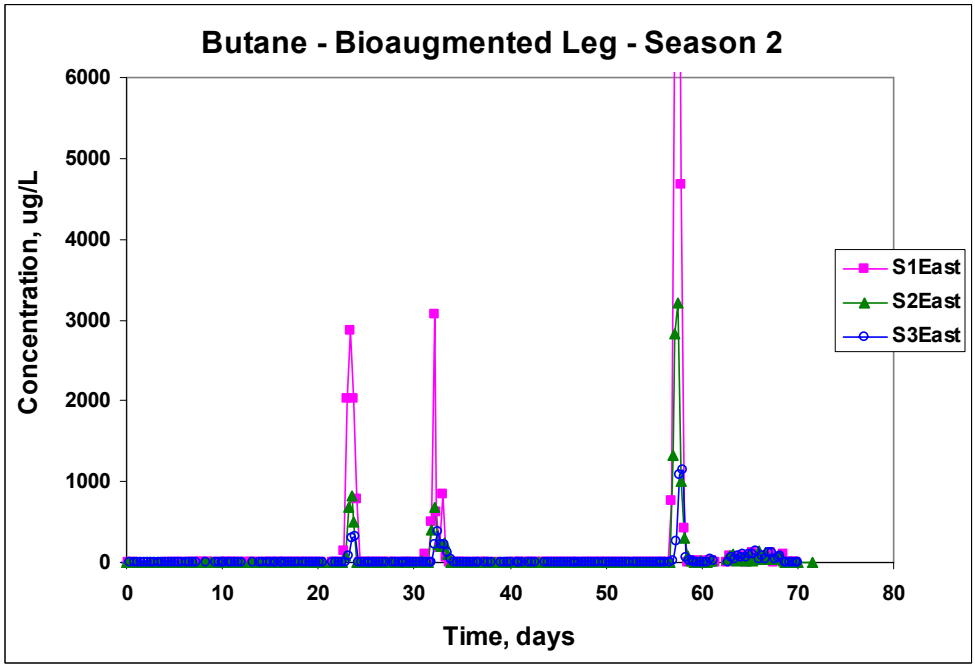

Figure 131. 1,1,1-TCA Concentrations in the West (Indigenous) Leg and the East (Bioaugmented) Leg during the Complete 70 Days of the Second Season of Field Testing

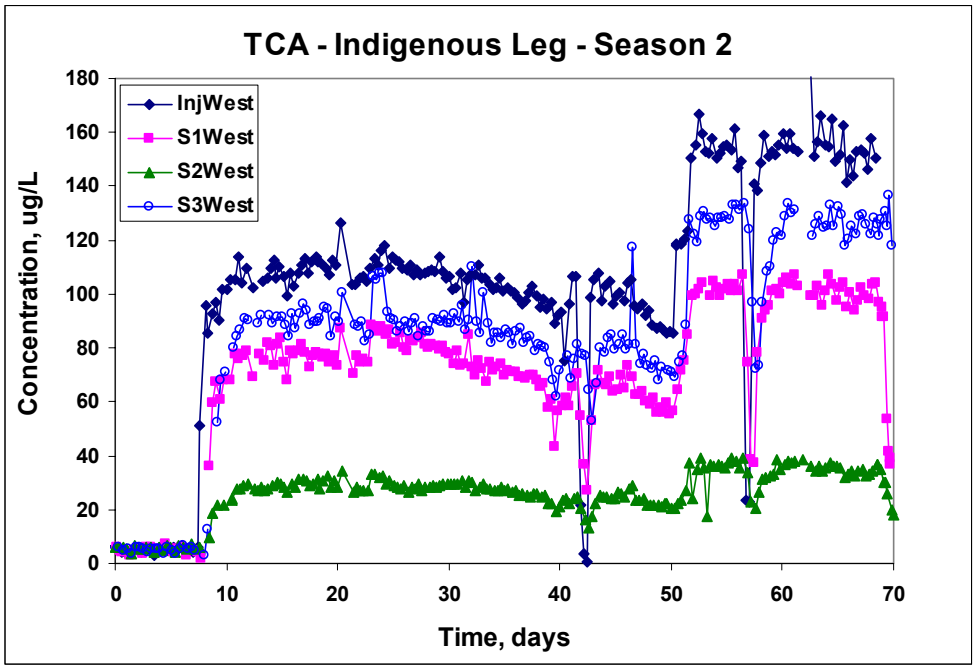

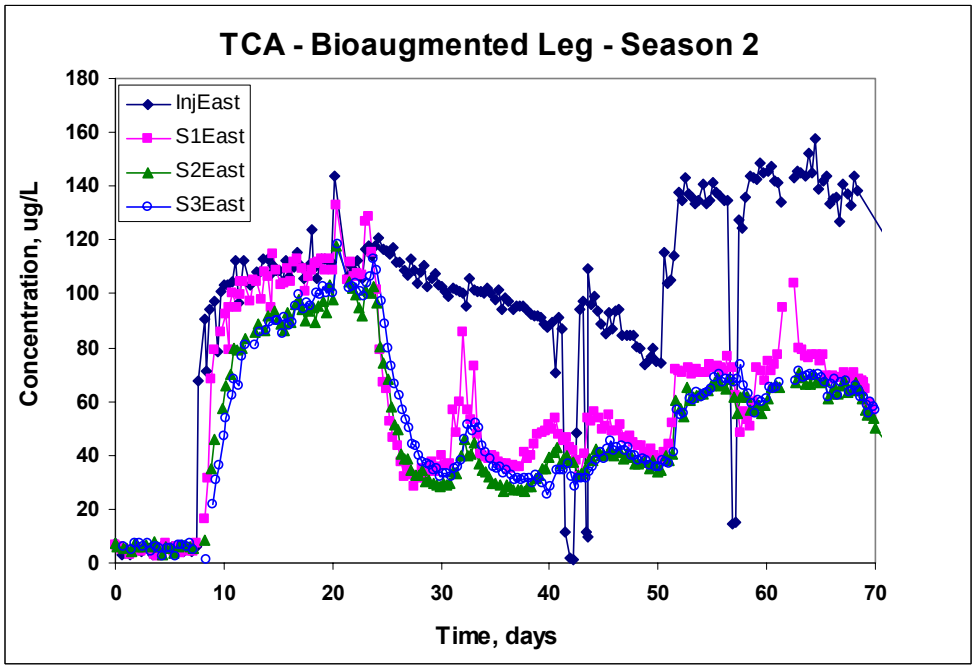

Figure 132. 1,1-DCE Concentrations in the West (Indigenous) Leg and the East (Bioaugmented) Leg during the Complete 70 Days of the Second Season of Field Testing

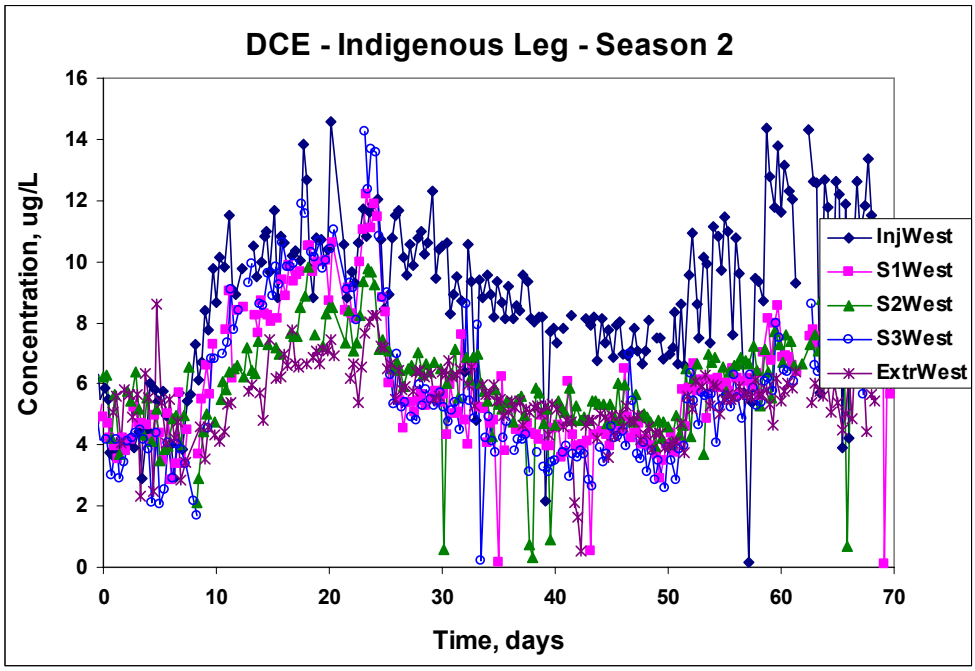

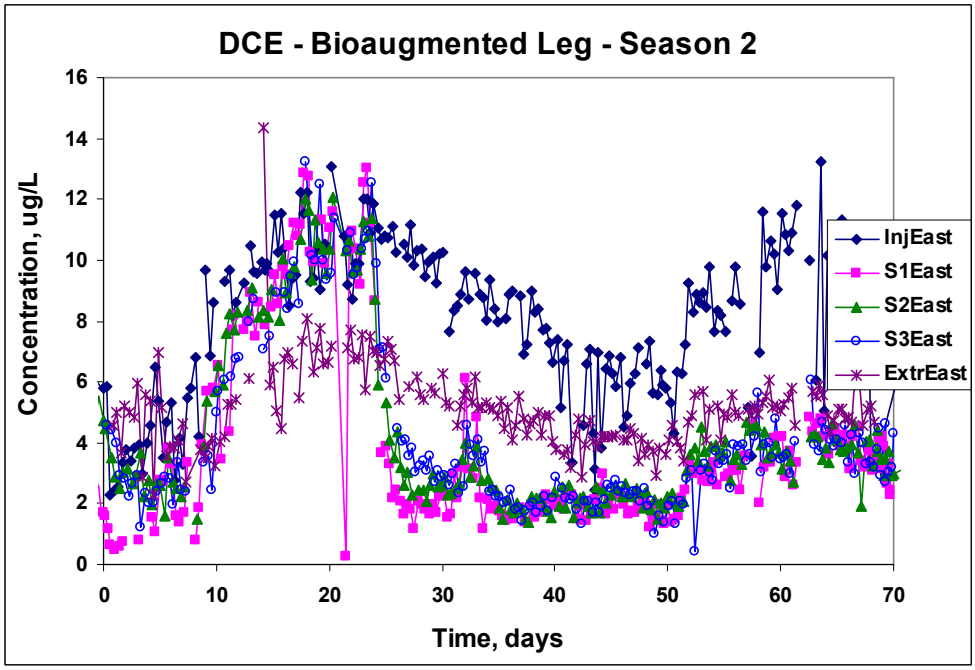

During the period of 30 days to 50 days the injection concentration of 1,1,1-TCA gradually decreased from 120 μg/L to 80 μg/L, while the 1,1,1-TCA concentrations at the monitoring locations remained constant, or increased slightly. The addition of hydrogen peroxide and increase in the butane pulse cycle to deliver more butane did not result in more effective 1,1,1-TCA transformation in the east leg. During this period, 1,1,1-TCA concentrations gradually decreased in the west leg, in response to the decrease in the injection concentrations. 1,1-DCE also remained relatively constant in the east leg, where it was being more effectively transformed, while the decreased in the west leg in response to the decrease in the injection concentration.

During the period of 52 to 68 days, the injection concentration of 1,1,1-TCA was increased to 145 μg/L in the east leg, and about 160 μg/L in the west leg. 1,1-DCE as a co-contaminant in the 1,1,1-TCA also increased in the injected groundwater. In response to the increase in the injection concentration, the concentrations of 1,1,1-TCA also increased at the monitoring locations in both the east and west experimental legs. As will be discussed the percentage removal remained relatively unchanged in the east leg, and the increases observed in the west leg are consistent with little or no transformation of 1,1,1-TCA. Similarly the percentage removals of 1,1-DCE remained relatively unchanged in both experimental legs.

5.2.3. Percentage Removals of 1,1,1-TCA and 1,1-DCE Achieved

The percentage removal of 1,1,1-TCA and 1,1-DCE were estimated for the different periods of the tests based on the average injection concentrations and the measured concentrations at the S3 monitoring wells. The results are presented in Table 52. The values were corrected for dilution by the native groundwater, based on the results of bromide tracer tests on the east leg and the concentration observed of 1,1,1-TCA observed in the west leg prior to biostimulation through butane addition. The estimates indicate that the best removals of both 1,1,1-TCA and 1,1-DCE, 80 % and 83 %, respectively, were observed on the east leg soon after bioaugmentation, around 30 to 35 days. The percentage removal efficiency decreased over the course of the experiment in the east leg to about 56 and 60 percent respectively. The removal efficiency remained about the same at the lower 1,1,1-TCA and 1,1-DCE injection concentrations, of 80 μg/L and 6 μg/L, respectively, at 50 days, as was observed at the higher injection concentrations of 140 μg/L and 10 μg/L, respectively. The west indigenous leg showed no measurable amount of 1,1,1-TCA removal, and about 40 % removal of 1,1-DCE. The addition of hydrogen peroxide and more butane in the latter stages of the test did not result in more effective transformation of 1,1,1-TCA or 1,1-DCE.

Table 52. Percentage Removals of 1,1,1-TCA and 1,1-DCE during Different Periods of the Second Season of Field Testing

Bioaugmented East Leg	1,1,1-TCA % Removal	1,1-DCE % Removal	**Indigenous West Leg**	1,1,1-TCA % Removal	1,1-DCE % Removal
30 days	70	83	30 days	0	43
50 days	52	66	50 days	0	48
65 days	56	60	65 days	0	38

Unfortunately no microbial samples were successfully analyzed from the second season of field testing. Problems were encountered with the method of fixing the groundwater samples prior to DNA extraction. The method of extracting and preserving DNA was corrected prior to the start of the third season of field testing.

5.2.4. Summary of Results from the Second Season of Field Testing

The second season of field testing demonstrated that 1,1,1-TCA could be transformed in the bioaugmented east leg, while transformation was not achieved in the west leg that was not bioaugmented. The consumption of dissolved oxygen and butane was comparable in the bioagumented and indigenous legs, thus the lack of 1,1,1-TCA in the indigenous leg could not be attributed to ineffective butane utilization. The results indicated that bioaugmentation did contribute to more effective transformation of both 1,1,1-TCA and 1,1-DCE. In addition transformation of 1,1,1-TCA and 1,1-DCE was maintained for a period of about 50 days, after bioaugmentation and biostimulation. This compares to the results of the first year of testing, where over a similar period of operation, 1,1,1-TCA transformation ability was lost. One difference between the first and second seasons of testing, is that 1,1-DCE concentration was much lower in the second season, and thus less transformation toxicity or inhibition, may have resulted. Also in the second season of testing, better efforts were made to maintain dissolved oxygen and butane concentrations in the injected groundwater. Consistent with the first season of testing, 1,1-DCE was transformed in both experimental legs, with more effective removal achieved in the bioaugmented leg.

Transformation was maintained when hydrogen peroxide was added to the test legs as a source of dissolved oxygen. Thus hydrogen peroxide did not prove to be toxic to the butane utilizers. Efforts to add more butane to the test legs did not result in more effective transformation of 1,1,1-TCA and 1,1-DCE. The reason why more effective transformation was not achieved is not known, but might be attributed to butane inhibition.

An interesting observation, is that the 1,1,1-TCA removal achieved in the field experiment was similar to that achieved in the continuous flow column study that was performed, as discussed in Section 4.8. Both tests showed that in the absence of 1,1-DCE transformation, 1,1,1-TCA could be maintained for a period of several months. In the continuous flow column the best percentage removal of around 80 % was achieved soon after bioaugmentation, and the removal decreased to about 60 % with time.

Unfortunately efforts to characterize the microbial community failed during the second season of testing. Thus direct observations of community structure and the survival of the bioaugmented microorganisms in the bioaugmented leg can not directly linked to the better transformation performance in that leg. Efforts to track better the augmented culture and to observe shifts in the microbial community, were addressed in the third season of field testing.

5.3 The Third Season of Field Testing

The third season of field bioaugmentation events commenced in late May 2003, approximately 170 days after Year Two tests were completed, during which time no amendments were added to the field. The following series of bioaugmentation events and test conditions were investigated.

1) Butane and oxygen cycle times were varied along with peroxide and nutrient amendment during the first bioaugmentation event with TCA, and later, DCA added to the field.
2) Butane addition was interrupted to determine the effect on CAH transformation.
3) Bioaugmentation of fresh inoculum after losing CAH transformation efficiency from the initial bioaugmentation under continuing field operation conditions
4) Addition of a bleach solution to both well legs to reduce the population of stimulated butane utilizers before the second bioaugmentation event.
5) Microbial characterization of groundwater samples taken over the course of the test from the first monitoring wells 0.5 m from the injection wells using T-RFLP for microbial community analysis and real time PCR for the enumeration of one of the bioaugmented strains, strain 183 bp.
6) Addition of a monoculture of strain 183 bp for the third bioaugmentation event with high concentrations of all three chlorinated solvents present.
7) Microbial characterization of groundwater samples taken over the course of the test from all of the monitoring wells using T-RFLP for microbial community analysis and real time PCR for the enumeration of one of the bioaugmented strains, strain 183 bp.

There were four separate bioaugmentation 'events' during the third field season. The test conditions and the processes investigated are shown in Table 53. The first event ran for 100 days and included bioaugmentation on days 0 and 86. The following three events included bioaugmentation only on day 0 and ran for shorter durations ranging from 10 to 28 days. Molecular analyses of groundwater samples obtained from the second and fourth events provided information about the transport and survival of the bioaugmented cultures and the dominant microbial community changes that occurred during stimulation with butane and oxygen and stress from the co-substrates 1,1,1-TCA, 1,1-DCA, and 1,1-DCE. After each bioaugmentation, CAH removal ability was successfully imparted to the subsurface, but was difficult to maintain over time. The butane-stimulated indigenous leg was capable of limited DCE transformation, but essentially no DCA or TCA transformation. CAH removal efficiencies in the bioaugmented leg were the highest for DCE and least for TCA. The four bioaugmentation events are discussed in detail in the following sections.

Table 53. Duration, Chemical Amendments, and Processes Studied during the Bioaugmentation Events in the Third Season of Field Testing

	Duration	Chemical Amendment	Average Concentration	Processes Studied
Event I	5/37 – 9/4/03	H_2O_2	50 ppm	Optimize O_2 and butane cycle times
	(100 days)	Nutrients	(See table 54)	
	Time since last	Oxygen	~ 10 – 20 mg/L	CAH removal in the absence of butane
	test: 170 days	Butane	~ 5 – 20 mg/L	
		1,1,1-TCA	160 µg/L	Re-bioaugmentation (day 86)
		1,1-DCA[1]	140 µg/L	
Event II	10/5 – 11/2/03	Bleach[2]	62 mg/L[2]	Track bioaugmented culture using molecular methods (SE0.5 well)
	(28 days)	Oxygen	30 mg/L	
	Time since last	Butane	3 mg/L	
	test: 30 days	1,1,1-TCA	200 µg/L	Pre-treat field with biocide to reduce active population
		1,1-DCA	200 µg/L	
		1,1-DCE[3]	130 µg/L	
Event III	11/19-11/29	Bleach[4]	62 mg/L[4]	Effects of high CAH concentrations
	(10 days)	H_2O_2	20 ppm	
	Time since last	Oxygen	20 mg/L	Augmentation of a monoculture (183 bp)
	test: 17 days	Butane	7 mg/L (calc)	
			16 mg/L (meas)	
		1,1,1-TCA	375 µg/L	
		1,1-DCA	260 µg/L	
		1,1-DCE	300 µg/L	
Event IV	12/20-1/7/04	Bleach[5]	20-40 mg/L[5]	Track bioaugmented culture in groundwater using molecular methods at all SE wells to determine extent of bacterial transport
	(17 days)	H_2O_2	varied	
	Time since last	Oxygen	30-60 mg/L	
	test: 21 days	Butane	7 mg/L (calc)	
			4 mg/L (meas)	
		1,1,1-TCA	160 µg/L	
		1,1-DCA	290 µg/L	
		1,1-DCE	170 µg/L	

1. DCA added from day 50 through day 97; 2. Bleach solution added to the field, allowed to sit, and pumped out approximately 1 month prior to bioaugmentation Event II; 3. DCE added from day 23 through day 28; 4. Bleach added at the end of Event II, from 11/4 – 11/5, 2 weeks prior to bioaugmentation Event III; 5. Bleach added at the end of Event III, from 12/1 – 12/5, 2 weeks prior to bioaugmentation Event IV r to bioaugmentation Event IV

5.3.1 First Bioaugmentation Event of the Third Field Season

The first bioaugmentation event of the third field season began on May 27, 2003, and ran for about 100 days. Initially, only 1,1,1-TCA was added to the test zone at approximately 160 μg/L, while 1,1-DCA was added from day 50 through day 97 at about 140 μg/L. A butane-utilizing mixed culture containing the 183 bp organism and at least five other dominant organisms was bioaugmented to the field on day zero. Good 1,1,1-TCA and 1,1-DCA removal efficiency was achieved in the bioaugmented leg early in the test, but then declined to near zero removal by the end of the 28-day test. However, 1,1-DCE was removed to below detection limits in the bioaugmented well leg even after 1,1,1-TCA and 1,1-DCA removal had essentially stopped. The non-bioaugmented control well leg exhibited little or no 1,1,1-TCA and 1,1-DCA transformation and limited 1,1-DCE removal.

Microbial results showed a community shift upon bioaugmentation and stimulation with butane and oxygen. Initially an organism with a TFL of 277bp dominated groundwater samples taken from the bioaugmented leg, but as butane was completely utilized and CAH transformation began an organism with a TFL of 126bp became dominant as long as butane was amended. An organism with a TFL of 277bp also was significant in the non-bioaugmented leg early in the test, and although it also fell in relative amplitude as the test proceeded, the organism with a 126bp TFL was not seen in the indigenous leg. Real-time PCR analyses were successful in enumerating the strain 183bp organism, but it was found to be present in small quantity compared to the total microbial community in the groundwater.

Table 54. Calculated Groundwater Concentrations of Amended Nutrient Solution

Nutrient	Calculated Field Concentration, μM
K_2HPO_4	1.31
NaH_2PO_4	0.80
$MgSO_4$	0.04
$MnCl_2$	0.02
$ZnSO_4$	0.01
H_3BO_3	0.01
Na_2MoO_4	0.005
$NiCl_2$	0.001
$CuCl_2$	0.001
$CoCl_2$	0.001

TCA was not significantly transformed in the indigenous well leg upon stimulation of an active butane-utilizing microbial population. Upon bioaugmentation of the east well leg, TCA concentrations fell rapidly, reaching maximum TCA removal efficiencies of approximately 75% between days 24 and 29. After day 29, TCA removal efficiency began to gradually drop in the bioaugmented leg. A short period of stable TCA removal occurred after switching to a lower time-averaged butane concentration on day 43; however, peroxide amendment concentration was

concurrently reduced to 15 ppm at the same time, so it is not certain that the reduction in butane concentrations was the reason for the observed increase in TCA transformation efficiency. In any case, the effect was small and short-lived, as TCA removal efficiencies continued to decline. DCA addition started on day 50, with little or no DCA transformation occurring in the indigenous leg. DCA removal efficiencies in the bioaugmented leg exhibited a trend of decreasing efficiency over time, with maximum removal efficiencies of about 75% achieved for a short period of time.

Butane addition was terminated on day 61 to see if continued CAH transformation in the absence of primary substrate would result in increased treatment efficiency. Both TCA and DCA treatment in the bioaugmented leg increased for about one week before dropping off to values experienced before stopping butane addition and eventually declining even further. Interestingly, 1,1-DCE, present as background contamination in both well legs, was treated to below quantification limits in the indigenous leg and below detection limits in the bioaugmented leg during the extended period of butane addition. However, concentrations rebounded in the indigenous leg when butane addition was stopped, but treatment to below the detection limit continued for the two weeks that butane was not added to the field in the bioaugmented well leg. Addition of another 2.5 g of a mixed butane-utilizing bioaugmentation culture to the field and the re-start of butane addition resulted in DCA transformation producing removal efficiencies of about 30%, or less than half of that attained from the initial bioaugmentation. TCA transformation activity was not re-gained with the second bioaugmentation.

5.3.1.1 Results from the First Bioaugmentation Event in the Third Field Season. The concentrations of bromide, 1,1,1-TCA, 1,1-DCA, 1,1-DCE, butane, and DO in the two injection wells (EI and WI) and the three monitoring wells (SE1, SE2, SE3, SW1, SW2 and SW3) on each leg were monitored semi-continuously for the 100-day duration of the test. Each sample required approximately 50 min to acquire, prepare, and analyze, resulting in approximately 25 samples and 3 standards run each day. Injection flowrates to both well legs was 1.25 l/min while extraction flowrate in the non-bioaugmented west well leg was approximately 7.5 l/min while that in the bioaugmented east well leg was about 5.9 l/min, resulting in faster residence times in the indigenous west leg.

Initially, TCA, at about 160 μg/L (Figure 134), and a peroxide solution were added to both well legs on day 0. A 150 mg/L bromide solution was also added to the west indigenous leg as a non-reactive tracer to compare TCA transport to and to determine if any cross-over flow to the bioaugmented east well leg was occurring. Times to reach 50% influent bromide concentrations at the west leg monitoring wells were approximately 0.3 d, 0.4 d, and 0.6 d for wells SW1, SW2, and SW3, respectively (Figure 142). The time to reach 50% influent TCA concentrations in the same wells were about 0.2 d, 0.4 d, and 0.7 d for wells SW1, SW2, and SW3, respectively. The TCA and bromide breakthrough times were quite close, considering the resolution of the data used to produce the breakthrough estimates, indicating that TCA transport was at most mildly retarded. Times to 50% TCA breakthrough in the east well leg were 0.7 d, 1.4 d, and 2.3 d for wells SE1, SE2, and SE3, respectively, or approximately 3 times those found for the west well leg. Bromide tracer was added to the east well leg later in the test from days 87 through 98 (Figure 142) and was found to have 50% breakthrough times of 0.5 d, 0.9 d, and 1.3 d for wells SE1, SE2, and SE3, respectively. Ratios of TCA to bromide breakthrough indicate a retardation

factor of approximately 1.6 for TCA in the east well leg. However, the TCA breakthrough times were obtained from day 1 through 15 and the bromide breakthrough from days 87 through 98, and as can bee seen in Figure 143, the TCA recovery profile in the west well leg begins to change around day 50 resulting in well SW1 having greater TCA recovery later in the test than occurred initially. Although the recovery data does not indicate as dramatic an effect in the east leg, a change in regional flow conditions could introduce errors in the east leg TCA retardation estimates.

In the west well leg, 65.7%, 18.1%, and 83.9 % bromide recoveries were obtained at wells SW1, SW2, and SW3, respectively, which were in very close agreement with TCA recoveries of 65.8%, 19.6%, and 81.3%. In the east well leg, TCA recoveries were found to be 98.2%, 94.5%, and 87.5% for well SE1, SE2, and SE3, respectively over days 10 to 15. Bromide recoveries obtained over days 92 to 98 were somewhat higher at 100.4%, 98.4%, and 91.8% for wells SW1, SW2, and SW3, respectively, but still in general agreement. Subsequent calculated CAH removal efficiencies were corrected for dilution based on bromide recovery values.

Late on day 13, oxygen and nutrient addition began. Oxygen was added at an approximate concentration of 20 mg/L and a nutrient solution was pumped into the injection streams for both well legs to achieve the injection concentrations described in Table 54. Butane addition in alternating pulses with oxygen addition began in the middle of day 15. Initially, the pulse cycles were set to 20 min butane followed by 4 min nitrogen to flush the system, and 34 min of oxygen followed by 4 min nitrogen, for a total cycle time of 1 hr. Although peroxide solution was also being added, inconsistencies in the strength of the stock peroxide solutions resulted in inconsistent production of dissolved oxygen in the aquifer as can be seen in Figure 136 for times less than 15 days. The calculated time-averaged butane concentration, based on butane solubility of 64 mg/L, was 21.3 mg/L during this cycle configuration. Measured butane concentrations were approximately 18.5 mg/L butane in the east well leg on day 18.5 and between 19 and 21 mg/L in the indigenous west well leg on day 17.6 (Figure 135).

Approximately 4.5 g of a mixed butane-utilizing culture was bioaugmented to the east well leg over a 45 min period about 1 hr after the initiation of butane pulses to the field. Butane concentrations rose over the next few days to peak values of 21 mg/L in the indigenous leg and to 18.5 mg/L in the bioaugmented leg. Butane was quickly consumed after the initial rise in both well legs with complete butane utilization occurring by day 23 in both legs. This rapid time to complete butane uptake in the indigenous leg indicated a significantly larger butane-utilizing microbial population was present at the start of the test compared to conditions encountered in the first season of field testing. As the butane was utilized in the bioaugmented leg, dissolved oxygen concentrations fell below 1 mg/L by day 17 and remained low throughout the east leg until day 23, when changes in the pulse cycling resulted in less butane and more oxygen delivery to the field. Dissolved oxygen concentrations in the indigenous leg also fell, but only dropped below 1 mg/L in SW3 briefly on day 21.

When oxygen limitations were observed in the east leg on day 18, cycle times were adjusted to increase oxygen delivery and reduce the amount of butane added. A change to cycle times of 17 min butane and 35 min oxygen in a 1 hr cycle was insufficient to overcome the oxygen deficit, so further adjustments were made in subsequent days until residual DO concentrations in the field exceeded 1 mg/L under the conditions of a 2 hr cycle with 15 min butane sparging and 97

min oxygen (Figure 133), or a ratio of 0.155 (min butane:min O_2) and a calculated time-averaged butane concentration of 8.0 mg/L. Butane pulses were gradually increased to 17 min and oxygen decreased to 95 min, providing a time-averaged butane concentration of 9.1 mg/L and residual DO concentrations greater than 2 mg/L in the indigenous leg and 3 mg/L in the bioaugmented leg. On day 37, the cycle time was increased to 3.15 hr with a butane cycle of 25 min and an oxygen cycle of 156 min, reducing the average butane concentration to 8 mg/L, in an attempt to push the bioactive zone further out from the injection wells. This resulted in an increase in residual DO in the east leg, so the cycle times were again adjusted to produce an average butane concentration of 11.3 mg/L on day 39, which in turn resulted in low residual DO in the both well legs. A final decision was made on day 43 to reduce the average butane concentration to eliminate the propensity to create anoxic conditions and to see if the reduced butane concentrations would result in greater TCA transformation as a result of lessened inhibition by butane. A cycle time of 13 min butane and 156 min oxygen separated by 4 min nitrogen pulses was used for the remainder of the test period resulting in a time-averaged butane feed concentration of 4.7 mg/L.

Figure 133. Butane and Oxygen Pulse Times and Total Cycle Times for the First Bioaugmentation Event of the Third Field Season

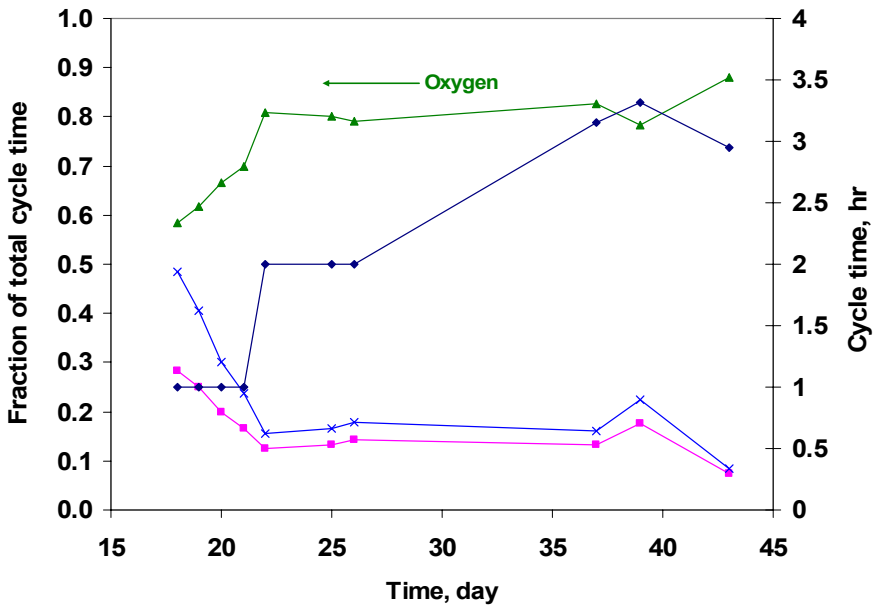

For the first 50 days of the test, TCA was the only CAH added to the field. Bioaugmentation was initiated after complete TCA breakthrough had been established to create the conditions of bioaugmentation to a contaminated site. Unfortunately, one day after bioaugmentation, mechanical problems with the CAH delivery pump caused a decrease in influent TCA concentrations, with problems persisting on the west leg through day 21 with failure of the CAH delivery tubing (Figure 137). Tubing was replaced and stable operation resumed on day 21. TCA removal in the bioaugmented leg increased steadily from day 18 through day 25 when minimum TCA concentrations of about 35-40 µg/L were achieved, corresponding to 75% influent TCA removal efficiency. The corresponding TCA removal efficiency in the west leg

was calculated to be 5%, a value to uncertain to conclude that significant TCA transformation was actually occurring.

TCA removal in the bioaugmented leg fell from a maximum of 75% removal around day 25 to 70% removal by day 32. Possibly related to the drop in efficiency, the amended nutrient solution was stopped on day 20 due to mechanical failure and re-introduced on day 30 when the appropriate parts arrived. Peroxide, at 5 ppm, was also added to the nutrient mix at this time to discourage biological growth in the stock solution. By day 32, TCA removal efficiency increased in the bioaugmented leg to about 75% removal, which was maintained for a few days. On day 34, peroxide concentration was increased to 15% and on about day 37, the same time the pulse cycle length was changed to 3 hr and the peroxide concentration in the nutrient mix was increased to 45 ppm, TCA concentrations begin a slight rise in the bioaugmented leg. On day 39, the cycle times were again changed to increase the butane levels in the field in an attempt to regain removal efficiency; however, a power failure on day 40 caused a momentary decrease in influent TCA concentrations and a significant reduction in field DO levels. On day 43, peroxide levels were dropped back to 15% and the pulse cycles were set to the values used for the reminder of the test, resulting in less butane to the field and higher residual DO concentrations. Under these conditions, TCA removal dropped to approximately 66% removal.

Beginning on day 50, DCA was added to the field at a concentration of about 140 μg/L (Figure 138). DCA concentrations began rising in the indigenous well leg significantly faster than in the bioaugmented leg. A disruption in the DCA supply on day 55 caused a temporary downswing in DCA concentrations, but the supply was stabilized the following day and concentrations rose in the indigenous leg to a steady value of about 110 μg/L through day 61, when butane addition was stopped. Using the bromide recovery data obtained under different flow conditions early in the test, these concentrations resulted in calculated removal efficiencies of -2% and 16% for wells SW1 and SW3, respectively. If the assumption is made that no TCA transformation is occurring in the indigenous leg and the DCA data is compared to the TCA data, estimates for DCA removal become 5.6% and 11% for wells SW1 and SW3, respectively. It is possible there was some DCA transformation in the indigenous leg, but the concurrent changes in regional flow patterns obscure the potential results. DCA concentrations in the bioaugmented leg increased at a slower rate than the indigenous leg. Just before the termination of butane addition, DCA removal efficiencies in the bioaugmented leg were 66% for wells SE1 and SE2, and about 77% in well SE3 based on bromide recoveries obtained later in the test from days 87-98. Inspection of the TCA data indicated recoveries in SE3 may have been over estimated during this portion of the test due to fluctuation of the regional groundwater flow pattern.

During this period of DCA addition, TCA in the indigenous leg appears as it did earlier in the test when no removal was taking place. However, recovery of TCA in well SW1 increased from 65.8% over days 10 to 15, to approximately 85% on day 69, while the recoveries in SW3 were essentially the same at 81.3% from day 10-15 and 82.2% on day 69, indicating a change in regional groundwater flow (Figure 137). TCA in the bioaugmented leg was still undergoing transformation, although transformation efficiencies were declining at about the same rate before DCA addition as it was after, indicating that DCA addition was not he sole cause of diminished TCA transformation. Before day 40, TCA recoveries in SE2 and SE3 were identical; however, after day 40, TCA recoveries in well SE3 were increasingly less than that in SE2, presumably

also due to changes in regional groundwater flow rather than onset of TCA transformation between wells SE2 and SE3. On day 50 at the onset of DCA addition, TCA removal efficiency was 50% in wells SE1 and SE2 (58% in well SE3), but by day 61 when butane addition was terminated, TCA removal had dropped to 25% removal in SE1 and SE2 (37% in SE3).

Butane addition was stopped on day 61 to see if greater CAH transformation efficiency would result from the lack of a competing primary substrate and if long-term CAH transformation in the absence of growth substrate, as was seen in some previous batch laboratory tests, was possible in the field. TCA in the indigenous leg appeared to increase in well SW1, but, as discussed previously, this was most likely due to a change in regional groundwater flow rather than a change in TCA transformation ability. TCA concentrations in the bioaugmented leg dropped about 20-30 μg/L over the next few days and then gradually increased to close to influent levels by day 69 when the injection/extraction crashed for a few days. DCA delivery to the indigenous leg was disrupted on day 61 just after butane addition was stopped, so it was difficult to conclude if enhanced transformation in the absence of butane occurred. After DCA delivery was restored the following day, DCA concentrations in the indigenous leg rose to pre-disruption levels immediately and to injection concentrations by day 65 or so, indicating a lack of significant transformation ability. DCA in the bioaugmented leg was also disrupted right after butane addition was stopped, but upon re-introduction of DCA, concentrations dropped to below those experienced just before the end of butane addition and continued to fall until day 64, when DCA concentrations began rising again. DCA removal efficiencies on day 64 were 68%, 65%, and 74% for wells SE1, SE2, and SE3, respectively, values equal to those just prior to when butane addition was stopped. By day 69 just before the crash of the injection/extraction system, DCA removal efficiencies had dropped to 30%, 26%, and 38% in wells SE1, SE2, and SE3, respectively, but influent DCA concentrations also dropped resulting in lower calculated removal efficiencies. DCA transformation continued in the absence of butane for at least 8 days, although not always at the removal efficiency encountered just before butane was stopped.

After the crash of the injection/extraction system on day 69, both extraction wells were swabbed, the chemical delivery tubing was changed, and the system was restarted on day 71. Between day 71 and day 86, CAHs, peroxide, and oxygen were augmented to the field without butane. CAH concentrations returned to influent values of approximately 175 – 200 μg/L of TCA and DCA in both legs, with the possibility of a very small amount of DCA removal in the bioaugmented leg during this time. Butane addition to the field began again on day 86. A brief spike of butane measuring 2 mg/L in the indigenous leg and 1 mg/L in the bioaugmented leg appeared in the first set of monitoring wells, but was completely removed within one day after the re-start of butane addition. Peroxide addition was stopped and nutrient solution to both legs and bromide amendment to the bioaugmented leg began one day after butane addition was started. About 8 hr later, on day 87, bioaugmentation was initiated by injecting a groundwater solution containing approximately 2.5 g of a mixed butane-utilizing culture into the east well leg. Peroxide addition was restarted to both legs on day 88. Stable TCA and DCA injection concentrations were maintained through the remainder of the test.

DO concentrations dropped in both well legs commensurate with butane utilization (Figure 136), but leaving residual DO levels from 5 to 15 mg/L for the remainder of the test. TCA concentrations in the indigenous leg were unchanged through the end of the test on day 100,

whereas a small amount of TCA transformation was seen in the bioaugmented leg (Figure 139). Calculated TCA removal efficiencies in the bioaugmented leg averaged over days 93 to 99 were quite low at 5%, 7%, and 9% for wells SE1, SE2, and SE3, respectively. Bromide was also being added to the bioaugmented leg at the same time so accurate estimates of removal efficiencies could be calculated. Although not conclusive, TCA concentrations in well SE3 appear to be slowly, but consistently, dropping compared to bromide values, possibly indicating a trend towards an increase in TCA removal efficiency over time rather than the gradual decline observed in many of the previous tests. Negative TCA removal efficiencies were calculated for the indigenous leg, but the calculation were based on flow characteristics determined early in the test, before the change in regional flow around day 50.

DCA concentrations in the indigenous well leg also unchanged throughout day 97, when DCA amendment was stopped (Figure 140). DCA concentrations in the bioaugmented leg dropped immediately after bioaugmentation and continued slowly down over the remaining 10 days of the test. DCA removal efficiencies averaged over days 93 to 97 were 22%, 29%, and 32% at wells SE1, SE2, and SE3, respectively, or approximately 40% of the DCA removal efficiency found on day 64. Thus, re-bioaugmentation, albeit with less inoculum, resulted in a small amount of TCA transformation and somewhere less than half of the original DCA transformation ability.

There was a small amount of 'background' 1,1-DCE contamination in the field. Values at the beginning of the test were about 10 mg/L in all of the wells in the indigenous leg (Figure 141). Butane addition was started and as the butane starts being utilized, DCE concentrations in well SW1 dropped to about 3 μg/L, while concentrations in well SW3 fell below the quantification limit of about 2 μg/L and stay there until the system crashed on day 69. After the second bioaugmentation on day 87, DCE in both SW1 and SW3 fell below the quantification limit. DCE concentrations in the influent stream, the extraction well, and monitoring well SW2 remained at about 6 μg/L.

In the bioaugmented leg, an initial DCE concentration of about 7 mg/L DCE was found in the extraction well, which pulls in approximately 80% 'background' groundwater and 20% injected solution. Values in the injection stream were about 10 μg/L, indicating the presence of some DCE in the influent TCA solution (Figure 141). Initial concentrations in wells SE1 and SE2 began at about 4 μg/L and rose over the first 15 days of the test to about 8 μg/L, with TCA addition in the absence of butane addition. After the onset of butane addition and the initial bioaugmentation, DCE concentrations fell below the detection limit in wells SE1, SE2, and SE3 through the 100 day test, including during the time when butane addition was stopped and through the injection/extraction system crash. A very transient DCE concentration of about 4 μg/L was observed in SE1 and SE2 after the re-start of butane addition and bioaugmentation on days 86-87, but immediately dropped below detection limits again. DCE values in the injection and extraction streams remained steady after the initial addition of butane at about 5 to 6 μg/L. Although it was not surprising to find the small amount of DCE present to be well remediated in the bioaugmented leg, removal was not anticipated to continue for two weeks in the absence of butane addition as was observed.

5.3.1.2 Summary of the First Bioaugmentation Event of the Third Field Season. In the first bioaugmentation event of the third field season a mixed butane-utilizing culture was bioaugmented in the presence of TCA contamination and enriched on oxygen and butane addition. A maximum TCA treatment efficiency of 75% removal of 160 mg/L TCA was achieved for a period of approximately 5 days followed by three weeks of good removal (~60-70%) before DCA addition began. Different combinations of butane and oxygen pulses and total cycle time were tried to determine the maximum amount of butane that could be added and still consistently keep the treatment zone aerobic. An operating condition of a 2hr cycle consisting of 15 min butane pulsing and 97 min oxygen pulsing with 4 min nitrogen addition between pulses was established and yielded sufficient residual oxygen (~5 mg/L or greater) and a time-averaged butane concentration of 8 mg/L. Maximum TCA transformation occurred during such a pulse cycle. Reducing the proportion of butane to result in an average concentration of 4.7 mg/L and lengthening the cycle to 3 hr resulted in slight initial gains in TCA removal followed by a slow decline in removal efficiency.

DCA was added to the influent stream along with the TCA on day 50, after the pulse cycle had been changed to 3 hr with a time-averaged butane concentration of 4.7 mg/L. Maximum DCA removal efficiencies of between 66% and 77% were attained for a short period. Butane addition was stopped on day 61, resulting in short-term greater TCA and DCA removal efficiencies for a few days before gradually declining efficiencies ensued. Re-bioaugmentation on day 86 resulted in little TCA removal, but approximately 35% DCA removal was re-gained. Interestingly, removal of both TCA and DCA was increasing until the test was stopped on day 100.

DCE was present as a background contaminant at levels between 6-10 mg/L. DCE was removed to below quantification limits in well SW3 in the indigenous leg during butane feeding and to non-detect levels in the bioaugmented leg. However, DCE treatment was lost in the indigenous leg in the absence of butane addition. In the bioaugmented well leg, complete DCE removal occurred through all perturbations through the end of the 100-day of the test.

Figure 134. TCA Breakthrough in the Absence of Butane Stimulation in the West (Indigenous) Leg and the East (Bioaugmented) Leg during the First Bioaugmentation in the Third Season of Field Testing

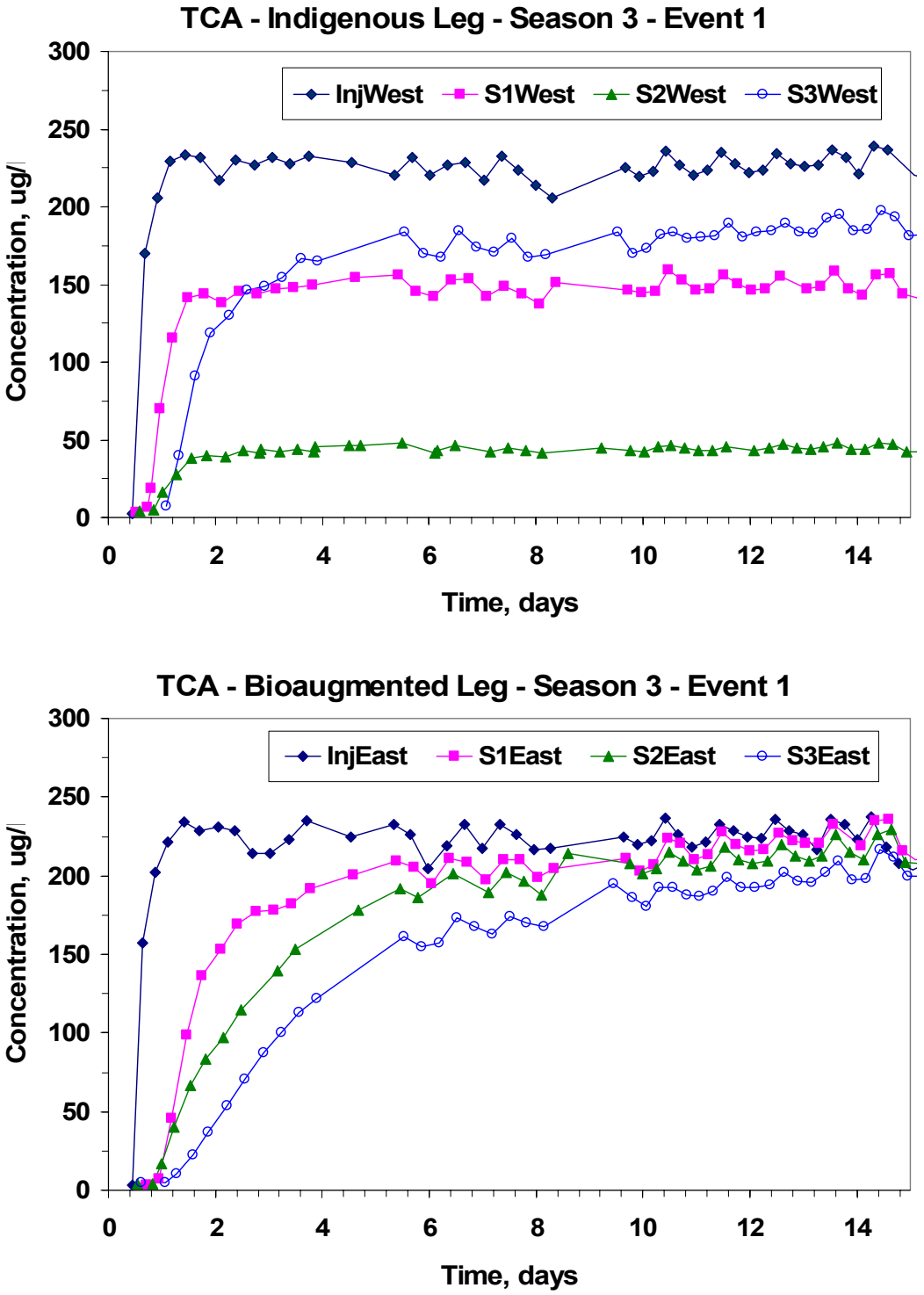

Figure 135. Butane Concentrations in the West (Indigenous) Leg and the East (Bioaugmented) Leg during the First Bioaugmentation in the Third Season of Field Testing

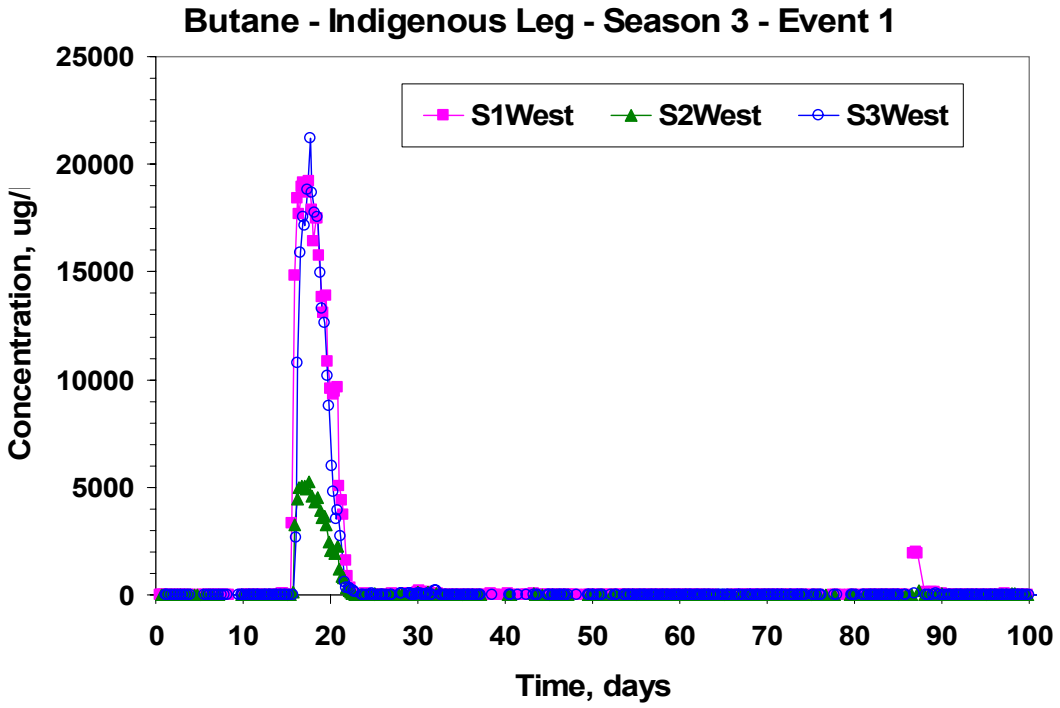

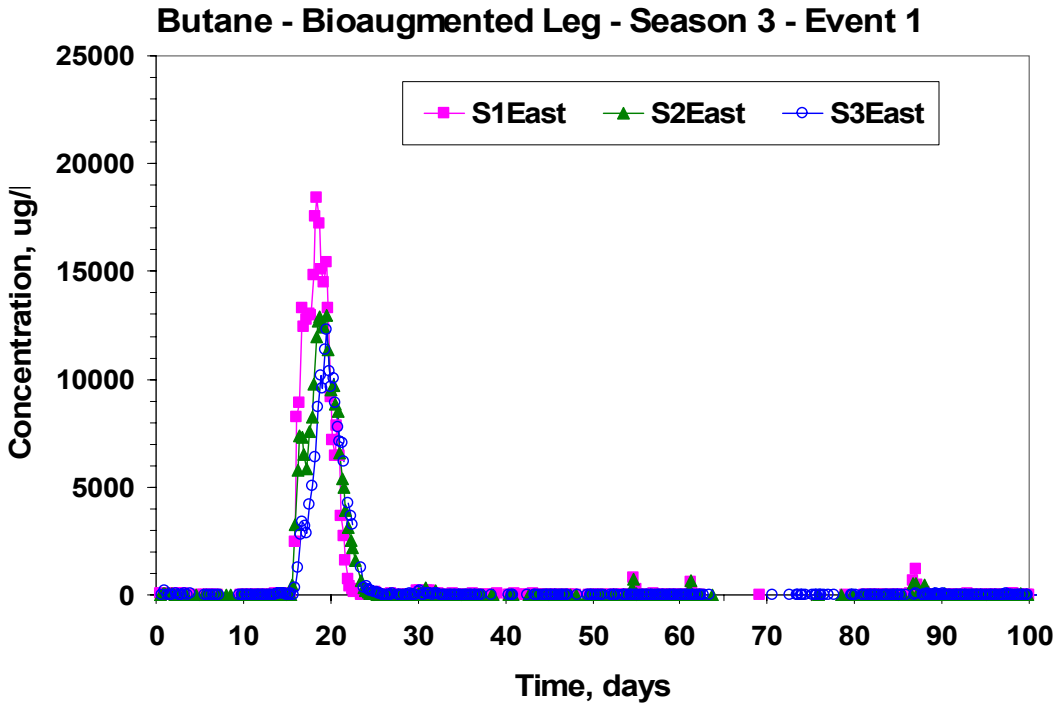

Figure 136. Dissolved Oxygen in the West (Indigenous) Leg and the East (Bioaugmented) Leg during the First Bioaugmentation in the Third Season of Field Testing

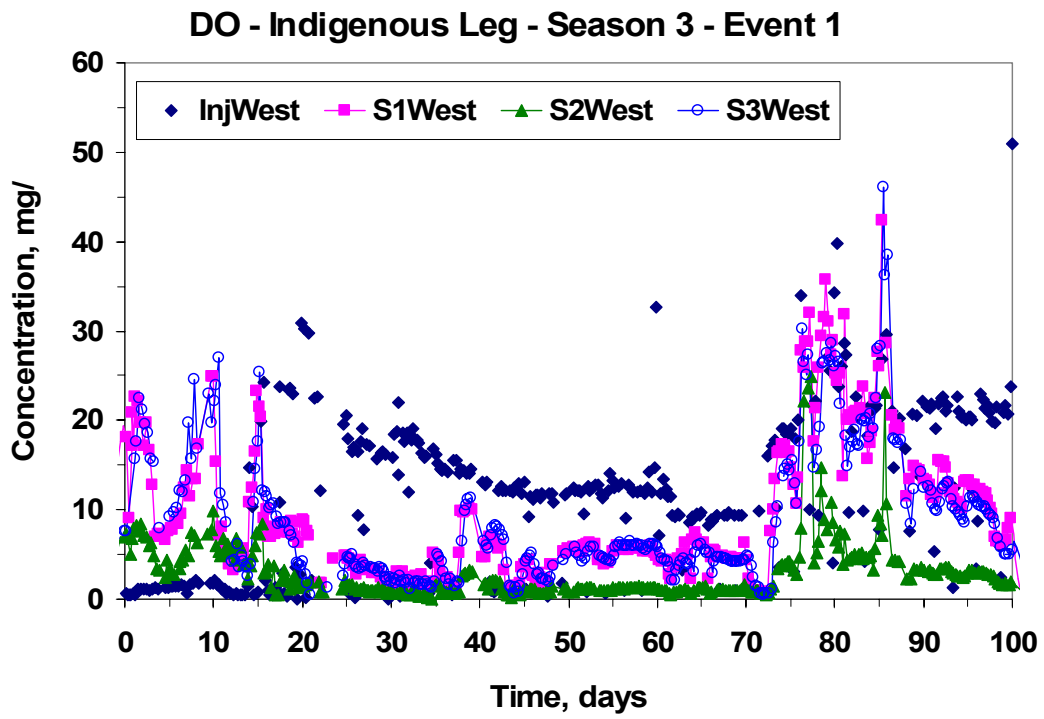

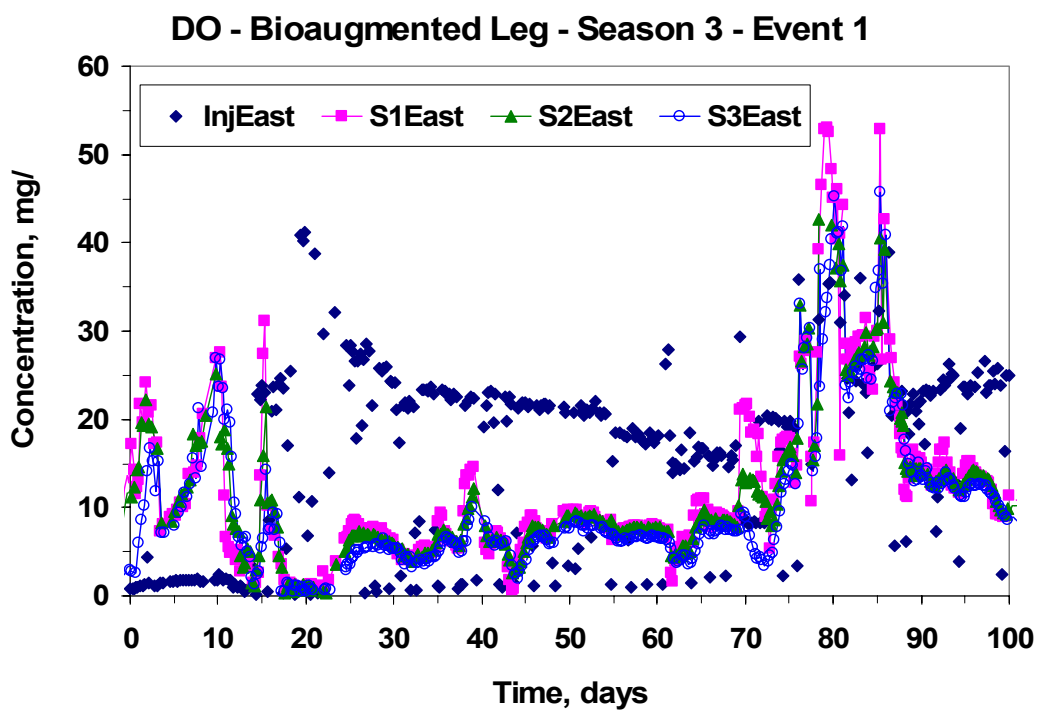

Figure 137. TCA Concentrations in the West (Indigenous) Leg and the East (Bioaugmented) Leg from Day 10 through Day 70 during the First Bioaugmentation in the Third Season of Field Testing

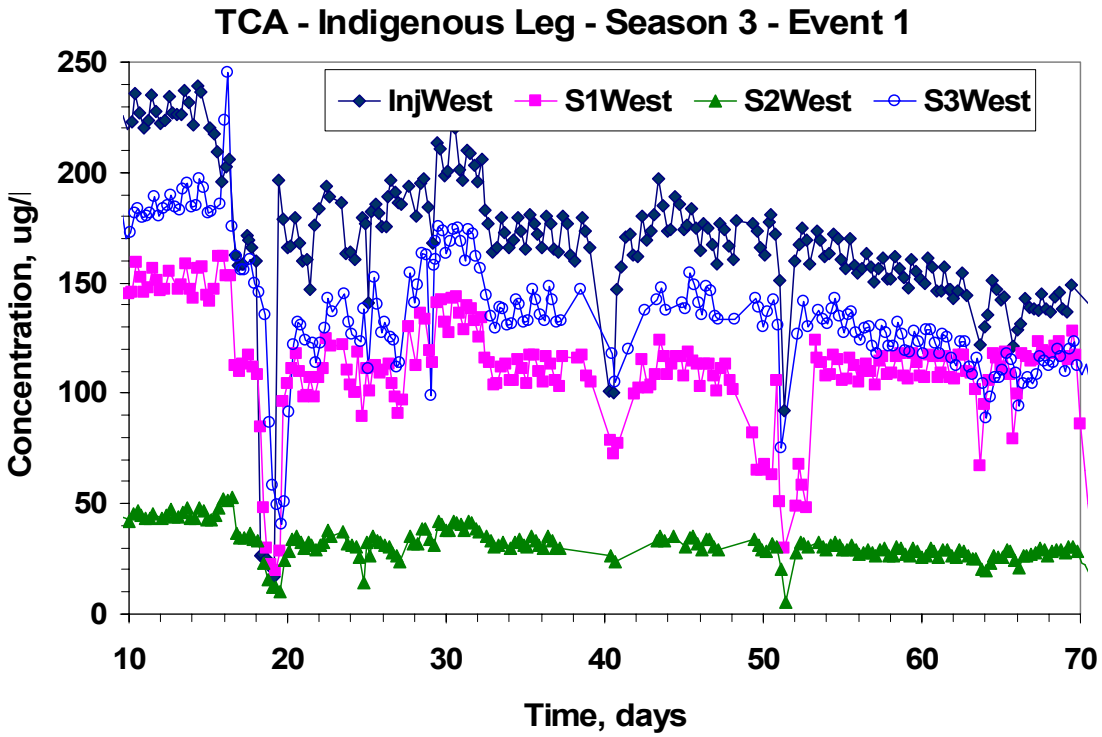

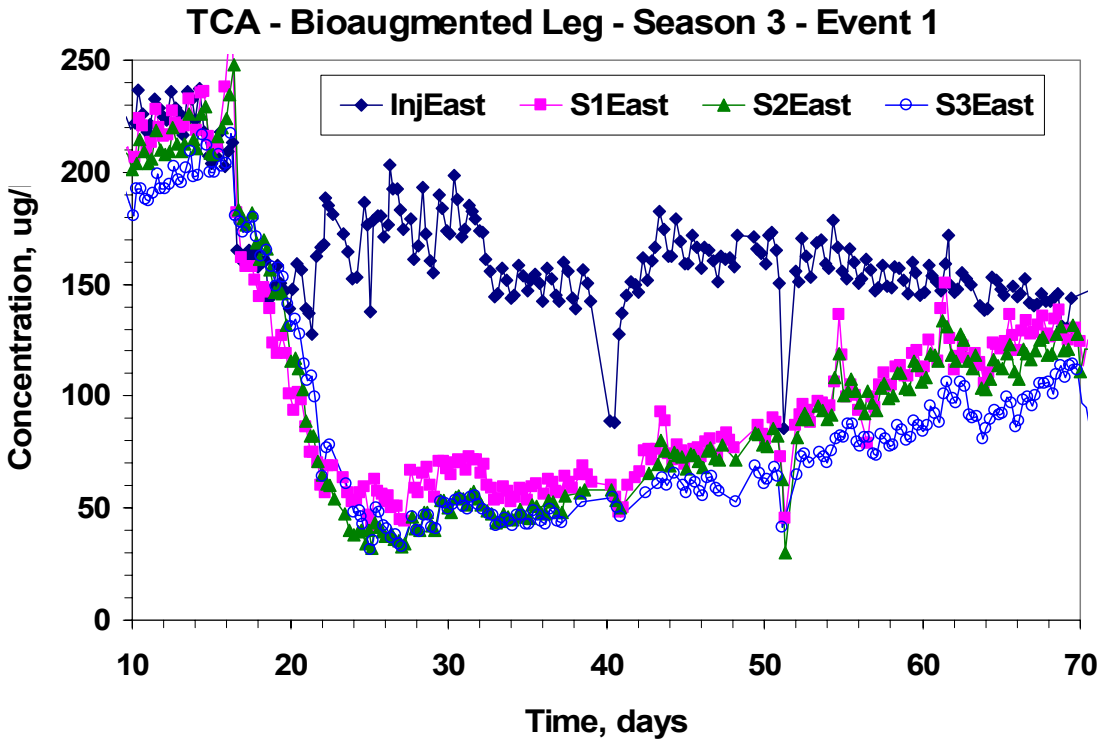

Figure 138. DCA Concentrations in the West (Indigenous) Leg and the East (Bioaugmented) Leg from Day 10 through Day 70 during the First Bioaugmentation in the Third Season of Field Testing

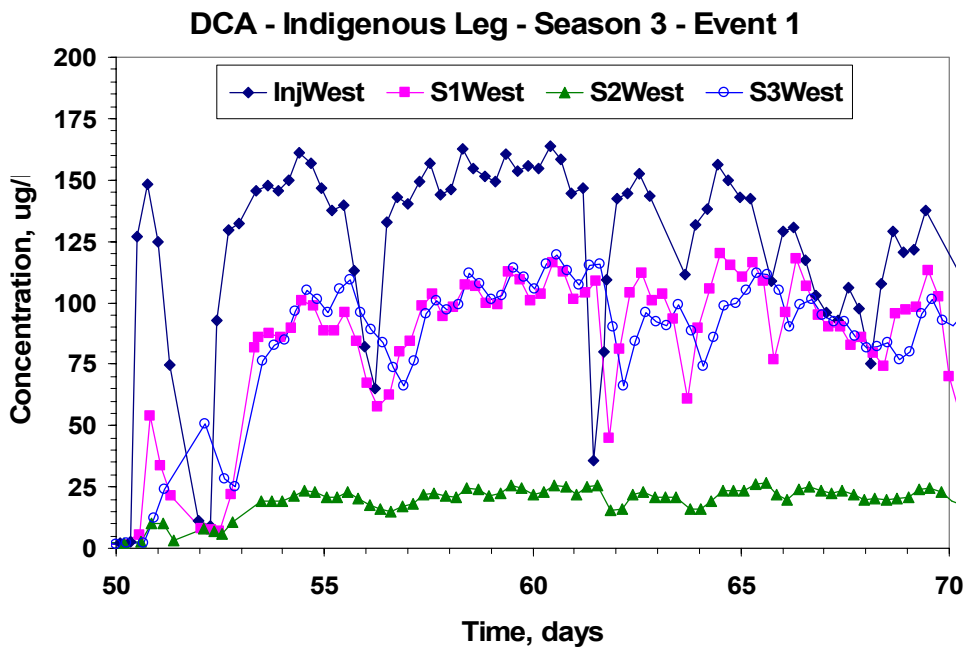

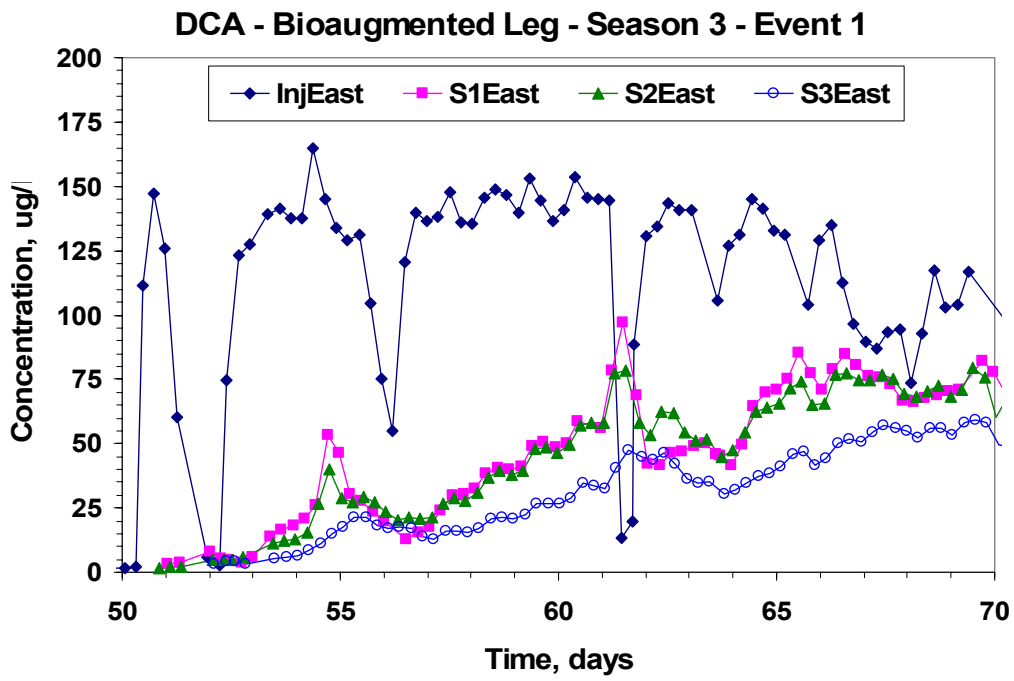

Figure 139. TCA Concentrations in the West (Indigenous) Leg and the East (Bioaugmented) Leg at the End of the First Bioaugmentation Test in the Third Season of Field Testing

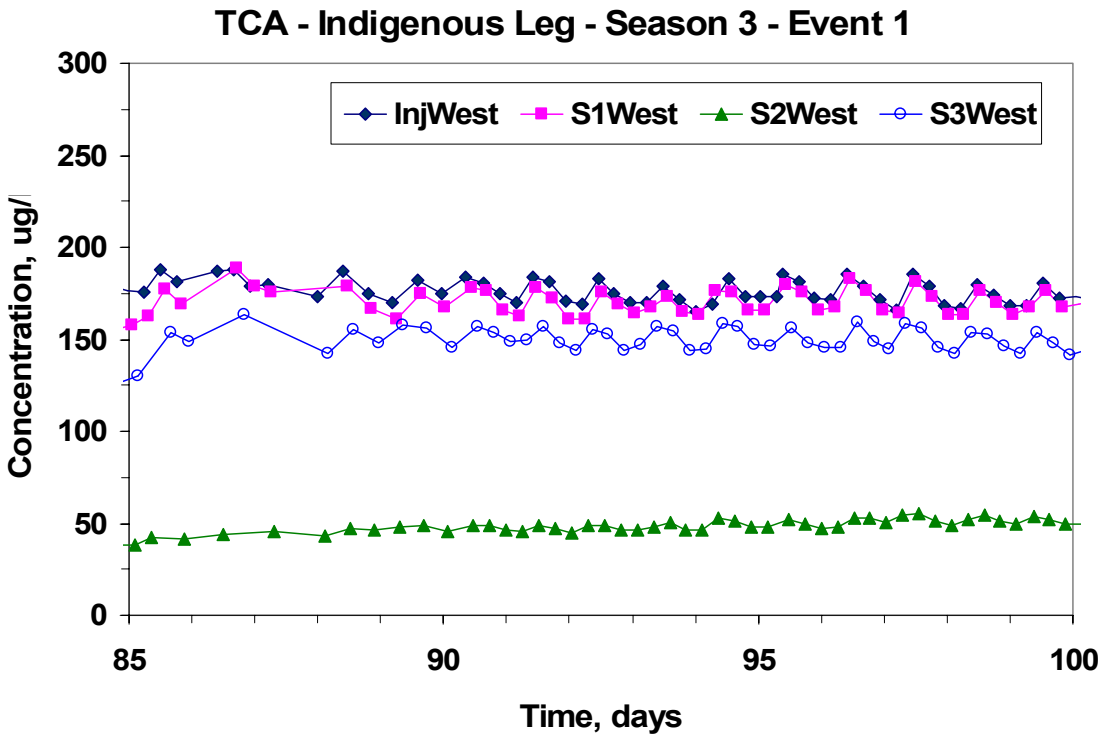

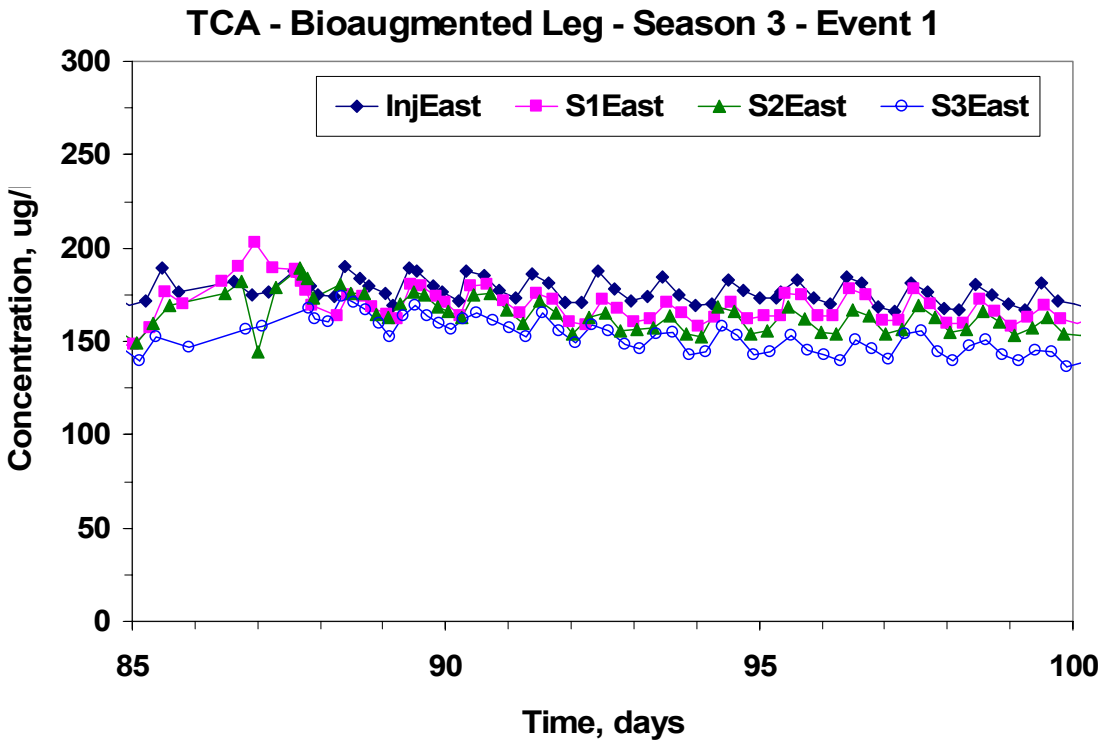

Figure 140. DCA Concentrations in the West (Indigenous) Leg and the East (Bioaugmented) Leg at the End of the First Bioaugmentation Test in the Third Season of Field Testing

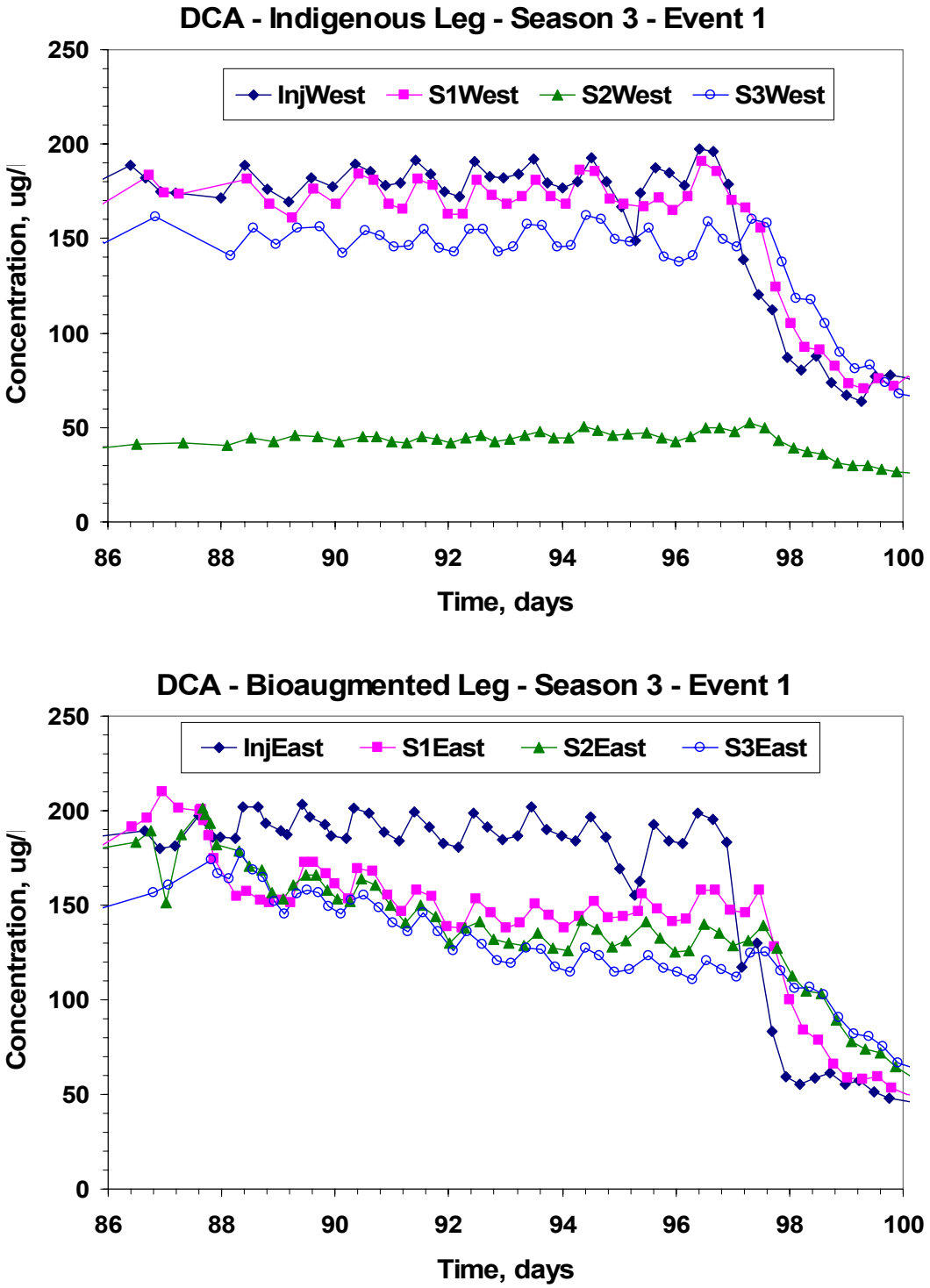

Figure 141. Background DCE Contamination Concentrations in the West (Indigenous) Leg and the East (Bioaugmented) Leg during the First Bioaugmentation Event in the Third Season of Field Testing

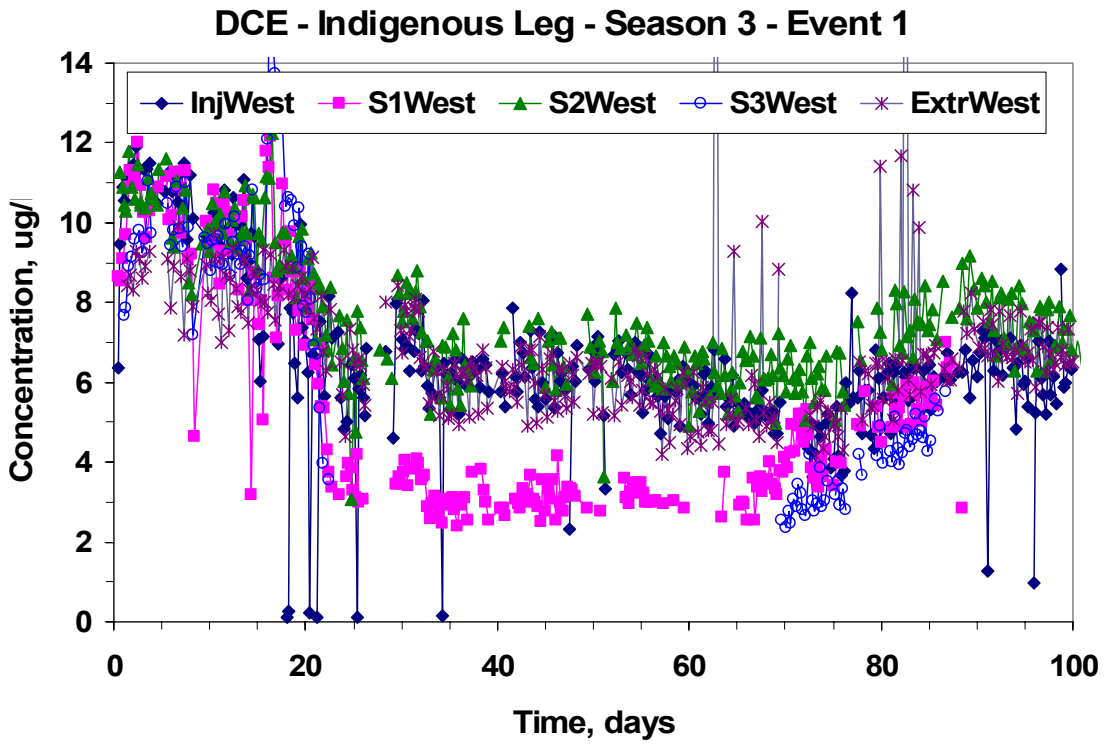

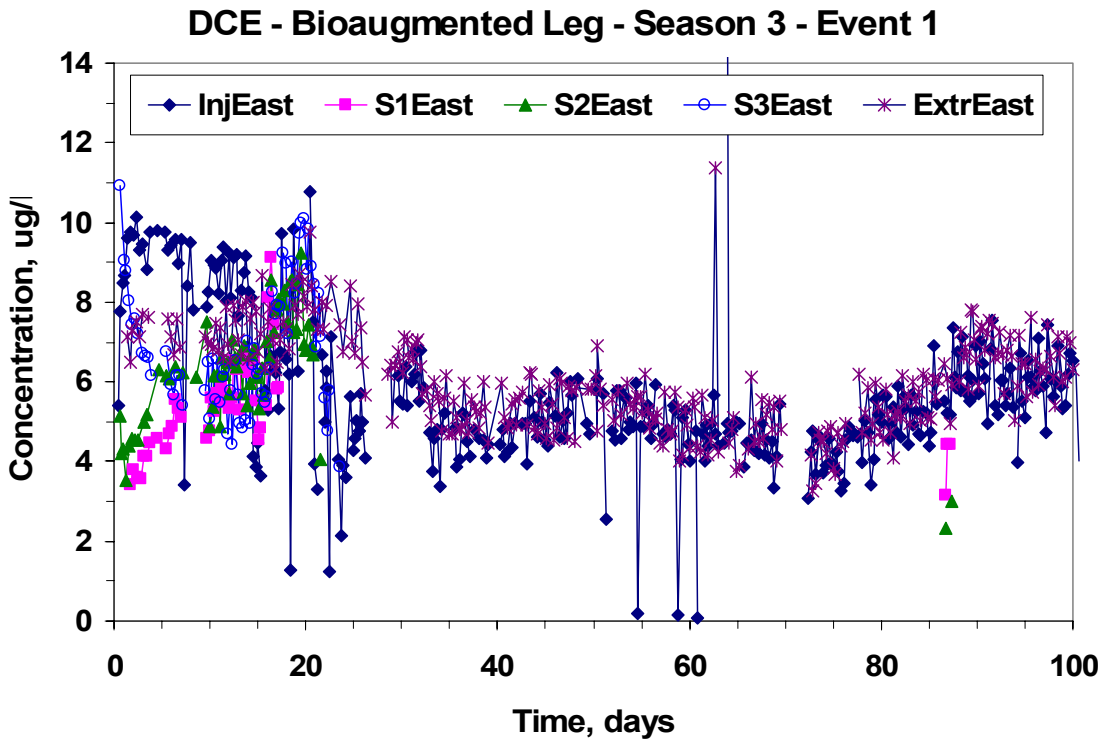

Figure 142. Bromide Concentrations in the West (Indigenous) Leg at the Beginning of the Test and in the East (Bioaugmented) Leg during the End of the First Bioaugmentation Event in the Third Season of Field Testing

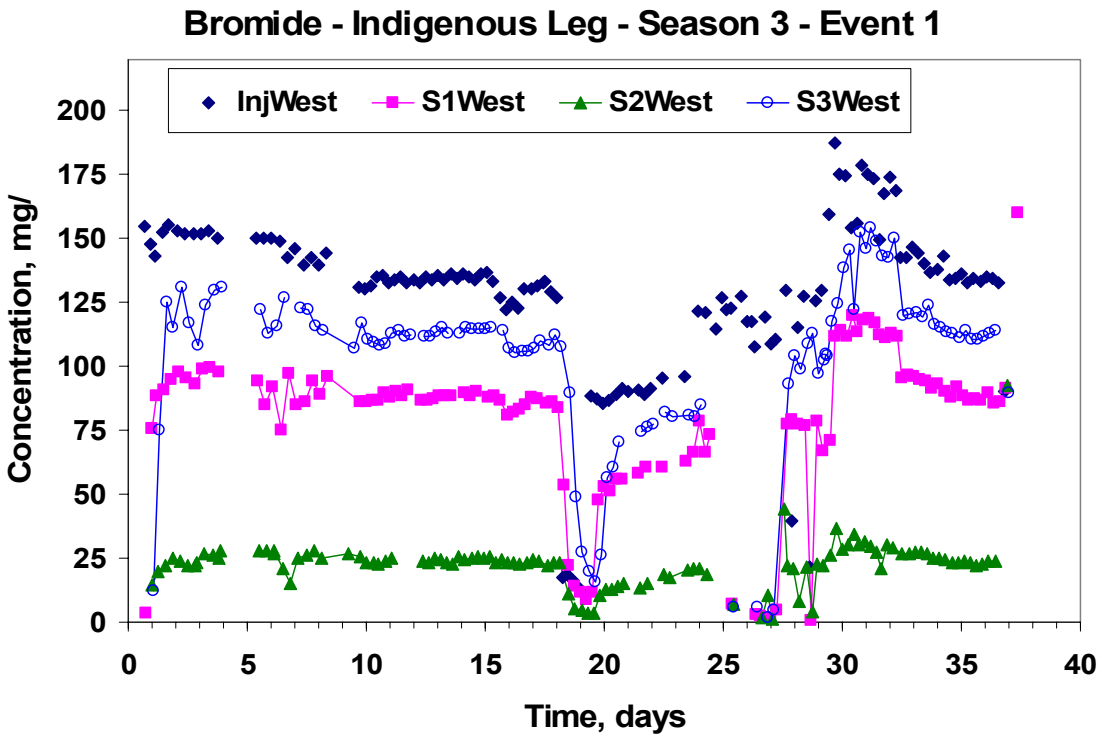

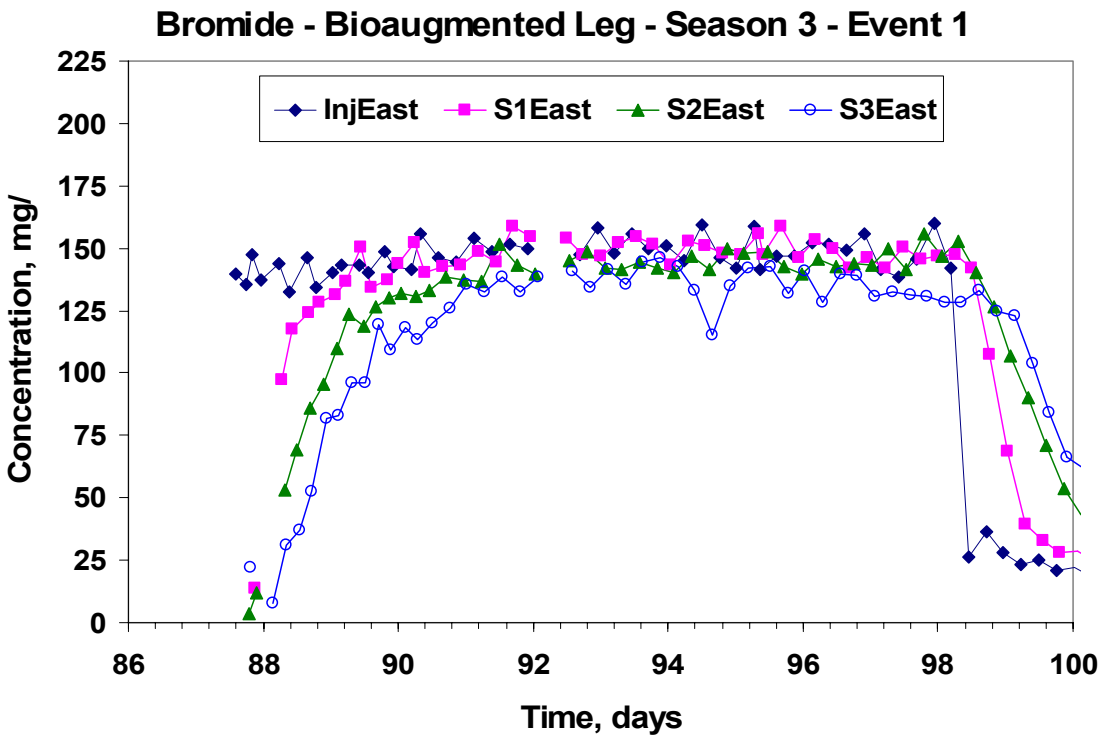

Figure 143. TCA Concentrations in the West (Indigenous) Leg and the East (Bioaugmented) Leg during the First Bioaugmentation Event in the Third Season of Field Testing

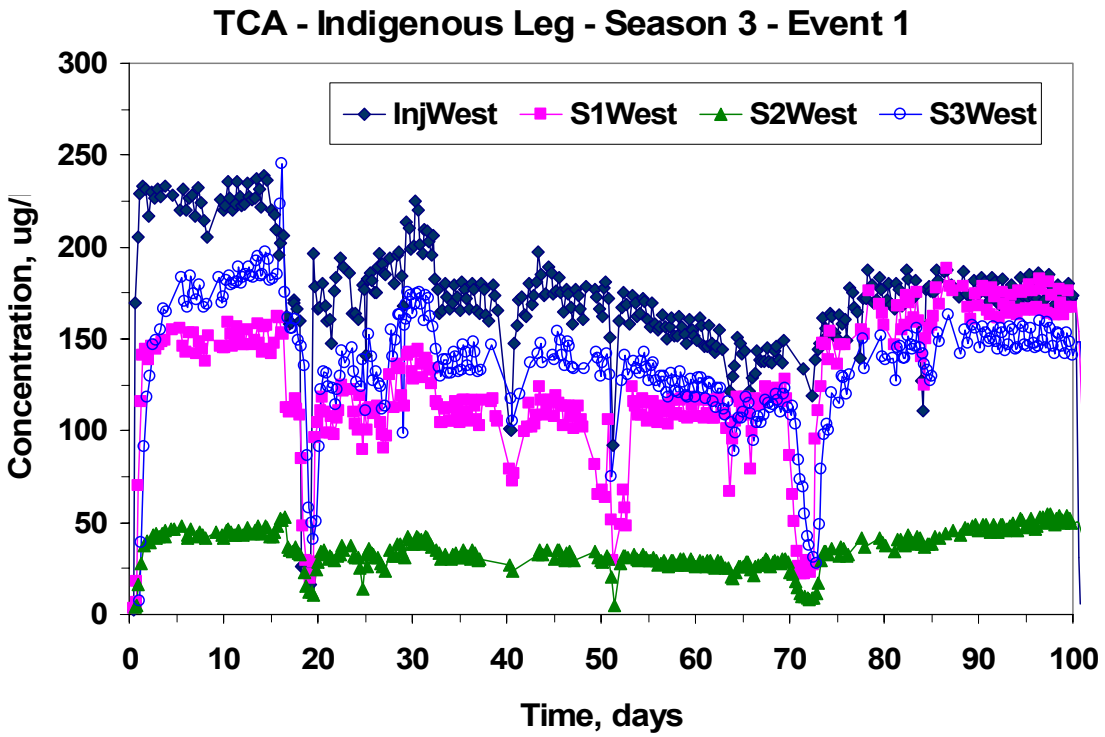

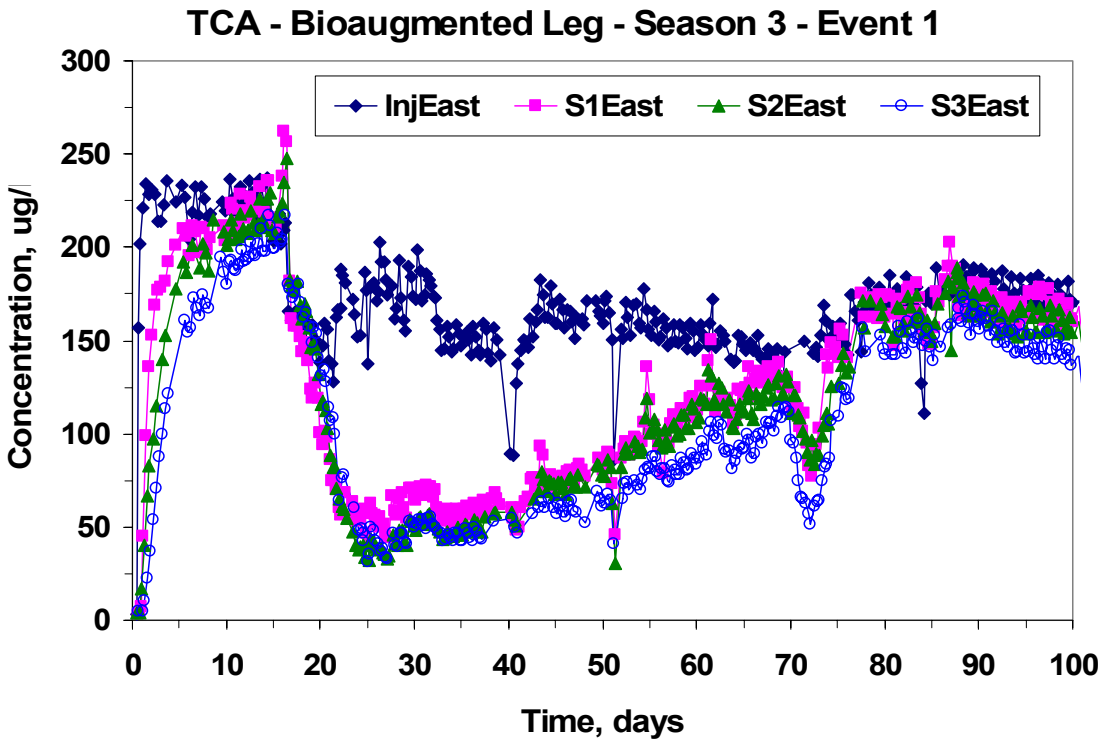

5.3.2 Second Bioaugmentation Event of the Third Field Season

The second bioaugmentation event of the third field season began on October 5, 2003, and ran for 28 days. Both 1,1,1-TCA and 1,1-DCA were added to the test zone at approximately 200 μg/L throughout the test, while 1,1-DCE was added at about 130 μg/L from day 23 through day 28. A butane-utilizing mixed culture containing the 183 bp organism and at least five other dominant organisms were bioaugmented to the field on day zero. Good 1,1,1-TCA and 1,1-DCA removal efficiency was achieved in the bioaugmented leg early in the test, but then declined to near zero removal by the end of the 28-day test. However, 1,1-DCE was removed to below detection limits in the bioaugmented well leg even after 1,1,1-TCA and 1,1-DCA removal had essentially stopped. The non-bioaugmented control well leg exhibited little or no 1,1,1-TCA and 1,1-DCA transformation and limited 1,1-DCE removal.

Microbial results showed a community shift upon bioaugmentation and stimulation with butane and oxygen. Initially an organism with a TFL of 277bp dominated groundwater samples taken from the bioaugmented leg, but as butane was completely utilized and CAH transformation began an organism with a TFL of 126bp became dominant as long as butane was amended. An organism with a TFL of 277bp also was significant in the non-bioaugmented leg early in the test, and although it also fell in relative amplitude as the test proceeded, the organism with a 126bp TFL was not seen in the indigenous leg. Real-time PCR analyses were successful in enumerating the strain 183bp organism, but it was found to be present in small quantity compared to the total microbial community in the groundwater.

5.3.2.1 Bioaugmentation Event 2: Chemical Results. The concentrations of bromide, 1,1,1-TCA, 1,1-DCA, butane, and DO in the two injection wells (EI and WI) and the three monitoring wells (SE1, SE2, SE3, SW1, SW2 and SW3) on each leg were monitored semi-continuously for the 30-day duration of the test. Each sample required approximately 50 min to acquire, prepare, and analyze, resulting in approximately 25 samples and 3 standards run each day. Injection flowrates to both well legs was 1.25 L/min while extraction flowrate in the non-bioaugmented west well leg was approximately 7.5 L/min while that in the bioaugmented east well leg was about 5.75 L/min, resulting in slightly faster travel times through the non-bioaugmented leg.

One hour prior to bioaugmentation, oxygen-sparged groundwater was introduced to both well legs. Approximately 5 g dry wt. of a mixed butane-utilizing culture was diluted in 4 L of groundwater and introduced into the injection stream to the east well leg over a period of ten minutes to initiate the test (t = 0 days). Immediately after bioaugmentation, chemical amendment of both well legs ensued. 1,1,1-TCA and 1,1-DCA were introduced continuously at approximately 200 μg/L and bromide was added at approximately 130 mg/L. Alternate pulses of butane-sparged and oxygen-sparged groundwater at influent concentrations of about 22 mg/L and 40 mg/L, respectively, were also initiated. Pulse cycles were 9 minutes of butane sparging followed by 4 minutes of nitrogen sparging, 156 minutes of oxygen sparging, and another 4 minutes of nitrogen sparging before repeating the cycle. In this way explosive gas mixtures were not formed and the alternating feed encouraged microbial growth farther from the injection well.

Bromide breakthrough in the bioaugmented east leg followed the pattern of 99% capture at SE1, 92% capture at SE2, and 89% recovery at SE3 (Figure 144). In the indigenous west leg, 90% bromide recovery was obtained in wells SW1 and SW3, while well SW2 appeared to be somewhat out of the flow path with only 21% bromide recovery. Consequently, data from SW2

were not included when analyzing treatment efficiencies in the west leg. It took about 0.4 day, 1.4 day, and 1.6 day to achieve 50% bromide breakthrough at wells SE1, SE2, and SE3 respectively. In the west well leg, 50% breakthrough occurred at about day 0.15 in SW1 and 0.65 d in SW3.

Organisms in the non-bioaugmented west leg took 9 days to grow to sufficient density to completely utilize the added butane (Figure 145). In contrast, only 3 days were required to achieve the same result in the bioaugmented east leg. Butane reached a maximum concentration of 3.5 mg/L at the first monitoring well in the non-bioaugmented leg and a maximum of 2.5 mg/L at SW3 and persisted for about one week. In the bioaugmented leg, immediate butane utilization resulted in a transitory maximum concentration of about 2.5 mg/L at the first monitoring well with significantly lower concentrations in wells SE2 and SE3, with complete removal occurring within 3 days. After initial enrichment, butane concentrations remained very low throughout the field for the duration of the test, with one exception. Beginning on day 24, butane delivery to the field was interrupted for 2 days. Upon the re-start of butane addition, butane levels in the field rose to approximately 0.5 mg/L in SE1 and 3 mg/L in SW1 before the butane-utilizing microbial populations responded and reduced concentrations to near zero values again. Similar to the initial start-up period, this process was much quicker in the bioaugmented leg than in the indigenous leg.

Oxygen utilization in both well legs occurred primarily between the injection well and the first monitoring well (Figure 146). Oxygen utilization was fairly stable throughout the test, except for transient declines in concentration around day 3 when oxygen delivery to the field was interrupted for about one day. Oxygen utilization averaged about 20 mg/L in the bioaugmented east leg and about 24 mg/L in the west leg throughout the first 20 days of the test. Calibration of a new DO probe on day 20 produced slightly lower DO readings, but the same general trend with DO utilization dropping to about 12 - 13 mg/L in both legs. A high residual of 15 to 25 mg/L DO was evident in both well legs throughout the test. The apparent slight utilization of oxygen in the east leg between the first and second monitoring wells is an artifact of incomplete capture of the flow path as evidenced by the bromide breakthrough data for the two legs.

In the non-bioaugmented west leg, TCA and DCA concentrations rapidly approached influent values and remained there throughout the test (Figures 147 and Figure 148). Bromide corrected concentrations for TCA and DCA at wells SW1 and SW3 showed from 3% to 7% removal compared to average influent values. Times to 50% TCA and DCA breakthrough were about 0.25 day and 0.9 day for wells SW1 and SW3, respectively, compared to 0.15 d and 0.65 d for bromide breakthrough, indicating little retardation in transport of the CAHs. In the bioaugmented east leg, TCA concentrations rose for the first three days followed by a decrease in concentration around day four corresponding to the time required for complete butane utilization (Figures 145, 146, and 147). Maximum treatment efficiencies of 95 % removal of DCA and 76% removal of TCA were achieved between days 4 and 7 in the bioaugmented leg. However, treatment efficiency began a steady decline after day 7. By day 21, TCA concentrations neared influent values, but about 53% DCA removal efficiency remained; however, by day 26, after a two-day interruption in butane addition to the field, DCA transformation had also essentially ceased.

On day 23, 125 μg/L 1,1-DCE was added to the CAH mixture injected to the field to determine if either the indigenous or bioaugmented well legs could still transform DCE even though TCA and DCA transformation had essentially stopped (Figure 149). The bioaugmented leg responded immediately with DCE transformation to below the detection limit (~3 μg/L). Butane was turned off from day 24 to day 26 and upon the re-start of butane addition, a "spike" of butane was observed before butane utilizers responded and began degrading the influent butane. During that butane pulse, a transient breakthrough of about 30 μg/L 1,1-DCE was observed at the first monitoring well, but was quickly degraded to below detection limits and remained there through the end of the test. In the non-bioaugmented west leg, initial DCE transformation delayed breakthrough at the monitoring wells, but either the inability of the microbial population to maintain transformation rates or the cessation of butane amendment caused DCE to build up to a concentration of about 85 μg/L in wells SW1 and SW3. The re-start of butane addition on day 26 did not result in greater transformation of 1,1-DCE in the west leg. A 1,1-DCE treatment efficiency of < 25% removal was obtained in the west leg, whereas complete removal (to < 3 μg/L) of 125 μg/L 1,1-DCE was attained in the bioaugmented leg.

Figure 144. Bromide Concentrations in the West (Indigenous) Leg and the East (Bioaugmented) Leg during the 28 Days of the Second Bioaugmentation in the Third Season of Field Testing

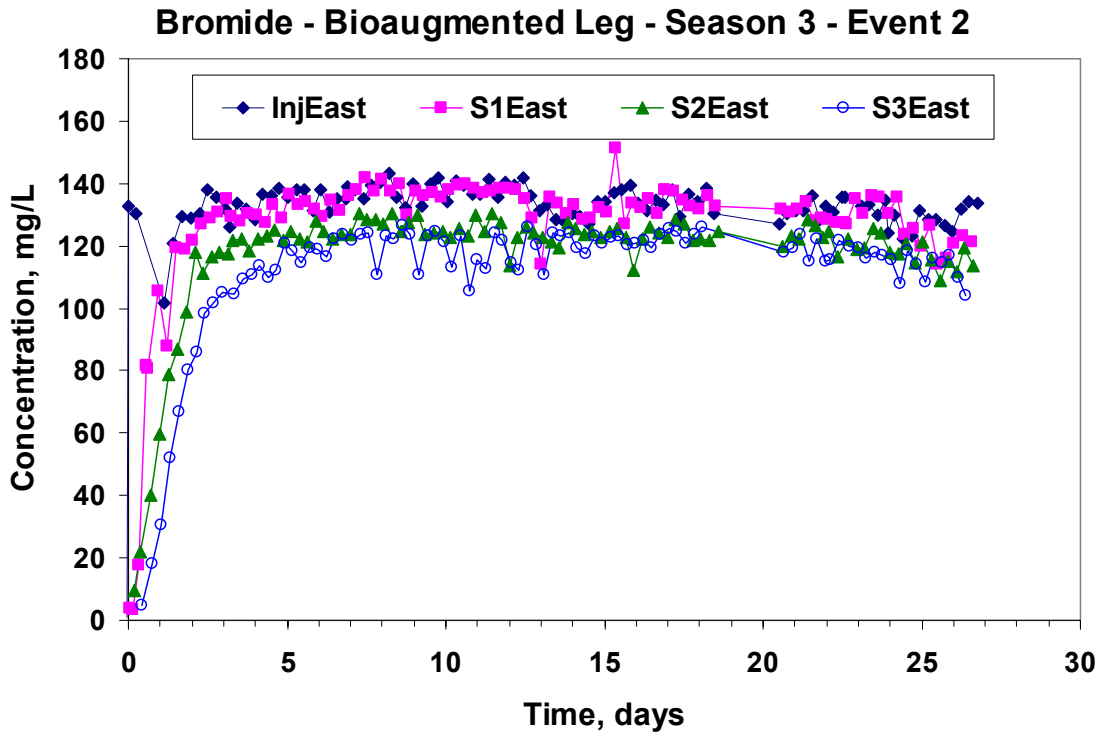

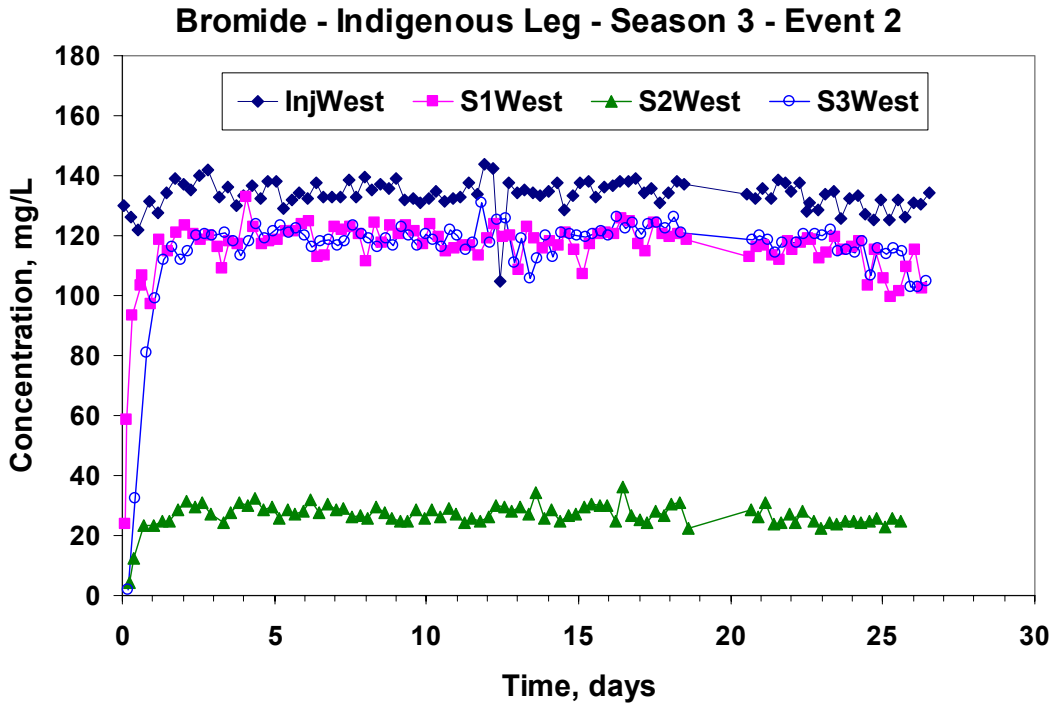

Figure 145. Butane Concentrations in the West (Indigenous) Leg and the East (Bioaugmented) Leg during the 28 Days of the Second Bioaugmentation in the Third Season of Field Testing

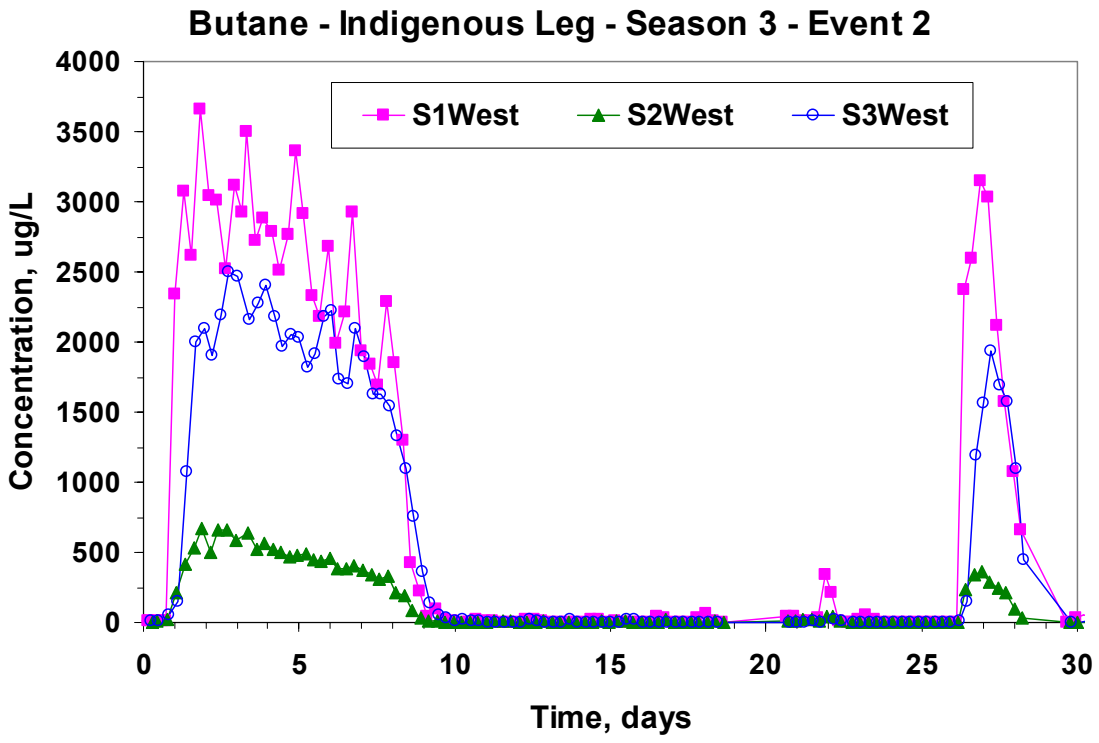

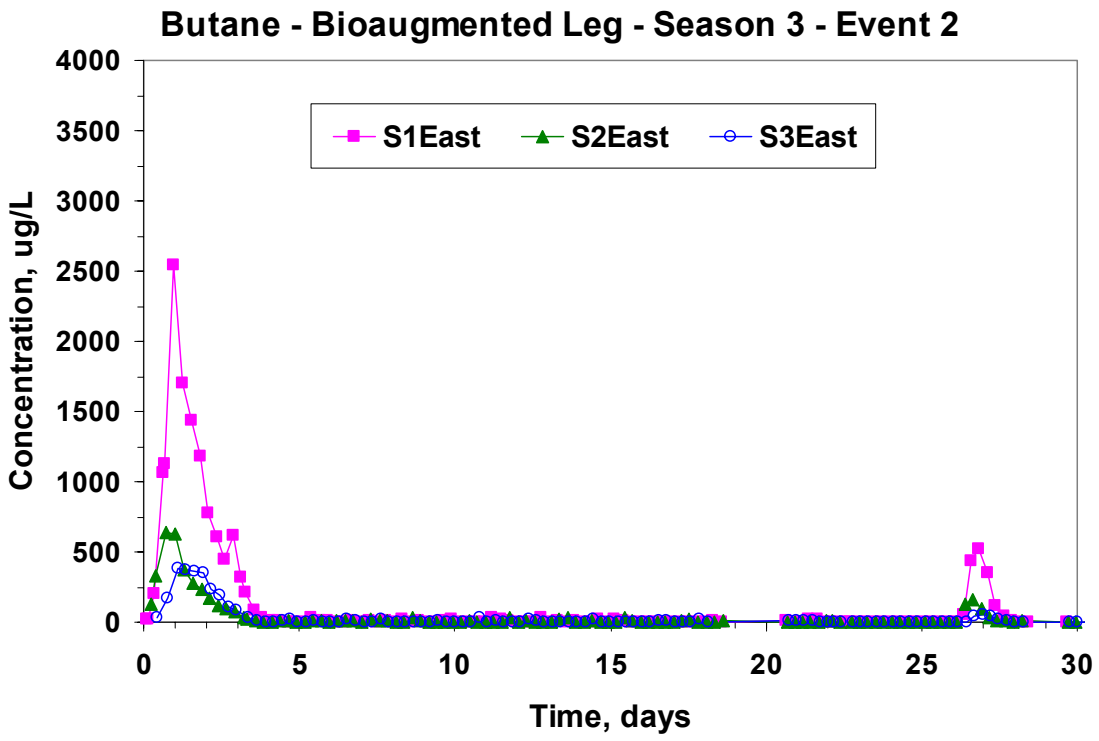

Figure 146. Dissolved Oxygen Concentrations in the West (Indigenous) Leg and the East (Bioaugmented) Leg during the 28 Days of the Second Bioaugmentation in the Third Season of Field Testing

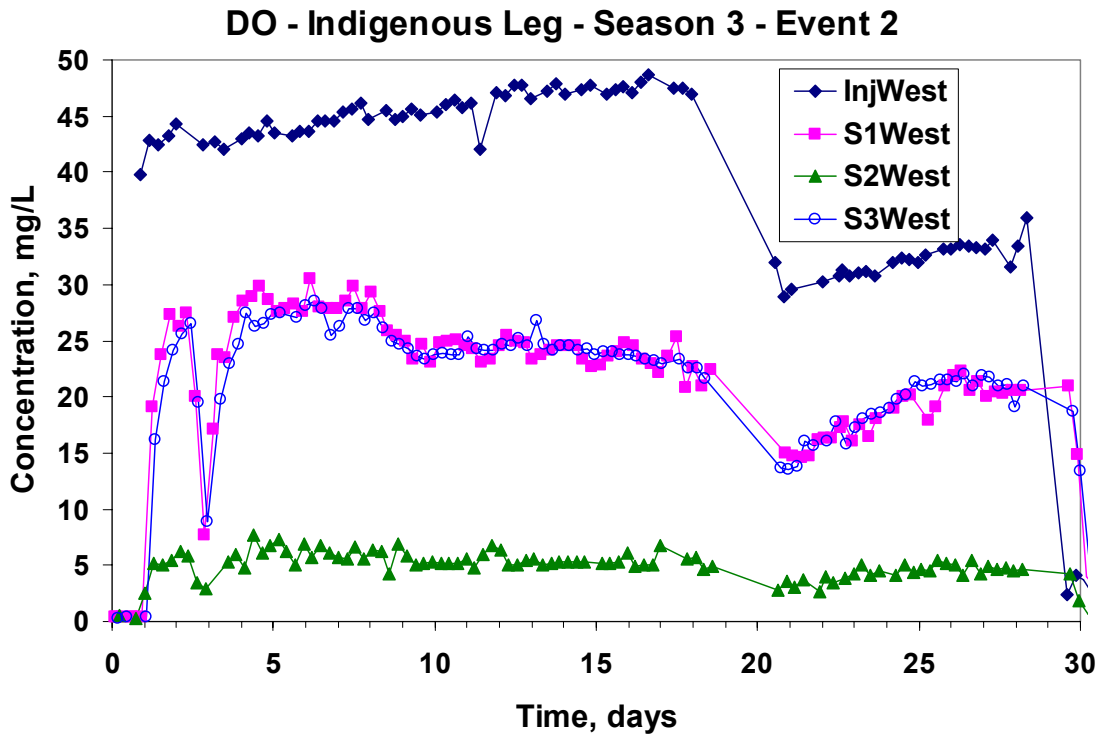

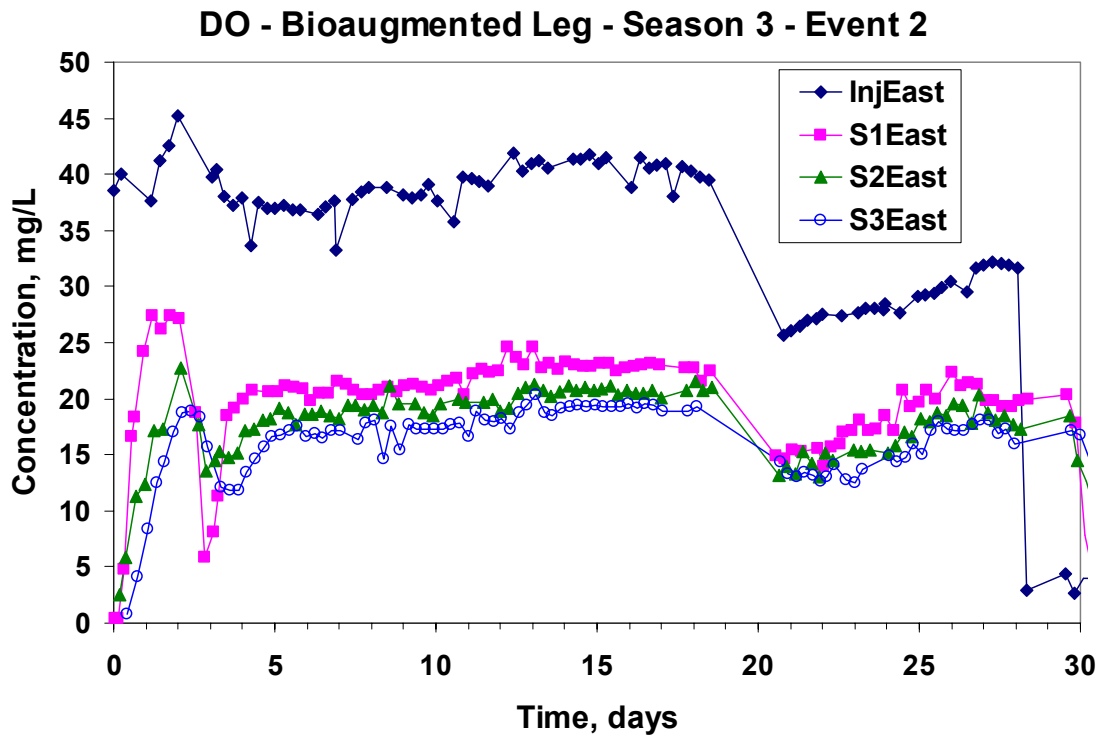

Figure 147. TCA Concentrations in the West (Indigenous) Leg and the East (Bioaugmented) Leg during the 20 Days of the Second Bioaugmentation in the Third Season of Field Testing

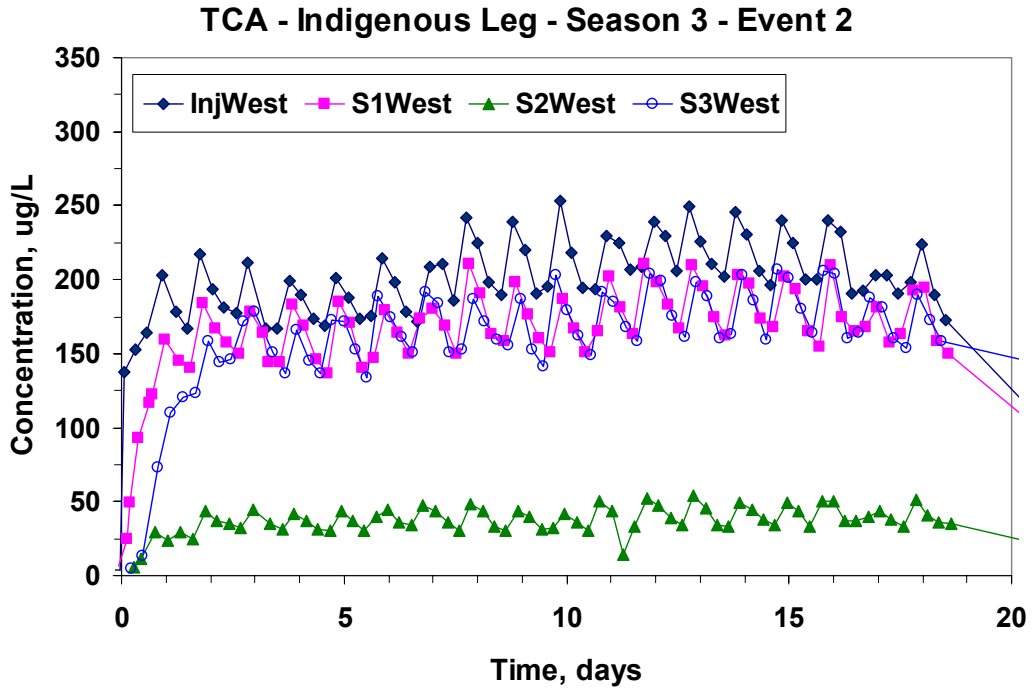

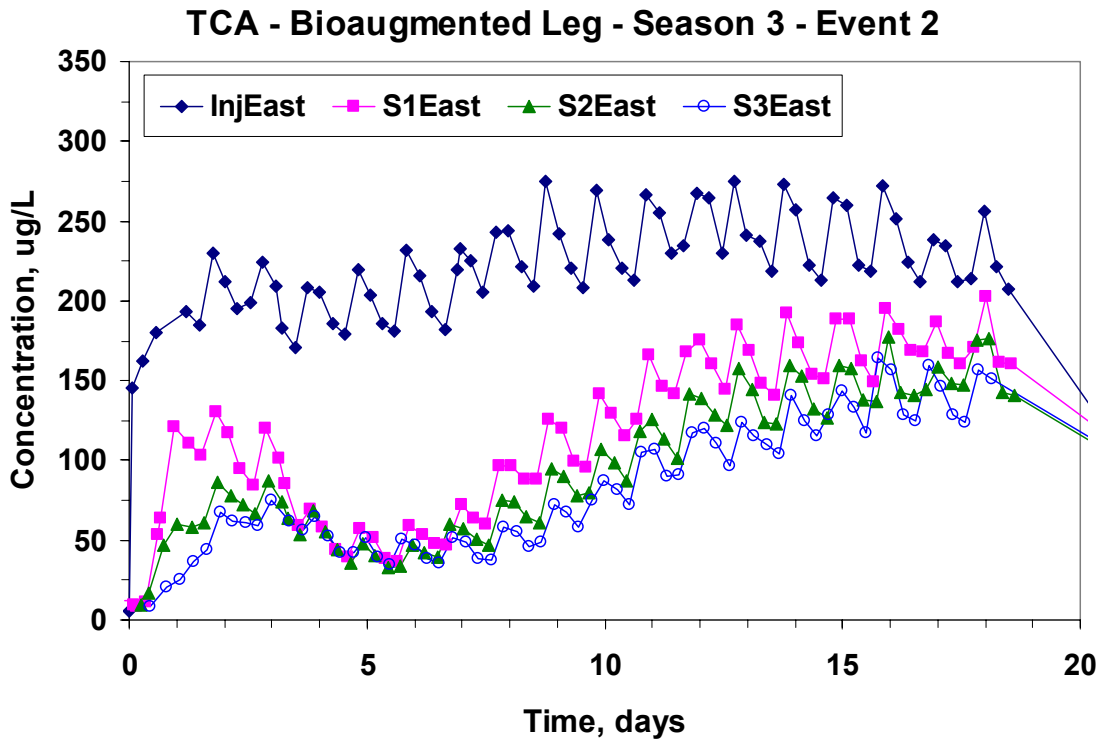

Figure 148. DCA Concentrations in the West (Indigenous) Leg and the East (Bioaugmented) Leg during the 20 Days of the Second Bioaugmentation in the Third Season of Field Testing

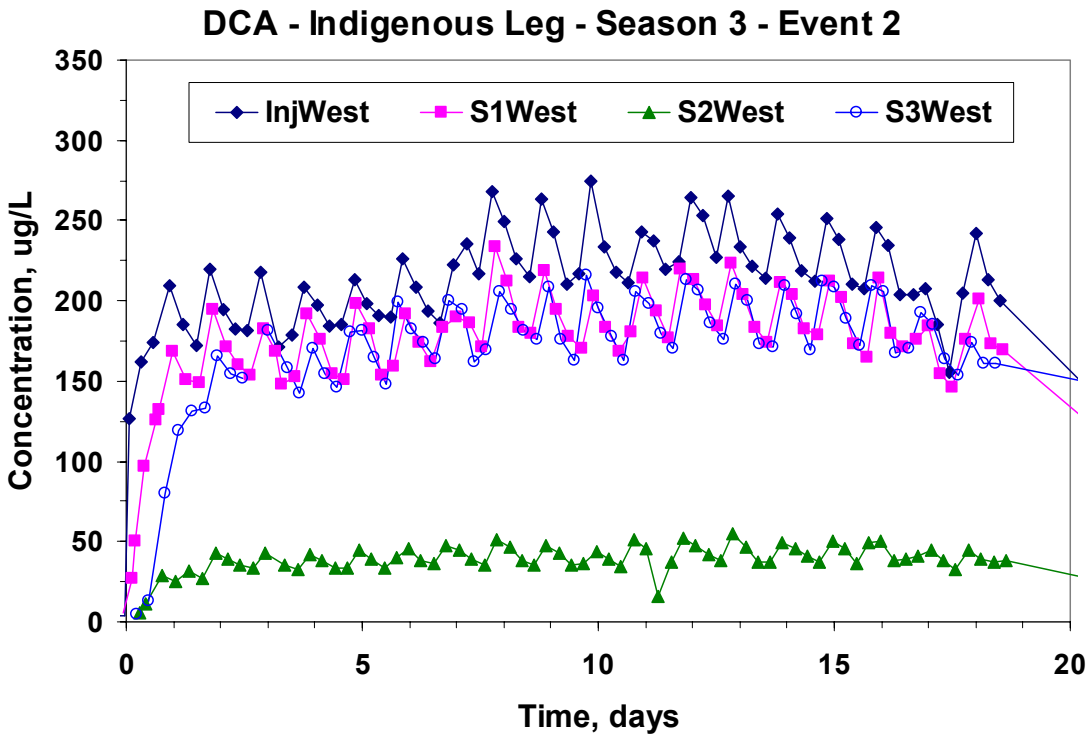

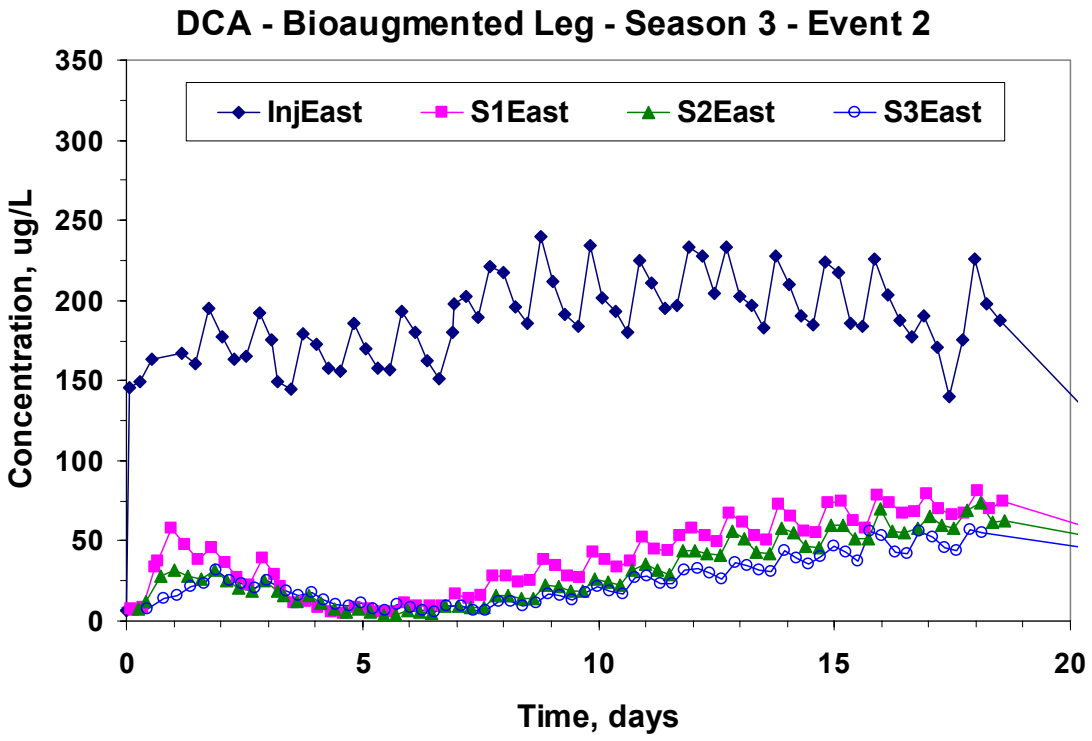

Figure 149. DCE Concentrations in the West (Indigenous) Leg and the East (Bioaugmented) Leg Late in the Second Bioaugmentation Test in the Third Season of Field Testing

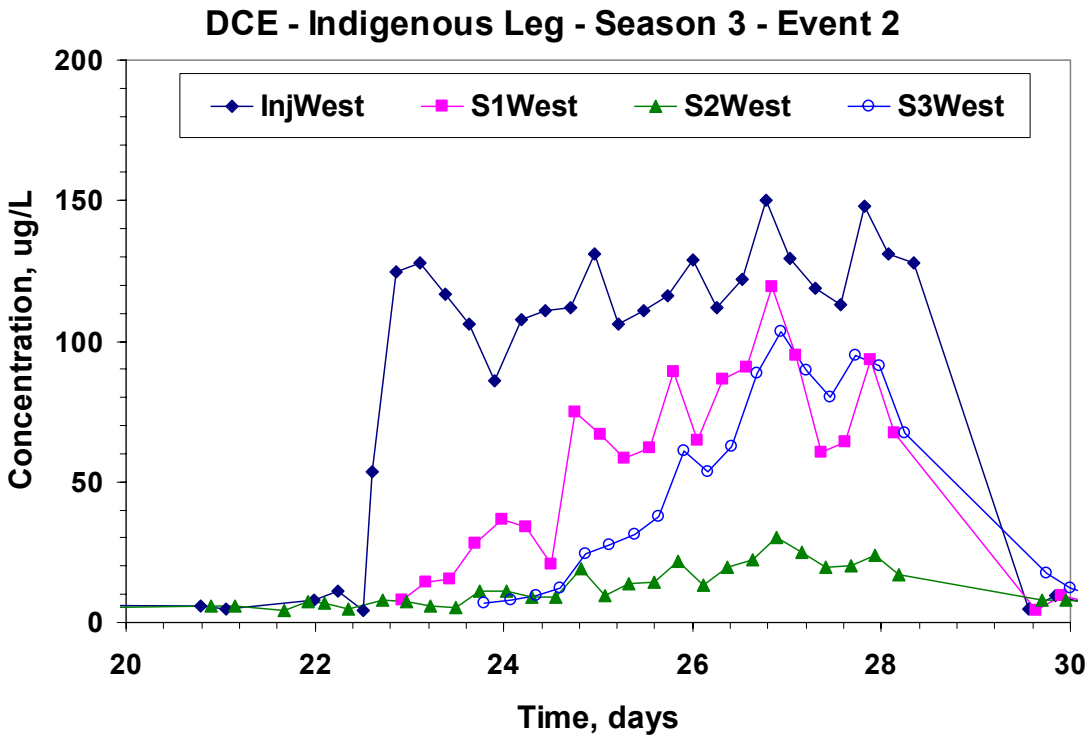

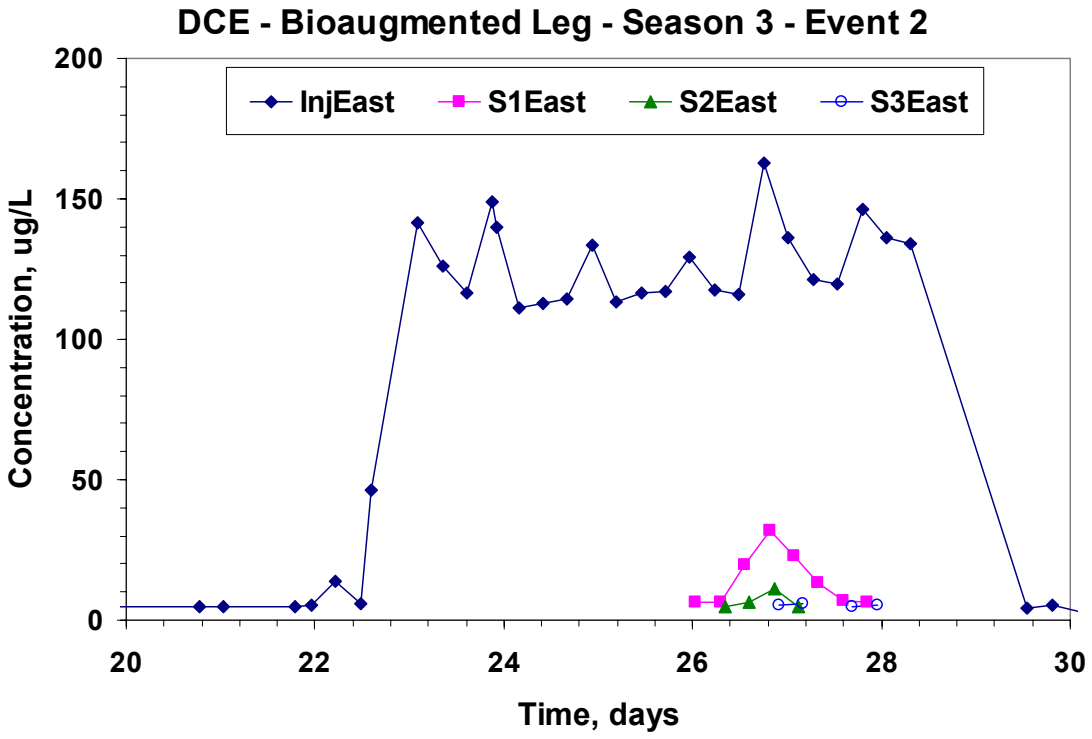

5.3.2.2 Bioaugmentation Event 2: Microbial Results. T-RFLP analysis of the mixed bioaugmentation culture showed that strain 183BP accounted for only 13.5% of the total peak area in the T-RFLP profile (Figure 151). Although the culture was not dominated by strain 183BP, based on representation in the T-RFLP profile up to 0.68 g dry wt. of strain 183BP was augmented to the east well leg. Groundwater samples were acquired for microbial analyses at monitoring wells SE0.5 and SE1 (Figure 150), in an attempt to track the transport and/or proliferation of one member of the bioaugmentation culture, strain 183BP, in the subsurface. prior to bioaugmentation, background groundwater samples taken from the east and west zones revealed that strain 183BP was below the real-time PCR detection limit (~10 cells/mL) in the groundwater.

In well SE0.5 groundwater, a significant increase in the 183bp cell density was observed at the first sampling interval 2 days after bioaugmentation. By day 2, the 183bp cell concentration reached its maximum measured concentration of $(1.46 \pm 0.29) \times 10^5$ cells/mL. Strain 183bp concentration declined until day 5 where it began to level out at about 10^3 cells/mL. Maximum TCA and DCA removal, 80 and 96% respectively, occur during this period from day 4 to day 7. The population appears to remain relatively stable at cell densities between 250 and 1000 cells/mL through day 15 when another period of cell decline occurs resulting in strain 183bp cell densities below the quantifiable detection limit by day 21. In contrast, 183bp cell densities at the SE1 monitoring well increased from less than 50 cells/mL on day 11 (the first sample taken from SE1) to approximately 600 cells/mL on days 15 and 21; however, the large variance in low cell density measurements precludes placing too much emphasis here. After day 21, no further groundwater samples tested positive for strain 183bp cells. Samples taken from the west well leg before bioaugmentation and on day 21 showed no evidence of 183bp cells.

Traditional PCR amplification of 16S rDNA extracted from groundwater samples taken from the SE0.5 well from day 5 to 11, and from the SE1 well on day 11 (data not shown) exhibited the same trend as the real-time PCR analyses. Quantification of band intensity using NIH ImageJ indicated that the concentrations of 16S rDNA amplified by the universal bacterial primers were approximately 15 ng/µL for all the samples; whereas, a decline in concentration of the 16S rDNA amplified from the 183bp-specific primers was observed in well SE0.5, from 8.5 ng/µL on day 5 to 3.9 ng/µL on day 11. These results are in general agreement with the real time PCR results marking a gradual decline in strain 183bp populations over the extent of the study.

Total cell counts on the same groundwater samples used for real time PCR indicated that the total microbial population in wells SE0.5 and SE1 remained greater than 10^5 cells/mL throughout the test (Figure 150). In well SE0.5, the total cell concentration ranged from a low of $(2.76 \pm 0.56) \times 10^5$ cells/mL on day 21 to a high of $(1.06 \pm 0.846) \times 10^7$ cells/mL on day 7. In well SE1, the total cell concentration showed a similar profile as that of well SE0.5. A clear three-orders-of-magnitude difference between the total cell concentrations and the 183bp cell concentrations was observed throughout most of the test. Only on days 2 and 3 did the 183bp count exceed 1% of the estimated total microbial population with values of 4.5% and 1.5% respectively.

Figure 150. Cell Densities Found in Groundwater Obtained from Wells SE0.5 and SE1 during the Second Bioaugmentation Event. Total cell densities were based on DAPI-stained cell counting and 183bp cell densities were estimated from real-time PCR analyses.

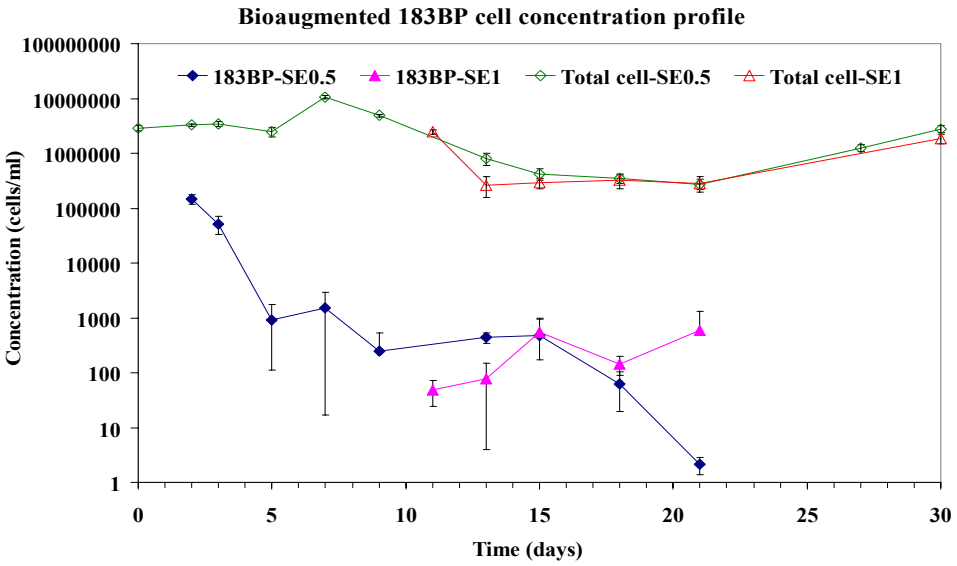

Figure 151. T-RFLP Profiles Generated from the Bioaugmentation Culture Grown in the Laboratory and Groundwater Samples Obtained from Wells SE0.5 and SW0.5 during the Course of the Second Bioaugmentation Event. Universal bacterial primers (27F-B-FAM and 338Rpl) were used in the PCR reactions and the restrictions were performed with the endonuclease *MnI*I (Fermentas, Inc).

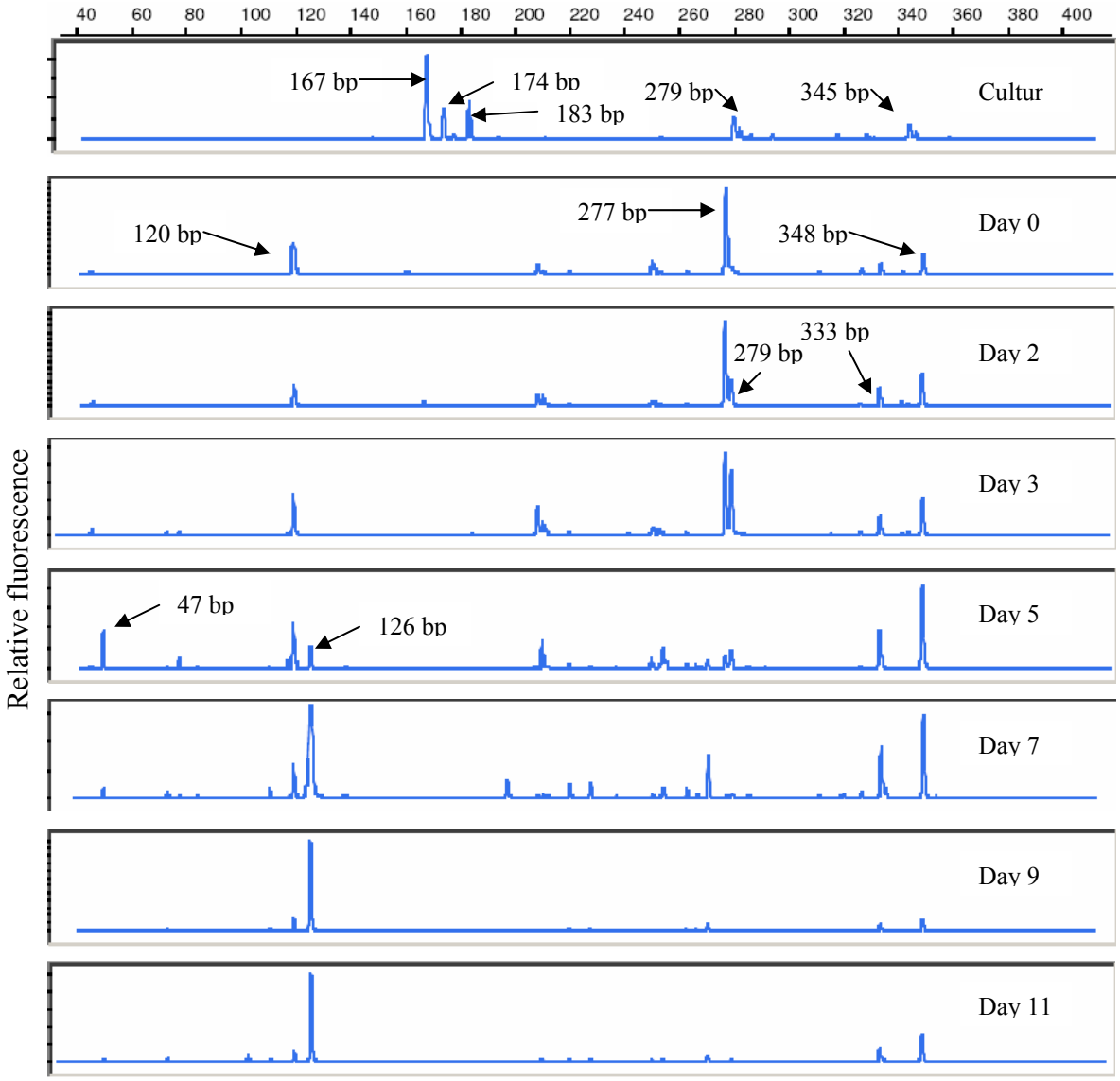

Figure 151 (continued) *Terminal restriction fragment length polymorphism (T-RFLP) profiles generated from the bioaugmentation culture grown in the laboratory and groundwater samples obtained from wells SE0.5 and SW0.5 during the course of the second bioaugmentation event. Samples from the bioaugmented leg were initially dominated by an organism with a TFL of 277bp, which was succeeded by an organism with a TFL of 126bp around day 7, when TCA and DCA removal efficiencies began to decline. An organism with a TFL of 277bp was also present in the west leg prior to butane utilization, but a different pattern emerges in the sample taken on day 21, with a peak at 348bp dominating the more complex profile.*

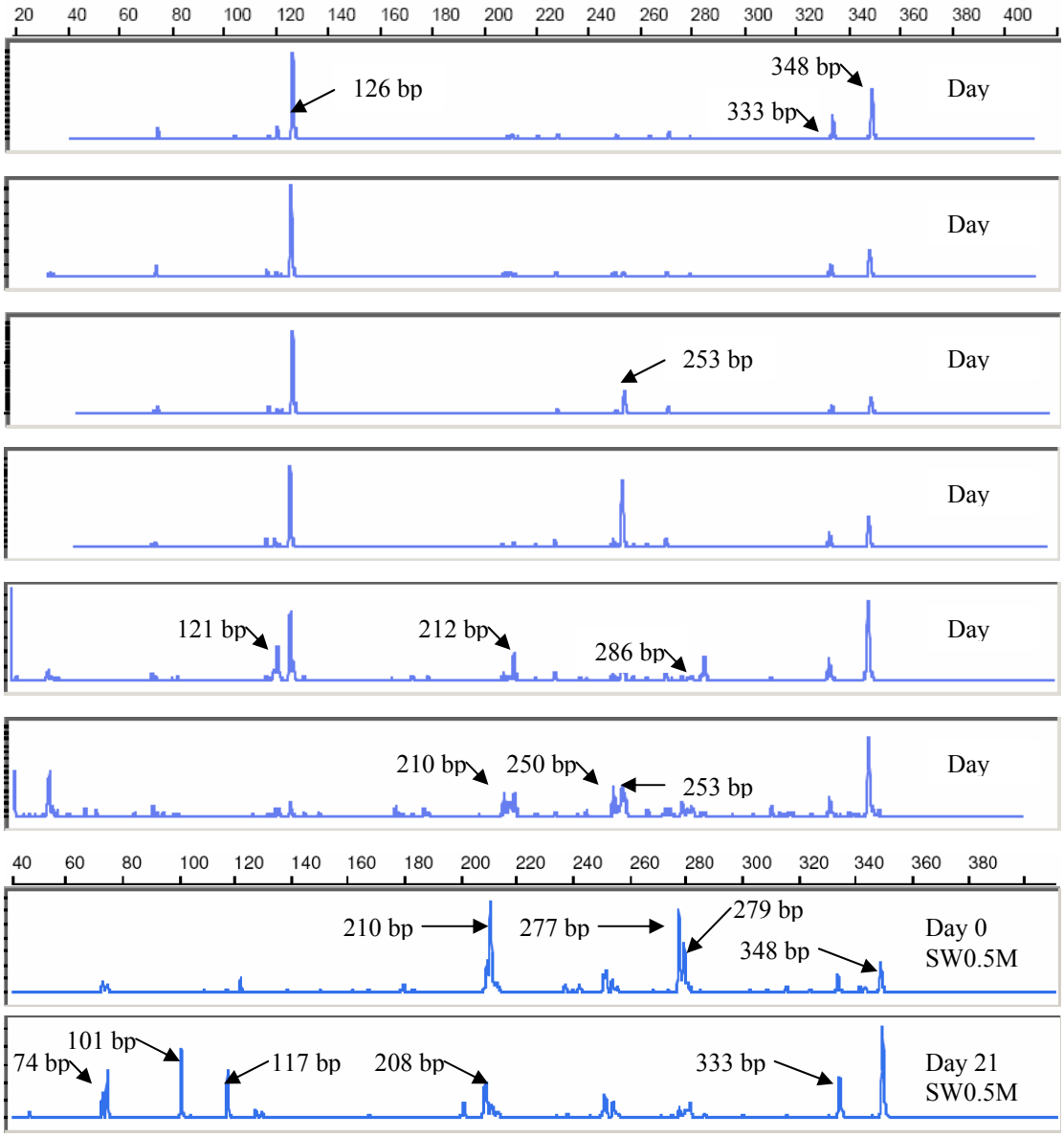

Figure 152. Bar Graph Representation of the Major Peaks Found in T-RFLP Analyses of Groundwater Samples Taken from the SE0.5 and SE1 Wells during the Second Bioaugmentation Event. Similar results were found in both wells with an organism with a TFL of 126bp dominating the profile after 7 -11 days of operation.

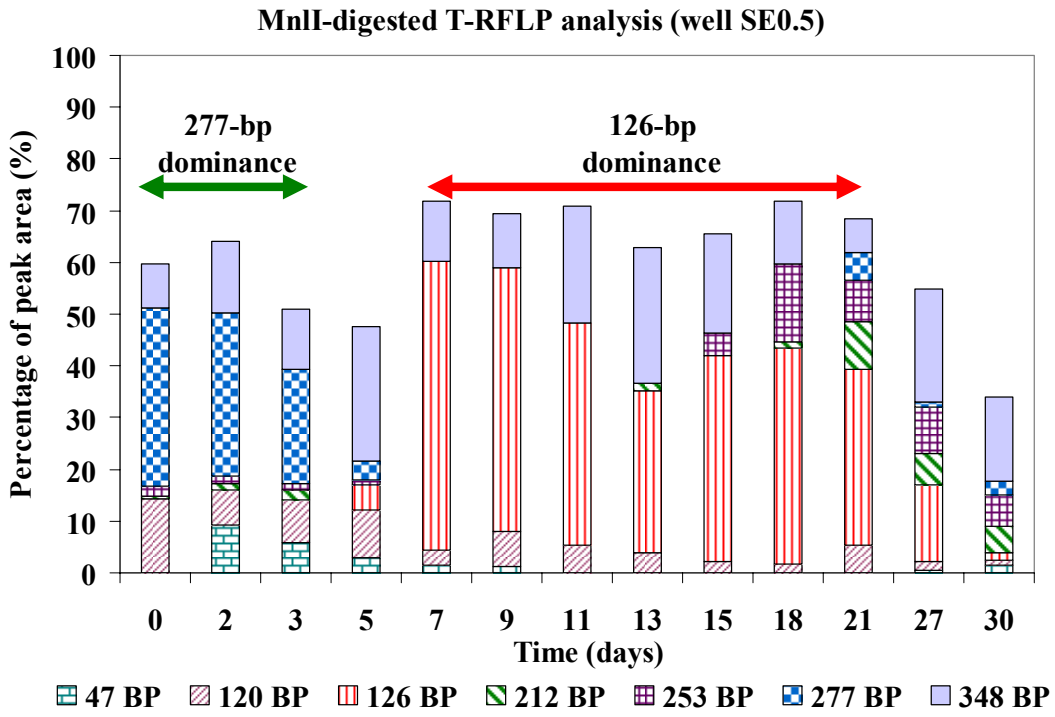

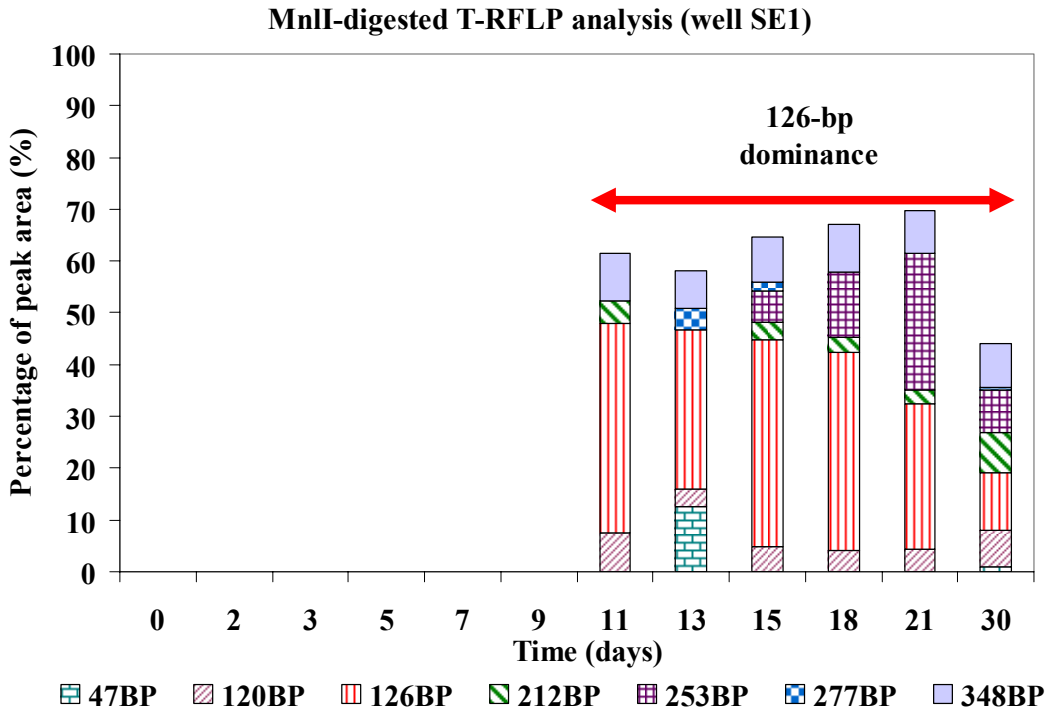

T-RFLP analyses of the bioaugmentation culture and groundwater samples acquired from the field were conducted using universal bacterial primers (27F-B-FAM and 338Rpl) and *Mnl*I and *Hin*6I restriction enzymes. The *Mnl*I T-RFLP profiles provided the highest discrimination of fragments due to increased frequency of recognition sites and the short length of the amplicons used. Considering members of the bioaugmentation culture, no fragments of 183 bp length were observed in any field groundwater samples and the other major peaks in the bioaugmentation culture profile at 167-, 174-, 279- and 345-bp accounted for only trace percentages of total peak areas throughout the test period (Figure 151). However, a clear succession from a major presence of an organism with a TFL of 277bp at the beginning of the study to dominance by an organism with a TFL of 126bp around day 7 occurred.

Before bioaugmentation, T-RFLP profiles of groundwater samples taken from well SE0.5 had major peaks at 120- and 277-bp. In the corresponding non-bioaugmented well leg, SW0.5, at the same time point, the dominant T-RFLP peaks were at 210-, 277-, 279-, and 348-bp. In the bioaugmented well leg, the 277-bp peak accounted for at least 30% of the total peak area on day 0 and day 2 (Figure 151). However, the 277-bp fragments declined to less than 1% of the total peak area by day 7. A clear transition occurs from dominance of the 277-bp fragment to dominance of a fragment with a length of 126-bp during the first 20 days of the study. From day 7 to day 21, the 126-bp peak accounted for at least 30% of the total peak area in all of the samples taken from the bioaugmented leg.

By day 27, a more diverse microbial community appears to have developed as the dominant 126-bp fragment approached the magnitude of the other fragments present, such as peaks at 121-, 210-, 212-, 250-, and 286-bp. A 348-bp fragment was present in every east leg sample analyzed and became the largest peak in T-RFLPs from day 27 and day 30. T-RFLP profiles from well SE1 on day 11, 13, 15, 18 and 21 displayed similar patterns to those of SE0.5 (data not shown). In the SE1 well, the T-RFLP profile of the groundwater samples beginning on day 11 showed that the bacterial community was dominated by the 126-bp fragment from day 11 to day 21 (Figure 152). Unfortunately, there was not a strong correlation between the dominance of any of the major peaks and maximum CAH treatment efficiency. The best treatment occurred between days 4 and 7 where the SE0.5 T-RFLP profiles show a transition from dominance of the 277-bp fragment to the 126-bp fragment. Both the 120-bp fragment and the 348-bp fragment were present throughout the study. As treatment efficiencies decrease from day 7 to day 21, there is not a similar recognizable pattern of decrease in any of the peaks found in the SE0.5 T-RFLP analyses.

Only two samples were obtained and successfully amplified from the non-bioaugmented well leg during the study, on days 0 and 21. On day 0, major fragments of 210-, 277-, 279- and 348-bp peaks were observed in a groundwater sample from the SW0.5 well. The 210- and 279-bp fragments accounted for approximately 32% of the total peak area in the west leg T-RLFP profiles at day 0, while they comprised less than 6% of the peak area in samples from the SE0.5 well. By day 21, the community composition in the SW0.5 well had shifted to a more diverse profile with major peaks at 74-, 101-, 117-, 208-, 333-bp, a dominant peak at 348-bp, and many more small peaks. Interestingly, the SW0.5 profile at day 21 is not too dissimilar to the SE0.5 profile at the end of the study. In both cases the 348-bp peak is the dominant peak, but additional major peaks at 74-, 101-, and 117-bp appear in the non-bioaugmented leg.

T-RFLP analysis was also conducted using *Hin6*I endonuclease (data not shown). It was found that peaks at 62- and 65-bp from *Hin6*I digests corresponded to 126- and 277-bp peaks from *Mnl*I digests. However, no definitive counterpart to the 120-bp peak from *Mnl*I digestion was observed in the T-RFLP from *Hin6*I digestion as it was not a mono-dominant peak in *Mnl*I-digested T-RFLPs. Unfortunately, none of the bacteria strains showing major peaks in *Mnl*I-digested T-RFLP profiles could be identified using in-silico digestion analysis (TAP T-RFLP, RDP II; available at http://rdp.cme.msu.edu/html/TAP-trflp.html#program for free).

5.3.2.3 Bioaugmentation Event 2: Discussion. During this test, effective treatment of chlorinated ethanes was achieved. The maximum removal efficiencies for 1,1,1-TCA and 1,1-DCA were approximately 75% and 95% of the influent values, respectively. In the bioaugmented east zone, butane was depleted within the first three days after bioaugmentation. During this period, increases in the concentrations of chlorinated ethanes were observed in the east monitoring wells. Since butane was present in abundance for organisms to use as primary growth substrate, chlorinated ethane biotransformation was inhibited. Transient maximum butane concentrations in wells SE2 and SE3 of approximately 500 μg/L was insufficient to support growth of a thriving butane-utilizing microbial population much beyond the first monitoring well. After the 3-day lag period, significant removal of 1,1,1-TCA and 1,1-DCA was observed as butane was reduced to near zero values, likely resulting in less CAH transformation inhibition. Upon correcting for dilution based upon bromide tracer concentrations, the concentration of chlorinated ethanes in all of the east leg monitoring wells was approximately the same; indicating no significant removal occurred past the first monitoring well.

Many factors may be associated with the loss of treatment during the late stage of the bioaugmentation test. The gradual loss of treatment efficiency began around day 6, which corresponds to the time required to grow a butane-utilizing microbial population in the indigenous well leg to sufficient density to utilize the added butane. Transformation product toxicity is common during cometabolism of CAHs and may have had a selective negative impact on butane-utilizing organisms capable of 1,1,1-TCA and 1,1-DCA cometabolism. Estimated transformation capacity values for the bioaugmentation culture were 0.11 mg TCA/mg cells and 0.20 mg DCA/mg cells based on previous microcosm tests and mathematical modeling (Mathias, 2002), which, when combined with a microbial yield, become transformation yields of 0.09 mg TCA/mg butane and 0.16 mg DCA/mg butane. Removal of up to 300 mg/L TCA and 530 mg/L DCA, predicted from microcosm studies, was not achieved in the field. This could have been the combination of many factors, including lower CAH concentrations used in the field study compared to the microcosm studies, predation in the subsurface environment, and out-competition by native butane-utilizing organisms.

Successful enumeration of one of the bioaugmented butane-utilizing, CAH co-metabolizing microorganisms, strain 183bp, was achieved by means of 183bp-specific primers using real-time SYBR Green I PCR. Two primers, Ran191F and Ran443R, were designed to be specific to strain 183bp, although specificity analysis indicated that the primer pair has a complete match to sequences of six other known bacterial strains, none of which were found in background sampling at the site. Melting curve analysis of real time PCR amplicons indicated that only one out of all of the samples generated identifiably significant non-specific amplicons; however, the six known organisms also targeted with the primers would result in amplicons identical to that of

strain 183bp, possibly over-estimating the presence of 183bp in groundwater samples. This assay allowed detection and quantification of strain 183bp in groundwater samples collected from the bioaugmentation test site at Moffett, CA.

The real-time PCR cell quantification method is subject to uncertainties due to specificity of primers, rDNA content of the target cells, DNA extraction efficiencies, and inhibition of PCR reactions by unknown sample constituents. In this study, cell quantification was performed by correlating threshold cycle values from SYBR-Green-I-bound 16S rDNA amplicons to sample cell densities. This conversion was based upon two assumptions: 1) each cell contains the same amount of rDNA under all environmental conditions; and 2), DNA extraction efficiency is the same for all sample types over a wide range of cell concentrations. However, since a number of environmental conditions such as nutrient limitation and chemical stress can affect cells' physiological state, the DNA content may vary among cells. Another challenge was the presence of unknown PCR inhibitors. Many of the PCR reactions using non-diluted template DNA did not amplify well. Comparison of non-inhibited undiluted sample amplification to results obtained with 1:10 and 1:100 dilutions showed good agreement, so 1:10 dilutions were used for sample analysis to minimize the effects of PCR inhibition.

A real-time PCR standard curve was performed on serial dilutions of DNA extracted from a pure strain 183BP culture and compared to a standard curve performed on DNA extracted separately from serial dilutions of the culture covering 7 orders of magnitude. Similar standard curves were produced with cell numbers predicted by DNA dilution being larger than those predicted by separate extractions for threshold cycle values less than 34. For cell counts from 1.5×10^3 cells/mL to 2.5×10^4 cells/mL the two standards produced less than 10% difference in cell estimates. For all threshold cycle values, the difference in cell estimates using the two standards was less than 50%, or one-half an order of magnitude. The method of DNA dilution was the chosen standard used for analysis in this study.

Groundwater samples analyzed by real-time PCR showed that strain 183bp concentration in well SE0.5 reached highest abundance of $(1.46 \pm 0.29) \times 10^5$ cells/mL at the first sample period, 2 days after bioaugmentation. Using a nominal cell weight of 2.8×10^{-13} g dry wt./cell (Rittman and McCarty, 2001), the maximum cell density translates to a mass concentration on the order of 0.04 mg cells/L, a population too small to provide the CAH treatment seen at the field site. Since butane was completely removed by the first monitoring well, microbial growth also preceded the first monitoring well. So, although the waterborne concentrations of strain 183bp were below a density required for effective treatment, there may have been significantly more cells attached to aquifer solids closer to the injection well providing a measure of treatment. The average total cell count was about 3×10^6 cells/mL, or using the same average weight per cell, approximately 0.8 mg/L, which is also low considering a time-averaged butane concentration of approximately 3.3 mg/L, possibly indicating that the majority of cells were attached to aquifer solids rather than suspended in the groundwater flow.

Since the 183bp-specific primers perfectly match the sequences of six other known organisms, melting temperatures of the 16S rDNA fragment sequences that can be amplified by these two primers were examined. It was determined from sequence information obtained from GenBank that all of the fragments were expected to have the same length and G+C content. The melting

temperatures were calculated using the equation as follows (Stahl and Amann, 1991): $T_d = 4N_{G+C} + 2N_{A+T}$, where N_{G+C} and N_{A+T} are the numbers of G and C bases and of A and T bases, respectively. The predicted melting temperatures for all fragments were 88 ºC, very close to the value (~88.3 ºC) observed from melting curve analysis. Thus, the melting curve analysis may distinguish non-target amplicons having different melting temperature, but not those originating from any sequence of the six known strains.

No treatment of the chlorinated ethanes was observed in the non-bioaugmented well leg, confirming the inability of the indigenous population to transform 1,1,1-TCA or 1,1-DCA. Additionally, the time to complete butane utilization was more than twice as long as that in the bioaugmented east zone, indicating a small existing population of butane-utilizers prior to chemical augmentation. T-RFLP and real-time PCR results of samples taken from the non-bioaugmented well leg before bioaugmentation and again after a robust butane-utilizing consortia had developed at day 21 showed no evidence of strain 183BP cells in the microbial population of the west well leg.

The T-RFLP pattern indicated that shifts in the native bacterial community structure likely resulted from bioaugmentation and chemical amendment. Although the community remained moderately conserved during the experiment, an organism(s) with a T-RFL of 277-bp that was present in some abundance before bioaugmentation and chemical amendment dominated the community profile for the first three days. Over the next 4 days, the microbial community transitioned to dominance by an organism(s) with a T-RFL of 126-bp that lasted through day 27 of the study (the end of butane addition). During this time, treatment efficiency initially increased and then decreased significantly from days 5-21. An organism with a T-RFL of 277-bp was evidenced in the non-bioaugmented west well leg, indicating that the organism was probably not active towards 1,1,1-TCA transformation. An organism with a T-RFL of 126-bp was not seen in the west well leg samples. Organisms with T-RFLs of 333- and 348-bp were present throughout the entire bioaugmentation test and seen in samples from both well legs and an organism with a T-RFL of 120-bp was present throughout the test in the east well leg. Unfortunately, none of the T-RFLs could be associated with a phylogenetic type using the RDPII 16S rDNA database and computer-simulated digestion analysis. A highly diverse community structure was observed at day 30 after the termination of butane addition to the field, presumably as part of a transition back to native environmental conditions.

5.3.3 Third Bioaugmentation Event of the Third Field Season

The third bioaugmentation event of the third field season began on November 19, 2003, and ran for only 8 days before CAH delivery to the field was halted. All three CAHs were added to the injection stream at the highest concentrations used during the field tests of 375 μg/L, 260 μg/L, and 300 μg/L for TCA, DCA, and DCE, respectively. A butane-utilizing isolate, strain 183bp, was bioaugmented to the east well leg to begin the test. The test ended prematurely after only eight days of CAH injection due to mechanical failure of the CAH and bromide injection systems. A 62 mg/L chlorox bleach solution in groundwater was pumped through both well legs at the end of bioaugmentation event III for approximately 12 hrs before flushing with recycled groundwater. The bleach was added as a biocide to reduce the butane-utilizing microbial populations that had developed after successive bioaugmentations and butane stimulation. A period of two weeks separated the biocide application and the third bioaugmentation of the season.

Butane was utilized to below 1 mg/L by day 3 in the bioaugmented leg and by day 6 in the indigenous leg. Very high butane concentrations, up to 20 mg/L, were recorded in the indigenous well leg in the first few days. It is uncertain if the butane concentrations were actually that high throughout the test. Butane concentrations calculated from influent concentrations and cycle times was 7.3 mg/L. Transformation efficiencies were difficult to establish for this test due to the short duration of the test and the inconsistency of influent CAH concentrations. TCA and DCA were not significantly transformed in the west control well leg and transformation in the bioaugmented leg was also minimal, most likely due to competition and toxicity from the high concentration of DCE at approximately 300 μg/L. DCE removal in the bioaugmented leg occurred out past the first monitoring well with calculated efficiencies of removal of 50%, 74%, and 83% for wells SE1, SE2, and SE3, respectively. DCE transformation in the indigenous leg was minimal through day 4 while butane was present, but picked up to approximately 35% and 58% removal for a short period from day 7 to day 9 in wells SW1 and SW3, respectively, before loss of CAH injection.

5.3.3.1 Bioaugmentation Event 3: Chemical Results. The concentrations of bromide, 1,1,1-TCA, 1,1-DCA, 1,1-DCE, butane, and DO in the two injection wells (EI and WI) and the three monitoring wells (SE1, SE2, SE3, SW1, SW2 and SW3) on each leg were monitored semi-continuously for the 10-day duration of the test. Each sample required approximately 50 min to acquire, prepare, and analyze, resulting in approximately 25 samples and 3 standards run each day. Injection flowrates to both well legs was 1.25 L/min while extraction flowrate in the non-bioaugmented west well leg was approximately 7.5 L/min while that in the bioaugmented east well leg was about 5.9 L/min, resulting in slightly faster travel times through the non-bioaugmented leg.

Nine hours prior to bioaugmentation, oxygen-sparged groundwater was introduced to both well legs along with approximately 20 ppm peroxide. Two hours before bioaugmentation, butane and CAHs addition began. Approximately 4 g dry wt. of a monoculture of butane-utilizing strain 183 bp culture was diluted in 4 L of groundwater and introduced into the injection stream to the east well leg over a period of ten minutes to initiate the test (t = 0 days). Bromide breakthrough data was obtained for both well legs with 50% of injection concentrations reached in 0.4 d, 1.0 d, and 1.4 d in wells SE1, SE2, and SE3, respectively, and 0.15 d and 0.5 d for wells SW1 and SW3,

respectively (Figure 153). Bromide recoveries of 98%, 88%, and 82% were found for wells SE1, SE2, and SE3, respectively, with 92% and 89% recovery in wells SW1 and SW3. Bromide injection was lost on day 4, possibly before the bioaugmented leg had reached pseudo-steady state operation.

While dissolved oxygen concentrations were stable in the bioaugmented leg, oxygen delivery to the indigenous leg was spotty for the first few days and high butane concentrations, up to 20 mg/L, were also recorded initially in the indigenous leg (Figure 154). The problem was fixed on day 3 and stable oxygen delivery was achieved for the remainder of the test. Butane levels in the indigenous leg fell to about 4 mg/L on day 3, closer to the estimated time-averaged butane concentration of 7.3 mg/L calculated from cycle times. It is possible that butane delivery exceeded the calculated value, but the DO data indicate that past day 3, DO utilization was approximately that found in previous tests.

1,1,1-TCA, 1,1-DCA, and 1,1-DCE were introduced continuously at approximately 375 μg/L, 260 μg/L, and 300 μg/L, respectively. Alternate pulses of butane-sparged and oxygen-sparged groundwater at influent concentrations of about 16 mg/L and 20 mg/L, respectively, were pulsed to the field for times of 27 minutes and 205 minutes, respectively, with a 4 minute nitrogen purge separating each pulse. In this way explosive gas mixtures were not formed and the alternating feed encouraged microbial growth farther from the injection well.

Complete butane utilization was achieved in bioaugmented well SE1 by about 6 days, but concentrations were below 500 μg/L by day 4 (Figure 154). Butane concentrations in the indigenous leg were initially much higher than anticipated at up to 20 mg/L at SW1 and 12 mg/L at SW3. Complete butane utilization was not achieved by well SW1 in the indigenous leg throughout the 10 days of the test, but residual concentrations were generally below 1 mg/L past day 5. The calculated time-averaged butane concentrations fed to the field based on influent concentrations and cycle times was about 7.3 mg/L. It is uncertain whether large amounts of butane made it to the indigenous leg, both legs, or whether an instrument malfunction resulted in the initial high butane concentrations. DO utilization calculated from cycle-corrected influent concentrations and an additional 10 mg/L attributed to peroxide decomposition ranged from 12 to 15 mg/L on both well legs, values similar to those obtained in previous tests.

Transformation efficiencies were difficult to establish for this test due to the short duration of the test and the inconsistency of influent CAH concentrations. In the non-bioaugmented west leg, TCA and DCA concentrations rapidly approached influent values and remained there throughout the test (Figures 156 and 157). Times to 50% TCA breakthrough were about 0.2 d and 0.7 d for wells SW1 and SW3, respectively, compared to 0.15 d and 0.5 d for bromide breakthrough, indicating little retardation in transport of the CAHs. In the bioaugmented east leg, times to 50% TCA breakthrough were about 0.8 d, 1.8 d, and 2.7d for wells SE1, SE2, and SE3, respectively, approximately twice those for bromide breakthrough, indicating TCA was somewhat transformed in the bioaugmented leg. TCA was at influent concentrations in the bioaugmented leg by day 6. DCA delivery was too intermittent to determine breakthrough times, but again, by day 6 influent values appear to be throughout the field.

DCE was added to the field at a concentration of approximately 300 μg/L (Figure 158). Although spotty delivery to the indigenous leg made interpretation difficult, significant DCE transformation was not observed until about day 4 when butane concentrations also fell to low values. Based on concentrations from day 7 to day 9, approximately 35% and 58% DCE removal was achieved by wells SW1 and SW3, respectively. However, DCE concentrations were rising in wells SW1 and SW3 when DCE addition was terminated on day 8. In the bioaugmented well leg, 50%, 74%, and 83% removal were found at wells SE1, SE2, and SE3, respectively, between days 4 to7 when influent DCE concentrations were fairly stable. Overall, up to 250 μg/L DCE was transformed in the bioaugmented leg while a maximum of 175 μg/L DCE was transformed in the indigenous leg. Significant DCE transformation appeared to be occurring in both legs past the first monitoring well, 1.0 m from the injection wells. This was most likely due to inhibition between the DCE and butane, both of which were found to have fast transformation kinetics in laboratory systems, and the effects of DCE transformation product toxicity. Due to the short duration of the test, the sustainability of DCE transformation was unable to be determined. However, DCE concentrations were rising in both legs at the end of the test indicating that DCE transformation product toxicity and/or other factors were probably leading to diminished transformation efficiencies.

Figure 153. Bromide Concentrations in the West (Indigenous) Leg and the East (Bioaugmented) Leg during the First 4 Days of the Third Bioaugmentation Event in the Third Season of Field Testing

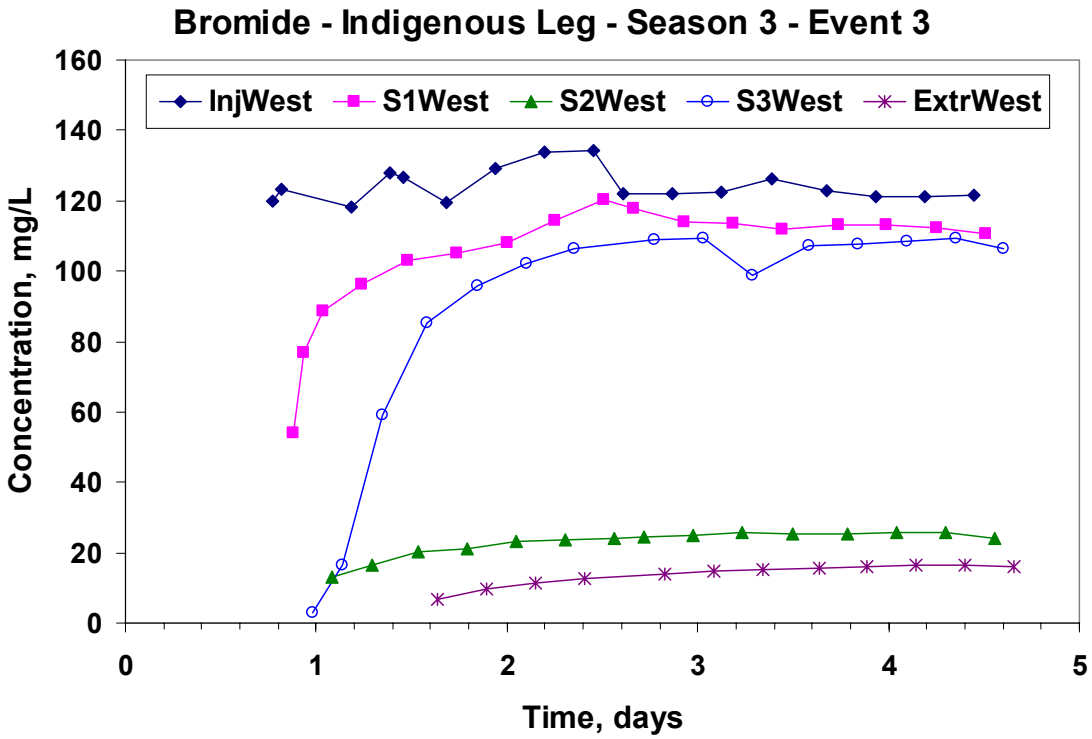

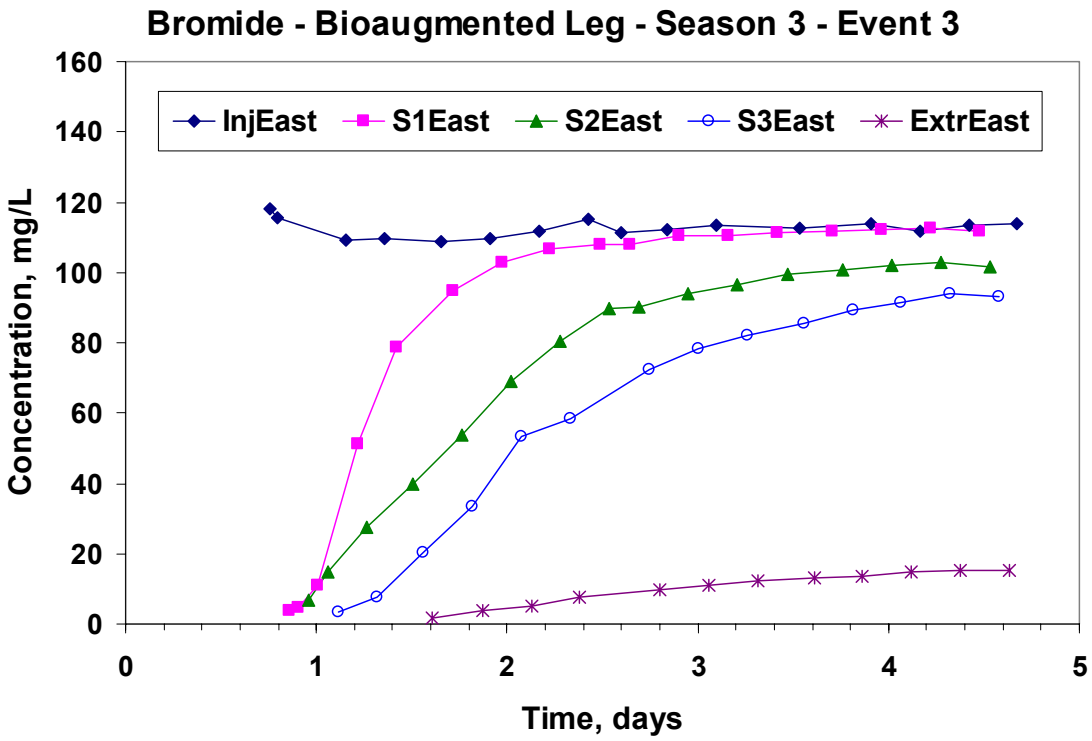

Figure 154. Butane Concentrations in the West (Indigenous) Leg and the East (Bioaugmented) Leg during the Third Bioaugmentation in the Third Season of Field Testing

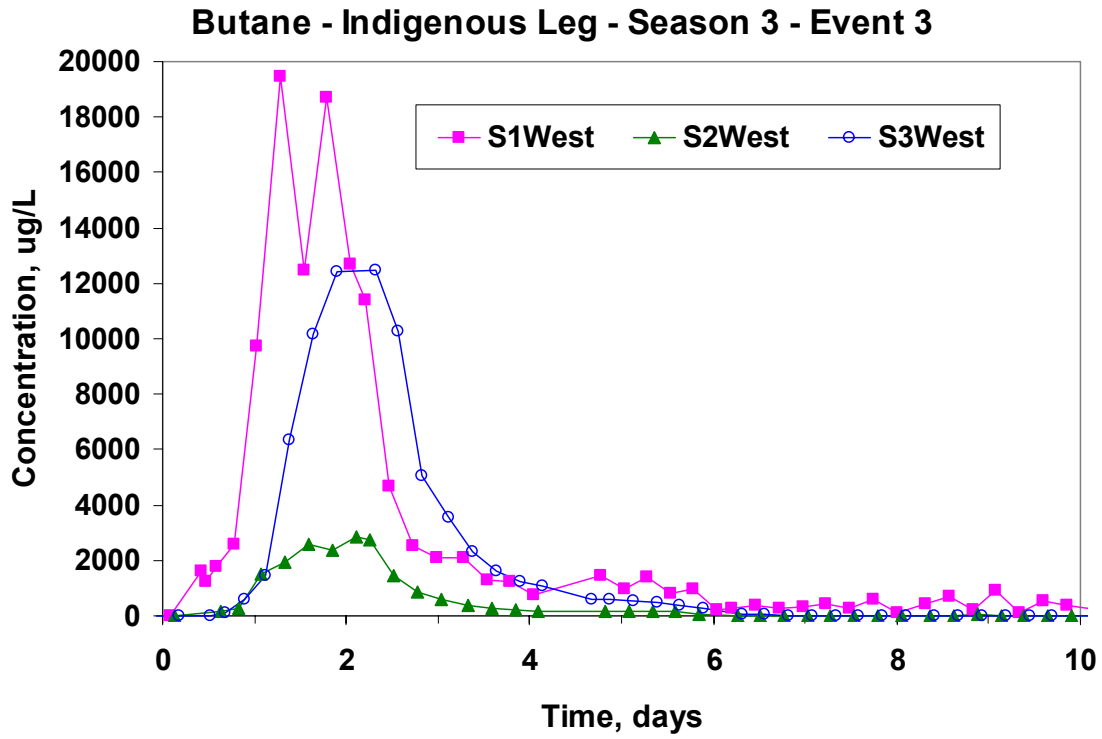

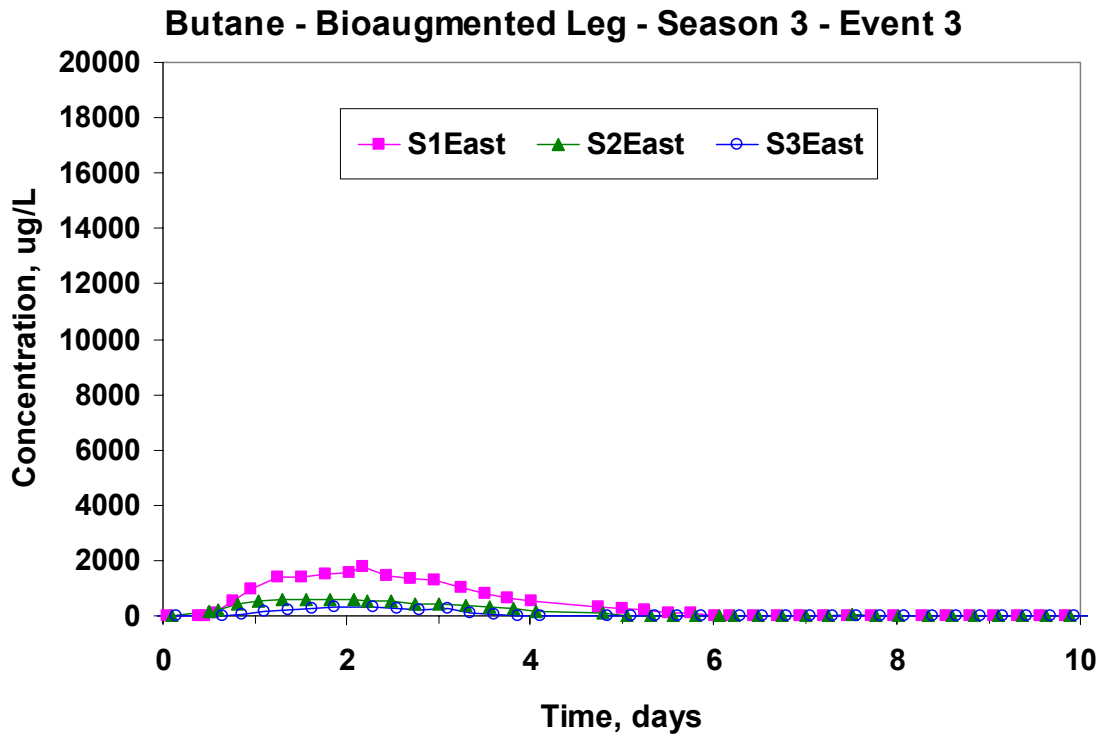

Figure 155. Dissolved Oxygen Concentrations in the West (Indigenous) Leg and the East (Bioaugmented) Leg during the Third Bioaugmentation in the Third Season of Field Testing

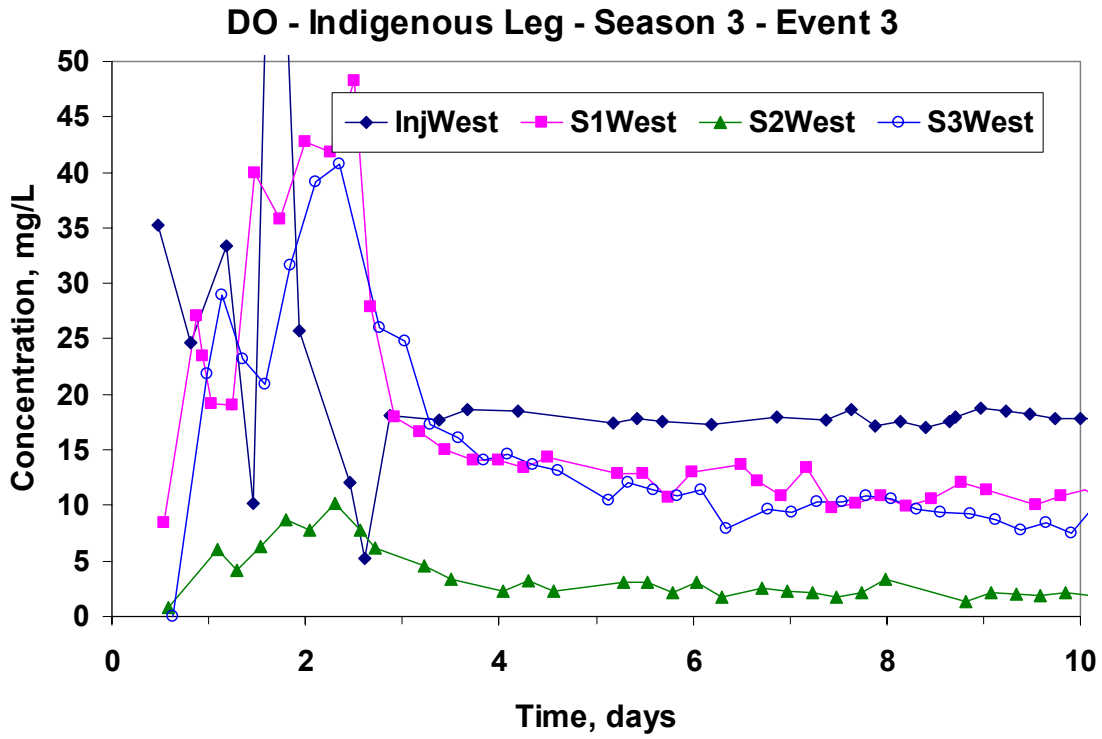

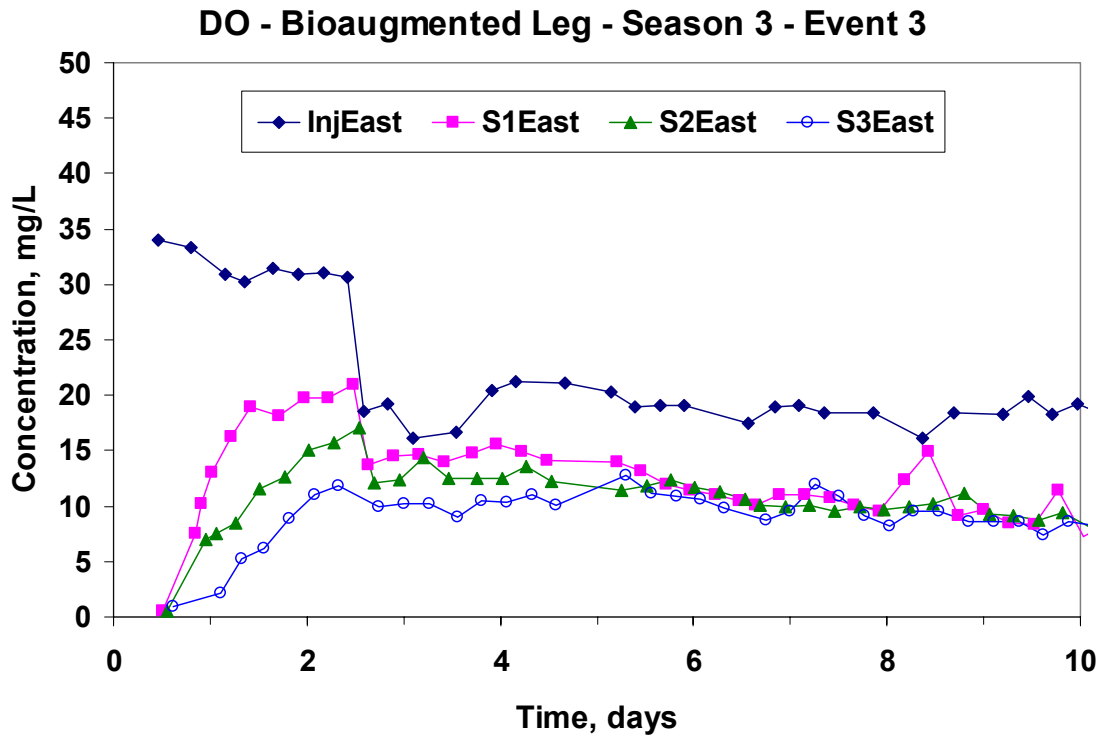

Figure 156. TCA Concentrations in the West (Indigenous) Leg and the East (Bioaugmented) Leg during the Third Bioaugmentation Event in the Third Season of Field Testing

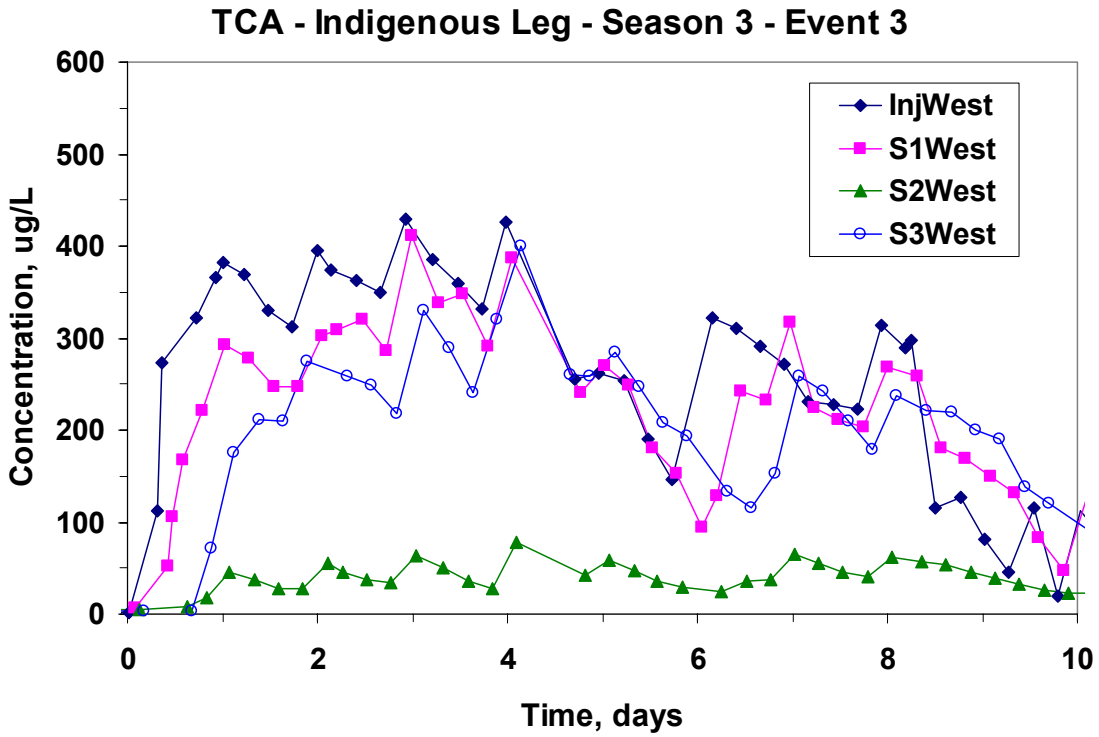

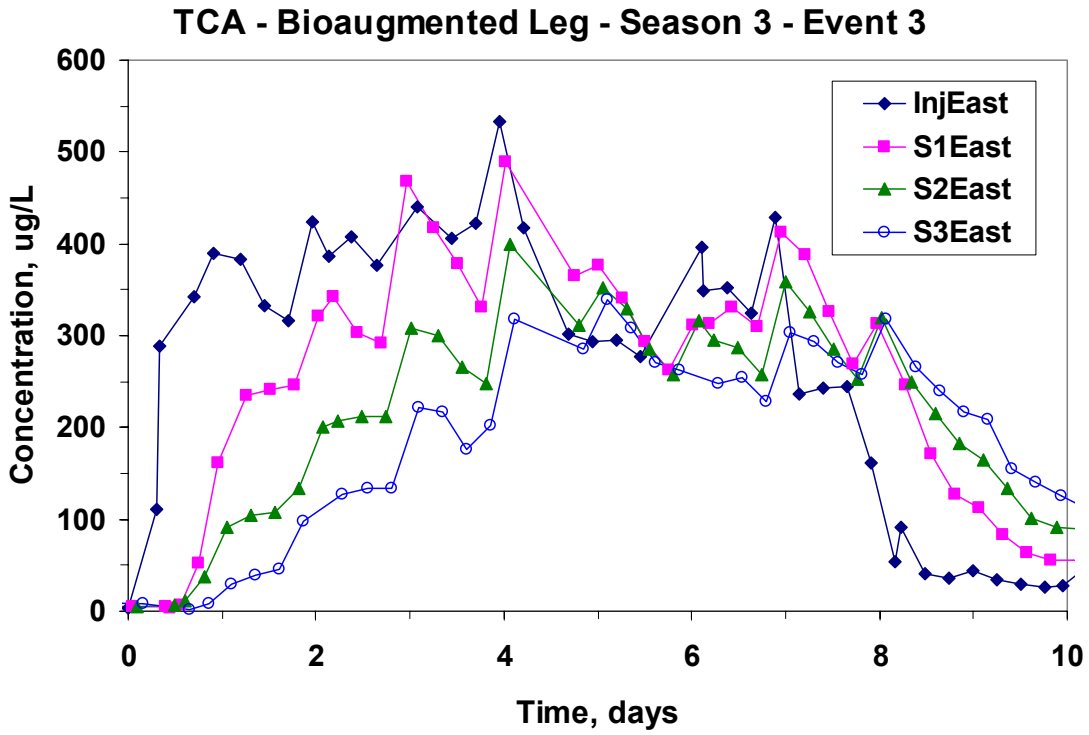

Figure 157. DCA Concentrations in the West (Indigenous) Leg and the East (Bioaugmented) Leg during the Third Bioaugmentation Event in the Third Season of Field Testing

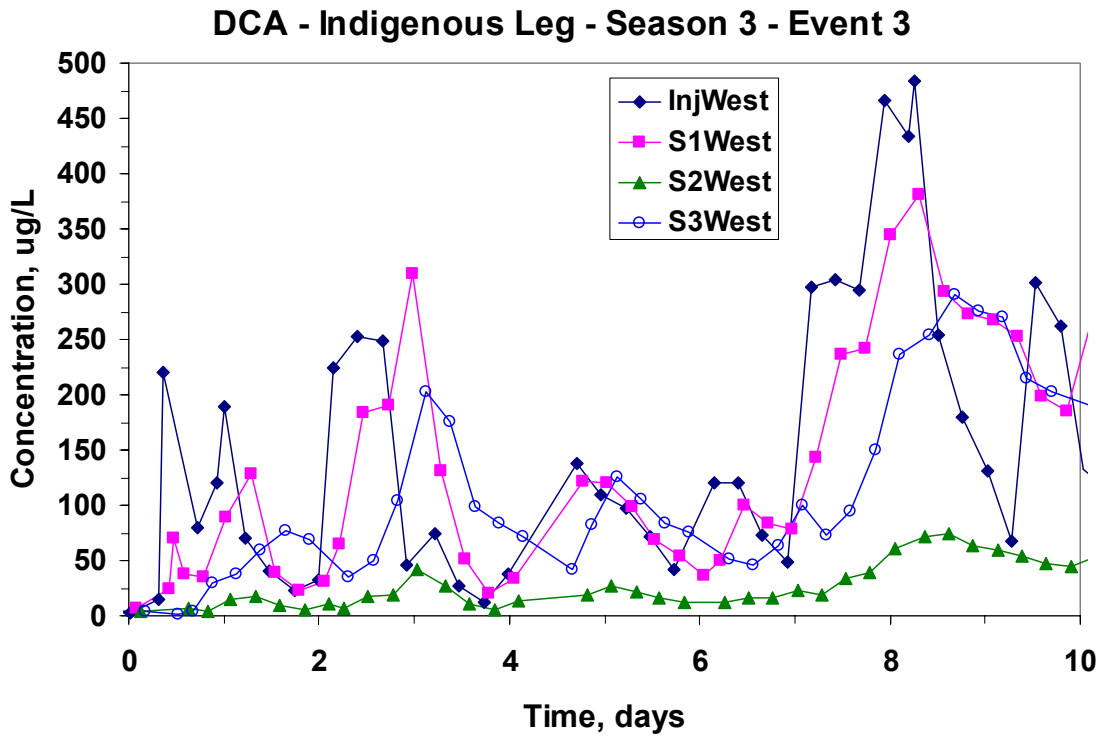

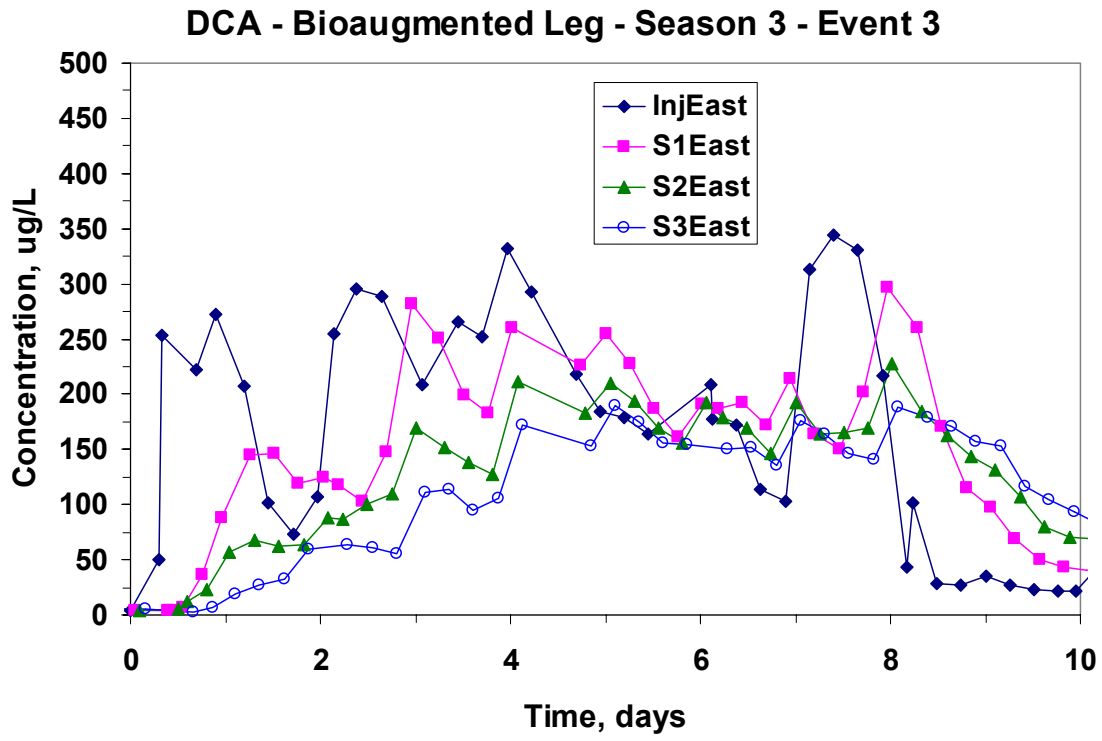

Figure 158. DCE Concentrations in the West (Indigenous) Leg and the East (Bioaugmented) Leg during the Third Bioaugmentation Event in the Third Season of Field Testing

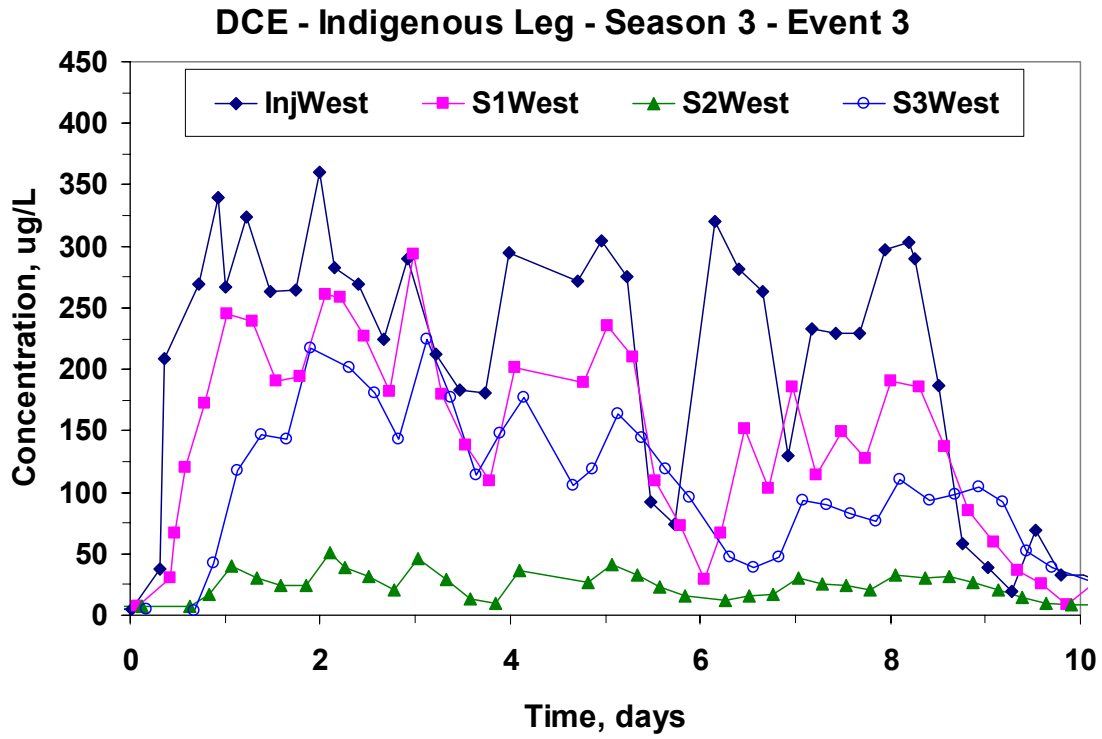

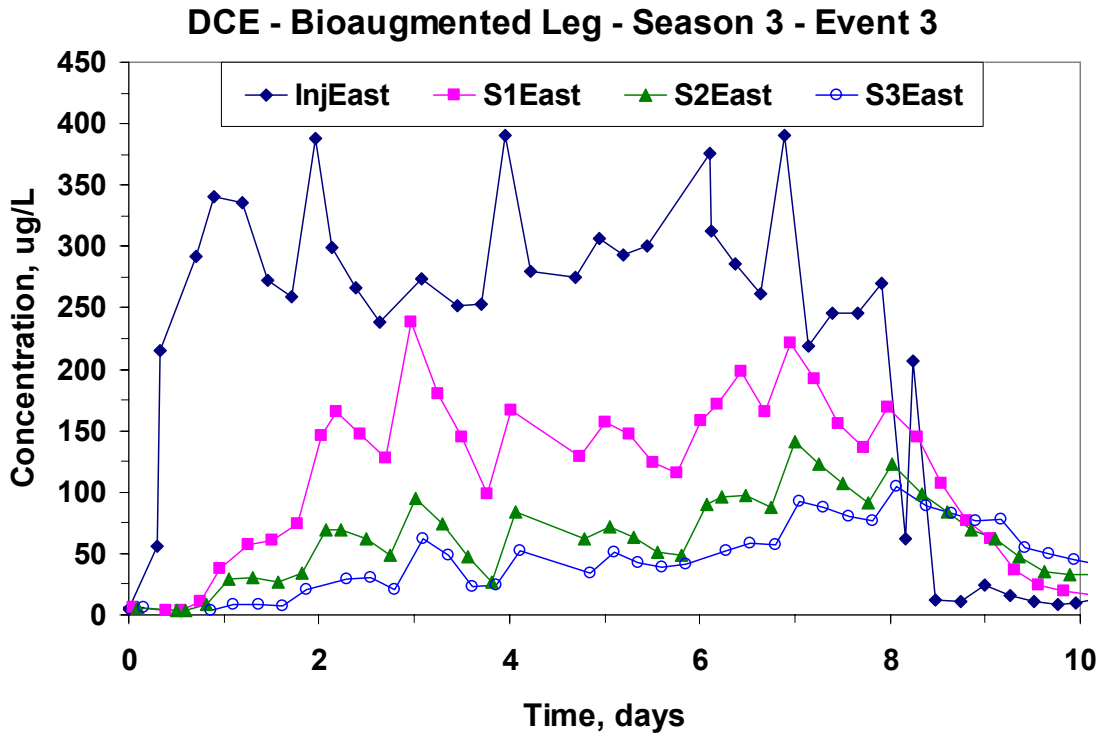

5.3.4 Fourth Bioaugmentation Event of the Third Field Season

The fourth bioaugmentation event of the third field season began on December 20, 2003, and ran for 17 days before weather and mechanical failure ended the test. The three CAHs, 1,1,1-TCA, 1,1-DCA, and 1,1-DCE were added to the test zone at concentrations of 200 μg/L, 290 μg/L, and 170 μg/L, respectively. A butane-utilizing mixed culture containing the 183 bp organism and a few other dominant organisms was bioaugmented to the field on day zero. Unlike previous tests, the bioaugmented leg was slow to reach complete butane utilization, with just less than 1 mg/L remaining at the third monitoring well when butane was shut off on day 10. Butane persisted at concentrations greater than 1 mg/L throughout the indigenous leg through day 8, with 1 mg/L remaining in third monitoring well when butane was shut off on day 10. This was most likely due to the high concentration of CAHs used, especially DCE which inhibits butane utilization and is toxic to the transforming bacteria, combined with a successful reduction in native microbial population prior to the test by passing a bleach solution through the test zone.

Significant TCA, DCA, and DCE transformation and butane utilization occurred beyond the first and second monitoring wells in the bioaugmented leg. No TCA or DCA transformation and very little DCE transformation occurred in the indigenous leg. Microbial results revealed a similar microbial community shift as was observed in the second event of the third field season with a 277bp organism dominating early to be succeeded by an organism with a TFL of 126bp until butane was terminated. This pattern was seen out to the second monitoring well. Strain 183bp was found in the bioaugmented leg in groundwater samples taken from wells SE0.5, SE1, SE1.5, and SE2. Again, strain 183bp did not show up in T-RFLP analyses and was estimated to be a small proportion of the total biomass at approximately 10^4 cell/mL at well SE0.5 based on real-time PCR analyses.

5.3.4.1 Bioaugmentation Event 4: Chemical Results. The concentrations of 1,1,1-TCA, 1,1-DCA, 1,1-DCE, DO, and butane were monitored routinely in all injection and monitoring wells. Six hours prior to bioaugmentation, oxygen-purged groundwater was injected into both well legs. Approximately 5 g dry wt. Of a mixed butane-utilizing culture was diluted in 4 L of groundwater and introduced into the injection stream to the east well leg over a period of ten minutes. Immediately after bioaugmentation, chemical amendment of both well legs began. CAHs and bromide were introduced continuously and alternate pulses of butane-sparged and oxygen-sparged groundwater at influent concentrations of about 30 mg/L and 40 mg/L, respectively, were also initiated. Gases were introduced into the injection flow upstream of CAH addition by alternately purging the recycled groundwater with butane and oxygen, with brief nitrogen purges in between to prevent formation of explosive gas mixtures and to limit biomass growth in the injection lines and in the immediate vicinity of the injection well. Sparge cycles were 9 minutes of butane sparging followed by 4 minutes of nitrogen sparging, 156 minutes of oxygen sparging, and another 4 minutes of nitrogen sparging before repeating the cycle. On day 10, the primary substrate was changed from butane to propane. Propane was added in a manner similar to butane, using the same cycle times. On day 15, primary substrate addition was stopped, but dissolved oxygen, CAH, and bromide addition continued.

Unfortunately, since the study was conducted in the lowlands near San Francisco Bay in the rainy season, hydraulic control of the flow field was transiently compromised a few times during the study. These events can be observed in the bromide breakthrough data for the two well legs

(Figure 159). In the bioaugmented east well leg, bromide breakthrough at the third monitoring well (SE3) was significantly affected by changes in the regional groundwater flow. On days 5, 9, and 12 bromide capture in SE3 dropped from its normal value of around 90% to lows of 68%, 45%, and 56%, respectively. There appears to be full recovery of hydraulic control at SE3 around day 8 before the second and third rain events ensue, resulting in diminished capture in SE3 from day 9 through day 13. Capture in wells SE1 and SE2 was unaffected on day 5, remaining at 97% or greater, but dropped slightly to approximately 87% and 83%, respectively, around days 9.5 and 12.5. Similarly on the west well leg, capture at SW3 was significantly affected around days 5, 10, and 13. Additionally, there were increases in bromide capture at SW2 on days 10 and 13, when the capture at SW3 decreased, indicating significant changes in the regional flow at these times. Capture at SW3 reached lows of 74%, 66%, and 46% on days 5, 9, and 13, respectively, and was significantly lower than its normal 87% recovery on days 4-6, 9-11, and 12-14. Capture at SW1 was also affected around days 5 and 9, but to a lesser extent. These deviations in recovery efficiency should be taken into account when interpreting chemical and microbiological data from the field test.

Times to 50% breakthrough of bromide in the east well leg were approximately 0.6 d, 0.9 d, and 1.8 d for wells SE1, SE2, and SE3, respectively. In the west well leg, 50% breakthrough occurred at approximately 0.15 d and 0.8 d at wells SW1 and SW3. These breakthrough values are similar to those obtained from the second bioaugmentation event in the third field season described earlier.

At monitoring wells SE1 and SW1, butane concentrations did not decrease to below detection during the 10 days of butane addition as they did during previous tests. The butane concentrations at well SW1 (~4000 μg/L) were nearly twice those of well SE1 (~2000 μg/L) prior to enhanced utilization from day 4 to day 10 (Figure 160). Butane concentrations in well SE2 and SE3 were significantly lower than in well SE1 indicating that a butane-utilizing microbial community was present past the first monitoring well. However, no significant difference in butane concentration was observed in the west well leg between wells SW1 and SW3. In contrast to the current bioaugmentation test, it took only 3 days to achieve complete butane removal in the bioaugmented east leg during the second bioaugmentation event that season. Toxicity caused by DCE transformation products may have inhibited microbial growth in the bioaugmented east leg during the test. On day 10, butane addition was stopped and the primary substrate was switched to propane.

Unlike the second bioaugmentation event, the oxygen utilization rate in the east leg was fairly low (Figure 161). The oxygen concentration in well SE1 reached a stable level of 30 mg/L after breakthrough, maintaining only about 10 mg/L oxygen removal between the injection well and the first monitoring well. There appeared to be about 5 mg/L oxygen utilization in the east leg between the first and second monitoring wells, which is consistent with the observed butane profile. Although the dissolved oxygen concentration in the west injection well was slightly higher than in the east, concentrations in wells SW1 and SW3 were similar to well those in SE1, with no oxygen removal observed beyond SW1. In the non-bioaugmented west leg, TCA and DCA concentrations reached 90% of the influent values within 3 days and remained at this level throughout the test (Figures 162 and 163). The difference in concentrations of chlorinated ethanes between the injection well and the monitoring wells was most likely due to dilution, as

indicated by the bromide capture recoveries for these wells. The sharp dip in TCA injection concentrations from day 2 to 3 and DCA concentrations on days 4 to 6 were caused by mechanical failures during field operation. Times to 50% TCA and DCA breakthrough were about 0.8 day for well SW1 and 1.4 day for well SW3. In the bioaugmented east leg, TCA concentrations gradually increased for the first 2 days followed by a dip in concentration around day 3.5 due to mechanical failures, and then a steady rise to influent concentrations by day 11.

Since butane was still present at a concentration around 1500 μg/L, cells were not in an optimum growth state and TCA transformation was inhibited by the presence of butane during this period. Unlike the second bioaugmentation event of the season in the absence of DCE contamination, biotransformation of TCA and DCA occurred beyond monitoring well SE1, as well as between the injection well and the first monitoring well.

Figure 164 shows DCE concentrations in the injection wells and in the monitoring wells during the 17-day operation period. In the east well leg, DCE transformation was observed out to the second monitoring well. Lower butane concentrations past the first monitoring well likely resulted in less inhibition of DCE transformation. With the DCE injection concentration at approximately 175 μg/L, about 93% reduction in the influent DCE was observed during the first 10 days of the study. When the primary substrate was changed from butane to propane on day 10, DCE concentrations increased throughout the test zone.

In the non-bioaugmented west zone, DCE was injected at the same levels as that of the east zone. In wells SW1 and SW3, DCE concentrations approached influent values within the first 4 days of the test. Based on bromide adjusted CAH concentrations, approximately 12-16% DCE removal was observed in the first monitoring well between days 4 and 10. The third monitoring well showed similar removal through day 8, but concentrations decreased to 20% of the injection concentrations at day 10, followed by a rapid rebound to concentrations roughly equivalent to those in SW1, with a similar dip occurring around day 13. It is difficult to determine if the DCE concentration drop in SW3 was the result of transformation or due to flow events. The increase in removal efficiency occurred at a time when the butane concentrations decreased to near zero values in SW3 (around day 8 to day 10), possibly resulting in less butane inhibition of DCE transformation. However, there was a flow event around day 9-10 that impacted other chemical concentration profiles, but not to the extent seen in the DCE concentrations for well SW3. Also, on day 13, the DCE concentration in well SW2 rises significantly, consistent with the concentration profiles of other chemicals indicating that a change in the regional flow field occurred. A similar increase in DCE concentrations in SW2 did not occur around day 9-10 during the period of increased DCE removal, suggesting that transformation may have been occurring. DCE removal dropped quickly after the switch to propane as a primary substrate, with influent values being reached at approximately day 11 and again on day 14.

Figure 159. Bromide Concentrations in the West (Indigenous) Leg and the East (Bioaugmented) Leg during the Fourth Bioaugmentation Event in the Third Season of Field Testing. Note the changes in bromide capture around days 5, 10, and 13.

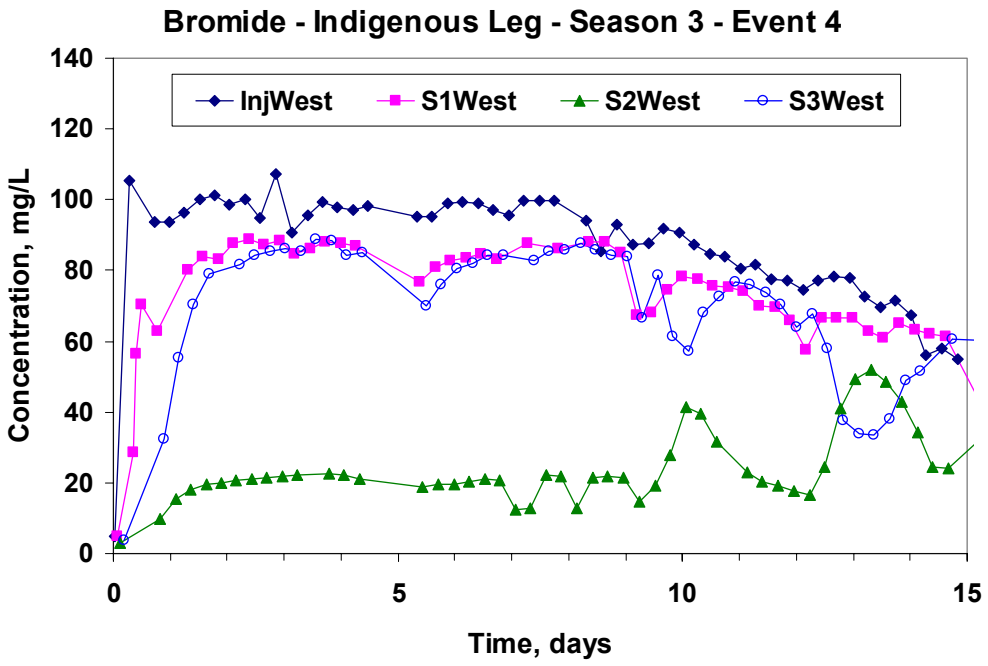

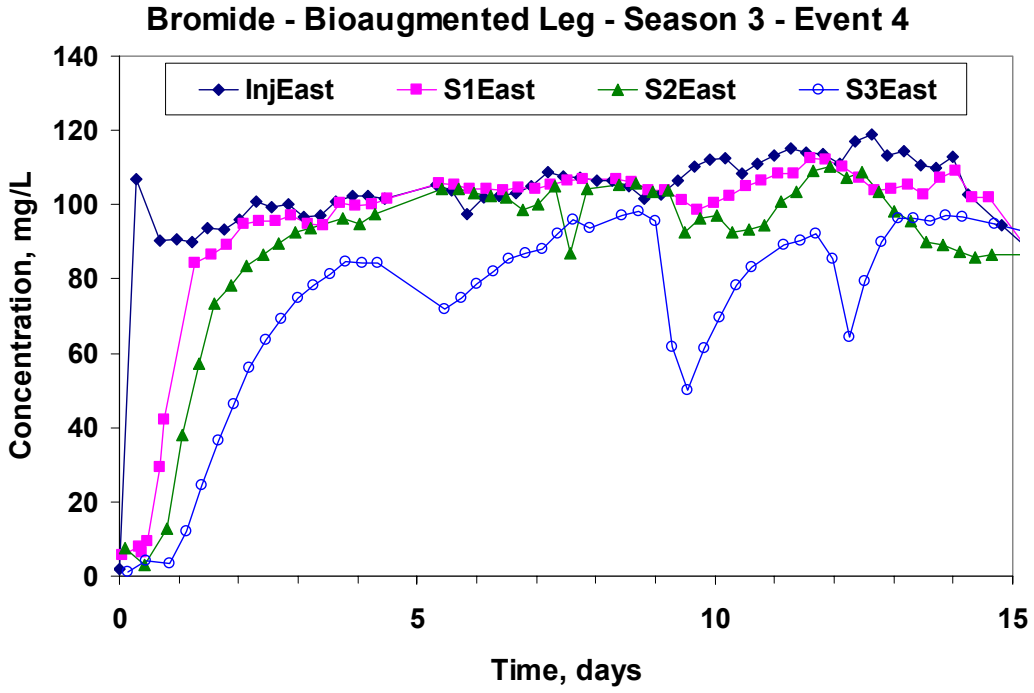

Figure 160. Butane Concentrations in the West (Indigenous) Leg and the East (Bioaugmented) Leg during the Fourth Bioaugmentation Event in the Third Season of Field Testing. Note the higher concentrations in the indigenous leg and the persistence in both legs.

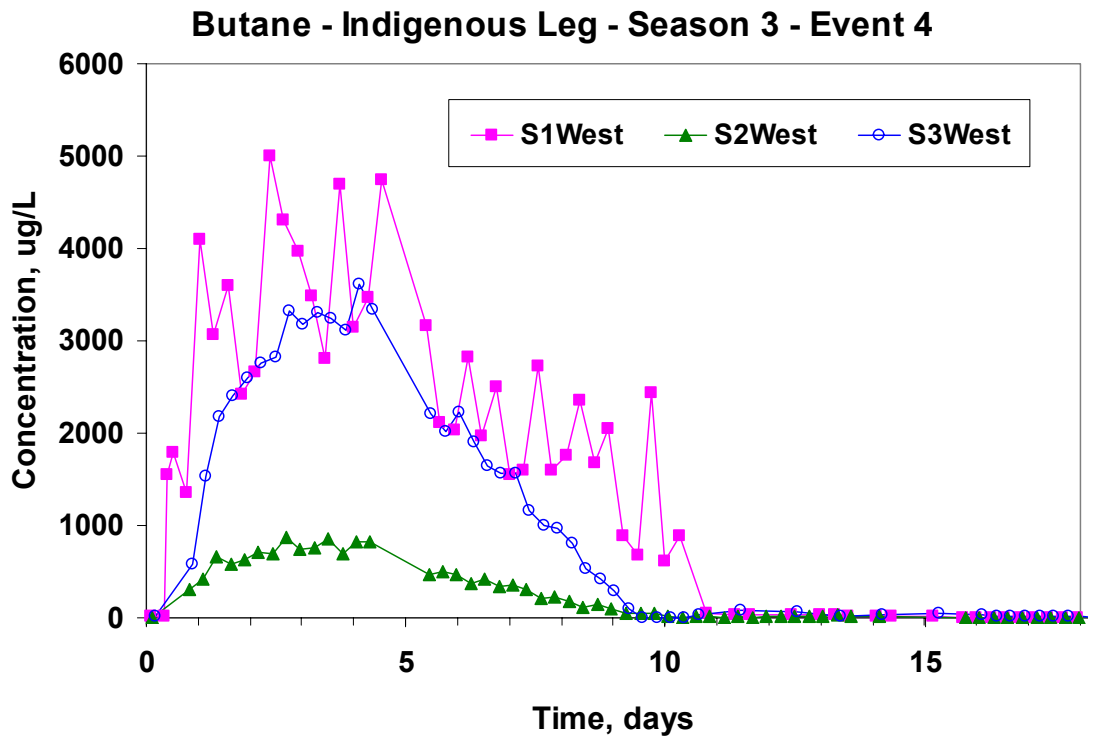

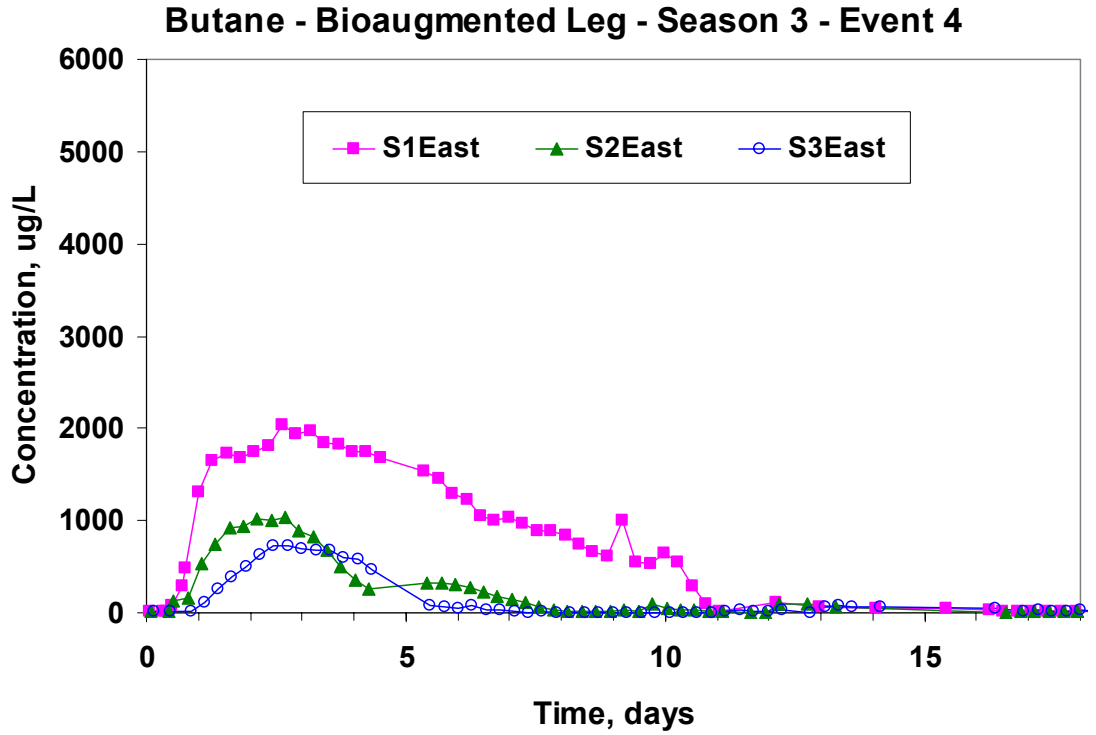

Figure 161. Dissolved Oxygen Concentrations in the West (Indigenous) Leg and the East (Bioaugmented) Leg during the Fourth Bioaugmentation Event in the Third Season of Field Testing. Note the additional removal between SE1 and SE3 not seen in SW1 and SW3.

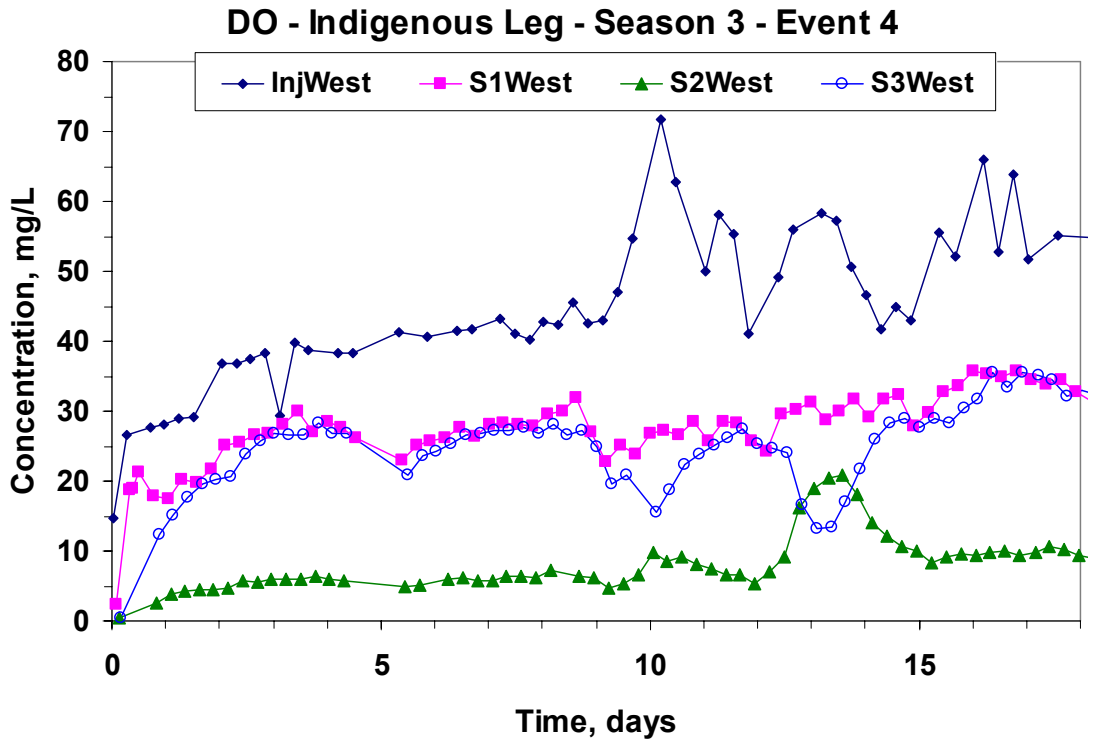

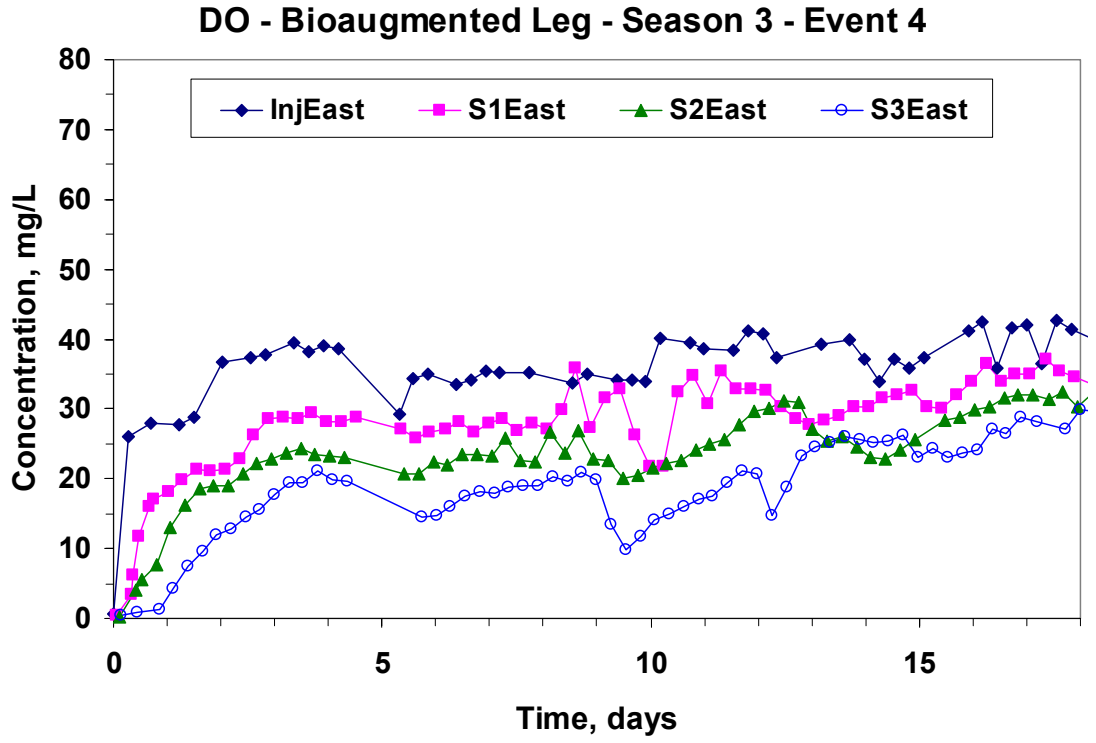

Figure 162. TCA Concentrations in the West (Indigenous) Leg and the East (Bioaugmented) Leg during the Fourth Bioaugmentation Event in the Third Season of Field Testing

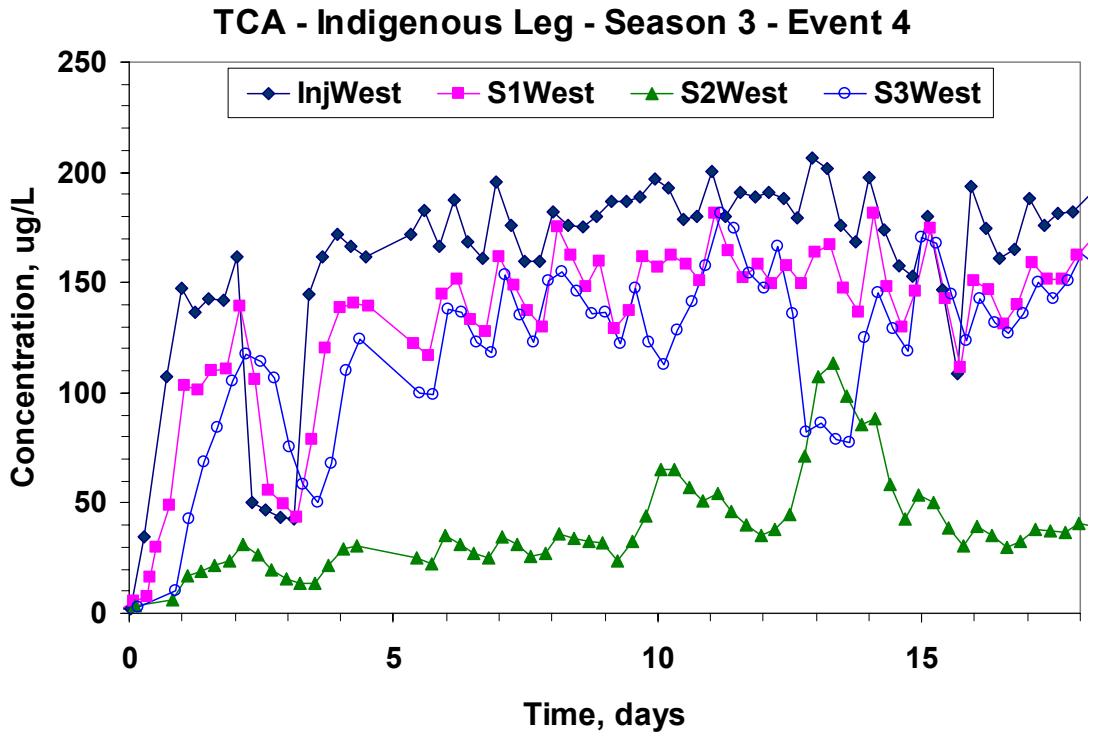

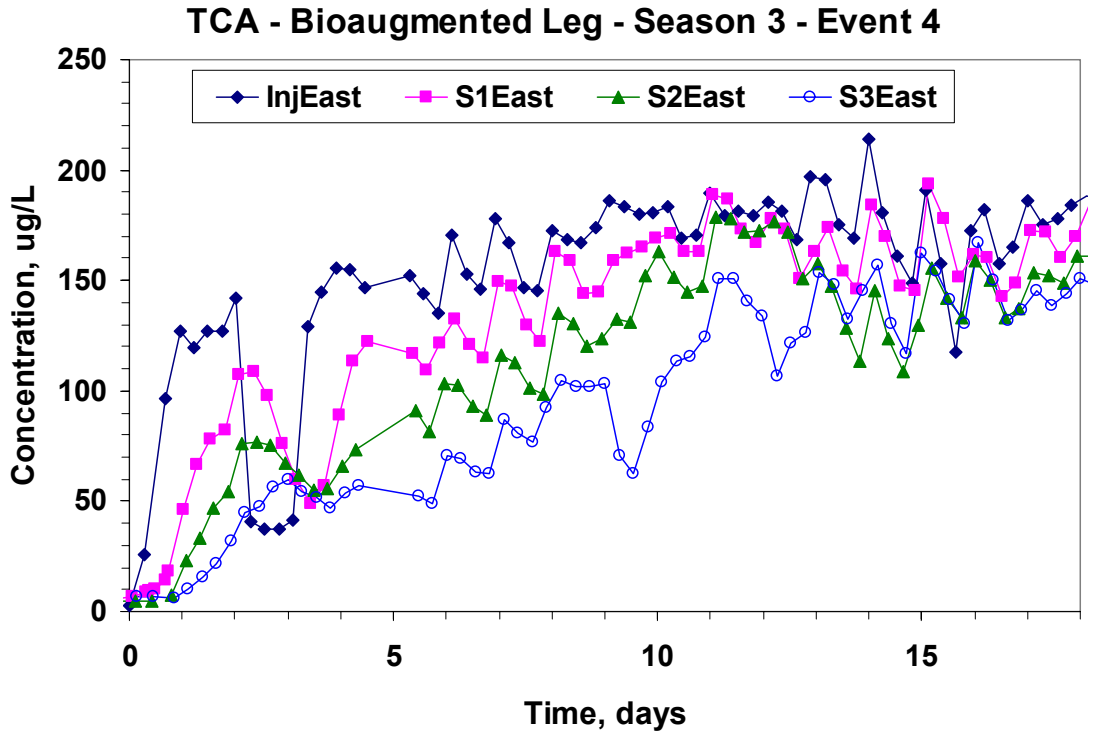

Figure 163. DCA Concentrations in the West (Indigenous) Leg and the East (Bioaugmented) Leg during the Fourth Bioaugmentation Event in the Third Season of Field Testing

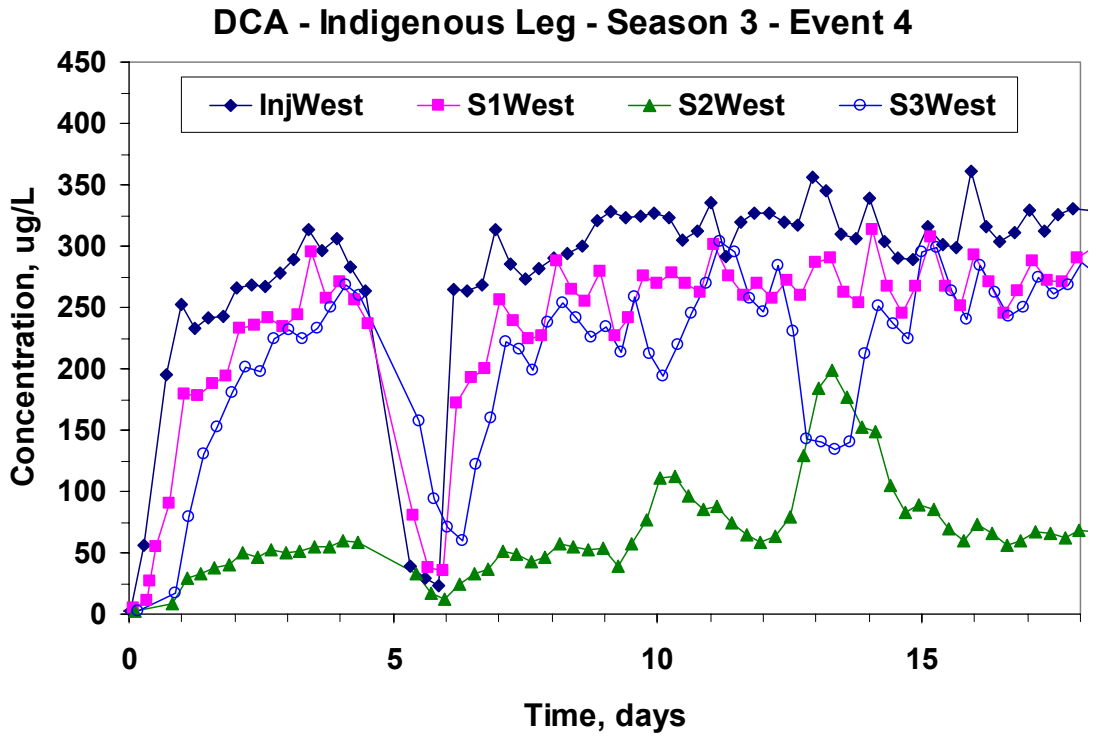

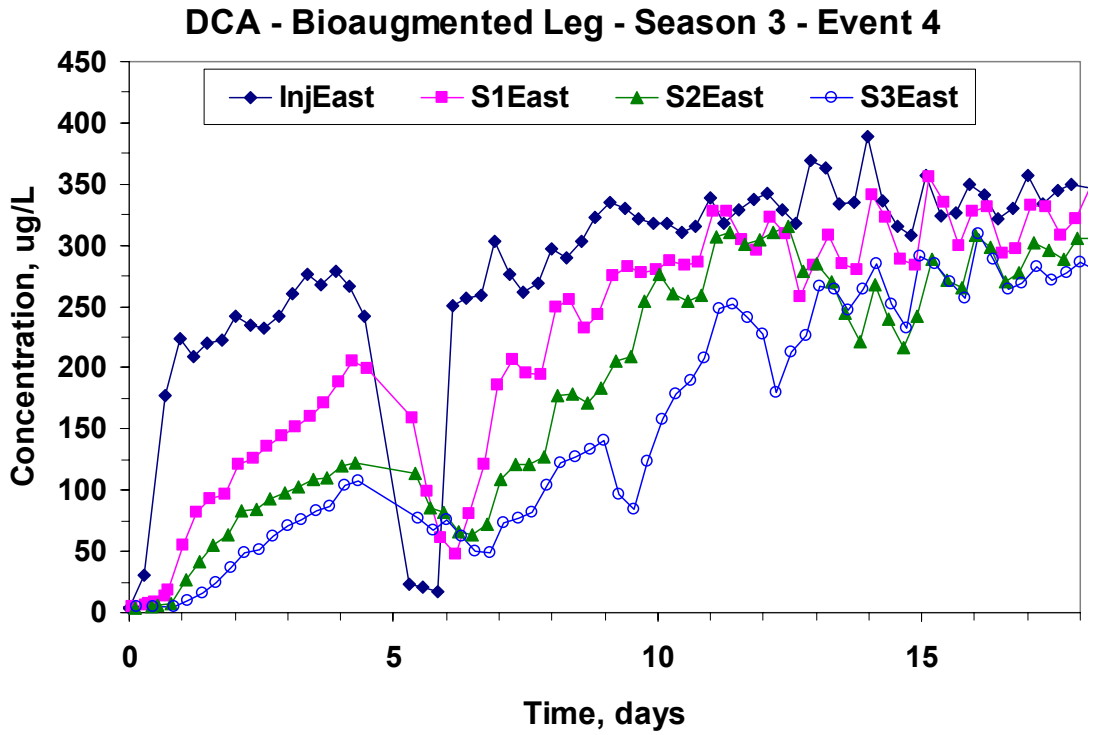

Figure 164. **DCE Concentrations in the West (Indigenous) Leg and the East (Bioaugmented) Leg during the Fourth Bioaugmentation Event in the Third Season of Field Testing. Butane was terminated on day 10 resulting in declining removal in the bioaugmented leg.**

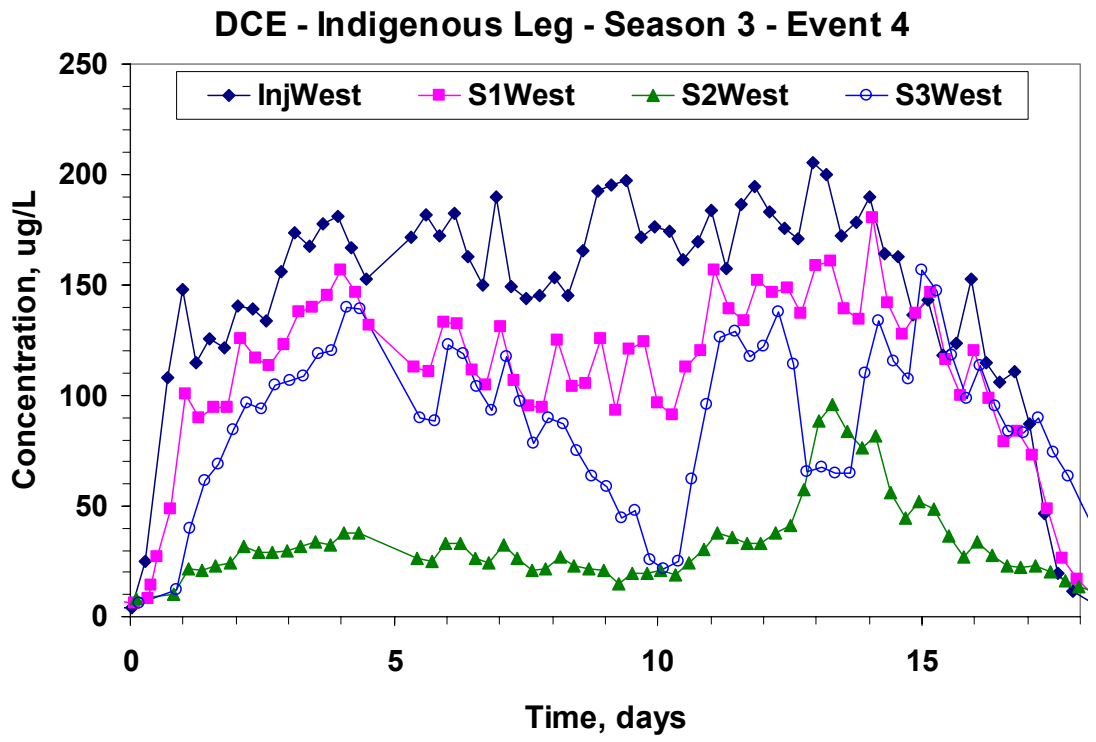

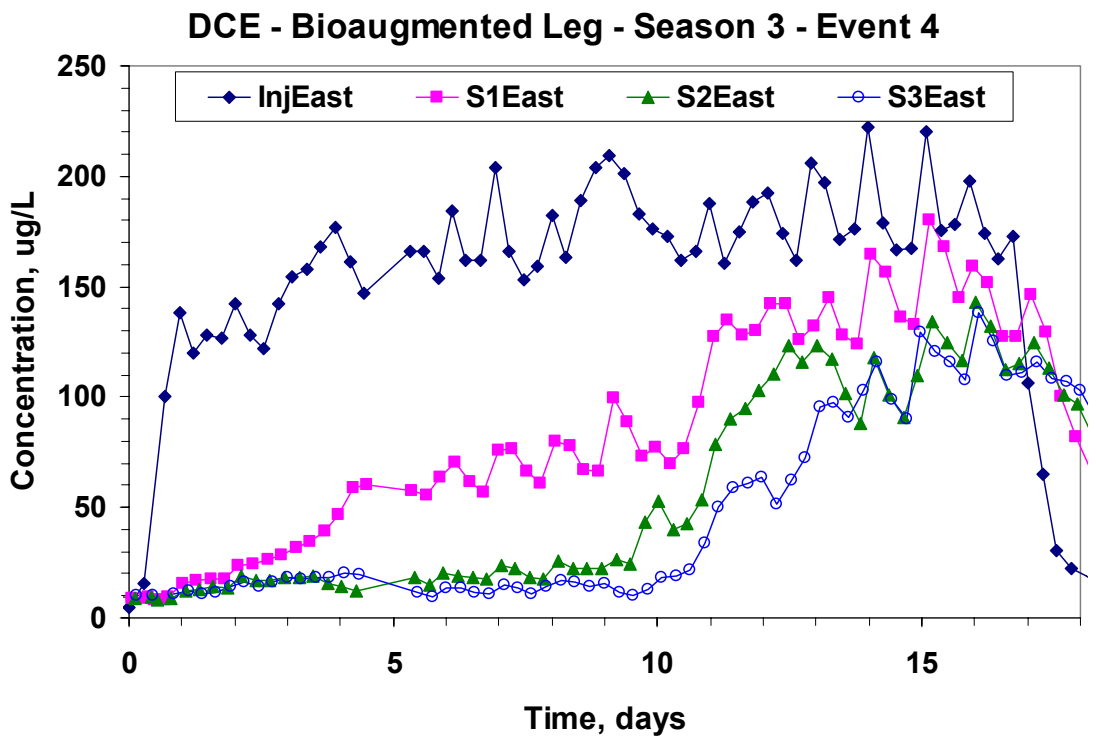

5.3.4.2 Bioaugmentation Event 4: Microbial Results. A T-RFLP analysis using the restriction endonuclease *Mnl*I showed four major peaks at 47-, 174, 183-, and 254-bp in community DNA extracted from the bioaugmentation culture (Figure 166, Culture). The 183-bp peak accounted for 13.5% of the total peak area and the 47bp peak dominated the T-RFLP profile.

Groundwater sampling for microbial analysis was conducted at all of the east groundwater monitoring wells (SE1, SE2, and SE3) as well as the fully penetrating wells SE0.5, SE1.5 and SW0.5. Prior to bioaugmentation, background samples taken from the east well legs revealed that strain 183bp was present at a density ranging from 10 and 500 cells/mL. These trace background levels were consistent with residuals found after previous bioaugmentation tests conducted at the site. In samples from well SE0.5, a greater than 2-log-order increase in strain 183bp cell concentrations was observed 0.4 day after bioaugmentation (Figure 165). After day 0.4, the cell concentration dropped to approximately 10,000 cells/mL and remained at this level through day 10. During this period, effective treatment of 1,1-DCE was achieved in the bioaugmented east zone. Higher cell concentrations were seen on days 15 and 17 after butane addition was terminated, which may have been the result of cell sloughing due to a switch in primary substrate, or due to the cessation of primary substrate addition on day 15.

The time to achieve the maximum cell concentration in wells SE1 and SE2 lagged that to well SE0.5 by about 0.3 days. Cell concentrations seen in wells SE1 and SE2 were also lower than those seen in SE0.5. Although further from the injection well, well SE2 had about a 1-log-order higher cell concentration than the fully penetrating well SE1.5. The densities of strain 183bp in well SE1.5 were below 600 cells/mL over the entire test and showed high variability, as these concentration levels were equal to the lowest concentration in the calibration curve. This may have been due in part to sampling procedures used during the test that resulted in flushing of the SE2 well during the acquisition of groundwater for chemical analyses at least once per day, while this flushing did not occur for well SE1.5. No positive real-time PCR signals were detected from samples collected from the SE3 well, indicating very few or no 183bp cells were transported that far or grew at this location. In the non-bioaugmented west zone, a sample taken from well SW0.5 on day 16.9 resulted in a positive signal with a calculated density of 19.4 cells/mL, below the quantifiable detection limit.

Figure 166 shows the T-RFLP profiles of the bioaugmentation culture and the community 16S rDNA in the monitoring well 0.5m from the injection well using universal bacterial primers (27F-B-FAM and 338Rpl) and *Mnl*I endonuclease. The T-RFLP profile of the bioaugmentation culture contained four major peaks at 47-, 174-, 183- and 254-bp; however, the same peaks accounted for less than 10% of the total peak area of any T-RFLP profile obtained from field samples at any time during the study. Similar to the results from the second bioaugmentation event of the season, T-RFLP analysis of groundwater samples showed no significant levels of 183-bp fragments in any of the samples. Also similar to the earlier test, an early stage dominance of the T-RFLP profiles by a fragment of 277-bp transitions to dominance by a 126-bp fragment after about five days of operation.

Before bioaugmentation, peaks at 120-, 277- and 348-bp dominated in the groundwater bacterial community. Immediately after bioaugmentation and the onset of chemical amendments, a reasonably large peak at 47-bp occurs in all of the east leg samples. However, the relative size of

the 47-bp peak diminishes quickly as fragments of 277-bp dominate the profile through day 2, accounting for at least 40% of the total peak area, while the peaks at 120- and 348-bp also diminished relative to the 277-bp peak. The primary community structure changed markedly from day 0 to day 0.4, but remained relatively unchanged from day 0.4 through day 2 when butane and DO were present in relatively high concentrations. At day 3.1, a more diverse microbial community appears to have developed or, since the analysis is relative to the largest peak present, perhaps the amount of 277-bp fragments diminished to that of the other organisms present. A similar community structure was observed on day 4.1, but by day 5.8 a distinctly different community structure emerged with a 126-bp fragment dominating the groundwater microbial community. The maximum percentage of the 126-bp peak occurred on day 7 (Figure 167). By day 10 the 126-bp peak appeared to be shrinking relative to the other peaks and by day 15 and day 16.9, again a relatively diverse population emerges (Figure 166).

The growth substrate was changed from butane to propane on day 10 and propane was shut off on day 15 possibly resulting in the community changes seen from day 10 to day 16.9. A peak arises at 242-bp that was not prominent before the substrate change. On day 16.9, the major peaks present in samples taken from the SE0.5 well and the SW0.5 well were different. Peaks at 71-, 73-, 120-, 126-, 212-, 242-, and 253-bp dominated the groundwater microbial community in well SE0.5. In well SW0.5, dominant peaks occurred at 74-, 241-, 253-, and 277-bp, with only the 253-bp fragment in common with profiles from well SE0.5 on the same day.

Figure 168 illustrates changes of the 47-bp fragment peak area in T-RFLP profiles of the groundwater samples. In the bioaugmentation culture, the 47-bp peak dominated the T-RFLP profile of the bioaugmentation culture and accounted for 23% of the total peak area. No TFLs of 47-bp were detected in groundwater samples taken prior to the bioaugmentation test, except in well SE1.5 where the 47-bp peak accounted for less than 0.7% of the total peak area. In all of the east leg monitoring wells, except SE3, the 47-bp fragment accounted for about 10% of the total peak area of the bacterial community members less than one day after bioaugmentation. The percentage of 47-bp fragments decreased rapidly to around 1% or less from day 3 through day 8 and then slowly increased to around 1% to 4% by the end of the test.

Figure 165. Cell Densities Found in Groundwater Obtained from the Bioaugmented Well Leg during the Fourth Bioaugmentation Event Based on Real-Time PCR Analyses. Total cell densities based on DAPI-stained cell counting averaged about 10^6 cell/mL. Concentrations peak within the first day or two from the bioaugmented cells being transported through the system. Note the reasonably stable 183bp populations at the different wells and the higher concentrations of 183bp found in well SE2 compared to well SE1.5.

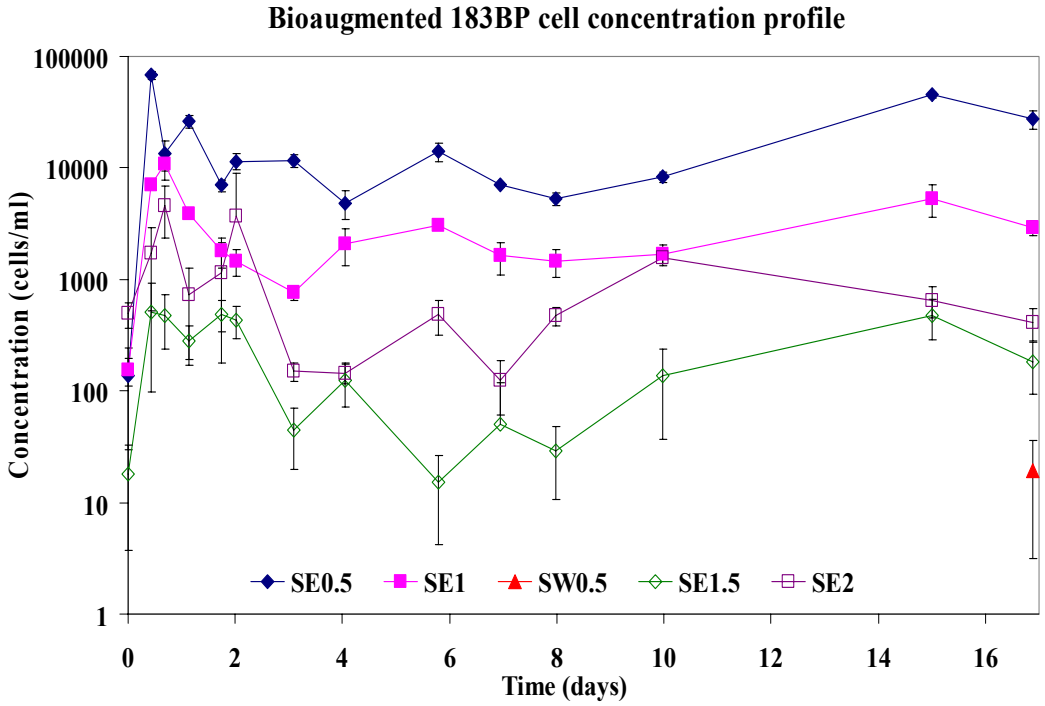

Figure 166. T-RFLP Profiles Generated from the Bioaugmentation Culture Grown in the Laboratory and Groundwater Samples Obtained from Wells SE0.5 and SW0.5 during the Course of the Fourth Bioaugmentation Event. Universal bacterial primers (27F-B-FAM and 338Rpl) were used in the PCR reactions and the restrictions were performed with the endonuclease *MnI*I (Fermentas, Inc).

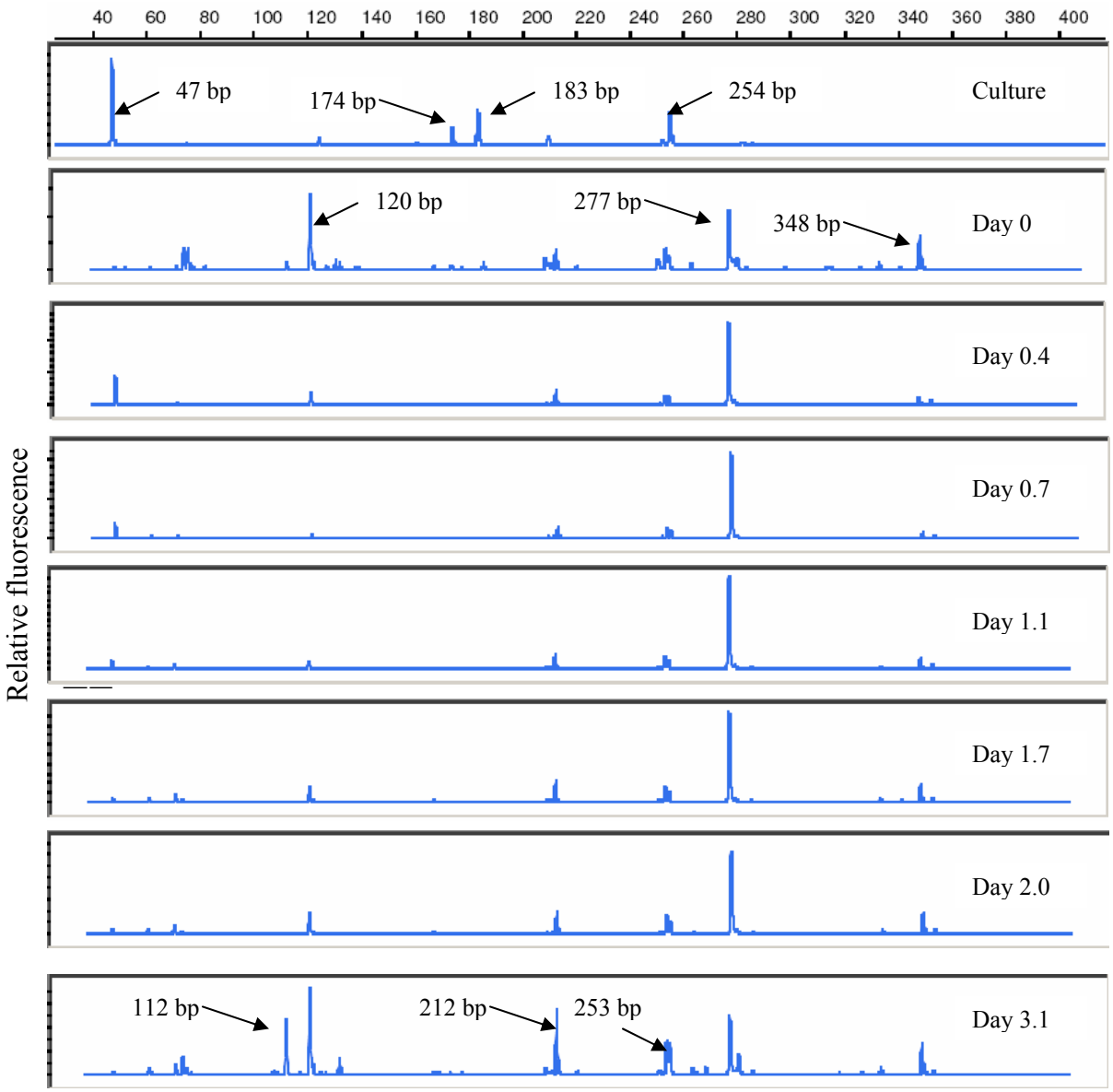

Figure 166 (continued) *Terminal restriction fragment length polymorphism (T-RFLP) profiles generated from the bioaugmentation culture grown in the laboratory and groundwater samples obtained from wells SE0.5 and SW0.5 during the course of the fourth bioaugmentation event. Samples from the bioaugmented leg were initially dominated by organisms with TFLs of 120bp and 277bp, which were succeeded by an organism with a TFL of 126bp around day 5. An organism with a TFL of 277bp was also present in the west leg prior to butane utilization and again at the end of the test 7 days after turning off butane addition. Note the way the 126bp peak diminishes after butane was terminated on day 10.*

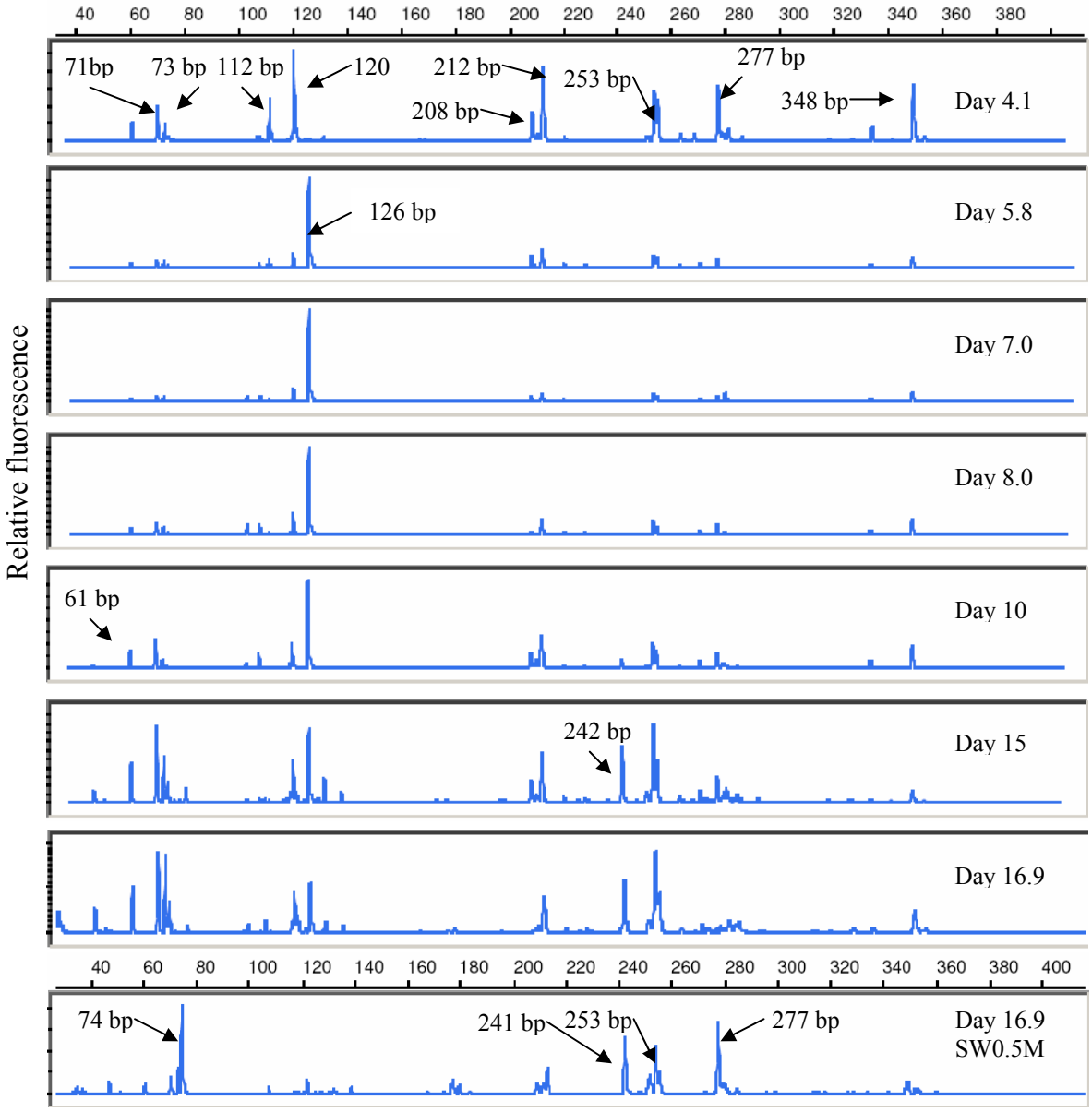

Figure 167. Bar Graph Representation of the Major Peaks Found in T-RFLP Analyses of Groundwater Samples Taken from the SE0.5 Well during the Fourth Bioaugmentation Event. Similar results were found in the first four wells in the bioaugmented leg with an organism with a TFL of 126bp dominating the profile after 5-7 days of operation.

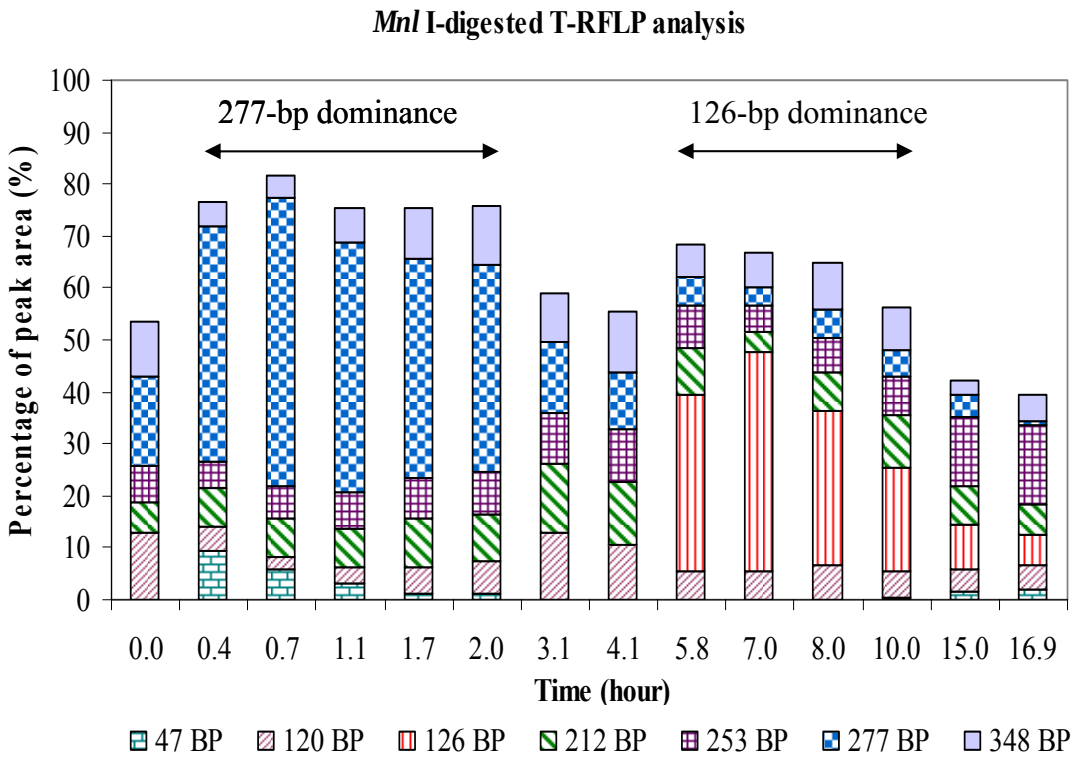

Figure 168. Qualitative Results Obtained from T-RFLP Analyses of the Amount of DNA in a 47bp Fragment, the Dominant Organism Present in the Bioaugmentation Culture, Compared to the Total DNA Obtained. The spike occurring in the first day shows successful transport of the organism out to the third monitoring well, 4 m from the injection well.

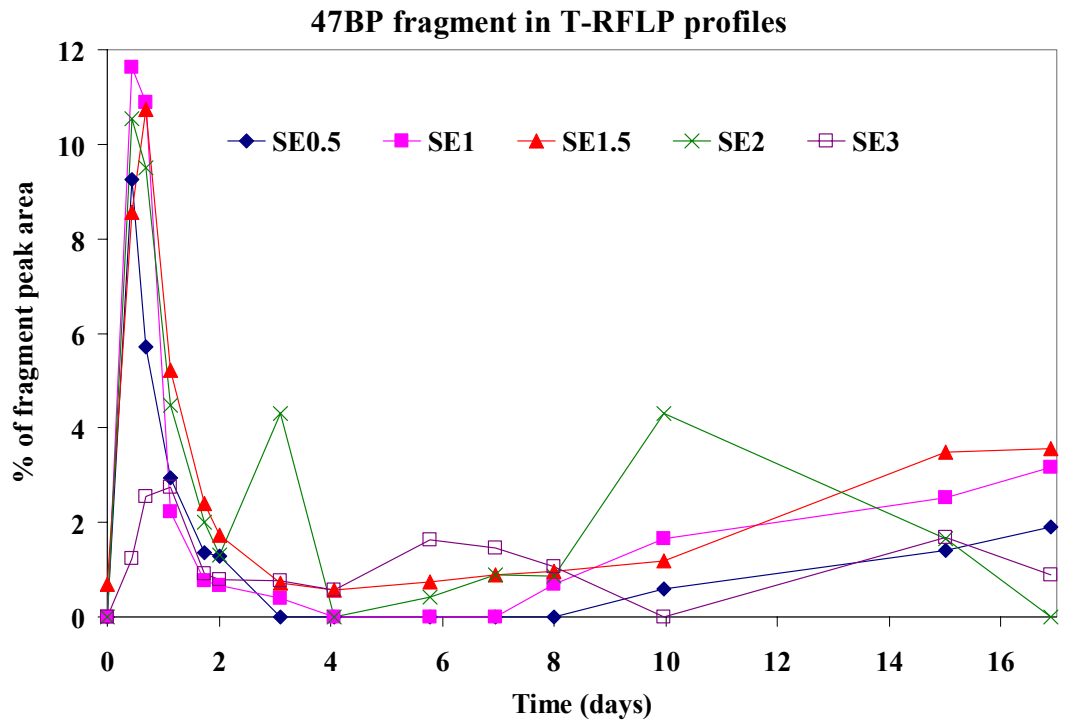

5.3.4.3 Bioaugmentation Event 4: Discussion. Although the test conditions and purposes for the fourth bioaugmentation study were only slightly different from the second bioaugmentation test of the season, the fourth test exhibited several characteristics which were not shown previously. In the second test, DCE was not added to the field until late in the test and the added butane was completely utilized by the first monitoring point within 3 days . In the fourth bioaugmentation, 175 µg/L DCE was added in conjunction with reasonably high TCA and DCA concentrations and butane was not completely utilized by the end of the 10 days of butane addition. The slower butane consumption may have been due to competition between the primary and cometabolic substrate for the monooxygenase enzyme and toxicity associated with CAH, especially DCE, transformation. In a previous study using microcosms bioaugmented with strain 183bp (Section 4.5), the maximum specific transformation rates for butane and 1,1-DCE by strain 183bp were estimated to be 2.5 µmol/mg/hr and 2.8 µmol/mg/hr respectively, which suggests the potential for significant inhibition, whereas the other CAHs exhibited lower maximum specific transformation rates of 0.49 µmol/mg/hr for DCA and 0.20 µmol/mg/hr for TCA.

Significant DCE degradation was observed during the first few days without any apparent lag period, unlike the second bioaugmentation of the season where a lag period of a few days was

required for maximum TCA and DCA transformation. In a previous study of microcosms bioaugmented with strain 183bp (Section 4.5)), DCE was quickly transformed concurrently with butane, followed by DCA and TCA transformation once the butane was almost completely utilized. In a separate study using a butane-grown mixed culture, Kim et al. (2002b) reported that the order of the half-saturation coefficients (K_s) from the highest to the lowest was 1,1-DCA, butane, 1,1,1-TCA and 1,1-DCE. The K_s of DCE was about one order of magnitude lower than those for the other compounds. Therefore, DCE may exert greater competition for the monooxygenase enzyme than butane or the other CAHs. When studying CAH toxicity on methane utilizers, Henschler et al. (1979) also stated that the affinity of TCE for methane monooxygenase was higher than TCA, which also was reflected by the higher degradation rate of TCE versus TCA.

During the second bioaugmentation test, maximum treatment efficiencies of 76% for 1,1,1-TCA and 95% for 1,1-DCA were achieved after butane was completely consumed as a growth substrate in the bioaugmented east leg. However, in this test, complete butane utilization was not achieved in the first monitoring well by the end of butane addition on day 10 and wells SE1 and SE2 only showed completed butane consumption beginning on day 9. A maximum of 48% TCA removal, 59% DCA removal, and 91% DCE removal was achieved by the third monitoring well while relatively little transformation of DCE only was achieved in the indigenous leg (Figure 169). Also unlike the second bioaugmentation event, considerable CAH removal occurred past the first monitoring well. For all three CAHs, about 30% of the removal efficiency occurs past the first monitoring well, with 3%, 7%, and 14% of DCE, DCA, and TCA being removed past the second monitoring well. Most likely this was the result of high initial DCE concentrations inhibiting complete butane utilization and the residual butane inhibiting DCA, and especially, TCA transformation as was witnessed in microcosm tests. Similar to previous tests, the DCA transformation efficiency declined somewhat over the 10 days of the test, while DCE treatment at the third monitoring well stayed essentially constant at 91% removal over the 10 days of butane addition.

Although 1,1-DCE itself is not toxic, its transformation products are highly toxic (Dolan and McCarty, 1995). In a recent survey of aerobic cometabolism of CAHs by a butane-grown mixed culture, 1,1-DCE was rapidly transformed, but 1,1-DCE transformation caused greater cell inactivation than the transformation of other chlorinated ethenes (Kim et al., 2000). According to a model developed by Anderson and McCarty (1996), transformation product toxicity appeared to be the most significant for 1,1-DCE among the CAH tested, including TCE and t-DCE. Although the 183bp cell concentrations in real-time PCR analyses was at least $(4.85 \pm 1.39) \times 10^3$ in well SE0.5, a gradual loss of CAH transformation ability was observed in TCA and DCA during the first ten days of the test. However, during the second bioaugmentation test, effective treatment of chlorinated ethanes was achieved under similar strain 183bp cell concentrations in the absence of DCE contamination. The CAH transformation activity loss may have been due to the toxicity presented by accumulated transformation products from CAHs, especially from DCE. A field evaluation of in situ CAH cometabolism by phenol-grown organisms conducted at the Moffett Field site in 1995 resulted in 50% transformation of the 65 μg/L influent 1,1-DCE and a 40% reduction in TCE removal efficiency due to DCE transformation (Hopkins and McCarty, 1995).

The primary substrate was switched from butane to propane on day 10. A rapid decline of transformation activity for DCE was observed in both well legs. Strain 183bp cell concentrations in the bioaugmented leg appear to increase from day 10 to day 15 (Figure 165). The increased cell concentration was inversely related to DCE removal efficiency and may have been the result of detached cells from solid phases for two reasons: 1), accumulated toxicity of transformation products of CAHs; and/or 2), deficient physiological state caused by the substrate replacement. A microcosm study using aquifer solids and groundwater from the Moffett Field site and bioaugmented with an enrichment culture developed from Hanford DOE site, WA, showed similar results (Section 4.3). It was found that the maximum transformation yields in microcosms bioaugmented with butane was 0.036 mg TCA/mg substrate whereas only 0.019 mg TCA/mg substrate was achieved using propane as the primary substrate.

With similar influent oxygen concentrations of approximately 40 mg/L, oxygen utilization was about 10 mg/L between the injection well and the first monitoring well in this test. This was only about 50% of the utilization rate found in the second bioaugmentation test, likely due to inhibition of butane oxidization by DCE. Another approximately 10 mg/L of DO was utilized between monitoring wells SE1 and SE3 indicating significant butane utilization occurred farther from the injection well than in other tests, which was consistent with the observed differences in butane concentrations at SE1 and SE3. In the indigenous leg, DO concentrations were the same in wells SW1 and SW3 indicating little microbial activity was occurring past the first monitoring well, which was also consistent with the butane concentration data from SW1 and SW3 that showed little differences.

The cell density profile from real-time PCR analyses revealed the spatial distribution of the 183bp cells throughout the bioaugmented leg. It was observed that increasing distances from the injection well corresponded to declines in the 183bp cell populations as would be expected due to decreases in butane concentrations further from the injection well. High bromide recovery was observed in the all the monitoring wells (from 81 to 99%, except for SW2), thus confirming that dilution of the cells with 'background' groundwater was not significant. However, it is noteworthy that the cell density in the well SE2 was higher than that of well SE1.5 for the duration of the experiment. The reason for this contradiction might be that well SE1.5 had incomplete capture of the groundwater flow path. Furthermore, the sampling frequency at SW2, used for groundwater chemical analyses, was much higher than at SE1.5, which was only sampled for microbial content, possibly resulting in a lack of complete flushing of the well casing before acquiring samples at SE1.5.

The T-RFLP profiles showed the community structure transition over the duration of the bioaugmentation test. Although organisms with TFLs of 47- and 254-bp were observed in community profiles and in the bioaugmentation culture, there was never a dominance or even strong representation of the augmented culture. However, CAH transformation ability was imparted via bioaugmentation, so some portion of the bioaugmentation culture was influential in CAH transformation. It may be that one of the less represented organisms in the laboratory-grown bioaugmentation culture responded favorably under field conditions, or possibly successful colonization of aquifer solids occurred, but few of the bioaugmented organisms were continually sloughed off to the aqueous phase where they could be quantified. Similar to the results from the second bioaugmentation test, the bacterial community in well SE0.5 shifted to

two alternately dominating fragments, 277- and 126-bp. Apparently, the 277-bp fragment was associated with the fast degradation phase, while the 126-bp fragment dominated during the period of diminishing CAH transformation. Another difference is that 277-bp could be detected in the background groundwater samples in both tests and in samples from the west well leg, whereas the 126-bp fragment was not not seen in the indigenous leg. Similar trends were also observed in the other monitoring wells in the bioaugmented east zone with extended dominance time for the 277-bp with increasing distance from the injection well. The 277-bp dominance was most likely due to favorable conditions established by the butane and oxygen additions; however, the 277-bp organism(s) may have been negatively affected by transformation products and diminished as the CAH transformation process proceeded. It is unknown why there was a distinct transition to dominance of the 126-bp fragment during the later phase of the experiment(s). CAH transformation efficiency decreased over the period of 126-bp dominance suggesting that the 126-bp organism(s) was unable to transform the CAHs or was inefficient at the process.

In a previous study conducted at the same site (Fries et al., 1997), groundwater samples from three successive treatments (phenol + TCE + 1,1-DCE, phenol + TCE, and toluene + TCE) were analyzed using amplified ribosomal DNA restriction analysis (ARDRA) with *Hae*III, *Hpa*II, and *Sau*3A as restriction endonucleases. The results showed decreased species diversity when 1,1-DCE was included in the influent stream. The original diversity was re-established after TCE + toluene conditions were re-instituted in the absence of 1,1-DCE. The similarity of the banding patterns indicated that the community structure remained fairly stable when the site was treated with phenol or toluene. The predominant microbial taxa were found to be the beta proteobacteria *Variovorax*, *Azoarcus*, and *Burkholderia* and three gram positive groups including *Bacillus*, *Nocardia*, and an unidentified group.

In the present study, when butane was fed as primary substrate, the community T-RFLP pattern of the groundwater samples shared approximately 80% similarity. As the substrate was switched to propane on day 10, the bacterial communities in the groundwater samples collected thereafter showed about 75% similarity with butane-fed communities, indicating relatively stable community structure under two different substrates. However, in a study of soil community structure during bioaugmentation treatment using PCR-single-strand-conformation polymorphism analysis, drastic changes was observed between samples collected in the first two weeks (Cho and Kim, 2000). The community in the sample collected in the first week of bioaugmentation treatment showed only about 50% identity to that of the second week, which was significantly lower than our observation at Moffett Field groundwater samples. This discrepancy may be due to the different habitats of the microbial communities and the experimental conditions at the two sites. No previous bioremediation studies in Moffett Field have reported the alternate dominance in microbial communities during a bioremediation test or similar phenomena.

Figure 169. CAH Removal Efficiency as a Function of Distance from the Injection Well for the Bioaugmented (closed symbols) and the Indigenous (open symbols) Well Legs during the Fourth Bioaugmentation Event of the Third Field Season

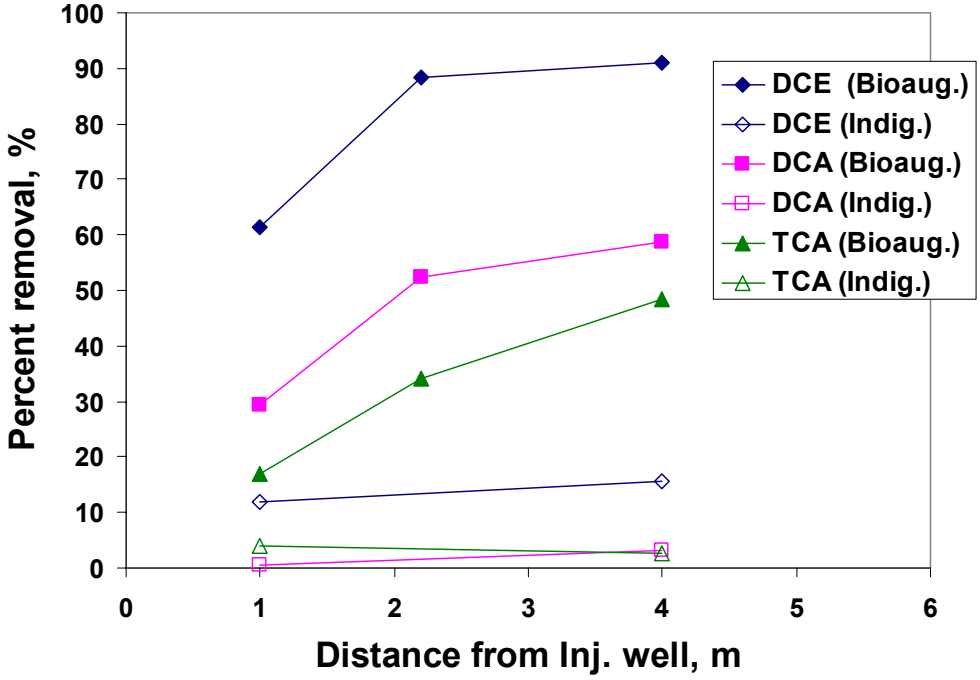

5.3.4.4 Summary of Third Field Season Bioaugmentation Tests. There were four separate bioaugmentation 'events' during the third field season (Table 55). Initially, transport of bromide and TCA were observed in both well legs in the absence of butane addition. Flow in the bioaugmented east well leg was slower than in the indigenous west well leg, with about 2 times the time required for bromide breakthrough and about 3 times the amount of time required for TCA breakthrough. TCA was found to be very slightly retarded compared to bromide transport in the indigenous leg; however, a calculated retardation factor of 1.6 was found for TCA transport in the bioaugmented leg.

Bioaugmentation of approximately 4-5 g of a butane-utilizing culture resulted in TCA and DCA transformation ability in the bioaugmented leg that was never observed in the indigenous leg. Maximum transformation efficiencies were attained within a few days after bioaugmentation, after the augmented culture had time to respond to butane stimulation (Table 55). Maximum transformation efficiencies were difficult to maintain over time, presumably due to competition from native butane-utilizing organisms that did not have the ability to transform TCA or DCA. Re-bioaugmentation of a butane-utilizing culture after a period of butane stimulation resulted in about 60-80% lesser treatment efficiency, most likely due to competition from butane-enriched

native populations. Generally, TCA transformation ability decreased the quickest, followed by DCA transformation ability. DCE was efficiently transformed over longer periods, often to non-detect values, although high DCE concentrations resulted in diminished transformation efficiencies over time presumably due to DCE transformation product toxicity. This was a good result in terms of meeting EPA MCL values, since DCE has the lowest MCL at 7 μg/L. DCA is not regulated and TCA has an EPA MCL of 200 μg/L, which was met during most of the field tests. However, inefficient TCA transformation results in residual concentrations that can undergo abiotic reactions that produce DCE, potentially re-contaminating the treated zone.

Butane and oxygen pulse cycles were varied to determine the maximum amount of butane that could be added and still maintain aerobic conditions in the treatment zone. Temperature variations and inconsistencies in peroxide solution concentrations resulted in inconsistent oxygen delivery to the subsurface, requiring excess oxygen delivery to ensure aerobic conditions at all times. Maximum time-averaged sustainable butane concentrations of around 8 mg/L were achieved with greater than 5 mg/L residual dissolved oxygen at all times. The system could be operated under higher butane concentrations, but reliability of oxygen delivery would need to be improved. Lower concentrations of butane appeared to result in similar removal efficiencies as was seen in Event II where butane concentrations were about 3 mg/L and high removal efficiencies were attained.

Nutrient addition appeared to have a minimal effect on survivability and CAH transformation activity of the bioaugmented culture. After turning nutrient addition off for about 10 days, re-addition of nutrients resulted in a 5% increase in TCA removal efficiency; however, this also corresponded to a decrease in peroxide concentrations so it was difficult to attribute the increase in efficiency directly to nutrient addition. Peroxide was effective at keeping delivery lines clear of biological growth and provided additional dissolved oxygen to the treatment zone. However, inconsistencies in peroxide concentrations (the peroxide appears to have been degrading to different extents during its 'shelf life') required a higher residual DO in the field to assure aerobic conditions at all times.

Table 55. Summary of CAH Removal in the Bioaugmented Leg during the Third Field Season

	TCA	DCA	DCE	Butane
Event 1 (100 day test)				
Injection Conc., μg/L	160	140	background	8[a] (4.7[a])
Maximum Removal, %	75	75	>80	100
Time, days	25-29	57-61	20-100	16-43 (43-100)
Event 2 (28 day test)				
Injection Conc., μg/L	200	200	130	3[a]
Maximum Removal, %	76	95	>98	100
Time, days	4-7	4-7	23-28	4-28
Event 3 (10 day test)				
Injection Conc., μg/L	375	260	300	7 – 16[a]
Maximum Removal, %	n/a[b]	n/a[c]	83	100
Time, days			4-7	4-10
Event 4 (17 day test)				
Injection Conc., μg/L	160	290	170	7[a]
Maximum Removal, %	48	60	91	100
Time, days	5-9	4-9	4-9	5-10

a) Concentration in mg/L
b) Delayed transport
c) Inconsistent delivery; delayed transport

Addition of a mild bleach solution to the field test zone several weeks before bioaugmentation was effective at reducing the butane-stimulated native populations, so the bioaugmented organisms had a better chance at successful colonization and competition for the supplied butane. The maximum effect was attained by leaving the 60 mg/L bleach solution in the subsurface for at least 48 hours or more in the absence of induced groundwater flow.

Molecular analysis of groundwater samples showed that the bioaugmented culture was transported at least 2.2 m in the subsurface. TCA transformation activity was recorded past the second monitoring well during a test using high DCE concentrations, indicating survival of some portion of the bioaugmented culture past 2.2 m from the injection well. Unfortunately, the bioaugmented organisms were not found when analyzing the samples for microbial community composition using T-RFLP analysis, indicating that the dominant organisms in the bioaugmented community when grown in laboratory conditions were not the same organisms that dominated or were stimulated in the subsurface, or that the bioaugmented organisms provided CAH transformation ability and yet were still less than 1% of the total microbial population, the approximate detection limit in T-RFLP analyses. The dominant organism in the community

before bioaugmentation and at the early stages of butane enrichment was an organism with TFL of 277 bp, consistent with an *Acidovorax* sp. found in the bioaugmentation culture and in indigenous field samples. After stimulation with butane, the microbial community shifted and an organism with a TFL of 126 bp dominated the samples in the later stages of butane enrichment when CAH transformation was declining. The microbial succession was observed in both Events II and IV, where microbial testing occurred. Real-time PCR targeting the 16S rDNA gene of one member of the bioaugmented culture indicated that the bioaugmented culture did transport well in the subsurface and survived in small numbers throughout the tests.

6. RESULTS AND ACCOMPLISHMENTS: FIELD STUDIES

6.1 Modeling of the First Season of Field Tests

This section presents the modeling results of field scale experiments conducted during the first season of field testing.

As discussed in Section 5.1, the enrichment culture containing the strain 183BP organism was inoculated in an east test leg and exposed to alternating pulses of butane and oxygen and constant sources of 1,1-DCE, 1,1,-DCA, and 1,1,1-TCA. The biotransformation/transport code was used to simulate the biostimulation of the butane culture and the transformation of the CAH mixture from the field experiment. Specific values for utilization rates, saturation constants, inhibition constants, transformation capacities, etc. defined from laboratory experiments (Section 8) were used as input values for the biotransformation kinetics of the combined model. Tracer tests prior to bioaugmentation allowed determination of aquifer characteristics and the model's advection, dispersion, and sorption parameter values.

This section discusses the simulations and output for determining transport parameters via tracer tests and for evaluating the model's ability to simulate cometabolic transformation, inhibition, and product toxicity by comparing model output to actual field observations.

As described in the Methods section, the test zone was confined to a 1.5 m thickness of alluvial sands and gravels between silty-clay aquitards. A schematic of the field test zone is presented in Figure 170.

Aquifer hydraulic characteristics (Table 56) were defined from previous experiments (Semprini and McCarty, 1991,1992) and from model simulations of recent tracer tests (Section 5.1.2). Since 1-D model simulations of these tests were performed, the groundwater velocity and a dispersion coefficient were obtained from bromide
tracer tests performed on the test leg.

Figure 170. Conceptual Model of Moffett Field Test Aquifer (not to scale)

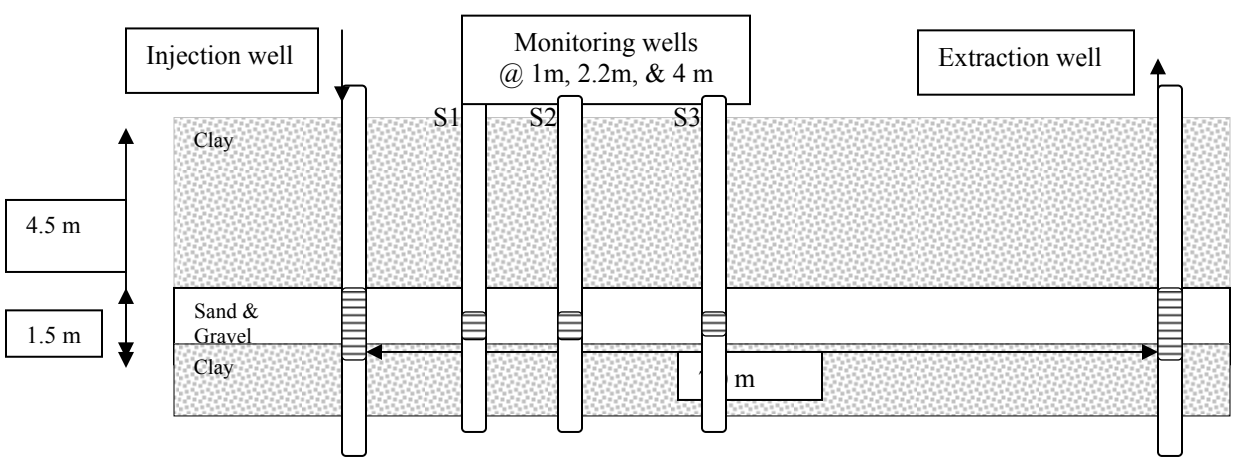

Table 56. Aquifer Hydraulic Characteristics

Average flow*, Q (m^3/day)	Aquifer Thickness, b (m)	Porosity, Φ (-)	Bulk Density, ρ_b (kg/L)	Dispersion Coeff., D_h (m^2/day)
1.0-1.5	1.5	0.33	1.6	0.31

**Defined from bromide tracer tests (Section 5.1.2), based on test zone with 1.5 m thickness and 1 m width.*

The injection system allowed for alternating, pulsed additions of butane and oxygen and continuous additions of 1,1-DCE, 1,1-DCA, 1,1,1-TCA. During the bioremediation experiment, concentrations and pulsing durations of butane and oxygen were varied periodically in attempt to improve bioremediation. Injection concentrations of the CAHs were held approximately constant. Specific details on injection concentrations and pulsing durations are provided in Section 5.1.

6.2 Determination of Flow Velocity

Bromide tracer tests were conducted in the test zone before bioaugmentation to determine flow and dispersion characteristics of the test zone. Bromide (150 mg/L) was injected into the site, and breakthrough concentrations were monitored from the monitoring wells S1, S2, and S3. Figure 171 presents the monitoring and injection wells' concentration histories. Times to 50% breakthrough of the bromide tracer observed for S1, S2, and S3 were 0.44, 1.12, and 1.42 days, respectively.

Figure 171. Bromide Tracer Test Data at the Three Monitoring Wells S1 (1m); S2 (2.2m); S3 (4m) and the Injection Well

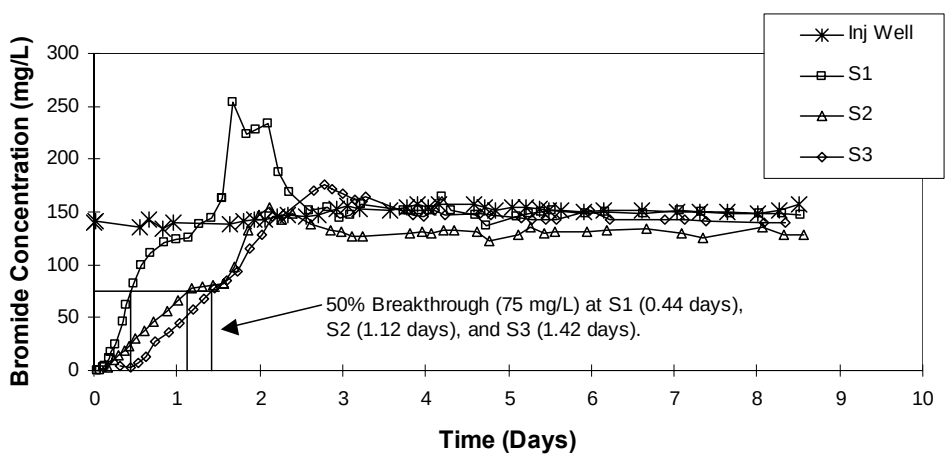

The tracer test was simulated using the transport model presented in Section 3. Results of tracer tests were simulated using the code with no transformation. This was done by setting utilization rates (k_m) to 0. Flow input values were varied and compared to the monitoring data at the first

and third sampling wells (S1 @ 1m and S3 @ 4m). Transport values for the simulations are provided in Table 56.

Comparison plots of the tracer data and model output for a 1.0 m^3/day volumetric flow (2.0 m/day average groundwater velocity) at S1 and 1.5 m^3/day flow (3.0 m/day average groundwater velocity) at S3 are presented in Figure 172. Note that there is a good match during the breakthrough period for each well, although different flow inputs were required to achieve this fit. Data from S1 showed some perturbations in bromide injection, resulting in high concentrations (days 1.3 to 2.6). The different flows may be explained by aquifer heterogeneities and the monitoring wells being partially penetrating. Similar observations were made by Semprini and McCarty (1991) for bromide tracer tests conducted on another test leg at the site. The combined model was run to simulate biotransformation seen at monitoring well S1 (1m from the injection well) using the flow rate determined at this location (1.0 m^3/day).

Figure 172. Comparison of Tracer Data to Model Output. Distances from the Injection Well: S1 (1m), S3 (4m). Groundwater velocities at S1 and S3 were 2.0 and 3.0 m/day, respectively, with aquifer porosity 0.33 width 1.0 m, and thickness 1.5 m.

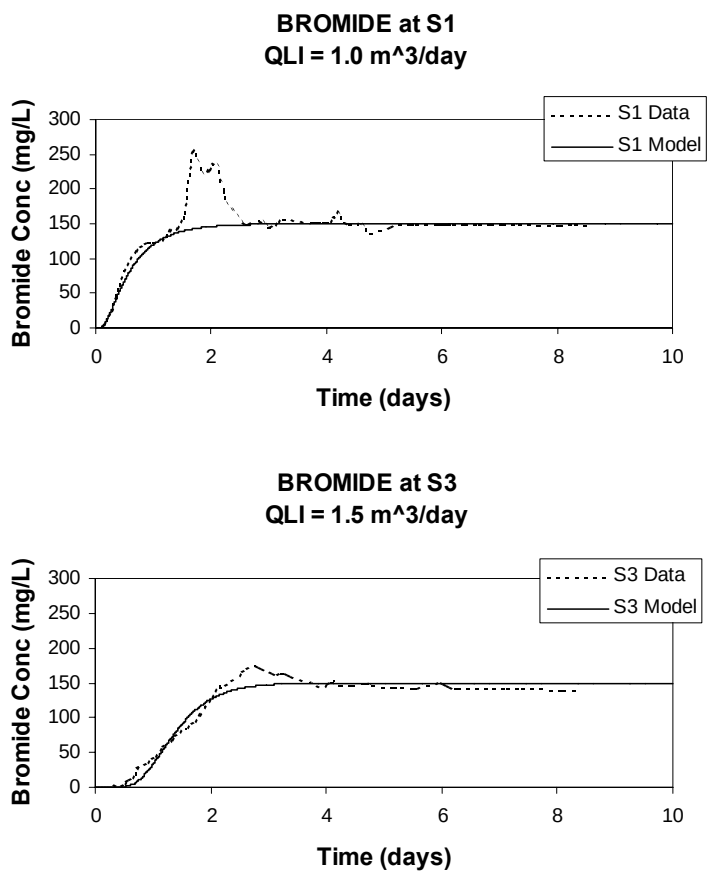

6.3 Determination of Sorption Parameter Value

Before bioaugmentation, 1,1-DCE, 1,1,1-TCA, and 1,1-DCA were injected into the aquifer to develop breakthrough curves of each compound. Injection concentrations of 1,1-DCE, 1,1-DCA,

and 1,1,1-TCA were approximately 45 μg/L, 130 μg/L, and 140 μg/L, respectively. Background 1,1-DCE in the aquifer was 5 μg/L. Concentrations over time were measured from the three monitoring wells, S1, S2, and S3. Breakthrough curves for the CAHs at the injection well, S1, and S3 are presented in Figure 173.

Compared to the bromide tracer data (Figure 172), the CAHs showed retarded breakthrough, indicating sorption was taking place. 1,1-DCA was sorbed with 50% breakthrough times (65 μg/L) at S1 and S3 of 1.5 and 3.1 days, respectively. Half of the 1,1,1-TCA injected concentration (70 μg/L)appeared at S1 and S3 at 1.5 and 3.2 days, respectively. Finally, 1,1-DCE showed 50% of the injection concentrations (22.5 μg/L) appearing at S1 and S3 at 1.9 and 3.2 days, respectively. Retardation factors based on these breakthrough times are presented in Table 57.

Figure 173. Breakthrough Curves of 1,1-DCE, 1,1-DCA, and 1,1,1-TCA. Distances from injection well: S1 (1m); S2 (2.2m); S3 (4m).

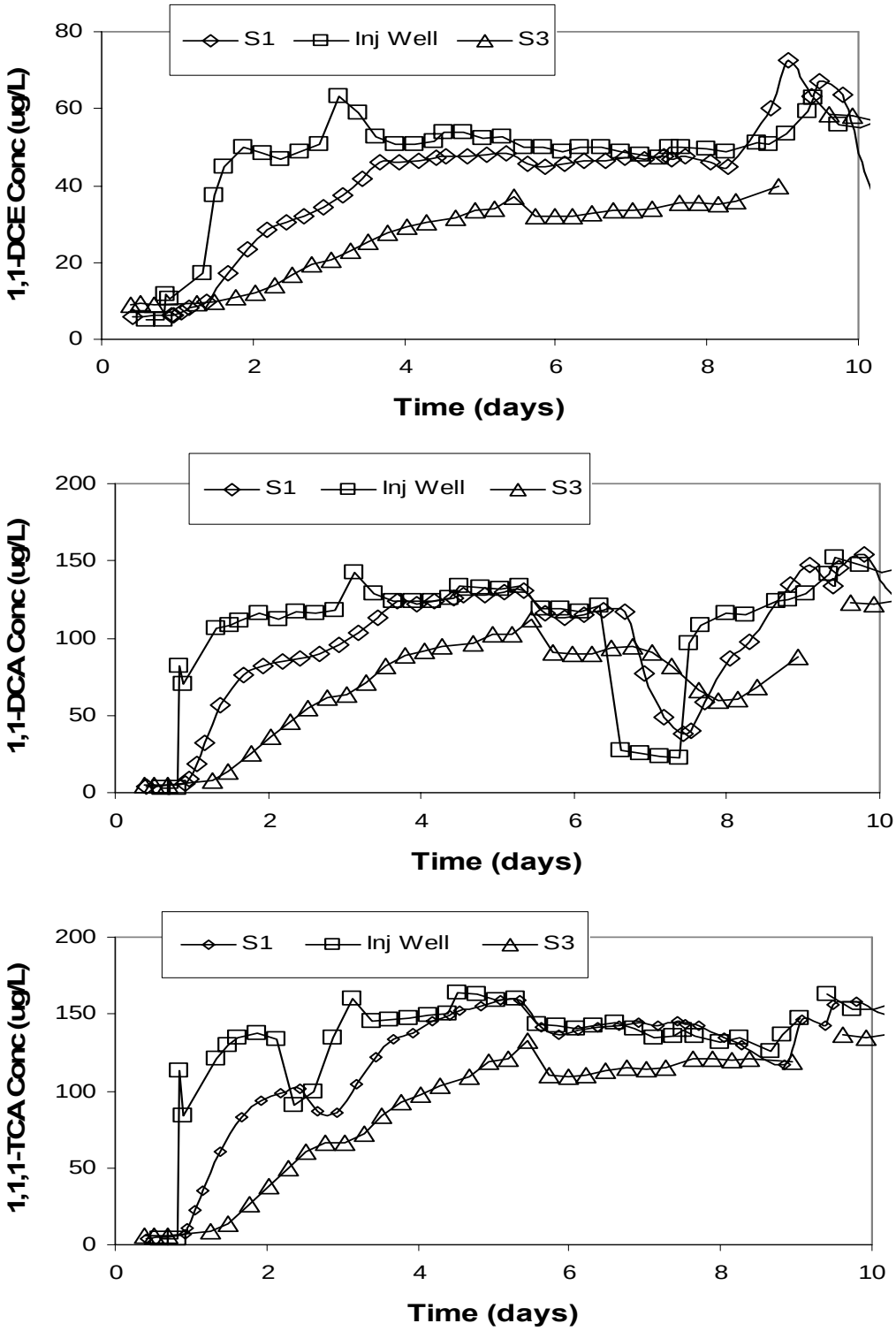

The breakthrough curves were used to determine initial estimates of sediment sorption coefficients (K_d) and the first order mass transfer rate coefficients (F_k). This was done by calculating a retardation value (R) for each CAH. The retardation value was defined as the time to 50% breakthrough of the CAH normalized to the time to 50% breakthrough of bromide.

Equation 6.1

$$R = T_{CAH} / T_{BR}$$

where: R = retardation factor
T_{CAH} = time for 50% of CAH injection concentration to reach well
T_{BR} = time for 50% of Bromide injection concentration to reach well

Approximate breakthrough times, 50% injection concentrations, and retardation factors at wells S1 and S3 are presented in Table 57. Partitioning coefficients (K_d) were then calculated by rearranging the relationship between R and K_d:

Equation 6.2

$$R = 1 + \frac{\rho_b k_d}{\phi}$$

Equation 6.3

$$k_d = \frac{\phi}{\rho_b}(R - 1)$$

where:
k_d = solids partitioning coefficient (L/kg)
ρ_b = bulk density (kg/L)
φ = porosity

Porosity (φ) and bulk density (ρ_b) listed in Table 56 (0.33 and 1.6 kg/L, respectively) were used with the retardation factors tabulated in Table 57 to calculate K_d. The K_d values determined from these calculations are also presented in Table 57. Note that there are differences between the retardation factors and sorption coefficients for each CAH at the two different wells. Like the variations seen in flow velocities, these differences may be attributed to non-homogenous conditions within the aquifer test zone.

Table 57. Retardation Factors and Solids Partition Coefficients

	Bromide	1,1-DCE	1,1-DCA	1,1,1-TCA
50% Inj. Conc. (μg/L)	75	22.5	65	70
Breakthrough time to S1 (days)	0.44	1.9	1.5	1.5
Breakthrough time to S3 (days)	1.42	3.2	3.1	3.2
Retardation Factor, R @ S1	-	4.3	3.4	3.4
Retardation Factor, R @ S3	-	2.3	2.2	2.3
Partition Coeff. , K_d @ S1 (L/kg)	-	0.69	0.50	0.50
Partition Coeff. , K_d @ S3 (L/kg)	-	0.27	0.25	0.27

Mass transfer rate coefficients (F_k) were determined by simulating the CAH breakthrough curves using the flows and sorption coefficients determined above. Figure 174 presents comparison plots of the S1 breakthrough data and two simulations with F_k values of 0.2 and 2.0 day^{-1} representing equilibrium and non-equilibrium cases, respectively. These values were assumed for all three CAHs. Simulations were also run for F_k values of 20.0 and 200 day^{-1}, with exactly the same results obtained with the 2.0 day^{-1} simulations.

With the quality of the data from the field demonstrations, it was difficult to determine if non-equilibrium (lower F_k) with higher partitioning (higher K_d) was occurring, or if equilibrium (higher F_k) with lower partitioning (K_d) was occurring. A value of 2.0 day^{-1} was used for all future field modeling for simplification. However, as seen in Figure 174, the F_k value of 0.2 day^{-1} gave a general "best fit" to the breakthrough data. Also, the work done by Harmon et al. (1992) would indicate that rate limited sorption was occurring under Moffett Field test zone conditions. Simulations shown in Figure 174 were therefore run to study the sensitivity of equilibrium versus non-equilibrium conditions.

Figure 174. Comparison of CAH Breakthrough Data with Model Output for Varying Mass Transfer Rate Coefficient (F_k) at S1 (1m)

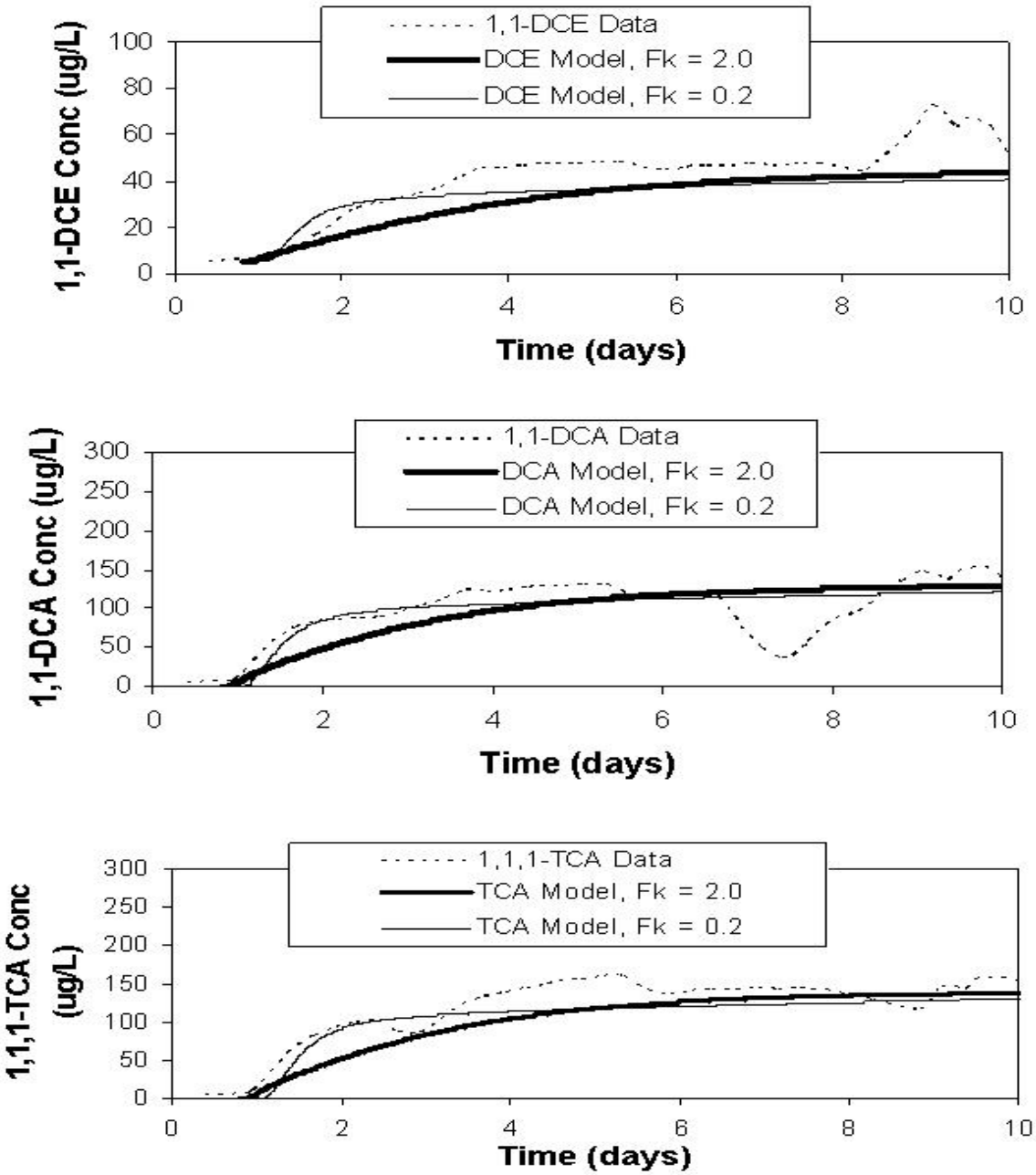

6.4 Results of the Modeling Analysis

Using the biotransformation parameter values determined from the laboratory experiments (Section 8) and the aquifer characteristics defined above, the first year tests were simulated with the model presented in Section 3. A summary of the biotransformation input values is listed in Table 58, while transport input is provided in Table 59. Kim et al's (2002) inhibition, rate, and half-saturation constant values were used. As with the microcosm experiments, cell decay was increased to a value of 0.1 day^{-1} which more accurately describes aerobes (Semprini and McCarty, 1991). Oxygen utilization parameters (f_d, and d_c) were used according to published values (Semprini and McCarty, 1991) and stoichiometry between butane and oxygen. Transformation capacity of 1,1-DCA (T_{cDCA}) as defined by Kim was incorporated along with that for 1,1,1-TCA (T_{cTCA}) used in modeling microcosm data. The lower transformation capacity of 1,1-DCE (T_{cDCE}) defined from laboratory experiments was also used. Microbial mass was assumed to be non-uniformly distributed, with most of the microbes existing within the first meter of the test zone. Injection concentrations and pulsing durations were input as listed in Tables 47 and 48.

Table 58. Biotransformation Values for Simulating Field Data

Parameter	Units	Value	Parameter	Units	Value
K_{ic}DCABUT	mg /L	39.88	X_0	mg/L	*
K_{ic}DCADCE	mg /L	1.78	Y	mg/mg	0.79
K_{ic}DCATCA	mg /L	1.58	b	day^{-1}	0.1
			Fa	-	0.8
K_{ic}DCEBUT	mg /L	0.84			
K_{ic}DCEDCA	mg /L	0.35	kmaxBUT	mg /mg/day	3.48
K_{ic}DCETCA	mg /L	0.11	kmaxDCA	mg /mg/day	1.16
			kmaxDCE	mg /mg/day	6.50
K_{ic}TCABUT	mg /L	41.79	kmaxTCA	mg /mg/day	0.64
K_{ic}TCADCA	mg /L	1.31			
K_{ic}TCADCE	mg /L	2.27	KsBUT	mg /L	1.11
			KsDCA	mg /L	1.90
K_{iu}BUTDCA	mg /L	0.23	KsDCE	mg /L	0.14
K_{iu}BUTDCE	mg /L	0.40	KsTCA	mg /L	1.63
K_{iu}BUTTCA	mg /L	0.03	KsO_2	mg /L	1
K_{ic}BUTDCE	mg /L	0.02	TcDCA	mg /mg	0.20
			TcDCE	mg /mg	0.017
f_d	mg/mg	4	TcTCA	mg /mg	0.11
d_c	mg/mg	1.42			

Nomenclature provided in Appendix A

**Microbial mass was assumed non-uniformly distributed (Appendix L)*

Table 59. Transport Parameter Values for Simulating Field Data

Average flow*, Q (m^3/day)	Aquifer Thickness, thick (m)	Aquifer Width, width (m)	Porosity, Φ (-)	Bulk Density, ρ_b (kg/L)	Dispersion Coeff., D_h (m^2/day)
1.0	1.5	1.0	0.33	1.6	0.31

Sorption Coefficient**, k_d (L/kg)			Mass Transfer Rate Coefficient**, F_k (day^{-1})		
1,1-DCE	1,1-DCA	1,1,1-TCA	1,1-DCE	1,1-DCA	1,1,1-TCA
0.69	0.50	0.50	2.0	2.0	2.0

**Defined from Bromide tracer tests*
***Defined from CAH breakthrough tests*

Because the model was limited to simulate only two CAHs, double simulations were run to create biotransformation/transport profiles of each of the 3 CAHs. The first simulations included the analysis of 1,1-DCE and 1,1,1-TCA. The second simulations evaluated 1,1-DCE with 1,1-DCA. These combinations were chosen because 1,1-DCE was the most toxic and most quickly transformed. It was therefore assumed that 1,1-DCE had the most influence on the 1,1-DCA and 1,1,1-TCA transformation, while these latter CAHs have minimal influences on one another.

To confirm this assumption, two additional runs were performed using the Stella model to simulate behavior of the laboratory microcosms in the absence of one CAH. One simulation included 1,1-DCE and 1,1,1-TCA in the absence of 1,1-DCA, while, the other included 1,1-DCE and 1,1-DCA in the absence of 1,1,1-TCA (results not shown). Both sets of output showed similar results to those from the laboratory simulations (Section 8), indicating that the presence/absence of 1,1-DCA or 1,1,1-TCA has minimal influence on CAH transformation and butane utilization.

The model was run to simulate the S1 monitoring data described in Section 5.1, using biotransformation values and transport values listed in Tables 58 and 59. The injection boundary conditions followed pulsing schedules listed in Tables 55 and 56. Model simulation output is compared to field data in Figure 175a-d. Plots of the cell concentration at the end of the simulation (day 75) and the microbial spatial distribution, as calculated from the model are included. As all models have limitations, the focus of this study was to capture trends interpreted from the field data. Overall, these trends were well simulated, particularly during the first 60 days of the experiments. Butane utilization decreased during longer pulsing durations (days 20-40) and limited oxygen availability (days 23-30). Oxygen was consumed with butane and when adequate quantities of oxygen were delivered to the test zone. During initial bioaugmentation (days 9-20) there was good transformation of 1,1-DCE, 1,1-DCA, and 1,1,1-TCA, with the latter two lagging behind until significant butane had been consumed and reduced to low concentrations. This follows the observations from the laboratory experiments, where 1,1-DCE

was quickly transformed (due to its high transformation rate) and 1,1-DCA and 1,1,1-TCA were inhibited by butane. Transformation of all three CAHs was lost when butane and oxygen pulsing cycles were elongated (days 20-40). 1,1-DCE transformation returned when pulsing was shortened again (days 40-75). Using equilibrium sorption (F_k = 2.0 day^{-1}) compared to lower first order mass transfer kinetics (F_k = 0.2 day^{-1}) likely resulted in a dampening of pulses due to competitive inhibition in the model.

The model predicted significantly more 1,1-DCA transformation for the latter period of the simulations (days 60-75) than was indicated by field data. It also predicted that slightly more 1,1,1-TCA should have been degraded. These contrasts were possibly due to a change in the microbial community within the test zone. It was speculated that an indigenous population was eventually stimulated and the bioaugmented population diminished. This was supported by data observed from a non-bioaugmented control test leg which had been treated in the same manner as the augmented leg. In the control leg, butane utilization was observed and 1,1-DCE was transformed at a later time, while 1,1,1-TCA and 1,1-DCA were not transformed. Based on this information, the modeling results would suggest that the indigenous microorganisms predominated at the later time.

There were other discrepancies between the model output and field data, indicating a number of possible complications. These may have been attributed to perturbations in field control, such as substrate delivery to the aquifer and fluctuations in hydraulics.

The cell concentration profiles (Figure 175d) provide additional understanding and interpretation of the model and field data. The upper plot depicts cell growth and decay during the entire simulation period, while the lower plot provides a blown-up scale for the first 40 days. Biomass peaked at the S1 well location when large amounts of butane were utilized (days 25-30 and 45-52). Cell death occurred after large amounts of 1,1-DCE were transformed and when butane consumption was limited (days 30-35 and 52-65). This is indicative of high 1,1-DCE product toxicity (as seen in the laboratory experiments, Section 8) and cell decay in the absence of a primary growth substrate. There was a greater magnitude of cell grown during the latter period. This was due to the greater amount of butane consumed and a lower mass of 1,1-DCE transformed. The lower transformation caused less cell inactivation. The spatial distribution plot for cell concentrations recorded at 20 days and 75 days (Figure 175e) both show that most cell mass exists within the first meter of the test zone.

Overall, the field transformation trends were well simulated by the biotransformation/transport model. This indicates the ability to successfully apply laboratory derived parameters to larger scale experiments.

Figure 175a. Comparison of Butane and Oxygen Field Data and Model Output at S1 (1m). The bioaugmented culture was introduced on day 9.

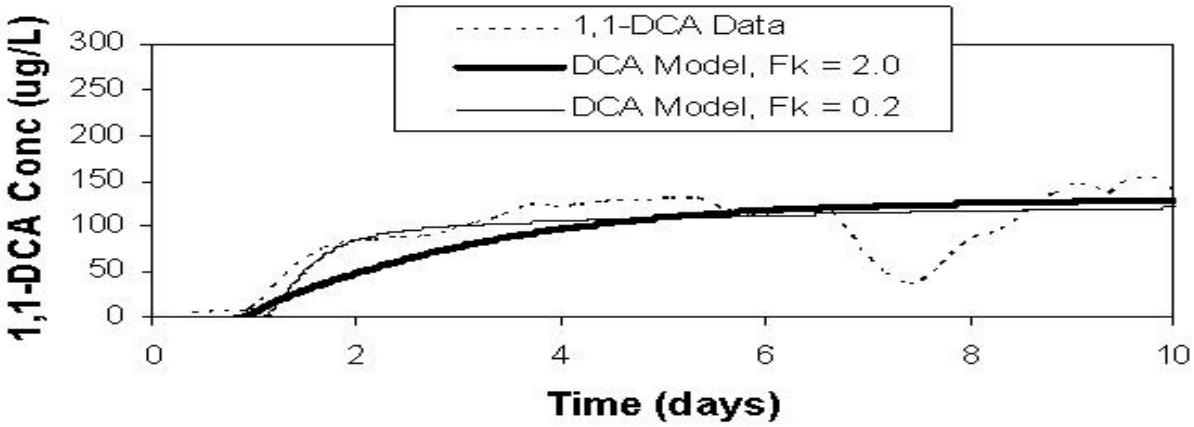

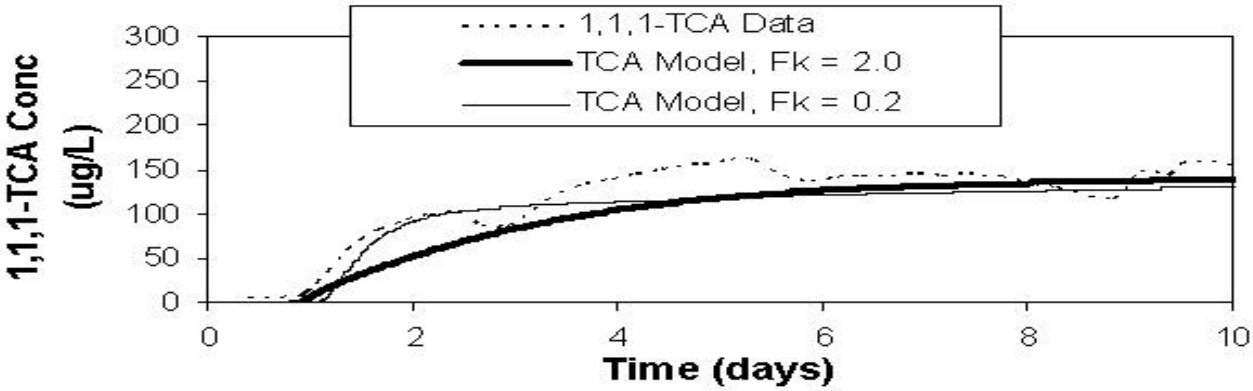

Figure 175b. Comparison of 1,1-DCE and 1,1,1-TCA Concentrations for the Field Data and Model Output at S1 (1m). The bioaugmented culture was introduced on day 9.

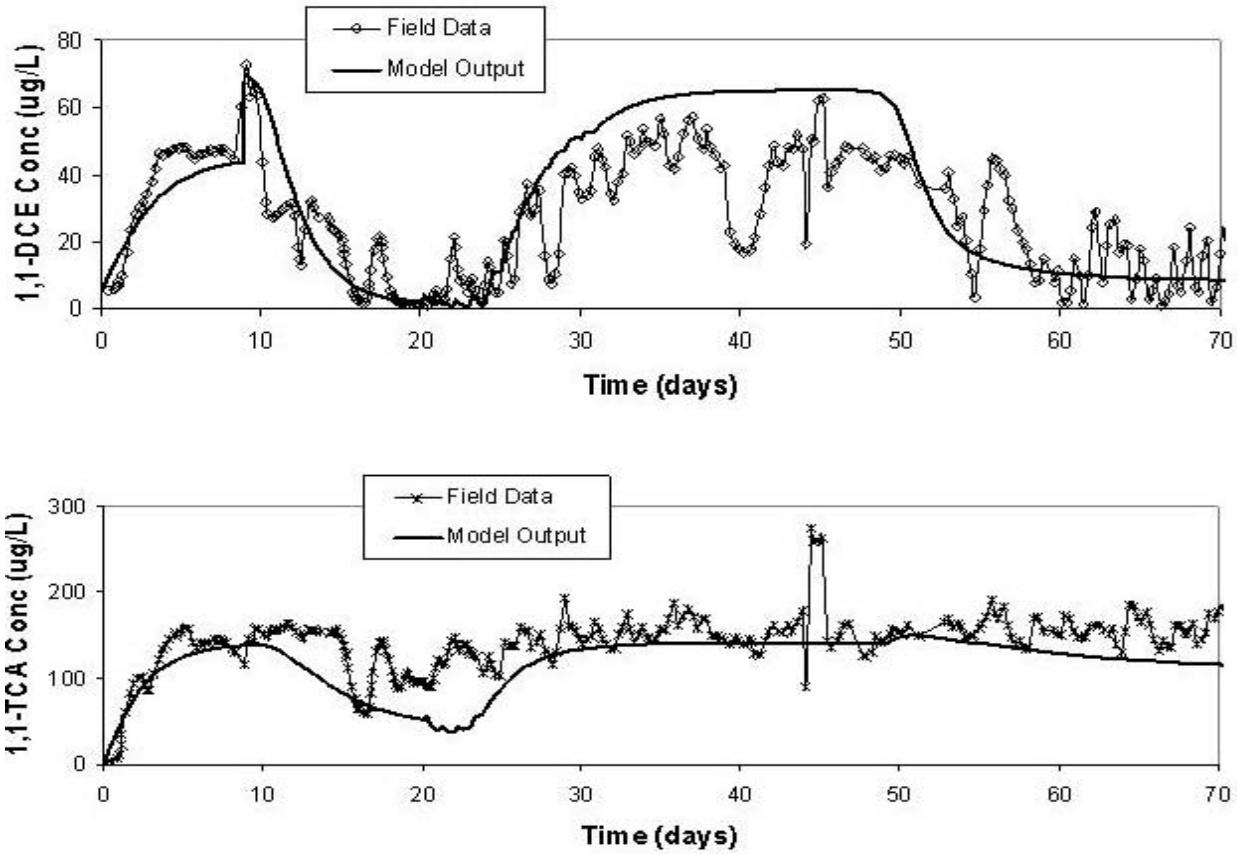

Figure 175c. Comparison of 1,1-DCA Concentrations for the Field Data and Model Output at S1 (1m). The bioaugmented culture was introduced on day 9. 1,1-DCA injection stopped at day 48.

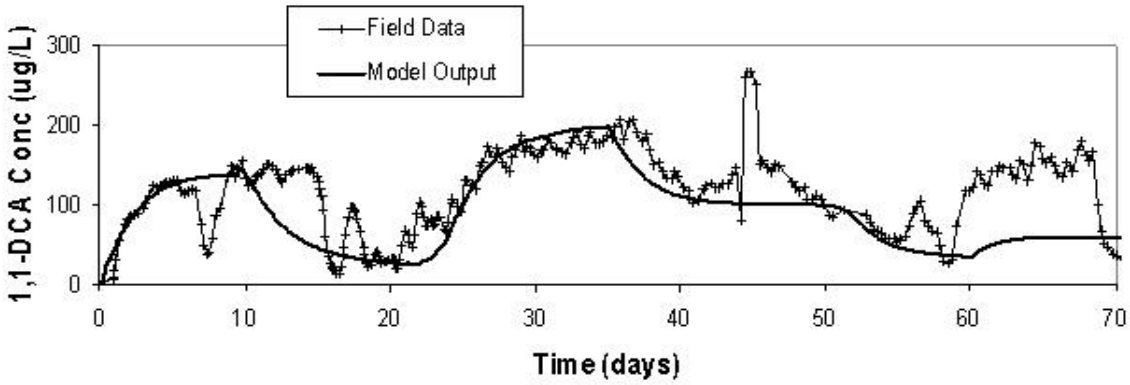

Figure 175d. Model Output of Cell Concentration at S1 (1m). The bioaugmented culture was injected on day 9. The lower figure is a blowup of cell growth, decay, and inactivation during the early part of bioaugmentation.

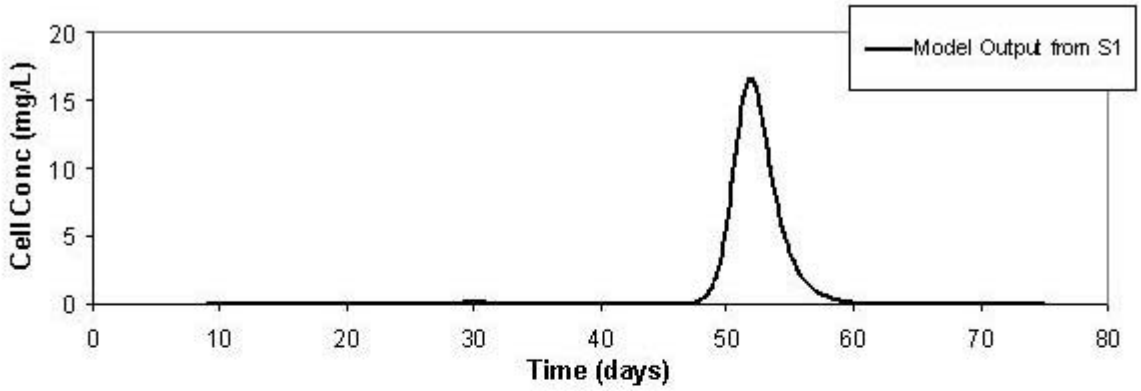

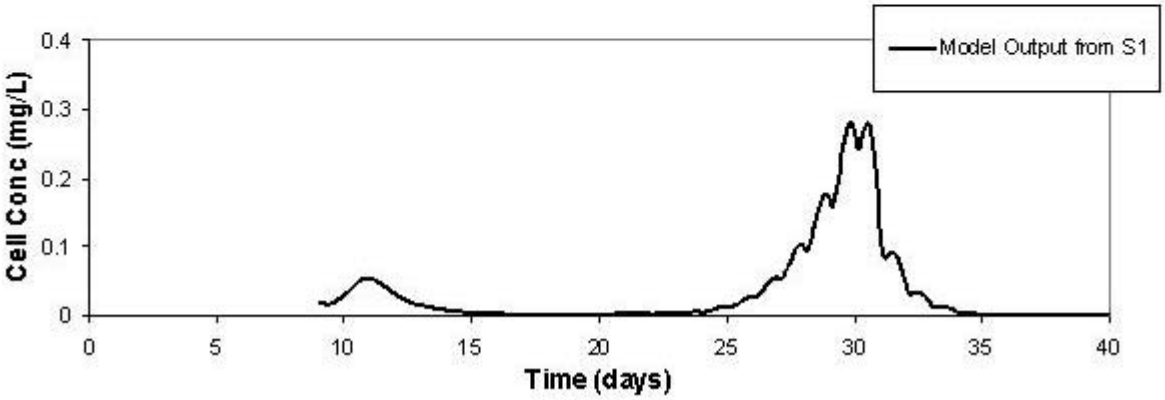

Figure 175e. Model Output of Cell Distribution over the First 2.6 m of the Test Zone on Day 20 and 75. The bioaugmented culture was injected on day 9. The lower figure is a blowup of cell concentration for day 20.

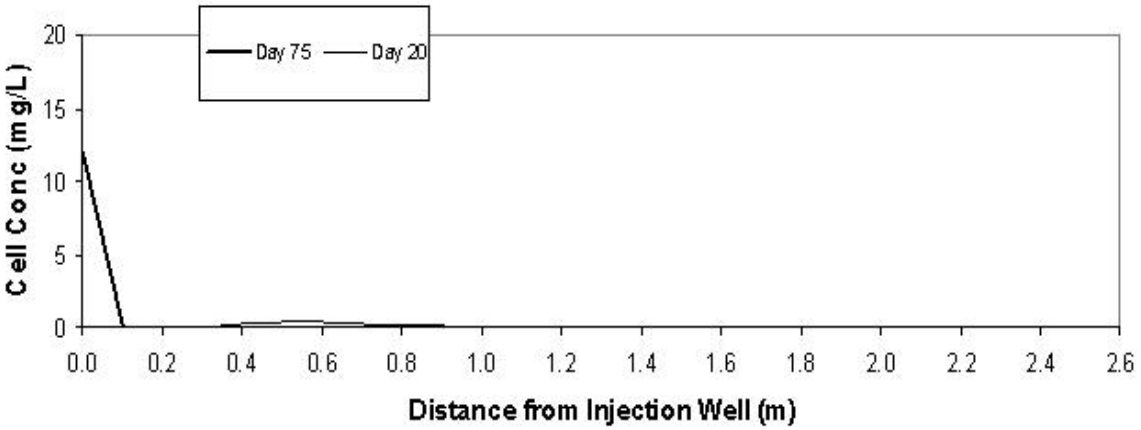

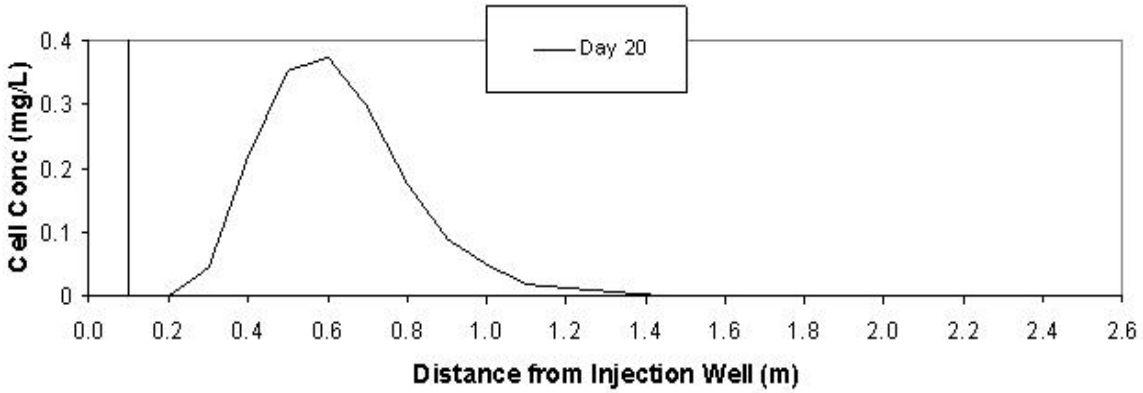

6.5 Simulations to Predict Activity after Bioaugmentation

Two simulations were run to predict activity within the test zone at S1 (1m from the injection well) after initial bioaugmentation ceased (day 75). This was done by expanding the simulation time to 90 days, with the first 75 days modeled for breakthrough and bioaugmentation seen in the field. After this period (days 75-90), the model was manipulated to simulate delivery of (1) oxygen alone and (2) elevated butane and oxygen concentrations. The simulations were run to observe transformation of only 2 of the 3 CAHs. 1,1-DCE was chosen to study because of its fast transformation ability and highly toxic effects on the culture. 1,1,1-TCA was chosen because it is the most recalcitrant of the three CAHs.

The first simulation included an oxygen injection concentration of 25 mg/L during days 75-90. This was pulsed every hour into the aquifer for 45 min durations. Results of the simulation are presented in Figure 176. Utilization and transformation during the first 75 days follow that seen in the previously discussed simulations. After day 75 there is rapid but short utilization of butane and transformation of 1,1-DCE and 1,1,1-TCA, followed by a rise in butane, oxygen, and CAH concentrations. This indicates that a large quantity of cells were inactivated during biotransformation of the highly toxic 1,1-DCE, leaving a nonviable population. The remaining cells were unable to transform the CAHs in the absence of butane.

The second simulation included butane and oxygen injection concentrations of 50 mg/L between days 75 and 90. This would represent much higher values with butane near its solubility limit. These were alternately pulsed into the aquifer, with butane being injected for 15 minutes followed by 45 minutes of oxygen. This shorter cycling time was chosen because the best transformation was observed in the field at this duration. Results of this simulation are presented in Figure 177. Utilization and transformation during the first 75 days follow that seen in the previous simulations. After day 75 there is rapid utilization and transformation, with particularly good degradation of 1,1,1-TCA due to 1,1-DCE having been reduced to low concentrations. This indicates that there is enough of a viable cell population at day 75 to restore transformation, once 1,1-DCE toxicity was eliminated. The results suggested that the addition of more butane and oxygen (through peroxide injection, H_2O_2) would be beneficial.

6.6 Sensitivity Analysis of 1,1-DCE Product Toxicity

As done with the laboratory data (Section 4), the field data were simulated using various 1,1-DCE transformation capacity values (T_{cDCE}). Biotransformation and transport values (Tables 58 and 59) were maintained from the previous simulations, with the exception of T_{cDCE}. This parameter was varied to represent three different product toxicities: 0.0167 (1.7%), 0.025 (2.5%), and 0.05 (5%) mg 1,1-DCE/mg cells. Note that the two extremes of this range are those studied in the laboratory modeling (Section 4).

Simulation results recorded at monitoring well S1 (1m from the injection well) are compared in Figure 178. The lower product toxicity (greater T_{cDCE} value, 0.05 mg DCE/mg cells) resulted in the most utilization and transformation. This observation is as expected, as lower product toxicity would inactivate less cells, allowing the microbial population to flourish. This

phenomena is depicted in Figure 178c., where the distributed biomass from lower product toxicity shows higher concentrations close to the injection well.

Figure 176. Model Output for Simulating Utilization and Transformation at S1 (1m) if 25 mg/L Oxygen is Injected between Days 75 and 90

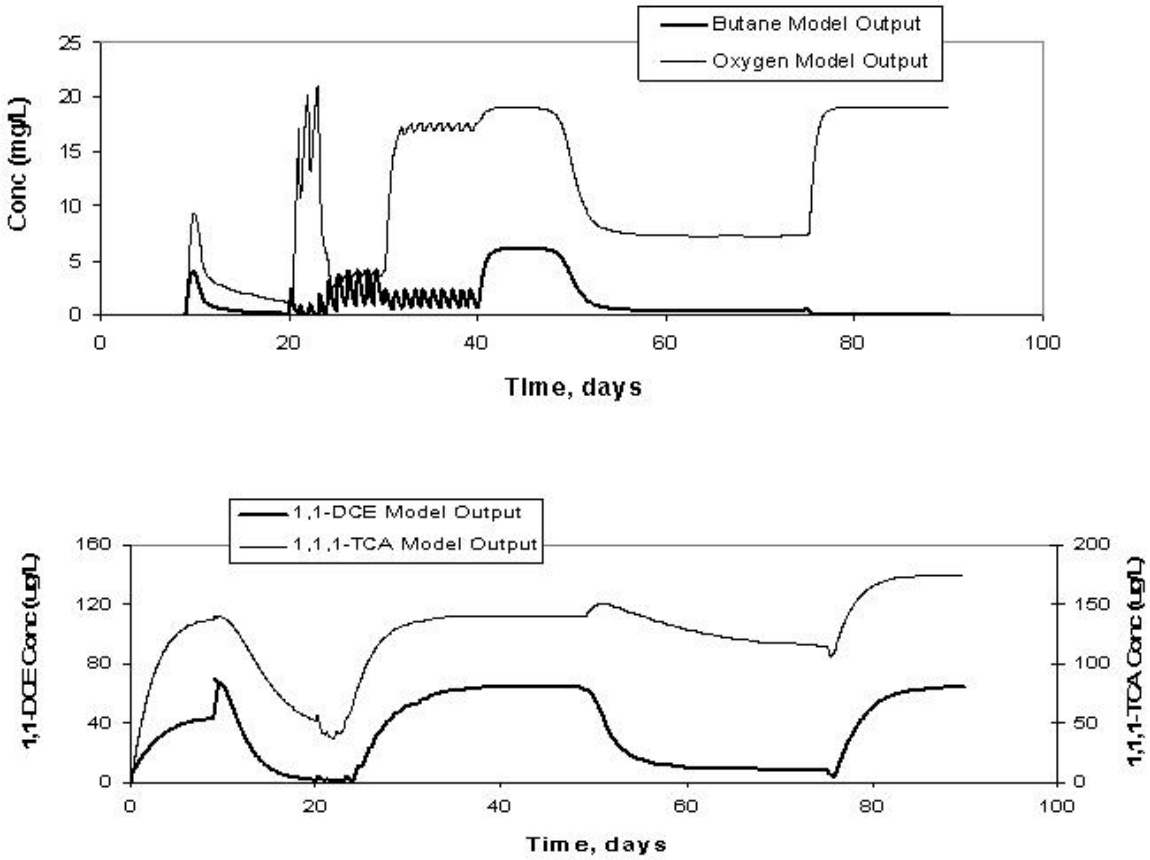

Figure 177. Model Output for Simulating Utilization and Transformation at S1 (1m) if 50 mg/L Butane and 50 mg/L Oxygen are Injected between Days 75 and 90

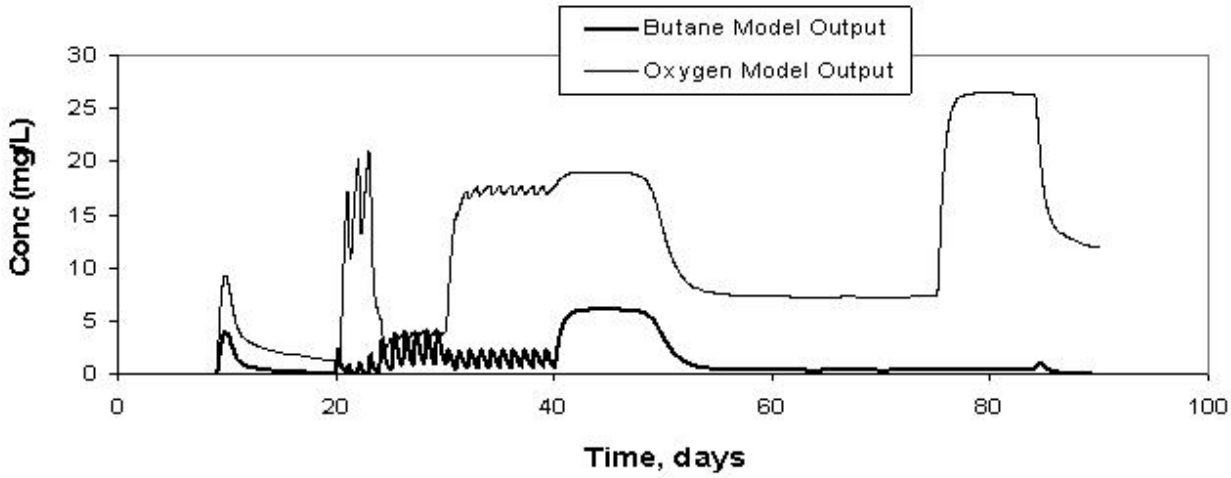

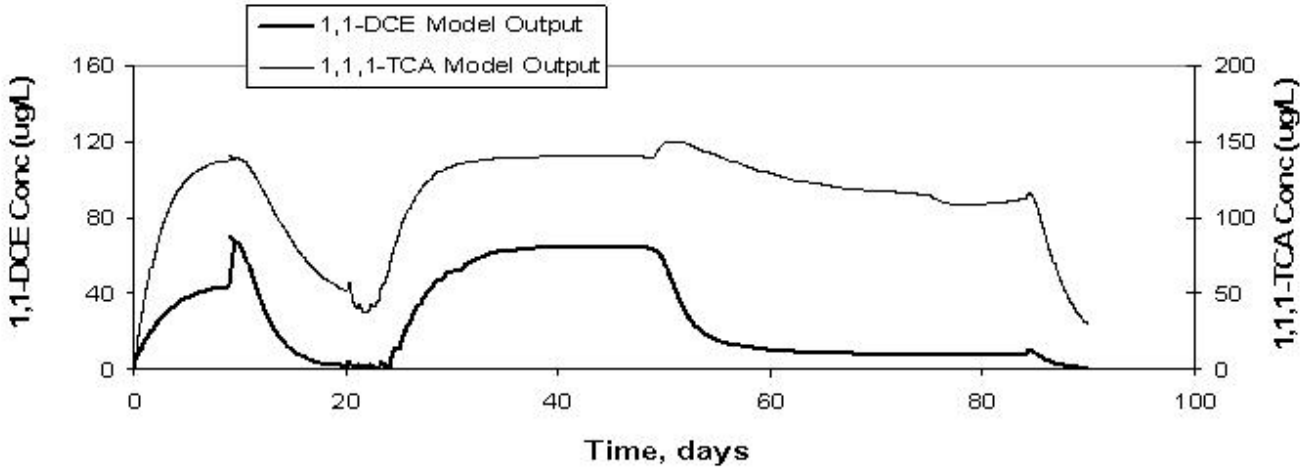

Figure 178a. Butane and Oxygen Output from Sensitivity Analysis of 1,1-DCE Product Toxicity at S1 (1m). Transformation capacities for 1,1-DCE (T_{cDCE}) values: 0.0167 (1.7%). 0.025 (2.5%), and 0.05 (5%) mg DCE/mg cells.

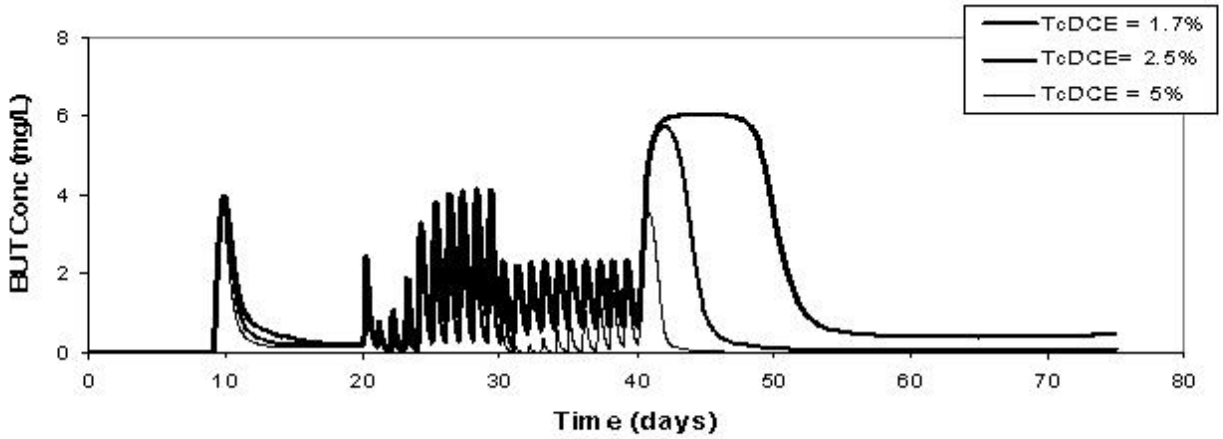

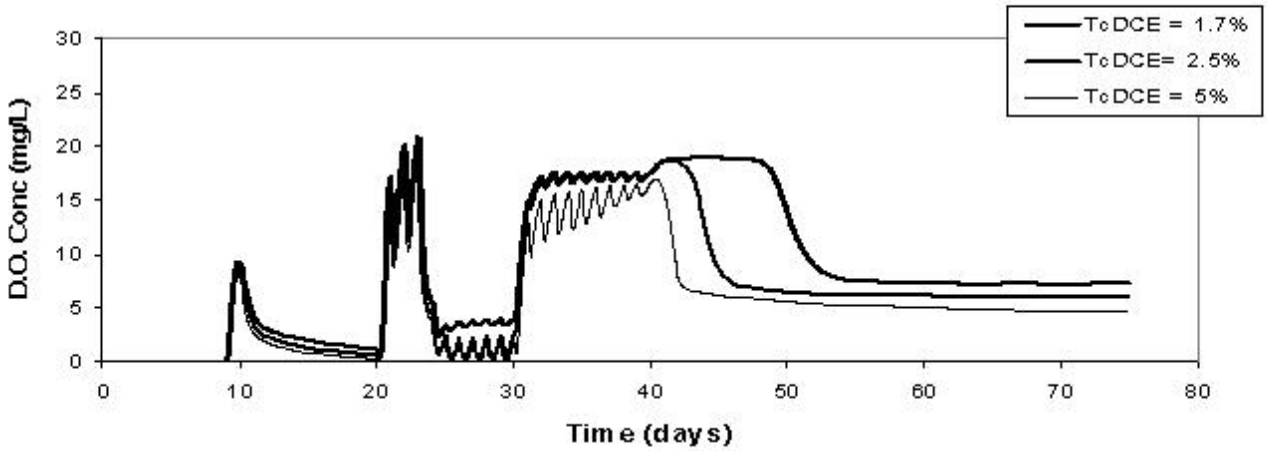

Figure 178b. 1,1-DCE and 1,1,1-TCA Results from Sensitivity Analysis of 1,1-DCE Product Toxicity at S1 (1m). Transformation capacities for 1,1-DCE (T_{cDCE}) values: 0.0167 (1.7%). 0.025 (2.5%), and 0.05 (5%) mg DCE/mg cells.

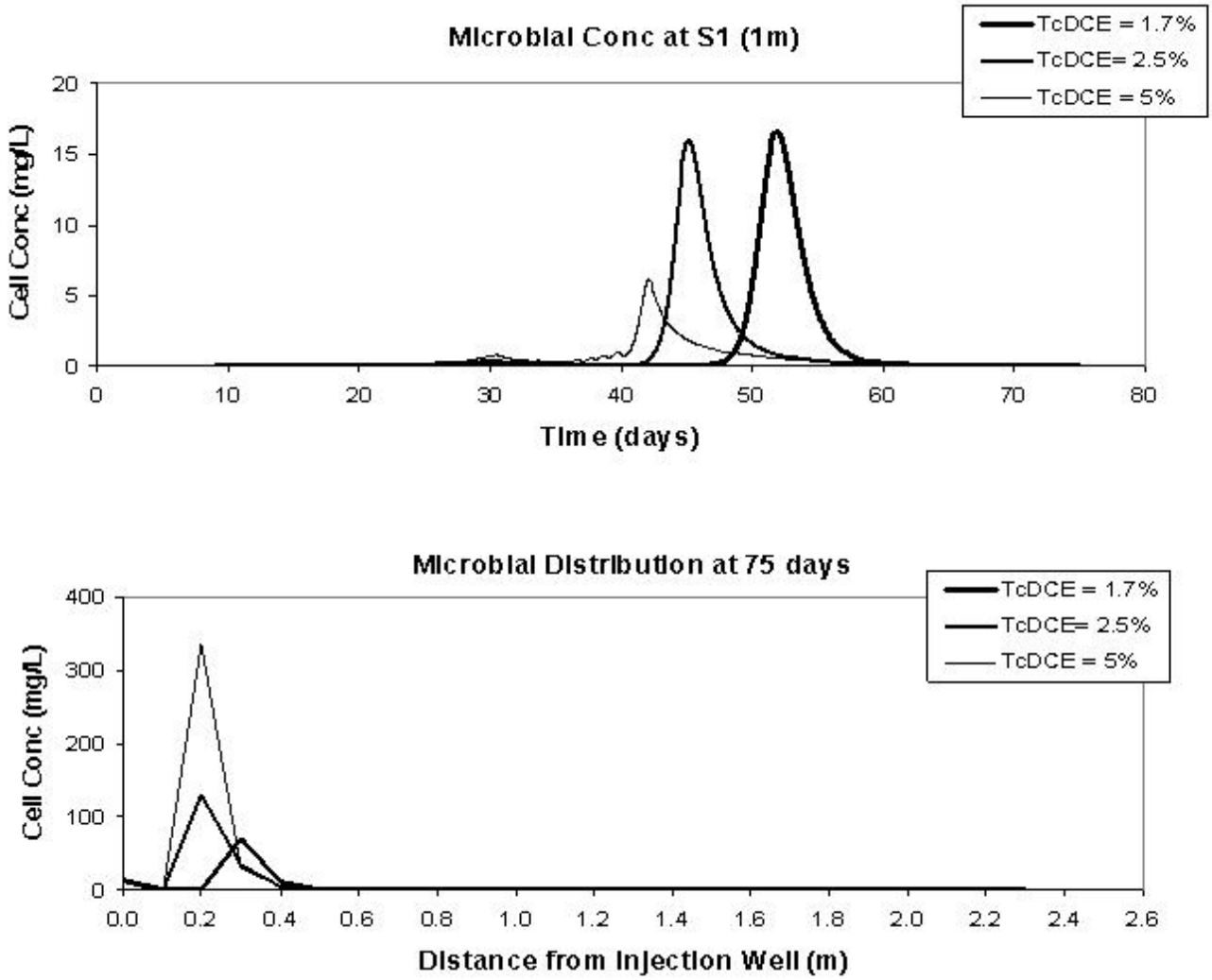

Figure 178c. Biomass Results from Sensitivity Analysis of 1,1-DCE Product Toxicity at S1 (1m). Transformation capacities for 1,1-DCE T_{cDCE}) values: 0.0167 (1.7%). 0.025 (2.5%), and 0.05 (5%) mg DCE/mg cells.

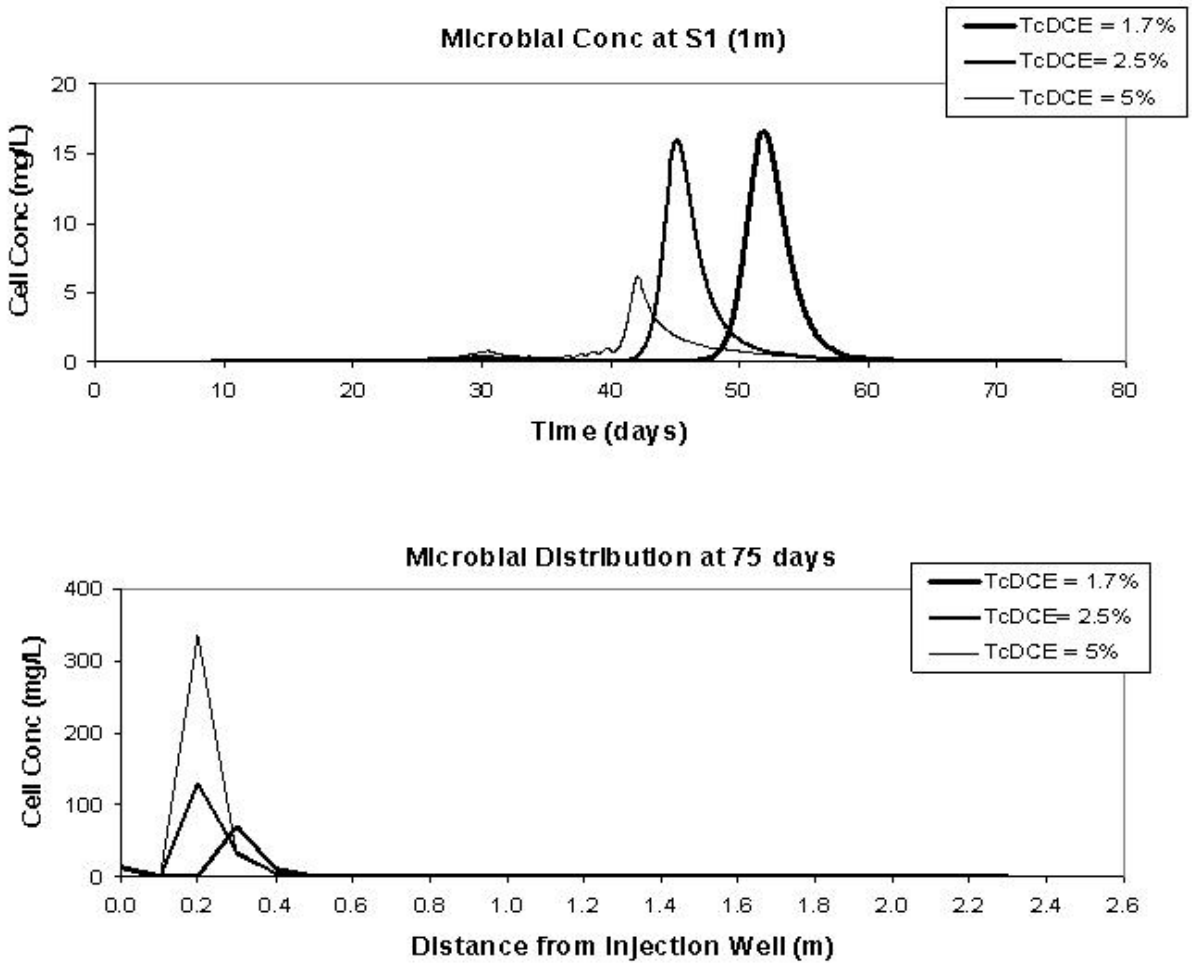

6.7 Sensitivity of 1,1-DCE Transformation Rate

Field simulations were also run using the lower 1,1-DCE transformation rate (k_{mDCE} = 0.1 μmol/mg/hr = 0.23 mg/mg/day) which had more closely fit the product toxicity laboratory data. This value was an order of magnitude lower than the k_{mDCE} value (2.8 μmol/mg./hr = 6.5 mg/mg/day) defined by Kim et al. (2002b). The model results are compared for both values of k_{mDCE}.. in Figure 179a. Other parameter values were the same as those presented in Tables 58 and 59.

The model output for transport and biotransformation is consistent with that from the Stella model. At the lower k_{mDCE} value, butane utilization and 1,1,1-TCA transformation became faster during the short butane and oxygen pulsing cycles (days 9 -20). During the later period (after day 20), 1,1-DCE transformation increased using the lower k_{mDCE} value (0.23 mg/mg/day). This

may have been caused by an increase in the microbial population at this location or inhibition by butane. Also note that the oscillations in CAH concentrations became more apparent. This observation suggested that the pulsing effect on CAH transformation was dampened using the higher $k_{mDCE..}$.

As with the simulations of the laboratory data for varying k_{mDCE}, the contrasts illustrate the complexity of the system and the sensitivity and limitations of the model. It is reasonable to suspect that because the culture used in this study was different from that used by Kim et al. (2002a, 2002b), other parameter values may also be different. A more useful approach in extrapolating model parameters from laboratory experiments to field experiments would have been to independently define the parameter values specific for our culture.

6.8 Sensitivity of First Order Mass Transfer Rate and Pulsing Cycle

Since sorption parameters were difficult to ascertain from simulating breakthrough data, a sensitivity analysis was run for variations in the first order mass transfer rate coefficient (F_k). The analysis included a variation in pulse durations, while maintaining the same butane to oxygen ratio. This was done because previous simulations for elongating pulsing durations included a decrease in the ratio of butane to oxygen that was being injected (15 min butane; 45 min oxygen at a 1:3 ratio, followed by 2 hrs butane; 22 hrs oxygen at a 1:10 ratio). It was suspected that, for actual field demonstrations and the previous simulations, it was not the longer pulse duration that caused transformation to cease (after day 20), but the reduction in the butane to oxygen delivery ratio, which made butane less available, resulted in transformation ceasing.

Figure 179a. Comparison of Butane and Oxygen Utilizations from Field Biotransformation Assuming Different 1,1-DCE Transformation Rates

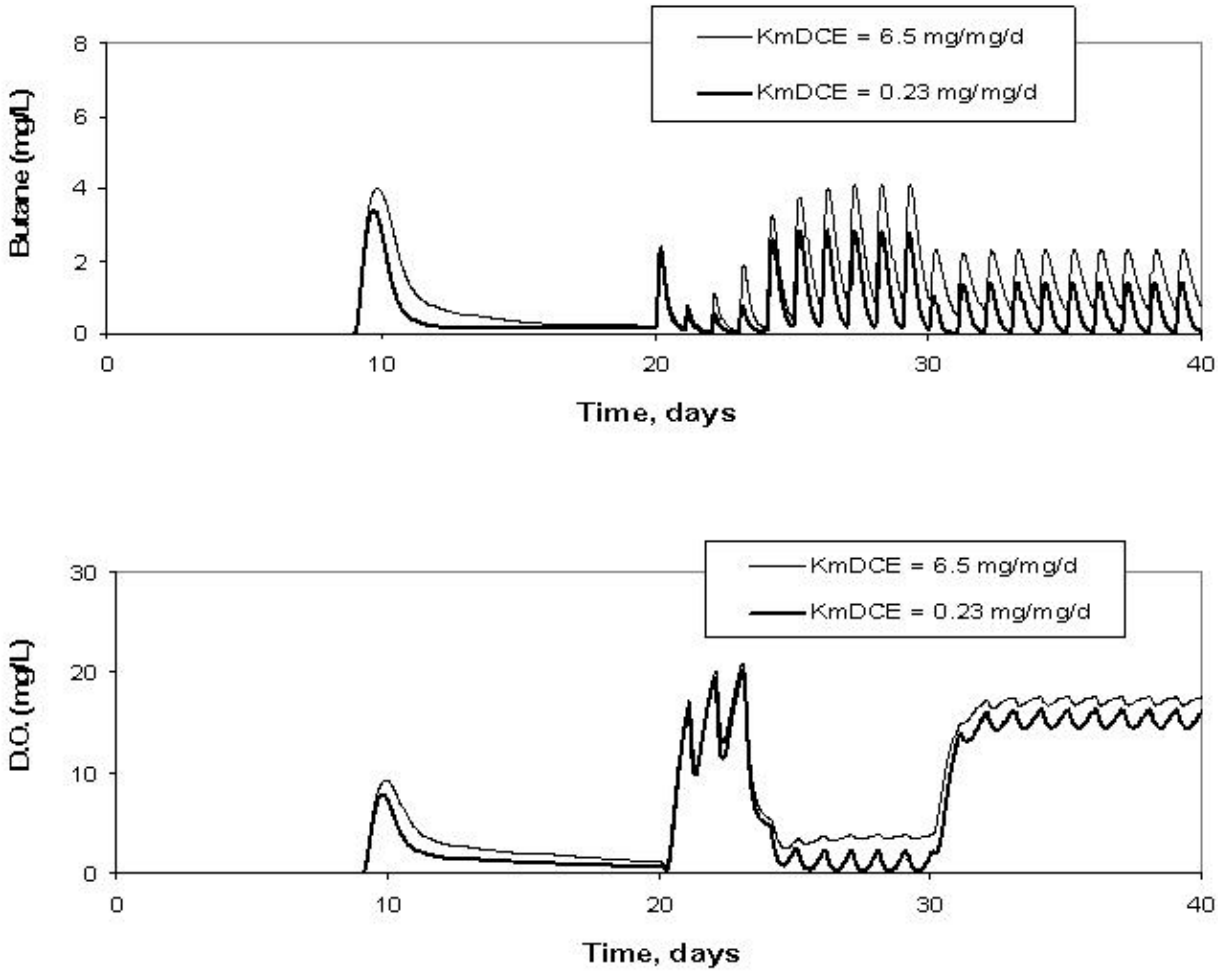

Figure 179b. Comparison of 1,1-DCE and 1,1,1-TCA Transformation from Field Biotransformation Assuming Different 1,1-DCE Transformation Rates

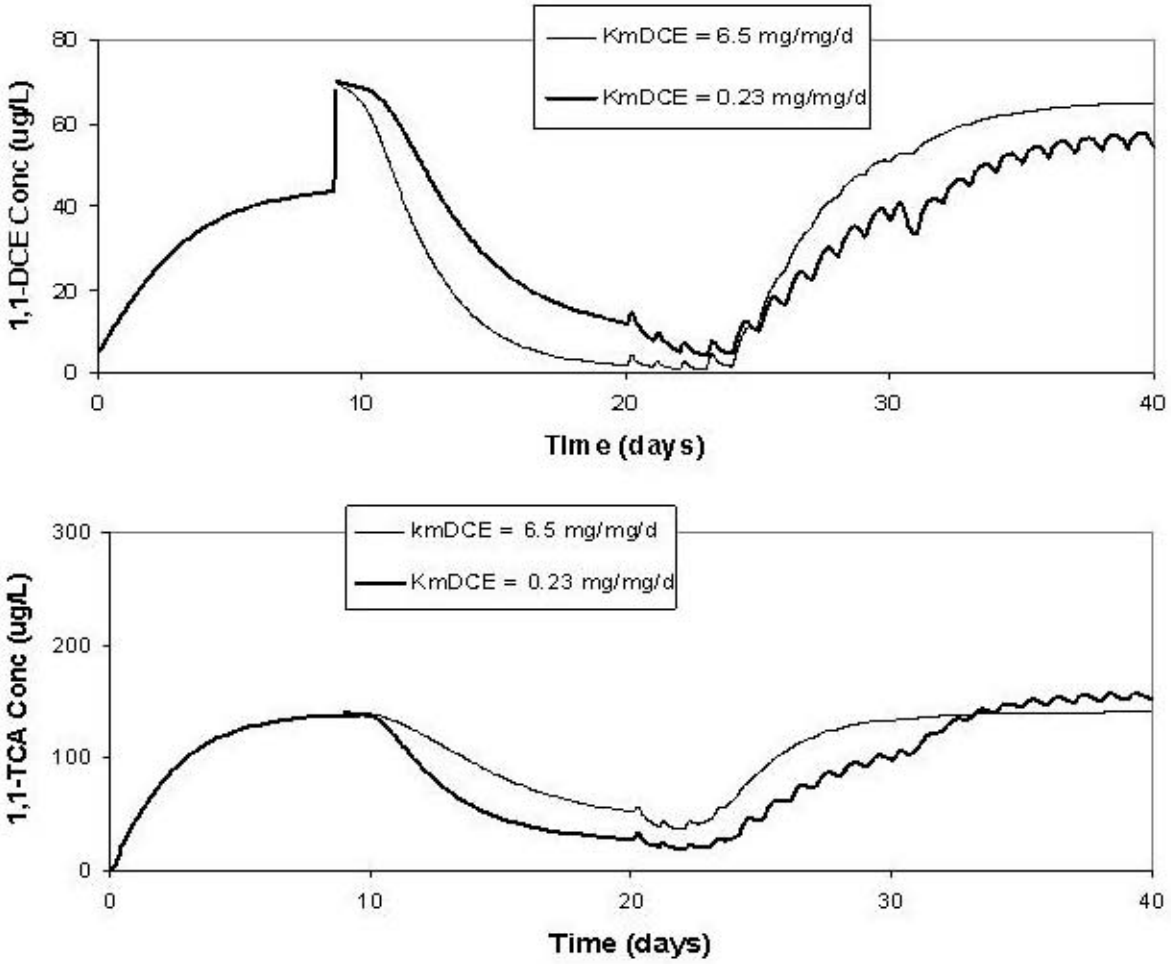

Simulations were therefore run to study the differences at monitoring well S1 between equilibrium and non-equilibrium sorption, with butane and oxygen pulsing durations elongated. The F_k value used in the previous simulations (2.0 day^{-1}) represented the case of equilibrium partitioning between the solid and liquid phases. A lower F_k value (0.2 day^{-1}) was incorporated to create a non-equilibrium case. All other biotransformation and transport parameters were maintained from the original 75 day simulations. For these simulations, butane and oxygen were initially pulsed (days 9-30) at a 1:3 butane to oxygen ratio for short durations (15 min butane;45 min oxygen). Later in the simulations, the pulse durations were elongated (3 hours butane; 9 hours oxygen), while maintaining the 1:3 butane to oxygen ratio. This allowed the same amount of butane to be delivered for both short and long pulse stages. This simulation included only the study of 1,1-DCE and 1,1,1-TCA transformation.

Figure 180 provides comparison plots of butane and oxygen utilization and CAH transformation for the variation in pulsing durations and the two different first-order mass transfer rates. There are two main points resulting from these simulations. The first is the influence of elongating the butane and oxygen pulsing durations (days 30-70). As seen in Figure 180a, when the duration was increased (3 hrs butane to 9 hrs oxygen) while maintaining the same oxygen to butane ratio (1:3) as the shorter cycle (15 min butane to 45 min oxygen), oscillations in the concentrations became more apparent. As oxygen became more available, transformation of 1,1-DCE (Figure 180c) and 1,1,1-TCA (Figure 180d) was maintained. This contrasted with the previous simulations in which both the butane to oxygen pulse durations and ratios changed (Figure 175) after day 40, making less butane available and stopping CAH transformation. From these simulations we can conclude that, had the butane to oxygen ratio been maintained during the field demonstration, CAH transformation may have continued.

The second point of understanding comes from observing the comparison plots of the equilibrium (2.0 day^{-1}) and non-equilibrium (0.2 day^{-1}) simulations. As seen in Figures 180c and 180d, when non-equilibrium was included during the longer pulsing cycles (days 30 to70), the oscillations in CAH concentrations became more exaggerated. This indicated the effect of equilibrium conditions dampening out the effects of competitive inhibition by butane. As the rate of CAH mass being sorbed onto and off of aquifer solids varied, less mass was exchanged between the liquid and sorbed phases over short time periods, causing greater variations in aqueous concentrations. This indicated that, based on the CAH oscillations observed during the field demonstration (Figure 175), non-equilibrium sorption was most likely occurring.

6.9 Summary from the Modeling of the First Season Tests

Simulations for flow and sorption using the transport model showed a good match to the field breakthrough data. The transport values determined from these simulations were incorporated into the combined model to simulate biotransformation and transport of the field data.

Bioaugmentation in the field showed similar results to the laboratory data when adequate butane and oxygen were delivered to the test zone. 1,1-DCE was quickly degraded with 1,1-DCA and 1,1,1-TCA more slowly transformed. The lag in transformation follows the phenomena of strong butane inhibition on these CAHs. When butane and oxygen pulsing was elongated, not enough growth substrate was available to maintain an effective cometabolic population, and

transformation ceased. Upon the reintroduction of shorter pulsing cycles, 1,1-DCE transformation was restored, although transformation of 1,1-DCA and 1,1,1-TCA ceased. This was most likely due to either a change in the microbial profile of the culture within the test zone, or an extreme product toxicity of 1,1,-DCE. 1,1-DCE transformation likely resulted from increased butane addition upon return to the shorter pulsing.

The model simulations reproduced many of these trends. During shorter injection pulsing of butane and oxygen, 1,1-DCE was quickly transformed. 1,1-DCA and 1,1,1-TCA were inhibited by butane, as transformation of these CAHs did not occur until a good portion of butane had been utilized. Elongating the butane and oxygen pulsing durations in the model reduced the amount of butane available to the organisms, and transformation ceased. However, the model predicted that upon restoring the shorter pulsing cycles, 1,1-DCA and slight 1,1,1-TCA transformation should have occurred. This discrepancy from the actual field data suggests that there was a shift in the microbial community with time.

Other inaccurate matches between the field data and model output were due to perturbations in the field system, such as inconsistent delivery of butane and oxygen to the site and heterogeneities within the test zone. Also, the bioaugmented culture was an enrichment from that used by Kim et al. (2002a, 2002b) from which many of the parameter values were taken. As the laboratory tests and modeling showed, there were likely variations in other parameters not studied here that would affect the simulations.

From these model simulations, improvements can be made for future bioremediation projects. Simulations indicated that maintaining short pulsing cycles of butane and oxygen were required in order to maintain CAH transformation and butane utilization. A less drastic elongation in cycling durations may have allowed further distribution of the microbes from the injection well without losing transformation.

The importance of this model, despite such complexities, is that trends observed in the field were well simulated, and the model permitted an analysis of the complex interaction of transport, biostimulation, and the transformation kinetics of cometabolism. This permitted us to determine what may have happened when changes were made in the pulsing duration, or the effect of different 1,1-DCE transformation capacities.

Figure 180a. Comparison of Butane Utilization at S1 (1m) for Equilibrium (F_k = 2.0 day^{-1}) and Non-Equilibrium (F_k = 0.2 day^{-1}) Sorption with Elongated Butane and Oxygen Pulsing Durations

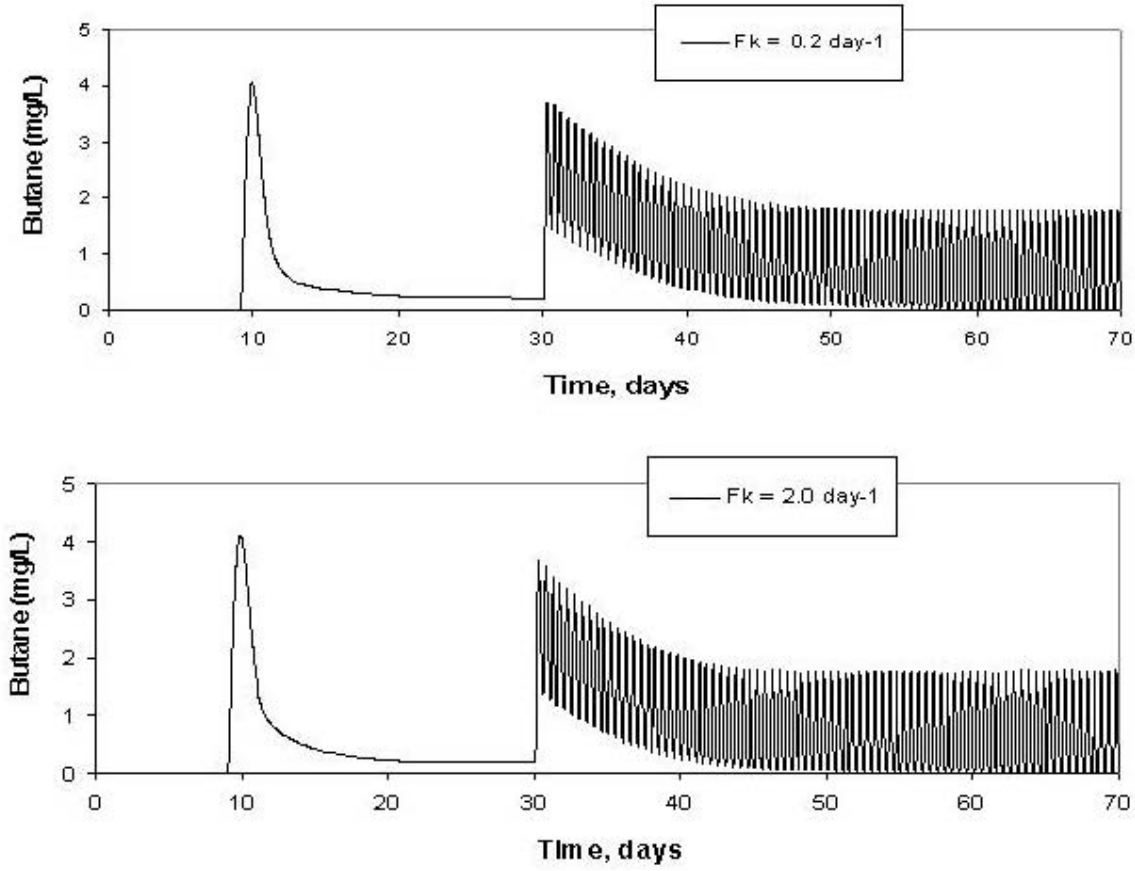

Figure 180b. Comparison of Oxygen Utilization at S1 (1m) for Equilibrium (F_k = 2.0 day^{-1}) and Non-Equilibrium (F_k = 0.2 day^{-1}) Sorption with Elongated Butane and Oxygen Pulsing Durations

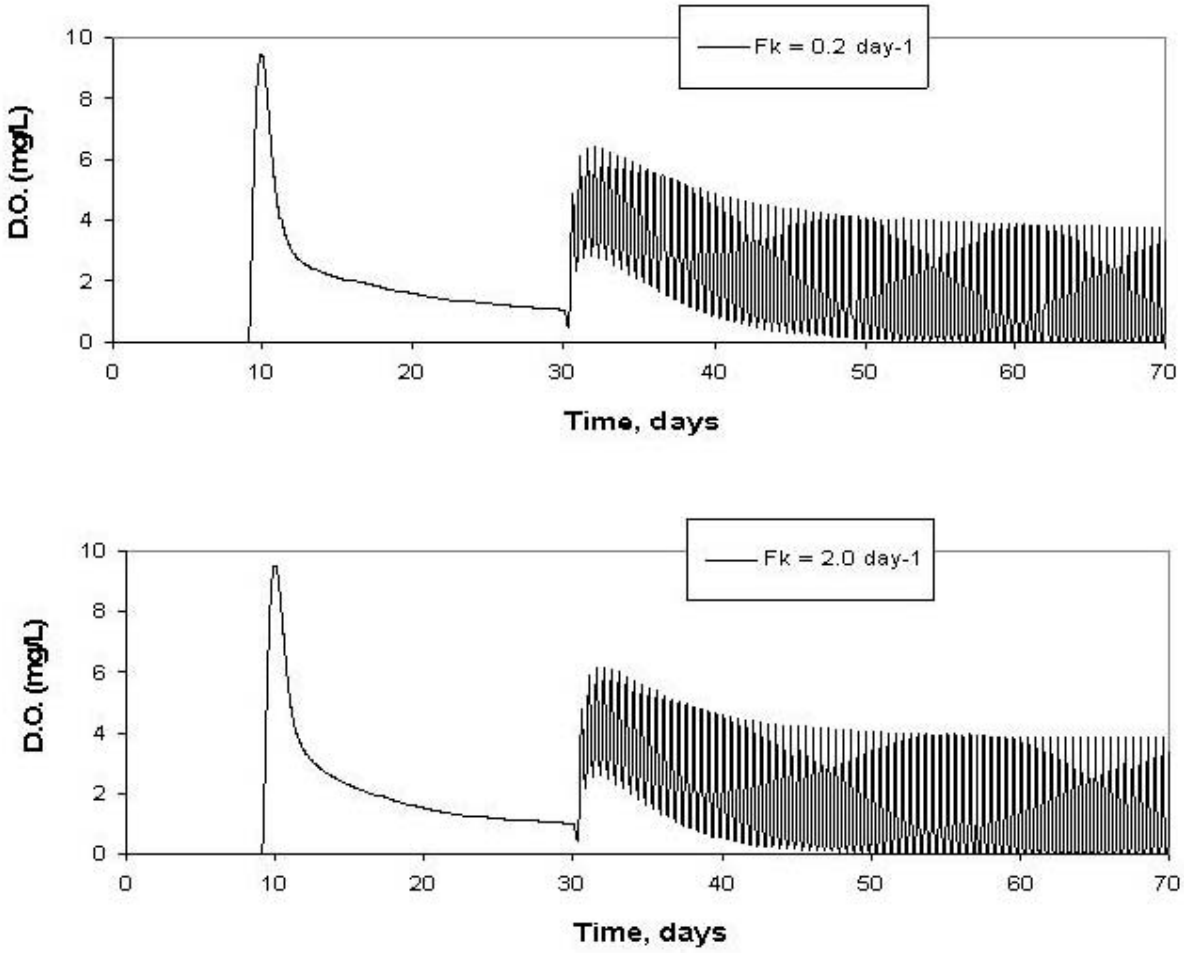

Figure 180c. Comparison of 1,1-DCE Transformation at S1 (1m) for Equilibrium (F_k = 2.0 day^{-1}) and Non-Equilibrium (F_k = 0.2 day^{-1}) Sorption with Elongated Butane and Oxygen Pulsing Durations

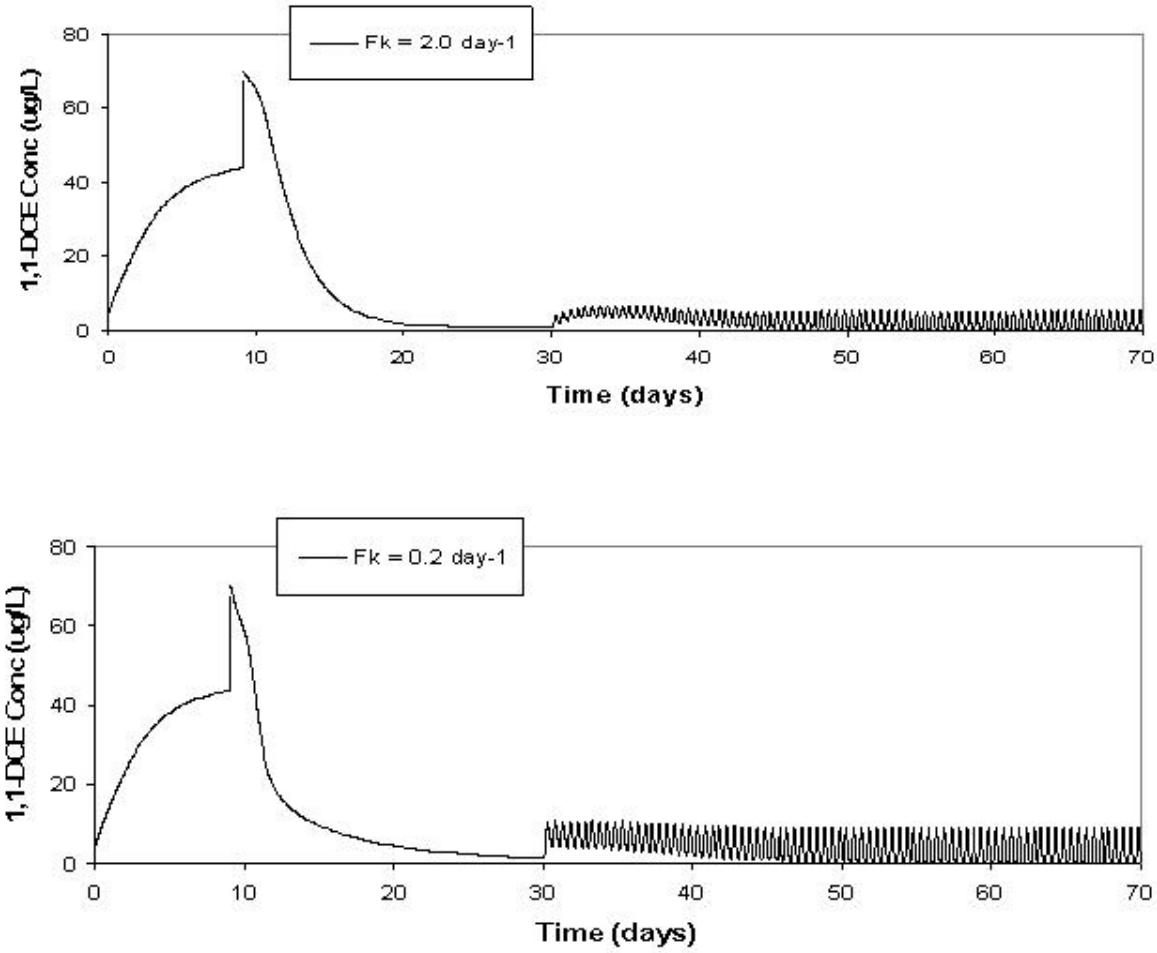

Figure 180d. Comparison of 1,1,1-TCA Transformation at S1 (1m) for Equilibrium (F_k = 2.0 day^{-1}) and Non-Equilibrium (F_k = 0.2 day^{-1}) Sorption with Elongated Butane and Oxygen Pulsing Durations

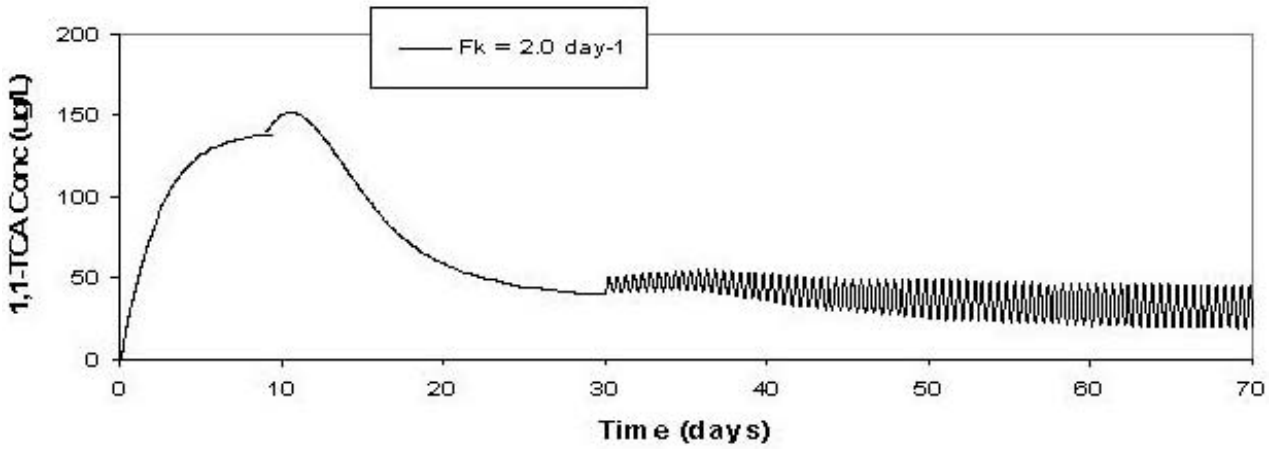

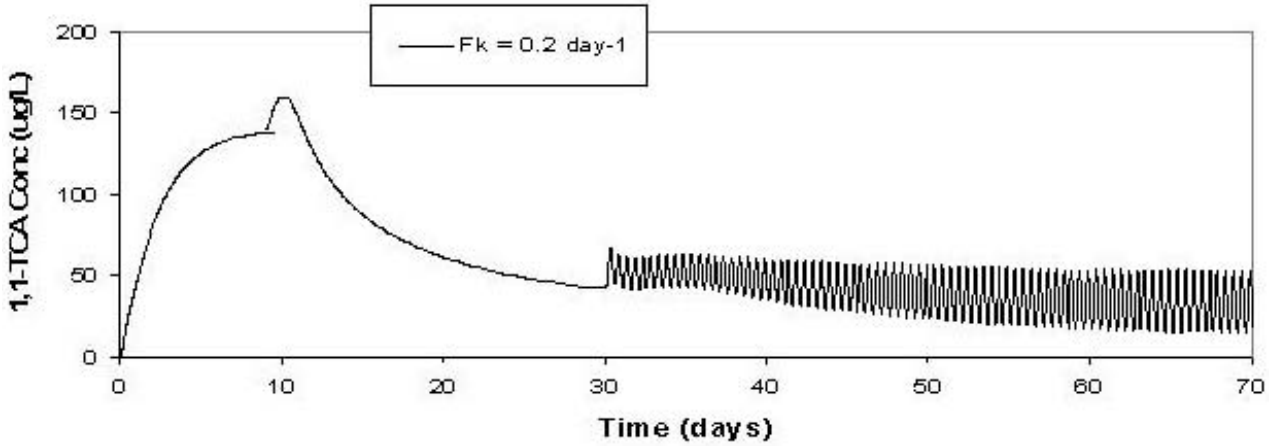

7. CONCLUSIONS

The following conclusions can be drawn from this study:

1) The transformation abilities of butane-utilizing organisms to cometabolize 1,1-DCE, 1,1-DCA, 1,1,1-TCA varies greatly.

2) 1,1-DCE is most rapidly transformed, followed by 1,1-DCA, and 1,1,1-TCA, and the transformation of these compounds is inhibited by butane, with 1,1,1-TCA being most strongly inhibited.

3) Cometabolic transformation models that include inhibition kinetics can be used to simulate the transformation of the CAH mixtures in batch kinetic studies and in microcosms, and do a reasonable job in predicting observed performance.

4) The bioaugmentation of butane cultures to microcosms resulted in effective transformation of mixtures of 1,1-DCE, 1,1-DCA, and 1,1,1-TCA, and decreased the lag times required for biostimulation.

5) Studies of bioaugmentation in continuous flow column study showed prolonged transformation of 1,1,1-TCA could be achieved if only 1,1,1-TCA was fed alone. When 1,1-DCE was also fed, 1,1-DCE was transformed and 1,1,1-TCA transformation essentially ceased. The continuous flow column study, although more difficult to perform than batch microcosm studies, proved a better predictor of the performance observed in the field tests than batch microcosm studies.

6) In the field, bioaugmentation results in shorter lag periods and better transformation of mixtures of 1,1-DCE, 1,1-TCA, and 1,1-DCA than mere stimulation with butane and oxygen. When 1,1-DCE was present, and being transformed, the transformation of 1,1,1-TCA and 1,1-DCA proved difficult to maintain for prolonged periods. This likely resulted from 1,1-DCE transformation product toxicity .

7) 1,1-DCE was most effectively transformed in the field tests with over 95% removal achieved. More effective and sustainable 1,1-DCE transformation was achieved in the bioaugmented leg than in the indigenous leg.

8) 1,1,1-TCA and 1,1-DCA were also transformed in situ, but at slower rates than 1,1-DCE. Removal was achieved in the bioaugmented leg, but not in the indigenous leg, despite effective butane removal in the indigenous leg. About 60 to 70 % removal of 1,1,1-TCA was achieved in prolonged tests in the bioagumented leg, but only when it was the primary contaminant present.

9) Real-time PCR analyses of groundwater samples obtained from the bioaugmented well leg resulted in successful enumeration of a single member of the bioaugmented culture. Although Strain 183 bp numbers were less than expected, a stable population of strain 183 bp was established in the bioaugmented leg and found throughout the test period.

10) Distinct microbial community succession from a dominant organism with a TFL of 277 bp to an dominant organism with a 126 bp TFL occurred upon stimulation of the bioaugmented well leg with butane and oxygen. The same succession was observed in two separate bioaugmentation events. The emergence and dominance of the 126 bp organism coincided with the gradual loss of CAH transformation efficiencies.

11) Results of the molecular analysis showed microbial population shifts occurred during the course of the field experiments, and these shifts appeared to be associated with changes in CAH transformation extents. Real time PCR analyses and T-RFPL analyses indicated that the dominant microorganisms in the bioaugmented culture represented only a minor fraction of the microorganisms present in groundwaters that were sampled from the test legs. Thus, while better performance was linked to bioaugmenation in the field tests, the results of the molecular analysis do not conclusively demonstrate a dominance of the bioaugmented microorganisms in groundwater samples taken during the tests.

12) Model simulations of the column studies and field tests proved to be useful in the interpretation of the results of the experiments. Kinetic parameters derived in laboratory batch studies gave reasonable estimates of the performance that was observed in the studies. Simulations also showed that processes, such as 1,1-DCE transformation toxicity, where important, and likely the cause of decreases in performance with prolonged bioremediation in the field tests.

13) The studies, although indicating that cometabolism of complex mixtures is possible, also demonstrated that bioaugmentation to enhance long term performance, is difficult to maintain, especially in the presence of indigenous organisms that consume the same substrate. Bioaugmentation however, did improve the long term performance for the transformation of 1,1-DCE, 1,1-DCA and 1,1,1-TCA. 1,1-DCA and 1,1,1-TCA were only transformed in the bioaugmented test leg.

14) Cometabolism is a complex process with many variables contributing to performance. If properly implemented it can be an effective process for treatment at low concentration levels of contaminants. For the conditions tested here, the enhanced treatment of 1,1-DCE, could be achieved.

8. REFERENCES

Alvarez-Cohen, L. and P.L.McCarty. (1991) Product Toxicity and Cometabolic Competitive Inhibition Modeling of Chloroform and Trichloroethylene Transformation by Methanotrophic Resting Cells. *Appl. Environ. Microbiol*. 57:1031-1037.

Alvarez-Cohen, L. and P.L.McCarty. (1991a). A Cometabolic Biotransformation Model for Halogenated Aliphatic Compounds Exhibiting Product Toxicity. *Environ. Sci. Technol.* 25: 1381-1387.

Alvarez-Cohen, L. and G.E. Speitel. (2001) Kinetics of Aerobic Cometabolism of Chlorinated Solvents. *Biodeg.* 12:105-126.

Anderson, J.E. and P.L. McCarty. (1996) Effect of Three Chlorinated Ethenes on Growth Rates for a Methanotrophic Mixed Culture. *Environ. Sci. and Technol. 30:3517-3525.*

Anderson, J.E.and P.L. McCarty. (1997) Transformation Yields of Chlorinated Ethenes by a Methanotrophic Mixed Culture Expressing Particulate Methane Monooxygenase. *Appl. Environ. Microbiol.* 63: 687-693.

Arp, D.J., C.M. Yeager, and M.R. Hyman. (2001) Molecular and Fundamental of Aerobic Cometabolism of Trichloroethylene. Biodegradation 12:81-103.

Aziz, C. E., G. E. Georgiou, and G. E. Speitel Jr. (1999) Cometabolism of Chlorinated Solvents and Binary Chlorinated Solvent Mixtures Using M. trichosporium OB3b PP358. Biotechnol. Bioeng. 65: 100-107.

Broholm, K., T. H. Christensen, and B. Jensen (1992) Modeling TCE Degradation by a Mixed Culture of Methane-Oxidizing Bacteria. *Wat. Res.* 26(9):1177-1185.

Chang, H.S.and L. Alvarez-Cohen (1995) Model for the Cometabolic Biodegradation of Chlorinated Organics. *Environ. Sci. Technol.* 29:2357-2367.

Chang, H.L. and L. Alvarez-Cohen. (1995) Transformation Capacities of Chlorinated Organics by Mixed Cultures Enriched on Methane, Propane, Toluene and Phenol. *Biotechnology and Bioengineering*. 45: 440-449.

Chang, H.S. and L. Alvarez-Cohen. (1996) Biodegradation of Individual and Multiple Chlorinated Aliphatic Hydrocarbons by Methane-Oxidizing Cultures. *Appl. Environ. Microbiol.* 62(9):3371-3377.

Chang, W.K. and C.S. Criddle, (1997) Experimental Evaluation of a Model for Cometabolism: Prediction of Simultaneous Degradation of Trichloroethylene and Methane by a Methanotrophic Mixed Culture. *Biotechnol. Bioeng.* 56: 492-501.

Cho, J.-C. and S.J. Kim. (2000) Computer-Assisted PCR-Single-Strand-Conformation Polymorphism Analysis fro Assessing Shift in Soil Bacterial Community Structure during Bioremediation Treatments. *World Journal of Microbiology & Biotechnology.* 16:231-235.

Connally, R., D. Veal, and J. Piper. (2002) High Resolution Detection of Fluorescently Labeled Microorganisms in Environmental Samples Using Time-Resolved Fluorescence Microscopy. *FEMS Microbiol. Ecology*. 41:125-129.

Cottrell, M. T. and D. L. Kirchman. (2000) Community Composition of Marine Bacterioplankton Determined by 16S rRNA Gene Clone Libraries and Fluorescence In Situ Hybridization. *Appl. Environ. Microbiol.* 66: 5116-5122.

Daims, H., N. B. Ramsing, K.-H. Schleifer, and M. Wagner. (2000) Cultivation-Independent, Semiautomatic Determination of Absolute Bacterial Cell Numbers in Environmental Samples by Fluorescence In Situ Hybridization. *Appl. Environ. Microbiol.* 67:5810-5818.

Dolan, M.E.and P.L. McCarty. (1995) Methanotrophic Chloroethene Transformation Capacities and 1,1-Dichloroethene Transformation Product Toxicity. *Ennviron. Sci. Technol*. 29: 2741-2747.

Dollopf, S. L., S. A. Hashsham, and J. M. Tiedje. (2001) Interpreting 16s rDNA T-RFLP Data: Application of Self-Organizing Maps and Principal Component Analysis to Describe Community Dynamics and Convergence. *Microbiol. Ecology.* 42:495-505

Domenico, P.A. and F.W. Schwartz, (1990) *Physical and Chemical Hydrogeology.* John Wiley & Sons, Inc.

Dunbar, J., L.O. Ticknor, and C. R. Kuske. (2000) Assessment of Microbial Diversity in Four Southwestern United States Soils by 16S rRNA Gene Terminal Restriction Fragment Analysis. *Appl. Environ. Microbiol.* 66: 2943-2950.

Ely, R.L., K.J. Williamson, R.B Guenther, M.R. Hyman, and D.J. Arp (1995) A Cometabolic Kinetics Model Incorporating Enzyme Inhibition, Inactivation, and Recovery: I. Model Development, Analysis and Testing. *Biotech. Bioeng.* 46:218-231.

Ely, R.L., K.J. Williamson, R.B Guenther, M.R. Hyman, and D.J. Arp (1997) Cometabolism of chlorinated solvents by nitrifying bacteria: kinetics, substrate interaction, toxicity effects, and bacterial response. Biotechnol. Bioeng. 54: 520-534.

Felske, A., A.D.L.Akkermans, and W.M.De Vos. (1998) Quantifications of 16S rRNAs in Complex Bacterial Communities by Multiple Competitive Reverse Transcription-PCR in Temperature Gradient Gel Electrophoresis Fingerprints. *Appl. Environ. Microbiol.*64: 4581-4587.

Ferris, M.J. and D.M.Ward, (1997) Seasonal Distributions of Dominant 16S rRNA-Defined Populations in a Hot Spring Microbial Mat Examined by Denaturing Gradient Gel Electrophoresis. *Appl. Environ. Microbiol*.63: 1375-1381.

Fetter, C.W. (1993) *Contaminant Hydrogeology.* Macmillan Publishing Company, New York.

Ficker, M., K. S. Krastel, Orlicky, and E. Edwards. (1999) Molecular Characterization of a Toluene-Degrading Methanogenic Consortium. *Appl. Environ. Microbiol.*65: 5576-5585.

Fry, V.A., J.D. Istok, L .Semprini., K.T. O'Reilly and T.E. Buscheck. (1995) Retardation of dissolved oxygen due to trapped gas phase in porous media. *Ground Water* **33** (3): 391-398.

Fuchs, B. M., G. Wallner, W. Beisker, I. Schwippl, W. Ludwig, and R. Amann. (1998) Flow Cytometric Analysis of the In Situ Accessibility of Escherichia coli 16S rRNA for Fluorescently Labeled Oligonucleotide Probes. *Appl. Environ. Microbiol.* 64:4973-4982.

Flynn, S.J., F.E. Löffler, and J.M. Tiedje. (2000) Microbial Community Changes Associated with a Shift from Reductive Dechlorination of PCE to Reductive Dechlorination of *cis*-DCE and VC. *Environ. Sci. Technol*. 34: 1056-1061.

Fox, B.G., J.G. Borneman, L.P.Wackett, and J.D.Lipscomb. (1990) Haloalkene Oxidation by the Soluble Methane Monooxygenase from *Methylosinus trichosporium* OB3b: Mechanistic and Environmental Implications. *Biochem* 29: 6419-6427.

Fries, M. R., G. D. Gary, P.L. McCarty, L. J. Forney, and J. M. Tiejie. (1997b) Microbial Succession during a Field Evaluation of Phenol and Toluene as the Primary Substrates for Trichloroethene Cometabolism. *Appl. Environ. Microbiol*. 63:1515-1522.

Giulietti, A., L. Overbergh, D. Valckx, B. Decallonne, R. Bouillon, and C. Mathieu. (2001) An Overview of Real-Time PCR: Applications to Quantify Cytokine Gene Expression. *Methods.* 25:386-401.

Gossett, J. M. (1987) Measurement of Henry's Law Constants for C1 and C2 Chlorinated Hydrocarbons. *Environmental Science and Technology* **21**(2):202-208.

Hamamura, N., C. Page, T. Long, L. Semprini, and D.J.Arp. (1997) Chloroform Cometabolism by Butane-Grown CF8, *Pseudomonas butanovora*, and *Mycobacterium vaccae* JOB5 and Methane-Grown *Methylosinus trichosporium* OB3b. *Appl. Environ. Microbiol.* 63: 3607-3613.

Hamamura, N., R. Storfa, L. Semprini, and D.J. Arp. (1999) Diversity in Butane Monooxygenases among Butane-Grown Bacteria. *Appl. Environ. Microbiol.* 65: 4586-4593.

Hamamura, N. and D.J. Arp. (2000) Isolation and characterization of alkane-utilizing *Nocardioides sp*. Strain CF8. *FEMS Microbiology Letters*. 186: 21-26.

Harmon, T.C., L. Semprini, and P.V. Roberts. (1992) Simulating Solute Transport Using Laboratory-Based Sorption parameters. *J. of Enviro. Engr.* **118**(5):666-689.

Head, I.M., J.R. Saunders, and R.W. Pickup (1998) Microbial Evolution, Diversity, and Ecology: A decade of Ribosomal RNA Analysis of Uncultivated Microorganisms. *Microb. Ecol*. 35: 1-21.

Hopkins, D.G., L. Semprini, and P.L. McCarty. (1993a) Microcosm and In-situ Field Studies of Enhanced Biotransformation of Trichloroethylene by Phenol-Utilizing Microorganisms. *Appl. Environ. Microbiol.* 59:2277-2285.

Hopkins, G.D., J. Munakata, L. Semprini, and P.L. McCarty. (1993b) Trichloroethylene Concentration Effects on Pilot Field-Scale In-Situ Groundwater Bioremediation by Phenol-Oxidizing Microorganisms. *Environ. Sci. Technol.* 27(12):2542-2547.

Hopkins, G.D., and P.L. McCarty. (1995) Field Evaluations of In Situ Aerobic Cometabolism of Trichloroethylene and Three Dichloroethylene Isomers Using Phenol and Toluene as the Primary Substrates. *Environ. Sci. Technol.*. 29(6):1628-1637.

Hugenholtz, P., C. Pitulle, K. L. Hershberger, and N. R. Pace. (1998) Novel Division Level Bacterial Diversity in a Yellowstone Hot Spring. *J Bacteriol.*180: 366-376

Hugenholtz, P., G. W. Tyson, and L. Blackall. (2001). Design and Evaluation of 16S rRNA-Targeted Oligonucleotide Probes for Fluorescence In Situ Hybridization. *Methods in Molecular Biology.* 17:29-41.

Hugenholtz, P. (2002) Exploring Prokaryotic Diversity in the Genomic Era. *Genome Biology.* 3:1-8.

Jenal-Wanner, U., and P. McCarty, (1997) Development and Evaluation of Semicontinuous Slurry Microcosms to Simulate *in situ* Biodegradation of Trichloroethylene in Contaminated Aquifer. *Environ. Sci. Technol.* 31: 2915-2922.

Jitnuyanont, P., L.A. Sayavedra-Soto, and L. Semprini. (2001) Bioaugmentation of Butane-Utilizing Microorganisms to Promote Cometabolism of 1,1,1-Trichloroethane in Groundwater Microcosms. *Biodegradation*. 12: 11-22.

Keenan, J.E., S.E. Strand, and H.D. Stensel. (1994) Degradation Kinetics of Chlorinated Solvents by a Propane Oxidizing Enrichment Culture. *Bioremediation of Chlorinated and Polycyclic Aromatic Hydrocarbon Compounds.* Lewis Publishers, Boca Raton, FL. pgs. 1-13.

Kim, Y., L. Semprini, and D.Arp. (1997) Aerobic Cometabolism of Chloroform and 1,1,1-Trichloroethane by Butane-Grown Microorganisms. *Bioremediation Journal.,* 1(2):135-148.

Kim, Y., D.J. Arp, and L. Semprini.(2000) Chlorinated Solvent Cometabolism by Butane-Grown Mixed Culture. *J. of Enviro. Engr*. 126: 934-942.

Kim, Y., D. Arp., and L. Semprini. (2002) A Combined Method for Determining Inhibition Type, Kinetic Parameters, and Inhibition Coefficients for Aerobic Cometabolism of 1,1,1-Trichloroethane by a Butane-Grown Mixed Culture. *Biotech. Bioeng.* 77(5):564-576.

Kim, Y., D.J. Arp, and L. Semprini. (2002) Kinetic and Inhibition Studies for the Aerobic Cometabolism of 1,1,1-Trichloroethane, 1,1-Dichloroethylene, and 1,1-Dichloroethane by a Butane-Grown Mixed Culture. *Biotech. Bioeng*. 80: 498-508.

Kindred, J.S. and M.A. Celia. (1989) Contaminant Transport and Biodegradation 2. Conceptual Model and Test Simulations. *Wat. Res*. 25(6): 1149-1159.

Lee, S.B., S.E Strand, and H.D.Stensel (2000) Sustained Degradation of Trichloroethylene in a Suspended Growth Gas Treatment Reactor by an Actinomycetes Enrichment. *Environ. Sci. Technol.* 34(15):3261-3268.

Lawrence Livermore National Laboratory. Historic Case Analysis of CVOC Plumes. UCRL-AR-133361, March 1999.

Liu, W.T., T.L Marsh, H. Cheng, and L.J. Forney. (1997) Characterization of Microbial Diversity by Determining Terminal Restriction Fragment Length Polymorphisms of Genes Encoding 16S RNA. *Appl. Environ. Microbiol.* 63: 4516-4522.

Liu, C.Y., J.R. Speitel and G.E.Georgiou. (2001) Kinetics of Methyl *t*-Butyl Ether Cometabolism at Low Concentrations by Pure Cultures of Butane-Degrading Bacteria. *Appl. Environ. Microbiol.* 67: 2197-2201.

Löeffler, F. E., Q. Sun, J. Li, and J. M. Tiedje. (2000) 16S rRNA Gene-Based Detection of Tetrachloroethene-Dechlorinating Desulfuromonas and Dehalococcoides Species. *Appl. Environ. Microbiol.* 66:1369-1374.

Mackey and Shui (1981) Review of Henry's Law Constants for chemicals of environmental interest. *J. Phys. Chem. Ref. Data* **10**(4):1175-1199

Mars, A.E., G.T. Prins, P. Wietzes, W.D. Koning, and D.B. Janssen. (1998) Effect of Trichloroethylene on the Competitive Behavior of Toluene-Degrading Bacteria. *Appl. Environ. Microbiol.* 64: 208-215.

Matheson, V.G., J. Munakata-Marr, G.D. Hopkins, P.L. McCarty, J.M. Tiedje, and L.J. Forney. (1997) A Novel Means To Develop Strain-Specific DNA Probes for Detecting Bacteria in the Environment. *Appl. Environ. Microbiol.* 63: 2863-2869.

Mathias, M.A. (2002) *Modeling Cometabolic Transformation of a CAH Mixture by a Butane Utilizing Culture*. Master Thesis. Oregon State University. Department of Civil, Construction and Environmental Engineering.

McCarty, P.L. and L. Semprini (1994) Ground-Water Treatment of Chlorinated Solvent in Groundwater Clean-Up Through Bioremediation. In *Handbook of Bioremediation Lewis Publishers Inc., Chelsea, MI*. pp. 87-116.

McCarty, P.L., G.D. Hopkins, J. Munakata-Marr, G. Matheson, M.E. Dolan, L.B. Dion, M. Shields, L. J. Forney, and J.M. Tiedje, "Bioagumentation with *Burholderia cepacia* $PR1_{310}$ for In-situ Bioremediation of Trichoroethylene Contaminated Groundwater, Final Report, The Gulf Breeze Environmental Research Laboratory, USEPA, January, 1997.

McCarty, P.L., M.N. Goltz, G.D. Hopkins, M.E. Dolan, J.P. Allan, B.T. Kawakami, and T.J. Carrothers. (1998) Full-Scale Evaluation of *In Situ* Cometabolic Degradation of Trichloroethylene in Groundwater through Toluene Injection. *Environ. Sci. Technol.* 32(1):88-100.

Munakata-Marr, J, P.L. McCarty, M.S. Shields, M. Reagin, and S.C. Francesconi. (1996) Enhancement of Trichlorethylene Degradation in Aquifer Microcosms Bioagumented with Wild Type and Genetically Altered *Burkholderia (Pseudomonas) cepacia* G4 and PR1. *Environ. Sci. Technol.* 30:2045-2052.

Munakata-Marr, J., V.G. Matheson, L.J. Forney, J.M. Tiedje, and P.L. McCarty. (1997) Long-Term Biodegradation of Trichloroethylene Influenced by Bioaugmentation and Dissolved Oxygen in Aquifer Microcosms. *Environ. Sci. Technol.* 31: 786-791.

Oldenhuis, R., J.Y. Oedzes, J.J. van der Waarde, and D.B. Janssen, (1991) Kinetics of Chlorinated Hydrocarbon Degradation by *Methylosinus trichosporium* OB3b and toxicity of trichloroethylene. *Appl Environ Microbiol* 57: 7-14.

Olsen, G. J., D. J. Lane, S. J. Giovannoni, and N. R. Pace. (1986) Microbial Ecology and Evolution: A Ribosomal RNA Approach. *Ann. Rev. Microbiol*. 40:337-365.

Peer, Y.V., S. Chapelle, and R.D. Wachter. (1996) A Quantitative Map of Nucleotide Substitution Rates in Bacterial rRNA. *Nucleic Acids Research*. 24: 3381-3391.

Ririe, K. M., R. P. Rasmussen, and C. T. Wittwer. (1997) Product Differentiation by Analysis of DNA Melting Curves during the Polymerase Chain Reaction. *Analytical Biochemistry.* 245:154-160.

Rittmann, B.E and P.L. McCarty. (2001) Environmental Biotechnology: Principles and Applications. *McGraw-Hill Companies, Inc. New York City, NY.*

Roberts, P. V., G. D. Hopkins, D. M. Mackay and L. Semprini. (1990) A Field

Evaluation of In-Situ Biodegradation of Chlorinated Ethenes: Part 1, Methodology and Field Site Characterization. *Ground Water*, 28(4): 591-604.

Rungakamol, D. (2001) Aerobic Cometabolism of 1,1,1-Trichloroethane and Other Chlorinated Aliphatic Hydrocarbons by Indigenous and Bioaugmented Butane-Utilizers in Moffett Field Microcosms. Masters Thesis. Oregon State University. Department of Civil, Construction, and Environmental Engineering.

Schramm, A., D. Beer, M. Wagner, and R. Amann. (1998) Identification and Activities In Situ of *Nitrosospira* and *Nitrospira* spp. As Dominant Populations in a Nitrifying Fluidized Bed Reactor. *Appl. Environ. Microbiol.* 64: 3480-3485.

Semprini, L., P. V. Roberts, G. D. Hopkins and P. L. McCarty. (1990) A Field Evaluation of in-situ Biodegradation of Chlorinated Ethenes: Part 2, Results of Biostimulation and Biotransformation Experiments. *Ground Water* 28:715-727.

Semprini, L., G. D. Hopkins, P. V. Roberts, D. Grbic-Galic, and P.L.McCarty. (1991) A Field Evaluation of In-Situ Biodegradation of Chlorinated Ethenes: Part 3, Studies of Competitive Inhibition. *Ground Water*. 29(2): 239-250.

Semprini, L. and P.L. McCarty (1991) Comparison between Model Simulations and Field Results for In-Situ Biorestoration of Chlorinated Aliphatics: Part 1. Biostimulation of Methanotrophic Bacteria. *Ground Water.* 29(3):365-374.

Semprini, L. and P.L. McCarty (1992) Comparison between Model Simulations and Field Results for In-Situ Biorestoration of Chlorinated Aliphatics: Part 2. Cometabolic Transformations. *Ground Water*. 30(1):37-44.

Semprini, L. (1997) Strategies for the Aerobic Co-Metabolism of Chlorinated Solvents. *Current Opinion in Biotechnology*. 8: 296-308

Shim, H., D. Ryoo, P. Barbieri and T.K. Wood. (2001) Aerobic Degradation of Mixtures of Tetrachloroethylene, Trichloroethylene, Dichloroethylenes, and Vinyl Chloride by Toluen-*o*-Xylene Monooxygenase of *Pseudomonas stutzeri* OX1. *Appl. Microbiol. Biotechnol*. 56:265-269.

Shim, J.H. (1998) Model Analysis of Trichloroethylene Cometabolism by Phenol-Utilizing Microorganisms under In-situ Conditions of the Moffett Field Test Facility. M.S. Project, Department of Civil, Construction, and Environmental Engineering, Oregon State University.

Sipkema, E. M., W. de Koning, J.G. Klaassien, D.B. Janseen, and A.C.M.B.Antonie. (2000) NADH-Regulated Metabolic Model for Growth of *Methylosinus trichosportium* OB3b. Model Presentation, Parameter Estimation, and Model Validation. *Biotechnol. Prog.* 16(2):176-188.

Squillace, P.J., J.C. Scott, M.J. Moran, B.T. Nolan, and D.W. Kolpin (2002) VOCs, Pesticides, Nitrate, and their Mixtures in Groundwater Used for Drinking Water in the United States. *Environ. Sci. Technol.* 36(9):1923-1930.

Steffan, R.J., K.L. Sperry, M.T. Walsh, S. Vainberg, and C.W. Condee. (1999) Field-Scale Evaluation of in Situ Bioaugmentation for Remediation of Chlorinated Solvents in Groundwater. Environ. Sci. Technol. 33: 2771-2781.

Strand, S. E., M.D. Bjelland, and H.D. Stensel. (1990) Kinetics of chlorinated hydrocarbon degradation by suspended cultures of methane-oxidizing bacteria. *Research Journal of the Water Pollution Control Federation.* 62: 124-129.

Tovannaboot, A. and L. Semprini. (1998) Comparison of Long-Term TCE Transformation Ability of Methane and Propane-Utilizing Microorganisms Stimulated from the McClellan AFB Subsurface," *Bioremediation J.*, Vol. 2, No. 2, 105-124.

United States Environmental Protection Agency (EPA). (1990) Office of Research and Development. Basics of Pump-and-Treat Ground-Water Remediation Technology. Document #: EPA-600/8-90/003.

United States Environmental Protection Agency (EPA). (2001) Integrated Risk Information System (IRIS). www.epa.gov/iris/

van Genuchten, M. Th. and W.J. Alves. Analytical solutions of the one-dimensional convective-dispersive solute transportequation. US Department of Agriculture, Technical Bulletin No. 1661, 1982, 151 pp.

van Hylckama Vlieg, J. E. T., W. de Koning and D.B. Janssen. (1996) Transformation kinetic of chlorinated ethenes by Methylosinus trichosporium OB3b and detection of unstable epoxides by on-line gas chromatography. *Appl. Environ. Microbiol.* 62: 3304-3312.

Vogel, T.M. and P.L. McCarty. (1987) Abiotic and Biotic Transformation of 1,1,1-Trichloroethane under Methanogenic Conditions. *Environ. Sci. Technol.* 21: 1208-1213.

Vogel, T. M. (1996) Bioaugmentation as a soil bioremediation approach. *Biotechnology*., 7: 311-316.

Wiegant, W. W., and J. A. M. deBont. **(**1980) A new route for ethylene glycol metabolism in *Mycobacterium* E44. *J. Gen. Microbiol.* **120:**325–331.

Westrick, J.J., J.W. Mello, J.W. and R.F. Thomas. (1984) The Groundwater Supply Survey. *AWWA.* 76:52-59.

Yeager, C.M., P.J. Bottomley, and D.J. Arp. (2001) Cytotoxicity Association with Trichloroethylene Oxidation in *Burkholderia cepacia* G4. *Appl. Environ. Microbiol.* 67: 2107-2115.

Theses Produced

Darin Rungkamol
Aerobic Cometabolism of 1,1,1-Trichloroethane and Other Chlorinated Aliphatic Hydrocarbons by Indigenous and Bioaugmented Butane-Utilizers in Moffett Field Microcosms
March 2001

This thesis has focused on developing a culture of butane-utilizing microorganics to be bioaugmented into the subsurface for the cometabolic treatment of 1,1,1-TCA, TCE and 1,1-DCE. The culture was tested in groundwater and aquifer solid microcosms that mimic conditions where a field test is to be performed. The butane mixed culture was selected from the existing microcosms (Jitnuyanont 1998) by comparing 1,1,1-TCA transformation abilities among these microcosms. Butane-utilizers that showed rapid 1,1,1-TCA transformation kinetics and long-term (10 - 44 days) 1,1,1-TCA transformation ability in the absence of butane utilization were selected. Modeling studies were performed and compared to the results of microcosm test to generate kinetic parameters for the microbial processes under conditions of the field.

Microcosms bioaugmented with the selected culture maintained effective transformation of 1,1,1-TCA, and mixtures of 1,1,1-TCA, TCE, and 1,1-DCE. Little 1,1,1-TCA transformation was found in microcosms where indigenous microorganisms were stimulated. The transformation of 1,1-DCE in the bioaugmented microcosms was the fastest, followed by 1,1,1-TCA and TCE. The limited transformation of chlorinated solvents and the cessation in butane utilization occurred after the transformation of the CAH mixtures.

The culture having the best 1,1,1-TCA transformation ability was developed for bioaugmentation studies for both the laboratory and the field tests. The culture was grown on mineral salts growth media, harvested, placed in 1 mL vials with 7%DMSO (Dimethyl Sulfoxide), and stored in –80 °C liquid nitrogen for future studies. The frozen cells were thawed, washed with growth media to rinse away DMSO and then grown in growth media. The microcosms bioaugmented with cell grown from the very frozen culture had reproducible performance, maintaining the long-term (13 days) 1,1,1-TCA transformation in the absence of butane utilization and transforming mixtures of 1,1,1-TCA, TCE, and 1,1-DCE. The transformation rates gradually decreased with continued additions of 1,1,1-TCA. The cell decay rates (b) determined with an analytical regression method were also similar to those obtained prior to using the frozen culture.

Half-saturation constants for butane and 1,1,1-TCA ($K_{s,But}$ and $K_{s,TCA}$) of bioaugmented cultures under microcosm conditions were determined using an analytical regression method that was developed. The bioaugmented microorganisms had $K_{s,But}$ and $K_{s,TCA}$ values of 0.11 mg/L and of 0.37 mg/L, respectively.

Kinetic parameters including maximum specific rate for butane utilization ($k_{max,But}$) and 1,1,1-TCA transformation ($k_{max,TCA}$), cell decay rate (b), and transformation capacity (T_c) for indigenous and bioaugmented microcosms were determined through simulations using a non-steady-state model. Reasonable fits between the model simulation and microcosm data at both low and high concentrations of both butane and 1,1,1-TCA were obtained. The values of kinetic parameters in all bioaugmented microcosms, which were inoculated with the media-culture from

batches of cells grown at different times, were similar. This indicates the reproducibility of bioaugmentation process. The bioaugmented microorganisms had high transformation capacity (0.1 – 0.3 mg 1,1,1-TCA/mg cells) and achieved ratios of $k_{max,But}$ and $k_{max,TCA}$, ranging from 0.05 to 0.09. The indigenous microorganisms potentially had lower transformation capacity (T_c), higher decay rate (b), higher butane and 1,1,1-TCA half-saturation constants ($K_{s,But}$ and $K_{s,TCA}$), and lower butane and 1,1,1-TCA maximum specific rates ($k_{max,But}$ and $k_{max,TCA}$) than the bioaugmented microorganisms.

Different butane-utilizing cultures are likely present in the indigenous and bioaugmented microcosms. A slower rate of 1,1,1-TCA transformation was probably due to the indigenous microorganism being less effective towards 1,1,1-TCA transformation. Unlike the bioaugmented microcosms, the enzyme present in the indigenous microcosms was not active over long periods of time. Augmentation with proven contaminant-degrading microorganisms having consistent transformation abilities will likely lead to improved bioremediation treatment processes.

Maureen Anne Mathias
Modeling Cometabolic Transformation of a CAH Mixture by a Butane Utilizing Culture.
September 2002

The goal of this research was to mathematically simulate the ability of bioaugmented microorganisms to aerobically cometabolize a mixture of chlorinated aliphatic hydrocarbon (CAH) compounds during in-situ treatment. Parameter values measured from laboratory experiments were applied to the transport model with biotransformation processes included. In laboratory microcosm studies, a butane-grown, enriched culture was inoculated in soil and groundwater microcosms and exposed to butane and several repeated additions of 1,1,1-trichloroethane (TCA), 1,1-dichloroethylene (DCE), and 1,1-dichloroethane (DCA) at aqueous concentrations of 200 μg/L, 100 μg/L, and 200 μg/L, respectively. Microcosms containing the bioaugmented culture showed 1,1-DCE to be rapidly transformed, followed by slower transformation of 1,1-DCA and 1,1,1-TCA. After most of the butane had been consumed, transformation of these latter CAHs increased, indicating strong inhibition by butane. With repeat biostimulations, butane utilization and CAH transformation accelerated, showing the increase in cell mass. These trends occurred in two sets of microcosm triplicates. No stimulation was observed in controls containing only the microorganisms indigenous to Moffett Field, confirming that activity seen in the bioaugmented microcosms was a result of the introduced culture's activity.

Batch reactor results were simulated using differential equations accounting for Michaelis-Menten kinetics, transformation product toxicity, substrate inhibition, butane utilization, and CAH transformation. The equations were solved simultaneously by Runge-Kutta numerical integration with parameter values adjusted to match the microcosm data.

Having defined the parameter values from laboratory studies, the biotransformation model was combined with 1-D advective-dispersive transport to simulate behavior of the culture and the substrates within an aquifer. The model was used to simulate the results of field studies where the butane-utilizing culture was injected into a 7 m subsurface test site and exposed to alternating pulses of oxygen and butane, along with the contaminant mixture studied in the microcosms. Monitoring wells spaced at 1 m, 2.2 m, and 4 m from the injection well allowed temporal and spatial changes in substrate concentrations to be determined. Model simulations of the field demonstration were performed to determine how well the biotransformation/solute transport model predicted actual field observations.

To model the influences of solute transport, simulations were run and compared to breakthrough test data (prior to bioaugmentation) to determine the values for advection, dispersion, and sorption. The simulations showed that flow ranged from 1.0 to1.5 m^3/day (average linear velocity of 2.0 m/day). Dispersion was estimated as 0.31 m^2/day. Sediment sorption partitioning coefficients for 1,1-DCE, 1,1,-DCA, and 1,1,1,-TCA were determined to be approximately 0.69, 0.50, and 0.50 L/kg, respectively. It was more difficult to determine an appropriate value of the mass transfer rate coefficient for non-equilibrium sorption, so simulations were run to compare equilibrium and non-equilibrium cases. Results indicated that non-equilibrium (with mass transfer rate coefficient of approximately 0.2 day^{-1}) better simulated the field data.

Using these transport parameters and the biotransformation values determined from the laboratory experiments, simulations of the field data showed that the model was capable of simulating the effects of transformation rates, butane inhibition, and 1,1-DCE product toxicity. Simulations for varying pulsing cycles and durations provided possible improvements for future field demonstrations.

Overall, this work proved that there is good potential in extrapolating laboratory based kinetics to simulate biotransformation at a field scale. Although the complexity of such systems makes modeling difficult, such simulations are useful in understanding and interpreting field data.

Hee Kyung Lim
Microcosm Studies of Bioaugmentation with a Butane-Utilizing Mixed Culture: Microbial Community Structure and 1,1-DCE Cometabolism.
February 2003

The 1,1-dichloroethene (1,1-DCE) cometabolic transformation abilities of indigenous and bioaugmented microorganisms were compared in microcosms constructed with groundwater and aquifer solids from the Moffett Field site, CA. Microbial community structure in the microcosms and possible community shifts due to 1,1-DCE transformation stress was evaluated by terminal restriction fragment length polymorphism method (T-RFLP). An existing biotransformation model was used to simulate the experimental data using parameter values determined by Kim et al. (2002) and Rungkamol (2001) with small adjustments to the parameter values.

The laboratory microcosm studies showed that both indigenous and bioaugmented butane utilizers were capable of transforming 1,1-DCE when fed butane as a primary substrate. A butane-grown enriched culture was bioaugmented into the microcosms and exposed to several repeated additions of butane and/or 1,1-DCE, ranging from 7.1 to 76 μmol and from 0.17 to 1.99 μmol, respectively. The bioaugmented butane-utilizers showed a reduced lag period compared to the indigenous butane-utilizers. The greatest ability to transform 1,1-DCE was observed in bioaugmented microcosms, simultaneously exposed to butane and 1,1-DCE. Very little 1,1-DCE was transformed in the bioaugmented microcosms that were not fed butane, presumably due to lack of reductant supply and/or product toxicity of 1,1-DCE transformation.

Microbial community analyses revealed similar results for replicate microcosms and differences in the community structure in microcosms subjected to different patterns of substrate addition and 1,1-DCE cometabolism. 1,1-DCE transformation resulted in temporal fluctuations in specific bacterial groups in the bioaugmented microcosms. It could be inferred that microorganisms, correlated with the T-RFL of 183 base pair (bp) were generally predominant in butane-fed bioaugmented microcosms simultaneously exposed to 1,1-DCE. Bioaugmented microcosms that were pre-exposed to 1,1-DCE for 29 days in the absence of growth substrate, followed by the addition of butane showed a significantly different microbial community from bioaugmented microcosms fed butane and 1,1-DCE simultaneously. Microorganisms with T-RFL of 179 or 277.8 bp dominated in these microcosms. These differences were possibly the result of extensive 1,1-DCE transformation product toxicity during the pre-exposure phase of the tests.

A model developed by Kim et al. (2002) was used to mathematically describe the rate and extent of butane utilization and the cometabolic transformation of 1,1-DCE in the microcosm tests. Using the kinetic parameter values previously determined by Kim et al. (2002) and Rungkamol (2001), heuristic fits were obtained between the experimental data and model simulations. The model successfully predicted the trend of the butane utilization and 1,1-DCE transformation. The model outputs were statistically quantified for their fit to the experimental data by estimating Standard Error of Estimate (SEE). A reasonable fit between model predictions and experimental observations was achieved.

A significant contribution of this study was developing the laboratory methods to evaluate the microbial abilities to cometabolize 1,1-DCE and determining the communities of microorganisms correlated with those biotransformation activities. Furthermore, the model comparison to experimental data indicated that there was a potential in using the existing model to predict and improve bioremediation strategies. The results showed the successful bioaugmentation of a butane-utilizing culture to improve transformation performance.

Ju Yong Jeong
Isolation and Molecular Characterization of Several Butane- and Butanol- Utilizing Microorganisms Obtained from a Bioremediation Test Site
July 2003

In this study, laboratory-grown, 183bp (Mnl1 digest) was introduced with butane and oxygen into the bioaugmented well leg at Moffet Field test site to stimulate CAH transformation. Sand, along with other solid materials, was put into the bioaugmented and indigenous well legs within stainless steel mesh coupons. Groundwater and solids samples from both bioaugmented and indigenous well legs were taken for use in this study.

For the microbial community analysis, sand samples and their enrichment cultures with butane were extracted and analyzed by T-RFLP. One of the sand samples from bioaugmented well leg (SE1) had the highest amount DNA, which meant this sand sample had the greatest number of microorganisms. T-RFLP of sand from SE1 and SE2 had 40 and 31 significant T-RFLs respectively while sand samples from SW1 and SW2 had only 10 and 4 significant peaks indicating higher microbial community diversity in the bioaugmented well leg. The microbial community in sand samples taken from the bioaugmented well leg (SE1 and SE2) was found to 60% similarity with each other. The T-RFLs (183bp by *Mnl*I) of the bioaugmented cells were not found in T-RFLPs of sand samples or cultures enriched with butane

The sand samples were cultivated to enrich butane and/or butanol utilizers with mineral media or filtered groundwater. All bottles containing mineral media with butane as a substrate used up butane and had relatively high turbidity, but bottles containing filtered groundwater utilized only a portion (30-50%) of butane (2.0mg) provided over 40days of incubation. This showed that groundwater could only support limited growth of butane-utilizing microorganisms, possibly due to nutrient limitations.

Butane and/or butanol-utilizing microorganisms were isolated through several selective growth steps. It was found that butane- and butanol-utilizing microorganisms were present in both bioaugmented and indigenous well legs. The isolates were characterized by molecular techniques including RFLP, T-RFLP and partial 16S rDNA sequencing. Thirty two cultures were analyzed by RFLP and 19 distinct RFLP patterns were identified. T-RFLP was conducted with *Mnl*I for 19 cultures and Hin61 for 9 cultures. 16S rDNA sequencing was performed to identify the 9 cultures that appeared to be isolates by RFLP and T-RFLP analyses. Among the identified isolates, three isolates Y1, Y3, W2 were relatively fast in butane utilization and Y3 was found to be able to transform TCA as well. Other isolates could utilize butanol relatively fast, but were very slow in butane utilization.

Among the nine isolates, three isolates were gram-positive bacteria group, *Rhodococcus* and *Mycobacterium.* There are a variety of *Rhodococcus* and *Mycobacterium* species that are able to degrade various contaminants including CAHs. SEO1, which has 179bp T-RFL by *Mnl*I, was found to be very close to *Rhodococcus erythropolis*, which was found in oil-contaminated site and chlorobenzene degrading *Rhodococcus sp* strain isolated from a chlorobenzene contaminated aquifer. Isolate SWO3 was found to be close to *Mycobacterium sp*. and this had a 278bp of T-RFL by *Mnl*I digestion. Isolate Y3 was close to *Mycobacterium* species which is capable of

degrading aromatic and gasoline hydrocarbons. T-RFL of Y3 was found in the electropherograms of sand samples and the enrichment cultures from bioaugmented well legs, this might reflect that enrichment cultures with sand samples from the bioaugmented well leg were able to degrade butane fast and transform TCA. This T-RFL was not found in sand samples and their enrichment cultures from indigenous well leg.

The six isolates belong to gram-negative *Proteobacteria* group. Isolate N10, the most common microorganism based on the RFLP analysis in the field, was found to be similar to *Methylobacterium mesophilicum.* Isolate NB1 was found to be similar to an *Acinetobacter calcoaceticus* that can degrade alkane such as octadecane and produce biosurfactants. Isolate NB6 was very close (99%) to *Varivorax* sp. WFF52 strain, which is able to degrade aliphatic polycarbonates. Isolate Y1 was close to *Stenotrophomonas maltophilia*. Isolate W2 was found to be similar to a *Nocardioides sp.* CF8 that can grow on alkane ranging from C_2 to C_{16} in addition to butane and other substrates such as primary alcohol, phenol and also similar to JS614 strain which can assimilate vinyl chloride. This organism was able to use butane slowly and might present in both bioaugmented and indigenous well leg.

Chakkrid Sattayatewa
Growth Characteristics and Chlorinated Hydrocarbon Transformation Ability of two Rhodococcus sp. Isolates
March 2004

Aerobic cometabolism of 1,1,1-TCA by a butane-grown microorganism, R183, was studied. The growth parameters, TSS, optical density (OD_{600}), protein concentrations, and nitrate consumption during butane utilization were measured. The relationships between growth parameters were developed and the yield coefficient of 0.73 ± 0.08 (95% confidence interval) of the R183 culture was evaluated. Butane was utilized as a primary substrate to aerobically cometabolize 1,1,1-trichloroethane (1,1,1-TCA) and 1,1-dichloroethene (1,1-DCE) and was found to also inhibit CAH transformation.

Acetate, succinate, and ethanol were evaluated as non-inhibitory alternate substrates for CAH cometabolism. Acetate was a good growth substrate for R183, but did not provide CHA cometabolic activity. A range of acetate concentrations were used in alternate feed cycles with butane in an attempt to increase the CAH transformation rate by finding an optimum mix of non-inhibitory, but non enzyme-inducing substrate with butane, the inhibitory, but enzyme-inducing substrate. However, results showed that the ability of the R183 culture to transform 1,1,1-TCA was only proportional to the mass of butane utilized. Strain R183 was efficient at transformation of 1,1,1-TCA concentrations as high as 1300 μg/L when fed butane.

Straight chain hydrocarbons (C1 through C6), methane, ethane, propane, butane, pentane, and hexane were also evaluated for growth and CAH transformation activity. The culture did not grow on methane and possibly ethane, but could on propane, butane, pentane, and hexane. However, 1,1,1-TCA transformation on propane was not successful, possibly due to nitrogen limitations. The maximum 1,1,1-TCA transformation rate of ≥ 9.9 μg/hr occurred when strain R183 was grown on butane. Pentane provided the greatest 1,1,1-TCA transformation capacity, T_C, of 26 μg TCA/mg cells, whereas T_c by butane and hexane inoculate culture were 16 and 11 μg TCA/mg cells respectively and the transformation yield, T_y, corresponded to transformation capacity. Lag time to reach 50% substrate removal and complete utilization was corresponded to solubility limit in water and Henry's constant of such substrate.

This study also compared the ability of another *Rhodococcus sp*., R179, to cometabolize 1,1,1-TCA, 1,1-DCE, and 1,1-DCA. Strain R183 transformed the CAHs more efficiently than did strain R179, with strain R179 taking approximately five times longer to completely transform a spike of 1,1,1-TCA. Transformation of 1,1-DCE by resting cells resulted in transformation product toxicity with a decrease in butane uptake rate, or percent inactivation, being proportional to the amount of 1,1-DCE transformed.

Bhargavi Maremanda

Aerobic cometabolism of 1, 1, 1-Trichloroethane and 1, 1-Dichloroethene by a bioaugmented butane-utilizing culture in a continuous flow column
June 2004

The transformation of 1,1,1-trichloroethane (1,1,1-TCA) and 1,1-dichloroethene (1,1-DCE) was evaluated in a continuous flow column reactor using a mixed culture that grew on butane. The column was packed with aquifer materials and groundwater obtained from the in-situ bioremediation test site at Moffett Field, CA. The pore volume of the column was 38 mL and the dispersion coefficient was 1.93E-3 cm^2/sec, based on the results of the bromide transport experiment. The 1,1,1-TCA transport test prior to biostimulation showed a retardation coefficient of 3.2.

The inoculum for bioaugmentation was a butane-utilizing *Rhodococcus Sp.* culture used in the Moffett Field experiments. The total mass of cells added was 0.9 mg on a dry mass basis. Three days after bioaugmentation, with the continuous addition of dissolved butane, dissolved oxygen, and 1,1,1-TCA (200 ug/L), decreases in all three of these solutes began. A maximum removal of 1,1,1-TCA of 84% was achieved 10 days after bioaugmentation and remained fairly constant for a period of 20 days. The ratio of dissolved oxygen to butane consumption during this period was 4.5 mg O_2: 1 mg Butane. The influent concentration of 1,1,1-TCA was then doubled, while dissolved oxygen and butane addition was maintained constant. The transformation of 1,1,1-TCA during this period fluctuated between 24%-84%. Upon restoring the 1,1,1-TCA concentration back to 200 ug/L the transformation stabilized at 59% removal. The butane-utilizers were then tested for their dependence on butane by turning the butane pulse off. The dissolved oxygen concentration doubled during this period and a residual transformation activity of 22% was observed. On restarting butane addition, 1,1,1-TCA transformation of 69% was achieved. In the final phase, 1,1-DCE was injected at 130 ug/L along with 1,1,1-TCA, dissolved butane and oxygen. The butane-utilizing culture transformed 70% of 1,1-DCE; however, the presence of 1,1-DCE inhibited 1,1,1-TCA transformation and approximately 50% of the butane injected was not consumed. The concentration of dissolved oxygen in the column also increased, which also indicating that 1,1-DCE transformation inhibited butane and dissolved oxygen utilization and 1,1,1-TCA transformation. Real-time PCR analysis conducted by Li (2004) indicated that during periods of low biotransformation of 1,1,1-TCA, bioaugmented cell densities observed in the column effluent was high. This corresponded to a period of anoxic conditions, which may have caused cell detachment from the aquifer solids.

The column reactor results were simulated using a combined biotransformation-transport model that uses Monod/Michaelis-Menten kinetics along with first-order sorption kinetics, to predict substrate utilization and chlorinated solvent transformation (Semprini and McCarty, 1992). The culture parameter values used to simulate biotransformation in the model were obtained from laboratory culture experiments conducted by Kim et al (2002) and Mathias (2002). Transport parameters (dispersion coefficient, porosity) were determined from modeling breakthrough test data with the CXTFIT2 transport model prior to bioaugmentation and biostimulation. Simulations of the column data using the transport and biotransformation parameters demonstrated that the model was able to simulate biotransformation of 1,1,1-TCA fairly well.

The model also indicated that 1,1-DCE transformation was toxic to the butane-utilizing culture and predicted the decreases in consumption of butane, and dissolved oxygen and in 1,1,1-TCA transformation.

This study showed that column experiments conducted on a small scale in a laboratory could be used to study the biotransformation capabilities of bioaugmented microorganisms. On the whole, the results suggest that the butane-utilizing culture could be successfully used in-situ for bioremediation, however transformation of mixtures of 1,1-DCE and 1,1,1-TCA could prove difficult.

Jun Li
Molecular Analysis of Bacterial Community Dynamics During Bioaugmentation Studies in a Soil Column and at a Field Test Site
June 2004

1,1,1-Tricholorethane (1,1,1-TCA), a widely used industrial solvents, is one of the most common subsurface contaminants. Transformation processes in the subsurface can result in the production of 1,1-dichloroethane (1,1-DCA) and 1,1-dichloroethene (1,1-DCE) from 1,1,1-TCA contamination, resulting in plumes of mixed chlorinated aliphatic hydrocarbons (CAHs). A butane-utilizing microorganism, strain 183BP, with the ability to cometabolically transform 1,1,1-TCA, 1,1-DCA, and 1,1-DCE was isolated from environmental samples taken from a CAH contaminated site. In laboratory microcosm studies (Rungkamol, 2001; Mathias, 2002; Lim, 2003), the results showed that microcosms bioaugmented with strain 183BP and fed butane as a primary substrate rapidly transformed 1,1-DCE, followed by slower transformation of 1,1-DCA and 1,1,1-TCA when all three CAHs were present. A 1-kb segment of the 16S rRNA gene sequence of strain 183BP was found to be identical to that of *Rhodococcus sp*. USAN-12 (Genbank accession number AF420413).

Two bioaugmentation treatment tests with strain 183BP as inoculum were conducted at the Moffett Federal Airfield In-Situ Bioremediation Test Site (Moffett Field), Mountain View, CA. Also, a soil column packed with aquifer solids and groundwater obtained from Moffett Field was inoculated with strain 183BP and operated under conditions similar to those used in the field tests.

Field groundwater samples and soil column effluent samples were analyzed using techniques based on 16S rRNA gene analysis. 183BP-specific primers were designed and used in real-time SYBR Green I PCR analyses to detect and quantify the inoculated microorganisms in the subsurface. Dynamics of the bacterial community composition were investigated using terminal restriction fragment length polymorphism (T-RFLP) methods and statistical analysis.

During the first bioaugmentation test in the absence of 1,1-DCE, maximum treatment efficiencies for TCA and DCA were approximately 80% and 96%, respectively in the bioaugmented well leg, while essentially no transformation occurred in the non-bioaugmented control leg. During the effective treatment period, the 183BP cell concentration was above 900 cells/mL in groundwater obtained 0.5 m from the injection well. In the second bioaugmentation test, 1,1-DCE was added to the influent CAH mixture and was effectively transformed in the bioaugmented well leg. Although 93% of the influent 1,1-DCE was transformed, 1,1-DCA and 1,1,1-TCA removal efficiencies were significantly reduced compared to the test in the absence of 1,1-DCE. The 183BP cell concentration was almost 1-log-order higher than that of the first test and clear spatial distribution of the cells among the monitoring wells was observed. The bioaugmented strain 183BP was not observed in T-RFLP analyses conducted on groundwater samples during either bioaugmentation test. The groundwater bacterial community profiles were alternately dominated by two peaks, 277-bp during the early stages of amendments and 126-bp during the later stages of both tests.

In the soil column, maximum treatment efficiencies for TCA and DCE were approximately 96% and 77%, respectively. Microbial results indicated that the decline in TCA concentrations was concomitant to an increase in the concentration of strain 183BP cells. The bacterial community had greater species diversity than field samples and did not follow the same succession trend as the field samples. However, addition of 1,1-DCE in the feed to the column resulted in a similar reduction of 1,1-DCA and 1,1,1-TCA transformation efficiencies as that observed in the field studies.

Presentations

2001 Fall General Meeting of the American Geophysical Union, San Francisco, CA

Assessing Subsurface Bioaugmentation of a Mixed Culture Capable of Chlorinated Solvent Cometabolism via Molecular Methods
Mark E. Dolan, Hee Kyung Lim, Lewis Semprini, Stephen J. Giovanonni, Kevin L. Vergin, Oregon State University.
Perry L. McCarty, Gary D. Hopkins, Stanford University.

The goal of this project was the successful bioaugmentation of a mixed culture capable of aerobic cometabolism of chlorinated solvent mixtures into an aquifer test zone at Moffett Federal Airfield, CA (Moffett). The test zone consists of two parallel well legs both fed butane and oxygen. One leg will be bioaugmented and the other will serve as an indigenous control. Injection and extraction wells and six (3 per leg) intermediately placed groundwater monitoring points will be frequently monitored for chlorinated solvents, butane, dissolved oxygen, and pH. Groundwater will also be periodically analyzed for microbial content using terminal restriction fragment length polymorphism (T-RFLP) and fluorescence in-situ hybridization (FISH) analyses. In each well leg, two fully-penetrating wells containing solid media will be periodically analyzed for microbial colonization (T-RFLP).

The mixed bioaugmentation culture originated from environmental samples taken from Hanford, WA. The culture was enriched on butane and tested for viability in Moffett groundwater and aquifer solids. A clone library was created from the 16S rDNA in the mixed culture and 86 clones were sorted based on RFLP patterns. Complete sequencing of the 16S rDNA gene from the three most prevalent clones revealed 45 clones similar to *Acidovorax* or Hydrogenophaga, gram negative proteobacterium, and 12 clones similar to *Rhodococcus*, a gram positive filamentous organism. Fluorescently-labeled rRNA probes were designed for FISH analyses and appropriate restriction enzymes were chosen for T-RFLP analyses based upon the sequence information.

Microcosm tests were conducted prior to the initiation of the field study to evaluate butane, 1,1-dichloroethylene (1,1-DCE), and 1,1,1-trichloroethane (TCA) degradation kinetics and microbial community composition. Bioaugmented microcosms began butane utilization sooner than non-bioaugmented ones in the presence and absence of 1,1-DCE, and were able to degrade more 1,1-DCE (up to 500 g/L) faster than non-bioaugmented microcosms. T-RFLP analyses of triplicate bottles produced very consistent results. An organism(s) with a T-RFLP signature of 183 bp was found to dominate in bioaugmented microcosms and was consistently absent from non-bioaugmented microcosms. T-RFLP and FISH analyses of groundwater and solid media during the bioaugmentation field demonstration are expected to reveal the extent of transport and subsurface colonization of the bioaugmentation culture.
SERDP and ESTCP Workshop, December 2001, Washington D.C.
Lewis Semprini, Mark Dolan, Oregon State University.
Gary Hopkins, Perry McCarty, Stanford University.

Molecular techniques were used to characterize the butane utilizing mixed culture that will be used for bioaugmentation and to track the culture in microcosm studies that mimic conditions of the field demonstration. A clone library analysis permitted the 16S rDNA sequencing of dominant microorganisms within the mixed culture, without the need to isolate the microorganisms as pure cultures. These sequences were used to develop rRNA probes for Fluorescent In-situ Hybridization (FISH) to track specific microorganisms in the mixed culture. PCR methods, to more easily evaluate community structure, were developed. The terminal restriction fragment length polymorphism (T-RFLP), a PCR method, was developed to evaluate microbial population dynamics in the microcosms studies, and to study the transport and fate of the bioaugmented culture in the field study. Microcosm tests were conducted prior to the initiation of the field study to evaluate butane, 1,1-dichloroethylene (1,1-DCE), and 1,1,1-trichloroethane (TCA) degradation kinetics and the fate of the bioaugmented culture. T-RFLP analysis indicated that specific microbes of the bioaugmented culture flourished in the microcosms over extended periods (100 days) of biostimulation with butane and transformation of 1,1-DCE, a contaminant that causes significant transformation product toxicity. Numerical model parameters, including expressions for microbial growth and decay, substrate and oxygen utilization, and cometabolism of dual contaminants, were determined independently in kinetic studies of the butane-utilizing culture and in microcosm studies. The model simulated well the repetitive utilization of butane and cometabolism of TCA and 1,1-DCE in the microcosms. Model simulations were then performed under the transport conditions of the field test with alternating pulses of dissolved butane and oxygen in the presence of 1,1-DCE (50 g/L) and TCA (250 g/L). Complete utilization of the butane occurred within 200-hrs of bioaugmentation. 1,1-DCE was much more rapidly transformed than TCA, and efficient TCA removal occurred only after 1,1-DCE and butane were decreased in concentration. The field demonstration test site at Moffett Field, CA has been instrumented to in order to conduct tests along two parallel test legs. One leg will be used for the bioaugmentation study, and the other leg will be used to stimulate indigenous microorganisms.

Proceedings from the Third International Conference on the Remediation of Recalcitrant Compounds May 20-23, 2002.

Molecular Characterization and Tracking of a Chlorinated Solvent Cometabolizing Mixed Bioaugmentation Culture

Mark E Dolan, Lewis Semprini, Stephen Giovanonni, Hee Kyong Lim, Kevin Vergin, Oregon State University.

The goal of this project is the successful bioaugmentation of a mixed culture capable of aerobic cometabolism of chlorinated solvent mixtures into an aquifer test zone at Moffett Federal Airfield, CA (Moffett). The test zone consists of two parallel well legs both fed butane and oxygen. One leg will be bioaugmented and the other will serve as an indigenous control. Injection and extraction wells and six (3 per leg) intermediately placed groundwater monitoring points will be frequently monitored for chlorinated solvents, butane, dissolved oxygen, and pH. Groundwater will also be periodically analyzed for microbial content using terminal restriction fragment length polymorphism (T-RFLP) and fluorescence in-situ hybridization (FISH) analyses. Two fully-

penetrating wells containing solid media in each leg will be periodically analyzed for microbial colonization (T-RFLP). Testing will begin this summer, with bioaugmentation slated for early fall.

The mixed bioaugmentation culture was enriched from environmental samples taken from Hanford, WA. The culture was enriched on butane and tested for viability in Moffett groundwater and aquifer solids. The microcosms were found to degrade trichloroethene (TCE), 1,1,1-trichloroethane (TCA) and 1,1-dichloroethene (1,1-DCE) alone and in mixtures when fed butane as a primary substrate. The culture was grown in mineral media with a butane-in-air headspace, concentrated, separated into 1 mL aliquots, and frozen in liquid nitrogen to serve as inoculum for microbial characterization and bioaugmentation tests.

The mixed culture was characterized using a clone library created from the 16S rDNA in a frozen aliquot of the mixed culture. Complete sequencing of the 16S rDNA gene from the three most prevalent clones (based on RFLP patterns) revealed 45 clones similar to *Acidovorax* or Hydrogenophaga, gram negative proteobacterium, and 12 clones similar to *Rhodococcus*, a gram positive filamentous organism. Fluorescently-labeled rRNA probes were designed for FISH analyses and appropriate restriction enzymes were chosen for T-RFLP analyses based upon the sequence information.

The mixed culture was thawed, rinsed, grown in mineral media, and augmented (0.5 mg dry weight in 100 mL groundwater and soil) into microcosms containing Moffett aquifer solids and groundwater. Bioaugmented microcosms began butane utilization sooner than non-bioaugmented ones in the presence and absence of 1,1-DCE, and were able to degrade more 1,1-DCE (up to 500 □g/L) faster than the non-bioaugmented microcosms. T-RFLP analyses of triplicate bottles showed very consistent results. The presence or absence of organisms with T-RFLP signatures of 179 (*Rhodococcus*) and 183 base pairs was found to correlate well with treatment conditions and may be predictive of field results.

2002 Fall General Meeting of the American Geophysical Union, San Francisco, CA

Bioaugmentation of an Aerobic Culture Capable of Chlorinated Solvent Cometabolism to a Subsurface Test Zone

Mark E. Dolan, Lewis Semprini, Oregon State University.
Gary D. Hopkins, Perry L. McCarty, Stanford University.

A butane-utilizing culture able to cometabolize chlorinated aliphatic hydrocarbons (CAHs) was bioaugmented into an aquifer test zone at Moffett Federal Airfield, CA. Microcosm bioaugmentation tests conducted with groundwater and aquifer solids collected from the test site indicated a strong potential for viability of the bioaugmented culture in the site subsurface. Microcosms bioaugmented with the butane-utilizing culture were able to degrade aqueous concentrations of 1,1-dichloroethylene (1,1-DCE) up to 1 mg/L and could successfully transform mixtures of 1,1-DCE, 1,1,1-trichloroethane (TCA) and 1,1-dichloroethane (DCA) when fed butane. T-RFLP analyses showed the presence of bioaugmented organisms within the microcosms throughout the 10-month test period. An isolate from the butane-utilizing culture was grown in batch bottles containing mineral media and a butane-in-air headspace. Approximately 4 g dry weight of culture was harvested and bioaugmented to the field site.

The site consisted of two parallel well legs, each with an injection well, two fully penetrating monitoring wells containing solid support media, three groundwater monitoring

wells and an extraction well. One well leg was bioaugmented with the isolate and the other was used as an indigenous control leg. A mixture of 1,1-DCE, TCA and DCA (~50 ug/L, 135 ug/L and 150 ug/L respectively) was continuously pumped through both well legs with alternate pulses of dissolved oxygen and butane. Fifty percent removal of 1,1-DCE occurred within one day in the bioaugmented leg; however, it took about 6 days to achieve complete butane utilization and 1,1-DCE removal to below 2 ug/L. During this period DCA and TCA were reduced by 70- 90 percent and 30-50 percent respectively. When the butane/oxygen pulses were changed from a 1-hr cycle to a 24-hr cycle 1,1-DCE removal fell to 50 percent and DCA and TCA concentrations increased to influent levels. Upon returning to short pulse cycles, 1,1-DCE removal efficiency returned to 95 percent while DCA and TCA were not effectively transformed.

Groundwater microbial samples obtained 1 m from the injection well did not show the presence of the bioaugmented organism. Butane uptake was observed in the non-bioaugmented leg after about 14 days of butane addition, but no CAH transformation was observed. Butane oxidation without CAH transformation continued through the period of longer pulse cycles; however, upon return to the shorter pulse cycles 1,1-DCE removal efficiencies similar to those obtained in the bioaugmented leg were achieved without significant removal of DCA or TCA. Comparison of initial groundwater microbial samples showed no significant differences between the two legs. Microbial analyses are ongoing and a second field season will begin in September 2003 to assess TCA transformation ability upon re-bioaugmentation of the site.

Workshop: SERDP-ESTCP Workshop, Nov. 2002, Washington.D.C.

Laboratory, Field, and Modeling Studies of Aerobic Cometabolism of 1,1-Dichloroethene, 1,1-Dichloroethane, and 1,1,1-Trichloroethane by Butane-Utilizing Microorganisms

Lewis Semprini, Mark Dolan, Maureen Mathias, Oregon State University.
Gary Hopkins, and Perry McCarty, Stanford University.

The ability of butane-utilizing microorganisms to aerobically cometabolize a mixture of chlorinated aliphatic hydrocarbons (CAHs) in laboratory microcosms and in an in-situ field demonstration was modeled using parameter values measured in laboratory experiments. This work was performed as part of a SERDP project (CU-1127) to develop effective aerobic cometabolic systems for the in-situ transformation of problematic chlorinated solvent mixtures. The butane grown culture was inoculated in soil and groundwater microcosms and exposed to butane with several repeated additions of 1,1,1-trichloroethane (TCA), 1,1-dichloroethylene (1,1-DCE), and 1,1-dichloroethane (1,1-DCA) at aqueous concentrations of 200 g/L, 100 g/L, and 200 g/L, respectively. The utilization of butane and the transformation of the CAH mixture in the batch microcosms were simulated using differential equations accounting for Michaelis-Menten kinetics with cell growth and decay, substrate utilization, transformation product toxicity, and substrate inhibition of CAH transformation. Both competitive inhibition kinetics and mixed inhibition kinetics, determined in prior laboratory studies, were included in the model construct. The equations were solved simultaneously using fourth-order Runge-Kutta numerical integration. The batch microcosm experimental results were simulated well with parameter values determined independently in culture kinetic studies, with some minor adjustments. Having adequately defined the parameter values from laboratory studies, the biotransformation model was combined with 1-D advective-dispersive transport to simulate the results of in-situ bioremediation tests conducted at the Moffett Field Test Facility in CA. The butane-utilizing culture was injected into a 7 m subsurface test site and exposed to alternating pulses of oxygen and butane, along with TCA (150 g/L), 1,1-DCE (50 g/L) and 1,1-DCA (150 g/L). The

model simulated well the transient transformation of the CAHs in response to different butane and oxygen pulse cycles and injection concentrations. Model simulations correlated well with field results and indicated that better remediation performance was achieved when more butane and oxygen were injected in the field test plot with short pulse cycles. 1,1-DCE was the most effectively transformed, followed by 1,1-DCA, and TCA, consistent with model predictions. The model simulations also indicated that as time proceeded, indigenous microorganisms were likely responsible for the effective transformation of 1,1-DCE and limited transformation of 1,1-DCA and TCA. This was consistent with PCR based molecular analysis of the microbial population that was stimulated.

Battelle Seventh Conference on In-situ and On Site Bioremediation, June 2003, Orlanda, FL

Laboratory, Field, and Modeling Studies of Aerobic Cometabolism of Cahs by Butane-Utilizing Microorganisms

Lewis Semprini, Mark E. Dolan, Maureen Mathias, Oregon State University.
Gary D. Hopkins, Perry L. McCarty, Stanford University.

The ability of butane-utilizing microorganisms to aerobically cometabolize a mixture of chlorinated aliphatic hydrocarbons (CAHs) in laboratory microcosms and in an in-situ field demonstration was modeled using parameter values measured in laboratory experiments. The butane grown culture was inoculated into soil and groundwater microcosms and exposed to butane with several repeated additions of 1,1,1-trichloroethane (TCA), 1,1-dichloroethylene (1,1-DCE), and 1,1-dichloroethane (1,1-DCA) at aqueous concentrations of 200 g/L, 100 g/L, and 200 g/L, respectively. The utilization of butane and the transformation of the CAH mixture in the batch microcosms were simulated using differential equations accounting for Michaelis-Menten kinetics with cell growth and decay, substrate utilization, transformation product toxicity, and substrate inhibition of CAH transformation. Both competitive inhibition kinetics and mixed inhibition kinetics, determined in prior laboratory studies, were included in the model construct. The equations were solved simultaneously using fourth-order Runge-Kutta numerical integration. The batch microcosm experimental results were simulated well with parameter values determined independently in culture kinetic studies, with some minor adjustments. Having adequately defined the parameter values from laboratory studies, the biotransformation model was combined with 1-D advective-dispersive transport to simulate the results of in-situ bioremediation tests conducted at the Moffett Field Test Facility in CA. The butane-utilizing culture was injected into a 7 m subsurface test site and exposed to alternating pulses of oxygen and butane, along with TCA (150 g/L), 1,1-DCE (50 g/L) and 1,1-DCA (150 g/L). The model simulated well the transient transformation of the CAHs in response to different butane and oxygen pulse cycles and injection concentrations. Model simulations correlated well with field results and indicated that better remediation performance was achieved when more butane and oxygen were injected in the field test plot with short pulse cycles. 1,1-DCE was the most effectively transformed, followed by 1,1-DCA, and TCA, consistent with model predictions. The model simulations also indicated that as time proceeded, indigenous microorganisms were likely responsible for the effective transformation of 1,1-DCE and limited transformation of 1,1-DCA

and TCA. This was consistent with PCR based molecular analysis of the microbial population that was stimulated.

SERDP/ESTCP Workshop December, 2003, Washington, D.C.
Bioaugmentation of an Aquifer Test Site for the Aerobic Cometabolic Transformation of a Chlorinated Solvent Mixtures by Butane-Utilizing Microorganisms Lewis Semprini, Mark E. Dolan, Perry L. McCarty, Gary Hopkins, Jun Li, Oregon State University.

This SERDP funded project assessed the cometabolic transformation of chlorinated solvent mixtures by native and bioaugmented butane-utilizing microbes. Field tests were performed in two parallel, but hydraulically separate, well legs installed at Moffett Federal Airfield, CA, One well leg was bioaugmented with approximately 5 g dry weight of a butane-utilizing enrichment culture known to cometabolically transform 1,1-dichloroethene (DCE), 1,1-dichloroethane (DCA), and 1,1,1-trichloroethane (TCA). The well legs were hydraulically controlled by separate injection/ extraction systems and were both fed pulses of butane and oxygen and were continually fed CAHs. Groundwater monitoring wells were located 1.0, 2.2, and 4.0 m from the respective injection wells and were semi-continuously analyzed for butane, chlorinated aliphatics, pH, anions, and dissolved oxygen. Periodically, samples were taken from the groundwater monitoring wells, or from two fully-penetrating wells placed 0.5 m and 1.5 m from the injection wells, for molecular microbial analyses including terminal restriction fragment length polymorphism (T-RFLP), real time quantitative PCR, and fluorescence in situ hybridization (FISH). Bioaugmentation stimulated butane uptake and CAH transformation with the greatest removal efficiencies observed within the first week, followed by declining CAH treatment efficiency over a period of days to months. DCE was at least partially transformed in both the indigenous and bioaugmented well legs. An injection concentration of 175 mg/L DCE was readily transformed in the bioaugmented well leg with a removal efficiency of greater than 90% while only 25-35% removal occurred in the indigenous well leg. Neither DCA nor TCA was transformed in the indigenous well leg, while both DCA and TCA transformation were obtained in the bioaugmented well leg. However, generally < 60% TCA transformation efficiency was obtained and it was difficult to maintain TCA transformation over time. A clear and repeatable microbial community transition from dominance of an organism(s) with a T-RFL of 277 bp, when restricted with MnlI, to an organism(s) with a T-RFL of 126 bp occurred upon bioaugmentation and stimulation of the aquifer test zone with butane and oxygen. However, the microbial succession was not well correlated to CAH removal efficiency and neither the 277 bp organism nor the 126 bp organism were present in dominant quantities in the bioaugmentation culture. A *Rhodococcus* sp. present in the bioaugmentation culture was quantified in samples taken from the field using real time PCR, but was found to be in insufficient quantity to appear in the T-RFLP analyses or to greatly influence CAH transformation.

May 2004 Oregon State University Crop and Soil Science Spring Seminar Series "A Microbe's View of Soil"
Bioaugmentation of an Aquifer Zone for the Cometabolic Transformation of Problematic Chlorinated Solvents

Invited Speaker: Dr. Mark E. Dolan

2004 Fall General Meeting of the American Geophysical Union, San Francisco, CA
In Situ Subsurface Cometabolic Transformation of Chlorinated Solvent Mixtures by Native and Bioaugmented Butane Utilizing Microorganisms
Mark E. Dolan, Lewis Semprini, Oregon State University.
Gary D. Hopkins, Perry L. McCarty, Stanford University.

An aquifer test zone at Moffett Federal Airfield, CA, was used to assess the cometabolic transformation of chlorinated solvent mixtures by native and bioaugmented butane-utilizing microbes. Two parallel, but hydraulically separate, well legs were controlled by separate injection/ extraction systems and were fed pulses of butane and oxygen and were continually fed chlorinated aliphatic hydrocarbons \(CAHs\). Groundwater monitoring wells were located 1.0, 2.2, and 4.0 m from the respective injection wells and were semi-continuously analyzed for butane, CAHs, pH, anions, and dissolved oxygen. One well leg was bioaugmented with approximately 5 g dry weight of a butane-utilizing enrichment culture known to cometabolically transform 1,1-dichloroethene \(DCE\), 1,1-dichloroethane \(DCA\), and 1,1,1-trichloroethane \(TCA\). Periodically, samples were taken from the groundwater monitoring wells, or from two fully-penetrating wells placed 0.5 m and 1.5 m from the injection wells, for molecular microbial analyses including terminal restriction fragment length polymorphism \(T-RFLP\), real time quantitative PCR.

Bioaugmentation stimulated butane uptake and CAH transformation with the greatest removal efficiencies observed within the first week, followed by declining CAH treatment efficiency over a period of days to months. DCE was at least partially transformed in both the indigenous and bioaugmented well legs. An injection concentration of 175 mg/L DCE was readily transformed in the bioaugmented well leg with a removal efficiency of greater than 90\% while only 25\% removal occurred in the indigenous well leg. Neither DCA nor TCA was transformed in the indigenous well leg, while both DCA and TCA transformation were obtained in the bioaugmented well leg. However, less than 80\% TCA transformation efficiency was obtained and it was difficult to maintain TCA transformation over time.

A clear and repeatable microbial community transition from dominance of organisms with a T-RFL of 277 bp, when restricted with MnlI, to an organisms with a T-RFL of 126 bp occurred upon bioaugmentation and stimulation of the aquifer test zone with butane and oxygen. Microbial community structure varied between the two parallel well legs while reasonably similar communities were observed along the flow path of the bioaugmented well leg. A *Rhodococcus* sp. present in the bioaugmentation culture was quantified in samples taken from the field using real time PCR. The organism was successfully transported at least 2 m through the subsurface, but was found to be present in insufficient quantity relative to the total microbial community to appear in T-RFLP analyses.

January, 2005 Montana State University Center for Biofilm Engineering Seminar Series
Field Bioaugmentation of a Butane-Utilizing Culture to Co-metabolize of a Mixture of Problematic Chlorinated Solvents
Invited Speaker: Dr. Mark E. Dolan